BNL-73534-2004
FORMAL REPORT

Proceedings of RIKEN BNL Research Center Workshop Volume 66

RHIC Spin Collaboration Meeting XXIX

October 8-9, 2004
Torino, Italy

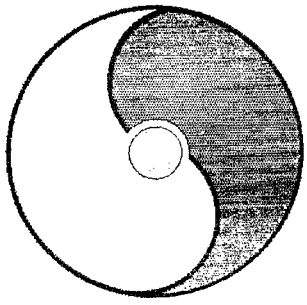

Organizer:
Akio Ogawa

RIKEN BNL Research Center

Building 510A, Brookhaven National Laboratory, Upton, NY 11973-5000, USA

DISCLAIMER

This report was prepared as an account of work sponsored by an agency of the United States Government. Neither the United States Government nor any agency thereof, nor any of their employees, nor any of their contractors, subcontractors or their employees, makes any warranty, express or implied, or assumes any legal liability or responsibility for the accuracy, completeness, or any third party's use or the results of such use of any information, apparatus, product, or process disclosed, or represents that its use would not infringe privately owned rights. Reference herein to any specific commercial product, process, or service by trade name, trademark, manufacturer, or otherwise, does not necessarily constitute or imply its endorsement, recommendation, or favoring by the United States Government or any agency thereof or its contractors or subcontractors. The views and opinions of authors expressed herein do not necessarily state or reflect those of the United States Government or any agency thereof.

FOR UNCLASSIFIED, UNLIMITED STI PRODUCTS

Available electronically at-

OSTI:

http://www.osti.gov/bridge

Available for a processing fee to U.S. Department of Energy and its contractors, in paper from-

U.S. Department of Energy
Office of Scientific and Technical Information
P.O. Box 62
Oak Ridge, TN 37831
(865) 576-8401
Facsimile: (865) 576-5728
E-mail: reports@adonis.osti.gov

National Technical Information Service (NTIS):

Available for sale to the public from-

U.S. Department of Commerce
National Technical Information Service
5285 Port Royal Road
Springfield, VA 22131
(800) 553-6847
Facsimile: (703) 605-6900
Online ordering: http://www.ntis.gov/ordering.htm

Printed on recycled paper

Preface to the Series

The RIKEN BNL Research Center (RBRC) was established in April 1997 at Brookhaven National Laboratory. It is funded by the "Rikagaku Kenkyusho" (RIKEN, The Institute of Physical and Chemical Research) of Japan. The Center is dedicated to the study of strong interactions, including spin physics, lattice QCD, and RHIC physics through the nurturing of a new generation of young physicists.

The RBRC has both a theory and experimental component. At present the theoretical group has 4 Fellows and 3 Research Associates as well as 11 RHIC Physics/University Fellows (academic year 2003-2004). To date there are approximately 30 graduates from the program of which 13 have attained tenure positions at major institutions worldwide. The experimental group is smaller and has 2 Fellows and 3 RHIC Physics/University Fellows and 3 Research Associates, and historically 6 individuals have attained permanent positions.

Beginning in 2001 a new RIKEN Spin Program (RSP) category was implemented at RBRC. These appointments are joint positions of RBRC and RIKEN and include the following positions in theory and experiment: RSP Researchers, RSP Research Associates, and Young Researchers, who are mentored by senior RBRC Scientists. A number of RIKEN Jr. Research Associates and Visiting Scientists also contribute to the physics program at the Center.

RBRC has an active workshop program on strong interaction physics with each workshop focused on a specific physics problem. Each workshop speaker is encouraged to select a few of the most important transparencies from his or her presentation, accompanied by a page of explanation. This material is collected at the end of the workshop by the organizer to form proceedings, which can therefore be available within a short time. To date there are sixty-six proceeding volumes available.

The construction of a 0.6 teraflops parallel processor, dedicated to lattice QCD, begun at the Center on February 19, 1998, was completed on August 28, 1998 and is still operational. A 10 teraflops QCDOC computer in under construction and expected to be completed this year.

N. P. Samios, Director
November 2004

*Work performed under the auspices of U.S.D.O.E. Contract No. DE-AC02-98CH10886.

CONTENTS

Preface to the Series..... i

RHIC Spin Collaboration Meeting XXIX ~ October 8-9, 2004 Torino, Italy

RHIC Status & Plan
M. Bai..... 1

Status of Polarized Ion Source
A. Zelinski..... 23

Polarized Beam at COSY and HESR
A. Lehrach..... 73

Measurement of the Analyzing Power for pp Elastic Scattering at CNI Peak Region for Absolute Polarimetry at RHIC
H. Okada..... 99

Measurement A_N in the Elastic pp-scattering with Small Momenta Transferred at $\sqrt{s}$=200 GeV at RHIC
I. Alekseev..... 123

Measurement of the Analyzing Power of Proton-Carbon Elastic Scattering in the CNI Region at RHIC
O. Jinnouchi..... 143

Energy Dependence of pp and pC CNI Analyzing Power
L. Trueman..... 167

Spin Dynamics for High Energy Protons
N. Buttimore..... 187

Transversity Measurements in SIDIS
R. Seidl..... 203

Short Comment on the HERMES A_{UT}
A. Efremov..... 231

CONTENTS

Disentangling the Sources of Single Spin Asymmetries
O. Teryaev 235

Suppression of Collins Mechanism for SSA in $p\uparrow p \rightarrow \pi X$
U. D'Alesio 245

Current and Future Transverse Spin at the PHENIX Experiment at RHIC
Y. Makdisi 263

Spin Effects in Large Rapidity Neutral Pion Production at STAR
A. Ogawa 281

Transversity Properties of Quarks and Nucleons in SIDIS and Drell Yan
L. Gamberg 297

Sivers Gluon Distribution in $p\uparrow p \rightarrow DX$ at RHIC
M. Boglione 329

A Critique of the Angular Momentum Sum Rules and a New Angular Momentum Sum Rule
E. Leader 339

Discussions
Sivers & Collins Mechanisms, *M. Anselmino* 347
Near-Term (<2 years) Experimental Opportunities, *L. Bland* 351

Physics at HERMES
D. Hasch 361

LEPTO and Polarized SIDIS
A. Kotzinian 397

Spin Asymmetries for high-p_T Pions and Jets
M. Stratmann 409

CONTENTS

$\pi 0$ A_{LL} Results from PHENIX
A. Bazilevsky..... 433

Measurement of Prompt Photon in $\sqrt{s}$=200 GeV pp Collisions
K. Okada..... 459

Longitudinal Progress at STAR
J. Sowinski..... 495

STAR Tracking Upgrades
M. Miller..... 511

Discussion:
Physics of Double Spin Asymmetries, *A. Deshpande & W. Voglesang*..... 525

PHENIX: Muon Trigger Upgrade and Nose Cone Calorimeter
K. Barish..... 541

PHENIX VTX Upgrade
Y. Goto..... 563

Jet Reconstruction Algorithms for RHIC
M. Miller..... 587

Plans for STAR Forward Calorimetry Upgrade
L. Bland..... 595

List of Registered Participants..... 608

Agenda..... 610

Additional RIKEN BNL Research Center Proceeding Volumes..... 612

Contact Information

RHIC Status and Plan

Mei Bai
Brookhaven National Laboratory

Outline

- Goal for RHIC pp RUN 5
  - Machine goals
  - RHIC pp projections
- Status
  - Machine status
  - Timeline
- RUN Plan
  - Set-up: 2 weeks
    - Physics data taking starts at the end of the setup
  - Ramp-up
    - Improve the machine performance
  - Physics run
    - Machine tuning saturates
- Machine developments for the future

RUN 5 Goal

- Physics data taking
- RHIC Machine developments
  - Spin tune measurement
  - Explore pp accelerating beyond 100 GeV towards 250 GeV
  - Spin flipping commissioning
  - Establish injection with both snake and spin rotators on at full field
- AGS cold snake commissioning

RHIC pp Run 5 projection

	bunch intensity [10^{11}]	# of bunch	# of collision points	$\mathcal{L}_{store\ average}$* [$10^{30}$ $cm^{-2}s^{-1}$]	$\mathcal{L}_{per\ week}$** [pb-1]	polarization at store
Run5 min	0.7	56	4	4.0	0.9	40%
Run5 max w/o cold snake	1.0	79	4	9.0	3.0	45~50%
Run5 max w cold snake	1.5	56	4	15.0	4.5	50~60%

Machine Parameters

RHIC			AGS		
Energy at injection	24.3	GeV/u	Energy at injection	2.2	GeV/c
Energy at Store	100.2	GeV/c	Energy at extraction	24.3	GeV/c
Interaction points	6 8 10 12 2 4	clock	Imperfection spin resonance	Warm snake	
β* at injection	10 10 10 10 10 10	m	4 strong intrinsic spin resonances at 0+Qy, 12+Qy, 36+Qy and 36-Qy	Ac dipole	
β* at store	1 1 10 10 3 10	m			
Working points	Inj & ramp: (28.73, 28.72) Store: (28.69, 29.68)				
Snakes current	DC		All the other spin resonances	No correction	
Spin rotator current	Ramp up after store				
Experimental magnets	STAR, PHENIX: on DC from inj. to top				
RF accelerating cavities	At injection: 100 kV ramp: 300 kV At store: 300 kV				
RF storage cavities	No rebucketing				

Machine Status

- RHIC in preparation for Cu run. Two dry runs are done.
- Snake no configuration change
- Online model
  - optimize the lattice fitting so that the β^* will be more close to 1m. In working progress.
- New applications
  - Skew quad modulation decoupling. This is will allow one to decouple the machine during the ramp. The application is expected to be commissioned during the Cu Run.
  - RHIC polarimeter application: working progress, expect to be ready around Nov.

Machine Status

- New survey was done along the ring and confirmed an additional 2mm sinking in IP12 between year 2002 and year 2004

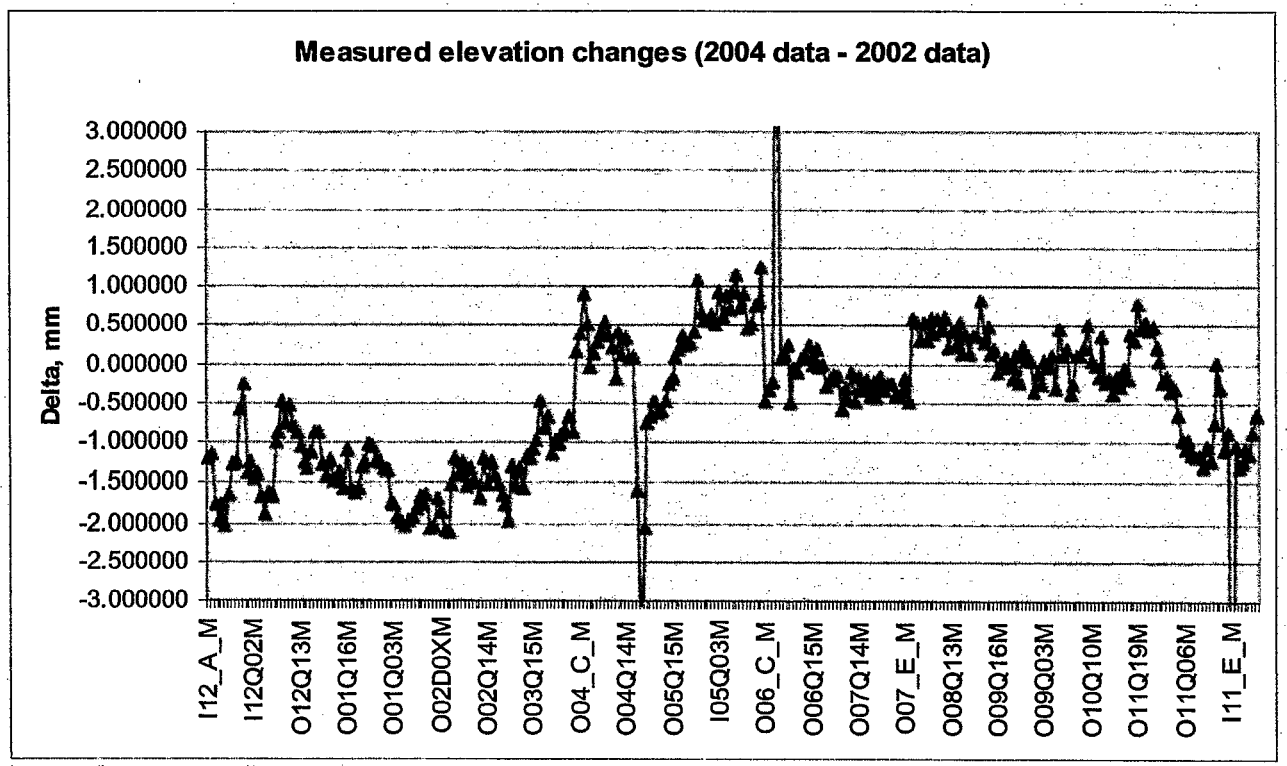

Plans for realignment

- Realign the quads and dipoles around IP12 & 2. A total of ~69 quads+ their adjacent dipoles/per ring will be involved. RHIC survey group plans to realign the IP12 first and then do IP2 if time allows

- also realign the following 4 additional quads:
  I12Q05, I05Q18
  O04Q04, O05Q09

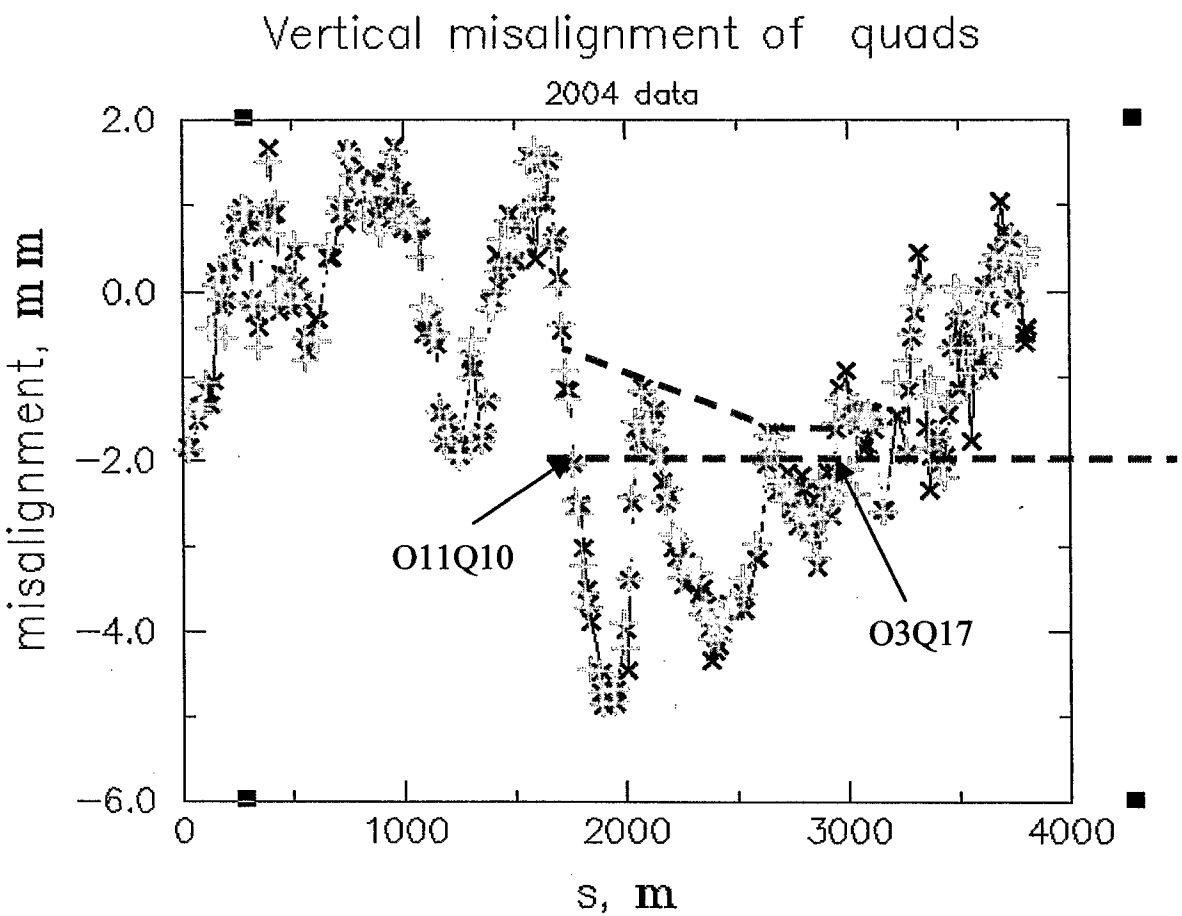

RHIC polarimeter Status

- Hardware
  - Targets will be installed around mid of Oct.
  - Silicon detectors will remain unchanged during the early part of the run
  - A new set of silicon detectors are under testing for replacement of the existing detectors during the Physics run to minimize the impact of radiation damage on the measurement
  - 25 new WFDs are expected to be delivered before the end of Oct. These WFDs will allow one to take polarization measurement in Blue and in Yellow at the same time

RHIC polarimeter Status

- software
  - WFD software. Still owned by Igo & Dima. C-AD has assigned an control expert to help Igo & Dima. It will be very beneficial for the technology transfer to have Igo & Dima over before the Run.
  - RHIC polarimeter application
    - Provides an user friendly interface
    - Consolidate many functionalities which used to require several pet page accesses
    - Auto-target scan
    - Auto-polarization profile measurement
    - Auto-entry to eLog
    - Transfer the banana plots as well as other quality factors to allow one to examine/log the quality of a particular measurement
  - Delivery date: end of January of 2005

AGS Cold Snake Status

- Short-to-ground was fixed

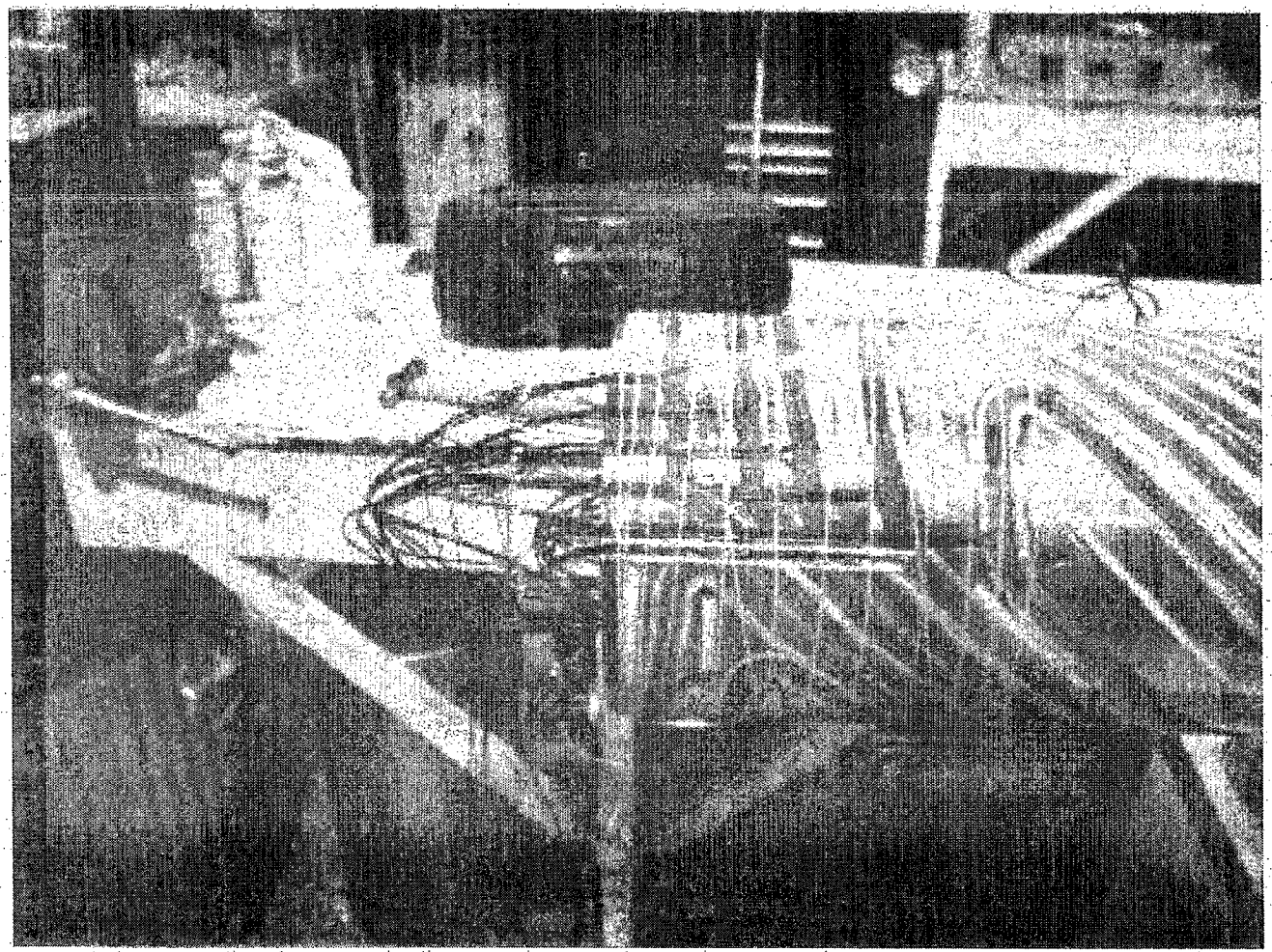

AGS Cold Snake Status: first cold tests

Axial Scans: Dipole Terms

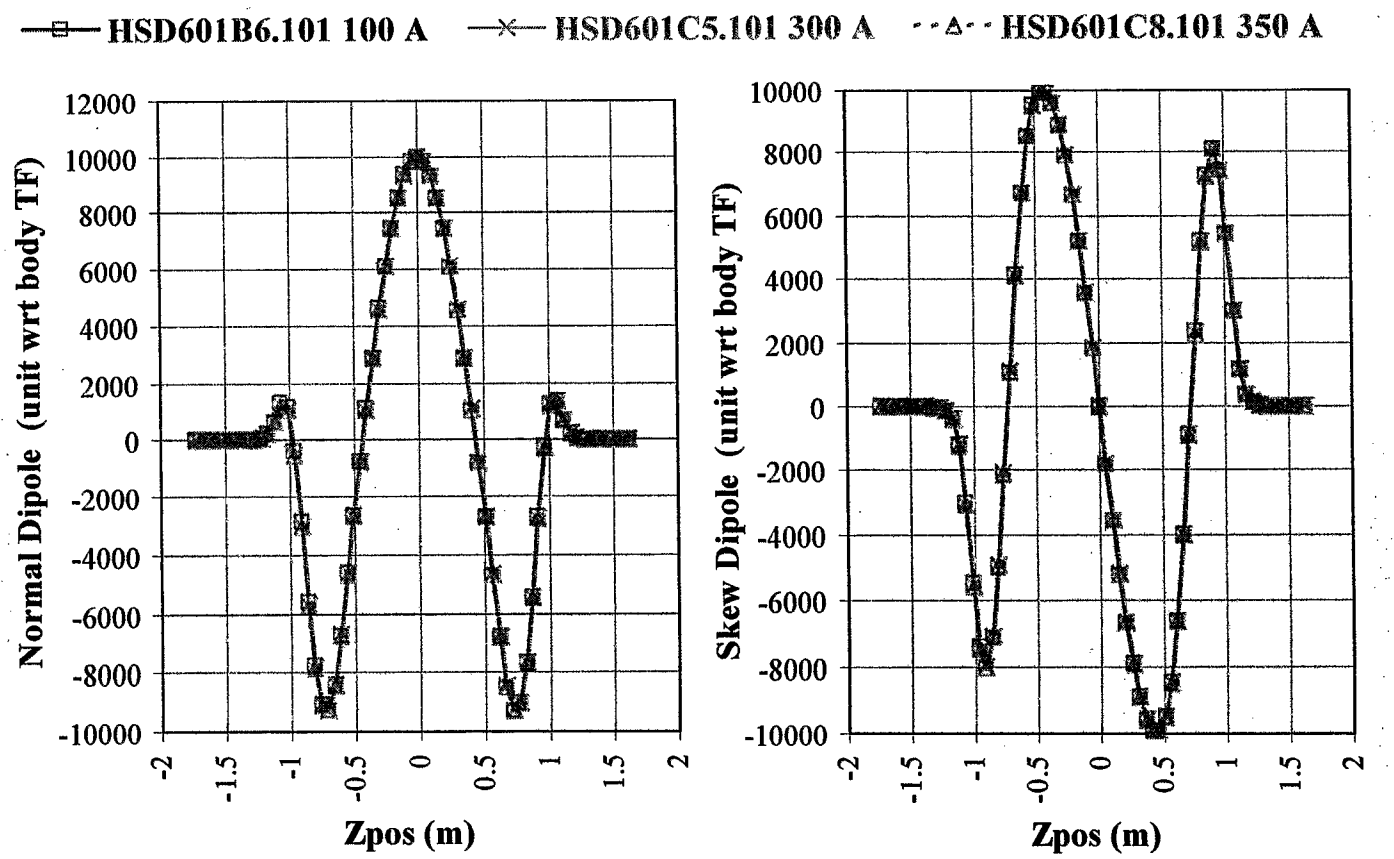

Courtesy of Animesh Jain

Plans for AGS Cold Snake

- Preparation for AGS cold snake cryostat has been started
- Cold mass into horizontal cryostat around mid of Nov.
- Cryostat is expected to be completed around the mid of Dec.
- Cool-down and cold test will get started around Christmas time
- System ready to be installed around early Feburary

Timeline

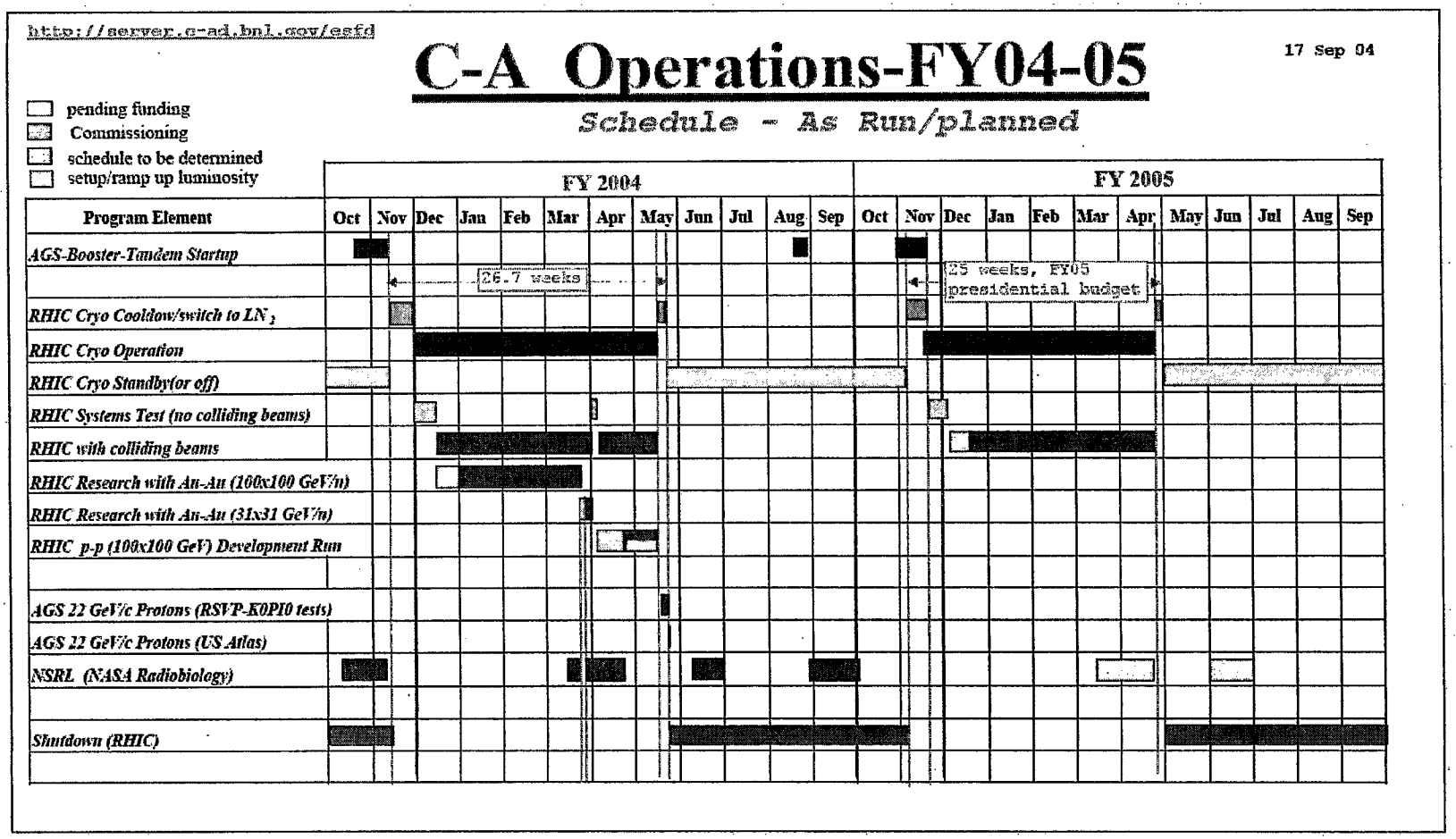
http://server.c-ad.bnl.gov/esfd
C-A Operations-FY04-05
17 Sep 04
Schedule - As Run/planned
pending funding
Commissioning
schedule to be determined
setup/ramp up luminosity
FY 2004
FY 2005
Program Element
Oct Nov Dec Jan Feb Mar Apr May Jun Jul Aug Sep
Oct Nov Dec Jan Feb Mar Apr May Jun Jul Aug Sep
AGS-Booster-Tandem Startup
26.7 weeks
25 weeks, FY05 presidential budget
RHIC Cryo Cooldow/switch to LN2
RHIC Cryo Operation
RHIC Cryo Standby(or off)
RHIC Systems Test (no colliding beams)
RHIC with colliding beams
RHIC Research with Au-Au (100x100 GeV/n)
RHIC Research with Au-Au (31x31 GeV/n)
RHIC p-p (100x100 GeV) Development Run
AGS 22 GeV/c Protons (RSVP-K0PI0 tests)
AGS 22 GeV/c Protons (US Atlas)
NSRL (NASA Radiobiology)
Shutdown (RHIC)

Timeline

Week	Monday of the week	Description	Remarks
1	08-Nov-2004	2 weeks cooldown,	Cooldown starts Nov 8
2	15-Nov-2004	80K->4K	First BLUE beam Nov 16
3	22-Nov-2004	2 weeks RHIC start-up	Beam in both rings Nov 23
4	29-Nov-2004		
5	06-Dec-2004	2 weeks RHIC ramp-up	Collisions overnight,
6	13-Dec-2004		starting Dec 6
7	20-Dec-2004	7 weeks Cu-Cu Physics,	Starts Dec 20
8	27-Dec-2004	200 GeV/u	
9	03-Jan-2004		
10	10-Jan-2005		
11	17-Jan-2005		
12	24-Jan-2005		
13	31-Jan-2005		
14	07-Feb-2005	3 weeks p-p Set-up	
15	14-Feb-2005		
16	21-Feb-2005		
17	28-Feb-2005	8 weeks p-p Physics	
18	07-Mar-2005		
19	14-Mar-2005		
20	21-Mar-2005		
21	28-Mar-2005		
22	04-Apr-2005		
23	11-Apr-2005		
24	18-Apr-2005		
25	25-Apr-2005	1 week Warm-up	

RHIC Cu Run

AGS pp setup

2-week setup

RHIC Jet target installation

AGS cold snake installation

1-week ramp up

8-week Physics Run + machine development

Run Plan: 2-week setup

- Goal: establish pp collision with reasonable polarization
  - 3-day shutdown
    - Jets target installation
    - AGS cold snake installation
    - AGS synchro setup
    - others
  - Injection setup
    - Establish Injection
      - Injection kicker timing, spin pattern confirmatioin
      - Circulating beam, capturing
      - Set the RF frequency based on Bρ and adjust the dipole field to center the beam
      - Rf loop setup
      - Orbit, chromaticity & coupling correction

Run Plan: 2-week setup

- Injection setup
  - Instrumentation setup
    - BPM, esp. the DX BPMs
    - Polarimeter: Blue and Yellow
    - PLL and Schottky
    - IPM
- Energy ramp development
  - use similar ramp as Run 4
  - Rf loop: Brho loop
  - Decoupling along the ramp. Adjust tunes/orbits/chromaticities to maximize beam/polarization transmission efficiency
  - Establish orbit/tune/chromaticity/decoupling at store
  - Cogging setup
  - Polarization ramp measurement

Run Plan: 2-week setup

- Rotator ramp development: 6 bunch
  - Establish tunes/chromaticities along the ramp, optimize the beam/polarization transmission efficiency
  - Adjust rf frequency at store to compensate the path length difference due to spin rotators
- Establish collisions
  - IR steering
  - Fine cogging tuning
- 56x56 bunch development
  - Provide stores for experiments
  - Collimator setup
  - Vernier scan

Run Plan: 1-week ramp-up

- Goal: improve the polarization as well as luminosity
  - Polarization tuning
    - Polarization ramp measurement
      - Locate the energy where polarization gets lost
      - Fine tuning the optics
    - Improve the orbit distortion
  - Luminosity tuning
    - Improve the beam transmission efficiency along the ramp

Machine development

- Polarimeter development
  - Turn-by-turn spin precession measurement
- Spin tune measurement
- Explore pp acceleration beyond 100 GeV towards 250 GeV
- Spin flipping commissioning
- Establish injection with both snake and spin rotators on at full field
  - This will allow us to save ~7 minutes per store.

Challenge of going beyond 100 GeV

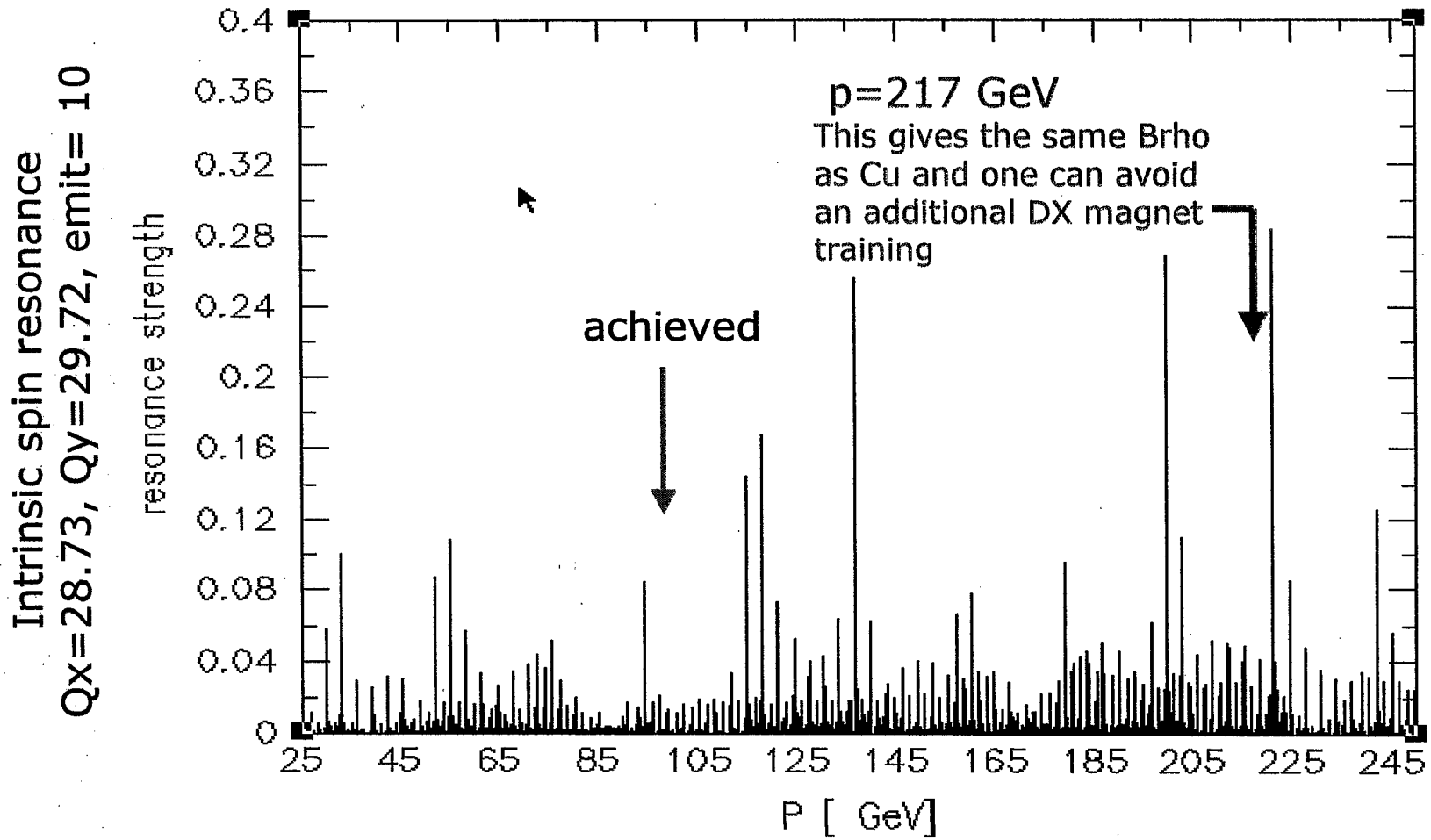

Status of polarized ion source.

A.Zelenski

- Summary of 2004 run.
- OPPIS upgrade for 2005 run.

Polarized injector, 200 MeV linac and injection lines.

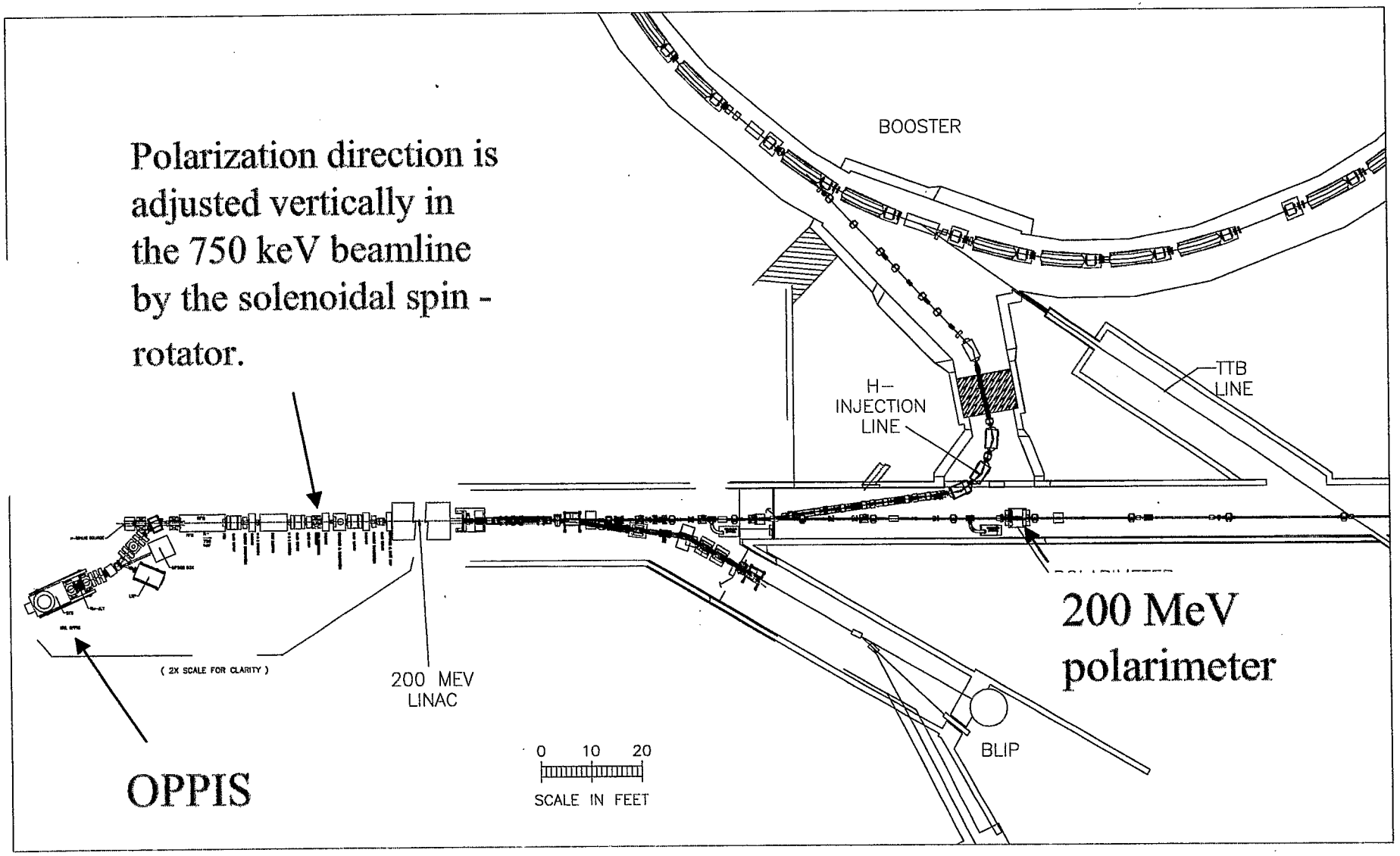

SCHEMATIC LAYOUT OF THE RHIC OPPIS.

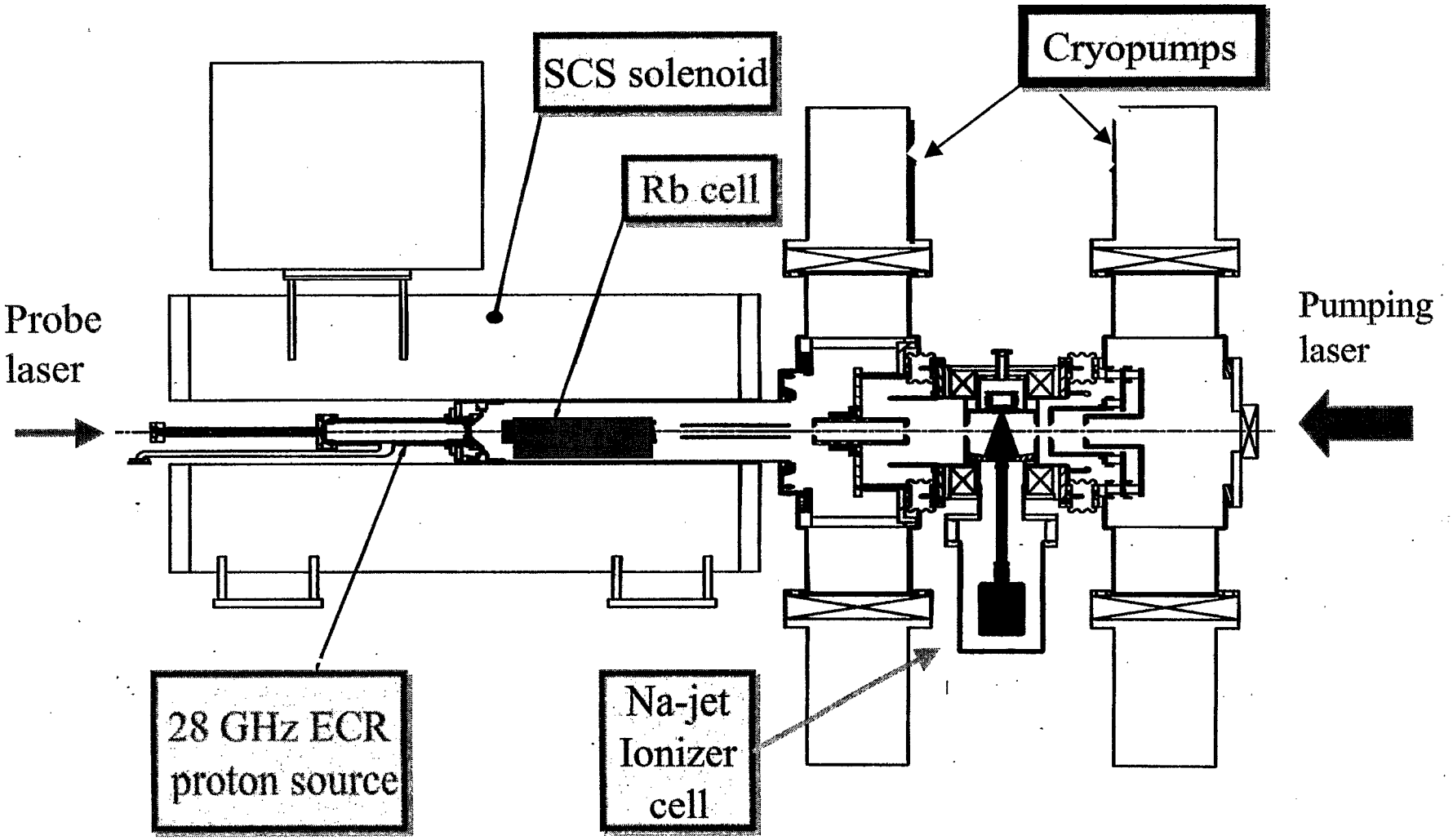

200 MeV p-Carbon and p-D polarimeter.

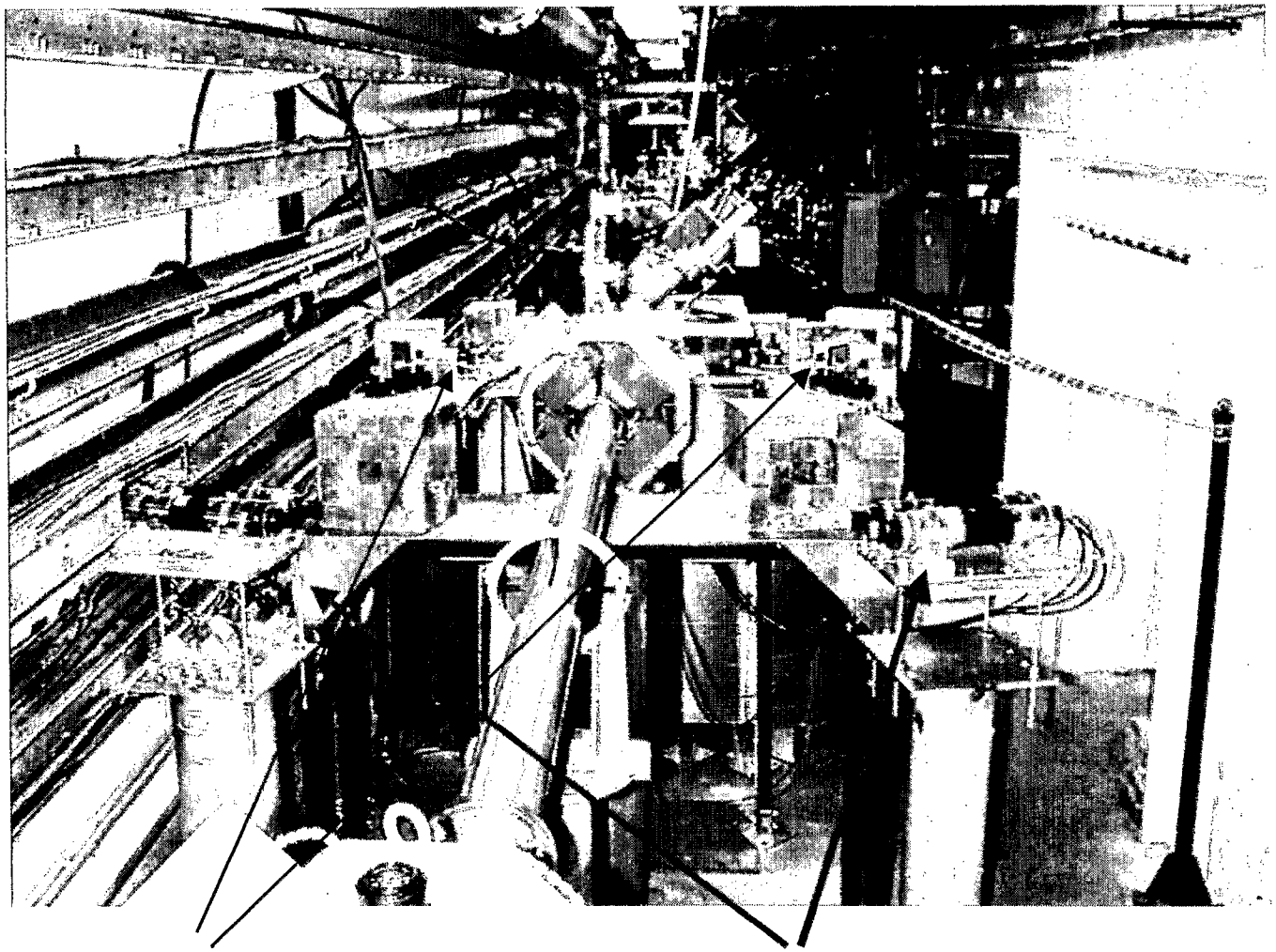

D-recoil arms

12 deg proton arms.

200 MeV polarization measurements.

Sequential measurements.

80%

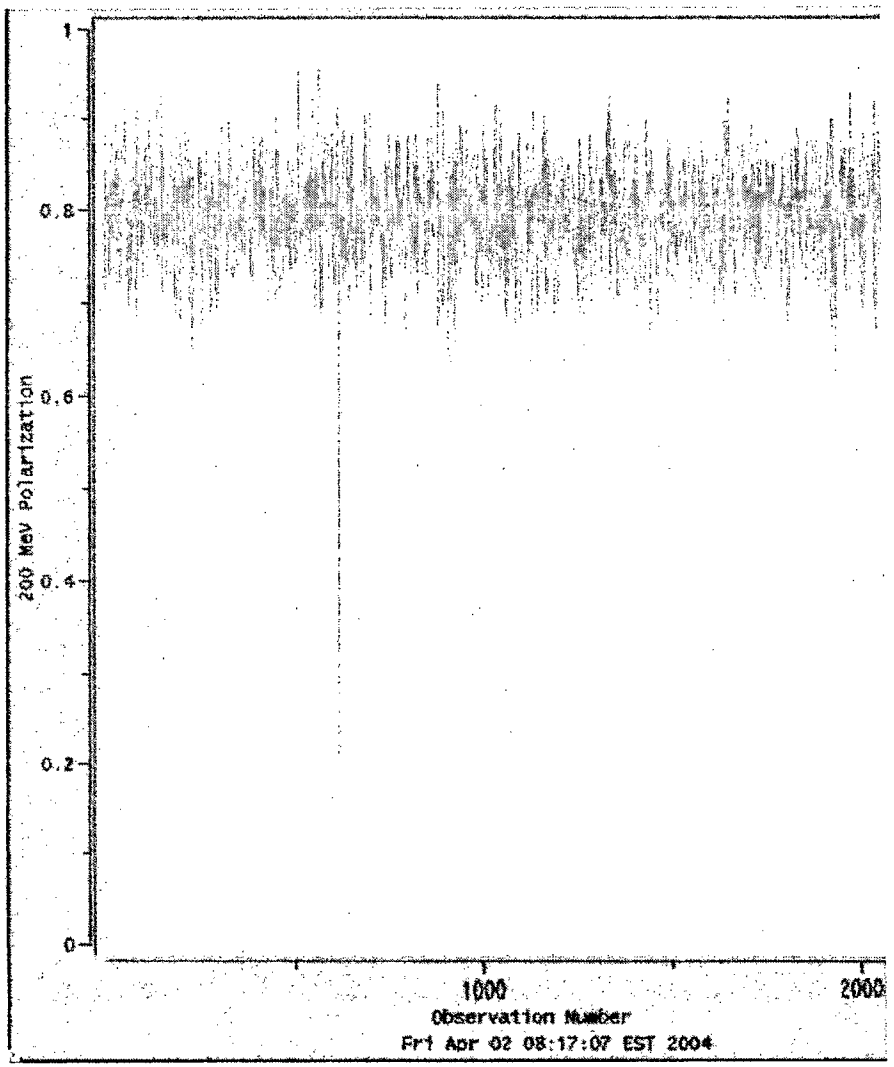

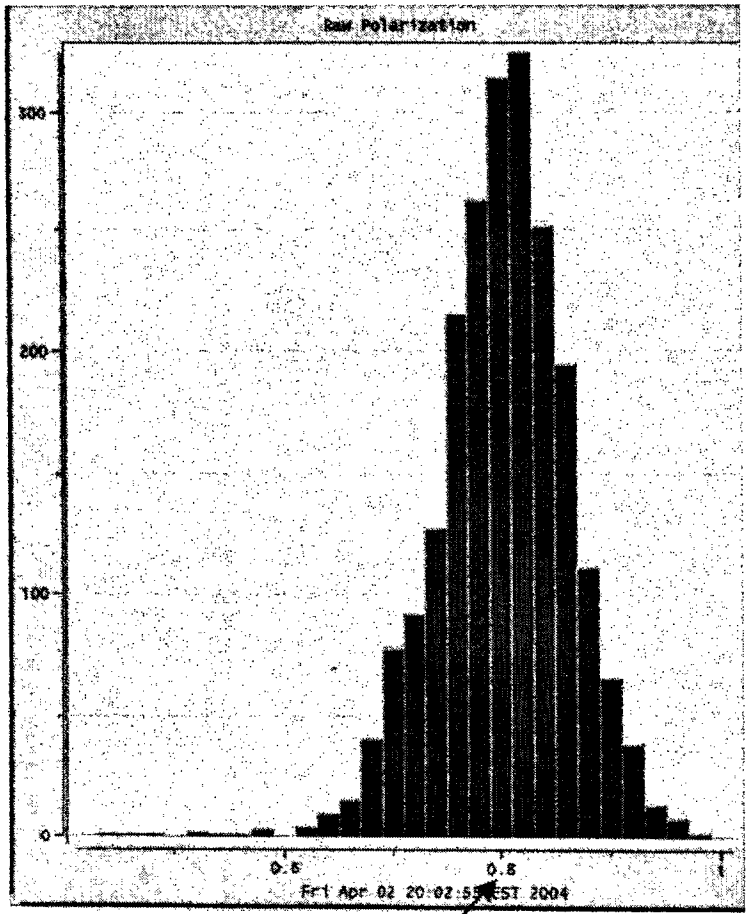

82%

Polarization histogramm,

maximum at 82%.

Polarization measurements fluctuations due to beam position "wondering" at the target.

80 % →

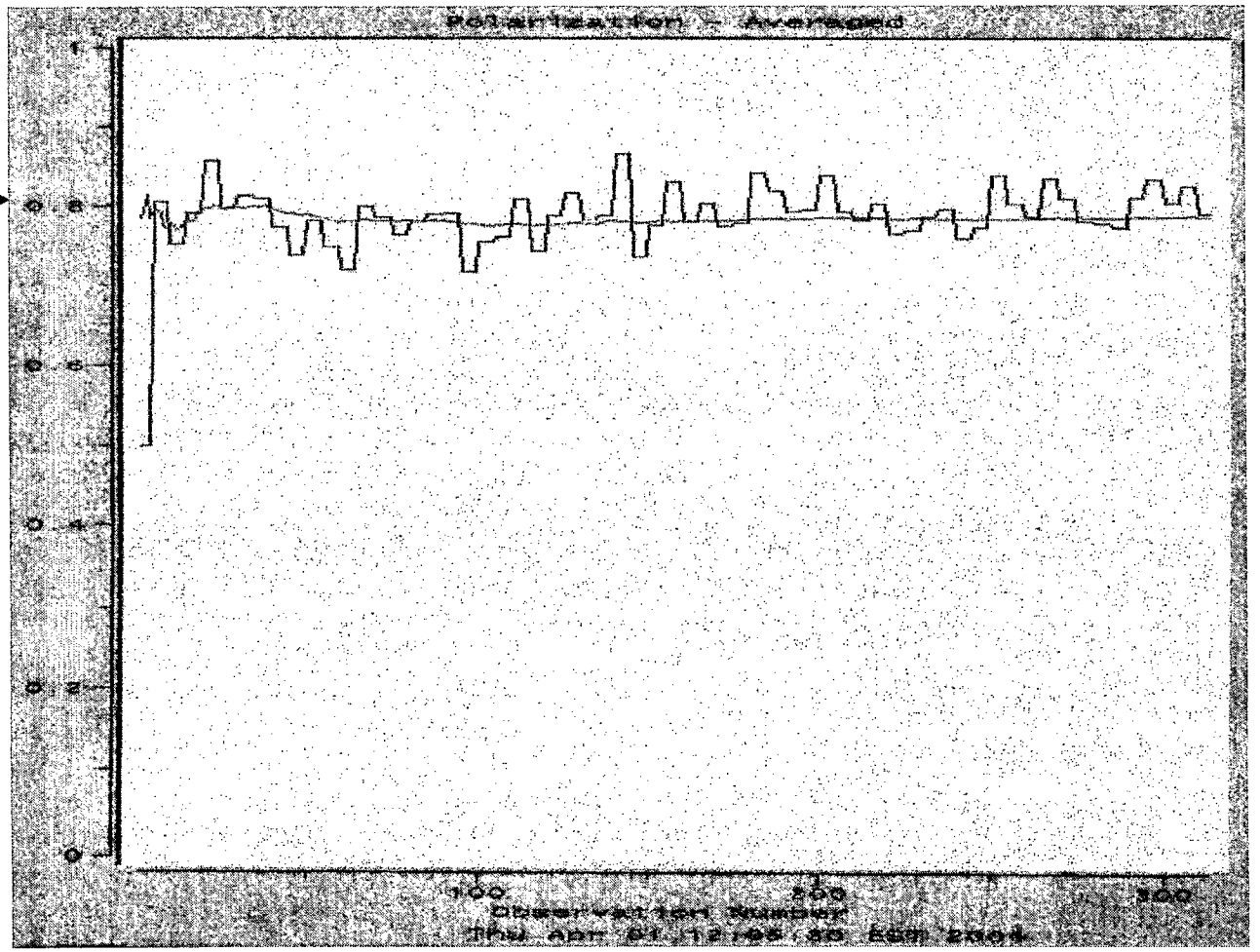

Polarization measurements at 300 keV at TRIUMF

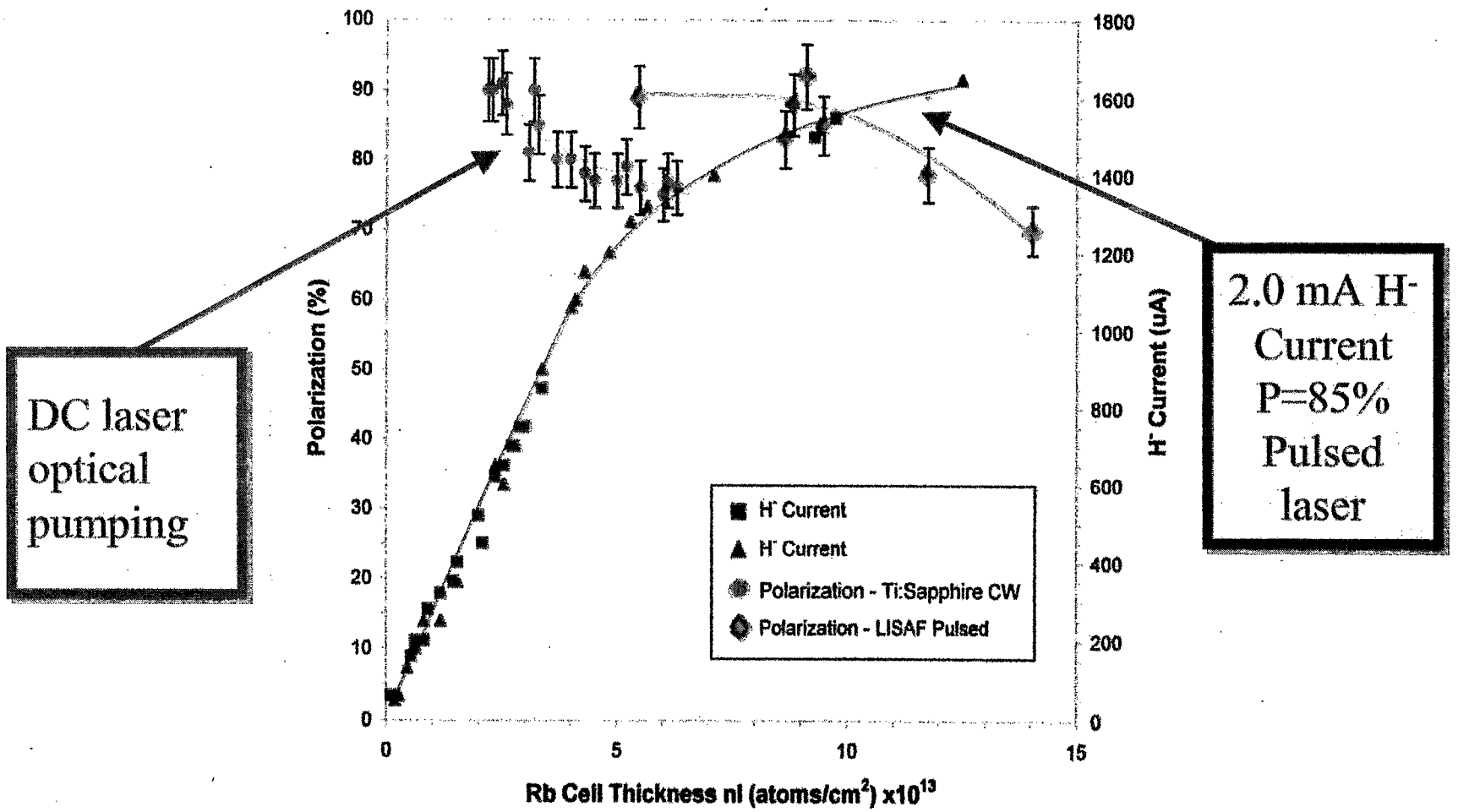

H^- ion beam current and polarization vs. optically-pumped Rb vapor thickness.

The Oxford Instr. superconducting solenoid at TRIUMF OPPIS.

- The solenoid has the cold yoke (lower transversal field).
- The field is more homogeneous and better confined.
- The solenoid had been shipped to BNL and will be installed for the 2005 run.

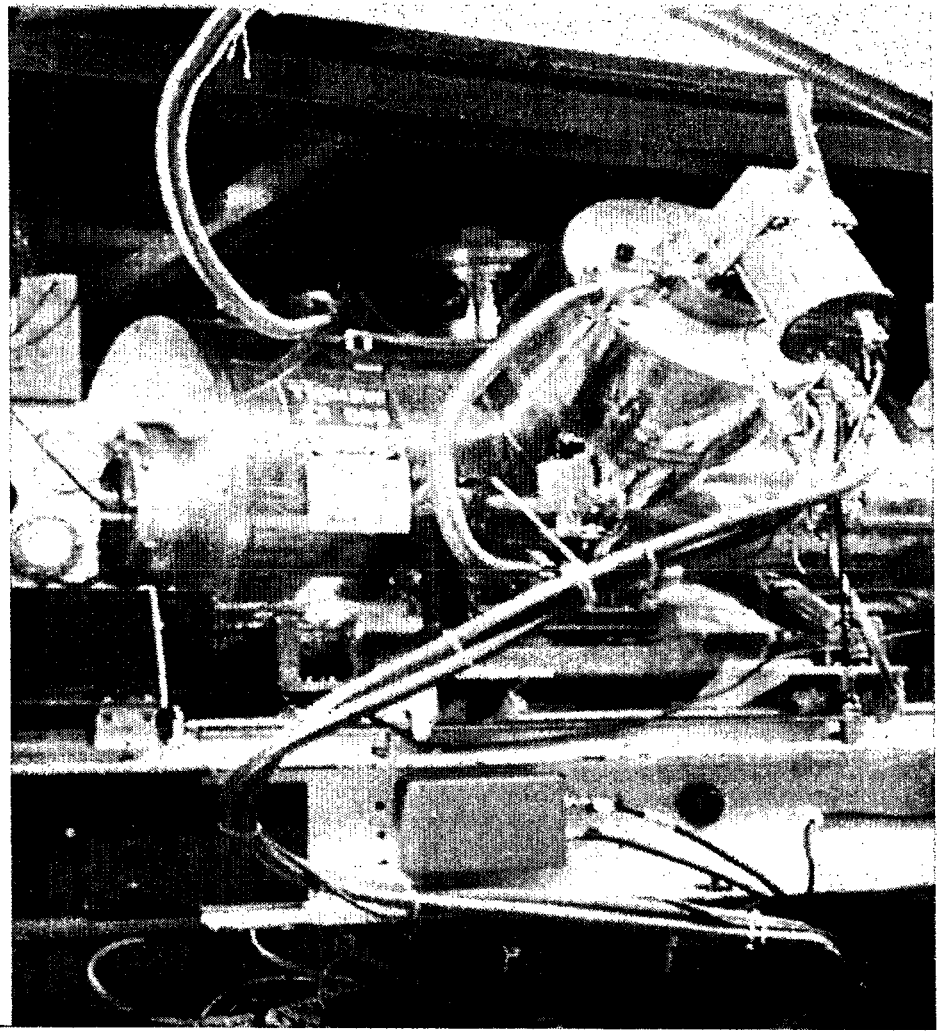

Upgrade status.

- The TRIUMF OPPIS superconducting solenoid had been shipped to BNL.
- At BNL in preparation for the solenoid arrival the operational OPPIS was completely refurbished.
- New support frame, a Na-jet ionizer power supply system was completely rebuilt, a new plumbing and wiring, realignment.
- At present, the source is back into operation with the old solenoid. A new solenoid will be initially assembled and fully tested at the separate test-bench.

A source layout at the new test bench and the Oxford Instr. solenoid.

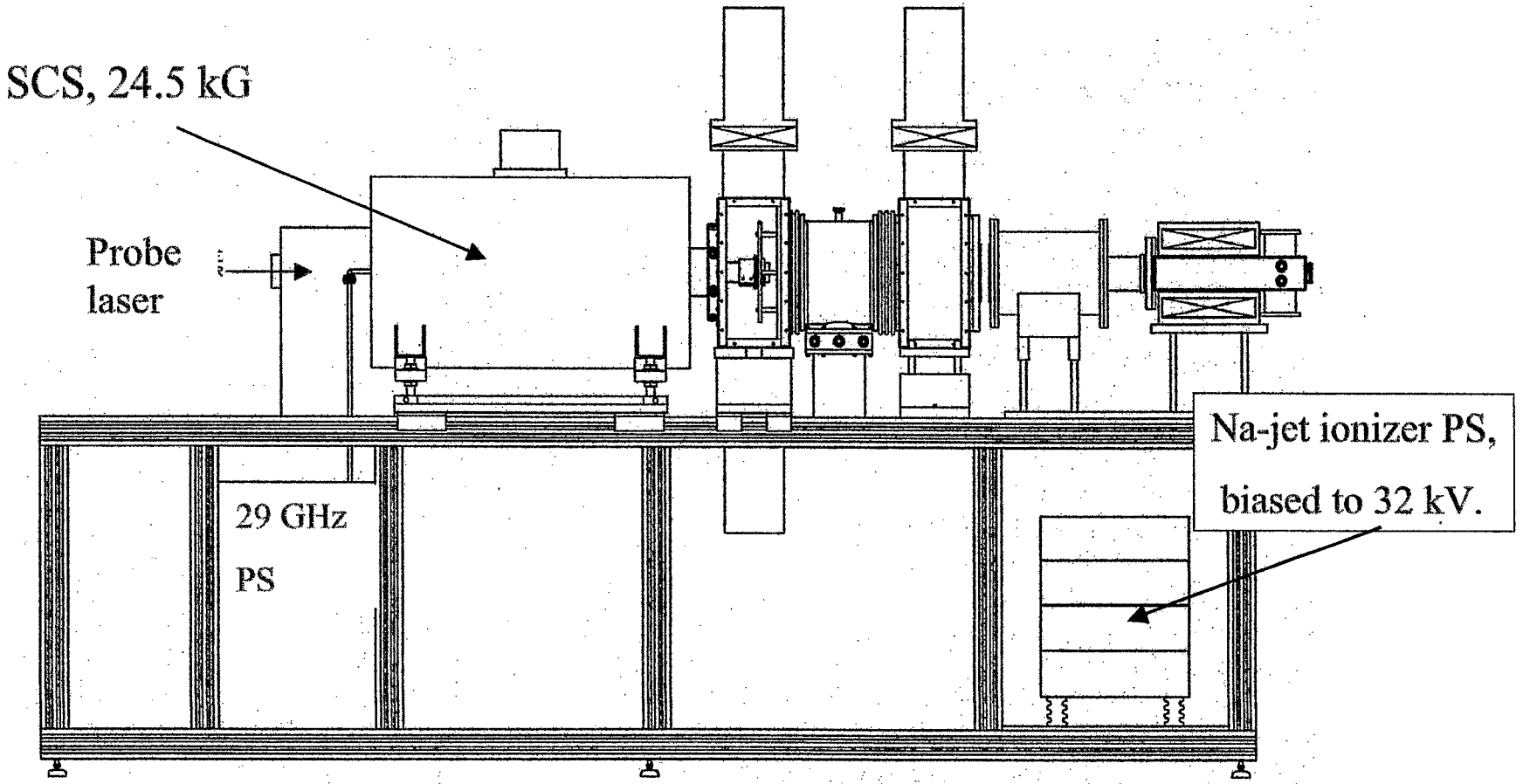

Conclusions.

- BNL OPPIS very reliably delivers polarized H^- ion beam (P = 80%) for the RHIC spin program.

- A beam intensity exceeds RHIC limit, which allowed strong beam collimation in the Booster, to reduce longitudinal and transverse beam emittances.

- The TRIUMF OPPIS superconducting solenoid (Oxford Instr.) was purchased to improve beam intensity and increase polarization to 85% value.

- This should provide sufficient intensity and higher polarization for the planned RHIC luminosity increase in run 2005.

H-jet polarimeter.

A.Zelenski, D.Graham, W.Haeberli, A.Kponou, G.Mahler, Y.Makdisi, A.Nass, J.Ritter, T.Wise, V.Zubets.

1. Dissociator design and operation.
2. Atomic beam intensity measurements and calibrations.
3. Atomic beam profile measurements.
4. QMA-quadrupole mass analyzer upgrade. QMA calibration.
5. H_2/ H – ratio measurements at the collision point.
6. Summary.

RSC meeting, Torino,
October 8, 2004

Set up @ IP12

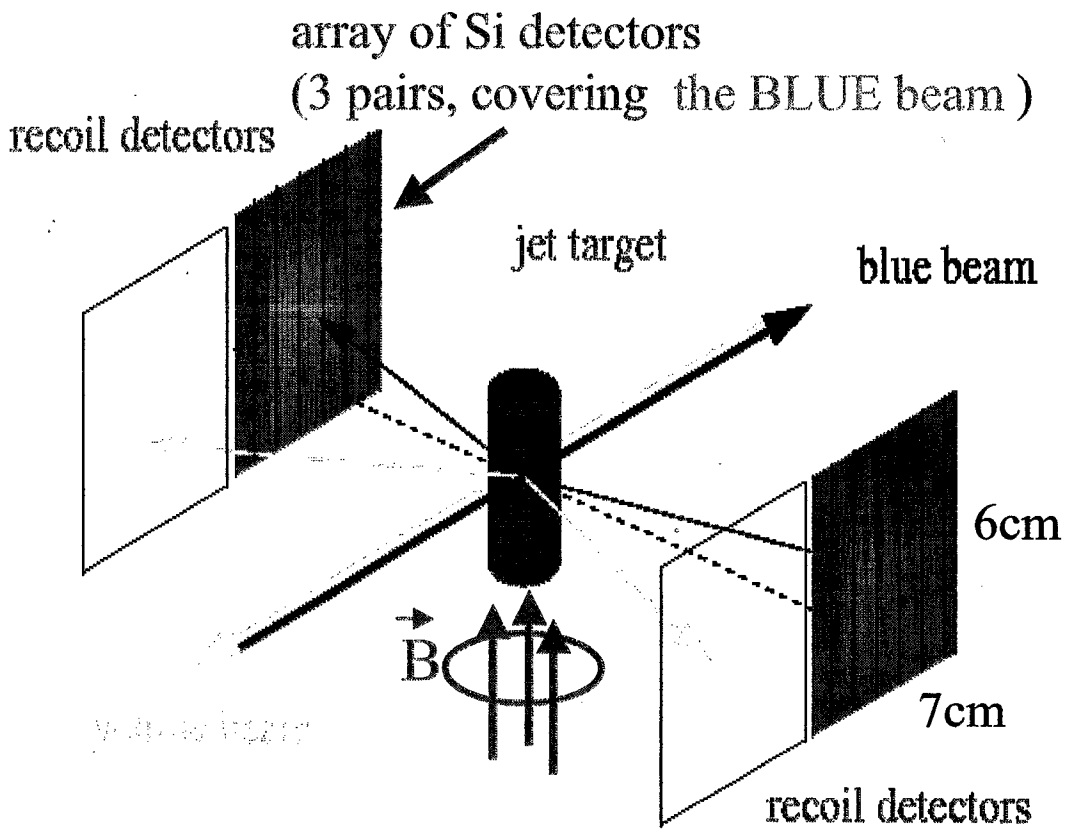

Polarized Hydrogen Gas Jet Target
polarization 0.924 +/- 0.018

Event rate ; ~6Hz (0.7~5MeV)

Si detector
7cm * 6cm / detector, 3 pairs
Acceptance 2 π /16
Measurement (recoil particle)
energy
(0.7~7MeV res. < 50 keV)
TOF (70~16ns res. < 2 ns)
Angle(10~100 mrad ,
res. <5mrad)

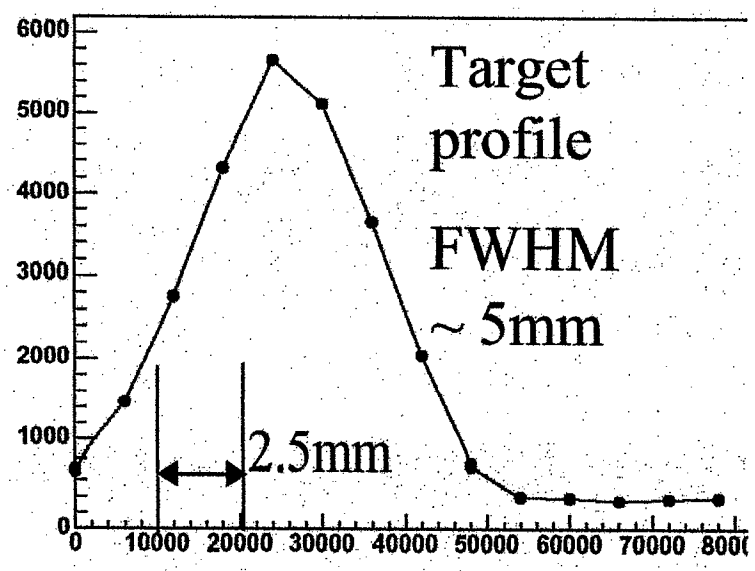

H-JET POLARIMETER SCATTERING CHAMBER

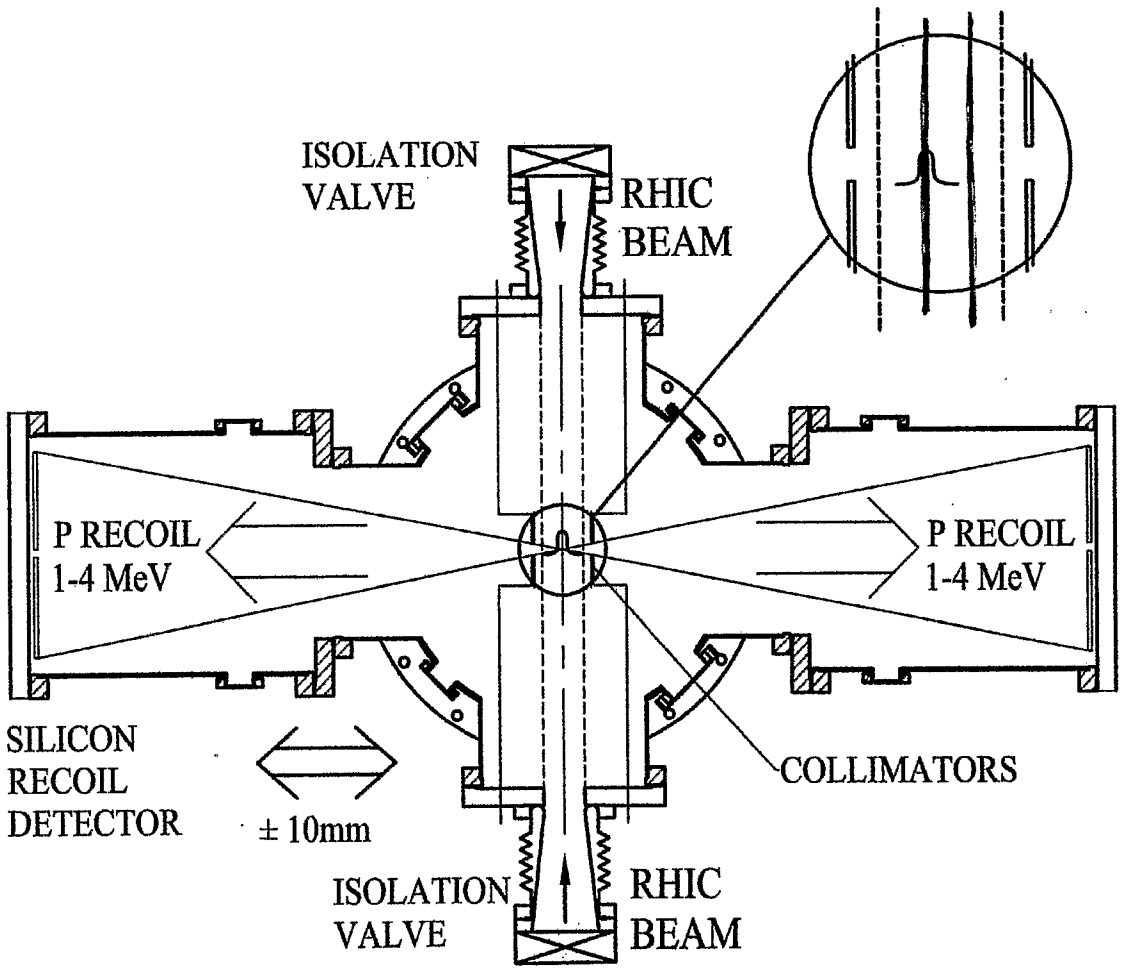

The absolute *proton* polarimeter.

Polarized H- jet Target

Thickness : $1.3+/-0.2 \cdot 10^{12}$ p/cm^2

Polarization: 93%

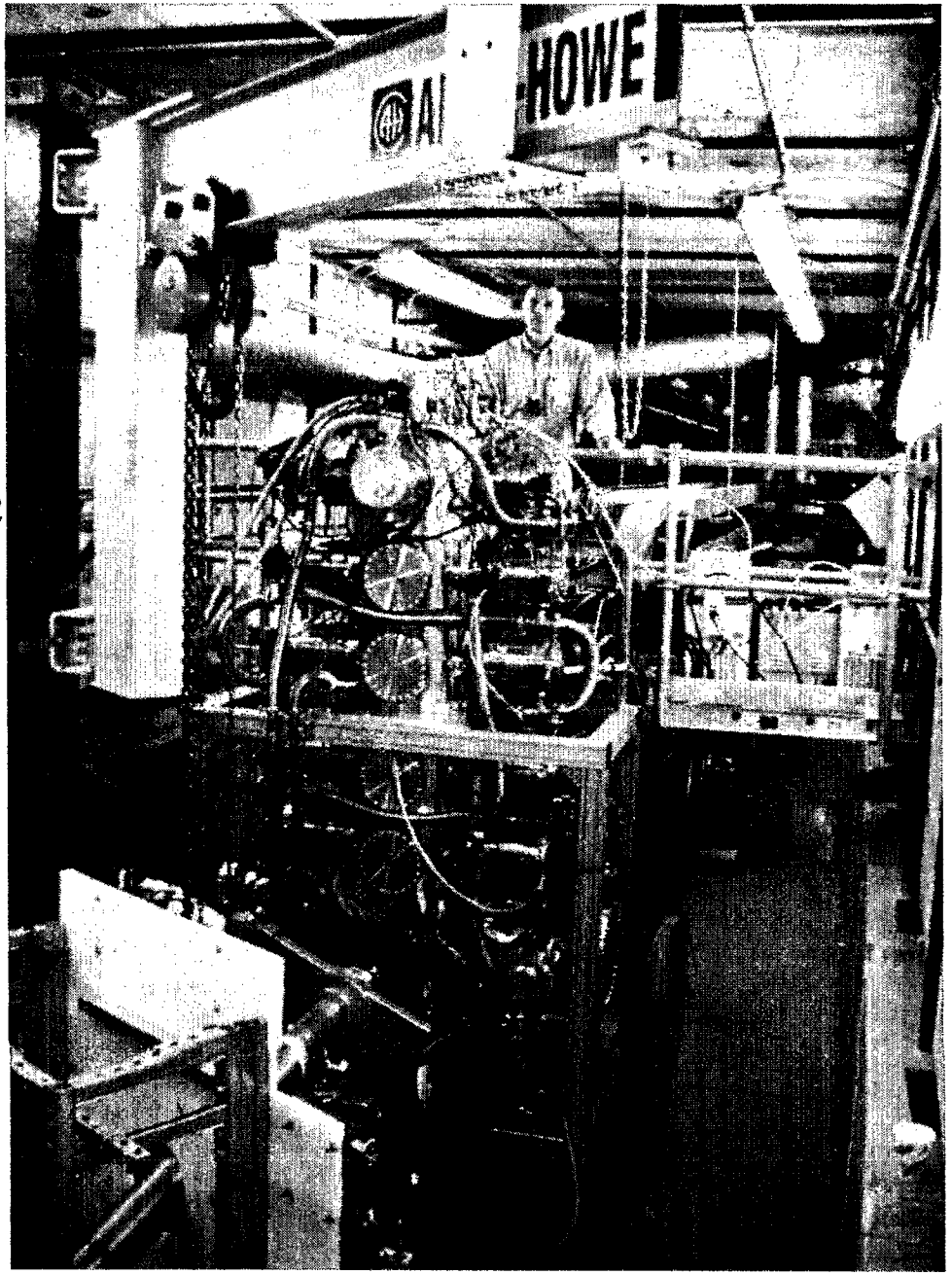

H-JET in the IR-12

Polarimeter vacuum system.

- The H-jet polarimeter includes three major parts: polarized Atomic Beam Source (ABS), scattering chamber, and Breit-Rabi polarimeter.
- The polarimeter axis is vertical and the recoil protons are detected in the horizontal plane.
- The common vacuum system is assembled from nine identical vacuum chambers, which provide nine stages of differential pumping.
- The system building block is a cylindrical vacuum chamber 50 cm in diameter and of 32 cm length with the four 20 cm (8.0") ID pumping ports.

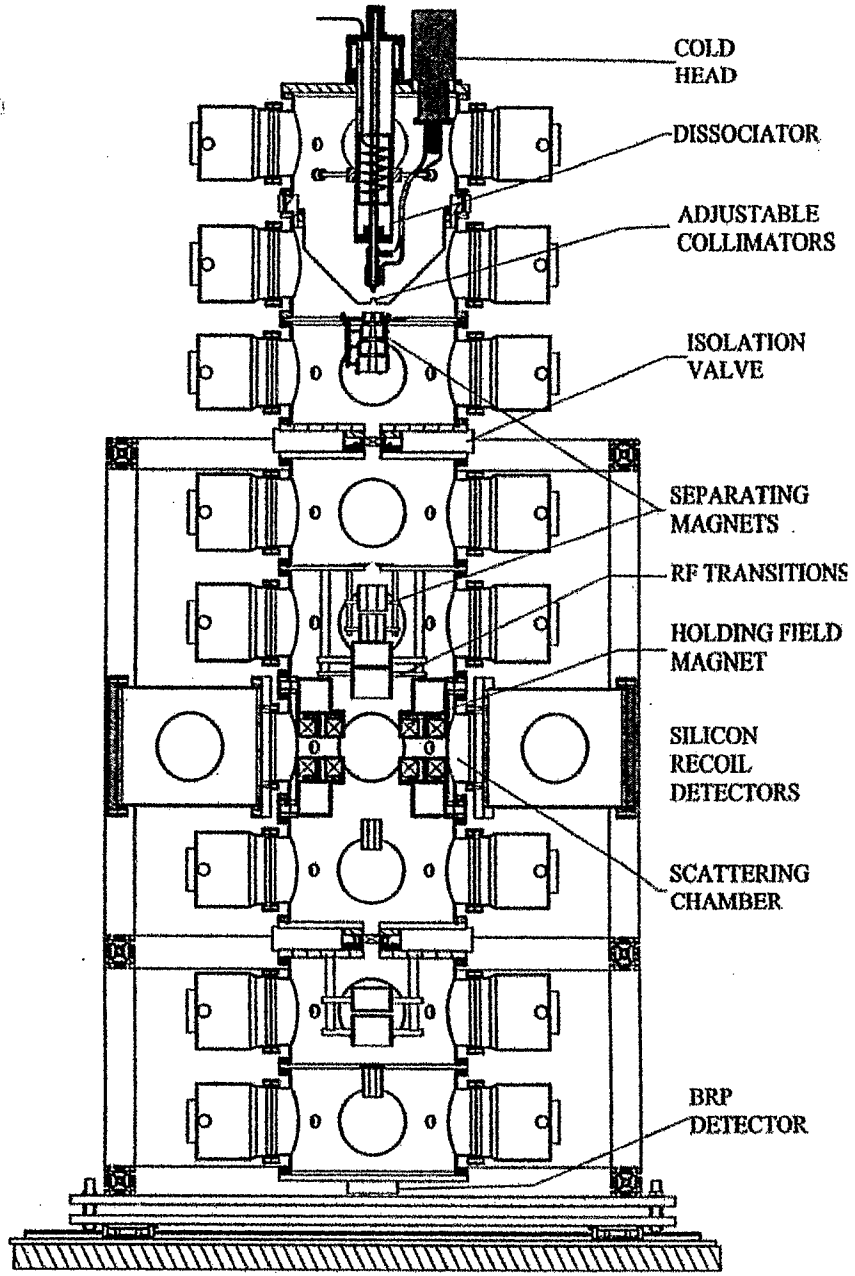

H-jet polarimeter can be moved and installed into the RHIC ring in one day.

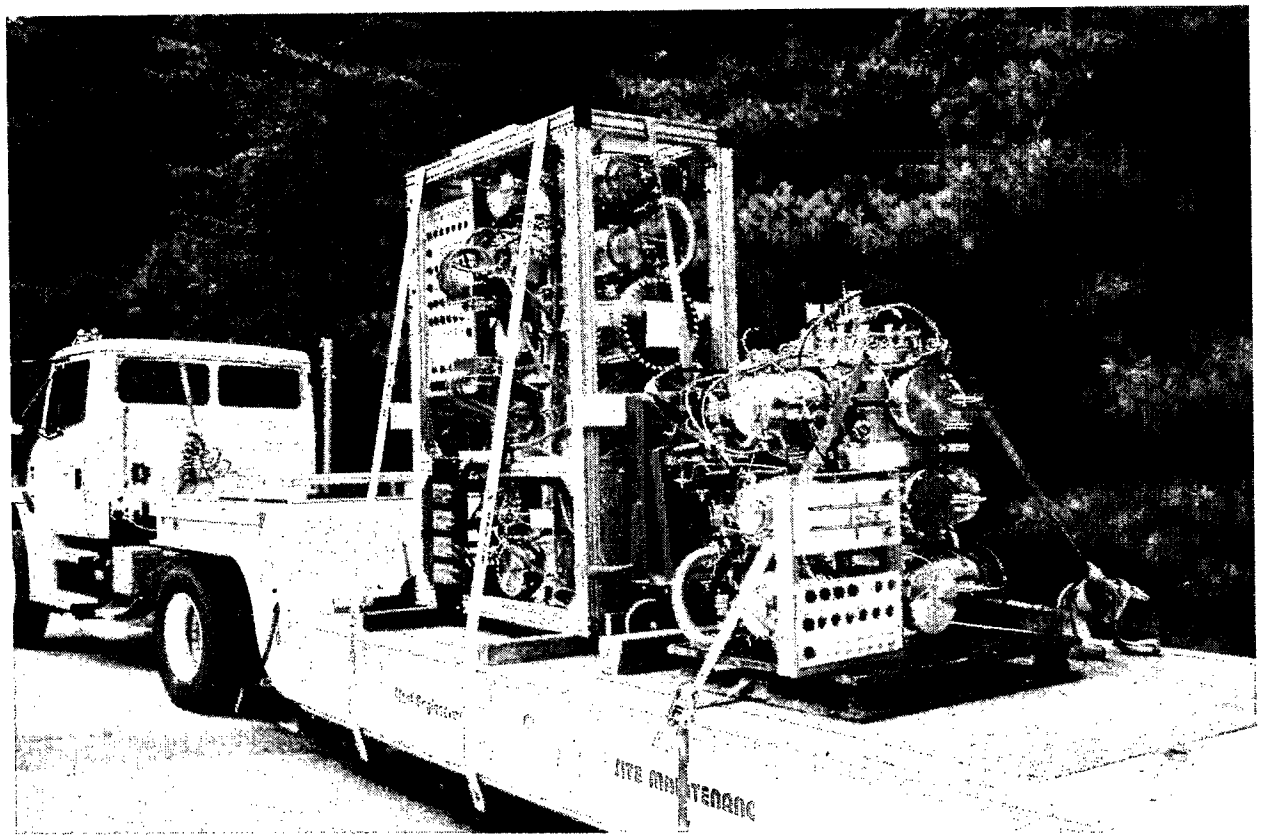

The power supply and control system is assembled in seven joint racks on the wheels.

H-jet layout at the IP-12.

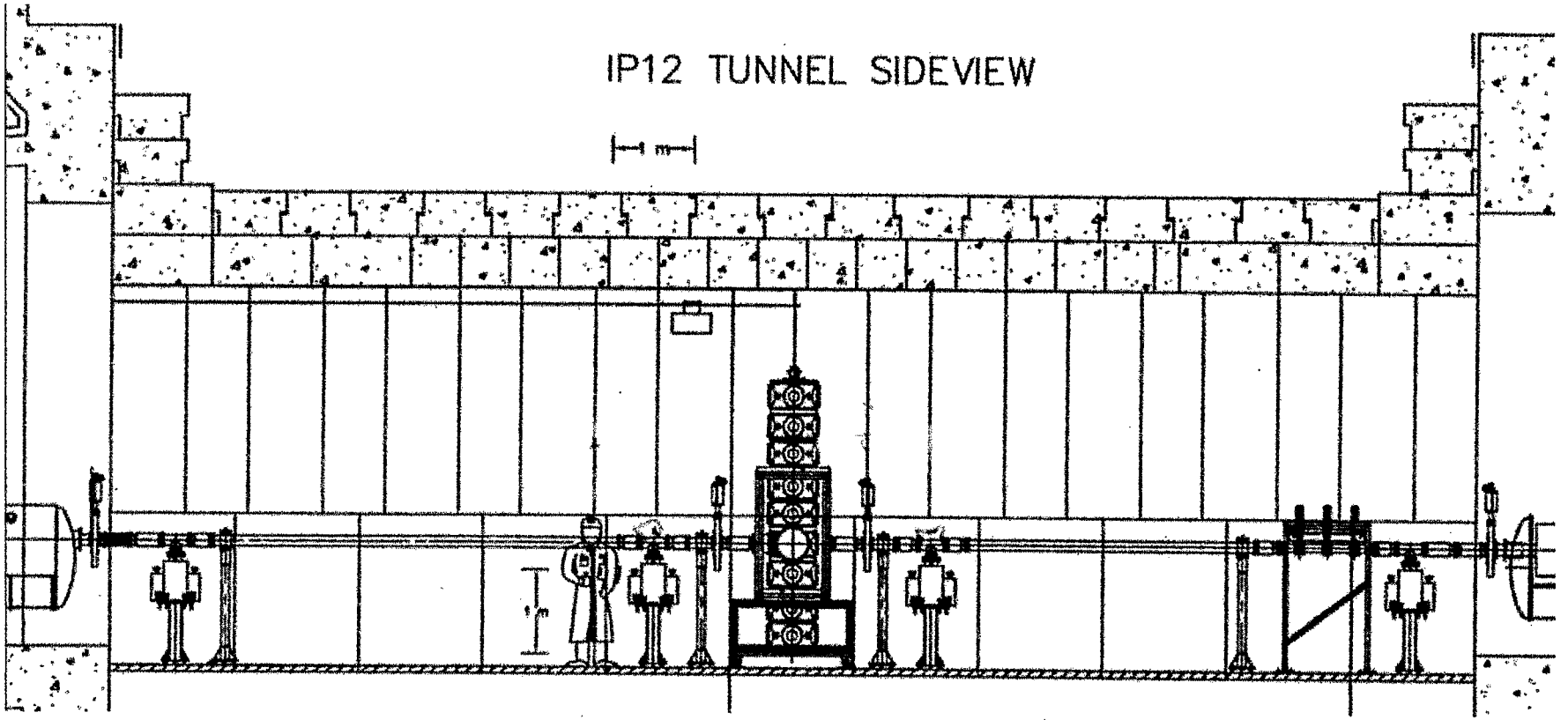

IR 12-vacuum schematic diagram

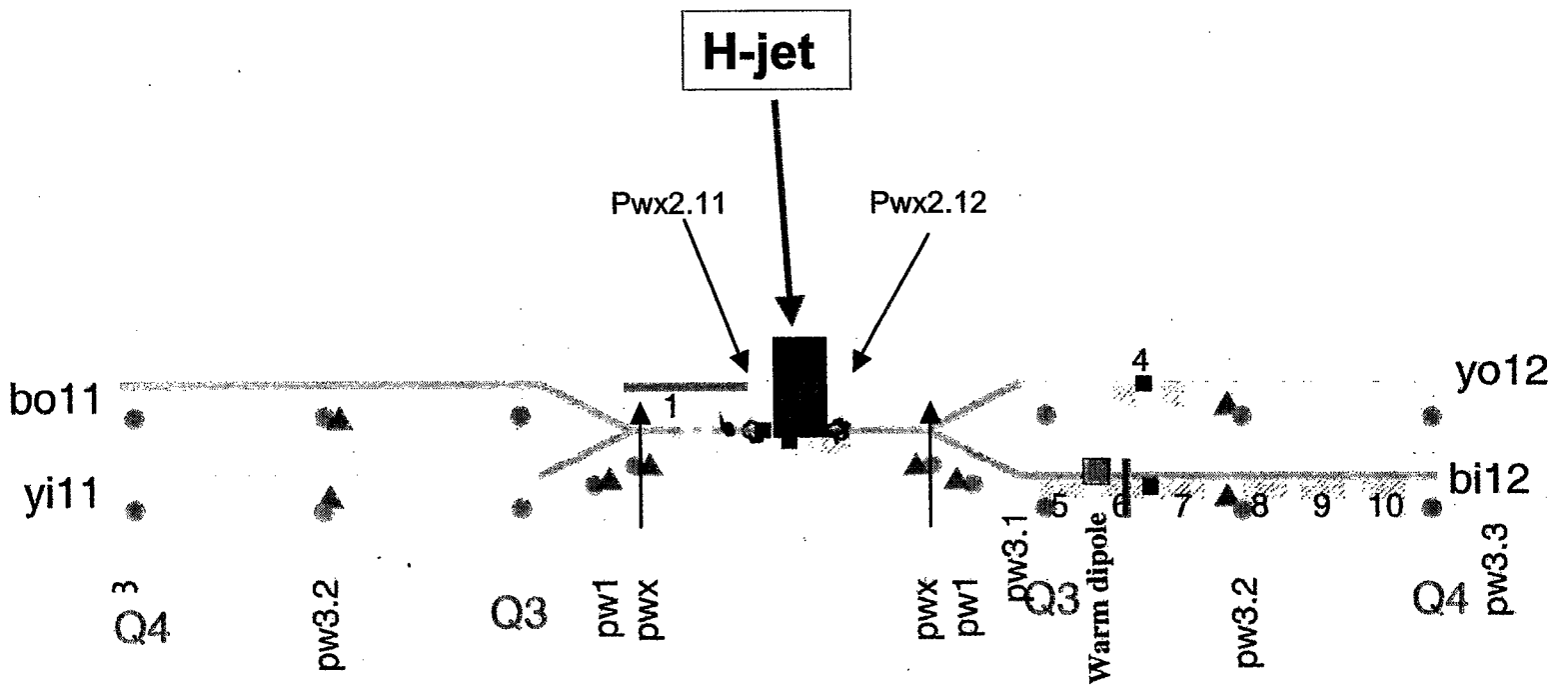

Vacuum spikes at the IP-12 during high intensity beam injection .

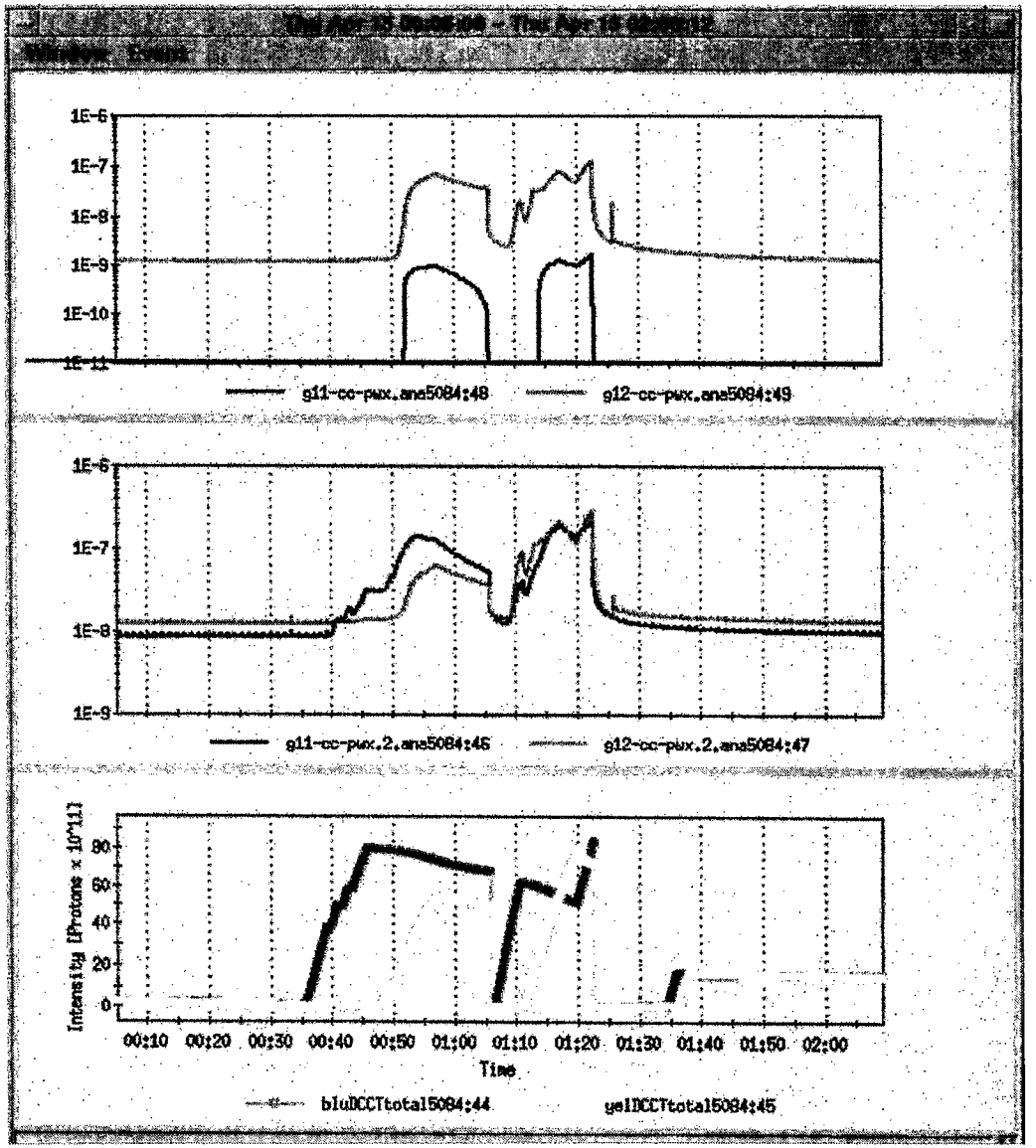

H-jet dissociator.

RF-cavity

Nozzle.

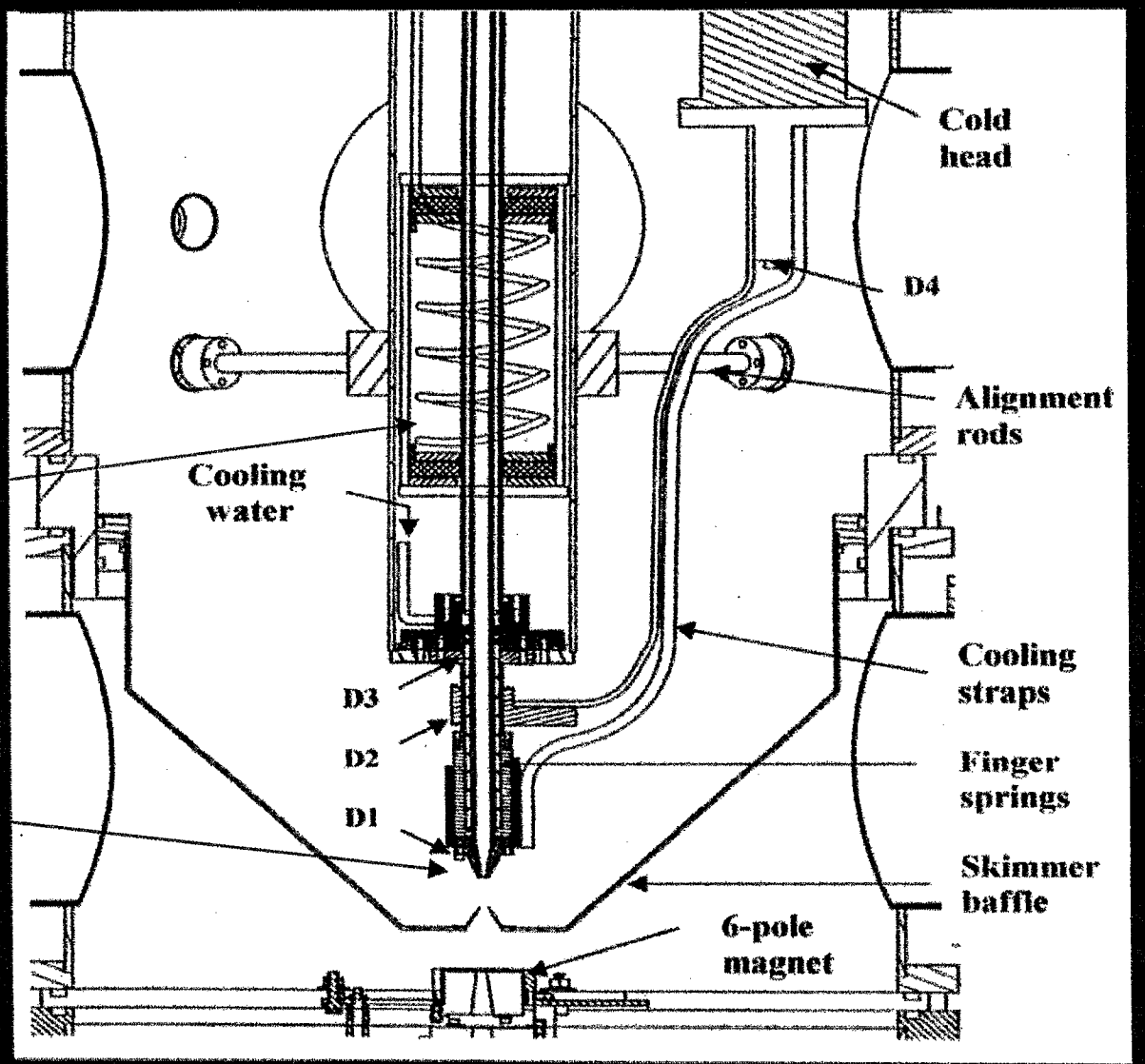

H-jet dissociator design.

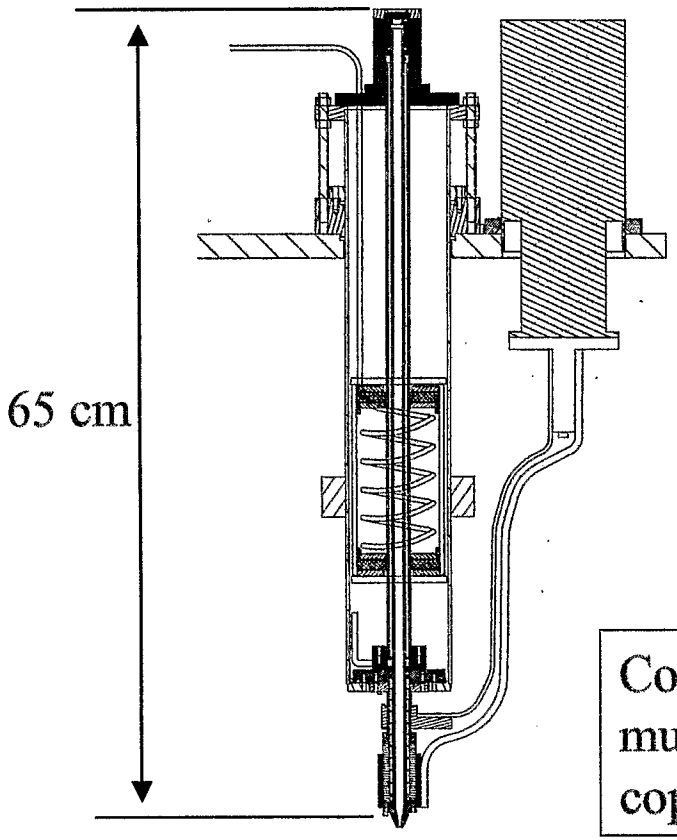

Cooling multifoil copper straps.

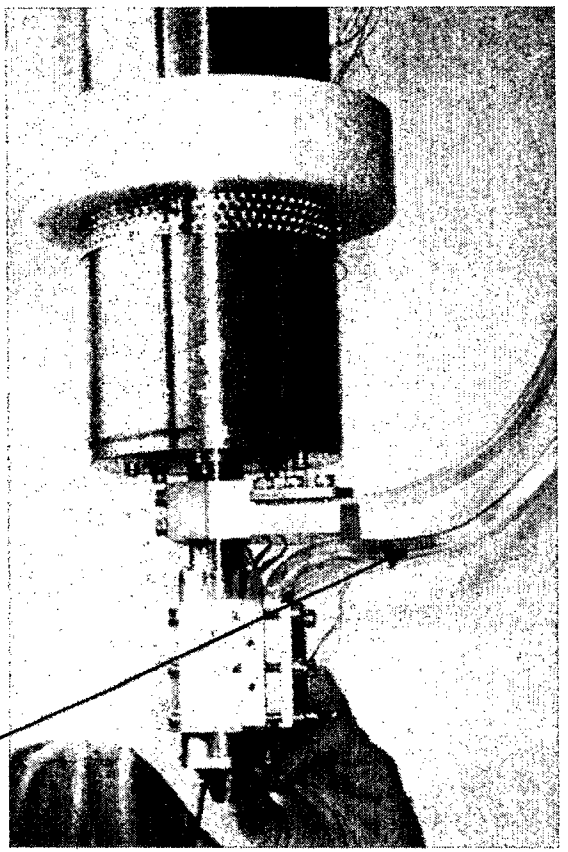

Movable skimmer baffle.

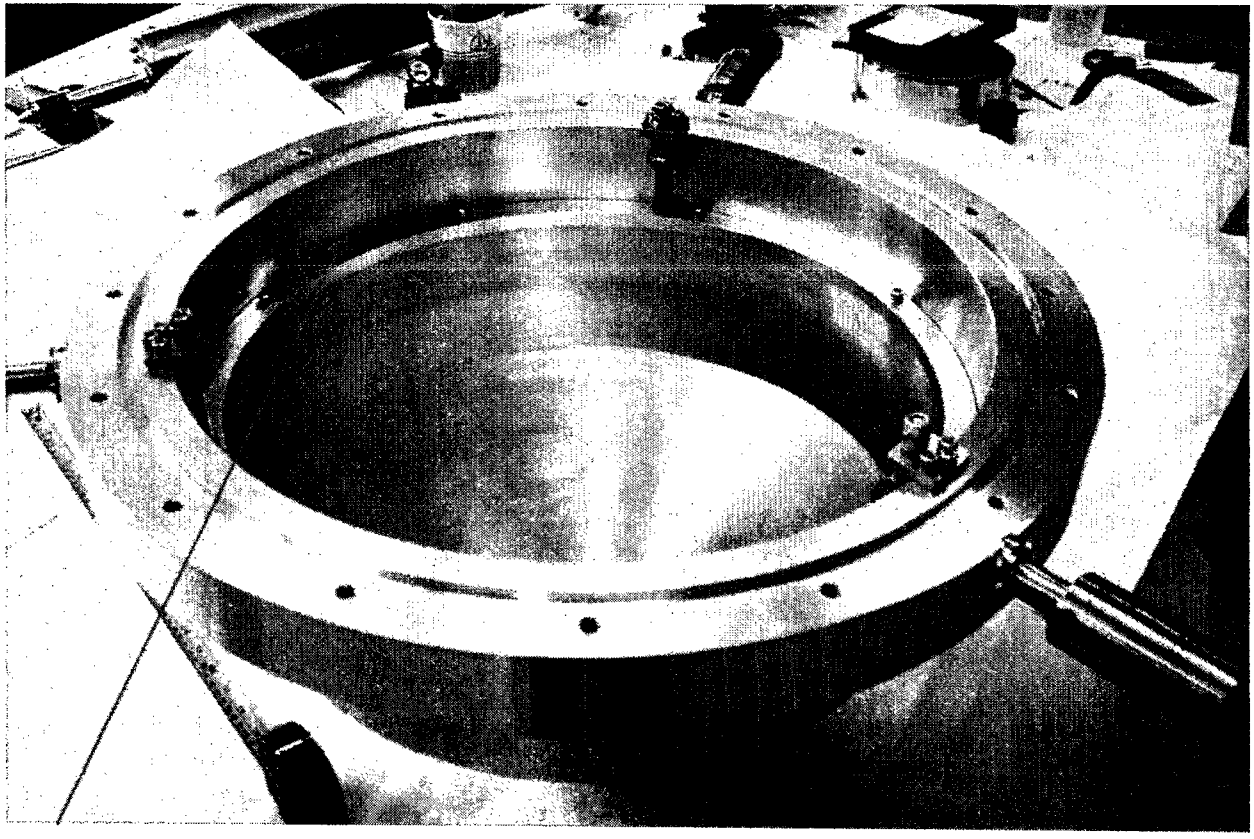

Driving worm-type gears allow +/-10 mm skimmer postion ajustment for the ABS intensity optimization. Optimal nozzle to skimmer distance is 15 mm, skimmer to 6-pole magnet distance is 40 mm.

H-jet sextupole separation magnet system.

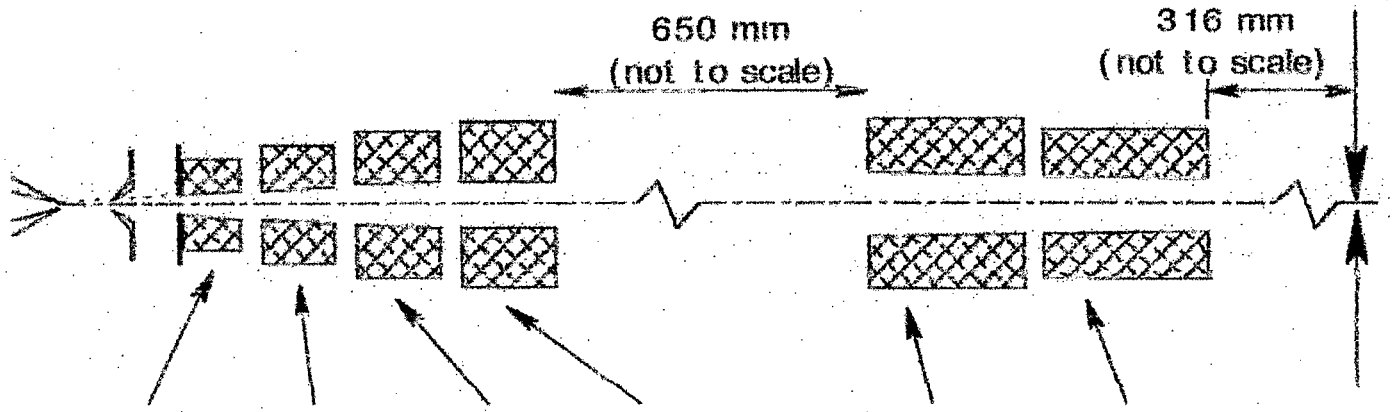

ri	5.2	7.5	9.7	11.5	16	14.5
rex	7.0	9.1	10.7	11.5	14.5	12.7
L	28.5	35.4	40.5	46.0	75	79.0
rout	22	29	35.7	40.3	41.2	36.7

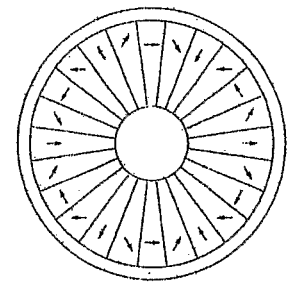

- Force on the atom:

$$\vec{F} = -\nabla E = -\frac{\partial E}{\partial B} \cdot \frac{\partial B}{\partial r}\vec{e_r} = -\mu_{eff} \cdot B_0 \frac{r}{2r_0^2}\vec{e_r}$$

Simulations of the 6-pole separating magnet system.

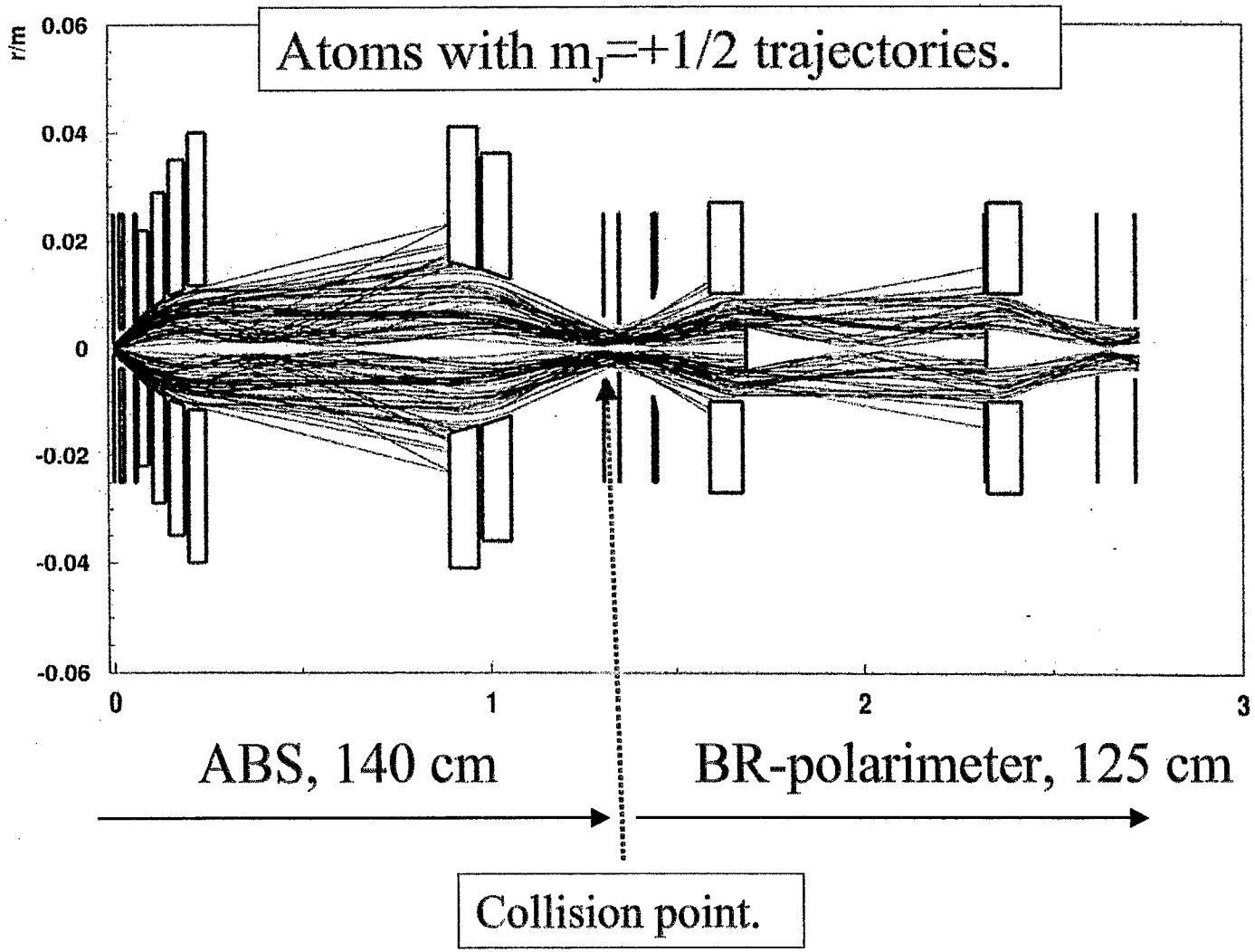

Compression tube calibration.

1. Hydrogen mass-flow controller MKS. Full range: 0.0-1.0 scc/min. Absolute accuracy 1-2%.
2. Conventional technique: pressure drop in calibrated volume.
3. Independent AB intensity measurement from the well known TMP pumping speed.

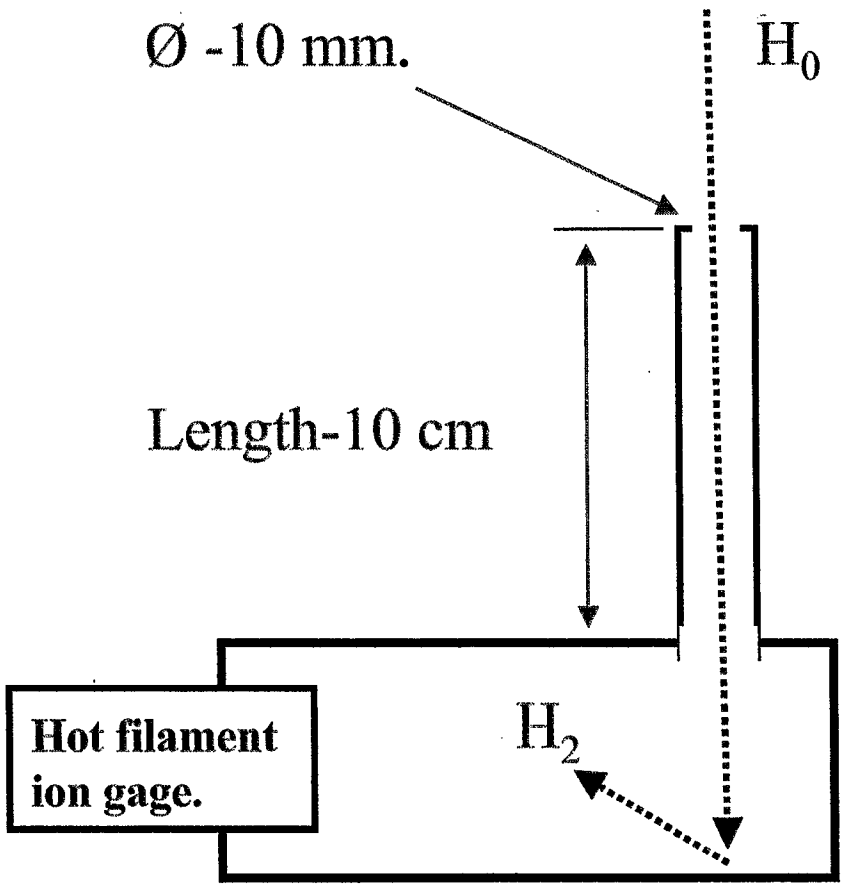

The compression tube calibration system for the absolute AB intensity measurements.

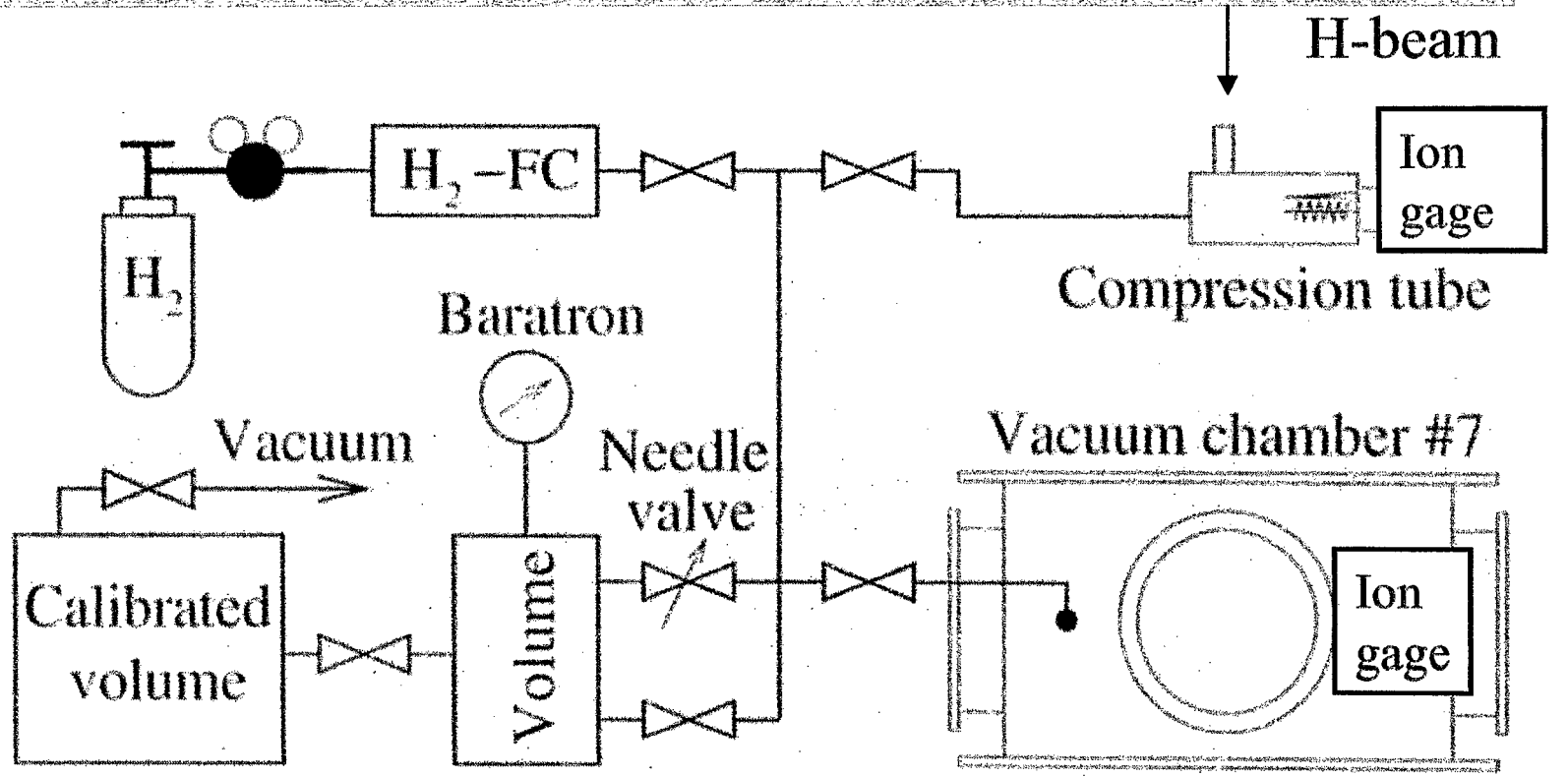

H2 mass-flow controller and a pressure drop measurement in the calibrated volume were used for compression tube calibration.

Atomic beam intensity dependence on H_2 flow in dissociator.

AB intensity at

65 scc/s H_2 flow is $12.5 \cdot 10^{16}$ at/s.

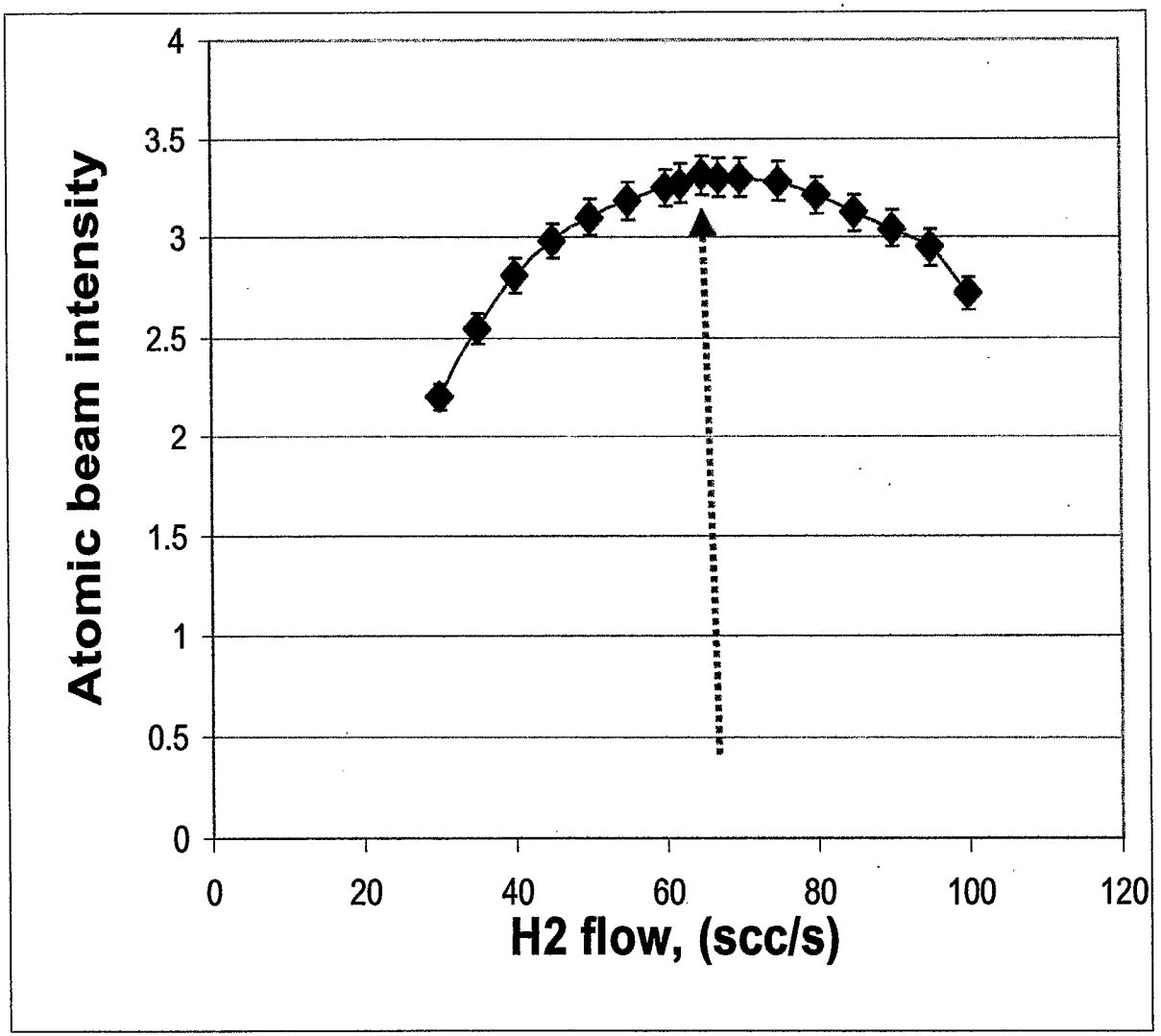

AB intensity vs. nozzle temperature.

The maximum AB intensity was measured at

T_{nozzle} =75 deg. K

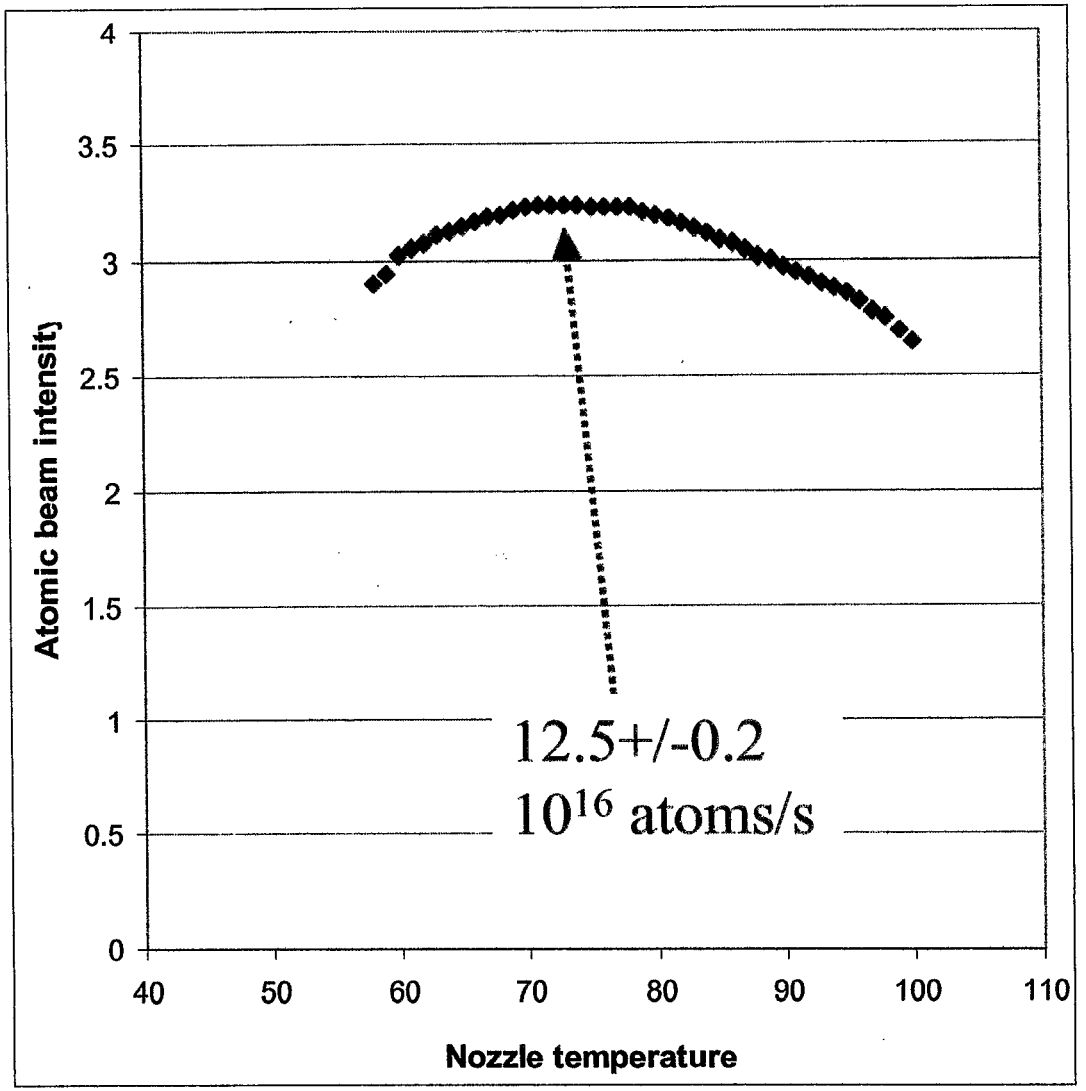

Operational atomic beam sources for polarized target applications.

- HERMES- at DESY, Hamburg
- PINTEX- at IUCF, Indiana (moved to IFNF, Italy)
- Cryogenic ABS - Novosibirsk
- EDDA - COSY, Julich
- ANKE - COSY, Julich
- BLAST – MIT, Bates
- H-jet polarimeter – BNL, New-York

- There are about 20 operational polarized ion sources based on atomic beam technique. All around the world.

Operational atomic beam sources intensities.

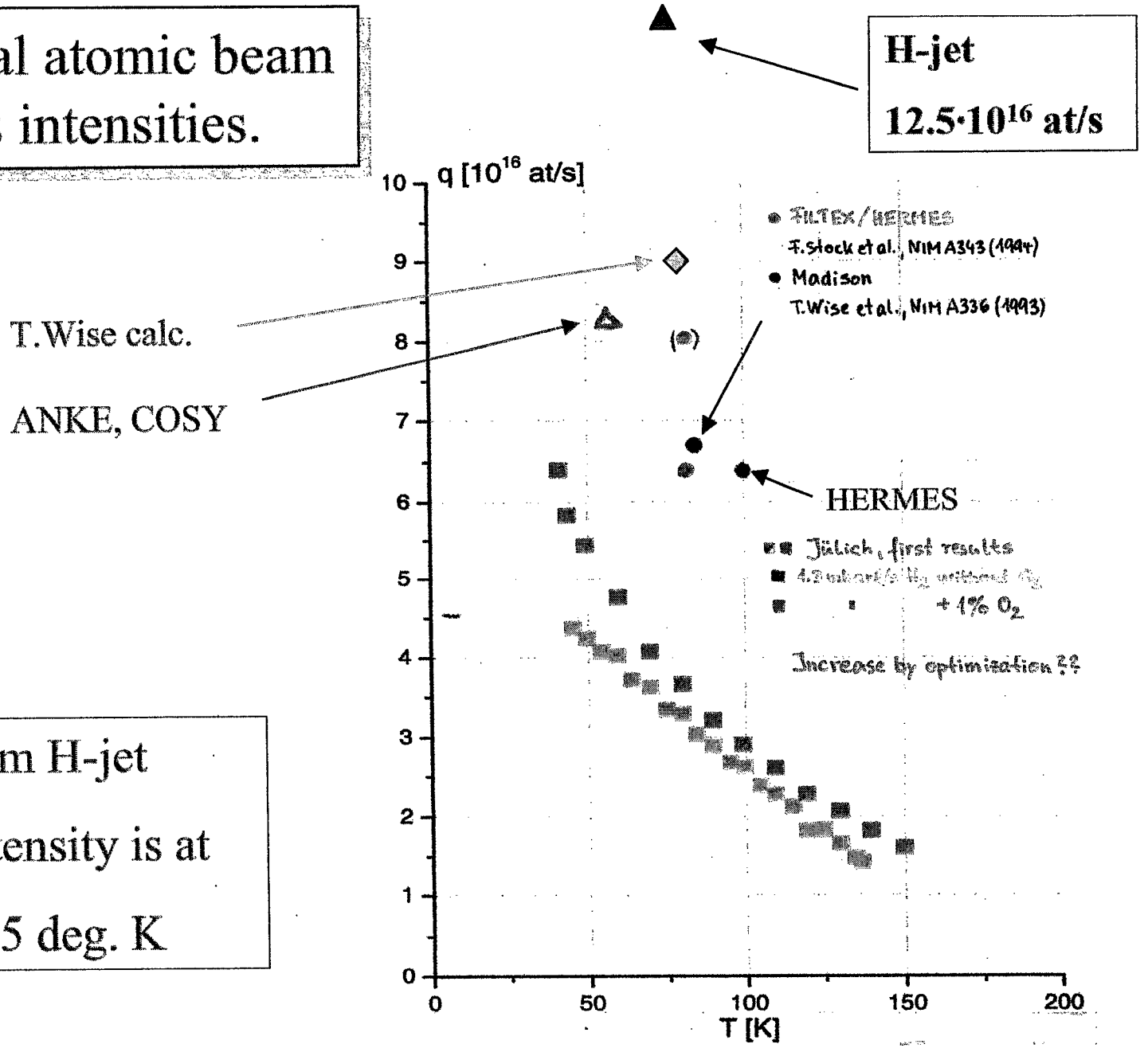

Maximum H-jet beam intensity is at T_{nozzle}~75 deg. K

Compression tube for the AB profile measurements.

Ø 2 mm collimator.

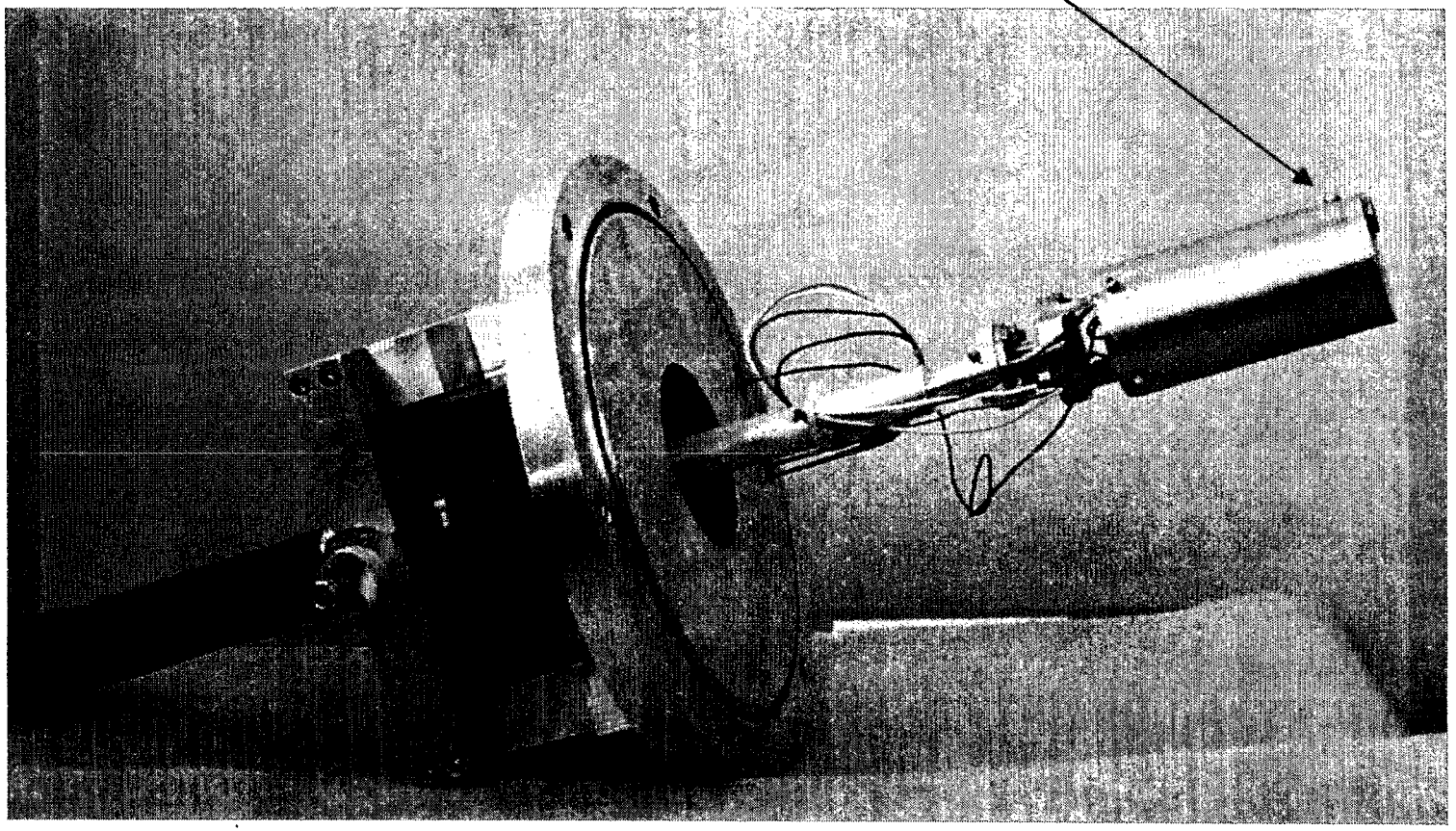

Atomic beam profile at the collision point.

- Atomic beam profile was measured with a 2.0 mm in diameter compression tube FWHM=5.5 mm

- 5 cm upstream the beam profile FWHM is about 4.5mm and 120 mm downstream FWHM is about 7.0 mm
- Atomic beam velocity is $1.6\text{-}1.8 \cdot 10^5$ cm/s.
- H - jet thickness at the collision point is about $1.3+/-0.2 \cdot 10^{12}$ atoms/cm^2 (as seen by 1.0 mm in diameter RHIC beam.

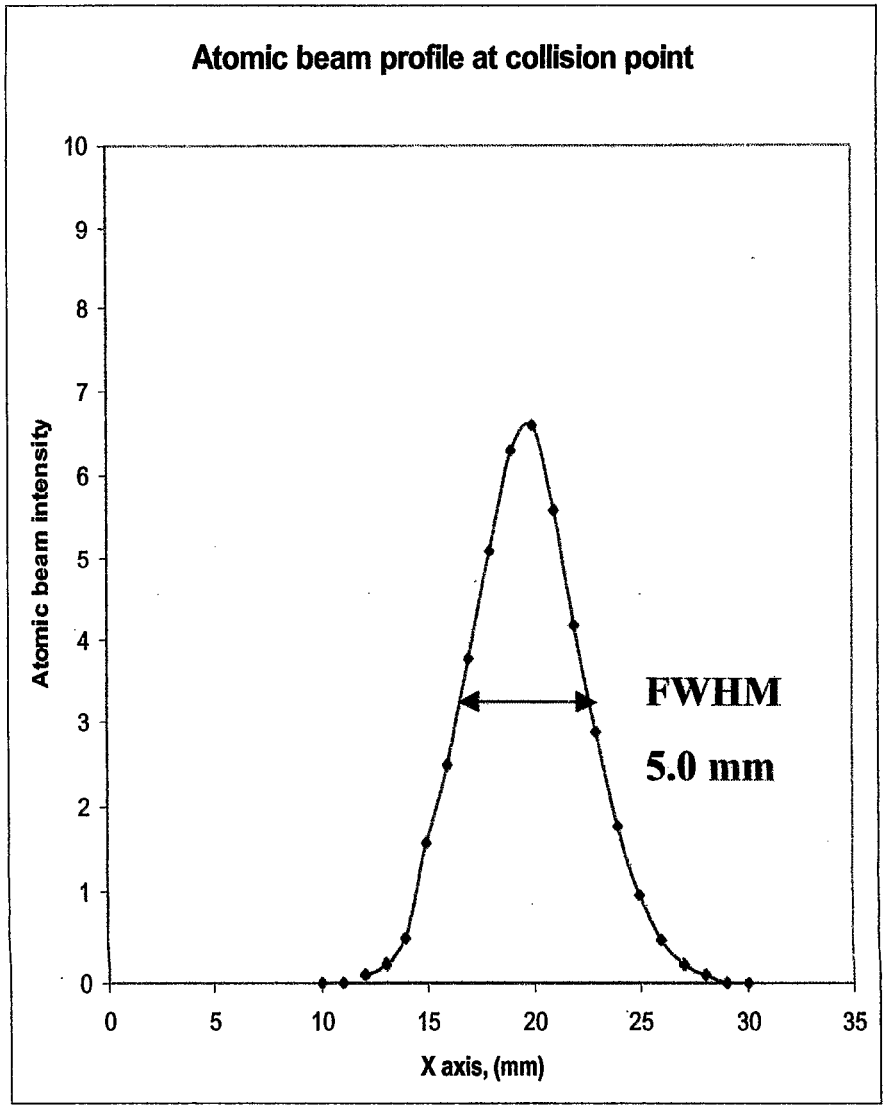

Atomic beam intensity profile measurements.

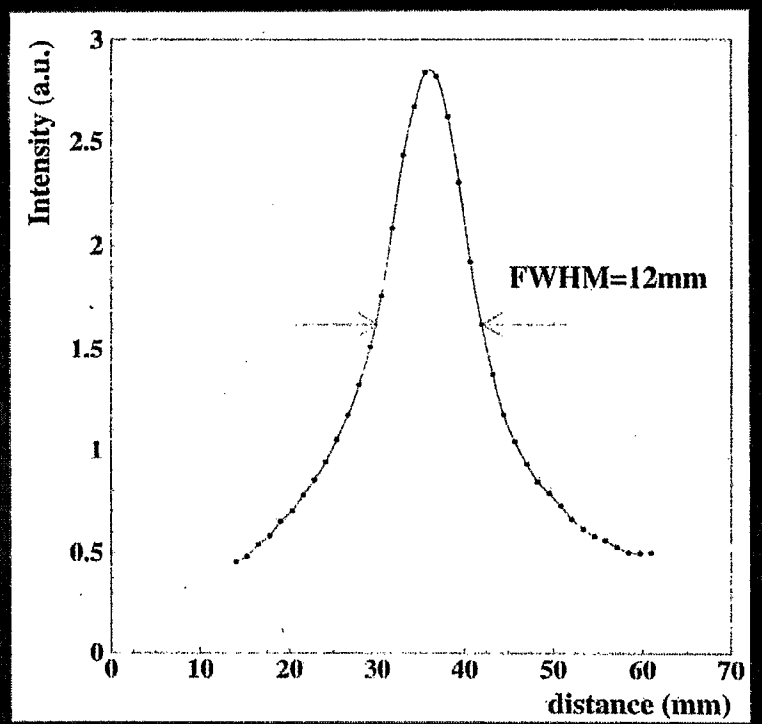

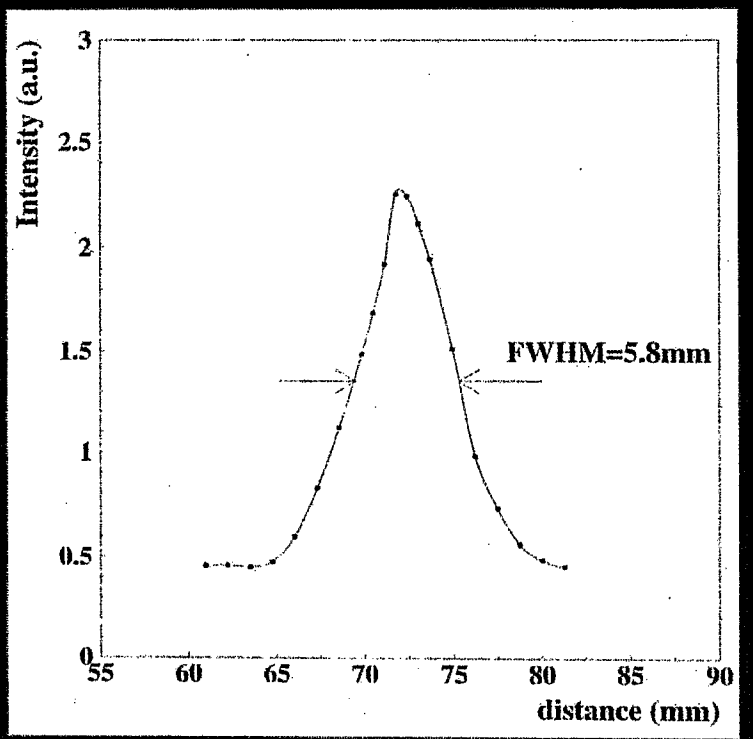

Beam profile at the entrance of 6-pole #5.

Beam profile at the RHIC beam collision point.

H-jet target intensity profile at the RHIC collision point.

Profile was measured from elastic *pp* scattering events.

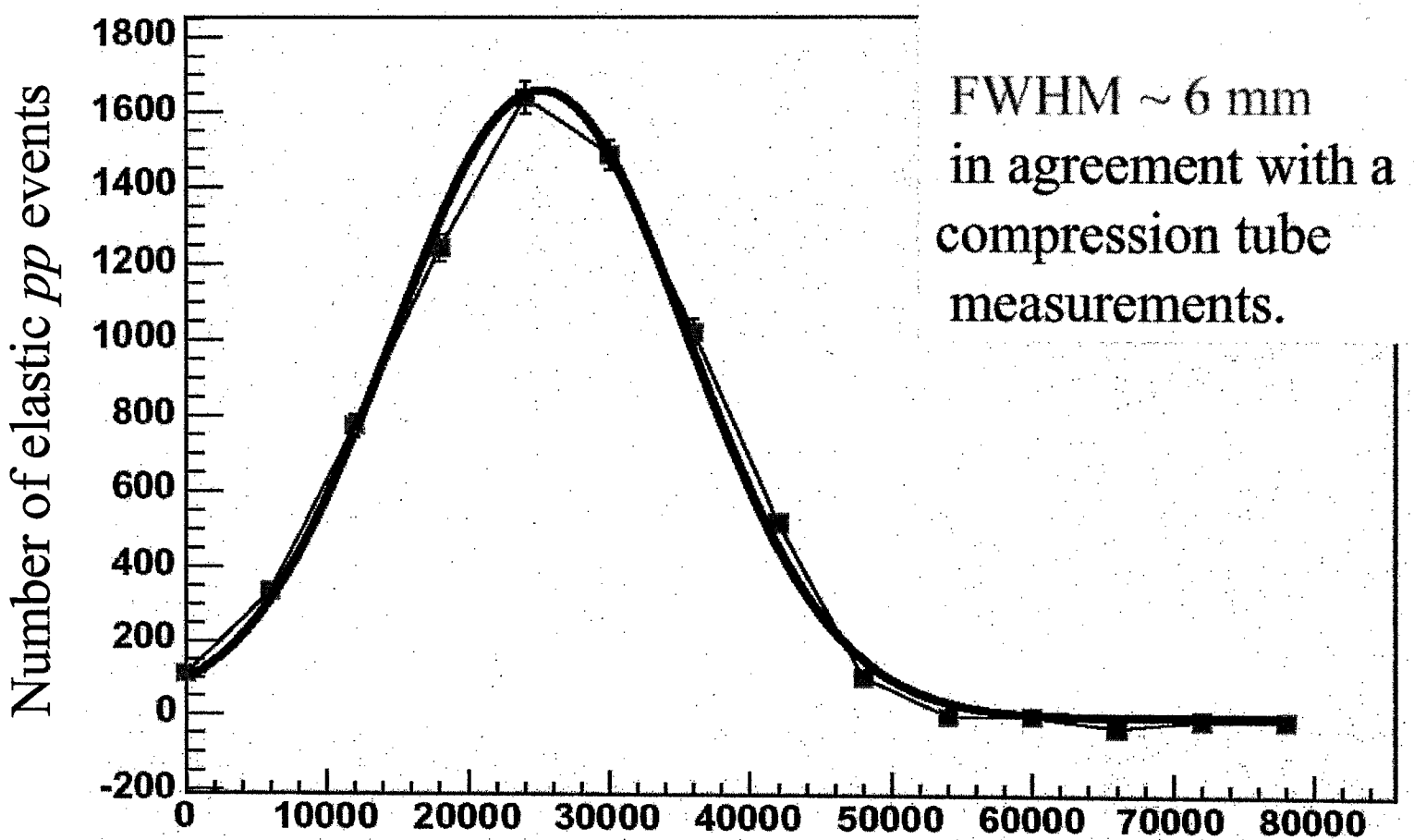

FWHM ~ 6 mm
in agreement with a
compression tube
measurements.

Hor. position of the JET ,10000 steps = 2.5 mm.

Atomic beam trajectories in BRP with both SFT and WFT – transitions are "on".

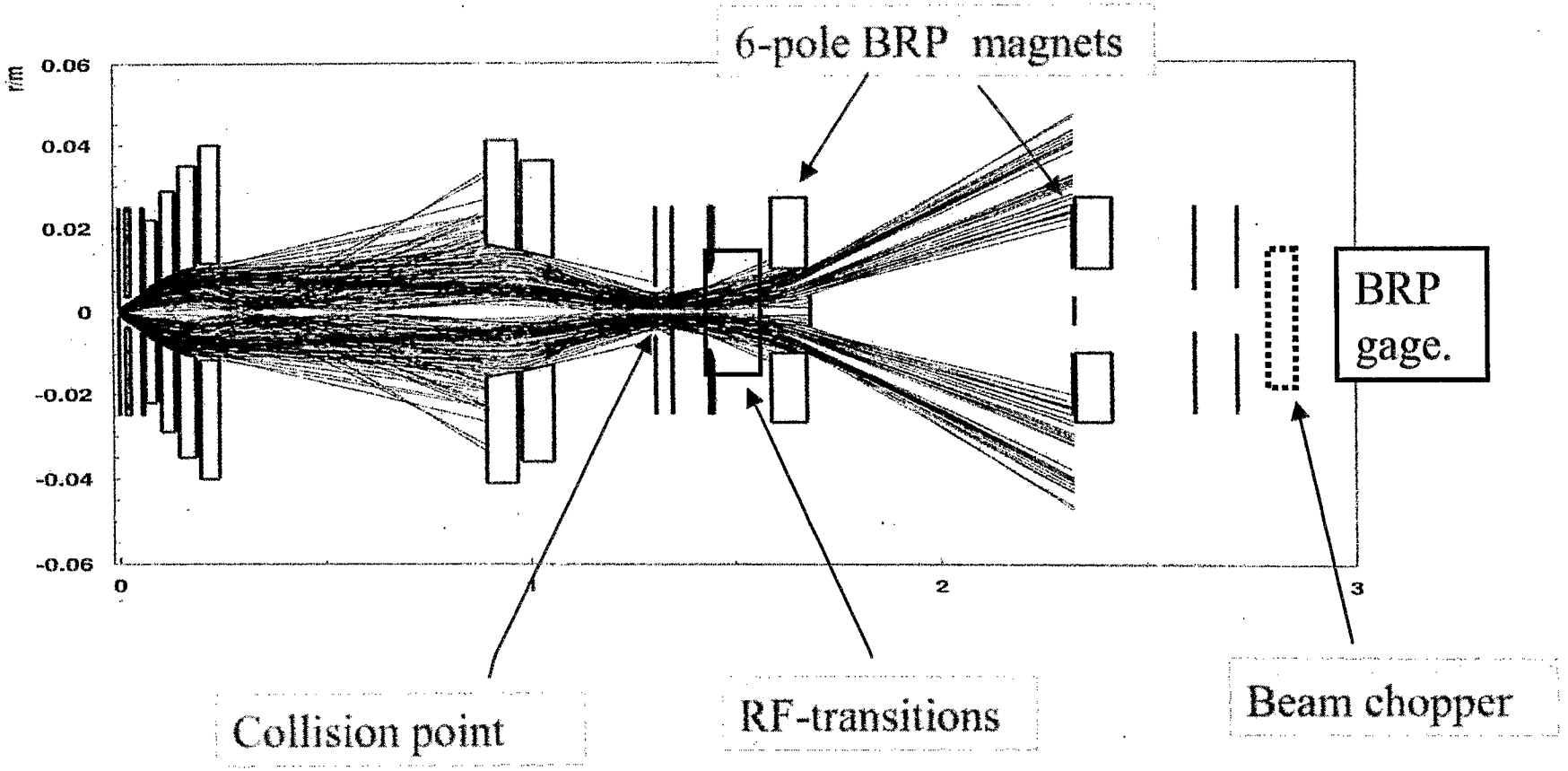

RF-transition operation. Atomic beam polarization reversal.

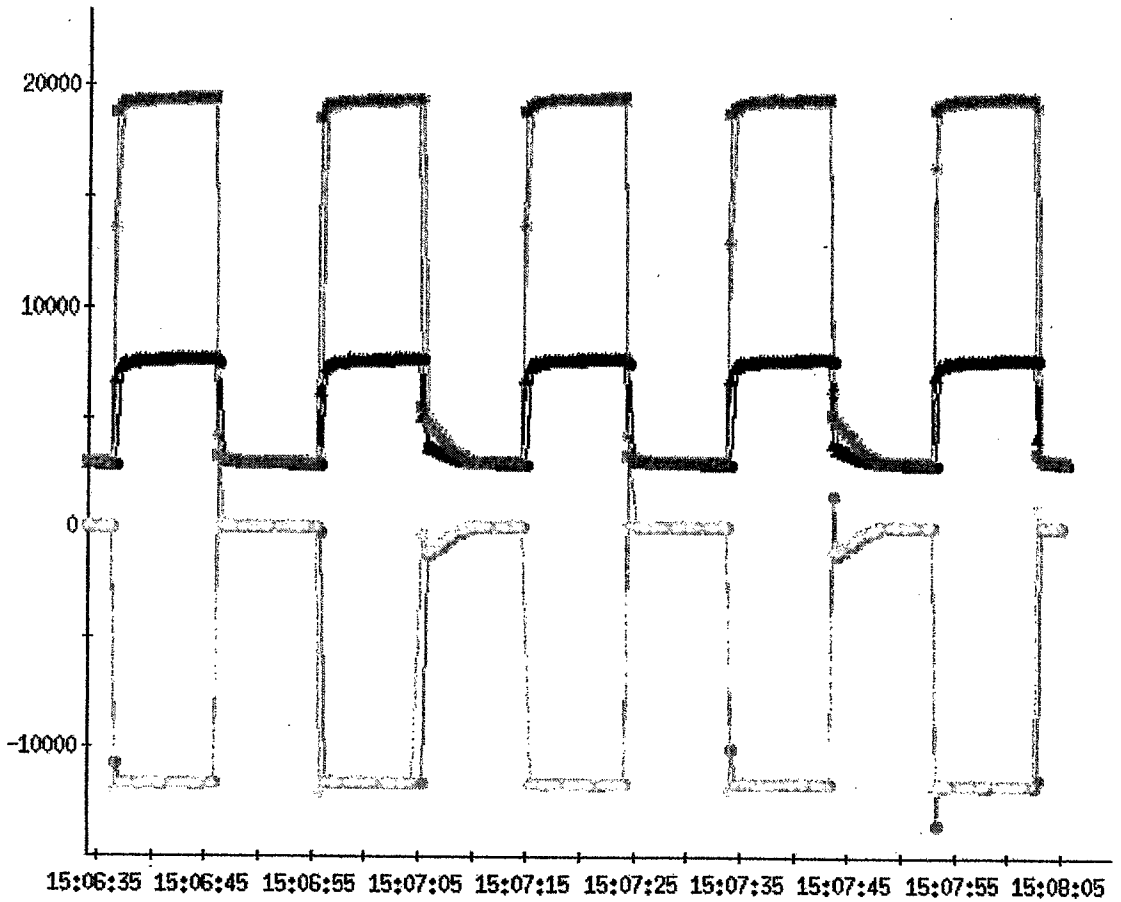

Efficiencies and nuclear polarization.

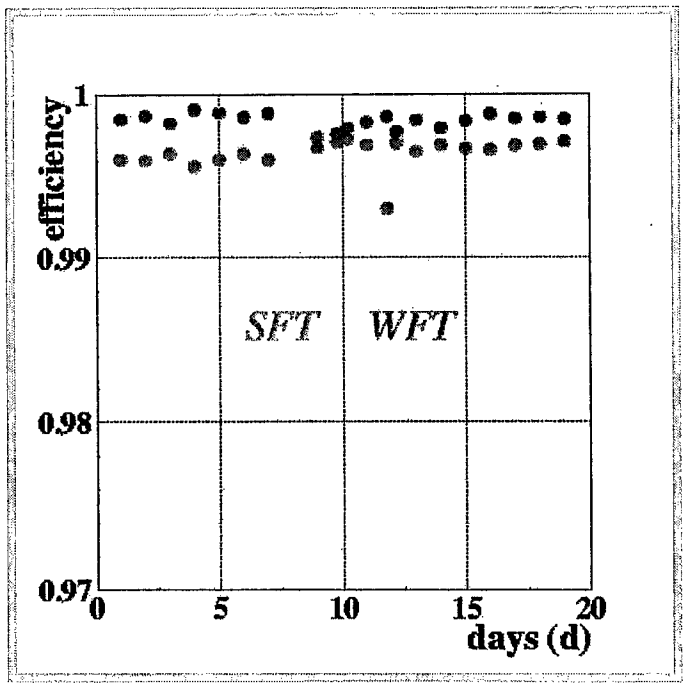

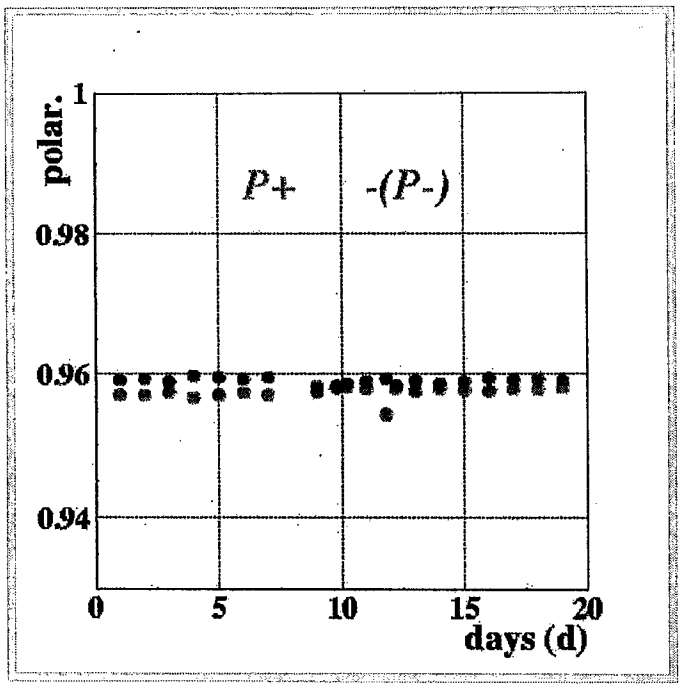

Stable behaviour over the whole 2004 run, mean values for nuclear polarization of the atoms:

$P^+ = 0.957 \pm 0.001$ and $P^- = -0.959 \pm 0.001$. More deatails in A.Nass talk.

Stability of nuclear polarization.

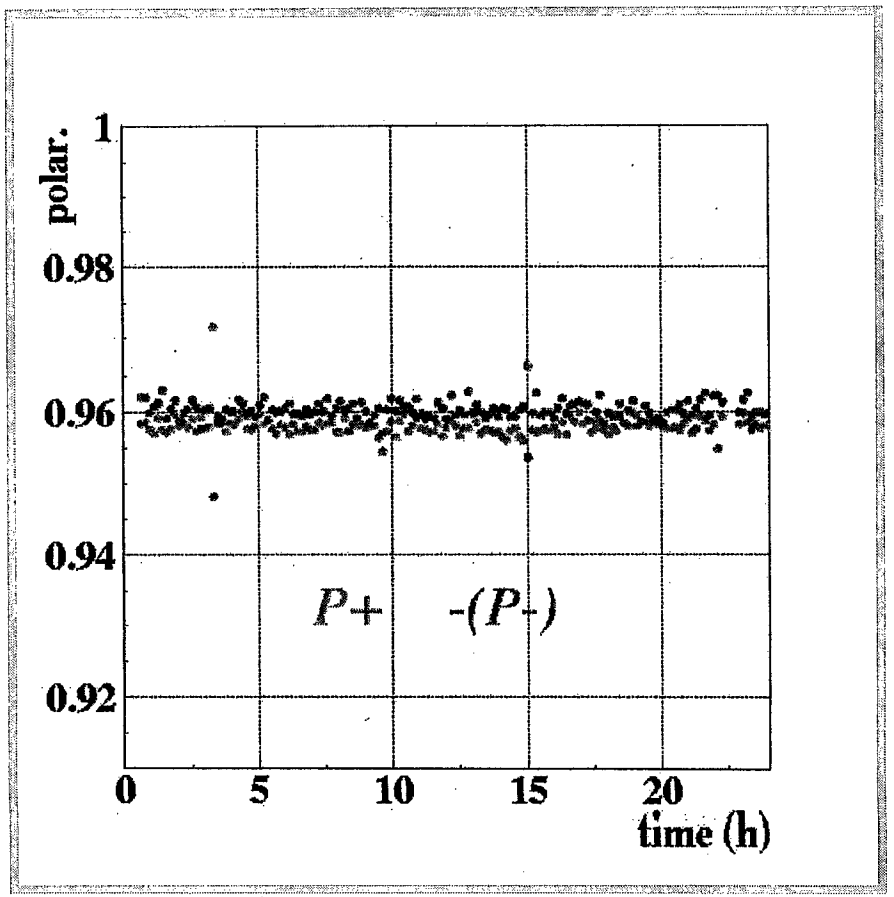

QMA upgrade for H-jet measurements.

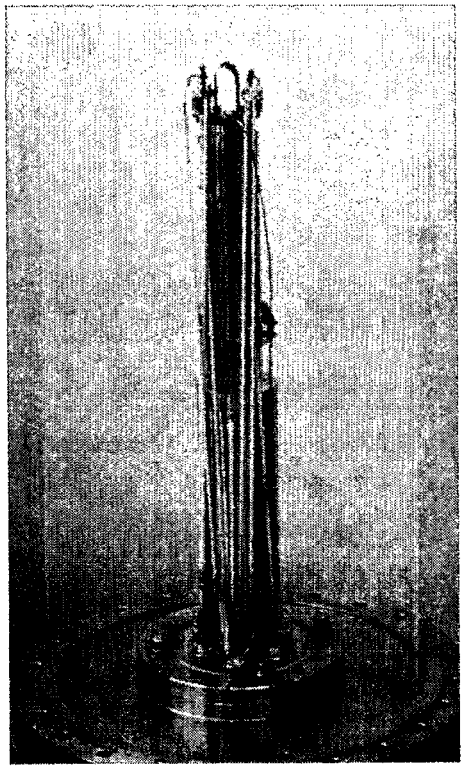

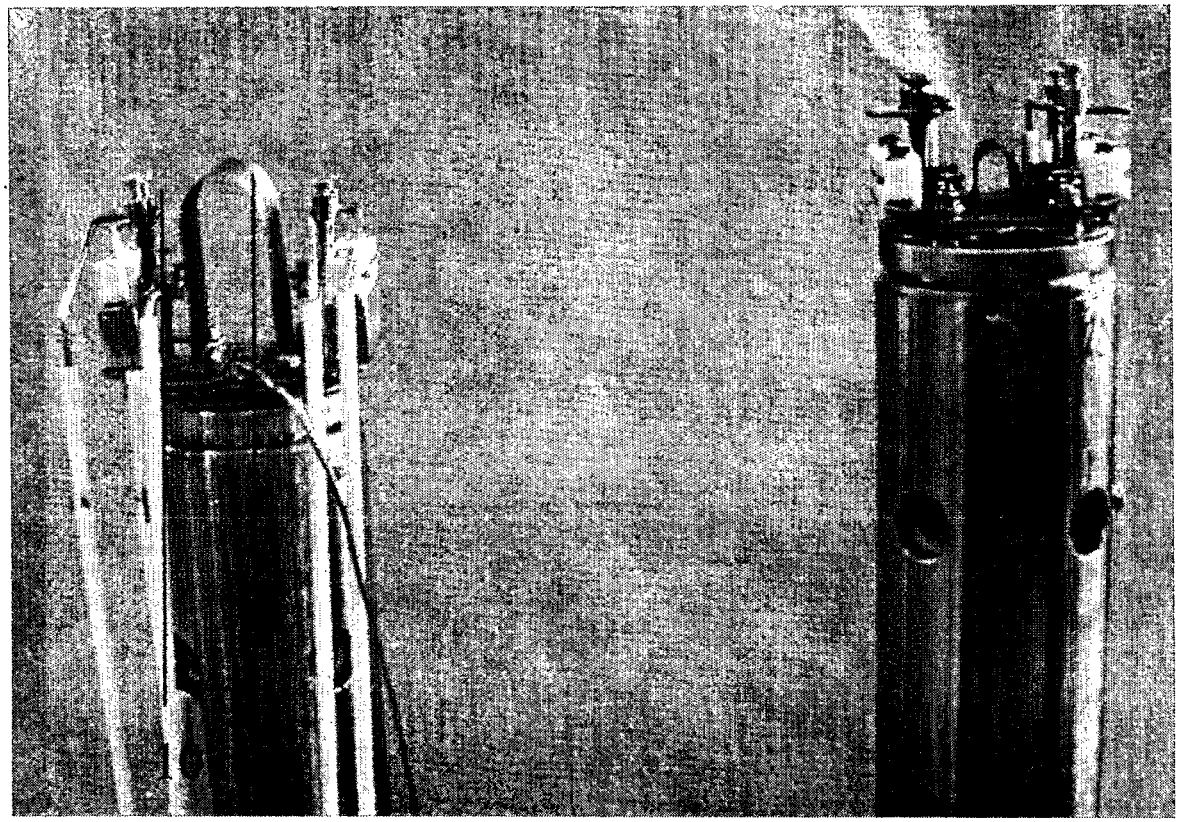

Original QMA geometry (right).

Expanded QMA sensitive volume (left).

Time –of - flight beam velocity and velocity spread measurements out of dissociator

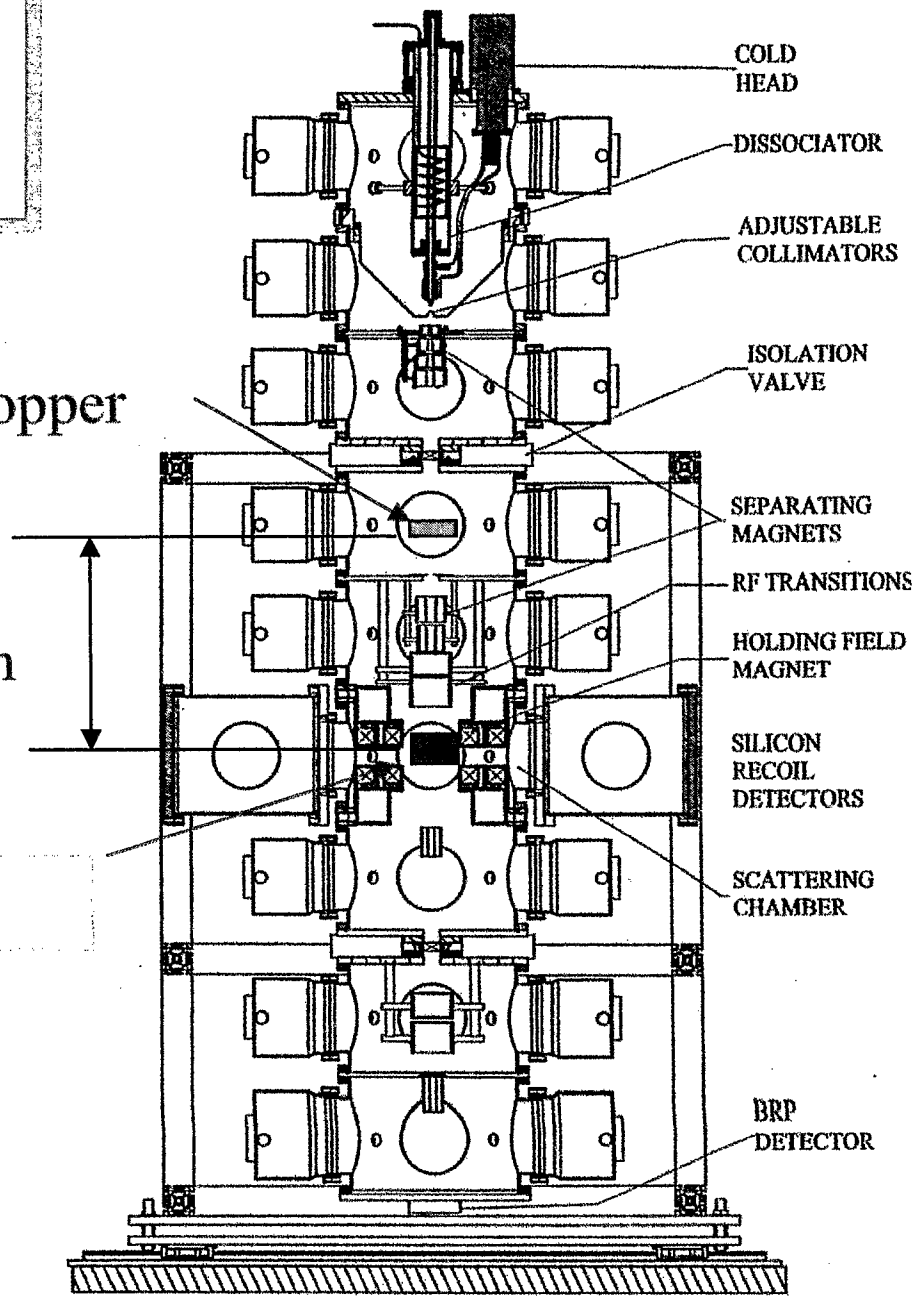

Beam chopper

69 cm

QMA

The narrow velocity spread is expected from the H-jet dissociator (due to long cooling "neck"), which can be a significant factor in the superior H-jet performance.

ABS separating magnets were removed for these measurements.

QMA atomic beam velocity measurements.

L=135 cm- drift length.

Vb ~1500-1800 m/s

Atomic beam intensity and density measurements in the collision region.

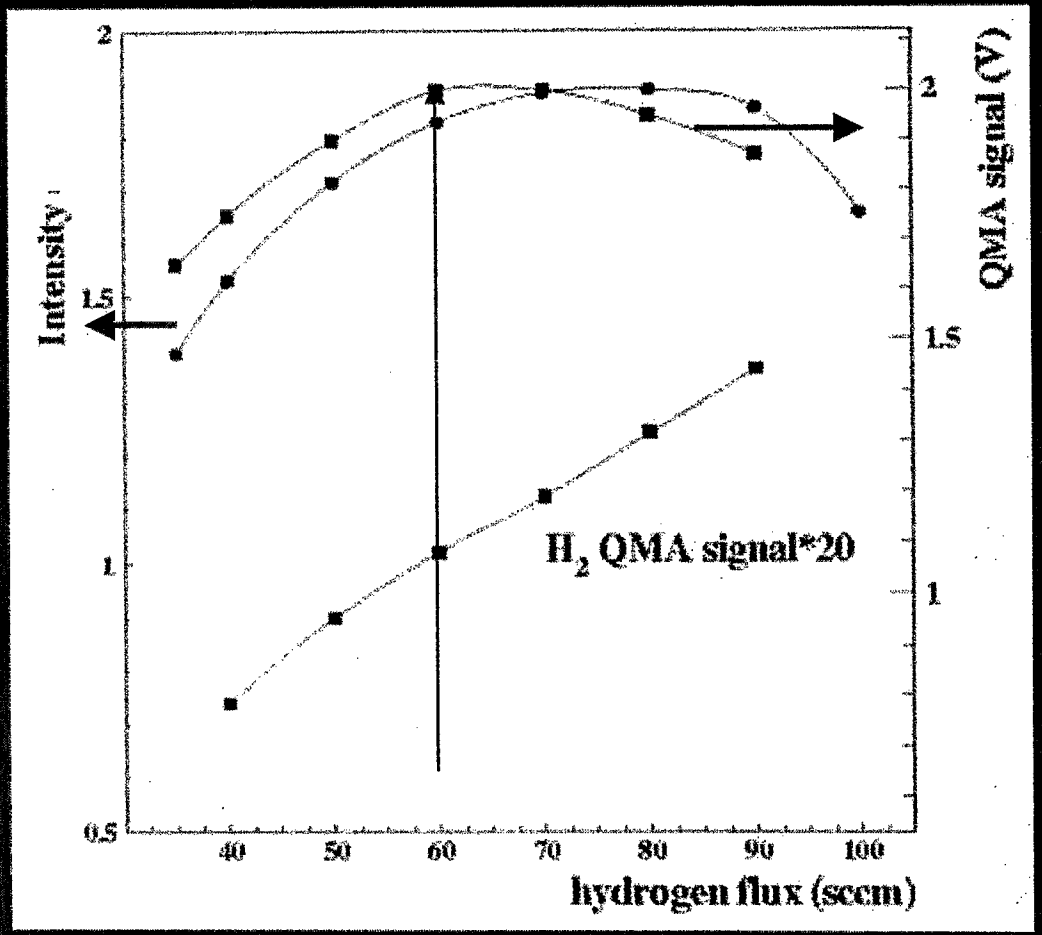

- H-beam intensity and density vs. H2 flow in dissociator.

QMA calibration.

10^{-7} torr.H_2 ⇔

0.98· 10 ^{10} H_2/cm3

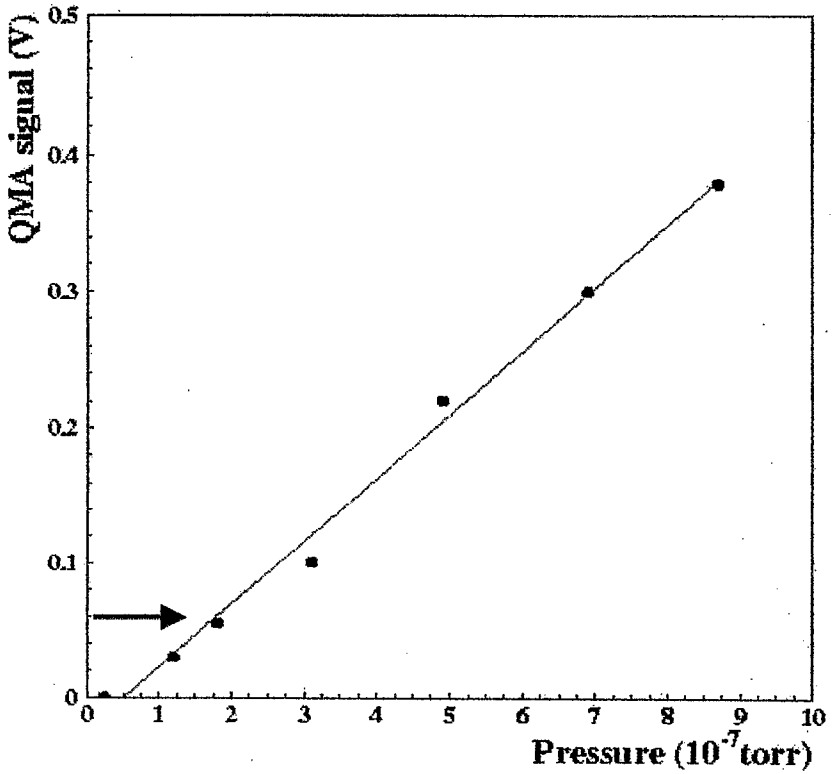

Measured H_2 / H density ratio:

~1.5%× 2 → 3%-polarization dilution.

- **QMA atomic beam signal vs. H_2 partial gas pressure in the collision chamber.**

Optical diagnostics for atomic and molecular hydrogen components.

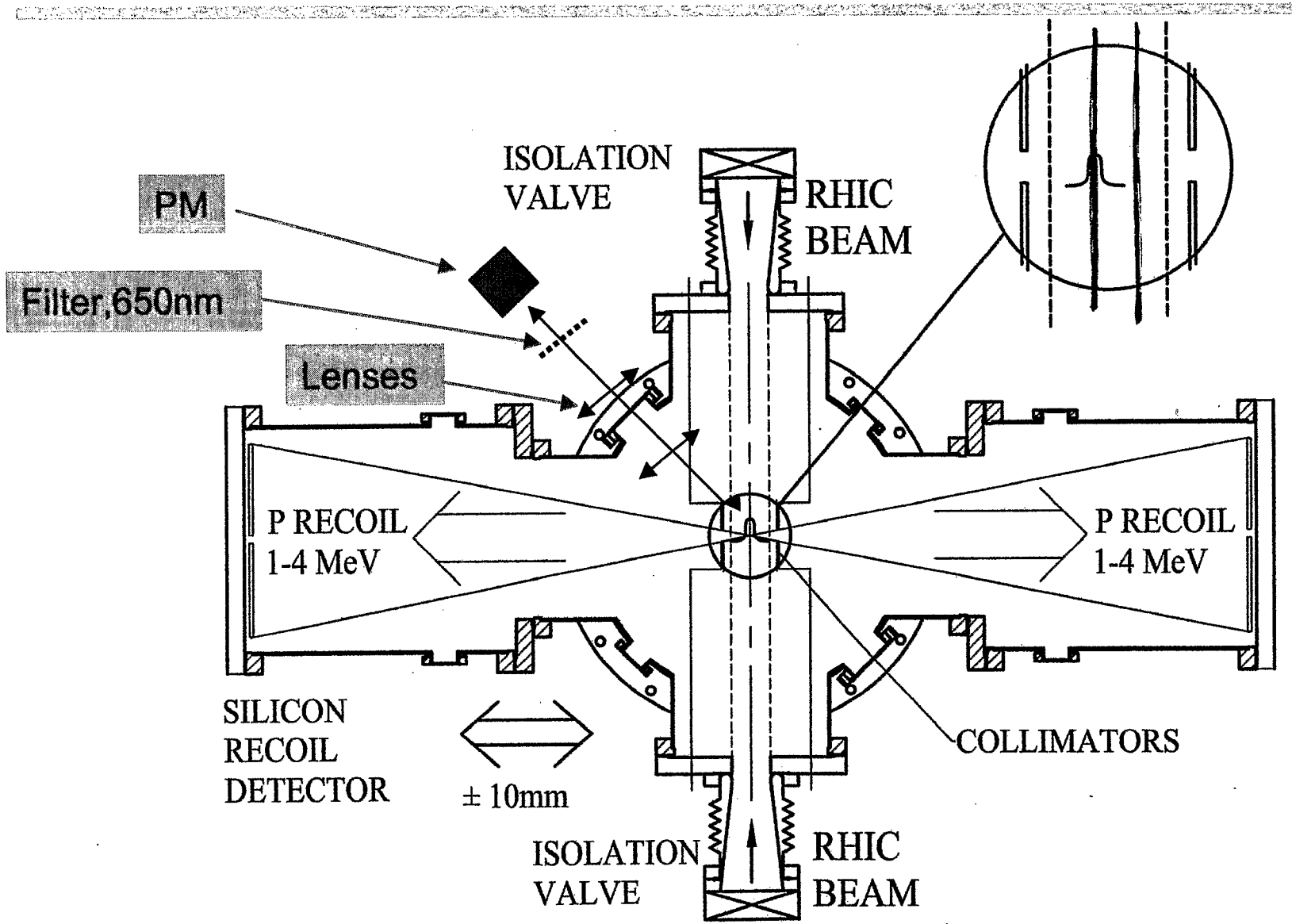

H/H_2 –measurements with the magnetic analyzer. T.Wise.

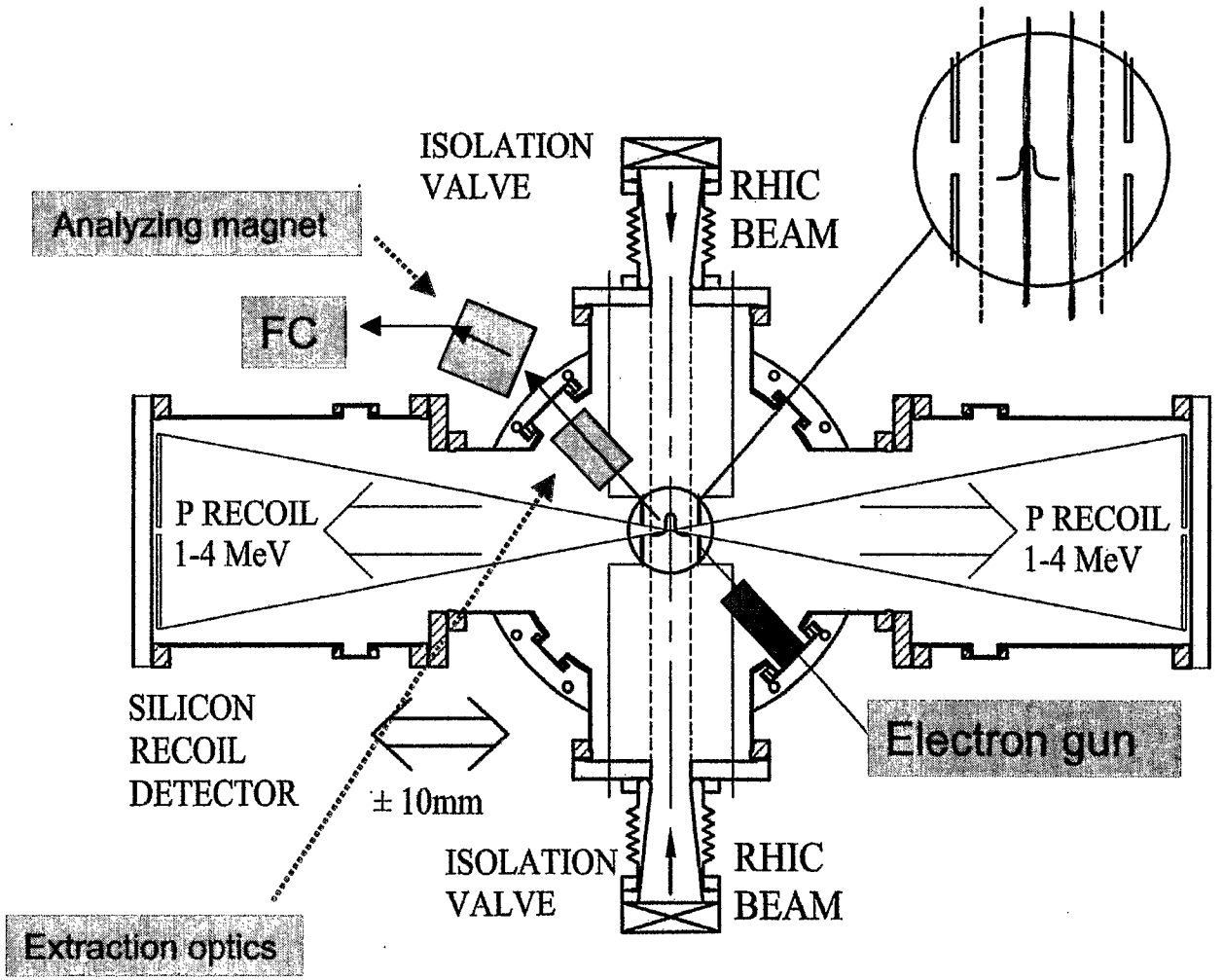

H-jet operation April 6 – May 14, 2004

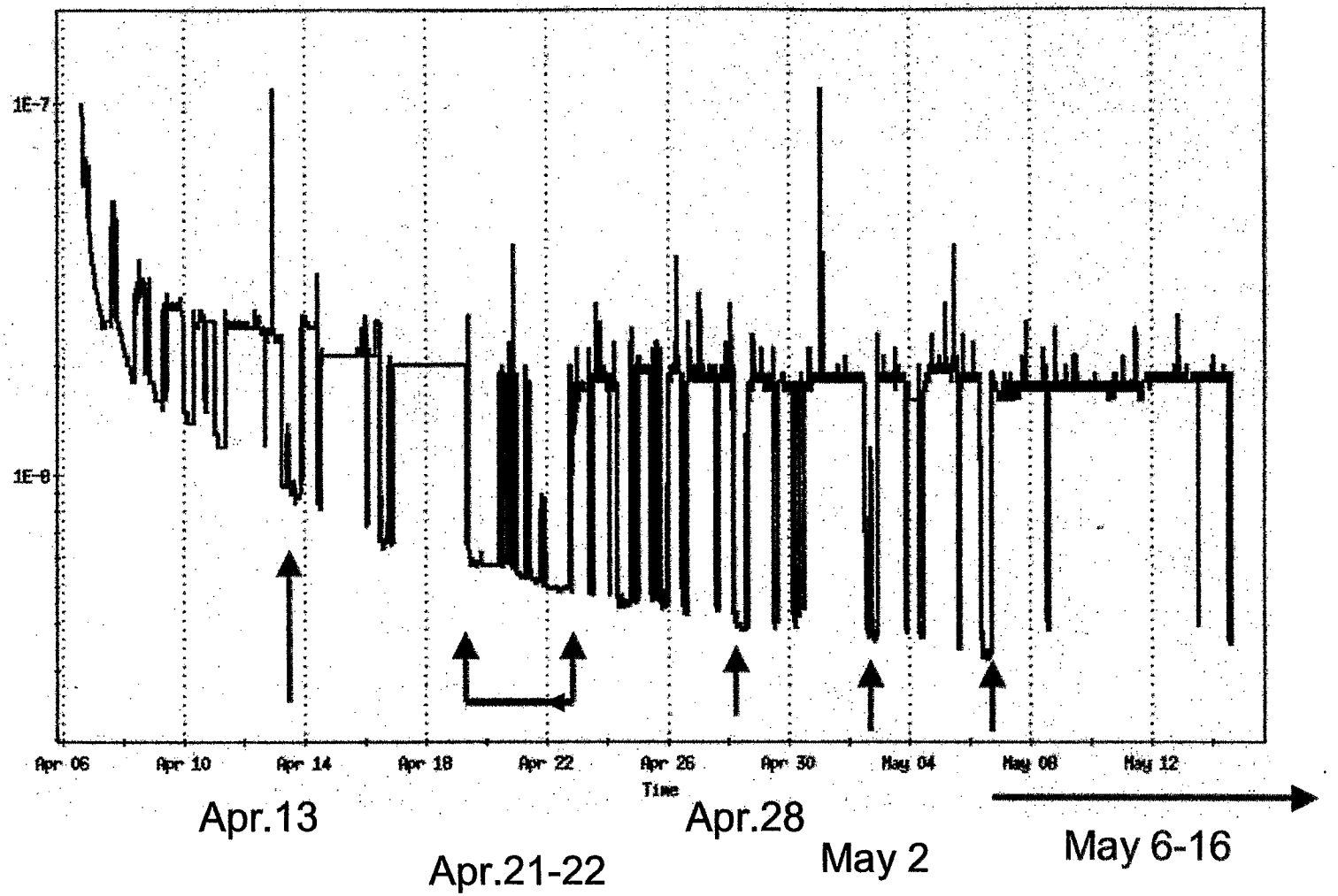

H-jet performance in 2004 run at RHIC.

- Overall H-jet operation was reliable in the first Apri-May 2004 run at RHIC.The atomic beam intensity was stable. The dissociator required maintanance about once a week.
- The first beam velocity measurements gives: $V \sim (1.6\text{-}1.9)\cdot 10^5$ cm/s. The total H-jet thickness is about $1.3\cdot 10^{12}$ atoms/cm^2.
- The RF-transitions efficiencies were measured with BRP polarimeter at $\sim 99.9\%$. SFT turn-on time has to be reduced.
- $H_2/H \sim 1.5\%$ -ratio was measured in the collision region with the QMA, which gives about 3% polarization dilution.
- It gives 93+1/-2 % effective proton polarization at 1.2 kG holding field and 94% polarization at 1.4 kG field.

Problems.

Turbopump failures.

- Frequent dissociator maintenance.

- Plans.
- Improve dissociator operation stability and lifetime between services. (Additional heater attached to the cold head reduced the maintenance time from 8 to 3 hrs).
- Measure atomic beam velocity to get a better accuracy for the target thickness.
- Develop diagnostics devices for molecular hydrogen component measurements.
- Design and build shutters for the r/a calibration sources.

RHIC Spin Collaboration Meeting, October 8 & 9, 2004, Torino (Italy)

Forschungszentrum Jülich
in der Helmholtz-Gemeinschaft

Polarized Beam at COSY and HESR

A. Lehrach, IKP, Forschungszentrum Jülich

Spin motion in circular accelerators

Polarized beams at COSY

Feasibility for polarized beams at HESR

Summary

Spin Motion in Circular Accelerators

Forschungszentrum Jülich
in der Helmholtz-Gemeinschaft

Thomas-BMT equation (Thomas [1927], Bargmann, Michel, Telegdi [1959]):

$$\frac{d\vec{S}}{dt} = \frac{e}{\gamma m} \vec{S} \times [(1+\gamma G)\vec{B}_{\perp} + (1+G)\vec{B}_{\parallel}]$$

Precession Equation in Laboratory Frame

Number of spin rotation per turn: $\nu_p = \gamma G$

$G_p = 1.792847337(29)$

$G_{\bar{p}} = 1.800(8)$

- **Pure vertical field:**

  Vertical bending field → vertical polarization preserved
  Spin rotates γG times faster than particle

- **Spin manipulation:**

  At low energy, use longitudinal fields
  At high energy, use transverse fields

First Order Depolarizing Resonances

Forschungszentrum Jülich
in der Helmholtz-Gemeinschaft

- **Imperfection resonance:** $\gamma G = k$

  Field and positioning errors of magnets

  k: integer

  Resonance strength ~ y_{rms}

  → **vertical orbit correction**

  → **partial snake**

- **Intrinsic resonance:** $\gamma G = (kP \pm Q_y)$

  Vertical focusing fields

  Resonance strength ~$\sqrt{\varepsilon_v}$

  P: super-periodicity

  Q_y: vertical tune

  → **vertical tune jumps**

  → **vertical coherent betatron oscillations**

COSY Accelerator Facility

Forschungszentrum Jülich
in der Helmholtz-Gemeinschaft

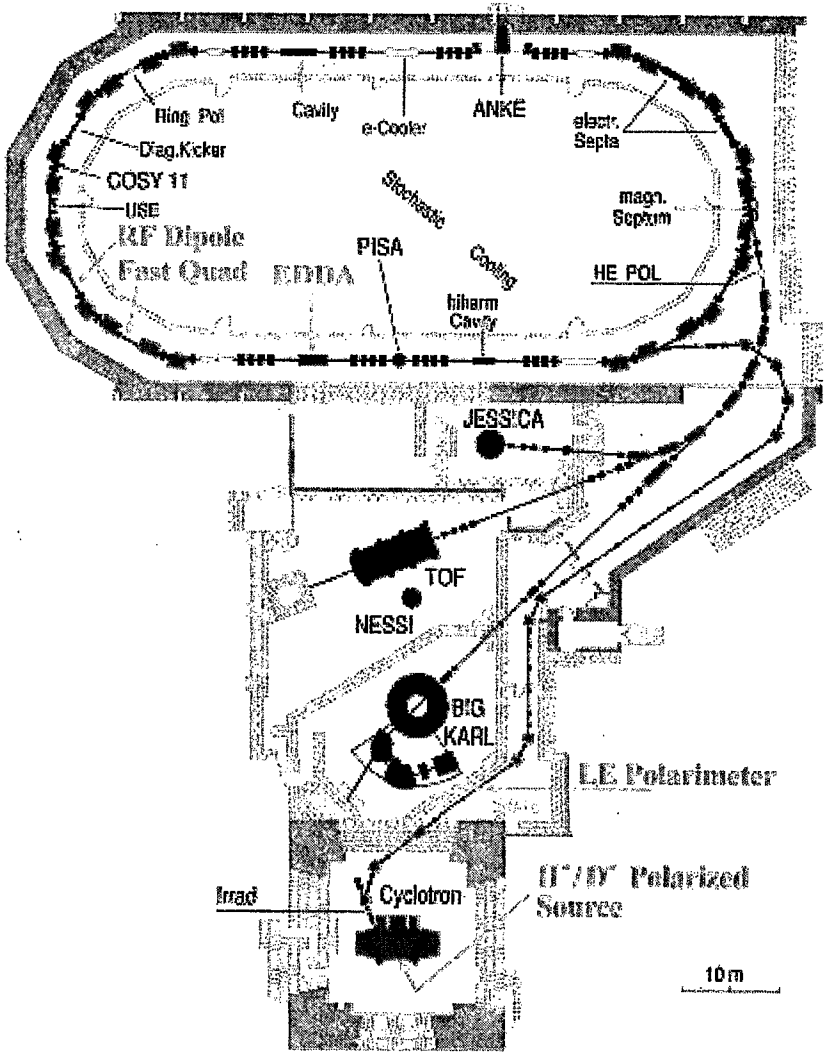

Ions: (pol. & unpol.) p and d

Momentum: 300 to 3650 MeV/c for p
540 to 3650 MeV/c for d

Circumference of the ring: 184 m

Electron Cooling at injection

Stochastic Cooling above 1.5 GeV/c

Targets:

- **Internal: solid, cluster, atomic beam**
- **External: solid, liquid**

Depolarizing Resonances at COSY

Forschungszentrum Jülich
in der Helmholtz-Gemeinschaft

Protons

Momentum GeV/c	Kinetic energy GeV	Imperfection resonance $\gamma \cdot G = \ldots$	Intrinsic resonance $\gamma \cdot G = \ldots \pm Q_y$
0.464	0.108	2	
0.835	0.318		6-
0.986	0.422		-1+
1.259	0.632	3	
1.512	0.841		7-
1.634	0.946		0+
1.871	1.155	4	
2.103	1.364		8-
2.217	1.469		1+
2.443	1.678	5	
2.666	1.888		9-
2.776	1.992		2+
2.997	2.202	6	
3.215	2.411		10-
3.324	2.516		3+

Deuterons

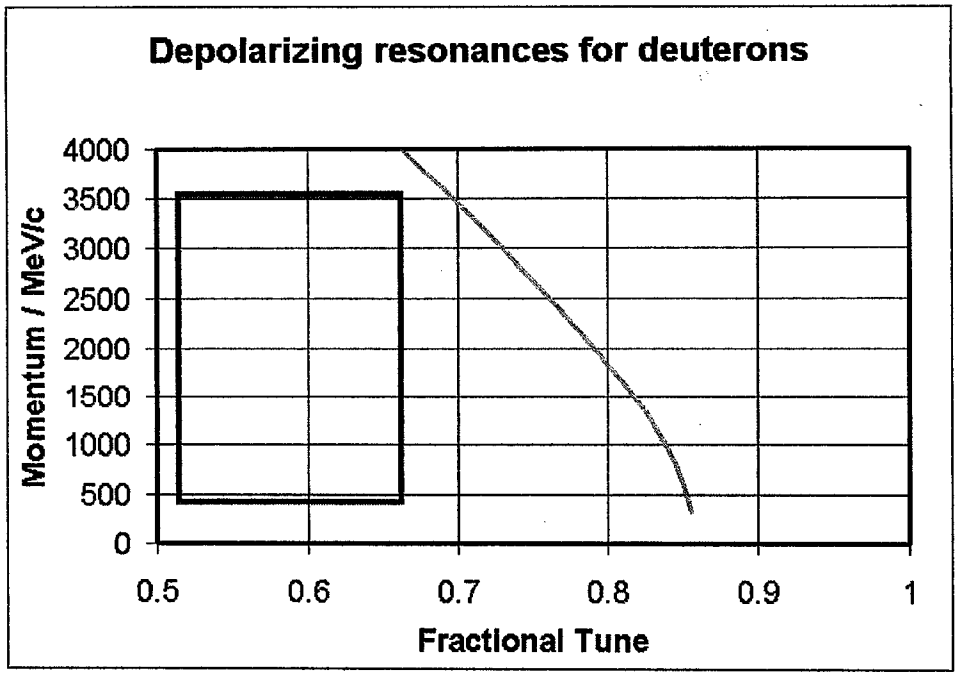

$Q_y = 3.60$

Resonance strength: 10^{-6} - 10^{-3}

Polarized Proton Beam at COSY

Forschungszentrum Jülich
in der Helmholtz-Gemeinschaft

Methods to preserve polarization

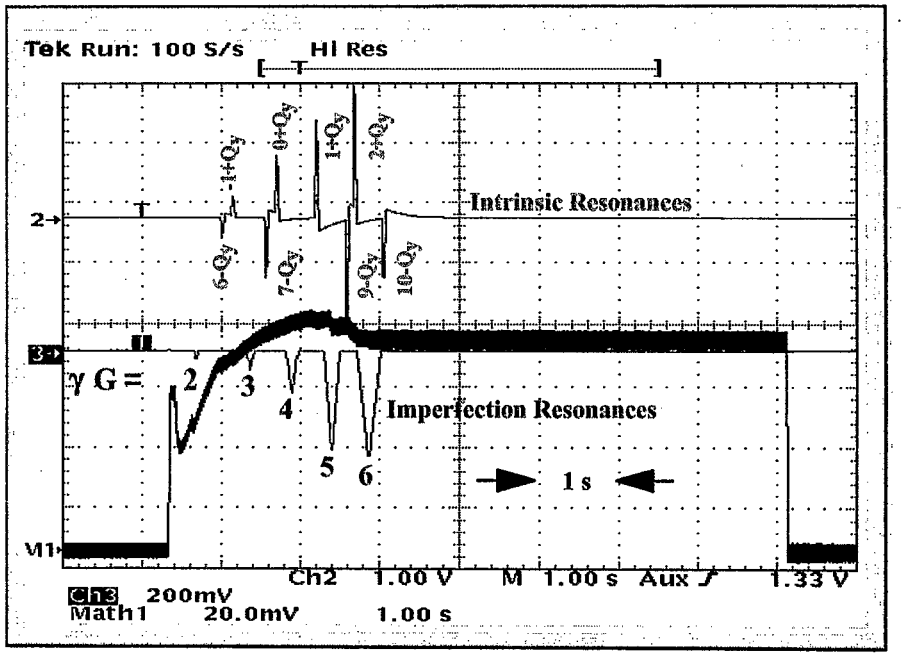

→ tune jumps

→ vertical orbit excitation

Polarization measurement during acceleration

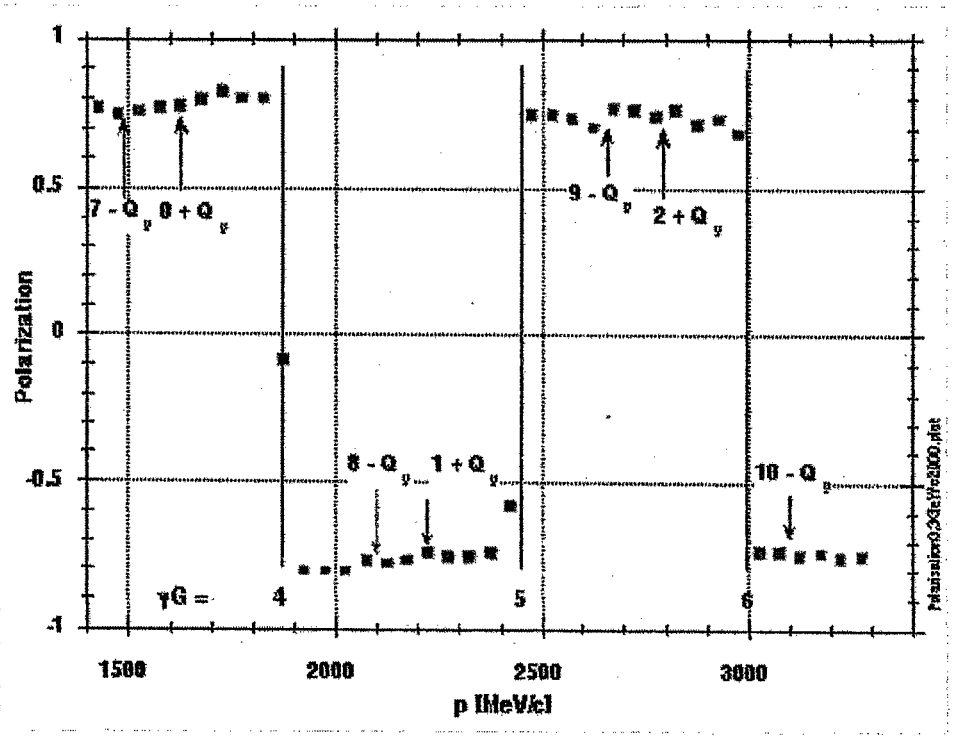

Polarized Deuteron Beam at COSY

Forschungszentrum Jülich
in der Helmholtz-Gemeinschaft

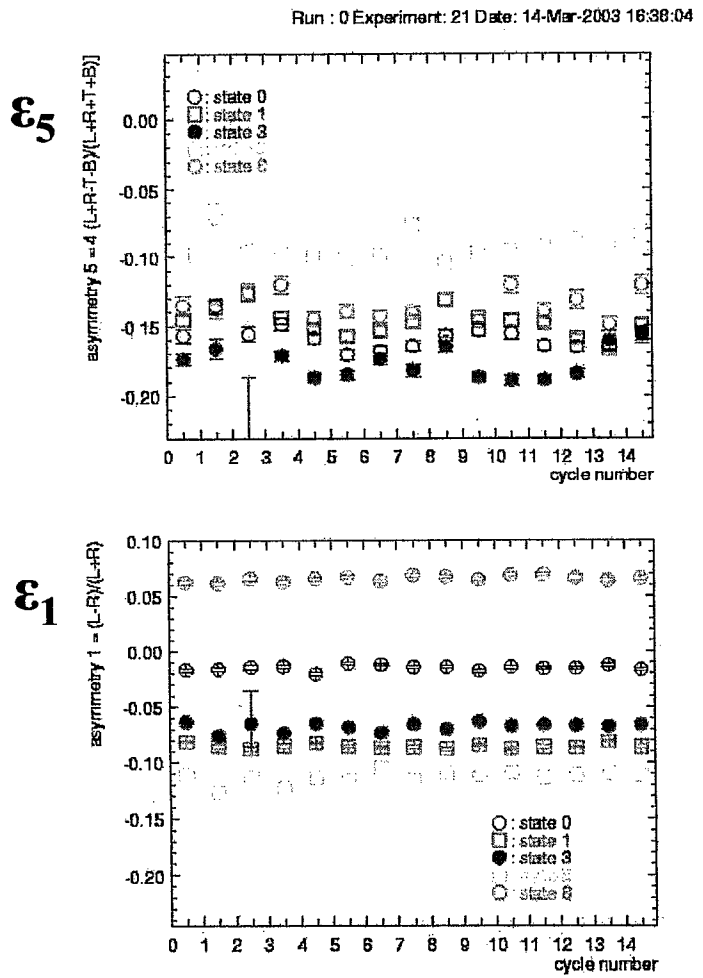

Asymmetries:

$$\varepsilon_5 = 4\,[(L+R) - (T+B)]/[(L+R) + (T+B)] =$$

$$p_{ZZ} * A_{xx-yy} / (1 - 0.25\, p_{ZZ}\, A_{zz}) \sim p_{ZZ}$$

$$\varepsilon_1 = (L-R)/(L+R) =$$

$$1.5 * p_Z * A_y / (1 - 0.25\, p_{ZZ}\, A_{zz}) \sim p_Z$$

- accelerated and stored at 1.85 GeV/c
- 5 polarization states

(vector and tensor polarized)

Facility for Antiproton and Ion Research

Forschungszentrum Jülich
in der Helmholtz-Gemeinschaft

FAIR

Future Accelerator Facilities

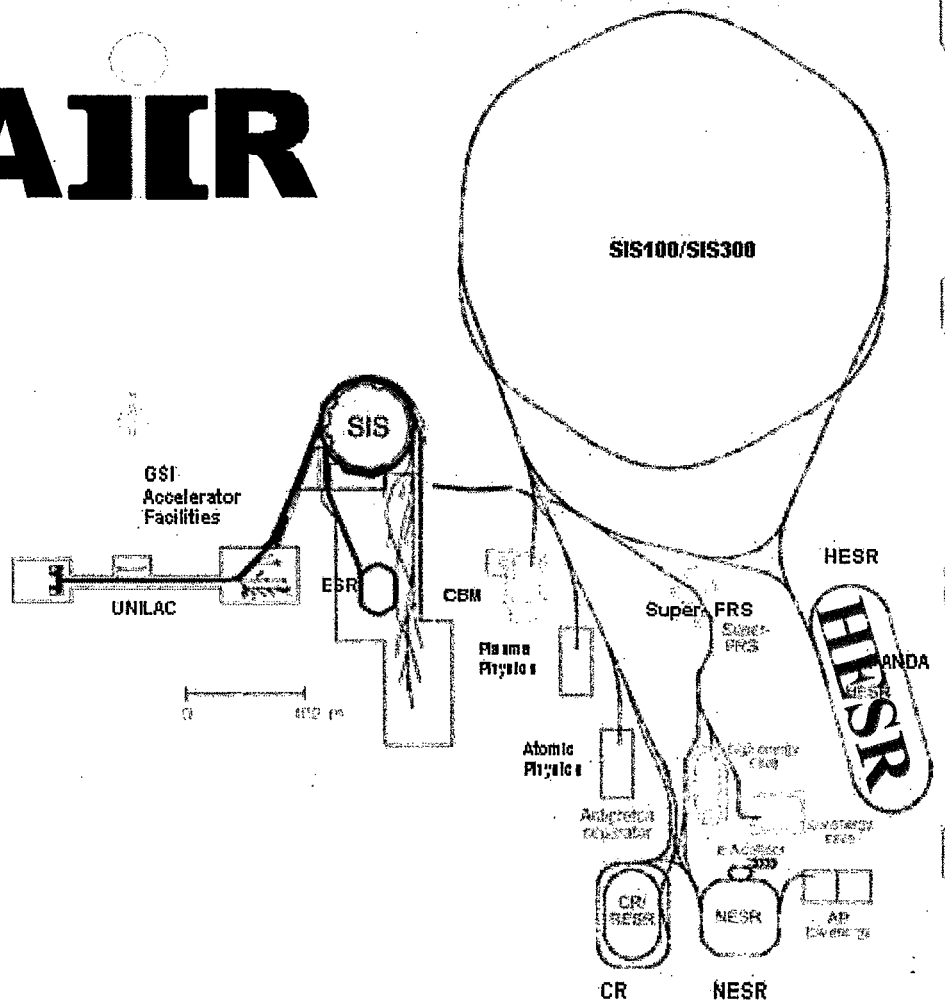

Primary Beams

- 10^{12}/s; 1.5-2 GeV/u; $^{238}U^{28+}$
- Factor 100-1000 over present intensity
- 4(2)x10^{13}/s 30 GeV protons
- 10^{10}/s $^{238}U^{73+}$ up to 35 GeV/u

Secondary Beams

- Broad range of radioactive beams up to 1.5 - 2 GeV/u; up to a factor 10 000 in intensity over present
- Antiprotons 3(0) - 30 GeV

Storage and Cooler Rings

- Radioactive beams
- e – A(RIB) collider
- 10^{11} stored and cooled 3(0) – 15 GeV antiprotons

Key Technical Features

- Cooled beams
- Rapidly cycling superconducting magnets

HESR Reference Design

Forschungszentrum Jülich
in der Helmholtz-Gemeinschaft

Conceptional design report

Beam Parameter:

0.8 - 14.5 GeV $\bar{p}$

$N_{max} = 5*10^{11}$

$L = 2x10^{32}\ cm^{-2}s^{-1}$

$N_{target} = 10^{15}\text{-}10^{16}\ cm^{-2}$

Beam Quality:

0.001 – 0.1 mm mrad

$\Delta p/p = 10^{-4} - 10^{-5}$

Beam Accumulation:

$1.4*10^{7}/s\ (5*10^{10}/h)$

Electrons: 1 A, 8 MV
Interaction length: 30 m
Long. B field: 1-5 kG

$-\Delta T_{\bar{p}} \propto \rho_e T_{\bar{p}}^{-3/2} \ln(B)$

Circumference: 443.4 m
Beam Rigidity: 50 Tm
Dipole field: 4T

$\Delta T_{\bar{p}} \propto \rho_{\bar{p}} T_{\bar{p}}^{-3/2}$

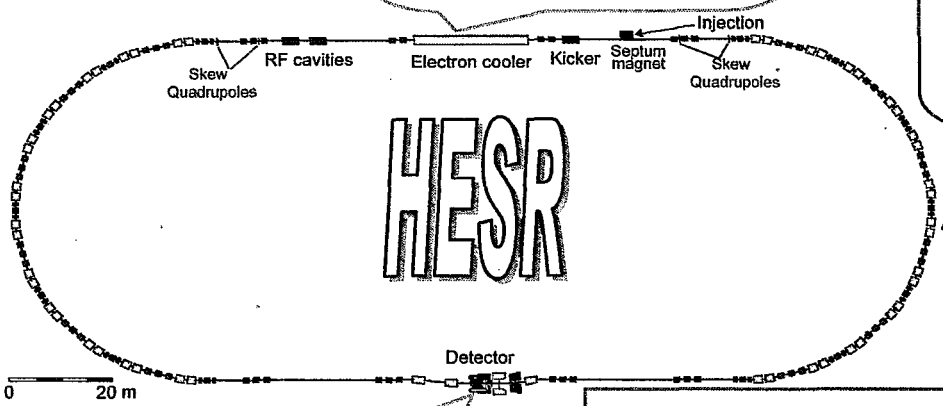

Pellet-Target

- H_2 (ρ=0.08 g/cm³)
- 70000 pellets/s

$\Delta T_{\bar{p}} \propto \rho_{H_2} d$

Accelerator R&D work:

- magnetized e-cooler (8 MV)
- stochastic cooling system
- broadband feedback system
- RF cavities, sc magnets
- impedance budget

Outline

Forschungszentrum Jülich
in der Helmholtz-Gemeinschaft

- General Features of Spin Filtering
- 1992 Filter Test at TSR in Heidelberg (23 MeV protons)

$$(\bar{p}+\overset{\sqcup\!\!\sqcup}{e} \rightarrow \bar{p}+\overset{\sqcup\!\!\sqcup}{e})$$

- Spin Transfer Cross Section
- Beam Lifetime Estimates
- AP Optimization
  - Space-Charge Limit
  - Optimum Filtering Energies
- Beam Transfer to HESR

Puzzle from the Filtex Experiment

Forschungszentrum Jülich
in der Helmholtz-Gemeinschaft

Observed polarization build-up: $dP/dt = \pm (1.24 \pm 0.06) \times 10^{-2}\ h^{-1}$

Expected build-up: $P(t)=\tanh(t/\tau_1)$,
$1/\tau_1=\sigma_1 Q d_t f = 2.4\times10^{-2}\ h^{-1}$
$\Rightarrow$ about factor 2 larger!

σ_1 = 122 mb (pp phase shifts)
$Q = 0.83 \pm 0.03$
$d_t = (5.6 \pm 0.3) \times 10^{13} cm^{-2}$
f = 1.177 MHz

Three distinct effects:

1. **Selective removal through scattering beyond Ψ_{acc}=4.4 mrad**
   $\sigma_{R\perp}$=83 mb
2. **Small angle scattering of target protons into ring acceptance**
   $\sigma_{S\perp}$=52 mb
3. **Spin transfer from polarized electrons of the target atoms to the stored protons** **$\sigma_{E\perp}$=-70 mb**

Horowitz & Meyer, PRL 72, 3981 (1994)
H.O. Meyer, PRE 50, 1485 (1994)

Spin Transfer from Electrons to Protons

Forschungszentrum Jülich
in der Helmholtz-Gemeinschaft

$$\boxed{p + \overset{\sqcup}{e} \rightarrow \overset{\sqcup}{p} + e}$$

$$\boxed{\sigma_{EM\perp} = -\frac{1}{2}\left[\frac{4\pi\alpha^2(1+\lambda_p)m_e}{p^2 m_p}\right] C_0^2\left[\frac{v}{2\alpha}\right] \times \sin\left[\frac{2\alpha \ln(2pa_0)}{v}\right]}$$

$$\boxed{\sigma_{EM\parallel} = 2 \cdot \sigma_{EM\perp}}$$

Horowitz & Meyer, PRL 72, 3981 (1994)
H.O. Meyer, PRE 50, 1485 (1994)

α	fine structure constant
$\lambda_p=(g-2)/2=1.793$	anomalous magnetic moment
m_e, m_p	rest masses
p	cm momentum
a_0	Bohr radius
$C_0^2=2\pi\eta/[\exp(2\pi\eta)-1]$	Coulomb wave function
$\eta=z\alpha/v$	Coulomb parameter (negative for antiprotons)
v	relative lab. velocity between p and e
z	beam charge number

PAX will exploit spin-transfer from polarized electrons of the target to antiprotons

Beam Polarization in a dedicated AP ring

Forschungszentrum Jülich
in der Helmholtz-Gemeinschaft

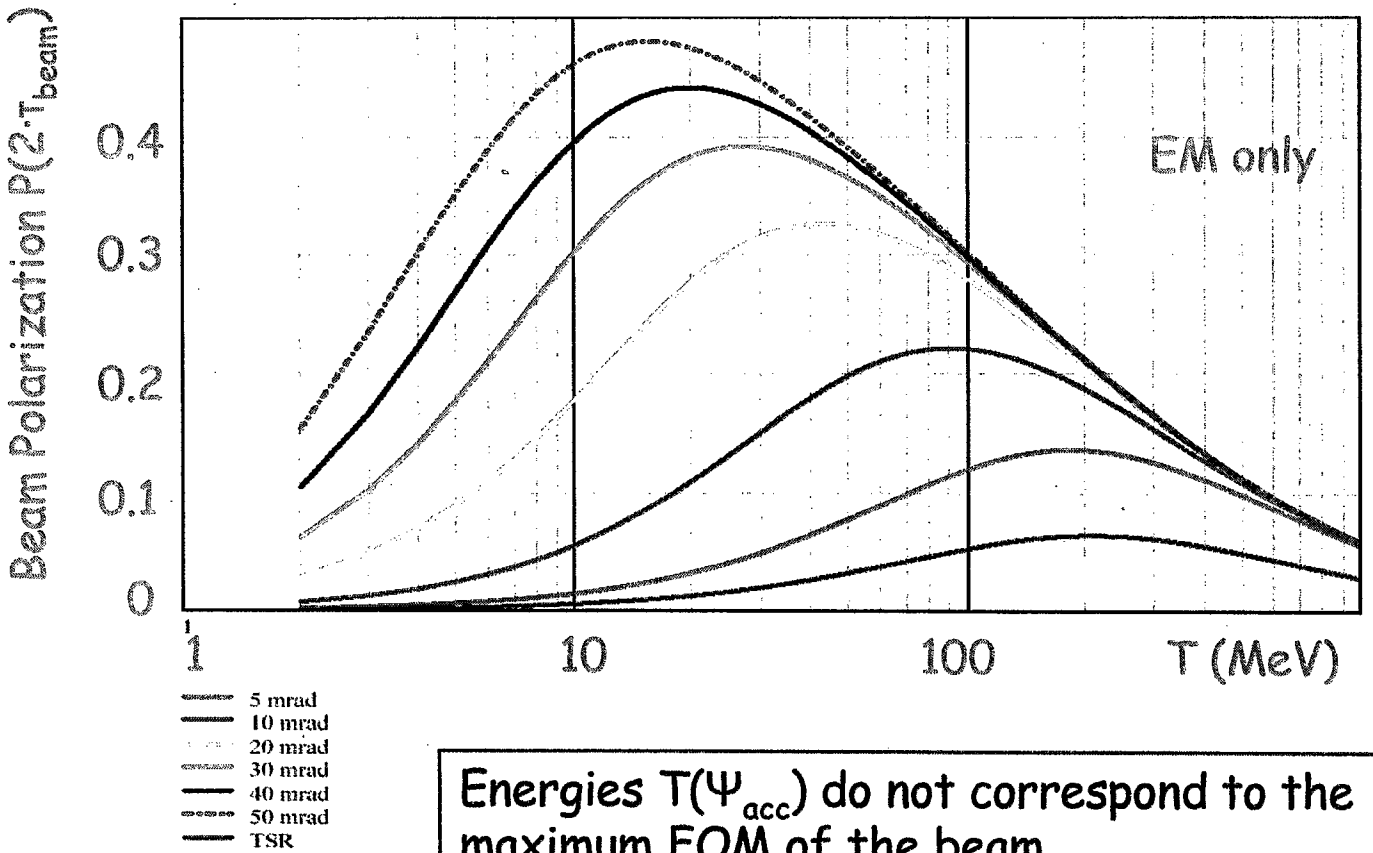

Energies $T(\Psi_{acc})$ do not correspond to the maximum FOM of the beam

Optimum beam energies for buildup in AP

Forschungszentrum Jülich
in der Helmholtz-Gemeinschaft

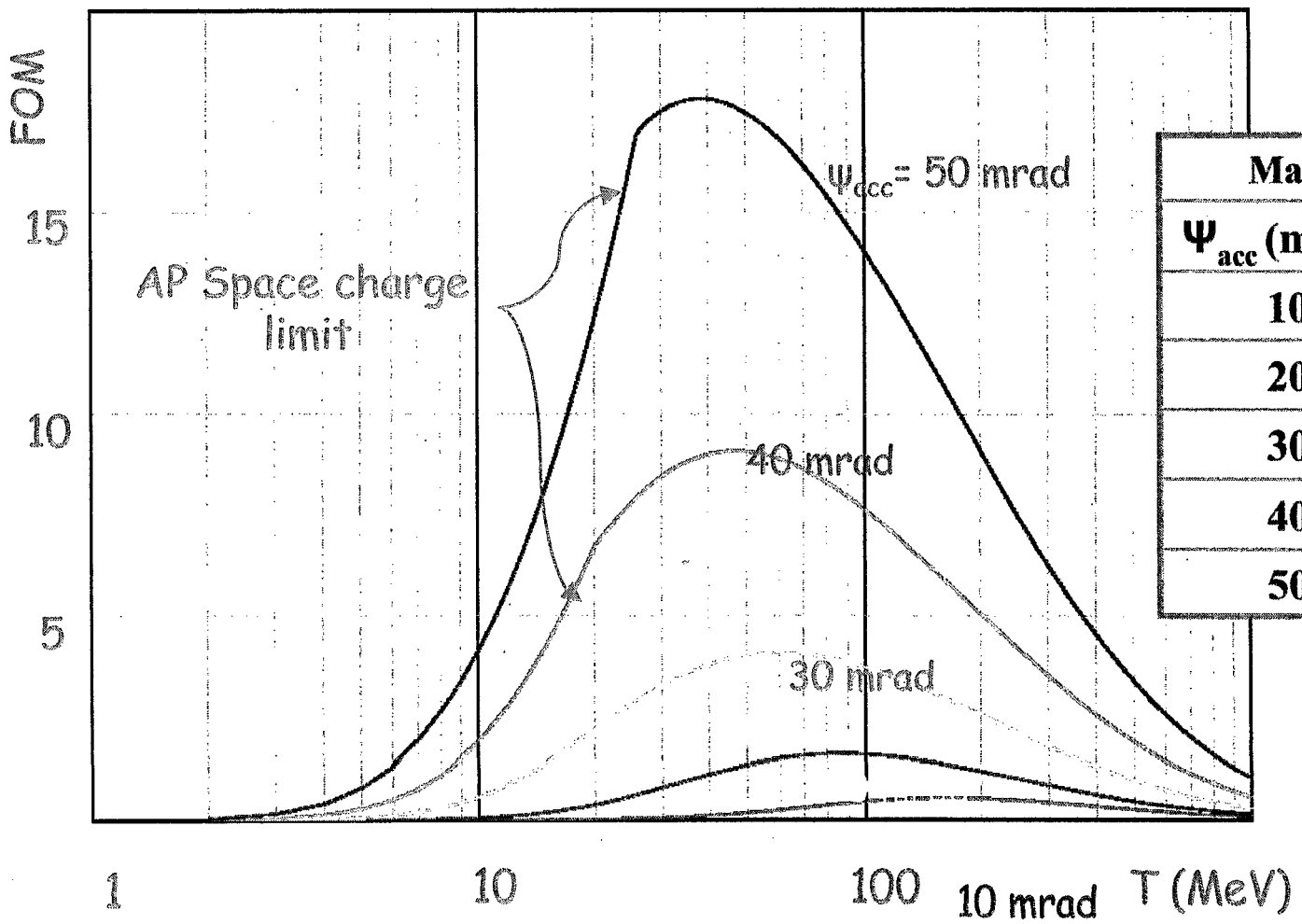

Maximum FOM	
Ψ_{acc} (mrad)	T (MeV)
10	163
20	88
30	61
40	47
50	38

Parameters for Calculation of Polarization Buildup

Forschungszentrum Jülich
in der Helmholtz-Gemeinschaft

- **Dedicated Ring AP (Antiproton Polarizer)**
  - 150 m circumference
- **β-function at polarizing target $\beta_{target} = 0.2$ m**
- **ABS H-Flow $1.5 \cdot 10^{17}$ atoms/s (2 states)**
  - (20% above existing performance)
- **Internal Target**
  - storage cell diameter $d_b = \psi_{acc} \cdot \beta \cdot 2$ → target density $d_t = d_t(\psi_{acc})$
  - length l_b=40 cm (=2·β), feed tube d_f=1 cm, l_f=15 cm
  - T=100 K
  - target polarization longitudinal $(\sigma_{EM\parallel} = 2 \cdot \sigma_{EM\perp})$
    - holding field (300 mT)

87

HESR Accelerator Complex for Polarized Beams

Forschungszentrum Jülich
in der Helmholtz-Gemeinschaft

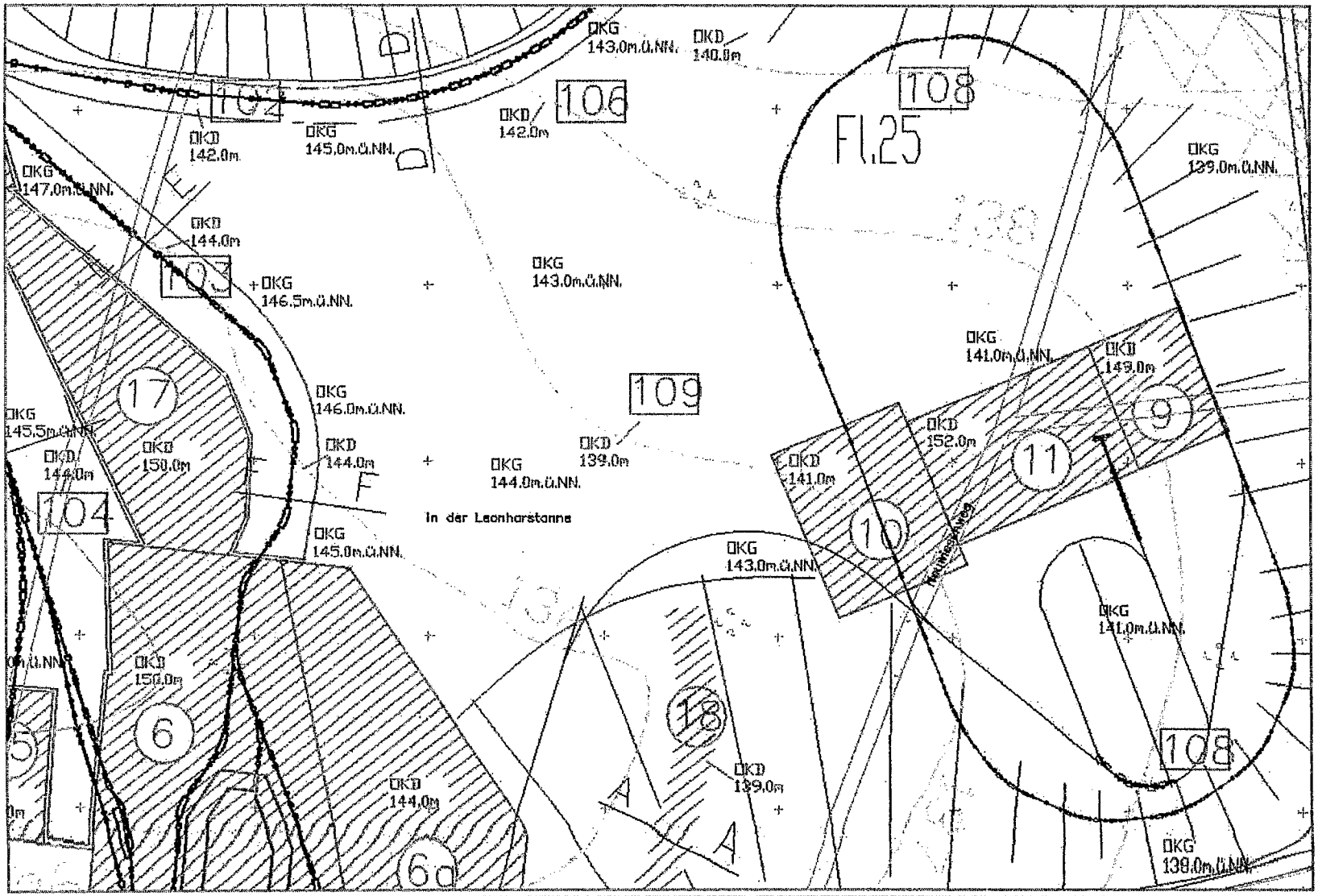

Depolarizing Resonances at HESR

Forschungszentrum Jülich
in der Helmholtz-Gemeinschaft

Momentum GeV/c	Kinetic energy GeV	Imperfection resonance $\gamma \cdot G = \ldots$	Intrinsic resonance $\gamma \cdot G = \ldots \pm Q_y$
1.789	1.082		12-
1.871	1.155	4	
1.953	1.228		-4+
2.364	1.605		13-
2.443	1.678	5	
2.521	1.752		-3+
2.920	2.129		14-
2.997	2.202	6	
3.073	2.275		-2+
3.465	2.652		15-
3.541	2.725	7	
3.617	2.798		-1+
4.005	3.175		16-
4.080	3.248	8	
14.172	13.265		19+
14.550	13.642		36-
14.624	13.715	28	
14.697	13.789		20+

$Q_y = 8.14$

Resonance strength:

$10^{-6} - 10^{-2}$

Depolarizing Resonances at HESR

Forschungszentrum Jülich
in der Helmholtz-Gemeinschaft

- **Imperfection:** **25 times**

  4, 5, 6, ... , 28

  Strong: **8, 16, 24**

- **Intrinsic:** **50 times**

  -4+, -3+, ... , 20+

  12-, 13-, ..., 35-

  Strong: **0+, 8+, 12+, 16+, 24-, 32+, 36-**

- **Coupling:** **50 times**

  -4+, -3+, ... , 20+

  12-, 13-, ..., 36-

Methods for Polarization Preservation

Forschungszentrum Jülich
in der Helmholtz-Gemeinschaft

- **< 5 GeV: Conventional methods**
  - → correcting dipoles
  - → tune jump quadrupoles
  - → Siberian snake (solenoid)
- **5 - 20 GeV: Adiabatic methods**
  - → partial snake (helical dipole or solenoid)
  - → ac dipole
- **> 20 GeV: Siberian snake concept**
  - → Siberian snakes (helical dipole)

Magnetic Field, Orbit and Spin

Forschungszentrum Jülich
in der Helmholtz-Gemeinschaft

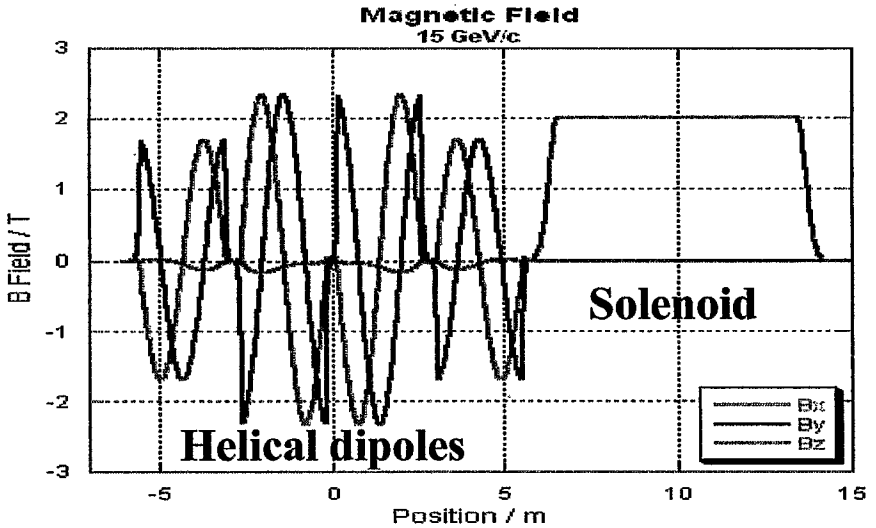

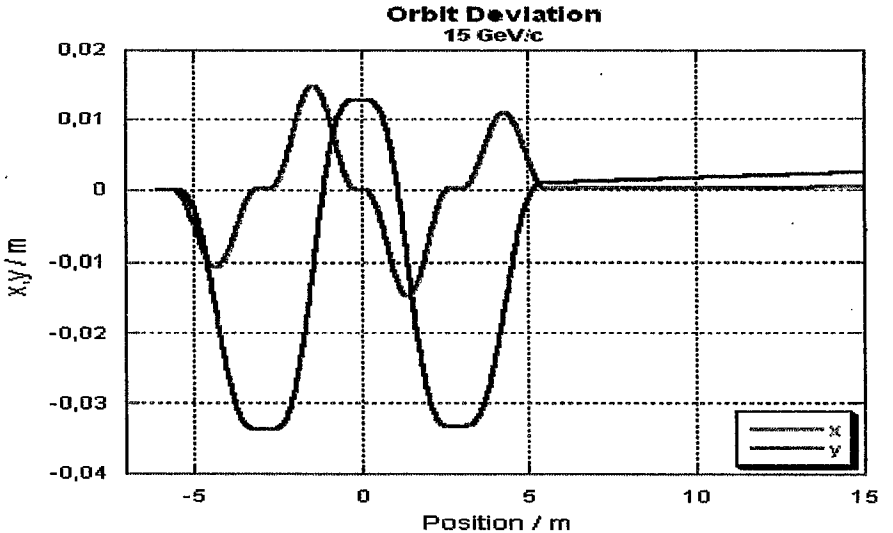

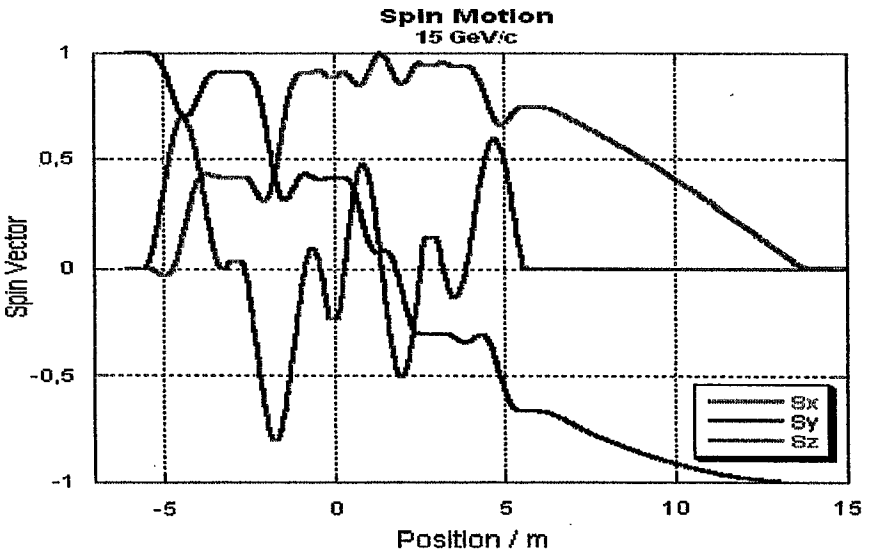

Siberian Snake for HESR (Solution I)

Forschungszentrum Jülich
in der Helmholtz-Gemeinschaft

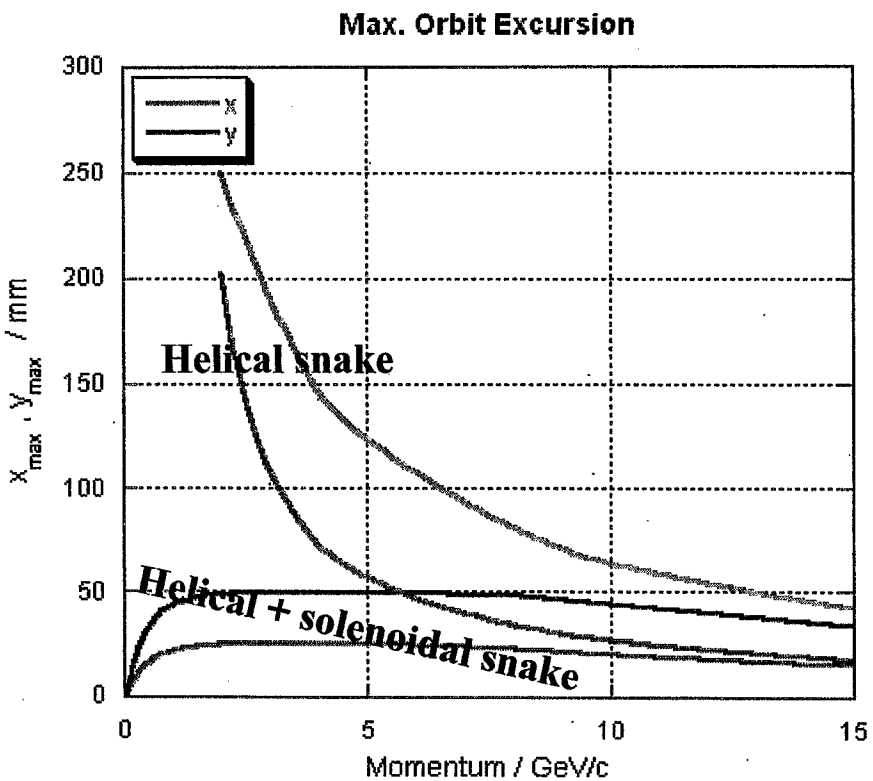

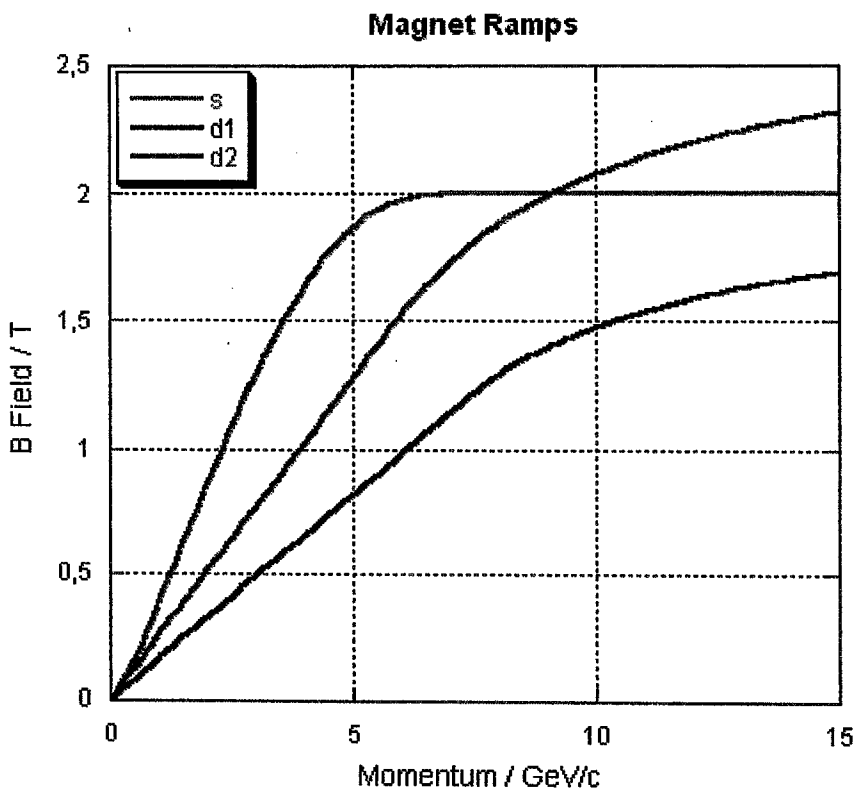

→ 4 helical dipoles (2.5 Tesla) and a 15 Tm solenoid

Siberian Snake for HESR (Solution II)

Forschungszentrum Jülich
in der Helmholtz-Gemeinschaft

- Together with the 15 Tm Cooler solenoid add one more solenoid in the same straight with same strength
- Both solenoids have to be decoupled.
- From injection up to some energy both solenoid will provide full spin flip. At higher energy they will work as the partial snake with about 50% snake at top energy.

Spin Tune with Partial Snake

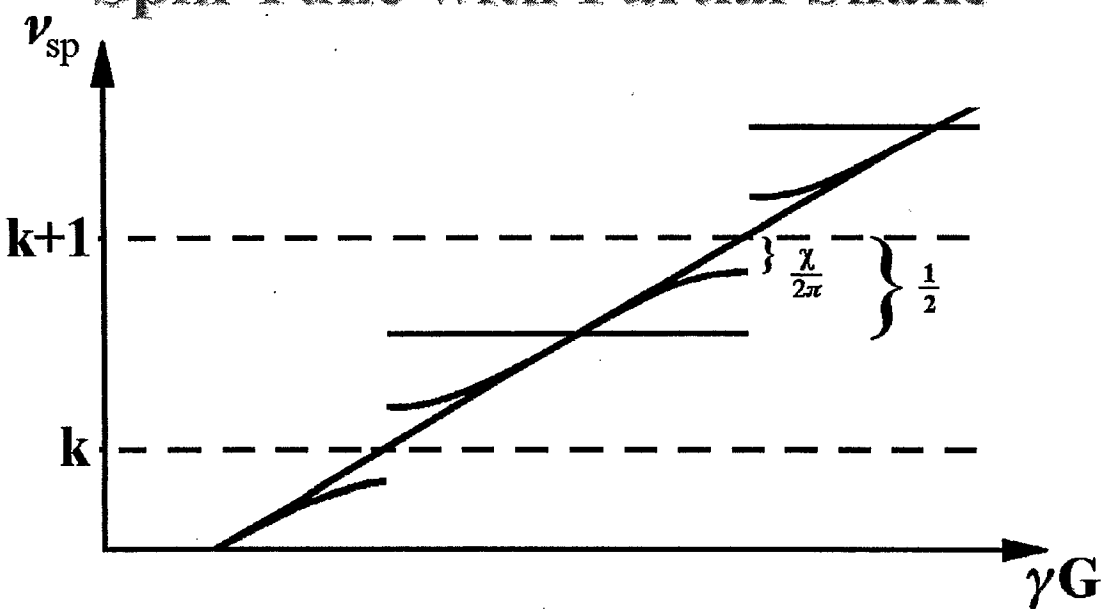

HESR Accelerator Complex for Polarized Beams

Forschungszentrum Jülich
in der Helmholtz-Gemeinschaft

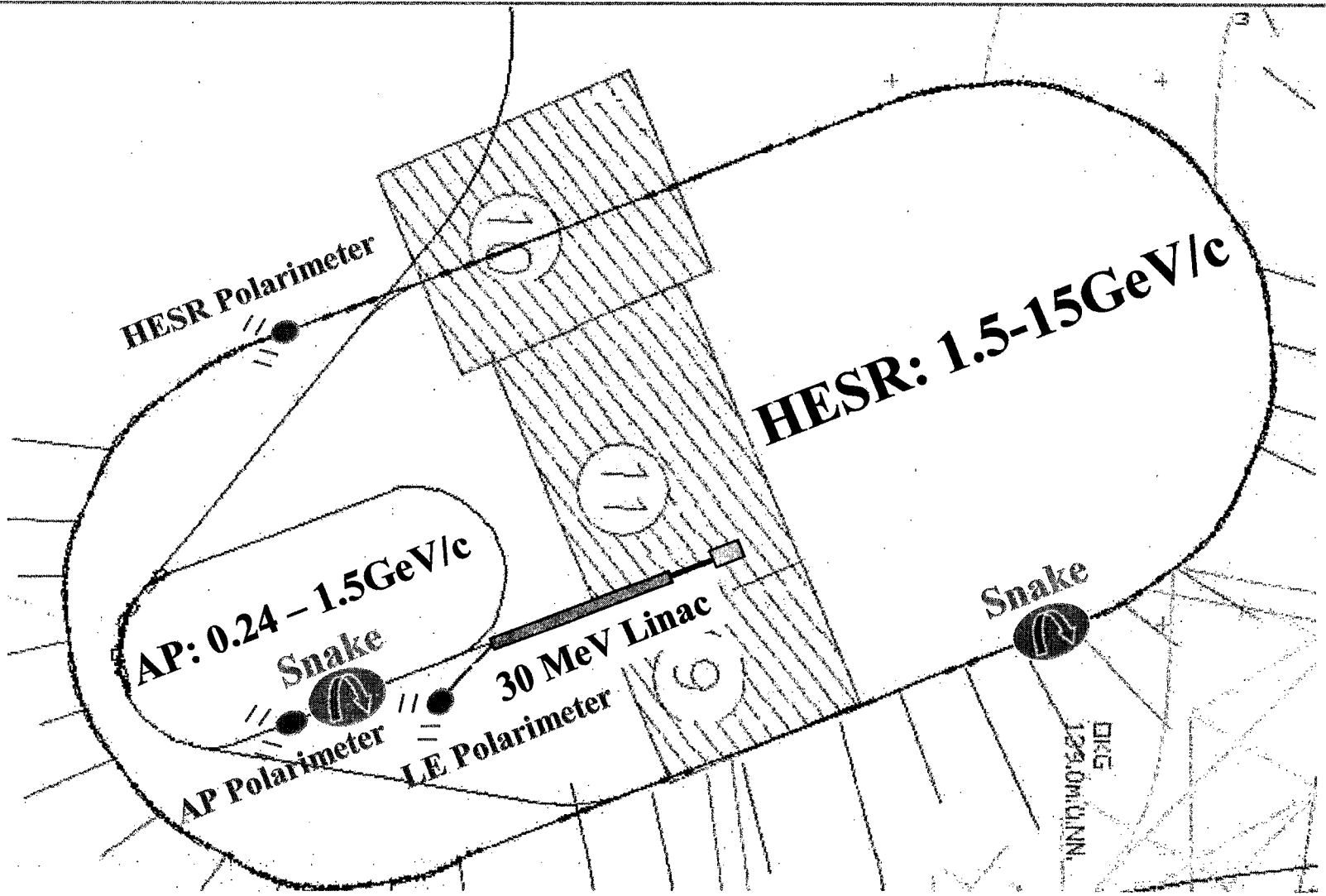

Conclusion

Forschungszentrum Jülich
in der Helmholtz-Gemeinschaft

- **Polarization Preservation at FAIR**

  Dedicated HESR/AP:

  → 6 Tm solenoid

  HESR:

  → 4 helical dipoles (2.5 Tesla) and 15 Tm solenoid

  or

  → 15 Tm solenoids to get a 50% snake

- **Other Equipment:**

  3 polarimeter, 1 spin flipper (ac dipole)

Stern-Gerlach Effect

Forschungszentrum Jülich
in der Helmholtz-Gemeinschaft

The Stern–Gerlach Interaction Between a Traveling Particle and a Time Varying Magnetic Field

M. Conte[1], M. Ferro[1], G. Genoese[1], W.W. MacKay[2], R. Parodi[1] and M. Pusterla[3]

97 -

6 A Few Numerical Examples

The spin-splitter principle requires a repetitive crossing of N_{cav} cavities distributed along the ring, each of them resonating in the TE mode. After each revolution, the particle experiences a variation, or *kick*, of its energy or of its momentum spread

$$\zeta = \frac{\delta p}{p} = \frac{1}{\beta^2}\frac{\delta E}{E} \simeq \frac{N_{cav}\Delta U}{E} \simeq \frac{2\sqrt{3}}{3} N_{cav}\frac{B_0}{B_{bb}}\gamma \tag{67}$$

having made use of eq. (54), further simplified by reasonably setting $\beta_{pb} = 2$, and with

$$B_{bb} = \frac{mc^2}{\mu^*} = \frac{1.503\times 10^{-10}\ \mathrm{J}}{1.41\times 10^{-26}\ \mathrm{JT}^{-1}} \simeq 10^{16}\ \mathrm{T} \tag{68}$$

for (anti)protons. From eq. (67) we may find as the number of turns needed for attaining a momentum separation equal to $2\left(\frac{\Delta p}{p}\right)$

$$N_{SS} = \frac{\left(\frac{\Delta p}{p}\right)}{\zeta} = \frac{\sqrt{3}}{2N_{cav}\gamma}\frac{B_{bb}}{B_0}\left(\frac{\Delta p}{p}\right) \tag{69}$$

Multiplying N_{SS} by the revolution period τ_{rev} we obtain

$$\Delta t = N_{SS}\tau_{rev} \tag{70}$$

as the actual time spent in this operation. For the sake of having some data, we consider RHIC [7] and HERA [8] whose essential parameters are shown in Table I together with what can be found by making use of eqs. (69) and (70) where $B_0 \simeq 0.1\ T$ and $N_{cav} = 200$ are chosen as realistic values.

Table I: RHIC and HERA parameters

	RHIC	HERA
E(GeV)	250	820
γ	266.5	874.2
$\tau_{rev}(\mu s)$	12.8	21.1
$\frac{\Delta p}{p}$	4.1×10^{-3}	5×10^{-5}
N_{SS}	6.67×10^{9}	2.48×10^{7}
Δt	$8.52\times 10^{4}\ s \simeq 23.7\ h$	523 s

In the example of the polarimeter we have to pick up a signal generated at cavity crossing. Therefore, making use of eq. (54) we have for a bunch train made N particles the total energy transfer

$$\Delta U \approx 2NP\mu^* B_0 \frac{b}{d}\gamma^2$$

where P is the beam polarization slightly modified with respect the definition (41)

$$P = \frac{N_{\rightarrow} - N_{\leftarrow}}{N_{\rightarrow} + N_{\leftarrow}}$$

The average power transferred will be

ΔU

Measurement of the analyzing power for pp elastic scattering at CNI peak region for absolute polarimetry at RHIC

Hiromi Okada from Kyoto-Univ. / RIKEN

I. Alekseev, A. Bravar, G. Bunce, S. Dhawan,
R. Gill, W. Haeberli, O. Jinnouchi, A. Khodinov,
A. Kponou, K. Kurita, Z. Li, Y. Makdisi, A. Nass,
S. Rescia, N. Saito, H. Spinka, E. Stephenson,
D. Svirida, T. Wise, A. Zelenski

contents

- Introduction
  - Spin dependent asymmetry (A_N) for elastic scattering in very small -t Region
- Set up (Hydrogen gas jet target & Si detectors)
- 2004 JET Commissioning RUN
  - Kinetics of elastic scattering and event selection
  - A_N plots
- Summary and Outlook

Elastic scattering process with Polarized target

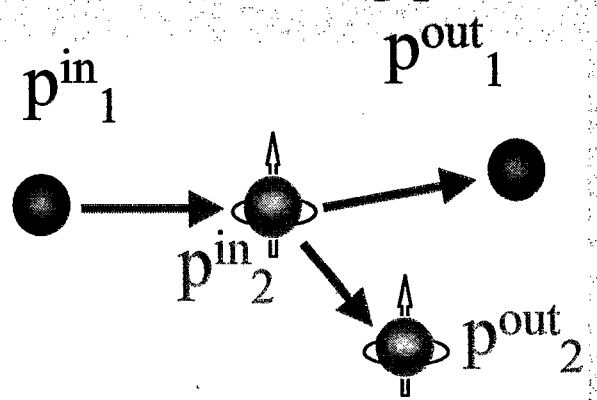

$$s = \left(p_1^{in} + p_2^{in}\right)^2$$

$$t = \left(p_1^{out} - p_1^{in}\right)^2 < 0$$

Physics of *pp* elastic scattering in very small -t region

- *pp* elastic scattering;
  Helicity Amplitudes $\phi_1 \sim \phi_5$

- Total cross section

$$\sigma_{tot} = \frac{4\pi}{s} \mathrm{Im}[\phi_1(s,t) + \phi_3(s,t)]\Big|_{t=0}$$

- Spin dependent left-right (up-down) asymmetry in very small –t region

$$\boxed{A_N \frac{d\sigma}{dt} = -\frac{4\pi}{s^2} \mathrm{Im}\{\phi_5^*(\phi_1 + \phi_2 + \phi_3 - \phi_4)\}}$$

$$A_{NN} \frac{d\sigma}{dt} = \frac{4\pi}{s^2} \{2|\phi_5|^2 + \mathrm{Re}(\phi_1^* \phi_2 - \phi_3^* \phi_4)\}$$

Spin ½ state

in1,in2 out1,out2

$$\phi_1(s,t) = \langle ++|M|++\rangle$$

$$\phi_2(s,t) = \langle ++|M|--\rangle$$

$$\phi_3(s,t) = \langle +-|M|+-\rangle$$

$$\phi_4(s,t) = \langle +-|M|-+\rangle$$

$$\phi_5(s,t) = \langle ++|M|+-\rangle$$

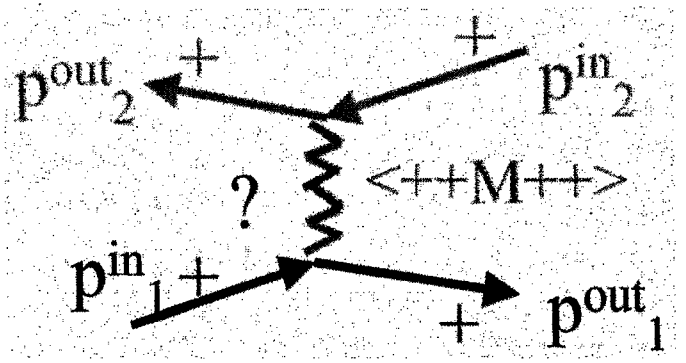

Motivation

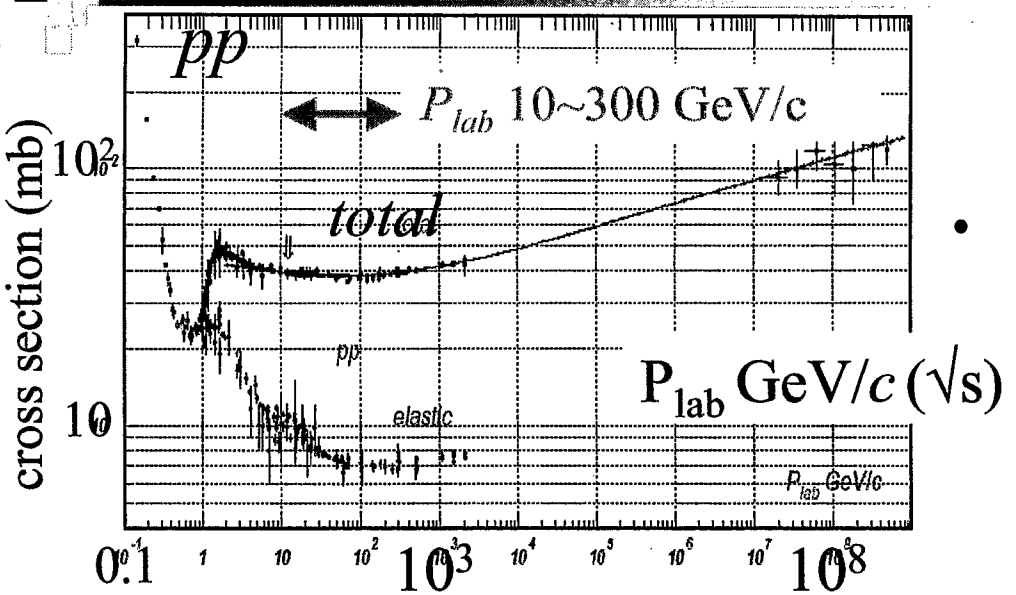

- A_N in very small –t range is very fundamental physics value as σ_{tot}

Phys. Rev. D 48, 3026 (1993)

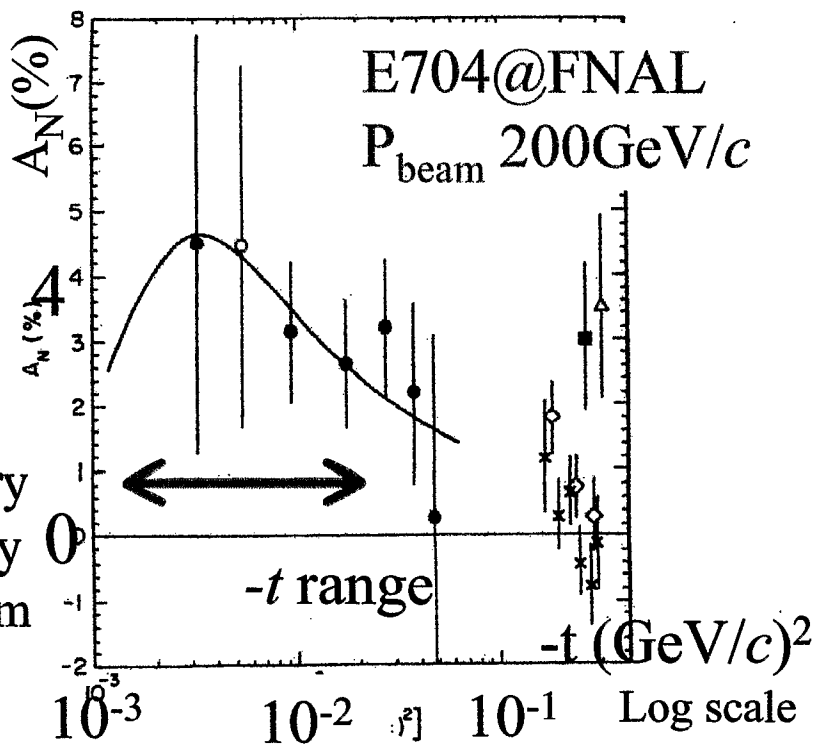

- Very small –t region →0.001 < -t < 0.02 (GeV/c)^2
- the helicity amplitude of hadronic part and electro-magnetic part become similar →Coulomb Nuclear Interference (CNI)
- A_N is predicted to have peak and its peak value and position are also predicted by theory
- The experiment in very small –t region is very difficult and the only experiment result is from E704

Set up @ IP12

array of Si detectors
(3 pairs, covering the BLUE beam)

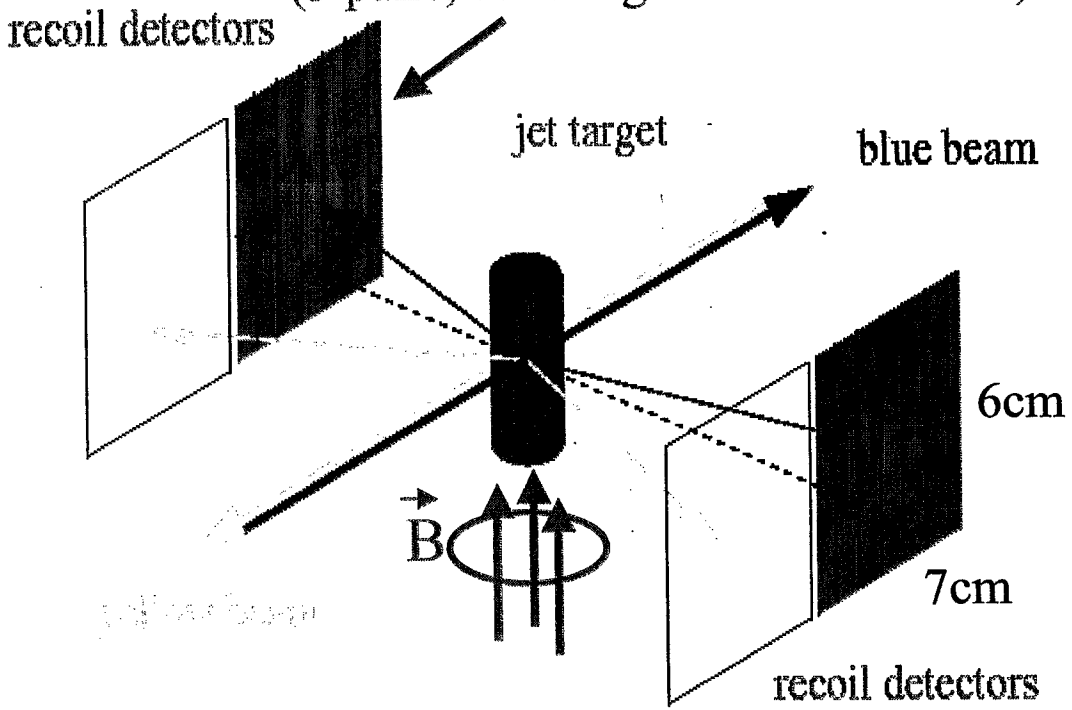

Polarized Hydrogen Gas Jet Target
polarization 0.924 +/- 0.018

Event rate ; ~6Hz (0.7~5MeV)

Si detector
- **7cm * 6cm / detector, 3 pairs**
- **Acceptance 2 π /16**

Measurement (recoil particle)
- **energy**
- **time of flight (tof)**
- **Angle**

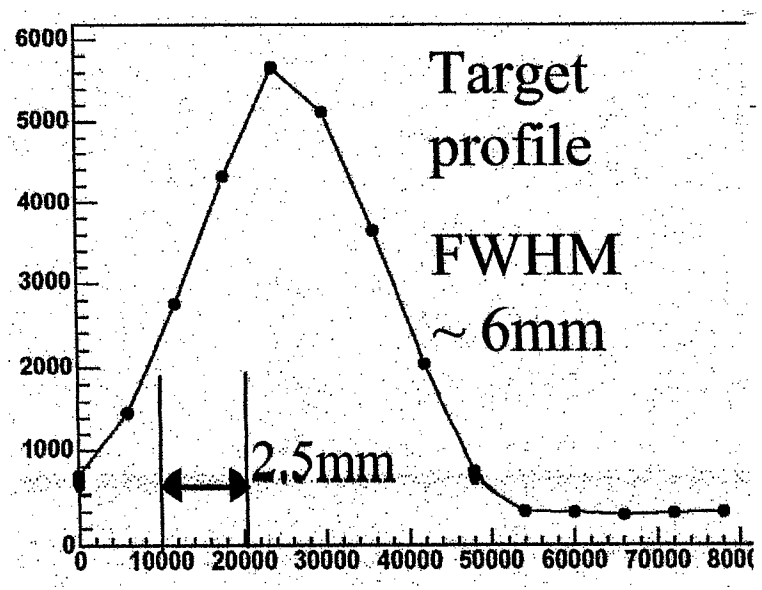

How to measure A_N ?

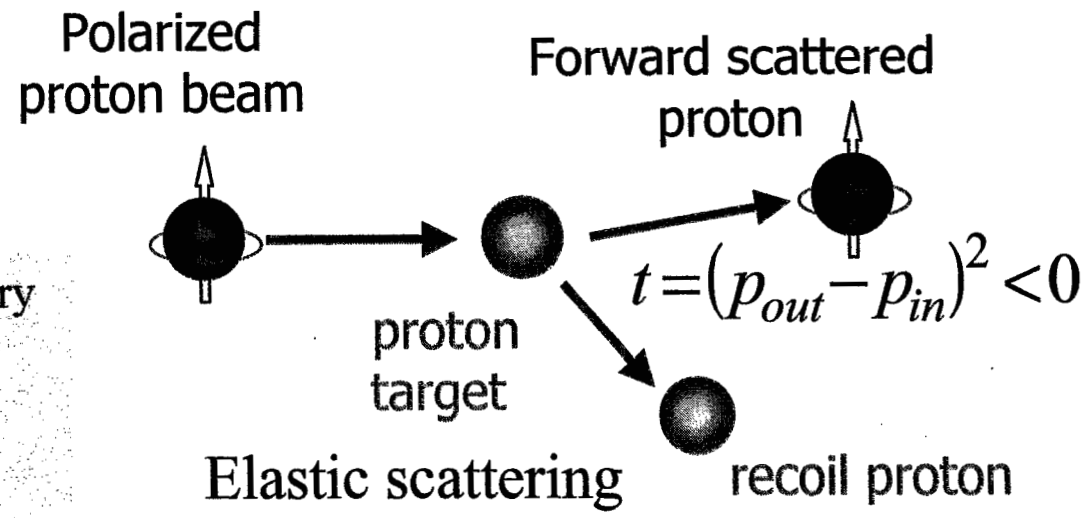

Event yield left-right asymmetry

$$\varepsilon = \frac{N_{left} - N_{right}}{N_{left} + N_{right}}$$

(by Square-root-formula)

$$A_N = \frac{\varepsilon}{P_{target}}, \quad \left(\frac{\Delta A_N}{A_N}\right)^2 = \left(\frac{\Delta P_{target}}{P_{target}}\right)^2 + \left(\frac{\Delta \varepsilon}{\varepsilon}\right)^2$$

(H-Jet target 0.924 +/- 0.018)

- During RUN2004, 90 good runs (~90 hours) @ 100GeV
- $0.0015 < |t| < 0.010$ (GeV/c)^2 1.85 M elastic pp events
  - expect similar statistics for $0.010 < |t| < 0.02$ (GeV/c)^2

Elastic event selection ; Kinetics and particle ID

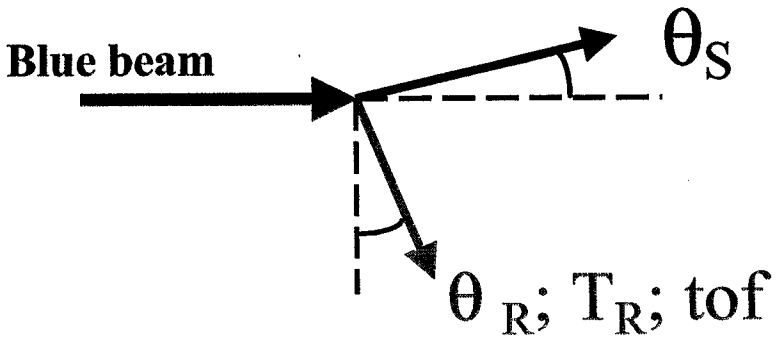

Particle ID ; recoil particle ,forward scattering particle → proton ?

(1) Correlation of **tof** and **energy (T_R)** for recoil particle ID

$$m_p \approx 2T_R \cdot \left(\frac{tof}{\text{Distance}}\right)^2$$

⇨ Recoil particle is proton

(2) Correlation of **position ($\propto \theta_R$)** and **T_R** for forward scattering particle ID

$$m_p \approx \frac{T_R}{2\sin\vartheta_R^{\,2}}$$

→ Forward scattering particle is proton

⇨ Elastic event

Recoil particle ID : Correlation of TOF and Energy

$$tof \approx \frac{1}{\sqrt{T_R}} \cdot \sqrt{\frac{m_p}{2}} \text{Distance}$$

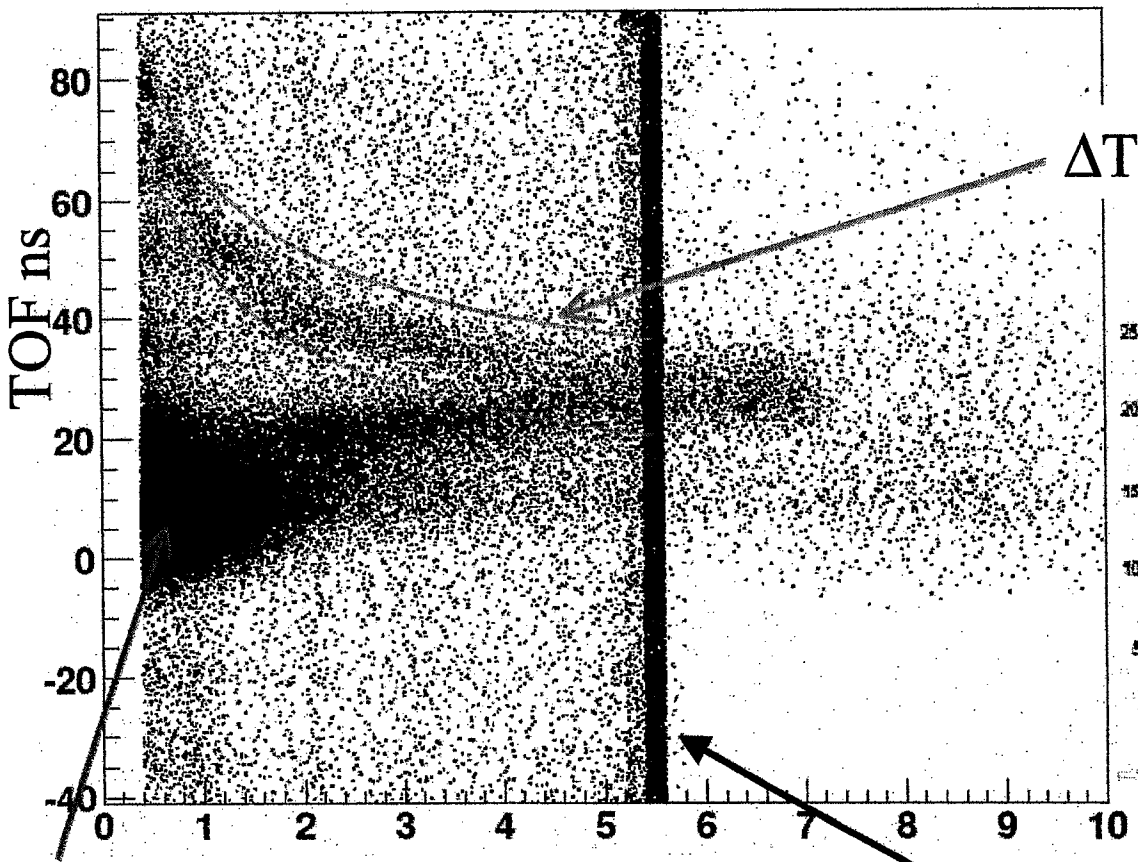

ΔTOF< +/-8 ns width line

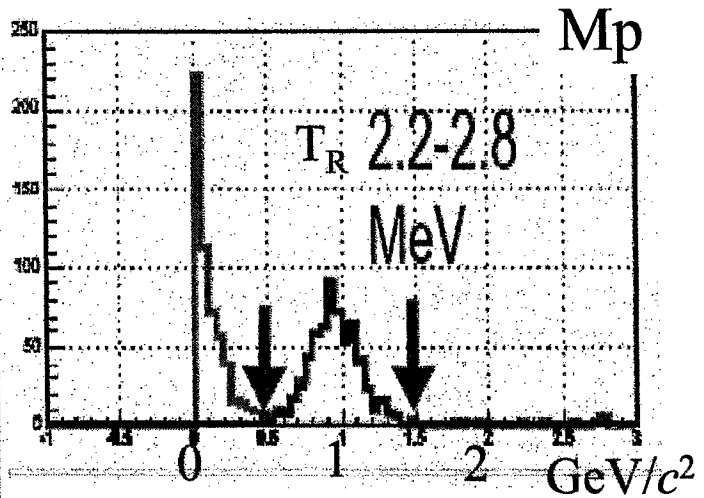

prompt events

T_R MeV

calibration alpha source (^{241}Am, 5.486 MeV)

Forward scattering particle ID ;
Correlation of Energy and position (ch#)

TOF vs T_R Si detector of 16channels

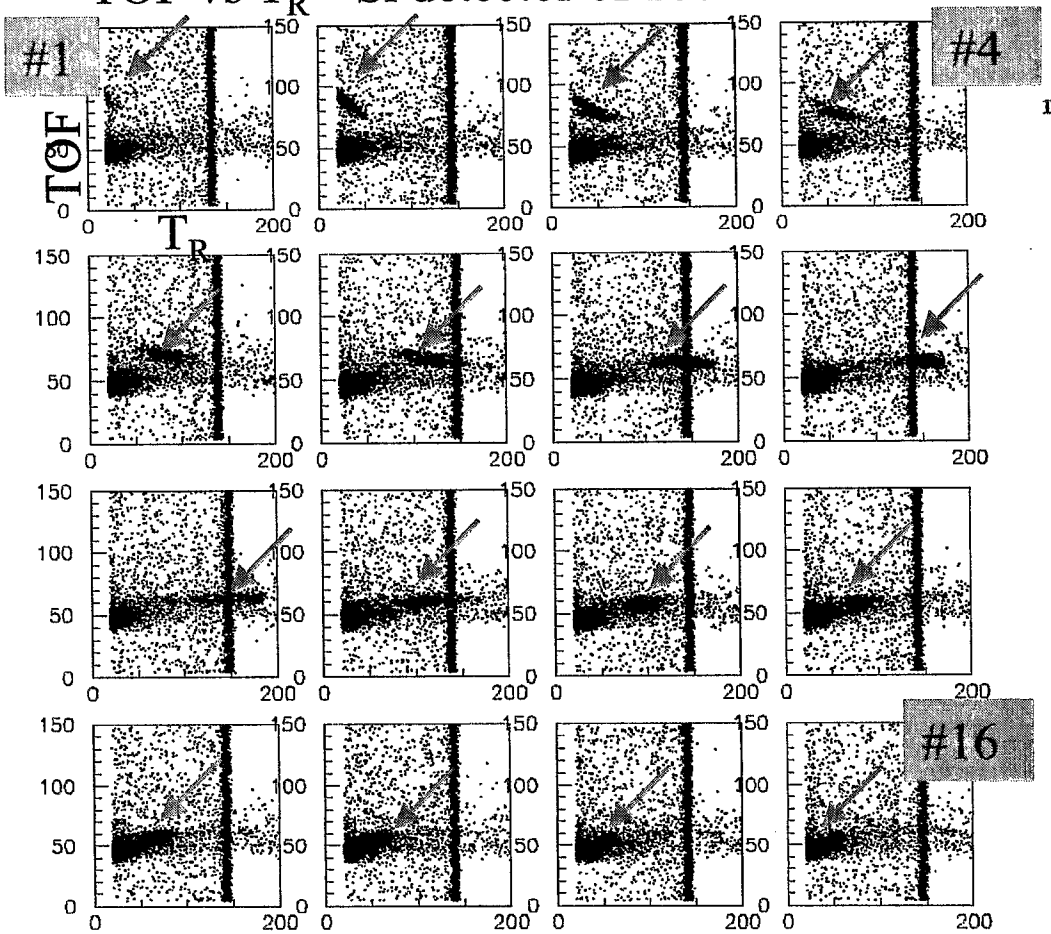

vertical strips → ch# → recoil angle

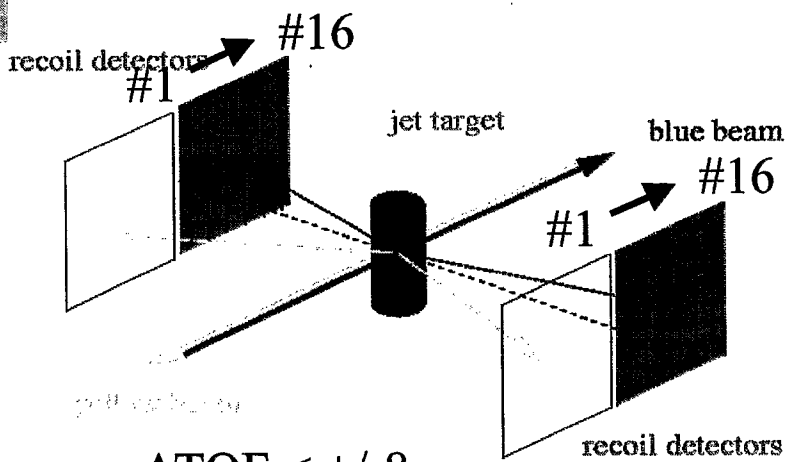

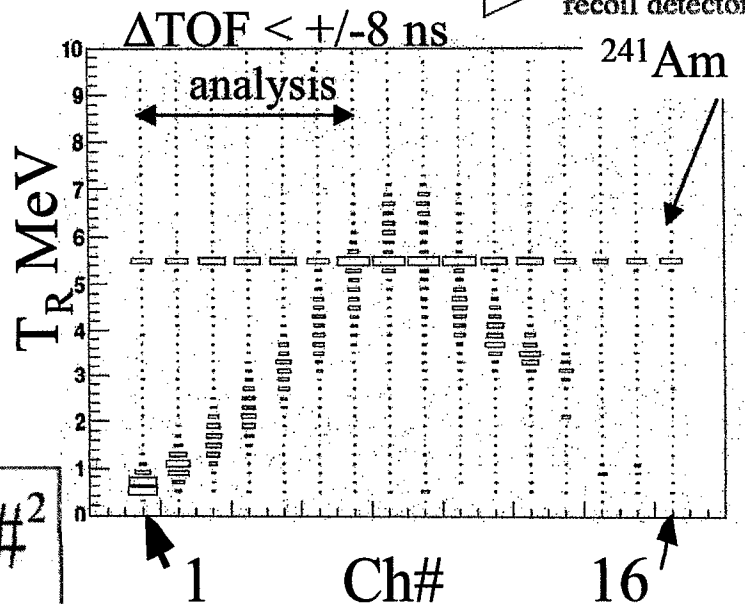

$$T_R \approx 2m_p \sin\vartheta_R^{\,2} \Rightarrow 2m_p ch\#^2$$

Elastic event selection

Energy vs. position (ch#)

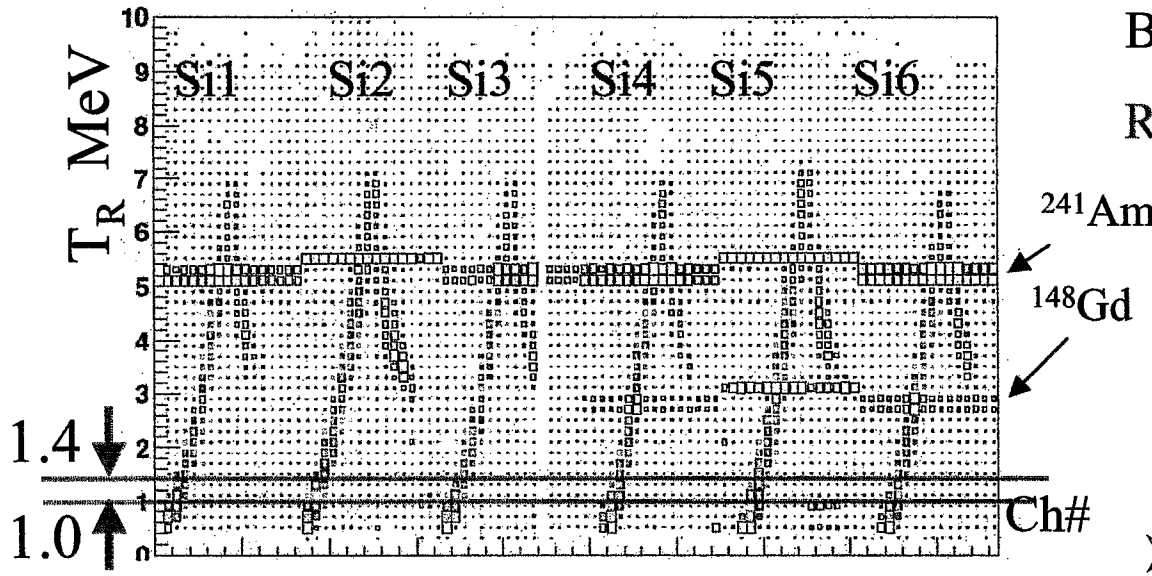

Black ; ΔTOF < +/-8 ns

Red ; ΔTOF < +/-8ns

^{241}Am & ch# select

^{148}Gd

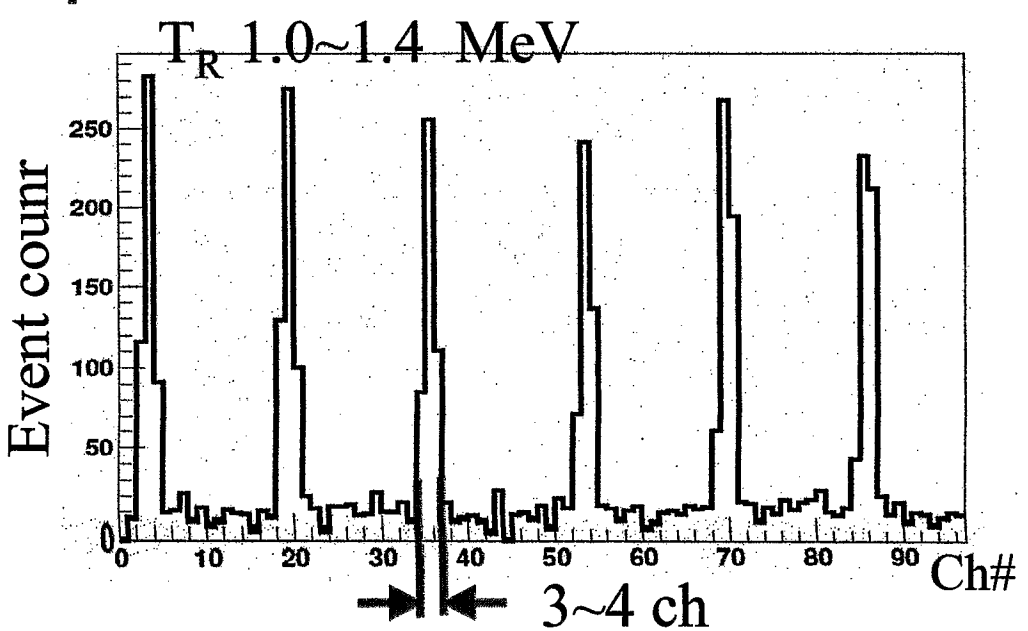

- Vertical strips
  - → ch# ∝ recoil angle
- Channel selection by eyes for every energy slice
  - → equivalent to missing mass cut for forward scattered particles

DAQ with WFD (Waveform digitizer) → same system with pC

- ADC 420MHz
- Synchronized with RHIC clock
- Waveform Output (for OFFLINE analysis)
- Algorithm on FPGA
  → waveform analysis (for ONLINE analysis)
  - ADC max
  - $TDC_{1/4}$

Energy calibration

- Tracking calibration constant with ^{241}Am(5.486 MeV) and ^{148}Gd(3.183 MeV)
  →very stable within +/- 1%
- Alpha spectrum σ ~70 keV

$$-t = 2m_p T_R$$

$$\Delta t \propto T_R < 100 \text{ keV}$$

Waveform data sample

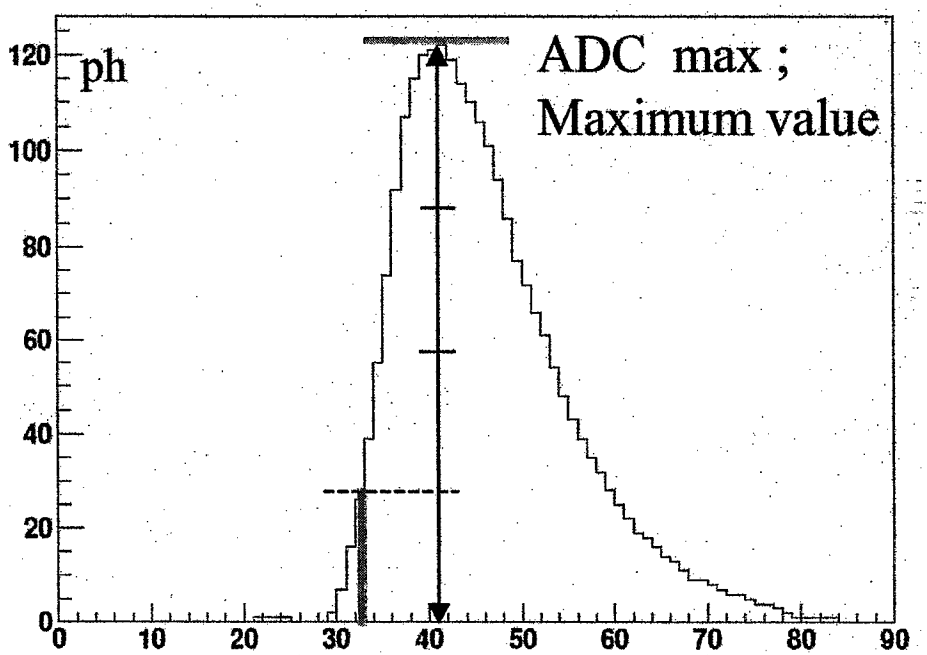

$TDC_{1/4}$; 1/4 of maximum timing

∝ time

1bin = 2.38 ns

A_N @ 100 GeV

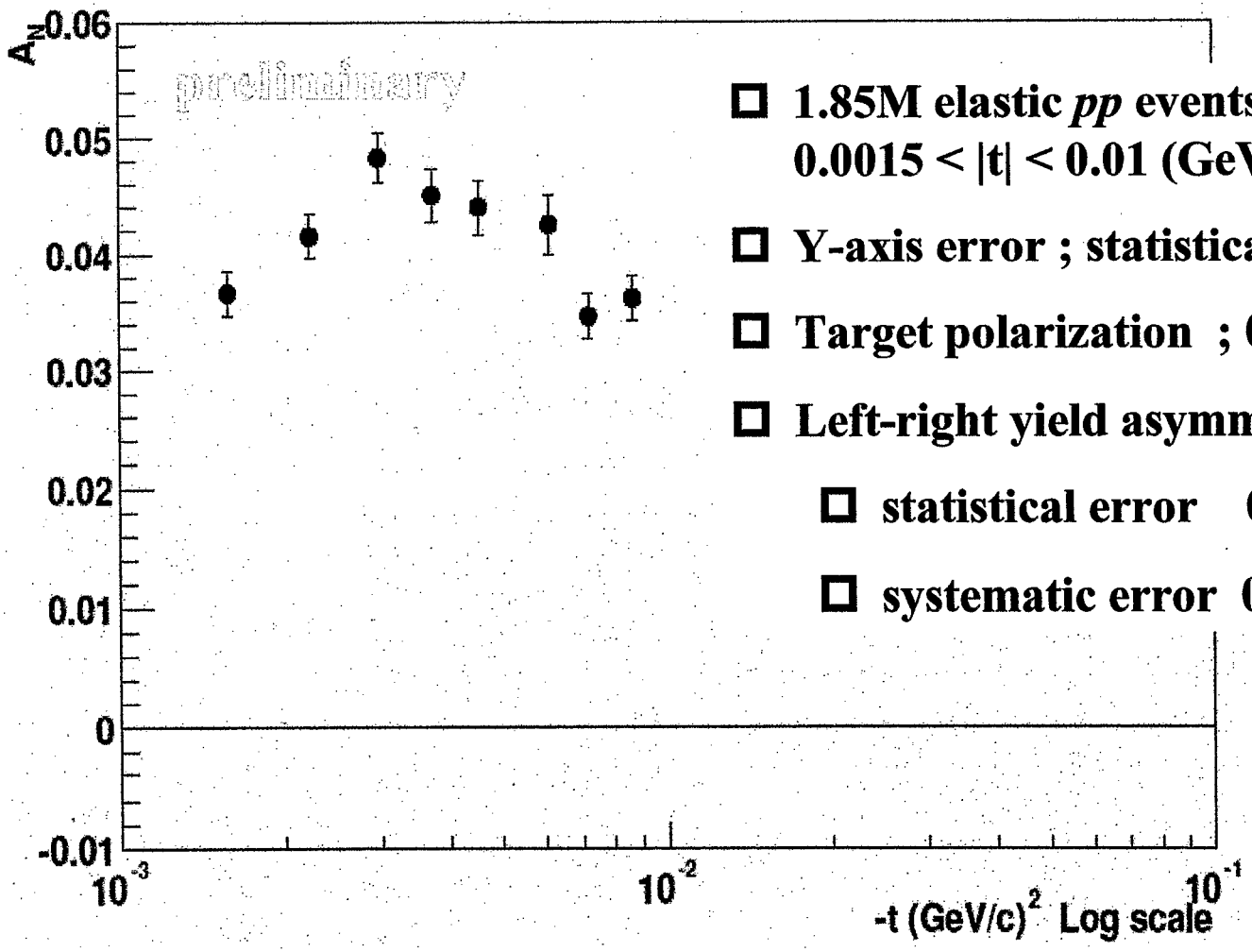

- 1.85M elastic *pp* events
  $0.0015 < |t| < 0.01$ (GeV/*c*)^2
- Y-axis error ; statistical only
- Target polarization ; 0.924 +/- 0.018
- Left-right yield asymmetry ε
  - statistical error 0.0025 (max)
  - systematic error 0.0015 for all bins

A_N @ 100 GeV and E704 data

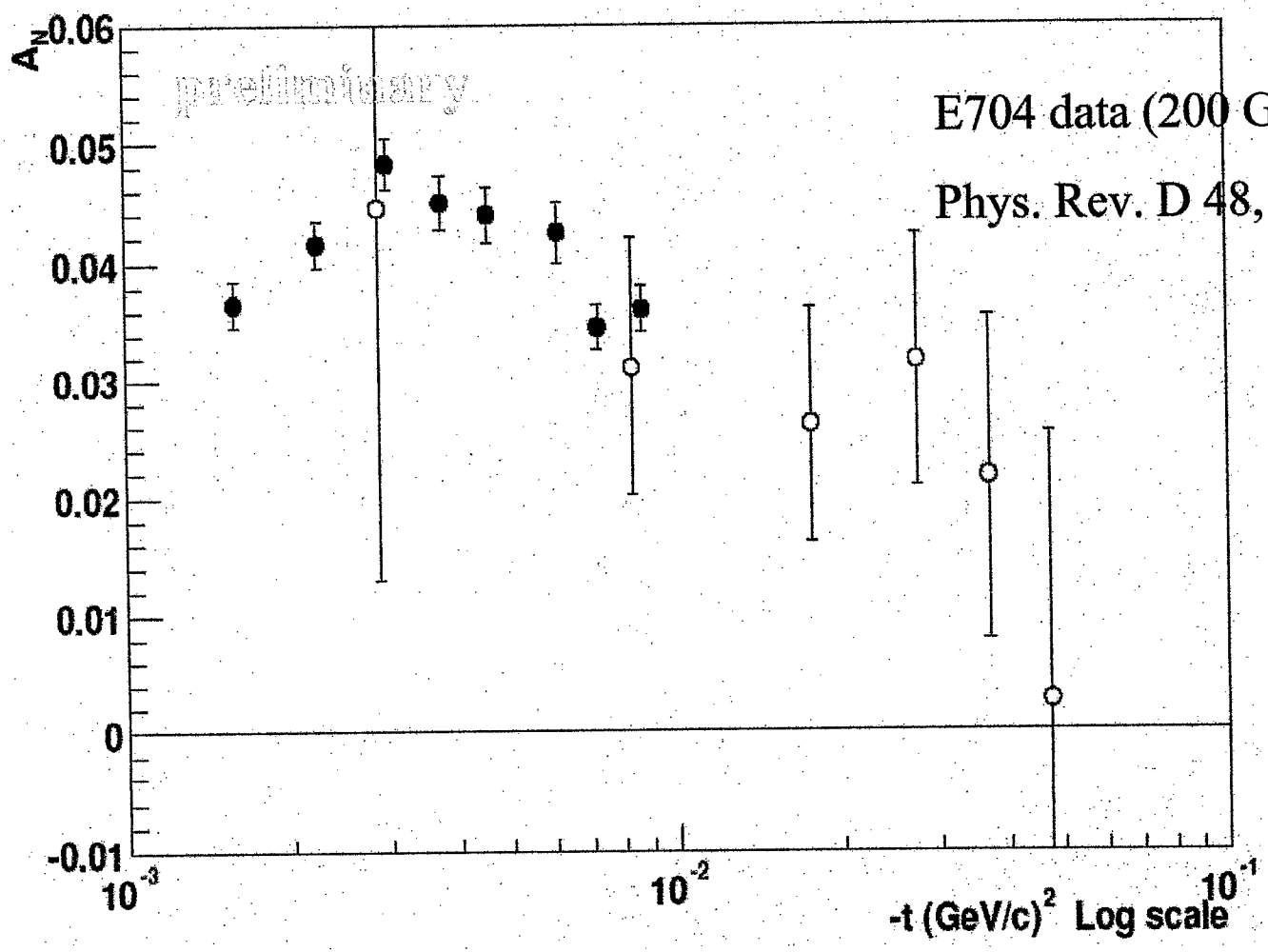

E704 data (200 GeV)

Phys. Rev. D 48, 3026 (1993)

Line color	Re r5	Teoretical function type
blue	0	Non-hadron spin flip δ=0, ρ=0
Green	-0.02	hadron spin flip δ =0.02, ρ =-0.08
red	+0.02	Im r5=0, Im r2=0, Re r2=0

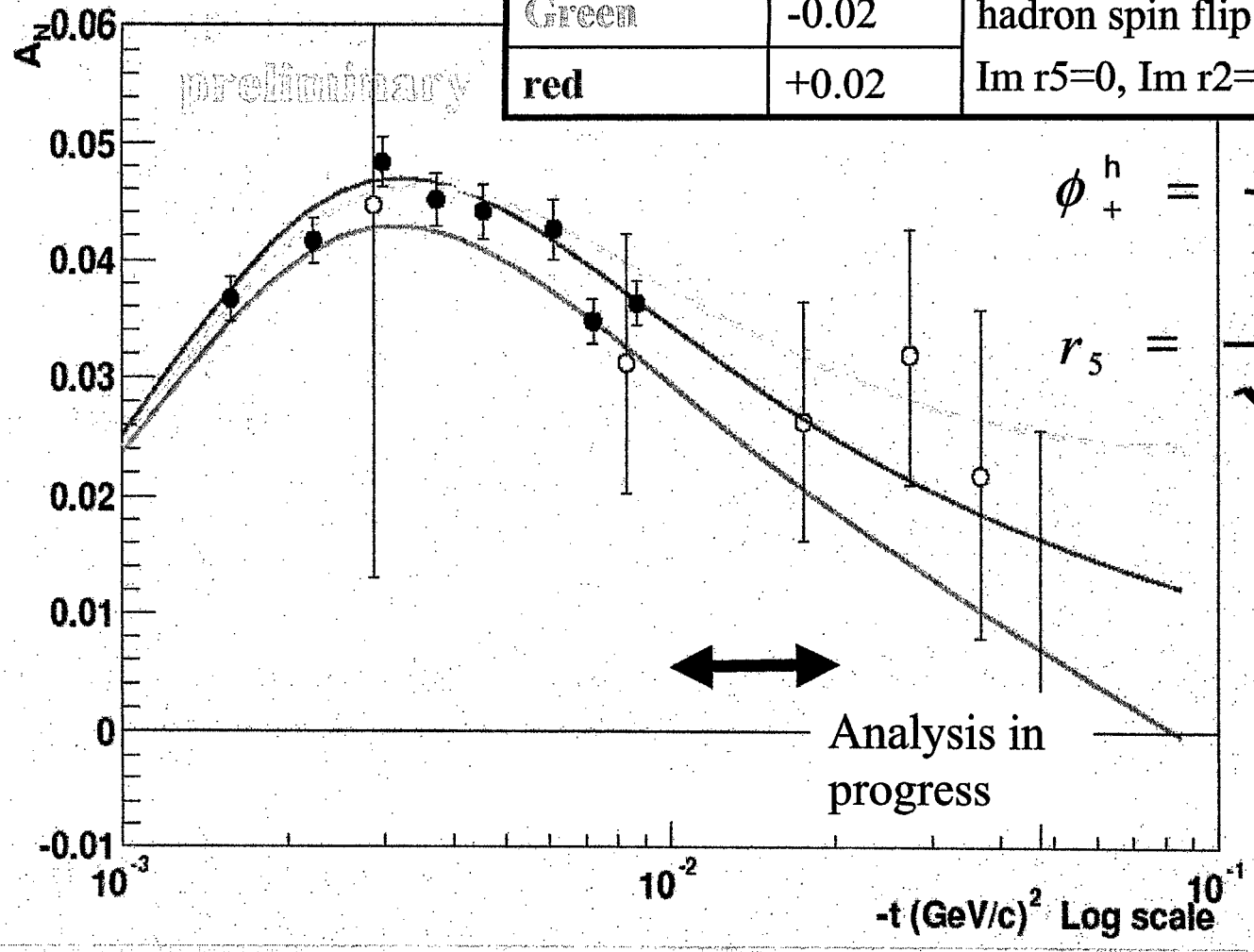

$$\phi_+^h = \frac{1}{2}\left(\phi_1^h + \phi_3^h\right),$$

$$r_5 = \frac{m_p \phi_5^h}{\sqrt{-t}\ \mathrm{Im}\ \phi_+^h}$$

Our results will severely constrain for poorly known r_5

Summary and Outlook

- During RUN4, we collected 1.85M *pp* elastic events of 100GeV beam data
- We have clear A_N peak shape of |t| from 0.0015 to 0.010 $(GeV/c)^2$ with a precision better than 0.0025⊕0.0015 for each A_N data point

- A_N analysis high -t ($0.01 < -t < 0.02$)
- A_N analysis of 24GeV blue beam
- A_{NN} analysis
- .....

These analysis results will severely constrain for poorly known ϕ_5

Backup

Asymmetry of prompt region and Am source region

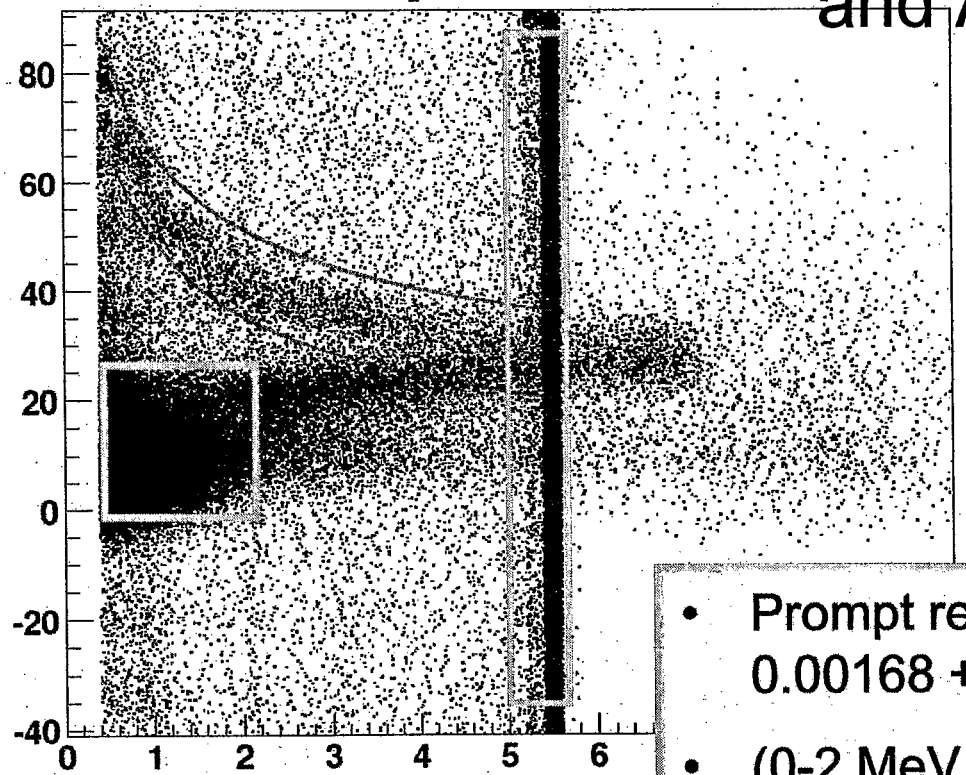

- Prompt region Physics-raw-asymmetry - 0.00168 +/- $1.075*10^{-4}$
- (0-2 MeV Mean=0.72 MeV, 86.5M prompt events in 90RUNs)
- Am region Phys-raw-asymmetry 0.000574 +/- $2.4*10^{-4}$
- (5.0-5.5 MeV Mean=5.25 MeV, 17.1M Am region events in 90RUNs)

Missing Mass M_X^2 @ 100 GeV ONLINE data

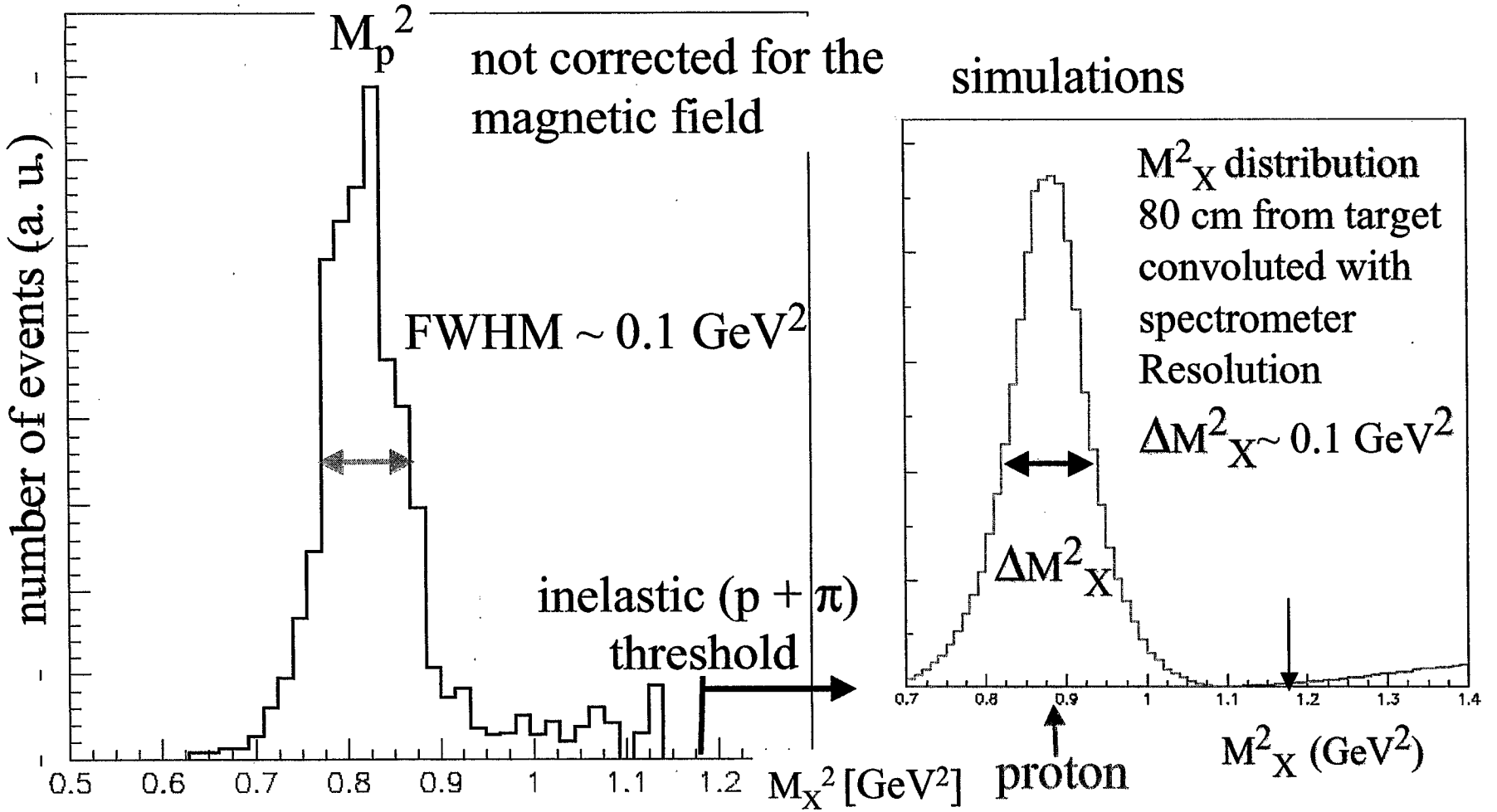

$$M_X^2 = \frac{(\sin\theta_{Xp} - \sin\theta_{el})}{2P_{beam}\sqrt{|t|}} + m_p^2$$

Background

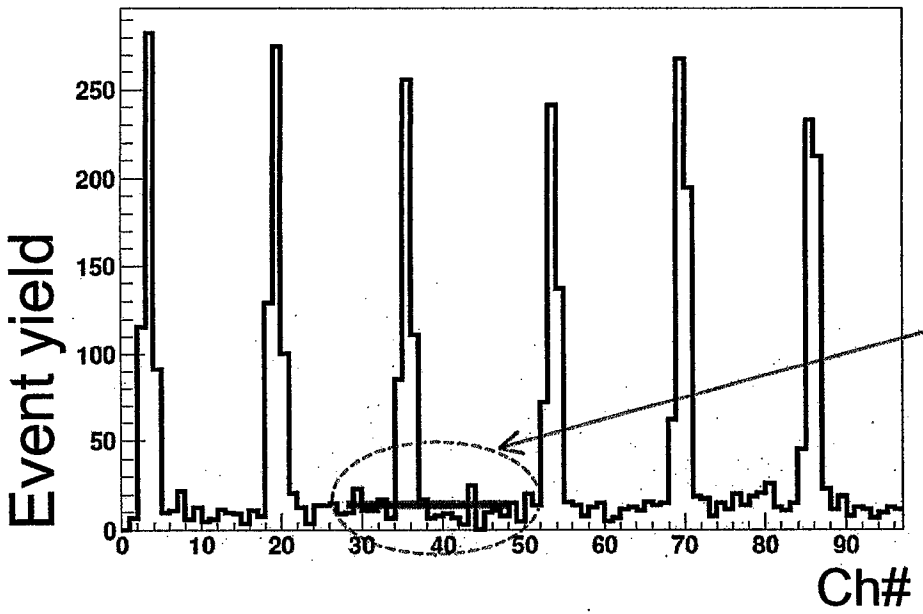

- α source ;2~4% depends on energy and width of energy slice

  →Done

- Beam – gas interactions: at 10^{-9} torr, ~ 10^{7} atoms / cm^{3}

  →Empty target RUN

- Beam – residual jet-target gas interactions

<u>α source correction</u>

$$\varepsilon\left(N_{proton}\right) = \varepsilon\left(N_{proton} + N_{alpha}\right) \cdot \left(1 + \frac{N_{alpha}}{N_{proton}}\right)$$

Measured value Correction factor

- From 90 good RUN (effective target period is 79.4 hour) and "Target+No_beam" 8 RUN, I estimated the ratio of N_{proton} and N_{alpha}

background (cont.)

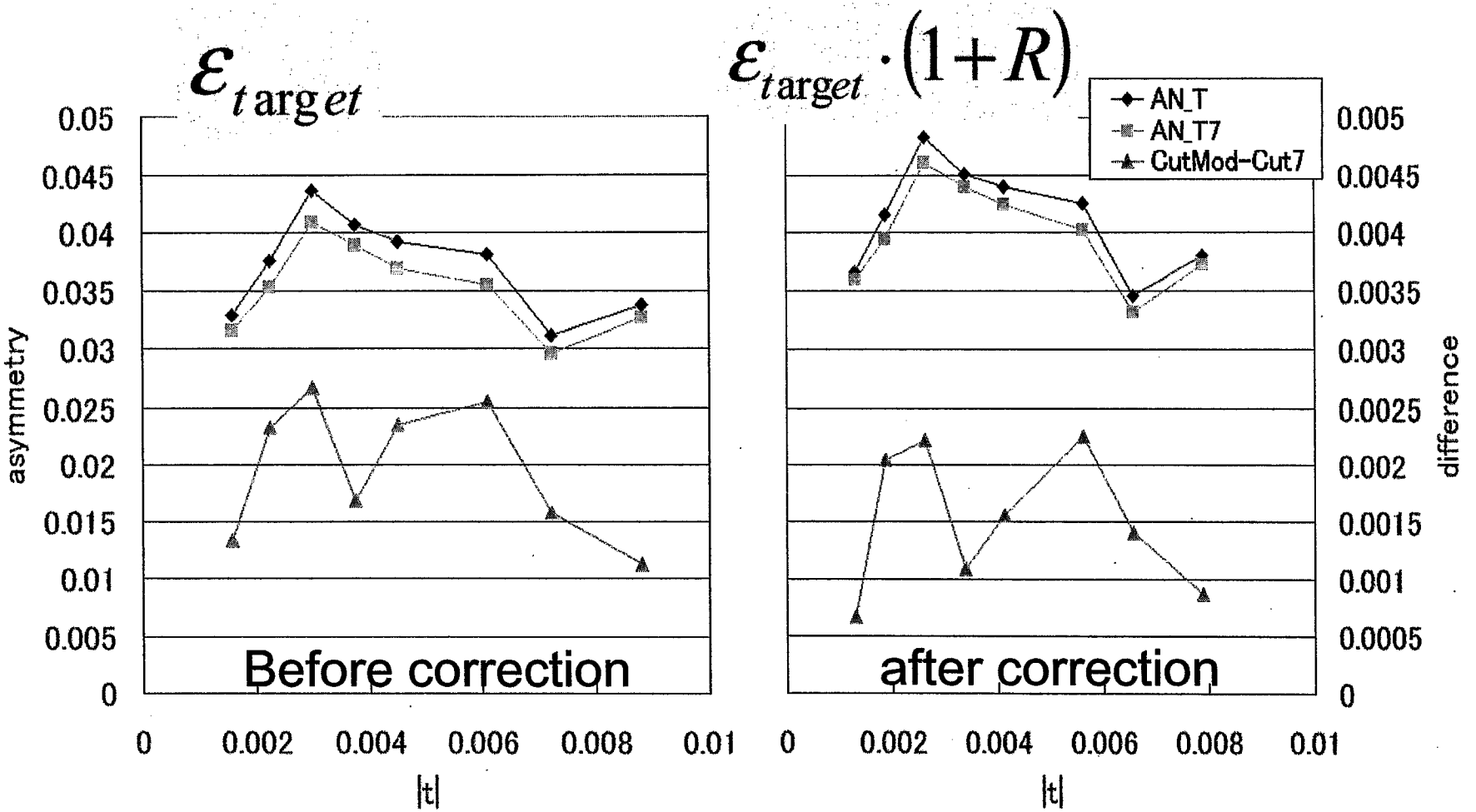

- If we can estimate all bkg correctly, cutMod and Cut7 result should be same
- The remaining discrepancy → "systematic" error

Photos

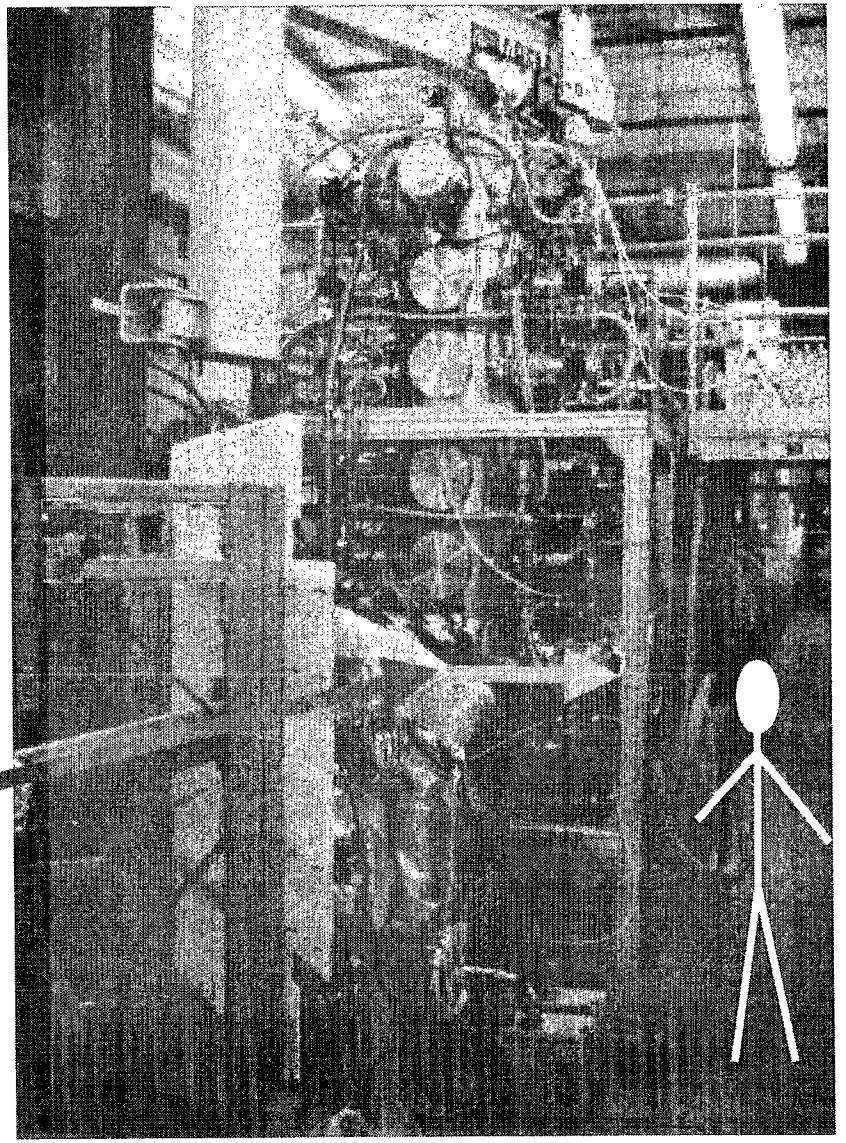

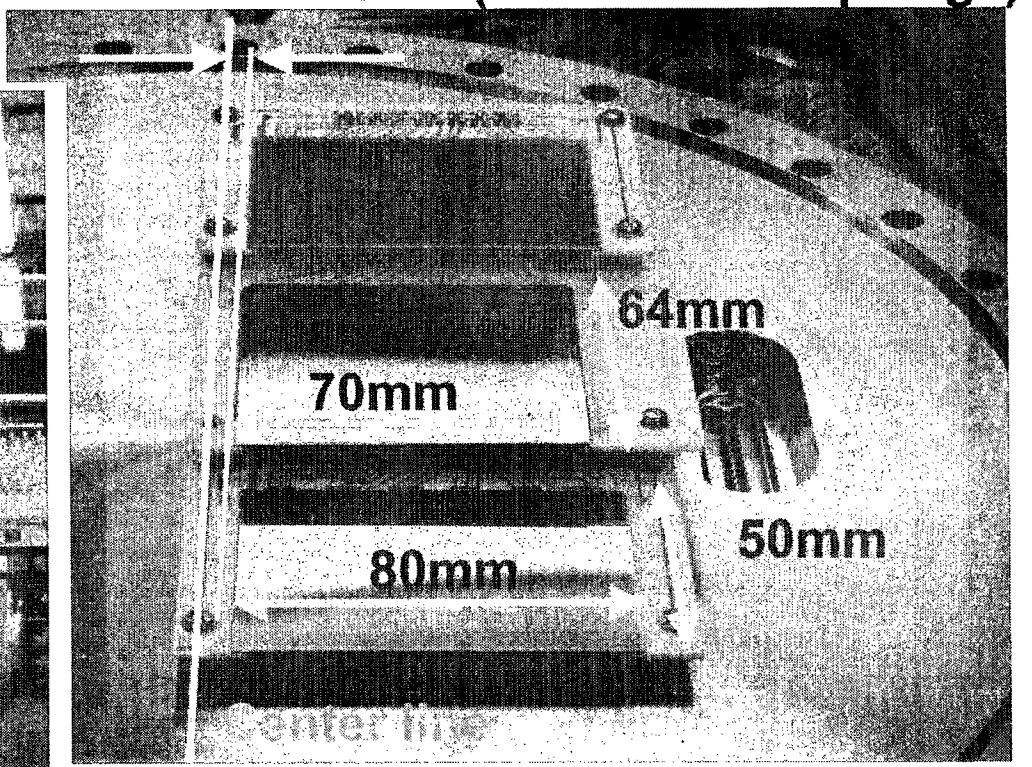

1ch ~4mm ; thickness 400 , 500[μm]

Operation voltage 200 [V], 160 [V]

Depletion capacitance ~80[pF]/ch
Leak current
- BNL 5-10nA /ch
- HAMAMATSU 1-10pA /ch

waveform data

Yellow beam anti-cogged

Amplitude

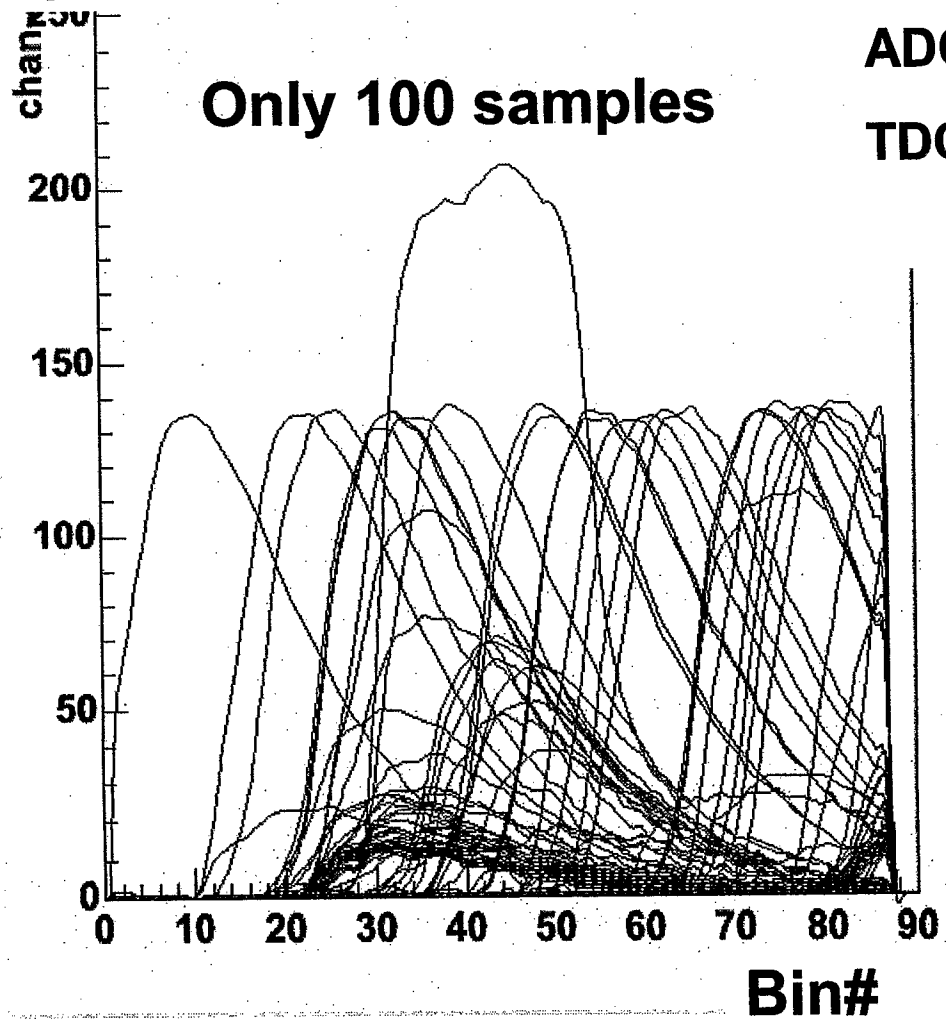

ADC=Maximum amplitude

TDC=1/4 timing of MAX bin# * 2

(TDC 1ch~1.2ns)

TDC

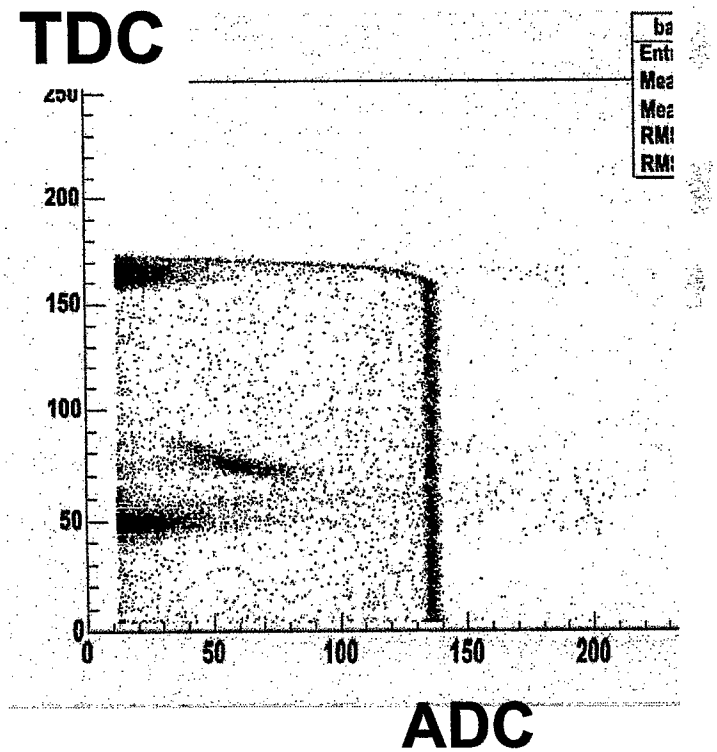

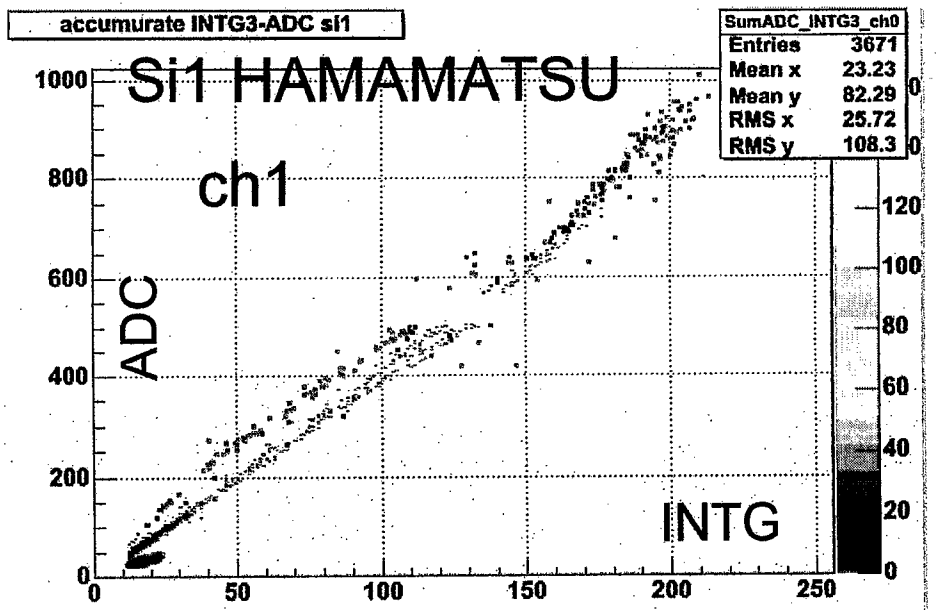

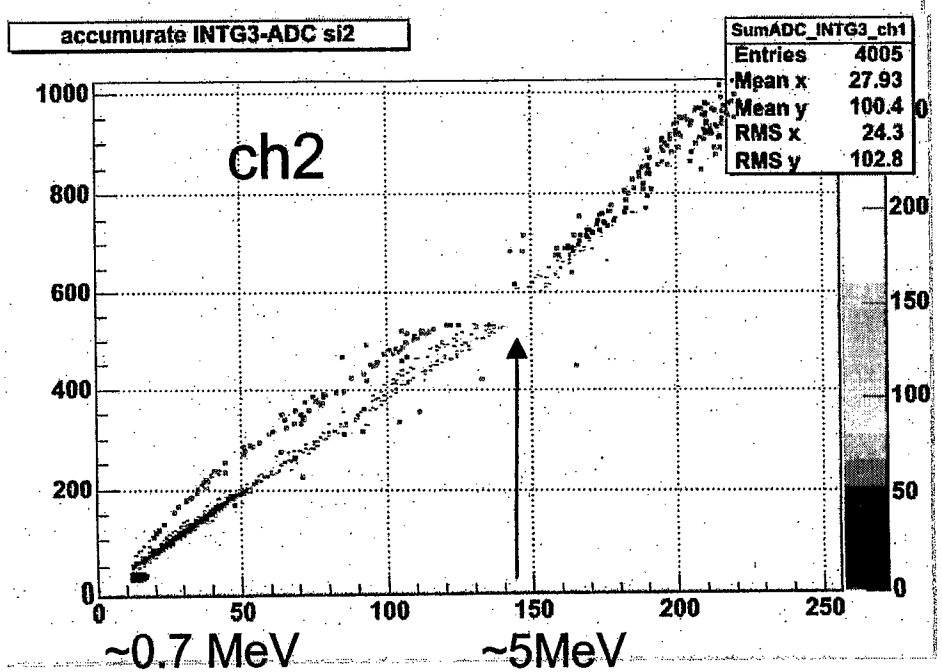

Bad Waveform rejection

By waveform fitting, we can separate good and bad waveform events (up to ~5MeV)

Rainbow color ; chi^2/ndf < 5

Black ; 5<= chi^2/ndf <10

Red ; 10<chi^2/ndf

- INTG-ADC correlation plots per channel
- Only BANANA region ; tof <15
- Bad waveform events come from mainly source fractions
- Bad waveform ratio increase by energy (up to ~5MeV)
- More than 5MeV, waveform shape is not same as lower energy one

$$A_N = \frac{\sigma_+ - \sigma_-}{\sigma_+ + \sigma_-}$$

A_N definition ;

$$A_{NL} = \frac{\sigma_{L+} - \sigma_{L-}}{\sigma_{L+} + \sigma_{L-}}, A_{NR} = \frac{\sigma_{R+} - \sigma_{R-}}{\sigma_{R+} + \sigma_{R-}}$$

Asymmetries from left and right detector

$$L_+ = N \cdot B_+ \cdot d\Omega_L (1 + P_+ A_{NL})$$
$$L_- = N \cdot B_- \cdot d\Omega_L (1 - P_- A_{NL})$$
$$R_+ = N \cdot B_+ \cdot d\Omega_R (1 - P_+ A_{NR})$$
$$R_- = N \cdot B_- \cdot d\Omega_R (1 + P_- A_{NR})$$

$$\varepsilon_A = \left| \frac{A_{NL} - A_{NR}}{A_{NL} + A_{NR}} \right|$$
$$\varepsilon_\Omega = \left| \frac{d\Omega_L - d\Omega_R}{d\Omega_L + d\Omega_R} \right|$$
$$\varepsilon_B = \left| \frac{B_+ - B_-}{B_+ - B_-} \right|$$
$$\varepsilon_p = \left| \frac{P_+ - P_-}{P_+ + P_-} \right|$$
$$PA_N = \frac{1}{2}(P_+ + P_-) \cdot \frac{1}{2}(A_{NL} + A_{NR})$$

$\varepsilon_A, \varepsilon_\Omega, \varepsilon_P, \varepsilon_B, PA_N$ are small and similar in magnitude

Square root formula

$$L_+ = N \cdot B_+ \cdot d\Omega_L (1 + P_+ A_{NL})$$
$$L_- = N \cdot B_- \cdot d\Omega_L (1 - P_- A_{NL})$$
$$R_+ = N \cdot B_+ \cdot d\Omega_R (1 - P_+ A_{NR})$$
$$L_- = N \cdot B_- \cdot d\Omega_R (1 + P_- A_{NR})$$

By use of this formula, we can cancel out the effect of ε and PA term up to the second order !

B_+, B_-; beam intensity

P_+, P_-; beam polarization

$d\Omega_L$, $d\Omega_R$; detector solid angle

$$\varepsilon = \frac{\sqrt{N_{L+} \cdot N_{R-}} - \sqrt{N_{L-} \cdot N_{R+}}}{\sqrt{N_{L+} \cdot N_{R-}} + \sqrt{N_{L-} \cdot N_{R+}}}$$
$$= PA_N \cdot \left[1 - 2\varepsilon_A \varepsilon_P (PA_N) + \left(\varepsilon_A{}^2 + \varepsilon_P{}^2\right)(PA_N)^2 + order(\varepsilon^5)\right]$$
$$\cong PA_N$$

$$\therefore A_N \cong \frac{1}{P} \frac{\sqrt{N_{L+} \cdot N_{R-}} - \sqrt{N_{L-} \cdot N_{R+}}}{\sqrt{N_{L+} \cdot N_{R-}} + \sqrt{N_{L-} \cdot N_{R+}}}$$

$$\left(\begin{array}{l} P = \frac{1}{2}(P_+ + P_-) \\ A_N = \frac{1}{2}(A_{NL} + A_{NR}) \end{array} \right)$$

PP2PP

SPIN-2004

Measurement A_N in the elastic pp-scattering with small momenta transferred at $\sqrt{s}$=200 GeV at RHIC.

I.G. Alekseev for pp2pp Collaboration

S. Bűeltmann, I. H. Chiang, B. Chrien, A. Drees, R. Gill, W. Guryn*, D. Lynn, J. Landgraf, T.A. Ljubičič, C. Pearson, P. Pile, A. Rusek, M. Sakitt, S. Tepikian, K. Yip: *Brookhaven National Laboratory, USA*

J. Chwastowski, B. Pawlik: *Institute of Nuclear Physics, Cracow, Poland*

M. Haguenauer: *Ecole Polytechnique/IN2P3-CNRS, Palaiseau, France*

A. A. Bogdanov, S.B. Nurushev, M.F Runtzo, M.N.Strikhanov: *Moscow Engineering Physics Institute (MEPHI), Moscow, Russia*

I. G. Alekseev, V. P. Kanavets, L.I. Koroleva, B. V. Morozov, D. N. Svirida: *ITEP, Moscow, Russia*

A.Khodinov, M. Rijssenbeek, L. Whithead: *SUNY Stony Brook, USA*

K. De, J. Li, N. Őztűrk: *University of Texas at Arlington, USA*

A. Sandacz: *Institute for Nuclear Studies, Warsaw, Poland*

*spokesperson

PP2PP

Main goal

SPIN-2004

Measurement of pp elastic scattering in collider regime with UNIQUE capability due to polarized proton beams.

Kinematical range: $50 < \sqrt{s} < 500$ GeV, $4 \times 10^{-4} < |t| < 1.3$ GeV^2

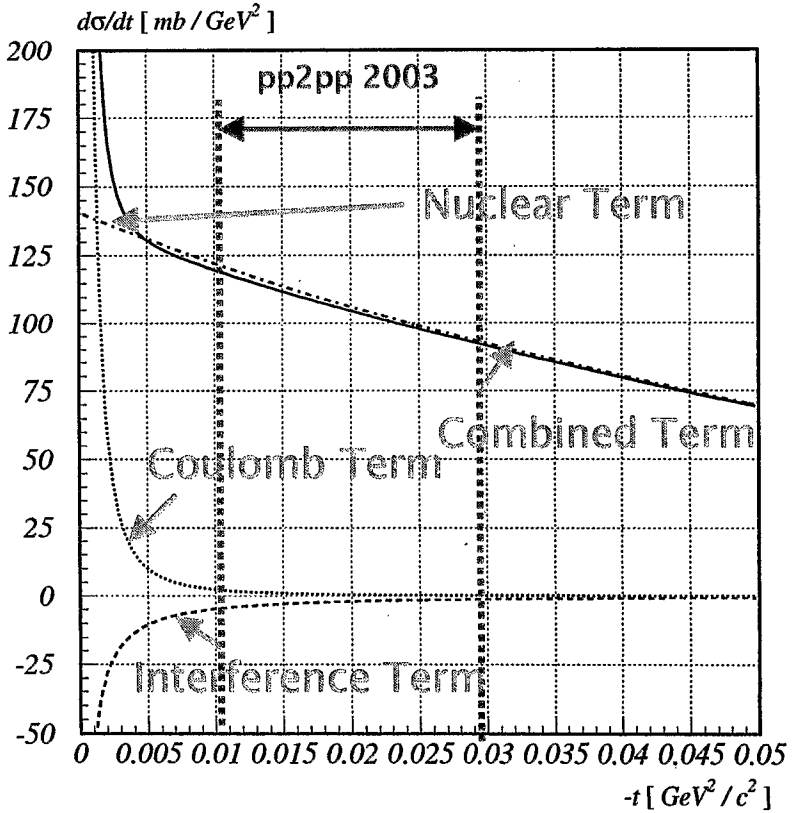

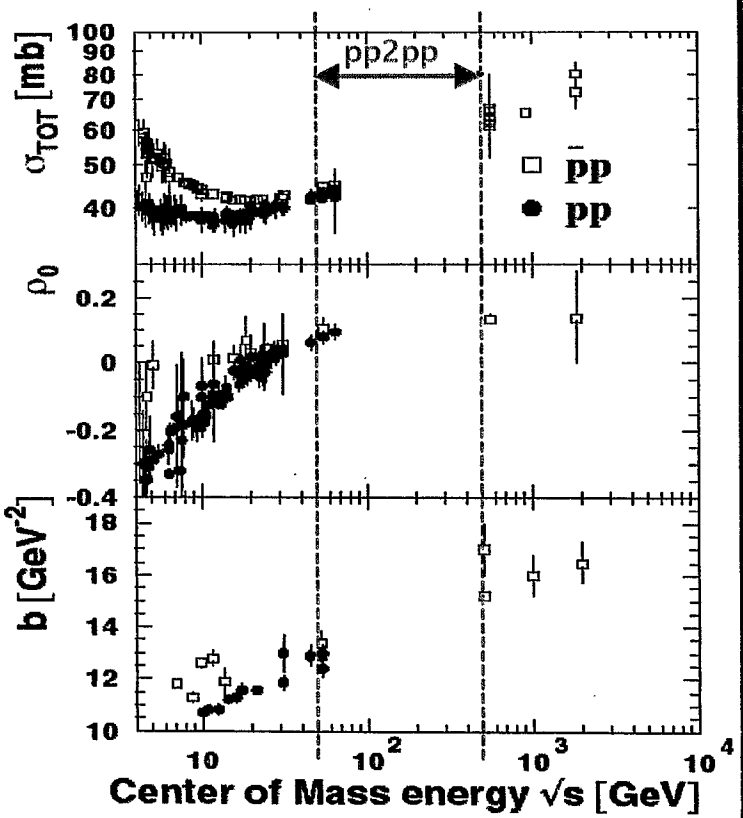

PP2PP

Formulas

SPIN-2004

$$\frac{d\sigma}{dt} = \frac{4\pi(\alpha G_E^2)^2}{t^2} + \frac{(1+\rho^2)\sigma_{tot}{}^2 e^{bt}}{16\pi} + \frac{(\rho+\Delta\Phi)\alpha G_E^2 \sigma_{tot} e^{\frac{bt}{2}}}{t}$$

Coulomb interaction	Hadronic interaction	Interference term
$\lvert t \rvert < 10^{-3}$ GeV^2	$5 \cdot 10^{-3} \le \lvert t \rvert \le 1$ GeV^2	(CNI)

Helicity amplitudes:

$\Phi \infty \langle h_3 h_4 | M(s,t) | h_1 h_2 \rangle$, where h_i – s- channel helicity of proton i

$\Phi_1 \infty \langle ++ | M | ++ \rangle$ no helicity flip, $\Phi_2 \infty \langle -- | M | ++ \rangle$ double helicity flip

$\Phi_3 \infty \langle +- | M | +- \rangle$ no helicity flip, $\Phi_4 \infty \langle +- | M | -+ \rangle$ double helicity flip

$\Phi_5 \infty \langle ++ | M | +- \rangle$ single helicity flip,

Frequently used: $\Phi_+ = (\Phi_1 + \Phi_3)/2$, $\Phi_- = (\Phi_1 - \Phi_3)/2$

$$\frac{d\sigma}{dt} = \frac{2p}{s^2}(|\Phi_1|^2 + |\Phi_2|^2 + |\Phi_3|^2 + |\Phi_4|^2 + 4|\Phi_5|^2)$$

$$A_N \equiv \frac{N_\uparrow - N_\downarrow}{N_\uparrow + N_\downarrow} \approx \frac{2\,\mathrm{Im}\,\Phi_+\Phi_5^*}{d\sigma/dt}, \quad A_{NN} \equiv \frac{N_{\uparrow\uparrow} + N_{\downarrow\downarrow} - N_{\uparrow\downarrow} - N_{\downarrow\uparrow}}{N_{\uparrow\uparrow} + N_{\downarrow\downarrow} + N_{\uparrow\downarrow} + N_{\downarrow\uparrow}} \approx \frac{2\,\mathrm{Re}\,\Phi_+\Phi_2^*}{d\sigma/dt}$$

PP2PP

Spin physics

SPIN-2004

N.H. Buttimore,
B.Z. Kopeliovich,
E. Leader, J. Soffer,
T.L. Trueman,
"The Spin Dependence of High-Energy Proton Scattering",
PR D59 114010 (1999)

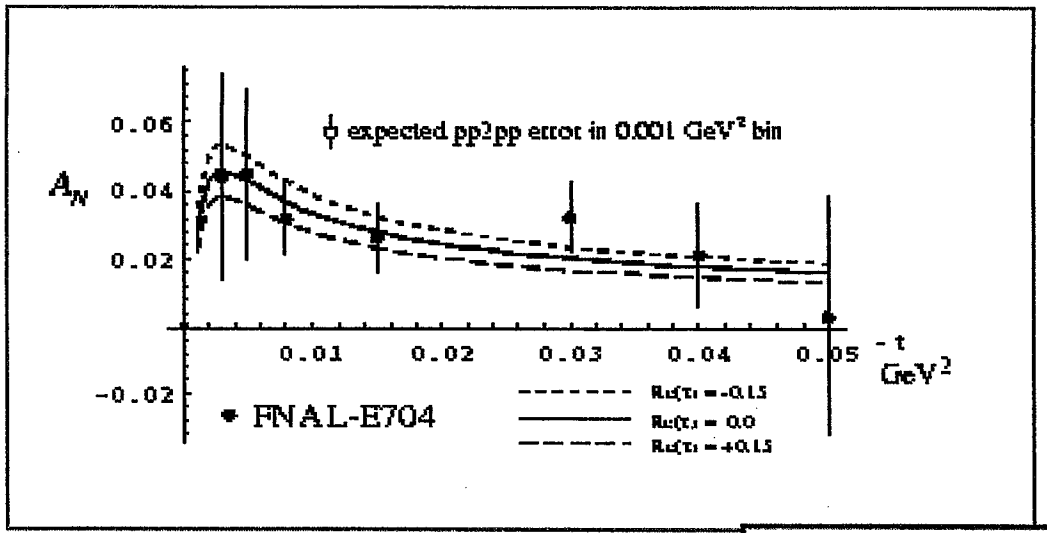

E.Leader, T.L.Trueman
"The Odderon and spin dependence of high-energy proton-proton scattering",
PR D61, 077504 (2000)

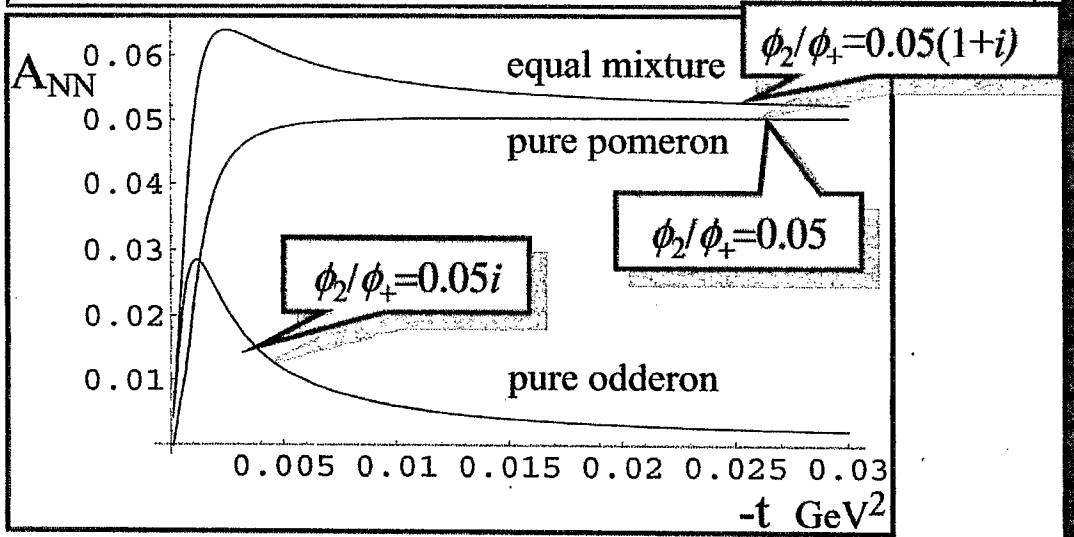

The AGS-RHIC complex

PP2PP

SPIN-2004

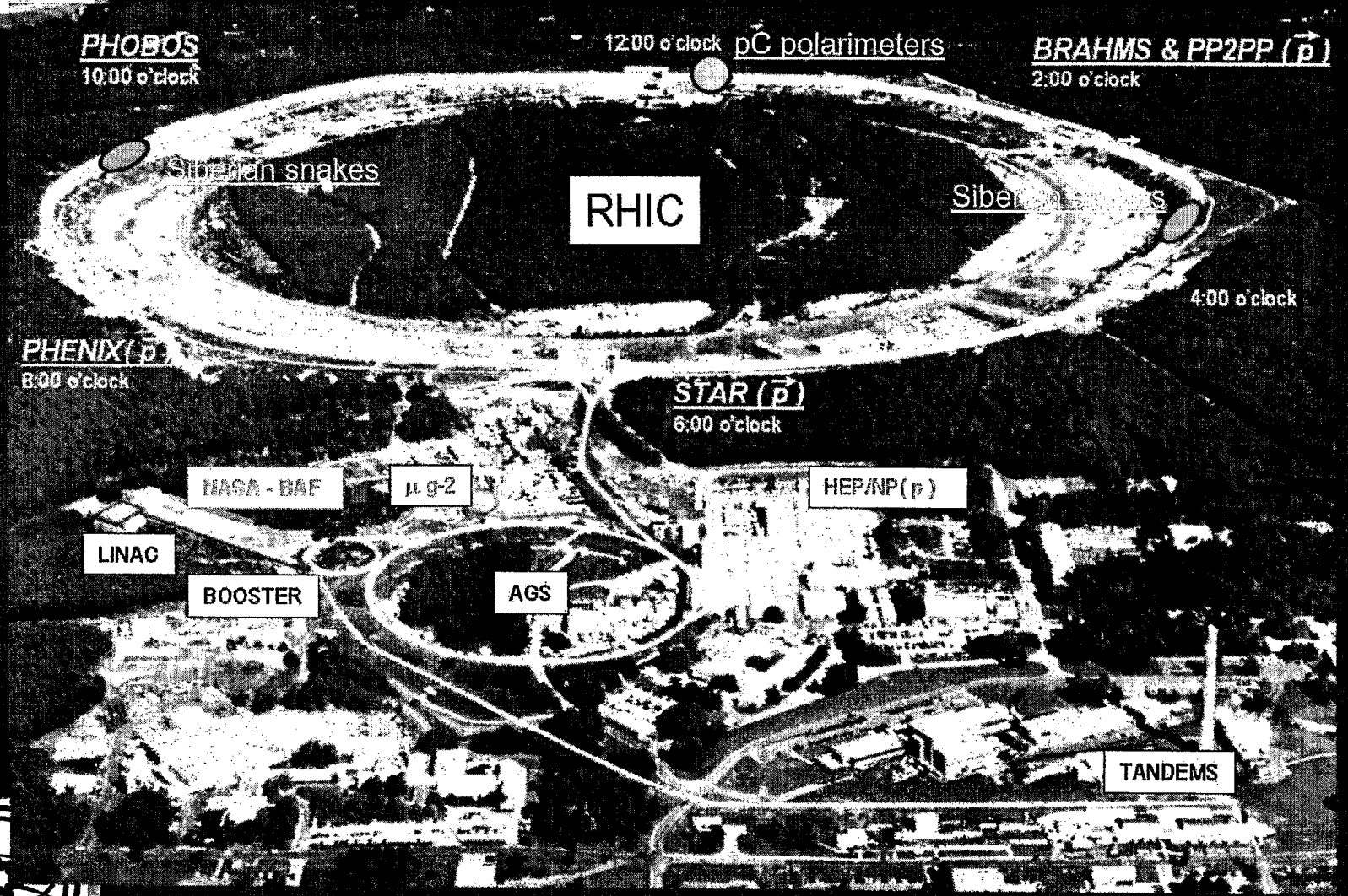

PP2PP

Experimental Idea

SPIN-2004

- MAIN IDEA
  - In colliding beam mode scattered proton follow trajectories determined by LATTICE of the collider because it has the same momentum as a beam proton and scattering angle is small.
  - The coordinates of scattered particles at the detector position with respect to the reference orbit are given by TRANSPORT EQUATION:

$$Y = a_{11}\, y^* + L_{eff}\, \theta^*_y$$

y^* is position of interaction vertex, θ^*_y is scattering angle

- OPTIMUM CONDITION --- " PARALLEL to POINT FOCUSING" :

$$\left.\begin{array}{l} a_{11} \approx 0 \\ L_{eff} \text{ - large} \end{array}\right\} \; y \approx L_{eff}\, \theta^*_y$$

$\beta^*=20m$

	RP1,3 (57m)	RP2,4 (60m)
a_{11}^y	0.156	0.044
L_{eff}^y	27.5m	26.2m
a_{11}^x	0.051	-0.041
L_{eff}^x	30.6	31.3

RHIC Insertion Functions $\beta^*=10m$

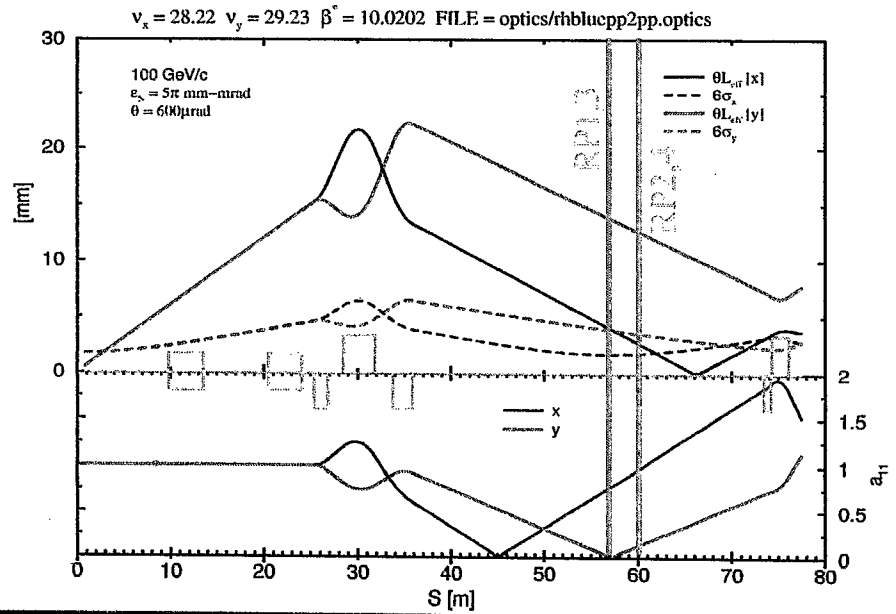

PP2PP

Experimental Setup

SPIN-2004

Need special tune of accelerator and detectors approaching the proton beams closely via Roman Pots to measure very small angles of elastically scattered protons

Two pairs of silicon microstrip detectors measuring (x,y) coordinates with 100 μm pitch plus one trigger scintillator per Roman Pot

One Roman Pot above and below the beam for each Roman Pot Station

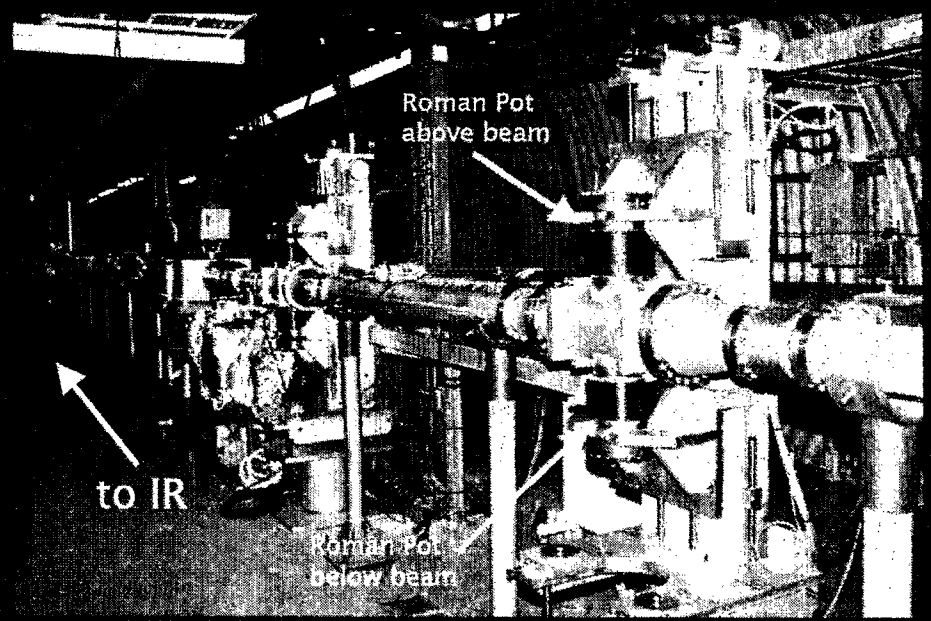

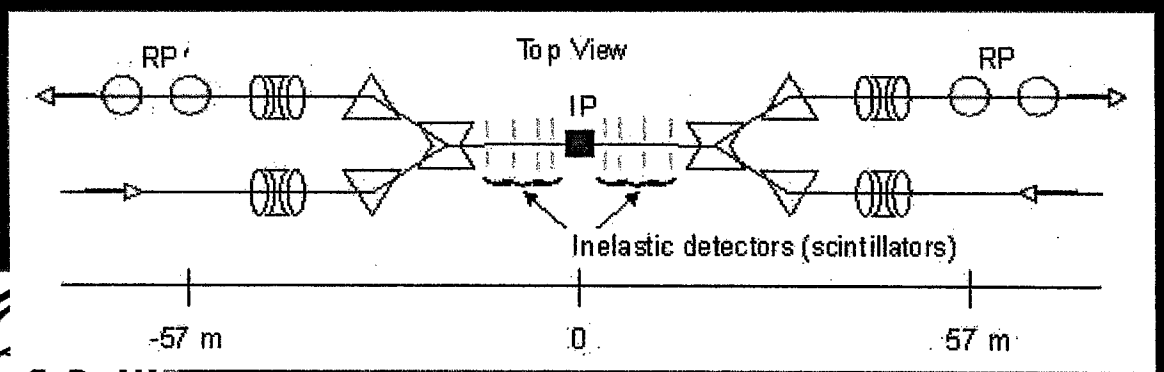

Inelastic Detectors:
Four planes of scintillation counters on either side of Interaction Region (IR) detecting particles from inelastically scattered protons

PP2PP

Si Detector Package

SPIN-2004

- 4 planes of 400 μm Silicon microstrip detectors:
  - 4.5 x 7.5 cm^2 sensitive area
  - good resolution, low occupancy
  - Redundancy: 2X- and 2Y-detectors
  - Closest proximity to the beam ~14 mm
  - 8 mm trigger scintillator with two PMT readout behind Silicon planes
- Run 2003: new Silicon manufactured by Hamamatsu Photonics.

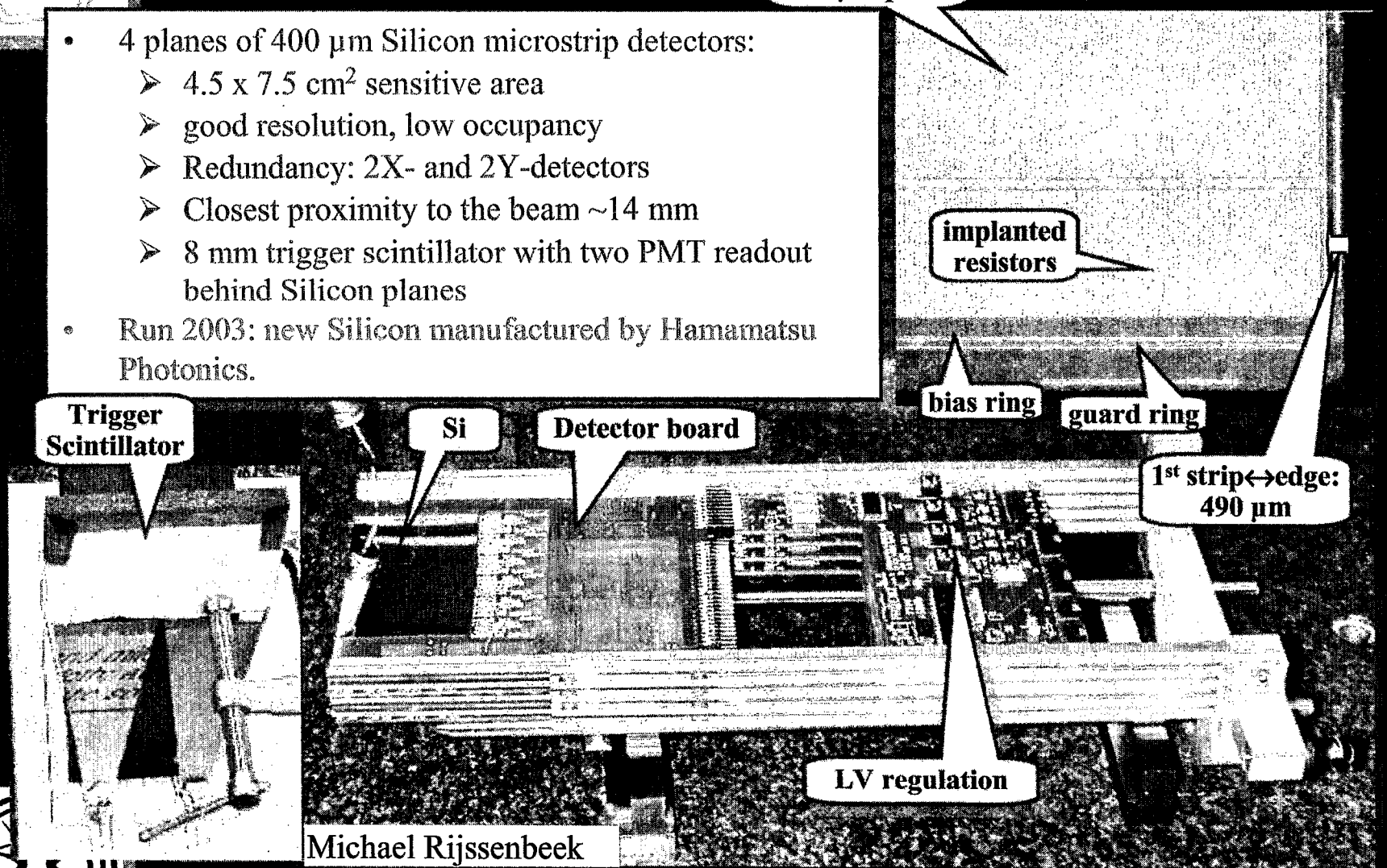

Michael Rijssenbeek

PP2PP

New silicon readout (2003)

SPIN-2004

New 4 channel sequencer to control SVXes was designed for run 2003.

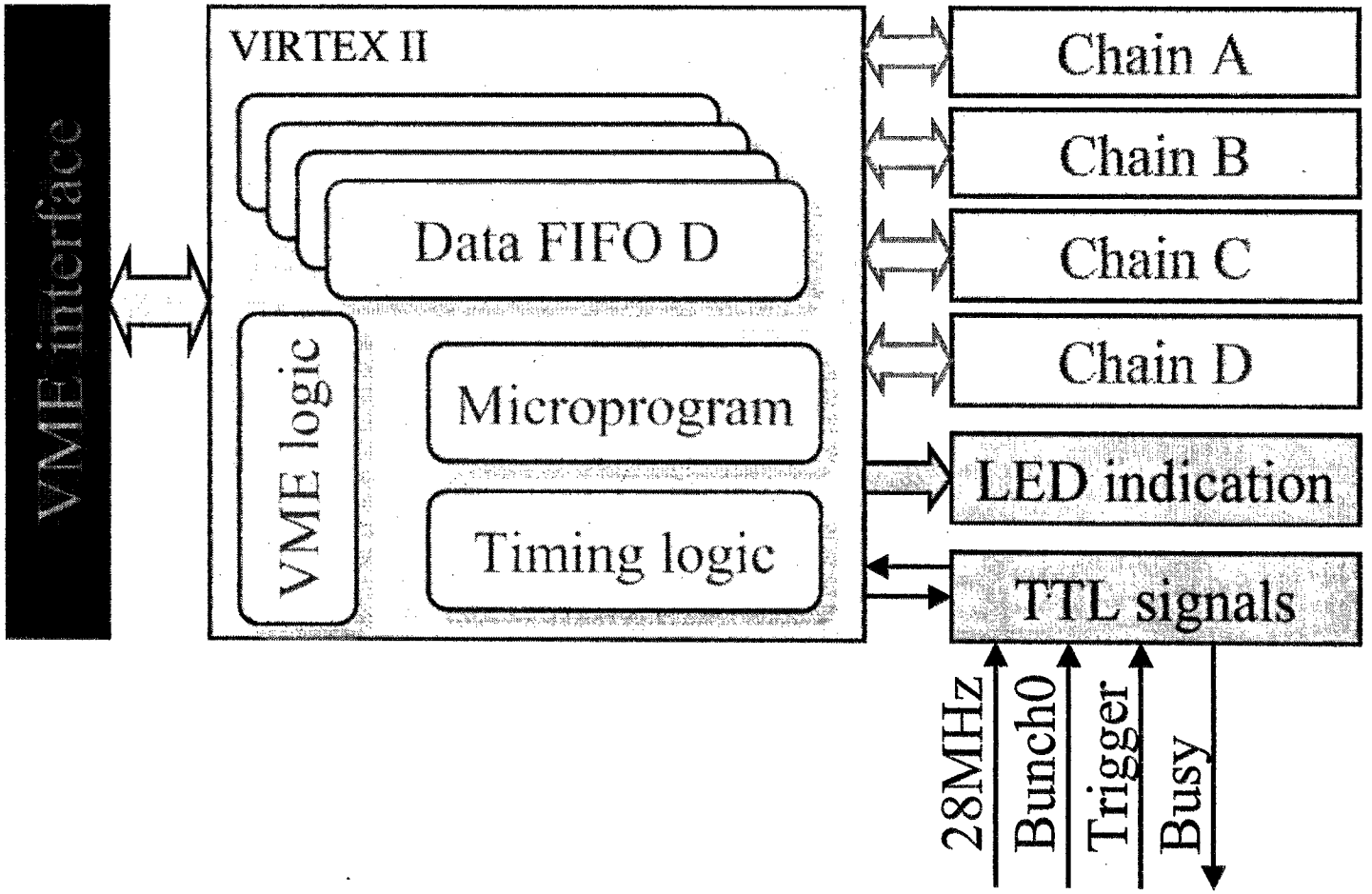

PP2PP

Hit selection

SPIN-2004

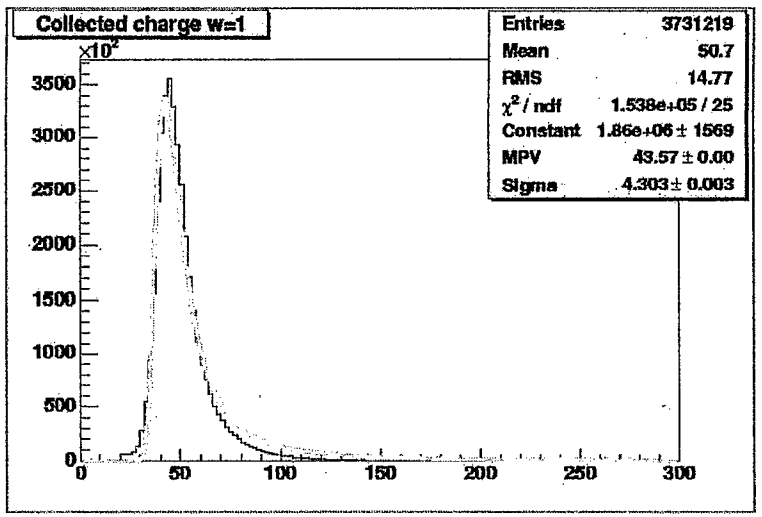

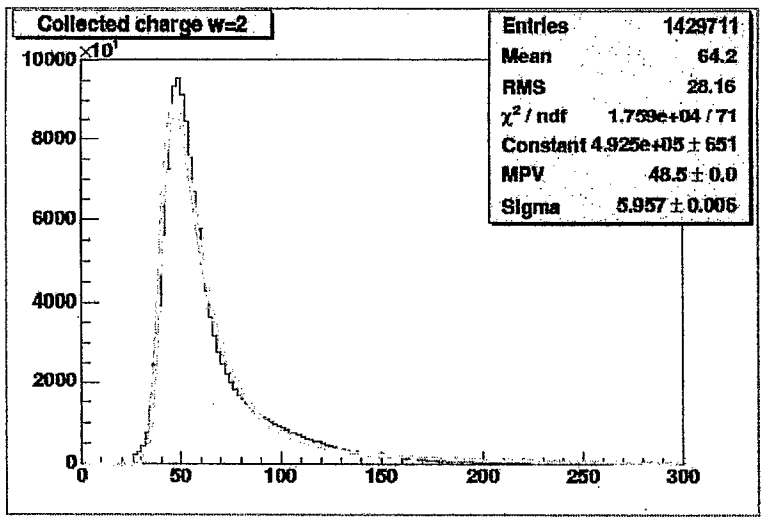

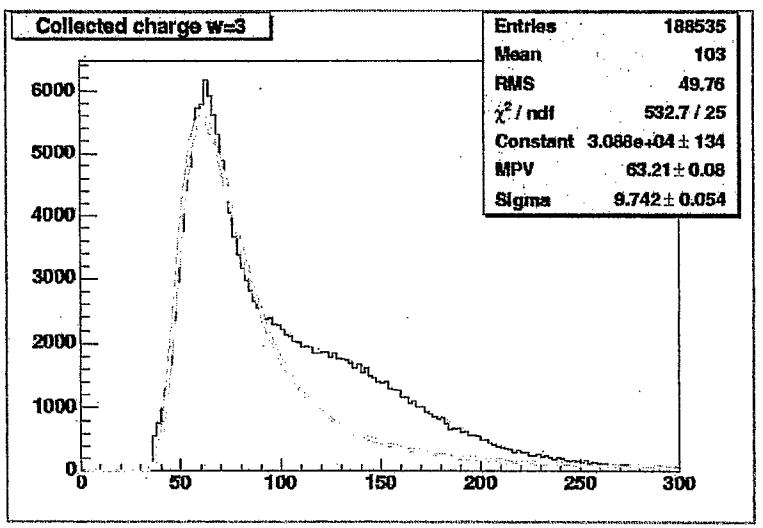

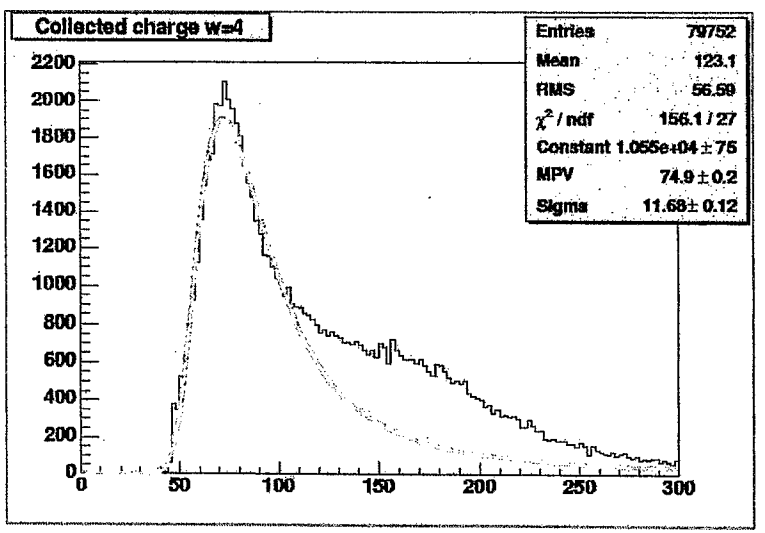

PP2PP

Detector performance

SPIN-2004

- Only 6 dead strips per 14112 active strips
- Average pedestal drift during the run 0.05-0.2
- Pedestal value variation 2.5-3.0
- Very large detectors efficiency

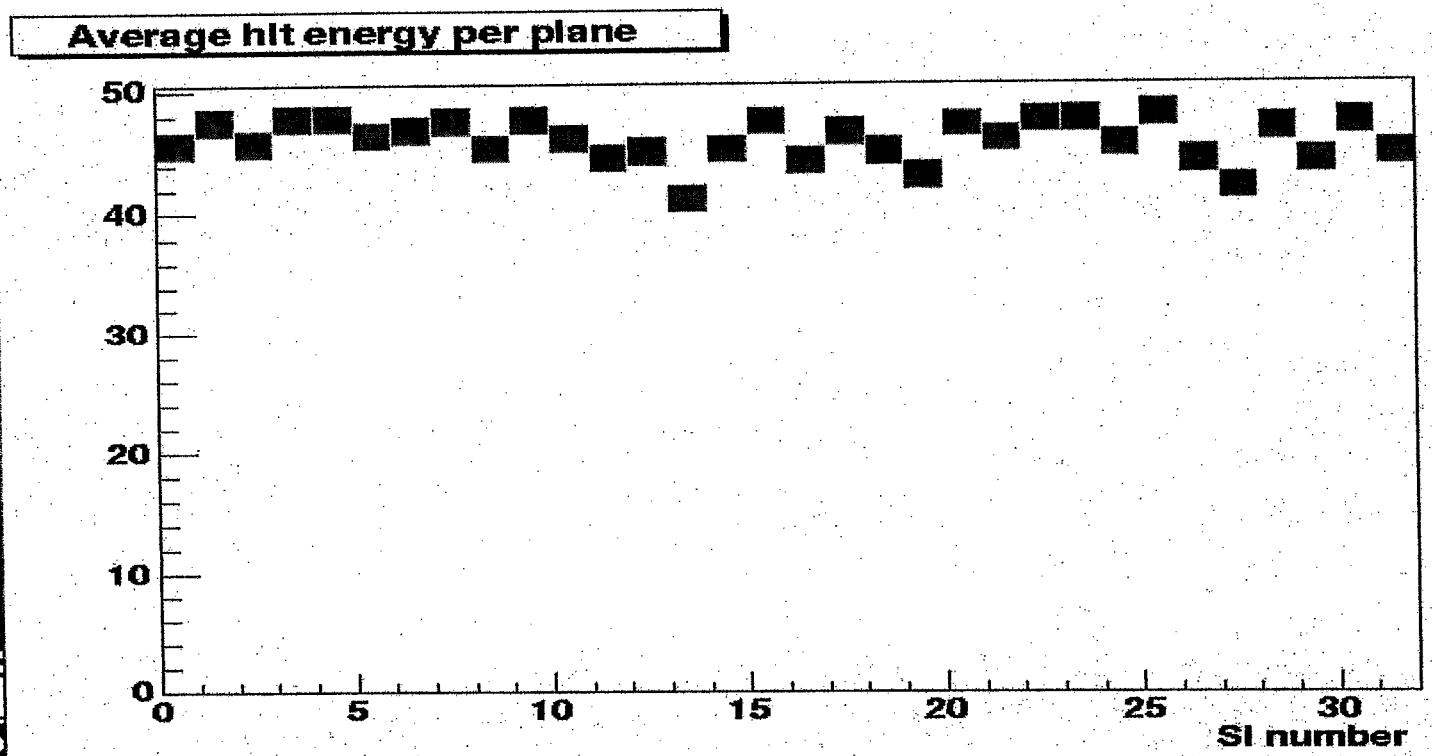

PP2PP

Elastic events selection

SPIN-2004

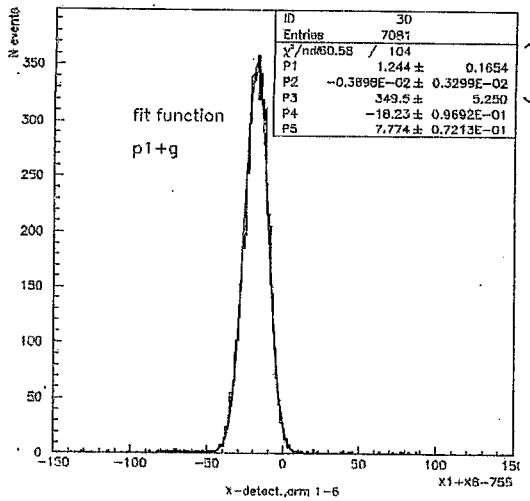

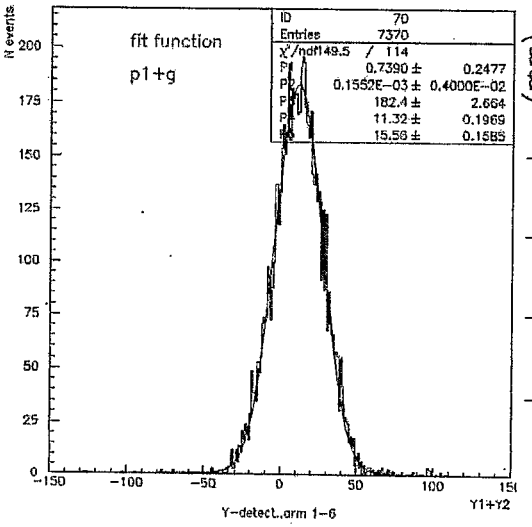

Distribution of hits for elastic events. POS.6

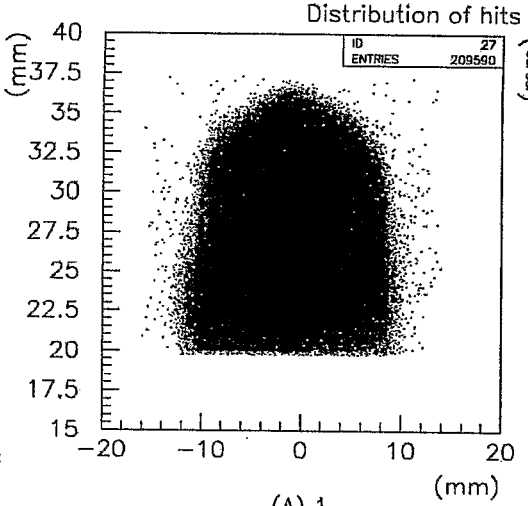

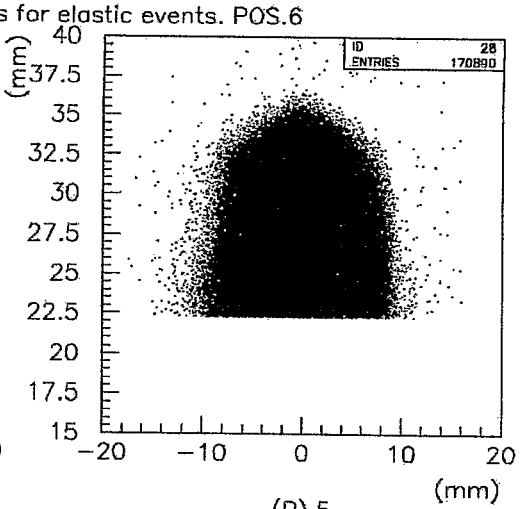

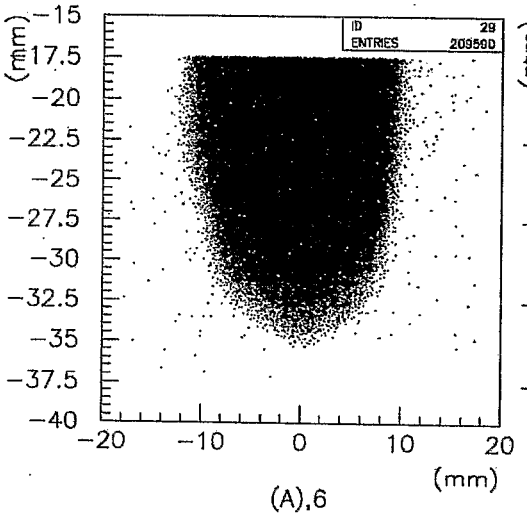

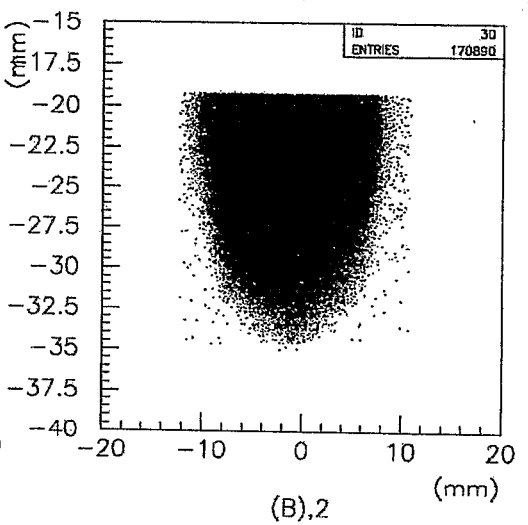

PP2PP

Run summary

SPIN-2004

Beam momentum	100 GeV
Number of bunches	55
β^*	10m
$\lvert t\rvert$*-range*	0.01-0.03 $(GeV/c)^2$
Proton intensity	$19 \cdot 10^{11}$
Proton polarization	P_B=0.36, P_Y=0.32
Number of Roman Pot stations	4
Number of Silicon planes	32
Number of triggers	6688363
Number of elastic triggers	6482751
Number of elastic events	2329177
Arm A	1403890
Arm B	925254

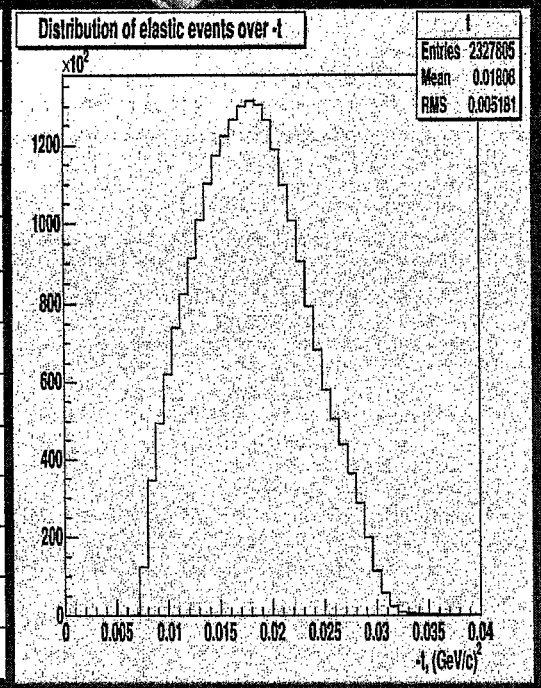

φ - cut

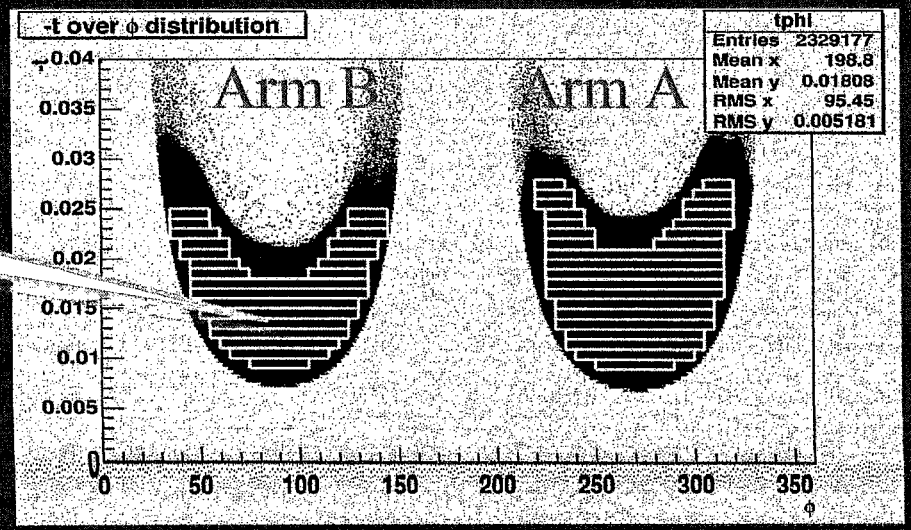

PP2PP

Calculation of asymmetries

SPIN-2004

$$N=C(1+(P_B+P_Y)A_N\cdot\cos(\varphi)+P_BP_YA_{NN}\cdot\cos^2(\varphi))$$

$$F_N(\varphi)=\frac{\sqrt{N^{++}(\varphi)N^{--}(180-\varphi)}-\sqrt{N^{--}(\varphi)N^{++}(180-\varphi)}}{\sqrt{N^{++}(\varphi)N^{--}(180-\varphi)}+\sqrt{N^{--}(\varphi)N^{++}(180-\varphi)}}$$

$$F_N(\varphi)=(|P_B|+|P_Y|)A_N\cdot\cos(\varphi)/(1+|P_B|\cdot|P_Y|\cdot A_{NN}\cdot\cos^2(\varphi))$$

Here N^{ij} are UNNORMALIZED counts,

$$|P_B|\cdot|P_Y|\cdot A_{NN}\cdot\cos^2(\varphi)<0.015$$

$$F_{NN}(\varphi)=\frac{(N^{++}(\varphi)+N^{--}(\varphi))-(N^{+-}(\varphi)+N^{-+}(\varphi))}{(N^{++}(\varphi)+N^{--}(\varphi))+(N^{+-}(\varphi)+N^{-+}(\varphi))}$$

where $N^{ij}(\varphi)=K^{ij}(\varphi)+K^{ij}(180-\varphi)+K^{ij}(180+\varphi)+K^{ij}(360-\varphi)$ and K^{ij} are counts NORMALIZED to the ij-polarization combination luminosity.

$$F_{NN}(\varphi)=\frac{C_x+|P_B|\cdot|P_Y|A_{NN}\cos^2(\varphi)}{1+C_x\cdot|P_B|\cdot|P_Y|A_{NN}\cos^2(\varphi)}$$

and C_X is unknown parameter, describing error in the normalization

PP2PP

Single spin asymmetry A_N

SPIN-2004

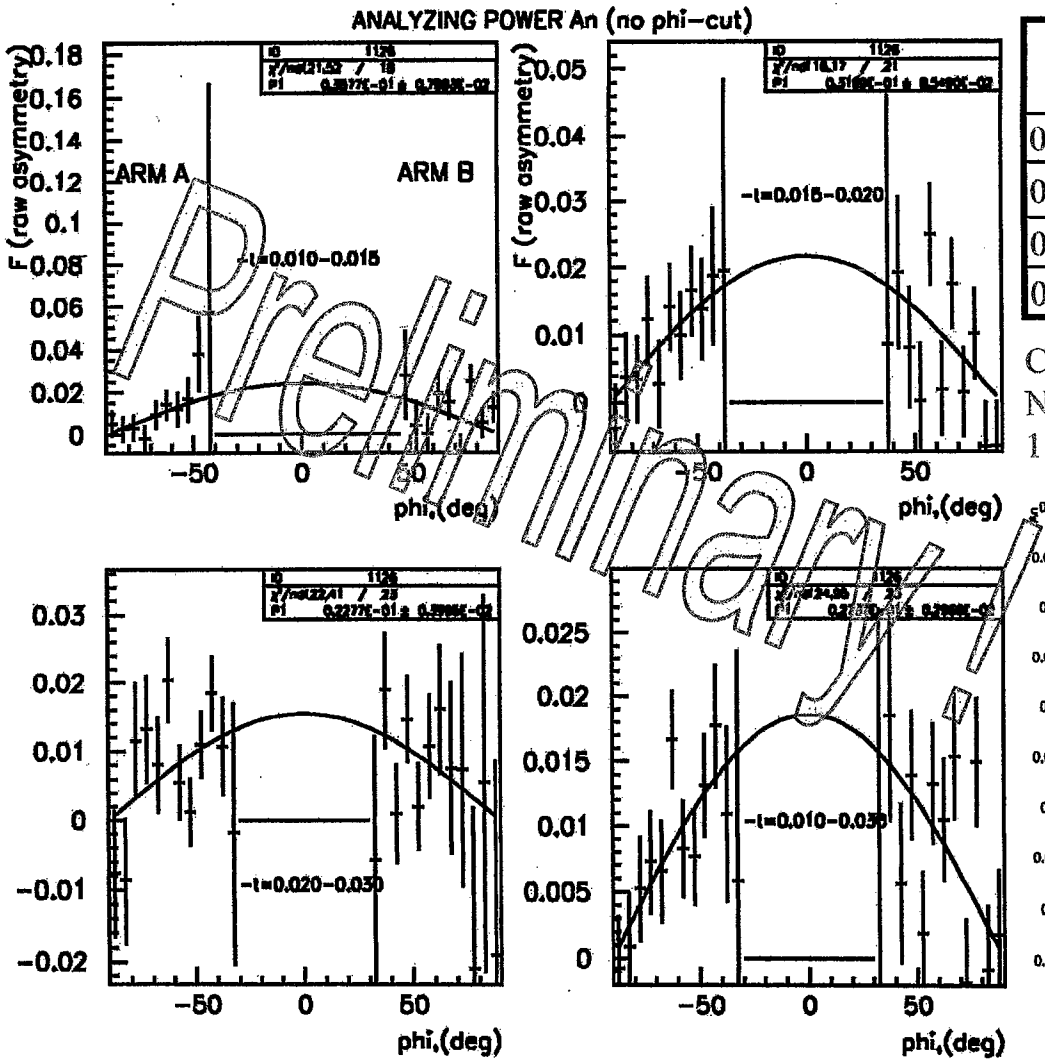

$\|t\|$-range, $(GeV/c)^2$	$\langle\|t\|\rangle$, $(GeV/c)^2$	A_N
0.010-0.015	0.013	0.036±0.008
0.015-0.020	0.018	0.032±0.006
0.020-0.030	0.024	0.023±0.004
0.010-0.030	0.020	0.027±0.003

CNI curve (no hadronic spin-flip)
N.H. Buttimore *et al.* PRD 59, 114010 (1999)

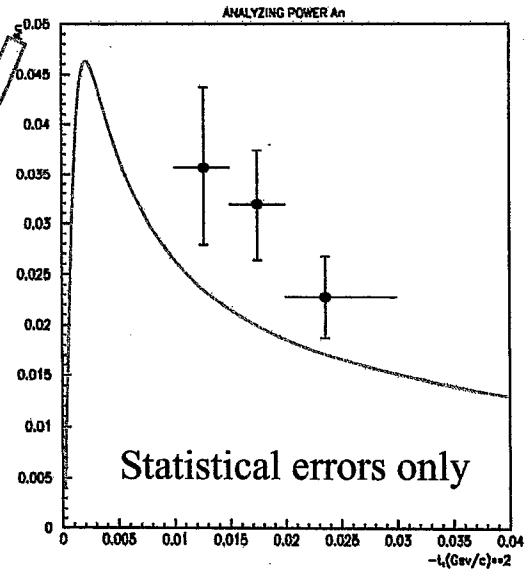

PP2PP

Normalization

SPIN-2004

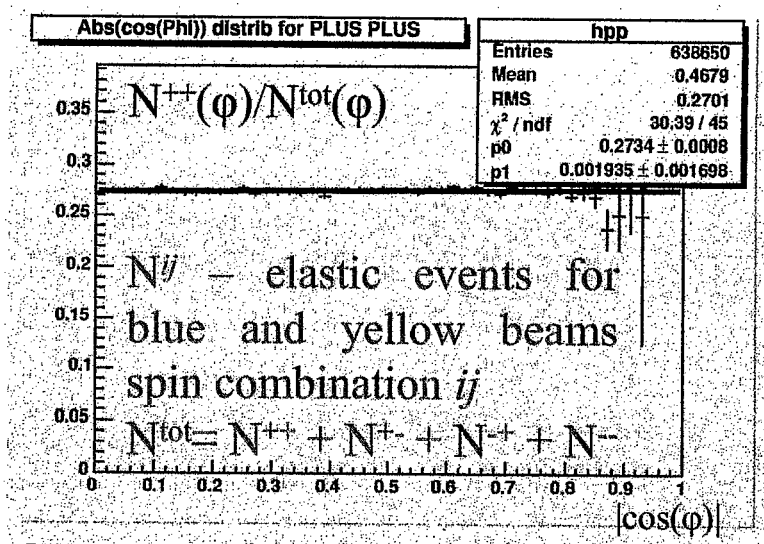

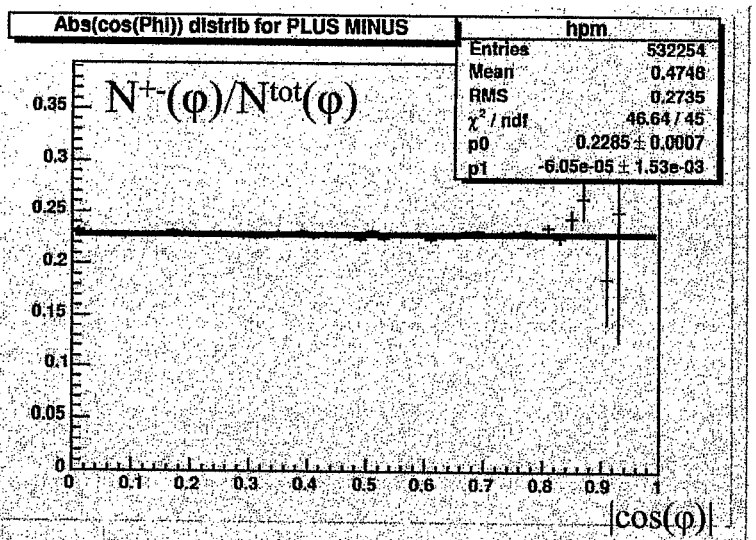

N^{ij} – elastic events for blue and yellow beams spin combination *ij*

$N^{tot} = N^{++} + N^{+-} + N^{-+} + N^{--}$

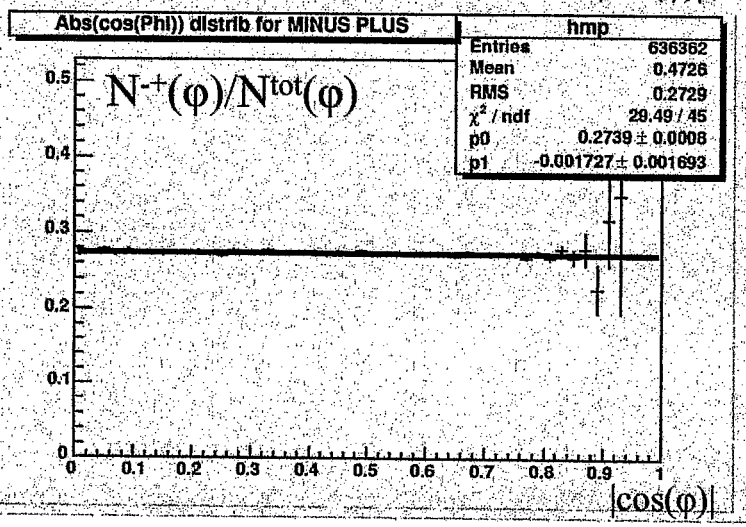

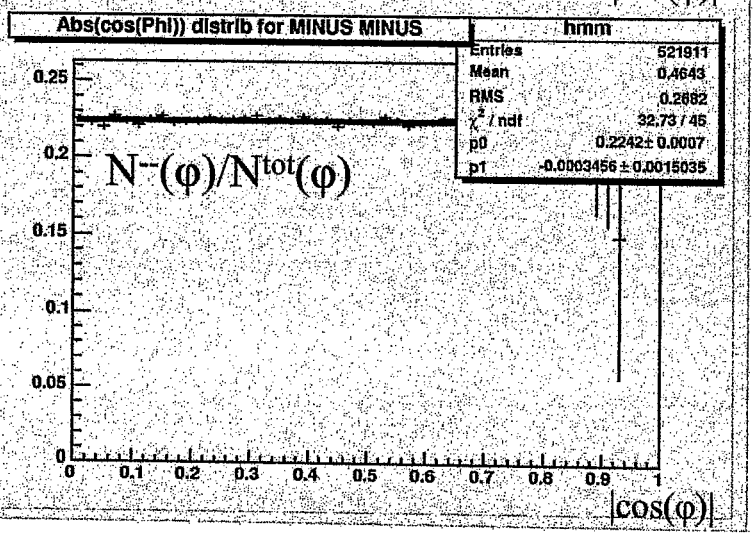

PP2PP

Double spin asymmetry A_{NN}

SPIN-2004

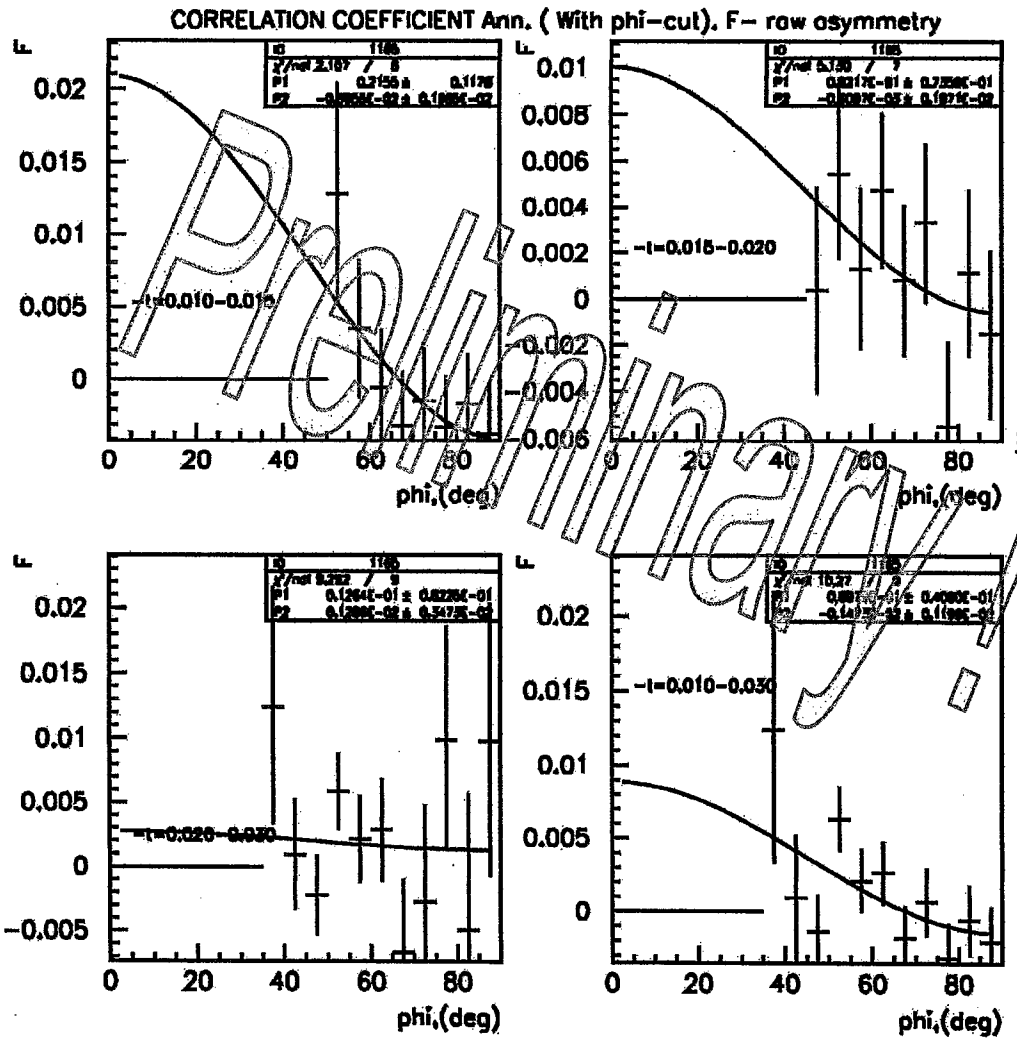

$\lvert t\rvert$-range, $(GeV/c)^2$	$\langle\lvert t\rvert\rangle$, $(GeV/c)^2$	A_{NN}
0.010-0.015	0.013	0.22±0.12
0.015-0.020	0.017	0.09±0.07
0.020-0.030	0.024	0.01±0.08
0.010-0.030	0.020	0.09±0.04

Statistical errors only

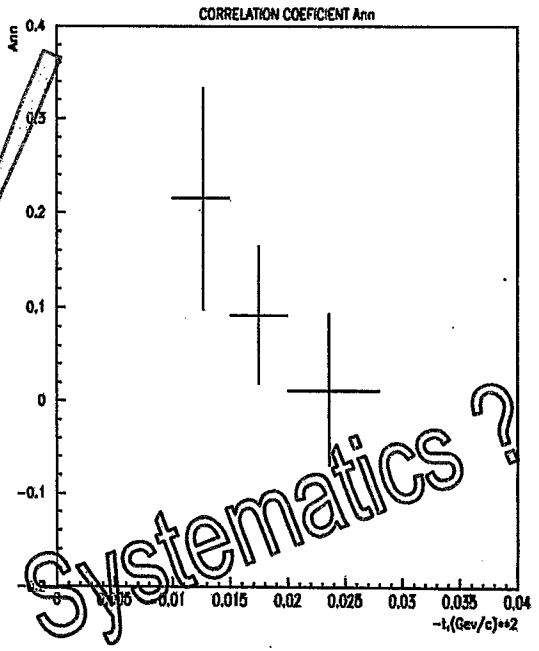

Preliminary!

Systematics ?

PP2PP

Systematic errors

SPIN-2004

- A_N:
  - We have 4 different data processings – three based on the formulas given above and one on the maximum likelihood method:
    - ✓ ITEP standard;
    - ✓ ITEP maximum likelihood;
    - ✓ BNL-Cracow;
    - ✓ S.Büeltmann's.
  - All processings give similar results in A_N.
  - Asymmetry is stable and doesn't significantly depend on the transport matrix or event selection criteria.
  - The main contribution to the systematic error for A_N is given by 15% uncertainty in the beam polarization.
- A_{NN}:
  - Result for A_{NN} is similar for both ITEP processings.
  - A_{NN} – result depends on the cut of the edges of the acceptance.
  - Observable effect is proportional to $P_B \cdot P_Y \cdot \cos^2(\varphi)$, which makes it small for current Roman pot position and beams polarization.
  - 15% of beam polarization scale uncertainty makes 30% systematic error in $P_B \cdot P_Y$

PP2PP

Conclusions and Plans

SPIN-2004

- Conclusions
  - Excellent silicon detector performance in physics run 2003
  - Our result in A_N is not compatible with absence of the hadronic spin flip
  - Result in A_{NN} suggest continue measurements
- What is next ?
  - Run with current setup (σ_{tot}, $d\sigma/dt$, b, ρ, A_N, A_{NN}) (rotate RP1,3 ?)
    - ✓ β^*=20m, p_{beam}=100 GeV/c $\Rightarrow$ $0.003<|t|<0.02(\mathrm{GeV/c})^2$;
    - ✓ β^*=10m, p_{beam}=250 GeV/c $\Rightarrow$ $0.025<|t|<0.12(\mathrm{GeV/c})^2$.
  - Put Roman Pots between DX and D0 magnets ($d\sigma/dt$, b, A_N, A_{NN})
    - ✓ β^*=3m, p_{beam}=250 GeV/c $\Rightarrow$ $0.2<|t|<1.3(\mathrm{GeV/c})^2$.
    - ✓ β^*=3m, p_{beam}=100 GeV/c $\Rightarrow$ $0.02<|t|<0.12(\mathrm{GeV/c})^2$.
  - Upgrade RHIC quadrupoles power supply at our IP to run with β^*=100m and move Roman Pots to 70m position (σ_{tot}, $d\sigma/dt$, b, ρ, A_N, A_{NN})
    - ✓ β^*=100m, p_{beam}=100 and 250 GeV/c $\Rightarrow$ $|t|$- *CNI region.*

This talk will be given in Spin2004 after the discussion in this RSC meeting

Measurement of the analyzing power of proton-carbon elastic scattering in the CNI region at RHIC

Osamu Jinnouchi (RBRC*)

On behalf of CNI Group (Polarimeter + Jet)

I.G.Alekseev[A] A.Bravar[B] G.Bunce[B*] S.Dhawan[D] R.Gill[B] H.Huang[B] W.Haeberli[E] G.Igo[F] V.P.Kanavets[A] K.Kurita[H] A.Khodinov[M] A.Kponou[B] Z.Li[B] W.Lozowski[I] W.W.MacKay[B] Y.Makdisi[B] A.Nass[B] H.Okada[G] S.Rescia[B] T.Roser[B] N. Saito[G] H.Spinka[L] E.J.Stephenson[J] D.N.Svirida[A] D.Underwood[L] C.Witten[F] T.Wise[I] J.Wood[F] A.Zelenski[B]

RBRC* ITEP[A] BNL[B] ANL[C] Yale U[D] Wisconsin U[E] UCLA[F]

Kyoto U[G] Rikkyo U[H] Indiana U[I] Indiana U[J] IUCF[K] Argonne U[L] StonyBrook U[M]

Elastic $\vec{p}C \rightarrow \vec{p}C$ scattering at very low $-t$ range

- Elastic scattering of hadron-Nucleus at RHIC has an important physics information on spin-dependent hadronic amplitude in high energy
- Elastic scattering process is identified by detecting recoil Carbon (inelastic fraction~10^{-2})

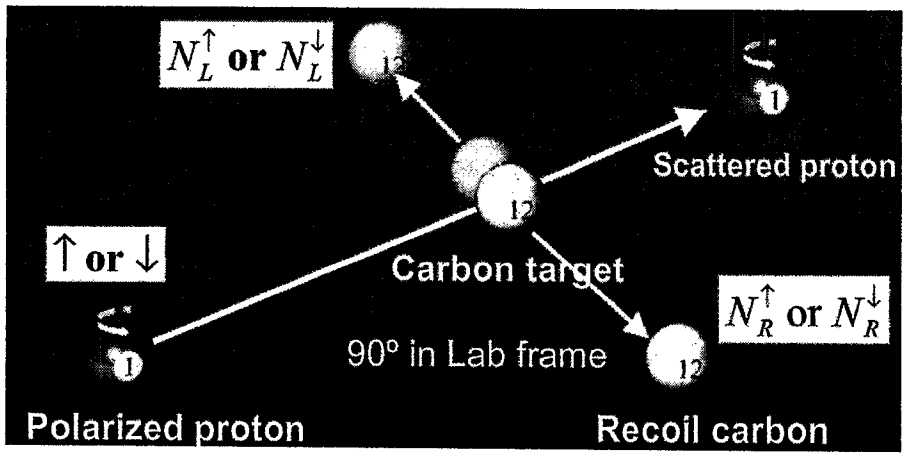

$$t = (p_{out} - p_{in})^2 \approx -2M_C T_{kin} < 0$$
$$0.005 < |t| < 0.05\ (GeV/c)^2$$

- Use single transverse spin asymmetry A_N of pC for RHIC polarimetry

A_N arises mainly from interference between ***EM spin-flip amplitude*** and ***hadronic non spin-flip amplitude*** (CNI = Coulomb – Nuclear Interference)

$$A_N = C_1 \phi_{em}^{flip} Im\phi_{had}^{nonflip} + C_2 \phi_{em}^{nonflip} \phi_{had}^{flip}$$

$\propto (\mu - 1)_p$ Pure CNI $\propto \sqrt{\sigma_{had}^{pp}}$

Regge poles /Pomeron exchange

A_N is also sensitive probe to hadronic spin flip amplitude

Helicity amplitude formalism and r_5 physics

Analogy to *pp* helicity amplitude formalism
pC process being described by two amplitudes

Non-flip $F_{+0}(s,t) =< +0|M|+0 >$

Spin flip $F_{-0}(s,t) =< +0|M|-0 >$

$$F_i = F_i^{em} + e^{i\delta} F_i^h \quad (i = +0, -0)$$

$$r_5^{pC}(t) = \frac{mF_{-0}^h}{\sqrt{-t}\ \mathrm{Im}F_{+0}^h}$$

spin flip amplitude ratio, $r_5^{pC}(t)$ for *pC* is translated into parameter r_5 for *pp*

$$r_5 = \frac{1 - i\rho_{pN}}{1 - i\rho_{pC}(t)} r_5^{pC}(t)$$

A_N can be described with two parameters

$$\mathrm{Re}r_5, \quad \mathrm{Im}r_5$$

s-dependence (E_B=24GeV, 100GeV)? phase?

Phys.Rev.Lett.,89,052302(2002)

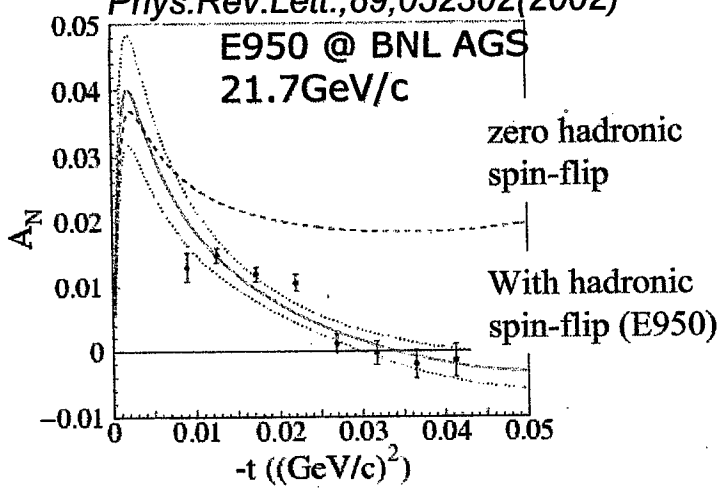

$r_5^{pC} \propto F_s^{had} / Im\ F_0^{had}$

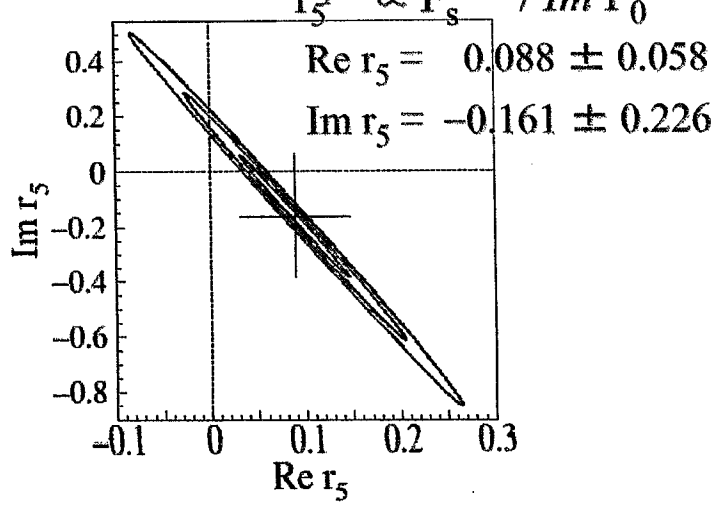

Detector setup + DAQ

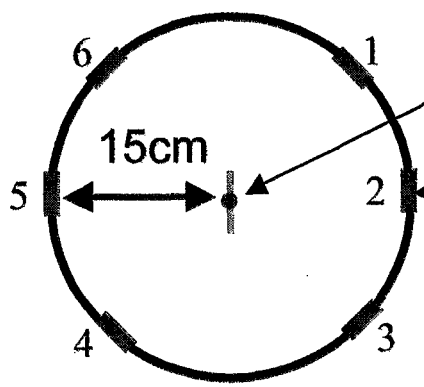

Ultra thin Carbon ribbon Target ($3.5\mu g/cm^2$)

Si strip detectors (TOF, E_C)

Thin dead layer for low energy carbon spectroscopy

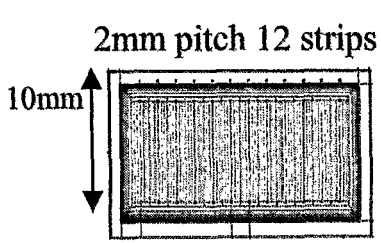

p^+ implants ~150 nm depth

72 strips in total

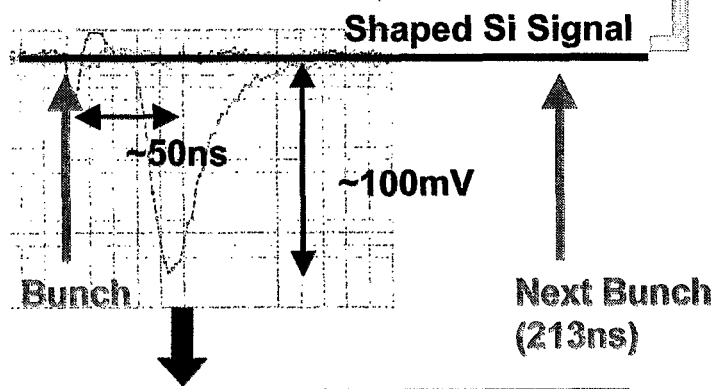

Wave Form Digitizer (WFD)

20M events / 20sec

- Pulse Height
- Bunch ID
- TOF
- Integral (Q)

online

Select carbons at on-board LUT

- Scaler data
- Asymmetry calculation
- Online results (to experiments)

offline

Event by event data

- Stored in on-board memory
- Used for offline detailed study

Recoil carbon PID → Asymmetry calculation

Particle ID (banana cut)

- Clear separation from backgrounds using TOF measurement

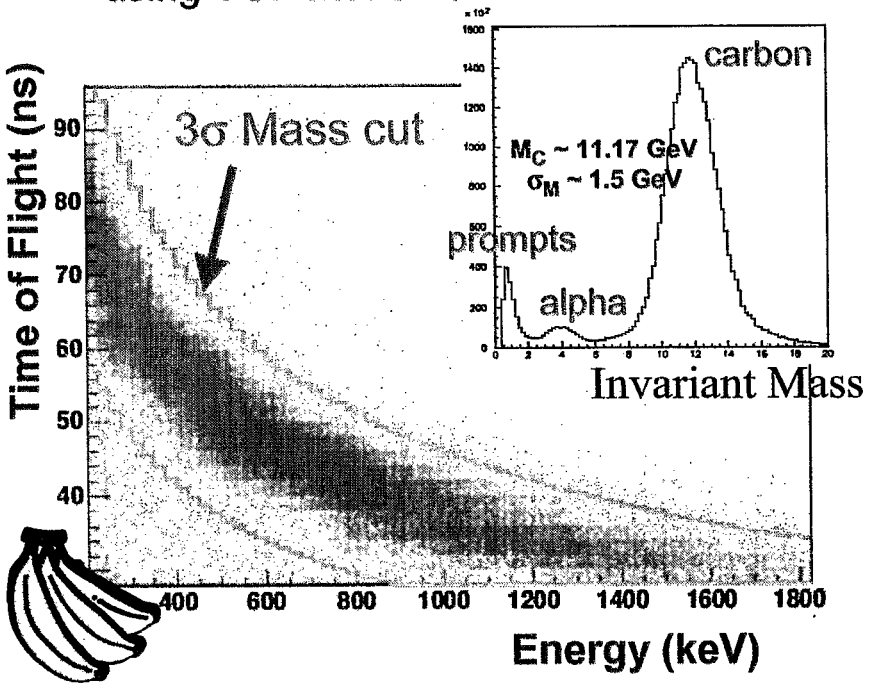

non-relativistic kinematics

$$tof = \sqrt{\frac{M_C}{2T_{kin}}}L$$

Asymmetry calculation

$$\varepsilon_N^{\uparrow} = -\frac{N_L^{\uparrow} - N_R^{\uparrow}}{N_L^{\uparrow} + N_R^{\uparrow}} \quad \text{for up spin}$$

$$\varepsilon_N^{\downarrow} = -\frac{N_R^{\downarrow} - N_L^{\downarrow}}{N_R^{\downarrow} + N_L^{\downarrow}} \quad \text{for down spin}$$

With alternating spin pattern (+,-,+,-) square-root formula

$$\varepsilon_N = -\frac{\sqrt{N_L^{\uparrow}N_R^{\downarrow}} - \sqrt{N_R^{\uparrow}N_L^{\downarrow}}}{\sqrt{N_L^{\uparrow}N_R^{\downarrow}} + \sqrt{N_R^{\uparrow}N_L^{\downarrow}}}$$

$$A_N = \varepsilon_N / P_{beam}$$

Offline analysis (1)

- Fit the carbon locus with the non-relativistic kinematics

$$Tof\ (ns) = \frac{1181.6}{\sqrt{E_{kin}(keV)}} + \underline{t_0}$$

$$E_{kin} = f(E_{deposit}, \underline{W_{dead\ layer}})$$

Non-linear function

  - Energy loss in the non-active layer on silicon surface
  - Width can be estimated from the degree of deformation against pure kinematics curve (2 parameters fit)

- Correction for energy loss in dead layer
  - Estimated to be 57 μg/cm² in average (±12 μg/cm²)
  - 6 detectors - from same wafer
  - Small variation from strip to strip

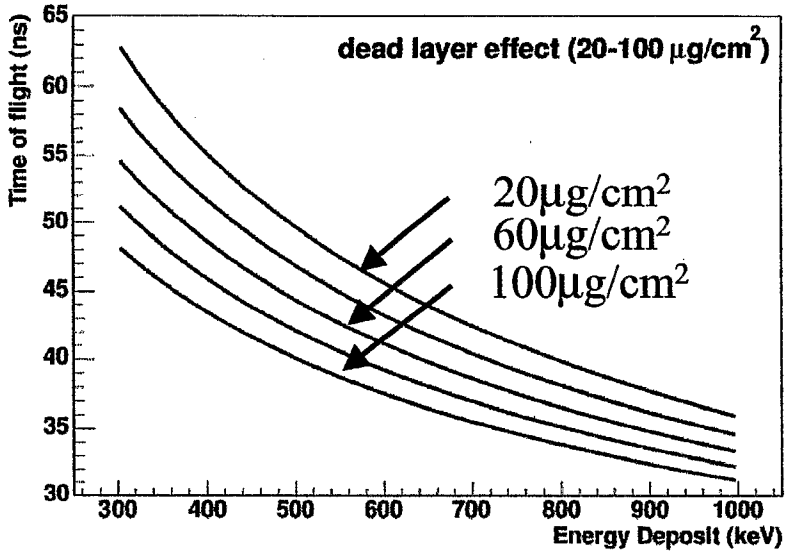

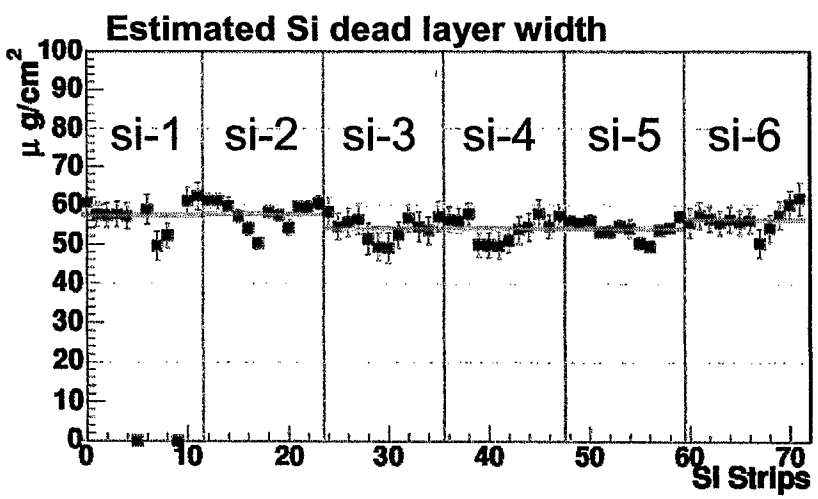

Offline analysis (2)

- Energy calibration
  - Tracking calibration constant using ^{241}Am (5.486MeV) sources inside chamber
  - Stable within ± 2% through run period
- Event selection with invariant mass
  - Better S/N ratio than timing cut
  - Mass distribution width evolves during fills (due to the change in bunch length)
  - 3σ cut applied

Mass distributions for all 72 strips

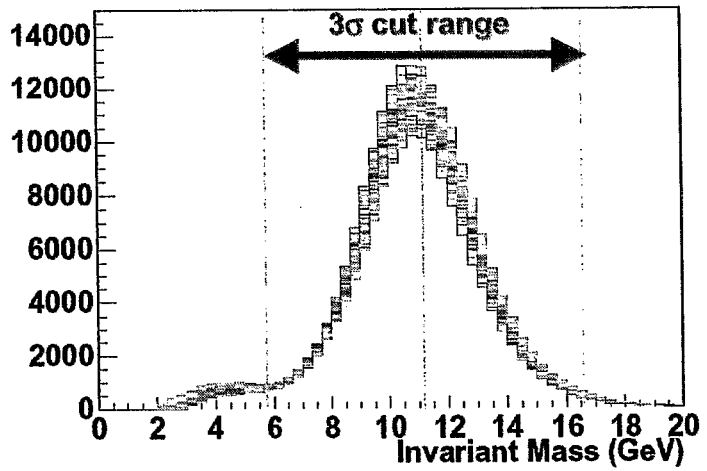

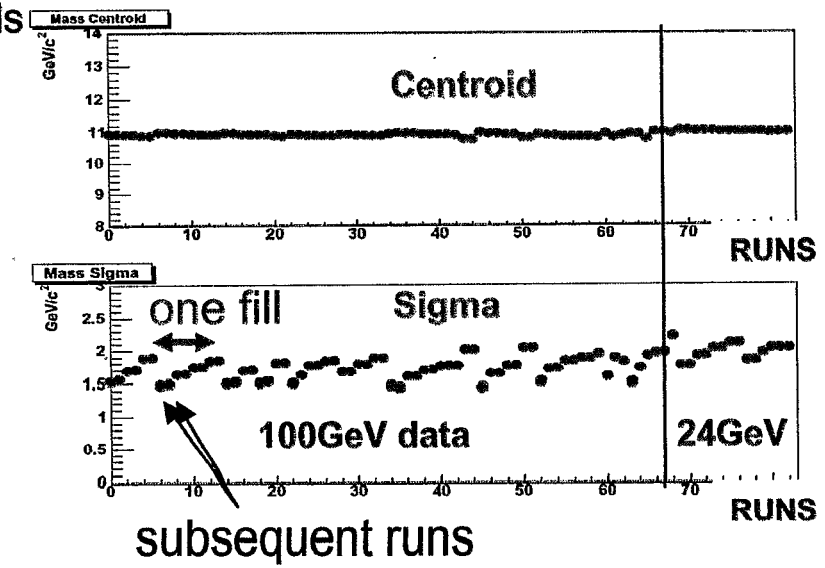

Strip by strip variations in asymmetry

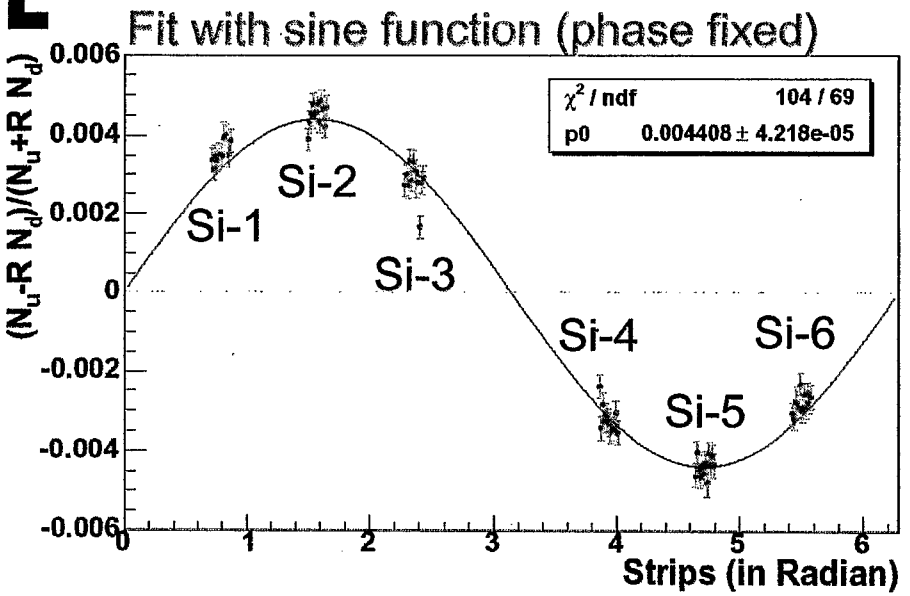

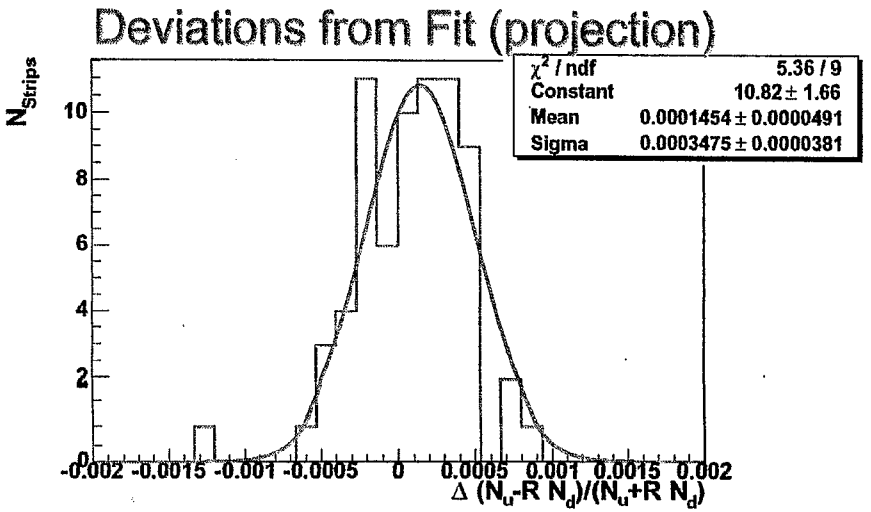

- Each strip can be considered as individual polarimeter

$$\varepsilon^{(i)} = \frac{(N_u^{(i)} - RN_d^{(i)})}{(N_u^{(i)} + RN_d^{(i)})} \quad R = \frac{\sum_i N_u^{(i)}}{\sum_i N_d^{(i)}}$$

$N_u^{(i)}, N_d^{(i)}$ Number of carbons in i-th strip for Up(Down) spin

- Variations more than statistical uncertainties are regarded as systematics of the measurement

$$\sigma_{sys} = \sqrt{\sigma_{total}^2 - \sigma_{stat}^2}$$

$$\sigma_{total} = 3.5 \times 10^{-4}$$
$$\sigma_{stat} = 2.8 \times 10^{-4}$$
$$\downarrow$$
$$\sigma_{sys} = 2.1 \times 10^{-4}$$

the same order of magnitude

Polarization measurements during RHIC fill

Online Results

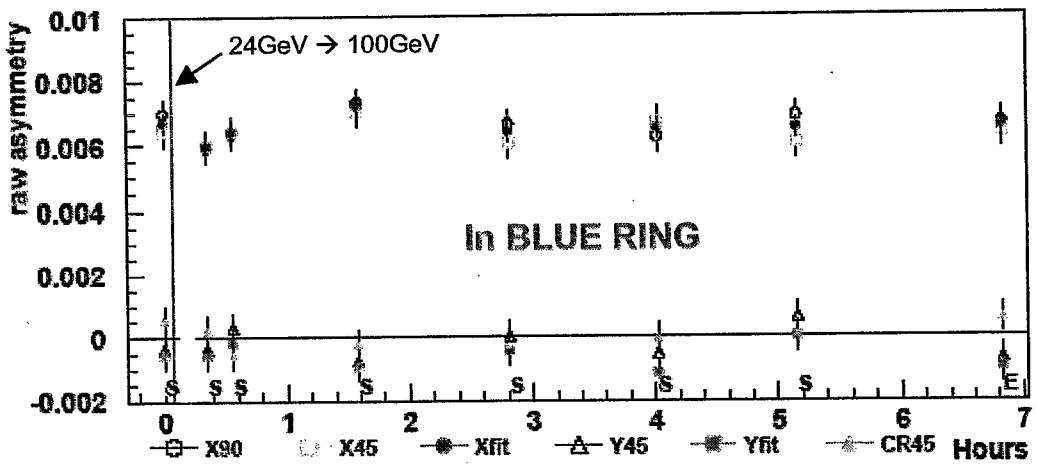

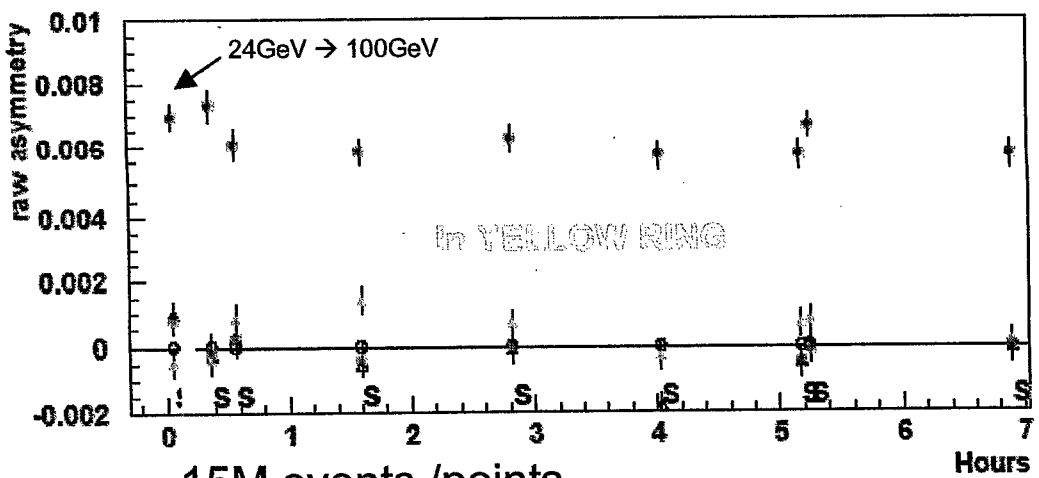

15M events /points

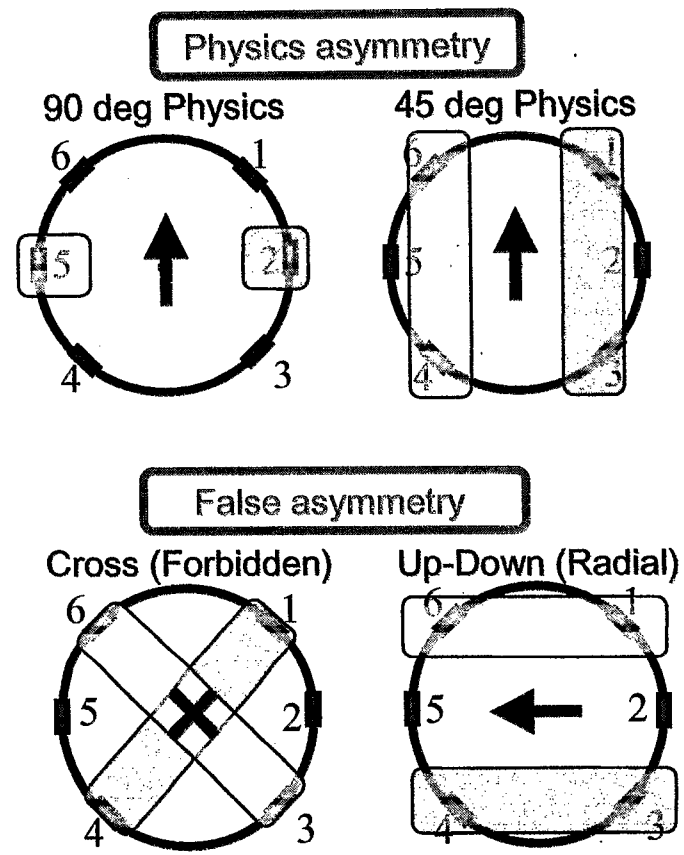

Raw asymmetry (t) in wide range

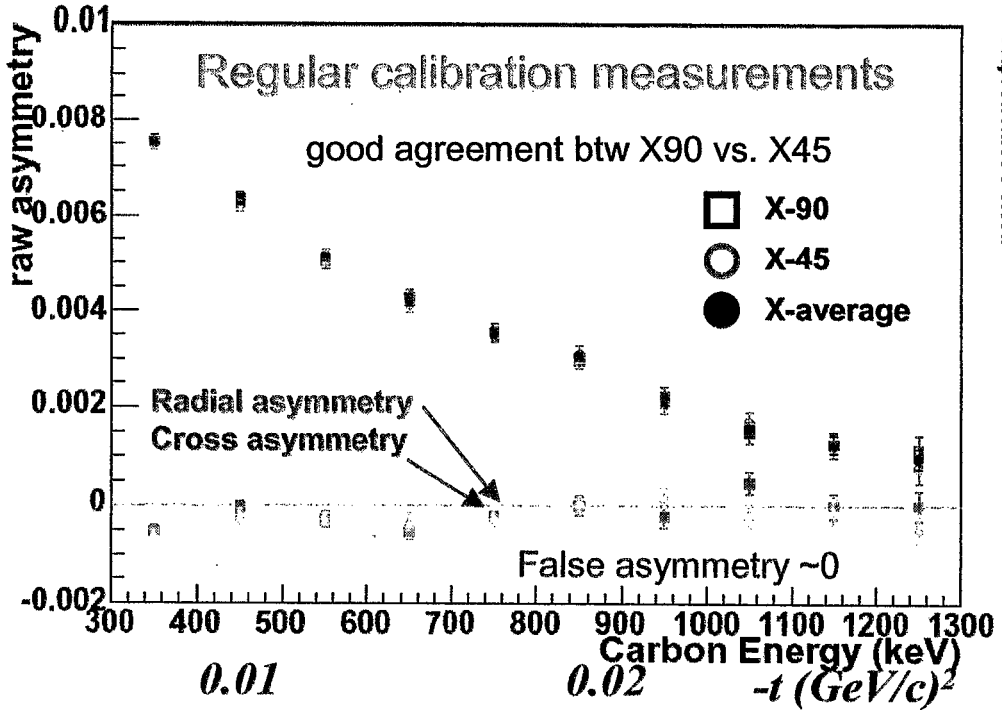

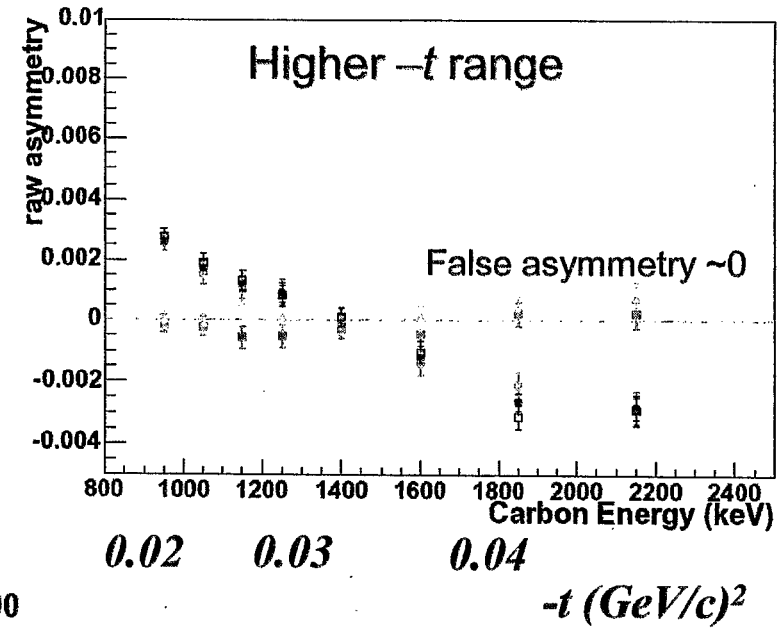

- Regular polarimeter runs
  - Measurements taken with running Jet-target in parallel
  - very clean asymmetry values

- Polarimeter dedicated runs (high -t)
  - Signal attenuation (x1/2) to reach higher –t
  - Normalized at overlap region to regular runs
  - *Zero crossing measured with large significance*

$A_N(t)$ at 100GeV and fit result with theoretical function

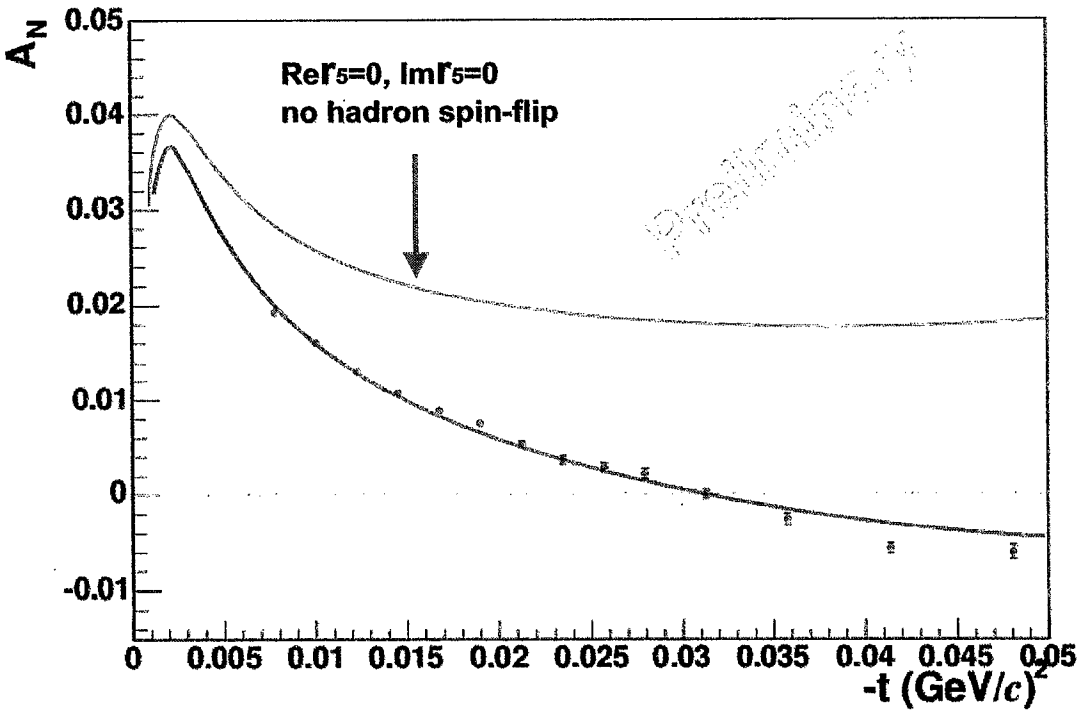

$$A_N(t) = \frac{\varepsilon_N(t)}{P_{beam}}$$

- 1.2 x 10^9 events are collected with P_B known from jet-target

  $P_B = 0.386 \pm 0.030$

- Fit with CNI theory function (hep-ph/0305085)

$A_N(t)$ at 100GeV and fit result with theoretical function

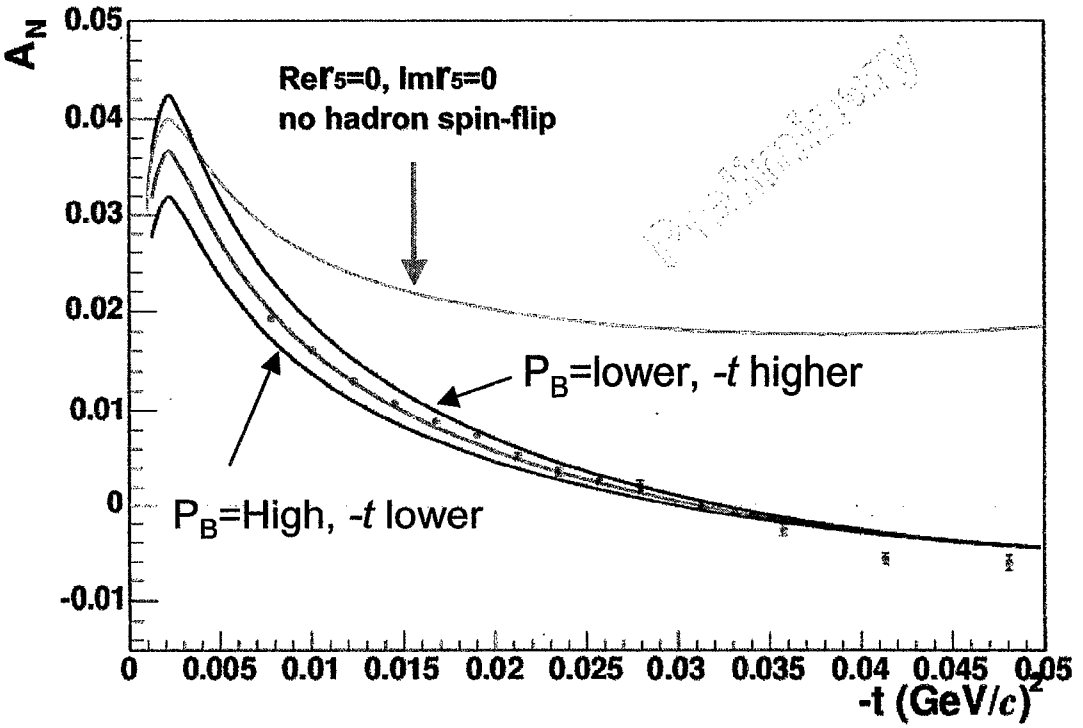

$$A_N(t) = \frac{\varepsilon_N(t)}{P_{beam}}$$

- 1.2 x 10^9 events are collected with P_B known from jet-target

  $P_B = 0.386 \pm 0.030$
- Fit with CNI theory function (hep-ph/0305085)
- Major sources for sys errors
  - Si dead layer on $-t$ ($\pm 12\mu g/cm^2$)
  - Propagation from error on P_B
  - The effects are scaling or shifting

$A_N(t)$ comparison between 24GeV vs. 100GeV

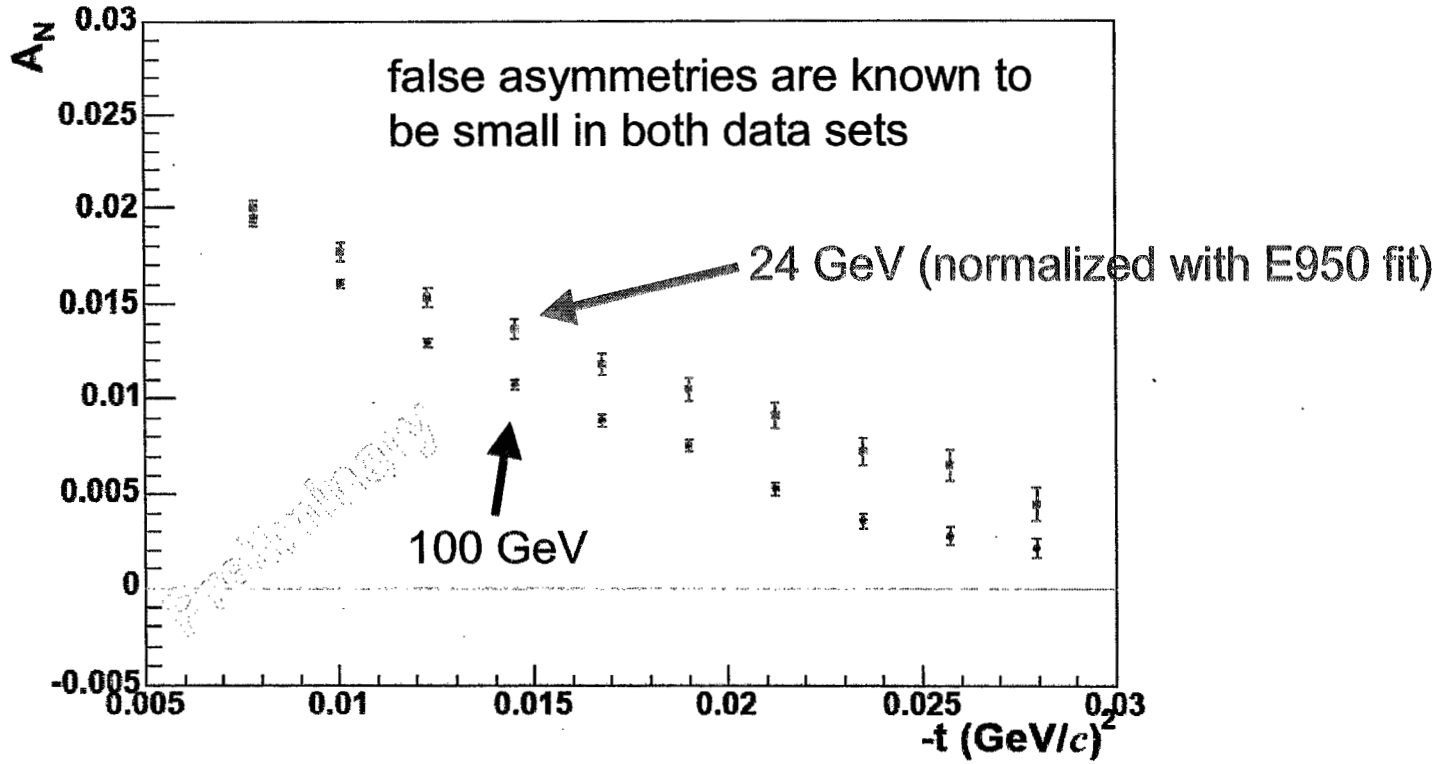

- Raw asymmetry for 24GeV data is available (Not calibrated yet)
- Raw asymmetries at 24GeV are normalized by $A_N(t)$ theory fit function to E950

Summary & Discussion

- A_N measurement of *pC* elastic scattering was carried out at E_B=100GeV with P_B measurement by Jet-Target
- The shapes of $A_N(t)$ are different between 24GeV and 100GeV
- r_5 parameter was measured at E_B=100GeV
  - Strong correlation (Im vs. Re)
  - Small (zero consistent) Im r5

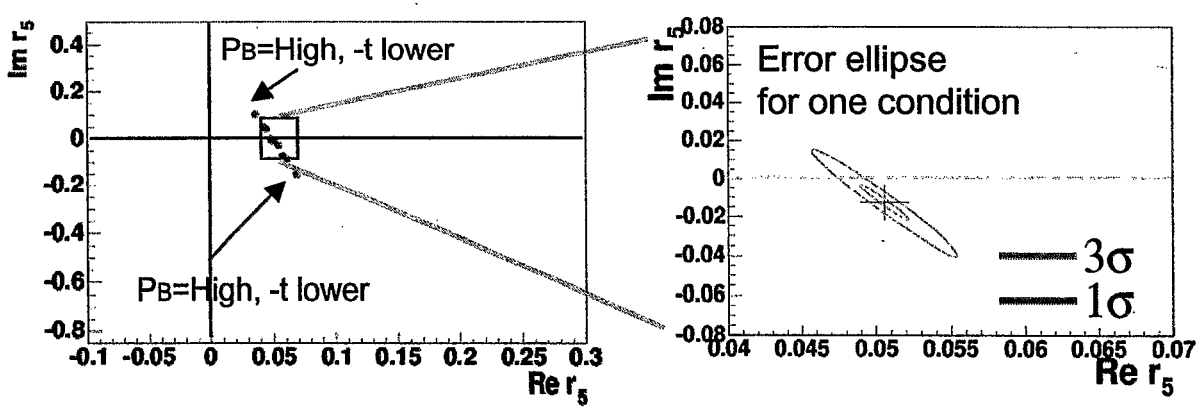

- A_N Calibration at E_B=24GeV is in progress

Back up slides ...

RHIC Proton Polarization measurements

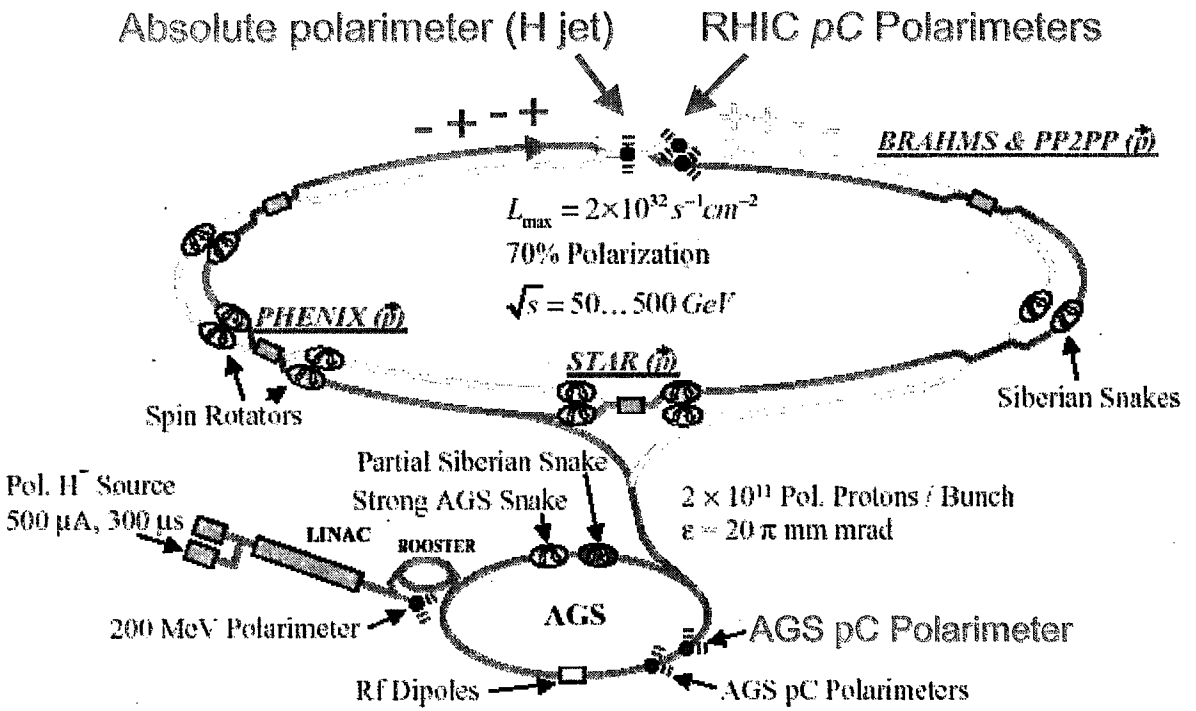

RHIC *pC* CNI Polarimeters :
- quick polarimeters used since Run-02
- determine relative P
- need A_N calibration

H jet *pp* polarimeter : (→ next speaker)
- commissioned at Run-04
- absolute polarization measurement
- calibrate pC CNI polarimeters

- Final goal is to achieve dP/P < 5%

AGS A_N : $pC \rightarrow pC$ at 3.9, 6.5, 9.7 & 21.7 GeV

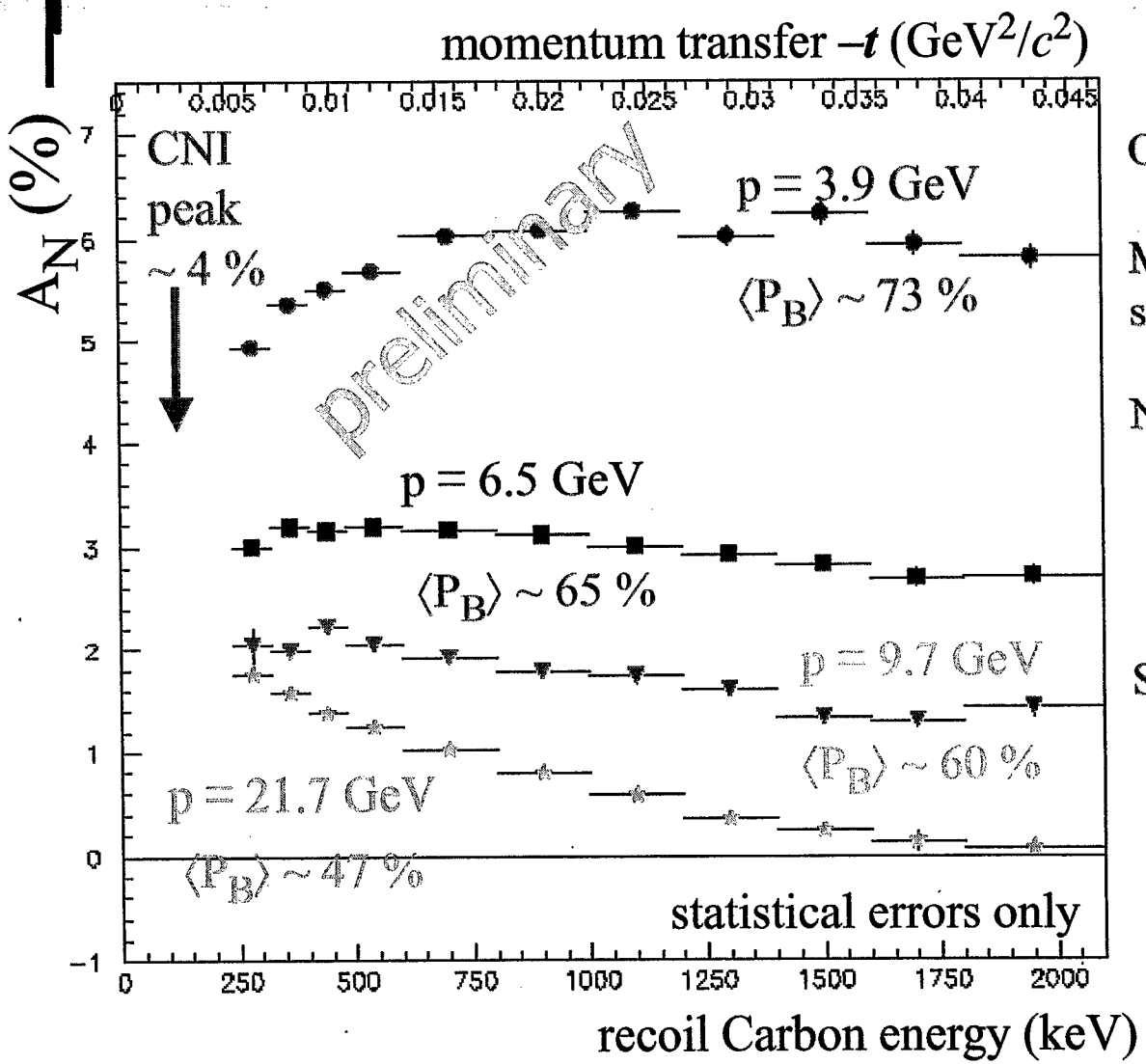

Only statistical errors are shown

Measure with E880 polarimeter simultaneously for normalization

Normalization errors:
- ~ 10 % (at 3.9)
- ~ 15 % (at 6.5)
- ~ 20 % (at 21.7)

Systematic errors:
- < 20 %
- backgrounds
- pileup
- RF noise

Comparison RHIC(100GeV) vs. E950(22GeV)

RHIC 100GeV (this data)

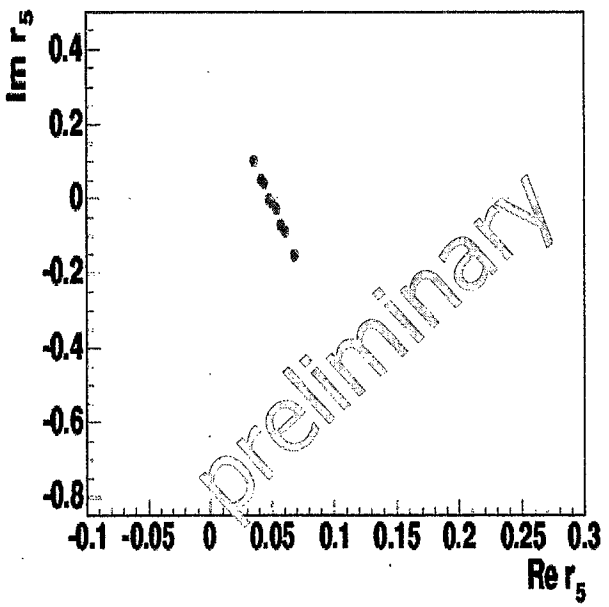

E950 22GeV

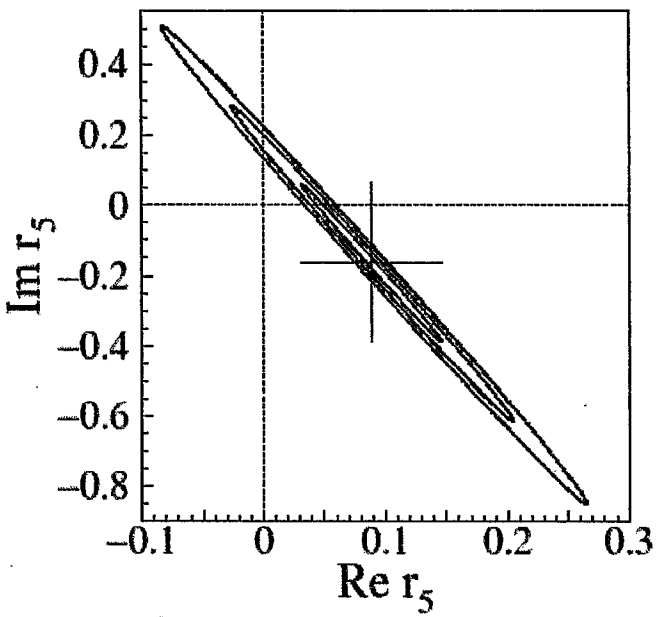

Phys.Rev.Lett.,89,052302(2002)

Strip by strip distribution back up

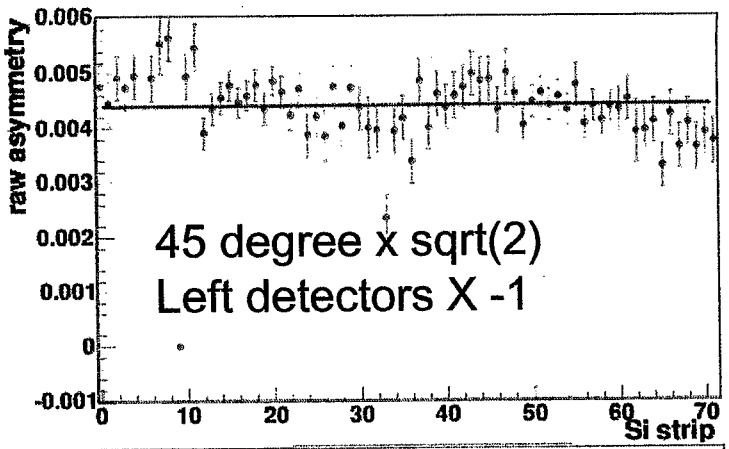

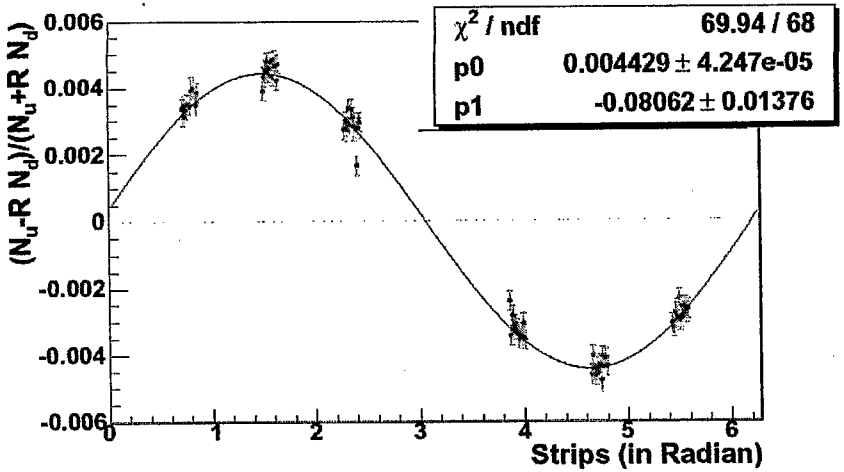

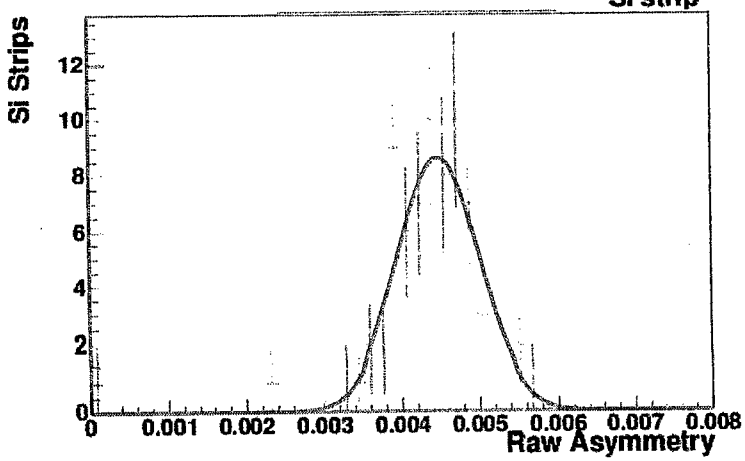

Fit with constant

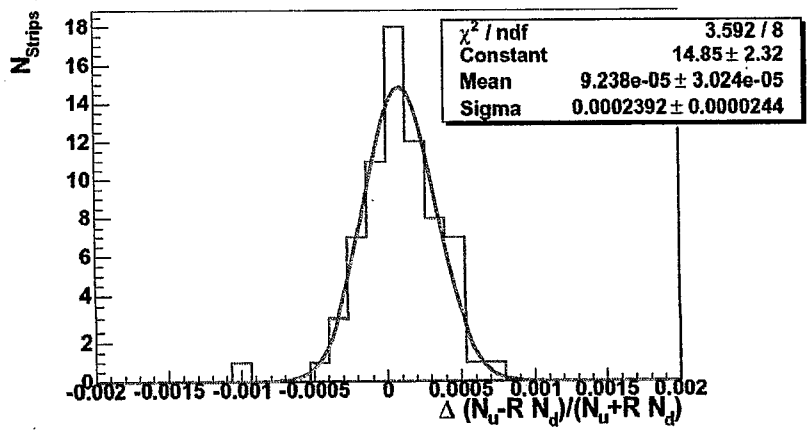

Fit with sine curve (2parameter fit)
Chisquare improved from 1parameter Sine fit

Determination of dead layer from fit

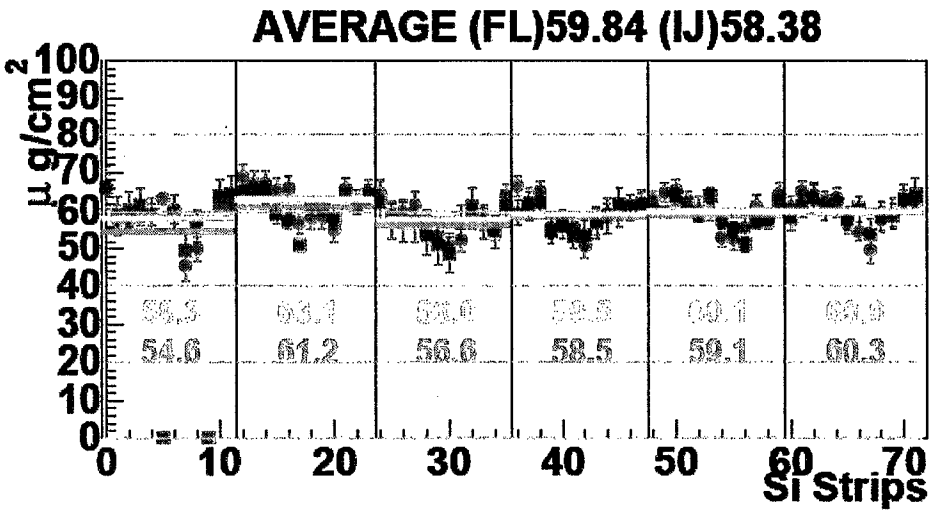

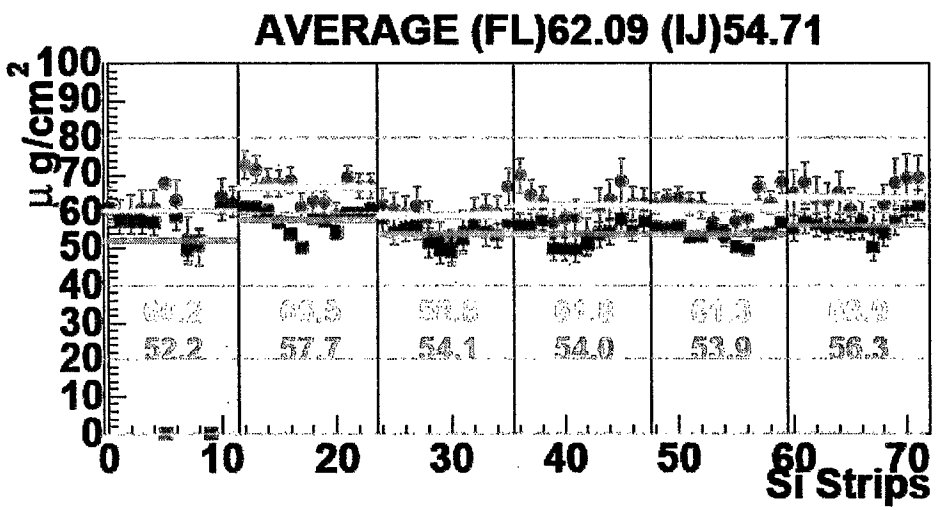

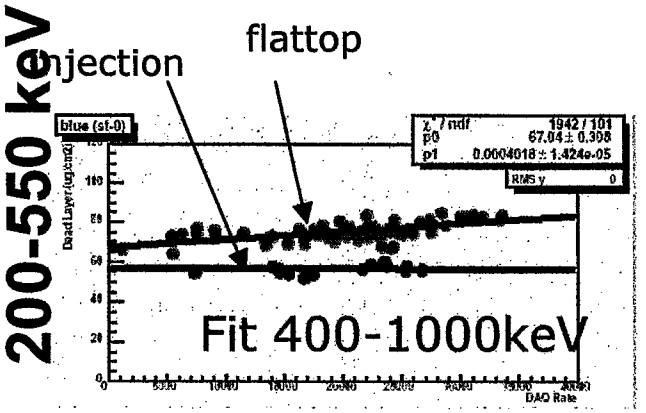

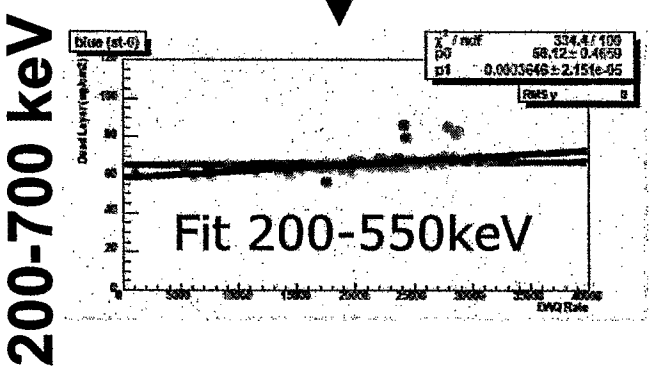

What makes difference in dead layer btw injection/flattop

RUN 5235.013 Hi Lumi 100GeV run dl=80.0

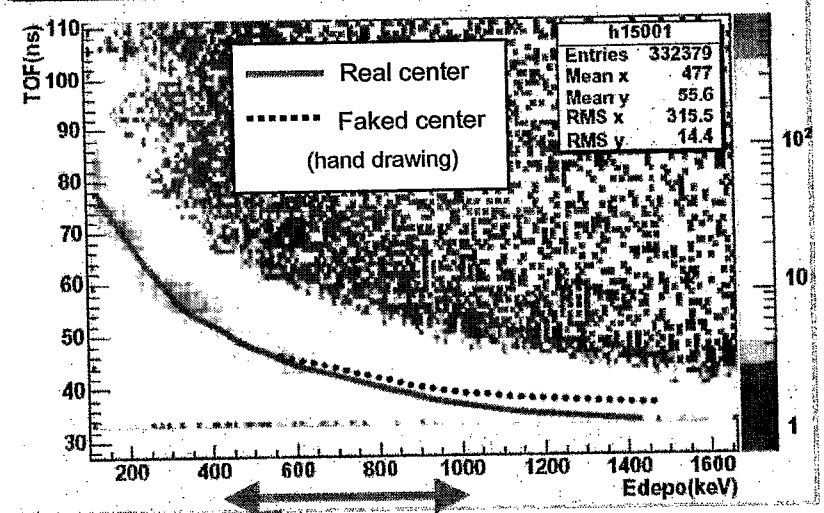

Fit range

RUN 5283.001 Hi Lumi 24GeV run dl=52.4

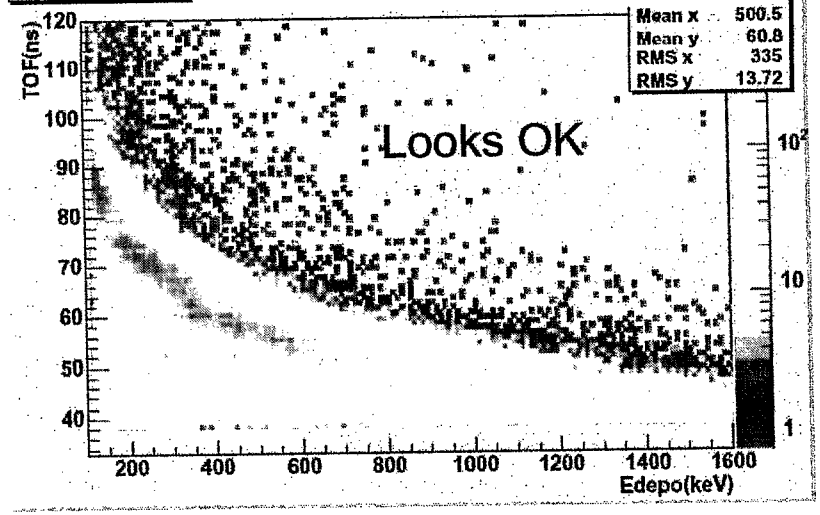

RUN 5220.001 Low Lumi 100GeV run dl=63.8

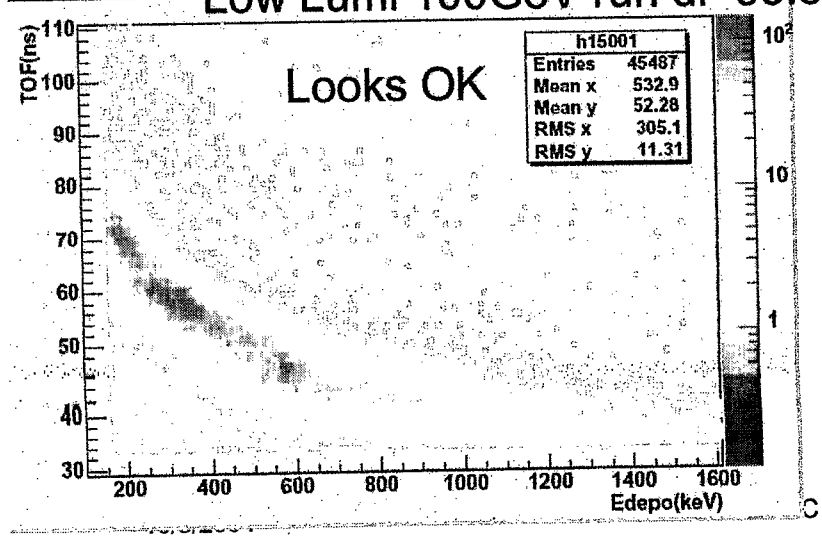

- At flattop the carbon locus is closer to the timing threshold
- At high luminosity, the real ridge is shifted from the distribution center (at higher carbon energy)
- Should use only lower carbon energy range to avoid the timing cut effect

Invariant mass distribution in high –*t* region

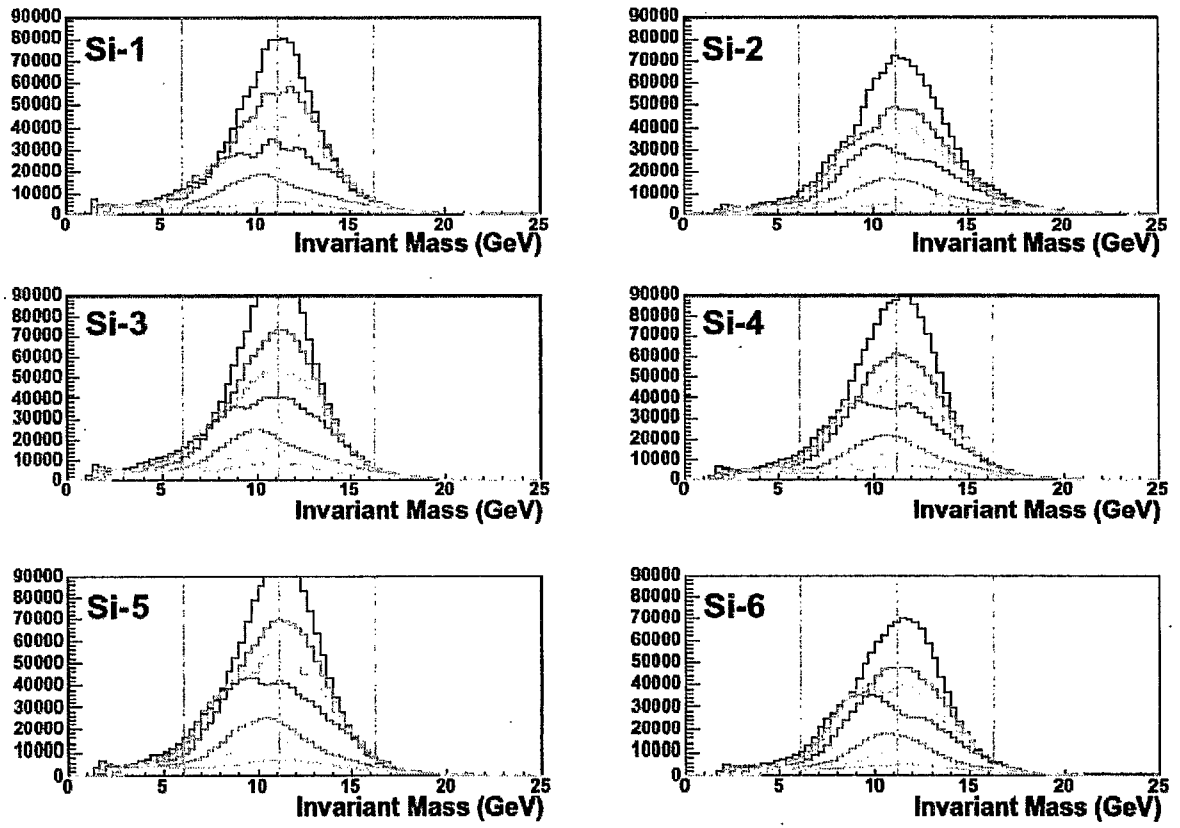

- Deformations of mass distribution are due to local non-linearity of ADCs
- Nevertheless the cuts preferentially select carbons
- Background contaminations are not negligible in the highest –t region

Invariant mass distribution in regular –*t* region

300-1100keV (100keV each)

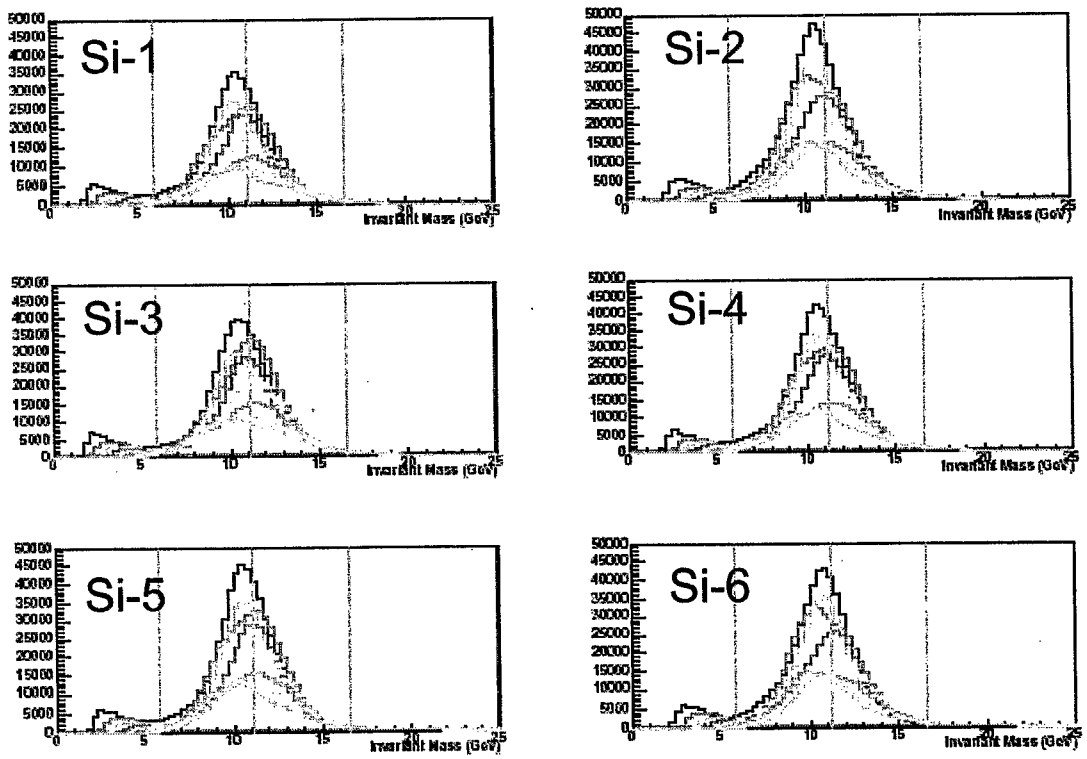

- Deformations of mass distribution are due to local non-linearity of ADCs
- Nevertheless the cuts preferentially select carbons
- Background contaminations are **negligible** even in the highest –t region

T.L.Trueman 10/8/04

Energy Dependence of pp and pC CNI Analyzing Power

1. Basic formulas

- Hadronic proton-carbon scattering amplitude

$$g(q) = g_o(q) + \vec{\sigma} \cdot \frac{\vec{k} \times \vec{k}'}{|\vec{k} \times \vec{k}'|} g_s(q)$$

For small momentum transfer q

$$g_s(q) = \tau(s) \frac{q}{m_N} g_o(q)$$

- Corresponding "Coulomb" amplitudes

$$Z\alpha F^{em}(q)(\frac{1}{q^2} + \vec{\sigma} \cdot \frac{\vec{k} \times \vec{k}'}{|\vec{k} \times \vec{k}'|} \frac{\kappa}{2m_N q})$$

$\kappa = 1.79$, the anomalous proton magnetic moment and $F^{em}(q)$ the carbon em form factor.

- Analyzing power

$$A_N(t,\tau) = \frac{2\,Im(g_s(q)g_0^*(q))}{|g_0(q)|^2 + |g_s(q)|^2}$$

$$\frac{A_N(t,\tau)}{A_N(t,0)} = 1 - \frac{2}{\kappa}Re[\tau(s)] + \frac{2}{\kappa}Im[\tau(s)]f(t),$$

with

$$f(t) = \Big((1+\rho_{pC}^2(t))(t/t_c)(F_C^h(t)/F_C^{em}(t)) - \rho_{pC}(t) - \delta_{pC}(t)\Big)/(1-\rho_{pC}(t)\delta_{pC}(t))$$

As usual $t = -q^2$, $\rho_{pC}(t) = Re(g_0(s,t))/Im(g_0(s,t))$, δ_{pC} is the Bethe phase and $t_c = -8\pi Z\alpha/\sigma_{tot}^{pC}$. F_C^h is the hadronic "form factor" equal to $Im(g_0(s,t))/Im(g_0(s,0))$.

- $f(t)$ is calculable by Glauber methods (cf. Kopeliovich & Trueman, Phys Rev D 64 034004) and so $1 - \frac{2}{\kappa}Re[\tau(s)]$ and $\frac{2}{\kappa}Im[\tau(s)]$ can be each determined from the raw asymmetry if polarization P is known. Otherwise P enters as a common scale factor in each.

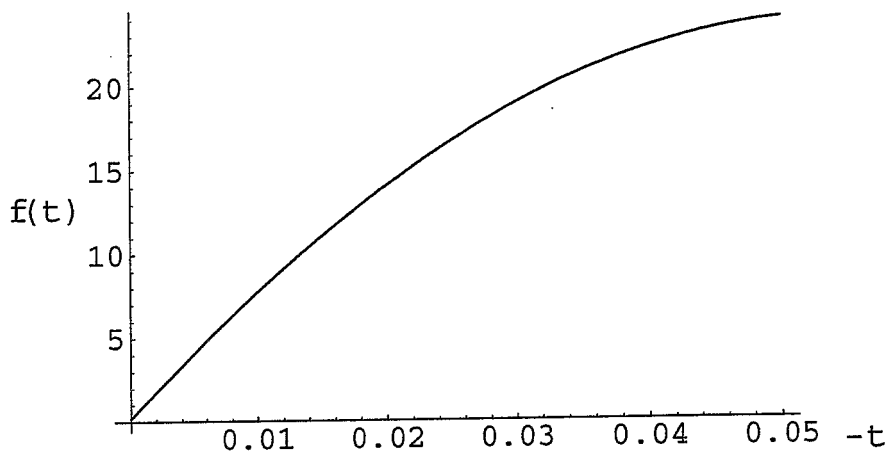
20
15
f(t)
10
5
0.01
0.02
0.03
0.04
0.05
-t

2. The Model

- is based on Regge fit to pp scattering over wide energy range (cf. Cudell et al) which fixes non-flip parameters for the Pomeron (simple or multiple pole), a $C = -1$ vector meson (mainly ω) and a $C = +1$ tensor meson (mainly f_2).

- The non-flip amplitude is

$$g_0(s,0) = g_P(s) + g_f(s) + g_\omega(s),$$

where the functions $g_R(s)$ have enery dependence and phase determined by standard Regge theory.

- The corresponding flip amplitude is determined by three real, energy independent constants

$$\begin{aligned} g_5(s,t) &= \tau(s)\frac{\sqrt{-t}}{m}g_0(s,t) \\ &= \frac{\sqrt{-t}}{m}\{\tau_P\, g_P(s) + \tau_f\, g_f(s) + \tau_\omega\, g_\omega(s)\}. \end{aligned}$$

so

$$\tau(s) = \{\tau_P\, g_P(s) + \tau_f\, g_f(s) + \tau_\omega\, g_\omega(s)\}/g_0(s,0)$$

From Berger et al (1978) the important properties of Regge pole contributions are displayed by

$$g^R_{\lambda'\lambda}(s,t) = (-t/m^2)^{|\lambda'-\lambda|}\beta^R_{\lambda'\lambda}(t)(1\pm e^{-i\pi\alpha^R})s^{\alpha^R}$$

$$g_0 = g_{++},\ g_s = g_{+-}$$

- The two constants in $\tau(21.7) = -0.213 - 0.054i$ determines two relations between the three constants $\tau_P, \tau_f, \tau_\omega$
- We need one more measurement to fix their values. If one measures the "shape" of the raw asymmetry over the CNI region *without knowing the value of P at that energy* one can obtain the needed information:

$$S(p_L) = \frac{PIm[\tau(p_L)]}{P(\kappa/2 - Re[\tau(p_L))]} = \frac{Im[\tau(p_L)]}{\kappa/2 - Re[\tau(p_L)]}$$

3. Test of the method

- The program is then to measure the asymmetry at one energy where the polarization is known, say at $p_L = 21.7$ GeV/c, and to measure the shape at some other energy where the polarization may not be known, say $p_L = 100$ GeV/c. From these three numbers one can calculate the three numbers τ_P, τ_f and τ_ω and thereby, if the model is correct, obtain the polarization at 100 GeV or any other energy where the model is valid.

- The numbers for $\tau(21.7)$ are published and preliminary data at 100 GeV has been reported at conferences during the past year. From fitting this data we find $S(100) = -0.052$, and with this value we can work through this process to get tentative values for the Regge residues. We find

$$\begin{aligned} \tau_P &= -0.02 \\ \tau_f &= -0.43 \\ \tau_\omega &= 0.03 \end{aligned}$$

- Using this preliminary data we can also work out tentative errors on these values. We will see that only the f spin-flip is significantly non-zero. Indeed, the often espoused assumption that the Pomeron spin-flip is zero is consistent with this determination.

- With these values we can tentatively calculated the polarization at 100 GeV in that experiment and find

$$P = 0.23.$$

The fact that this number is about 10% below the value measure at 24 GeV may indicate a limitation on this method already.

- The newest 100 GeV data was taken in conjunction with the p-jet determination of the beam polarization so we have a very accurate and absolutely normalized A_N. Here it is along with the prediction using the Regge parameters just determined and the best fit to the data showing the same 10% between the model and the data.

Comparison of recently measured A_N at RHIC (from Osamu Jinnouchi) for pC scattering at 100 GeV/c with model prediction (upper curve) and best fit to data (lower curve).

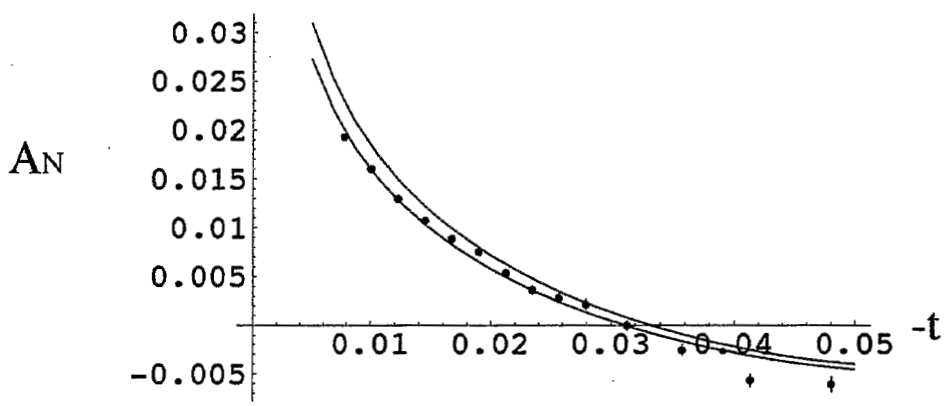

Model τ = -0.130 -0.053 i

Best fit τ = -0.017 -0.049 i

4. Regge couplings

- Here we give the revised Regge couplings using the new 100 GeV data and the shape of the E950 21.7 GeV data. A new revision is underway using the shape of the new 24 GeV data but not yet complete. We find

$$\begin{aligned} \tau_P &= +.09 \\ \tau_f &= -0.30 \\ \tau_\omega &= 0.19 \end{aligned}$$

- The next figure shows a comparison between the E950 data, the original fit and this prediction. It looks pretty good, but examination of the crucial peak region again indicates a 10% discrepancy. The following figure shows again the original error ellipses for the Regge residues with the new central values marked with x (errors not worked out yet). Agreement is O.K.. The new 24 GeV data looks at first sight to have a rather different shape from the earlier data and this might lead to bigger changes.

Checking Regge model

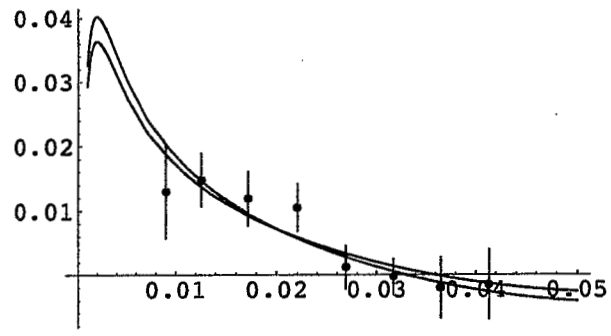

21.7 GeV data and E950 fit with known P(upper) and Regge prediction based on fit to 100 GeV data and 21.7 GeV shape (lower)

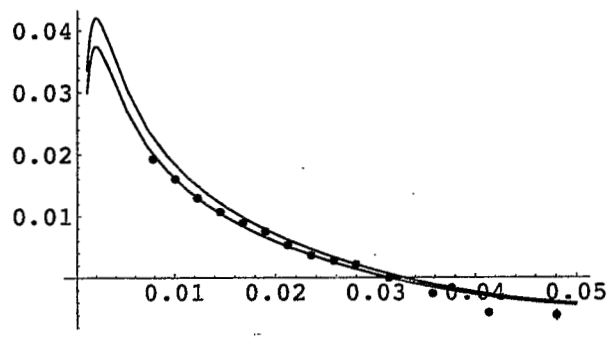

new 100 GeV data, best fit with known P(lower) and Regge prediction based on E950 fit and 100 GeV shape (upper)

New values of Regge I=0 spin-flip coupling and the "old" ellipses

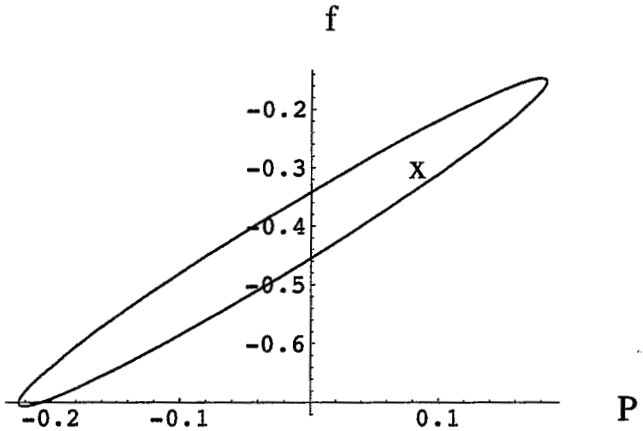

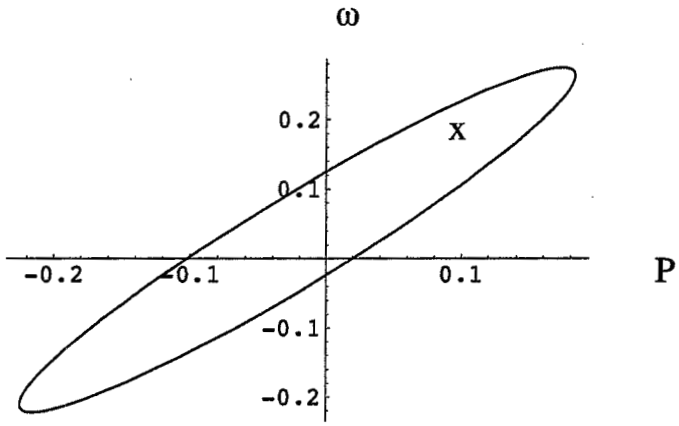

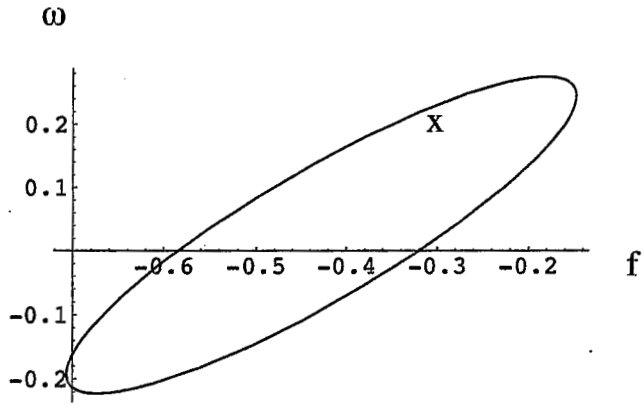

$\tau P = 0.09,\ \tau f = -0.30,\ \tau\omega = 0.19$

may require revision with new data

5. New 24 GeV data

Just last week I was given the preliminary 24 GeV data from the latest RHIC run. The polarization was not directly measured at that energy so the plot shows the raw asymmetry ϵ, which is enough to determine the shape. If we use this shape, which is very different from E950,

$$shape950 = -0.048, \; newshape = -0.036$$

the Regge couplings are changed to

$$\begin{aligned} \tau_P &= +.115 \\ \tau_f &= -0.336 \\ \tau_\omega &= 0.397 \end{aligned}$$

This determines $newP(24) = 0.35$. This is a little low given that the nominal polarization at 100 GeV from the jet is about 0.39, but it could be this low (Jinnouchi).

New (October 2004) 24 GeV data from RHIC for ε(t)

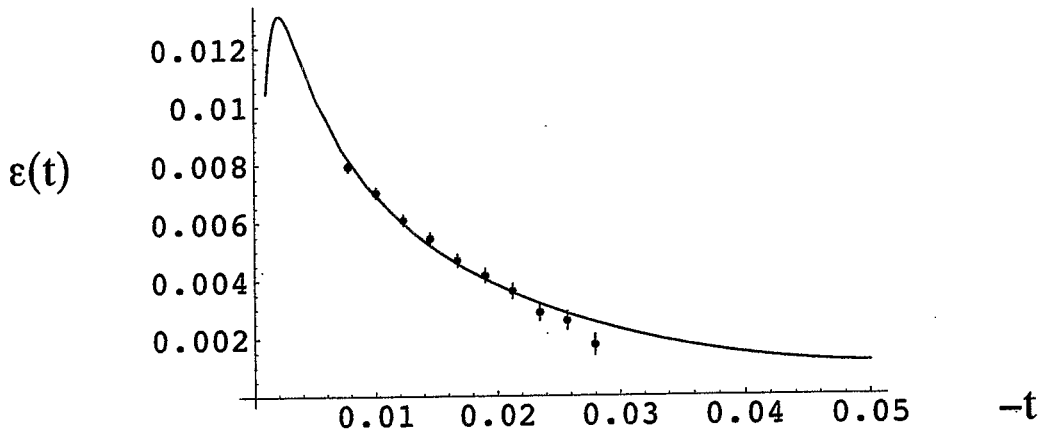

best fit for shape = -0.036

We can also use these numbers to predict the analyzing power at 250 GeV. This is shown for two cases : one with the new Regge couplings I just showed (upper) and the other a first look at the effect of the new 24 GeV data. Very little difference here. The corresponding tau values are

$$\text{new} \quad \tau(s) = 0.015 - 0.0407i$$

$$\text{new new} \quad \tau(s) = 0.025 - 0.0427i$$

Note the zero crossing moves in because the shape of the new new fit is larger than the shape of the "new" fit. The crossing occurs at the t-value when $f(t)$ in the analyzing power formula, about 20 and increasing in the range around 0.04, is equal to $1/S(p_L)$.

Analyzing power predicted for 250 GeV/c:
upper curve shows prediction prior to newest 24 GeV data,
lower curve uses the newest data to determine Regge couplings

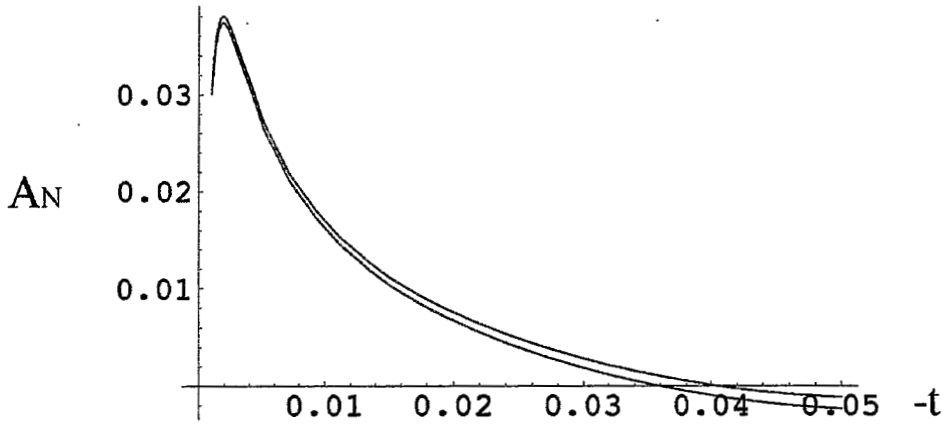

6. $I = 1$ couplings and proton-proton elastic scattering

- Because pp scattering involves the exchange of of $I = 1$ Regge poles, the ρ and the a_2 in particular, we cannot simply use the results above to make predictions for this case. But we can use the beautiful new p-jet data and a couple of reasonable assumptions to achive this. We assume (1) at these energies the proton-proton and neutron-proton unpolarized scattering amplitudes are approximately equal and (2) the two $I = 1$ Regge poles are degenerate with the corresponding $I = 0$ Regge pole of the same Charge Conjugation parity, $C = -1$ for ω, ρ and $C = +1$ for f, a_2. Then we can describe pp scattering in terms of 3-parameters: τ_+, τ_- and the pomeron coupling τ_P. Since we already know τ_P, in some sense, from the pC analysis and we can determine two parameters from the real and imaginary parts of τ obtained by fitting the p-jet data, we are in business.
- I fit the data that Sandro Bravar gave me to the standard CNI asymmetry formula. It is much simpler for pp because the functions and the

parameters involved are all measured. The only uncertainty is the ρ value at this energy which is not directly measured, but from fits over a big energy range it looks that one can reasonably interpolate the value $\rho = -0.082$. If you use a different value, like 0, you will get a different τ. I obtain then

$$\tau_{pp}(100) = -0.065 - 0.0124i$$

and from this and using $\tau_P = 0.09$ we find

$$\begin{aligned} \tau_P &= +.09 \\ \tau_+ &= -0.324 \\ \tau_- &= 1.06 \end{aligned}$$

I remind for the $I = 0$ Reggeons

$$\begin{aligned} \tau_P &= +.09 \\ \tau_f &= -0.30 \\ \tau_\omega &= 0.19 \end{aligned}$$

New p-jet data

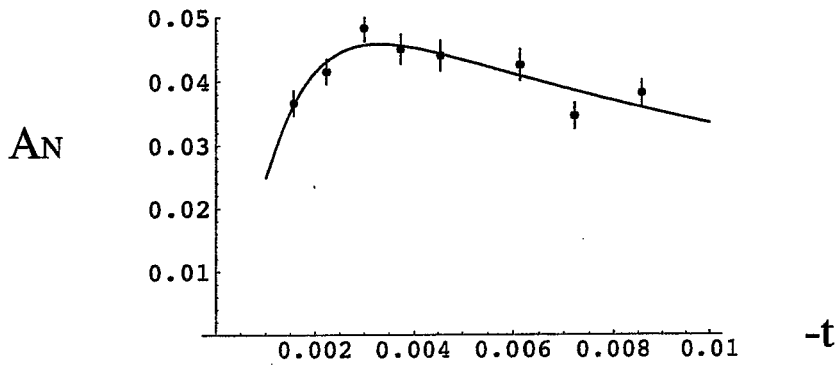

τ from p-jet fit = -0.0625 -0.011 i

τ from E704 fit = 0.185 + 0.024 i

so the f coupling is not much modified by the a_2 but the the $C = -1$ is changed by a factor of 10! This is not too much of a surprise: the ancient fit of Berger et al shows just such a pattern.

- Finally, we have also gotten some small-t data from the pp2pp experiment, and equipped with these couplings we can calculate

$$\tau(s = 4 * 10^4) = 0.08 - 0.007i.$$

The last plot shows pp2pp data from colliding beams of protons at 100 GeV each together with calculated A_N assuming (a) no hadronic flip-very low, (b) model prediction -even lower and (c) the best fit which gives an enormous spin-flip of $\tau = 1.2 - 0.042i$. I don't know what to make of this. All attempts to estimate a bound on this helicity, cf. Buttimore et al, come up with a number of about 0.15. More hard work is needed.

Analyzing Power for pp2pp at s=200[2]

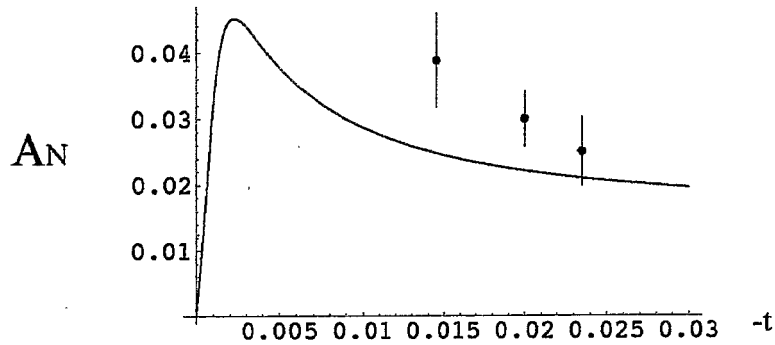

no hadronic spin flip
$\tau=0$

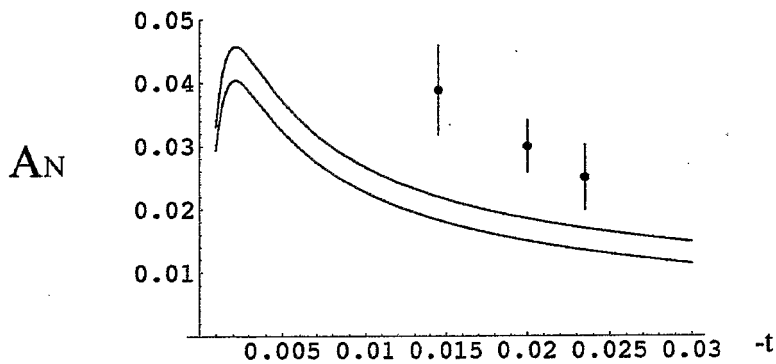

Model predictions

$\tau P = -0.02 \quad \tau = -0.025 - 0.0027\,i$

$\tau P = +0.09 \quad \tau = +0.076 - 0.0072\,i$

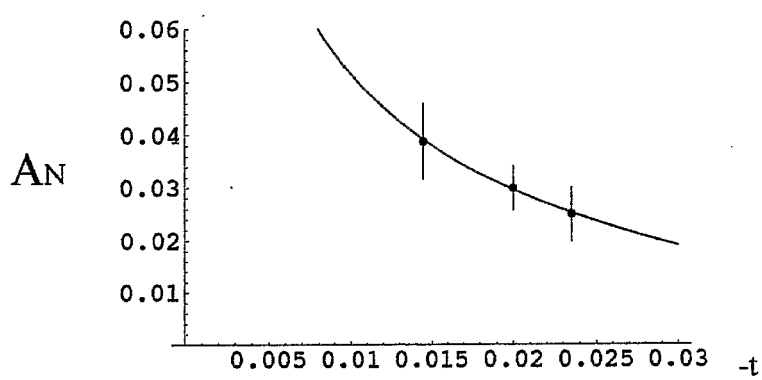

Best fit

$\tau = -1.2 - 0.042\,i$

Spin dynamics for high energy protons

Nigel Buttimore

University of Dublin

Trinity College

October 8, 2004

RSC 2004 October 8 – 9 Torino

Lagrange

born at via Lagrange within Torino, 1736

worked in Torino, Berlin, and Paris, 1813

Hamilton

born in Dublin at 12pm, August 3, 1805

worked all his life near Dublin until 1865

events: www.hamilton.tcd.ie

Summary

- New spin frontier from RHIC pp collider
- Partonic spin structure of the nucleon
- Scaled proton proton helicity amplitudes
- Rôle in understanding analyzing powers
- Longitudinal and transverse asymmetries
- Spin dependence studies for polarimetry
- Conclusions

Introduction

Polarized proton beams facilitate a study of the spin dependent amplitudes of pp elastic scattering, particularly

$$\phi_+(s,0) \propto \sigma_{\rm tot}\,(i+\rho)$$

$$\phi_-(s,0) \propto \Delta\sigma_L\,(i+\rho_-)$$

$$\phi_2(s,0) \propto \Delta\sigma_T\,(i+\rho_2)$$

$$\phi_5(s,t) \propto \sqrt{-t}$$

with the definitions, $\phi_\pm = (\phi_1 \pm \phi_3)/2$ where ϕ_+ here refers to the dominant spin averaged proton proton amplitude.

Proton carbon elastic scattering has been successfully used by the E950 Collaboration as a polarimeter for RHIC. Polarized neutron studies could use forward deuteron carbon elastic scattering or helium-3 carbon elastic scattering for polarimetry. Understanding the hadronic spin dependence would increase the effectiveness of each polarimeter.

Kopeliovich, Lapidus, YaF 19 (1974) 340

Bourrely, Soffer, DW, NP B91 (1974) 386

NHB, Gotsman, Leader, PR D18 (1978) 694

Akchurin, NHB, Penzo, PR D51 (1995) 3944

NHB, BK, EL, JS, TLT, PR D59 (1999) 114010

NHB, Leader, Trueman, PR D64 (2001) 094021

JT IA MB BB GB AD .., PRL 89 (2002) 052302

Scaled amplitudes

Introduce ratios of amplitudes relative to the dominant imaginary proton proton amplitude Im ϕ_+

$$R_2 + i\,I_2 = \frac{\phi_2}{2\,\mathrm{Im}\,\phi_+}$$

$$R_- + i\,I_- = \frac{\phi_-}{\mathrm{Im}\,\phi_+}$$

$$R_5 + i\,I_5 = \left(\frac{m}{\sqrt{-t}}\right)\frac{\phi_5}{\mathrm{Im}\,\phi_+}$$

as such ratios are expected to have a variation in t that is less pronounced near the forward direction of scattering.

To first order in small quantities ρ, R_5, I_5, and Coulomb phase δ, the maximum of the pC asymmetry A_N occurs at t value

$$\frac{t_{\max}}{t_c} = \sqrt{3} - \rho - \delta - \frac{8}{\mu - 1} R_5 + \cdots$$

where $t_c = 8\,\pi\,\alpha/\sigma_{\rm tot}$ near interference. The maximum of $A_{\rm N}$ to first order is

$$\frac{4\,m\,A_{\max}}{\sqrt{-3\sqrt{3}\;t_c}} = (\mu - 1)\left[1 + \frac{\sqrt{3}}{2}(\rho + \delta)\right]$$

$$- 2\sqrt{3}\,R_5 - 2\,I_5 + \cdots$$

Similar expressions appear for the pp asymmetry A_N but with additional terms R_2, I_2, R_-, I_-, reflecting the more elaborate pp spin dependence.

- A positive value of ρ, about 0.10 over the RHIC energy range, would enhance the single spin asymmetry maximum

- A positive real or imaginary part of the single helicity flip amplitude would reduce the maximum of the asymmetry

- It would be helpful to know more about the augmented helicity flip amplitudes, R_5 and I_5, and generally R_2, I_2, R_-, I_- in the case of pp elastic scattering.

The spin dependent amplitudes of proton proton collisions are, in fact, accessible from asymmetry measurements undertaken in the interference region with both initial protons spin polarized.

Spin asymmetries

A_N, A_{NN}, A_{SS}, A_{LL}, A_{SL} have singular terms in t arising from CN interference. The scaled pp differential cross section

$$\mathcal{I}_0 \equiv \left(\frac{t}{e^{2Bt}\,\sigma_{\text{tot}}} \right) \frac{d\sigma}{dt}$$

with a logarithmic slope parameter $2B$ has a singular expansion in powers of t

$$\mathcal{I}_0 = \frac{4\pi}{\sigma_{\text{tot}}} \frac{\alpha^2}{t} + \alpha\, a_0 + \frac{\sigma_{\text{tot}}}{8\pi} b_0\, t + \cdots$$

where it is assumed here that coefficients like a_0, b_0 are essentially t-independent.

For initial protons both polarized along axis, N (normal to the scattering plane), or L (longitudinal), the t expansion is

$$A_{NN}\mathcal{I}_0 = \alpha\, a_{NN} + \frac{\sigma_{\rm tot}}{8\pi} b_{NN}\, t + \cdots$$

$$A_{LL}\mathcal{I}_0 = \alpha\, a_{NN} + \frac{\sigma_{\rm tot}}{8\pi} b_{LL}\, t + \cdots$$

Spin observables with both initial protons polarized along perpendicular axes S, L have a similar power series expansion in t

$$-A_{SL}\mathcal{I}_1 = \alpha\, a_{SL} + \frac{\sigma_{\rm tot}}{8\pi} b_{SL}\, t + \cdots$$

In identical pp scattering, $A_{LS} = A_{SL}$ and near the forward direction one could check the expected equality $A_{NN} \approx A_{SS}$.

Like A_{SL}, the spin asymmetry with one of the initial protons polarized has a $\sqrt{-t}$ factor and so in

$$-A_N \mathcal{I}_1 \;=\; \alpha\, a_N \frac{\sigma_{\rm tot}}{8\pi} + b_N\, t + \cdots$$

it is convenient to define another scaled unpolarized differential cross section

$$\mathcal{I}_1 \equiv \frac{m\sqrt{-t}}{e^{2Bt}\sigma_{\rm tot}} \cdot \frac{d\sigma}{dt}$$

The eight expressions for the measurable coefficients, a_j, b_j, of the asymmetry expansions are sufficient to determine

$$R_j,\, I_j, \quad j = +,\, -,\, 2,\, 5$$

or at least bounds on these amplitudes.

Table 1: The expansion coefficients a_j

Observable	a_j
$\mathcal{I}_0$	ρ
$A_{NN}\mathcal{I}_0$	R_2
$A_{LL}\mathcal{I}_0$	R_-
$-A_{SL}\mathcal{I}_1$	$\kappa(R_2 + R_-)/2$
$-A_N\mathcal{I}_1$	$I_5 - \kappa(1 + I_2)/2$

Recall that for A_N , the occurence of the single helicity flip value I_5 in the coefficient a_N presented a difficulty for polarimeter normalization as does, incidentally, a non-zero value of I_2 .

Only the single helicity flip amplitude represents a problem for proton carbon elastic scattering with just two helicity amplitudes or for deuteron carbon elastic scattering with four helicity amplitudes.

Table 2: The expansion coefficients b_j

Observable	b_j
$\mathcal{I}_0$	$(1+\rho^2+R_-^2+I_-^2)/2+R_2^2+I_2^2$
$A_{NN}\mathcal{I}_0$	$R_2(\rho+R_-)+I_2(1+I_-)$
$A_{LL}\mathcal{I}_0$	$\rho R_- + I_- + R_2^2 + I_2^2$
$-A_{SL}\mathcal{I}_1$	$R_5(R_2+R_-)+I_5(I_2+I_-)$
$-A_N\mathcal{I}_1$	$I_5(\rho+R_2)-R_5(1+I_2)$

Analyzing power

- The analyzing power for polarized protons has a maximum in the Coulomb interference momentum transfer region.
- Spin effects change the value of the maximum expected on theoretical grounds in the absence of such effects.
- Many spin dependent terms can be obtained from double spin asymmetry measurements near forward angles.
- A study of the energy dependence of individual terms via interpolation, or

through the use of analyticity relations, would assist the understanding of their contribution to other processes such as deuterium or helion carbon elastic scattering

- The dipole magnetic moment of the deuteron $\mu_{\mathrm{d}} = 0.8574$ is less than the proton's $\mu_{\mathrm{p}} = 2.7928$ changing the maximum in the pC analyzing power to a small minimum in the dC analyzing power near the interference region.

- Isolating helicity dependent terms could elicit their energy and momentum transfer dependence and facilitate the understanding of proton spin structure.

Conclusions

- Understanding hadronic spin dependence assists polarimetry
- Change in maximum analyzing power at interference
- Implications for polarized deuteron and helion beams
- Causality test via analyticity of spin dependent amplitudes
- Measurement of double spin asymmetries near forward direction

Transversity measurements in SIDIS

RHIC-SPIN Meeting

Oct, 8-9,Torino, Italy

Ralf Seidl
(University of Illinois at UC, RBRC)

Outline

- Motivation: Transversity
- Measuring Transversity in SIDIS
  transverse momentum dep. functions ⇨SSA
- HERMES
- Interpretation of the results
- COMPASS
- Towards a global analysis
- Outlook

Measuring Transversity

Leading Twist quark distributions

- Unpolarized quarks in unpolarized nucleon
- Momentum fraction q(x) of the quarks
- Related to vector charge of the nucleon

$$\langle PS|\overline{\psi}\gamma^{\mu}\psi|PS\rangle = \int_0^1 dx(q(x)-\overline{q}(x))$$

Well known

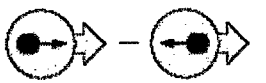

- Longitudinally polarized quarks in longitudinally polarized nucleon
- Helicity difference $\Delta q(x)$ of the quarks
- Related to axial charge of the nucleon

$$\langle PS|\overline{\psi}\gamma^{5}\gamma^{\mu}\psi|PS\rangle = \int_0^1 dx(\Delta q(x)+\Delta\overline{q}(x))$$

known

- Transversely polarized quarks in transversely polarized nucleon
- Transverse spin difference $\delta q(x)$ of the quarks
- Related to vector charge of the nucleon

$$\langle PS|\overline{\psi}\sigma^{\mu\nu}\psi|PS\rangle = \int_0^1 dx(\delta q(x)-\delta\overline{q}(x))$$

unknown

Transversity properties

- Helicity flip amplitude
- Chiral odd
- Since all interactions conserve chirality one needs another chiral odd object
- Does not couple to gluons ⇨different QCD evolution than $\Delta q(x)$
- Valence dominated⇨ Comparable to Lattice calculations

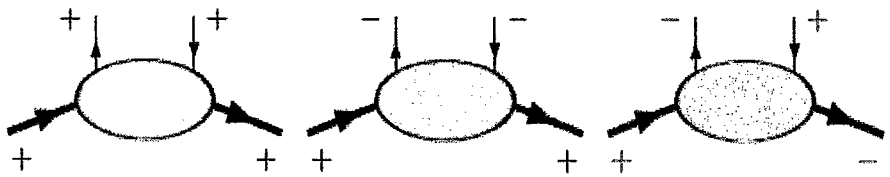

$$q(x) = q_+(x) + q_-(x) \sim Im(\mathcal{A}_{++,++} + \mathcal{A}_{+-,+-})$$
$$\Delta q(x) = q_+(x) - q_-(x) \sim Im(\mathcal{A}_{++,++} - \mathcal{A}_{+-,+-})$$
$$\delta q(x) = q_\uparrow(x) - q_\downarrow(x) \sim Im\mathcal{A}_{+-,-+}$$

Positivity bound:

$$|\delta q(x)| \leq q(x)$$

Soffer bound:

$$|\delta q(x)| \leq \tfrac{1}{2}(q(x) + \Delta q(x))$$

Finding another chiral odd object in SIDIS
⇨ Collins fragmentation function

Cross section factorizes: $\sigma^{ep\to ehX} = \Sigma_q q^{p\to q}(x) \quad \sigma_{QED} \quad D^{q\to h}(z)$

Transverse momentum dependent Distribution functions

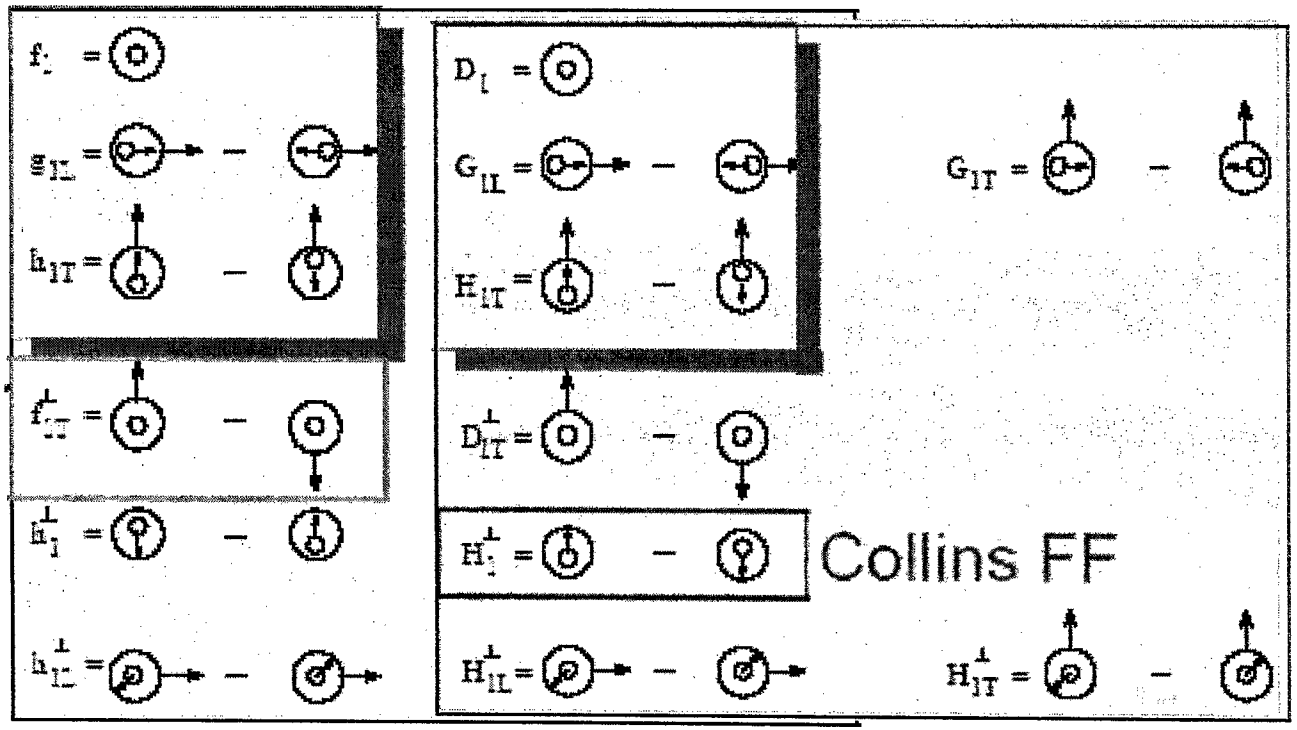

Both Sivers and Collins Effect create azimuthal asymmetries

Azimuthal Asymmetries

- Sivers and Collins effect are not distiguishable with longitudinally polarized target
- Higher Twist effects are kinematically favored in longitudinal case
- With transversely polarized target a 2nd angle allows to distinguish

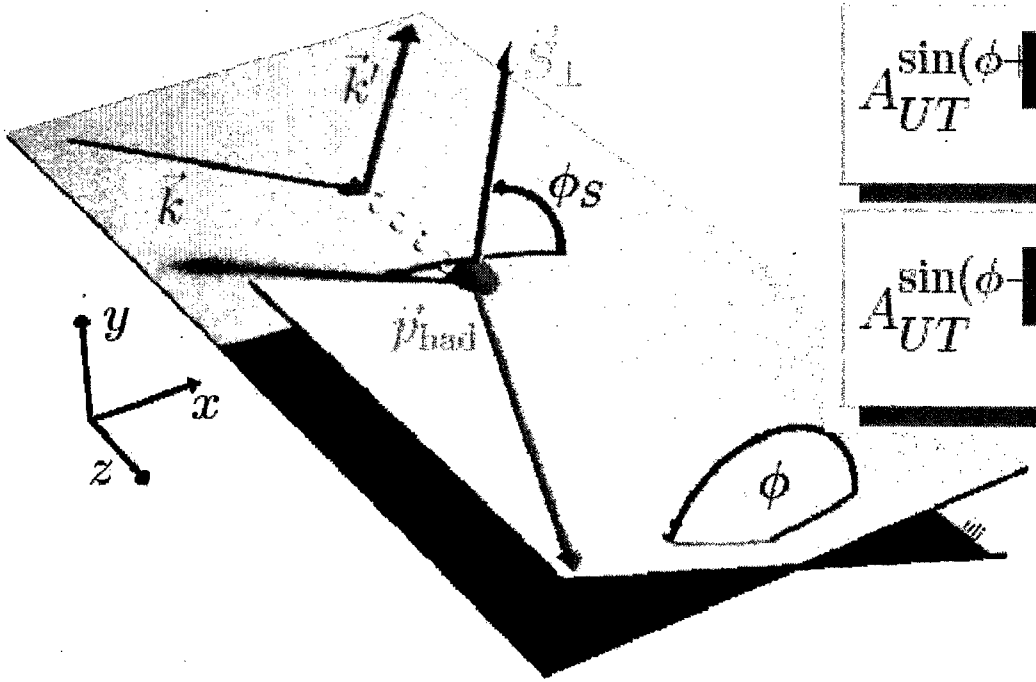

$$A_{UT}^{\sin(\phi+\text{[redacted]})} \propto S_\perp \frac{\sum_{q,\bar{q}} e_q^2 \delta q(x)\, H_1^\perp(z)}{\sum_{q,\bar{q}} e_q^2 q(x)\, D_1(z)}$$

$$A_{UT}^{\sin(\phi-\text{[redacted]})} \propto S_\perp \frac{\sum_{q,\bar{q}} e_q^2 f_{1T}^{\perp,q}(x) \cdot D_1(z)}{\sum_{q,\bar{q}} e_q^2 q(x)\, D_1(z)}$$

U: unpolarized beam
T: transversely polarized target

The HERMES experiment

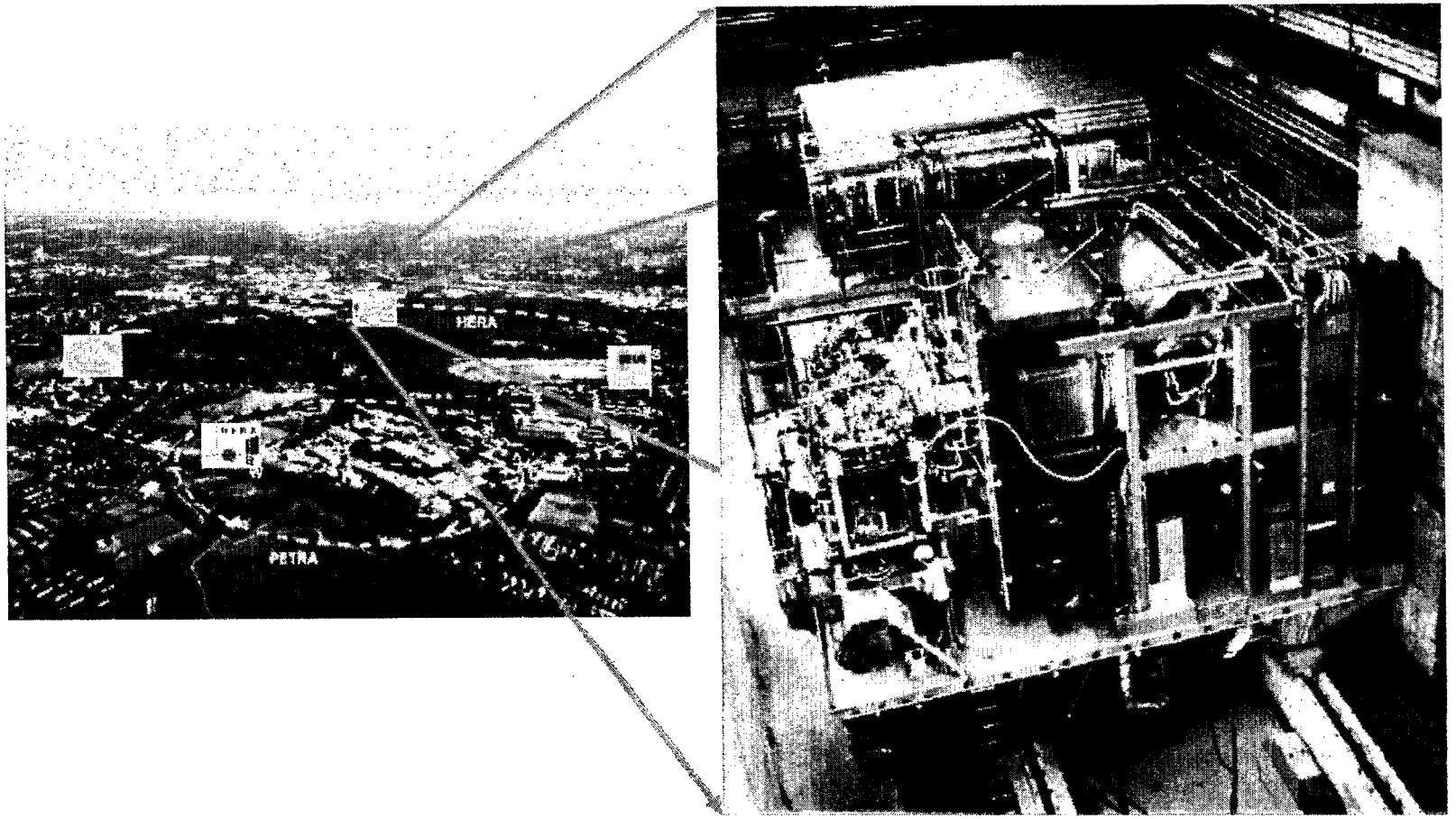

The HERMES spectrometer

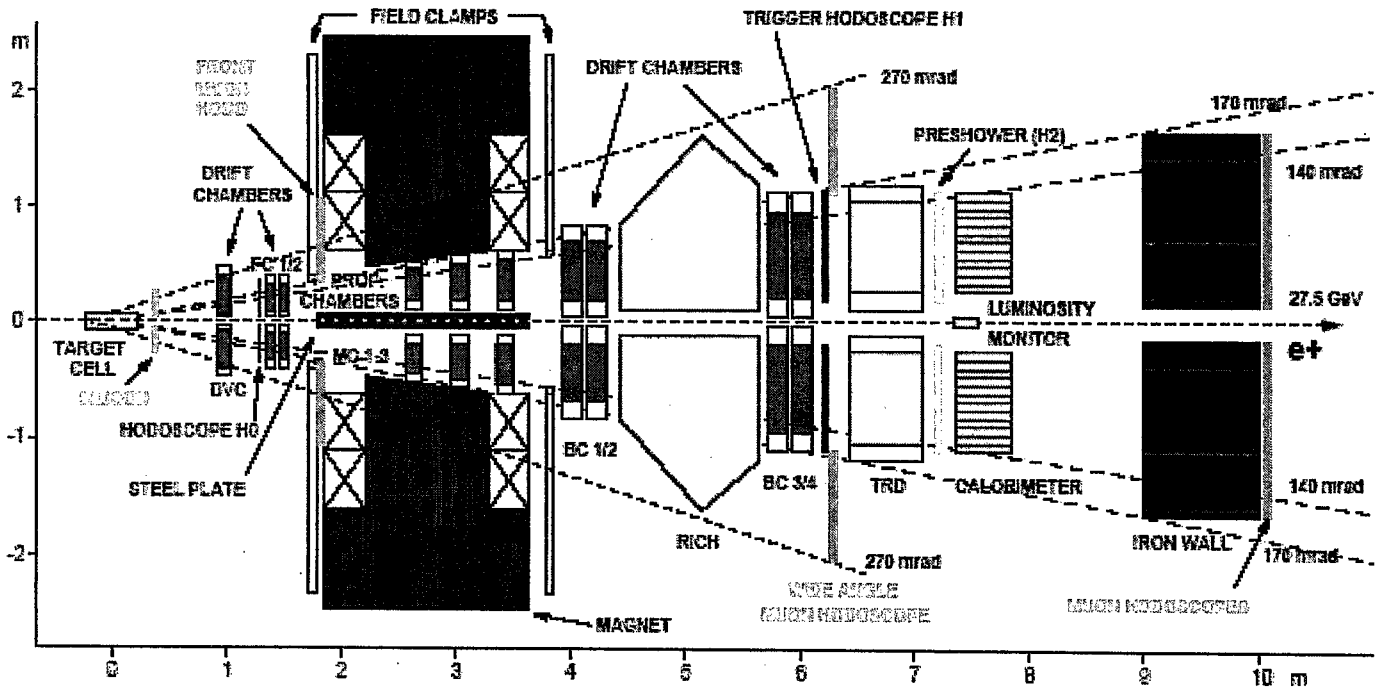

- Kinematic range $0.023 < x < 0.8$ for $Q^2 > 1$ GeV^2 and $W > 2$ GeV
- Momentum resolution $\Delta p/p = 1.4..2.5\%$, angular resolution $\Delta\theta < 1$ mrad
- Particle Identification: and (>1998)

Asymmetry reconstruction

$$A^h_{UT}(\phi,\phi_S) = \frac{1}{S_T}\frac{N^{\uparrow}_h(\phi,\phi_S)-N^{\downarrow}_h(\phi,\phi_S)}{N^{\uparrow}_h(\phi,\phi_S)+N^{\downarrow}_h(\phi,\phi_S)}$$
$$= \bar{A}^h_C \sin(\phi+\phi_S) + \bar{A}^h_S \sin(\phi-\phi_S)\cdots$$

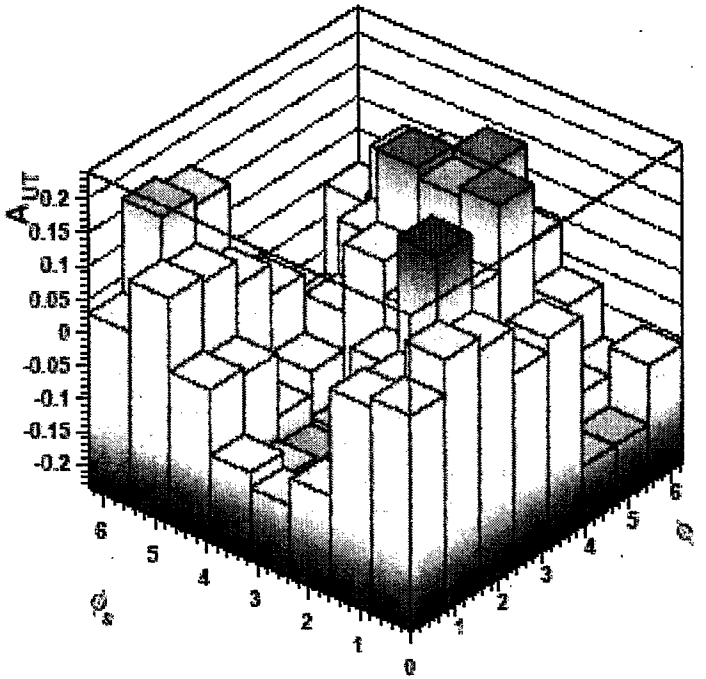

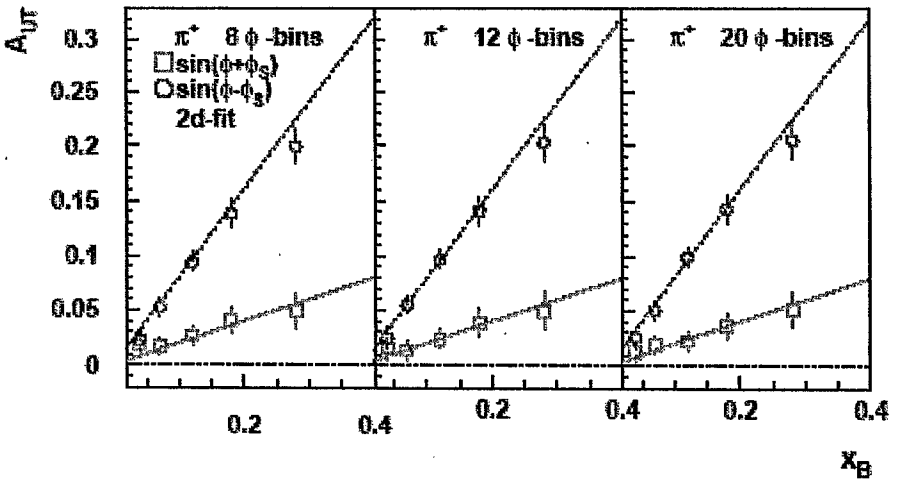

fit both asymmetries simultaneously

Unweighted results

Collins Type Moments

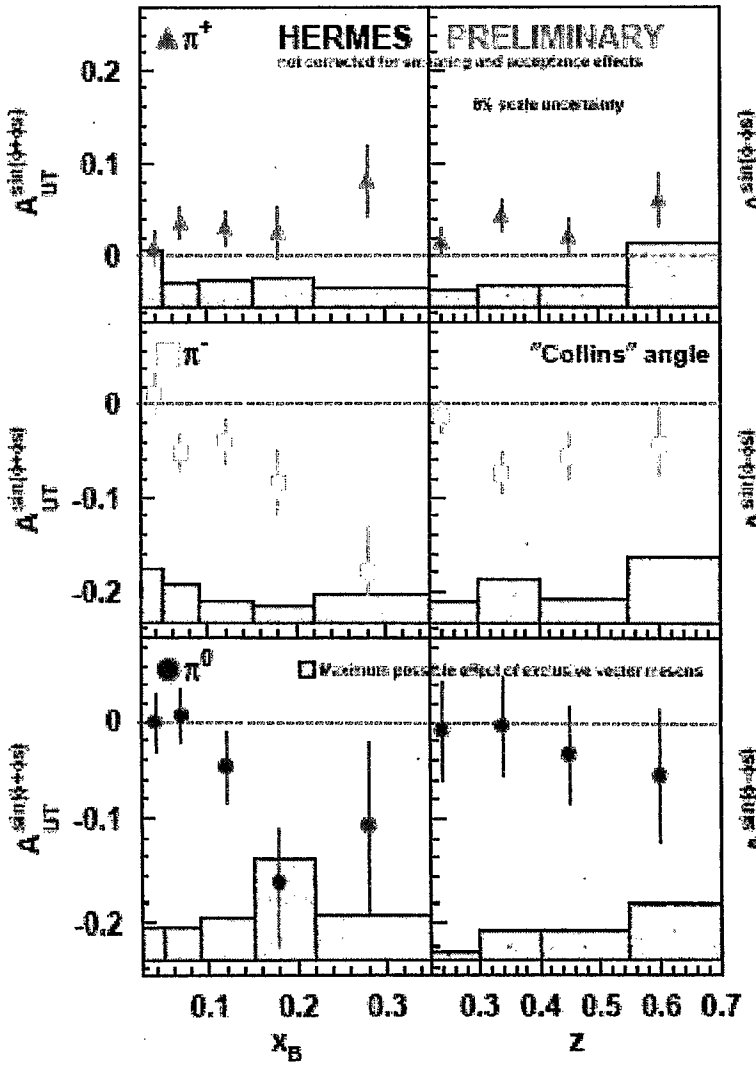

Sivers Type Moments

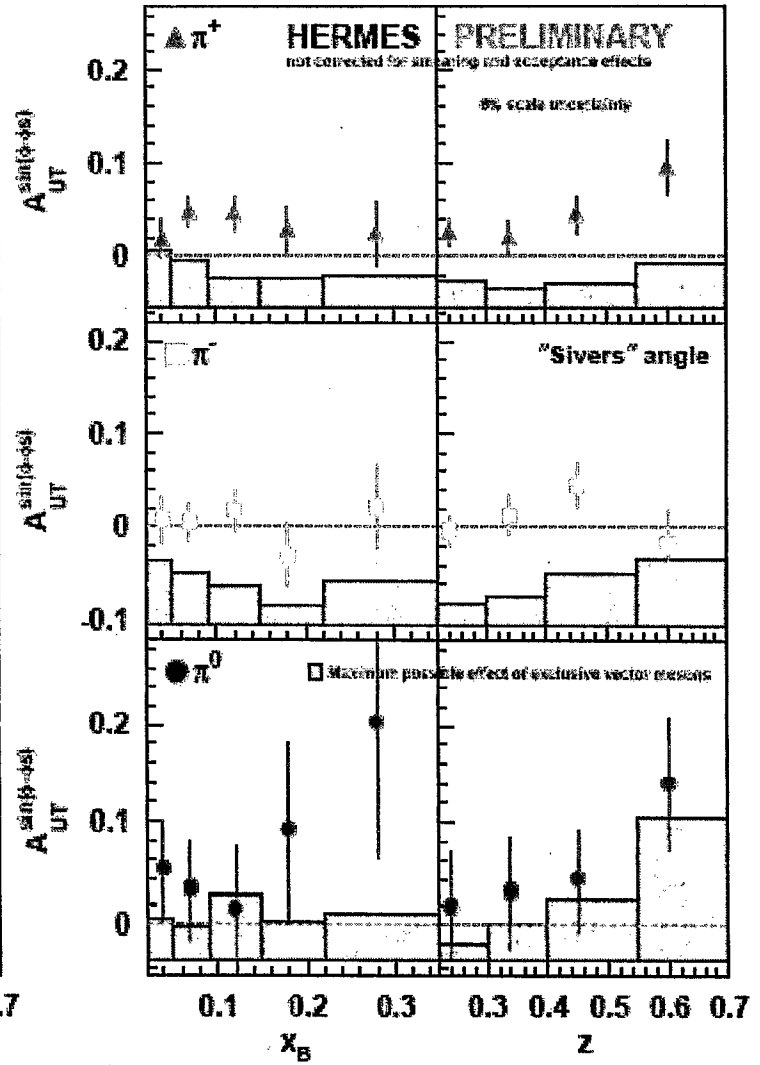

...of signs and moments

transverse cross section contains convolution integrals over intrinsic transverse momenta:

$$d^6\sigma_{UT} \approx |S_T| \sum_q e_q^2 \left(B(y)\sin(\phi+\phi_S)\mathcal{I}\left[\frac{\mathbf{k}_T\cdot\hat{P}_{h\perp}}{M_h}\delta q H_1^{\perp,q}\right] + A(y)\sin(\phi-\phi_S)\mathcal{I}\left[\frac{\mathbf{p}_T\cdot\hat{P}_{h\perp}}{M_N} f_{1T}^{\perp,q} D_1^q\right] + \cdots \right)$$

$$H_1^{\perp(1)}(z) \equiv \int d\boldsymbol{k}_T^2 \left(\frac{k_T^2}{2M_h}\right) H_1^{\perp}(z, \boldsymbol{k}_T^2)$$

$\frac{P_{h\perp}}{M}$ weighted moments decouple integrals:

$$A_C^h \approx 2|S_T| \frac{\sum_q e_q^2 \delta q H_1^{\perp(1),q}}{\sum_q e_q^2 q D_1^q}$$

$$A_S^h \approx -2|S_T| \frac{\sum_q e_q^2 f_{1T}^{\perp(1),q} D_1^q}{\sum_q e_q^2 q D_1^q}$$

- Unweighted moments can only be decoupled using assumptions on $\mathbf{k}_T$ or $\boldsymbol{p}_T$ distributions
- Signs come from integration and angle definition (HERMES' definition taken)

$\frac{P_h^{\perp}}{zM_h}$ -weighted results

Collins Type Moments

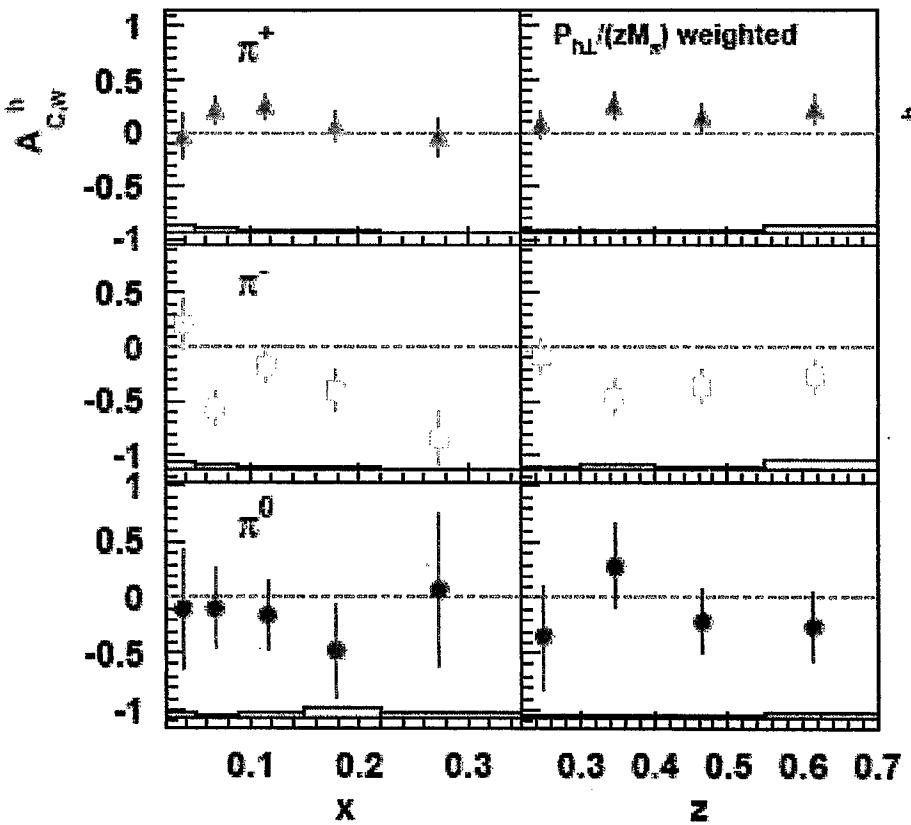

Sivers Type Moments

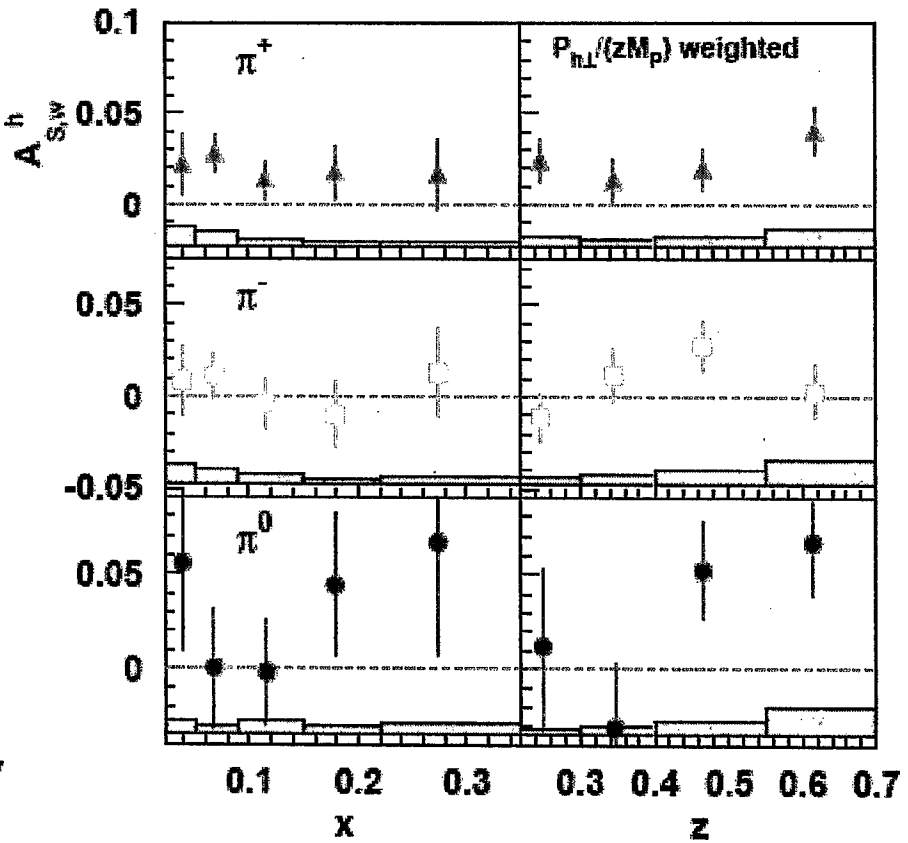

Integrated Sivers results

Assumptions/Input:

- Asymmetry is leading Twist
- Take only light quarks
- Favored / disfavored Isospinsymmetry

$$D_{fav} \equiv D_1^{u\to\pi^+} = D_1^{d\to\pi^-} \cdots$$
$$D_{dis} \equiv D_1^{u\to\pi^-} = D_1^{d\to\pi^+} \cdots$$

- Calculate FF from Kretzer LO parameterization **[Eur.Phys.J.C22:269-276,2001]**
- CTEQ6LO for unpol. q PDFs

$$A_S^{\pi^+} = -2\frac{(4f_{1T}^{\perp,(1),u}+f_{1T}^{\perp,(1),d})D_{fav}+(f_{1T}^{\perp,(1),d}+4f_{1T}^{\perp,(1),\bar{u}})D_{dis}}{(4u+d)D_{fav}+(d+4\bar{u})D_{dis}}$$

$$\cdot$$

$$\cdot$$

$$\frac{f_{1T}^{\perp,(1),u}(x)+1/4f_{1T}^{\perp,(1),d}(x)}{u(x)+1/4d(x)} = -0.035 \pm 0.011$$

$$\frac{f_{1T}^{\perp,(1),d}(x)+4f_{1T}^{\perp,(1),\bar{u}}(x)}{u(x)+4\bar{u}(x)} = 0.056 \pm 0.036$$

- Clear nonzero values for Sivers functions
- Large Sivers function for negative light quarks, but sea contribution might be sizeable
- Theory predictions favor small *d* -Sivers function

Sivers interpretation

- Attractive rescattering of hit quark by gluon creates transverse momentum
- M.Burkardt [hep-ph0309269] – impact parameter formalism
- Orbital angular momentum at finite impact parameter
- observed and true x differ
- Observable left/right asymmetry

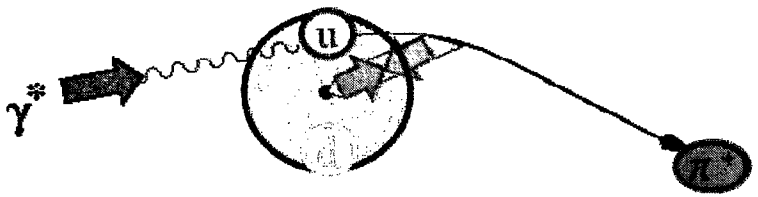

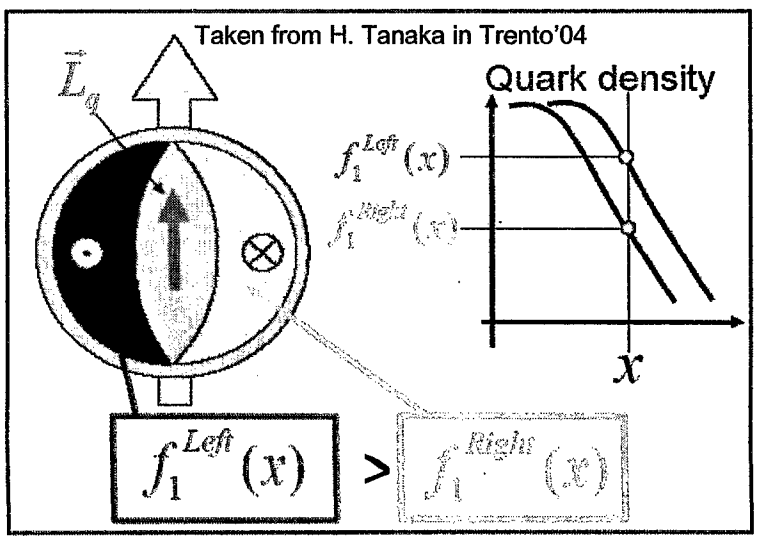

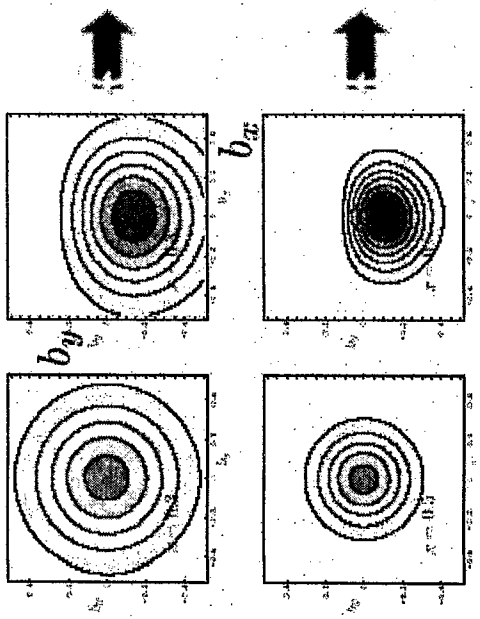

Interpretation of the HERMES Collins results

The Collins results for π^+,π^- and π^0 show an unexpected behavior...
Expectation: u-quark dominance in Quark distributions
$\delta u > 0, \delta d < 0 \Rightarrow A^{\pi^+} > A^{\pi^0} > 0$
and $A^{\pi^-} \leq 0$ and $|A^{\pi^-}| < |A^{\pi^+}|$
New data for $A_{UT}^{Collins}$ shows $A^{\pi^+} > 0$
but $A^{\pi^0} \simeq A^{\pi^-} < 0$ and $|A^{\pi^-}| > |A^{\pi^+}|$

- Internal consistency check depending on known quantities fulfilled for weighted and unweighted Asymetries within 1σ
- Take unpolarized quantities from Parameterizations and sample around measured Asymmetries to fill solution space in:

$$\delta r = \frac{\delta d + 4\delta\bar{u}}{\delta u + 1/4\delta d} \qquad \eta_H = H_{1,dis}^{\perp}/H_{1,fav}^{\perp} \qquad \mathcal{K} = \frac{\delta u + 1/4\delta\bar{d}}{u + 1/4\delta\bar{d}} \frac{H_{1,fav}^{\perp}}{D_{1,fav}}$$

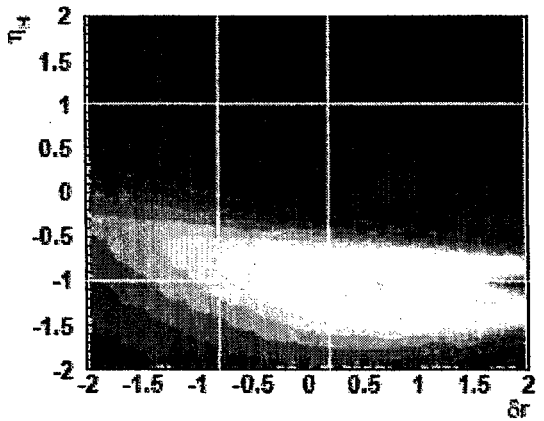

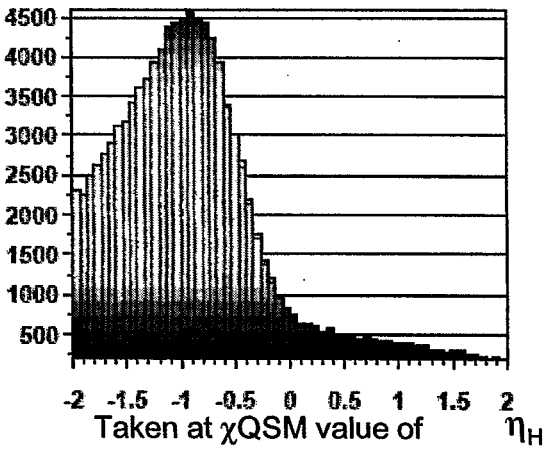

Taken at χQSM value of δr = -0.30 of Schweitzer and Wakamatsu

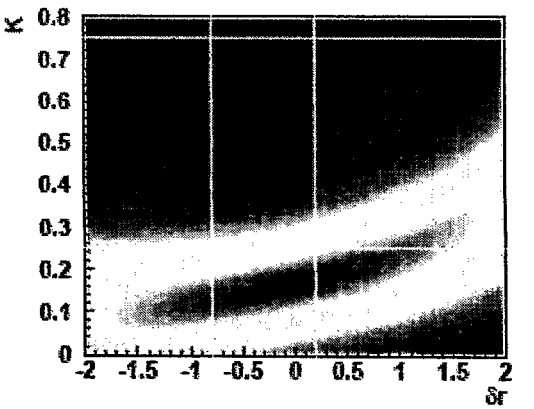

Interpretation of the HERMES Collins results

Possible explanation: $H^{\perp}_{1,\mathrm{dis}} \approx -H^{\perp}_{1,\mathrm{fav}}$?

Artru model

[hep-ph9310323]

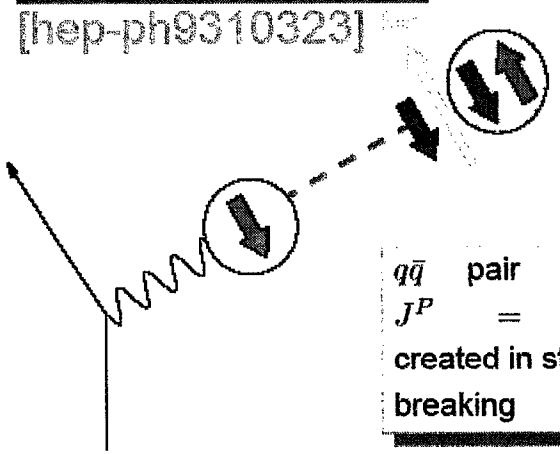

First π heads into the plane

$q\bar{q}$ pair with $J^P = 0^+$ created in string breaking

unpol. Lund MC

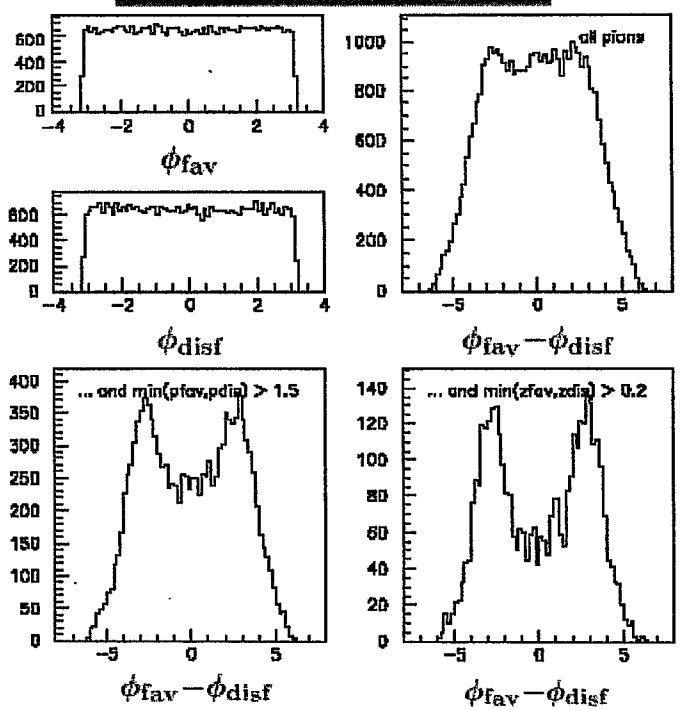

The COMPASS experiment@CERN

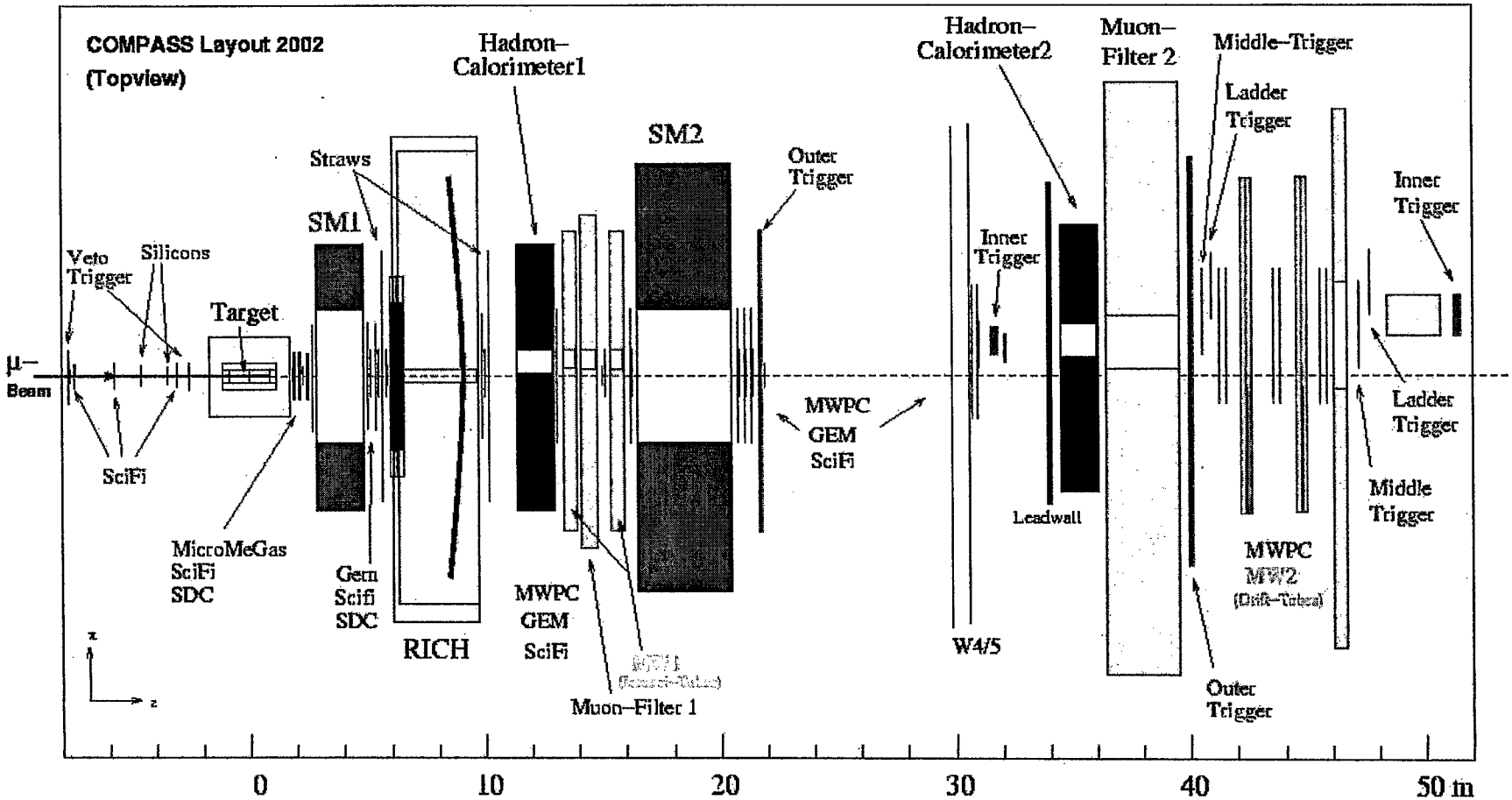

Beam: $2 \cdot 10^8$ μ^+/ spill (4.8s/16.2s) **Beam momentum:** 160 GeV/c

Luminosity: $\sim 5 \cdot 10^{32}$ cm^{-2} s^{-1} **Beam polarization:** -76%

Unweighted Collins results

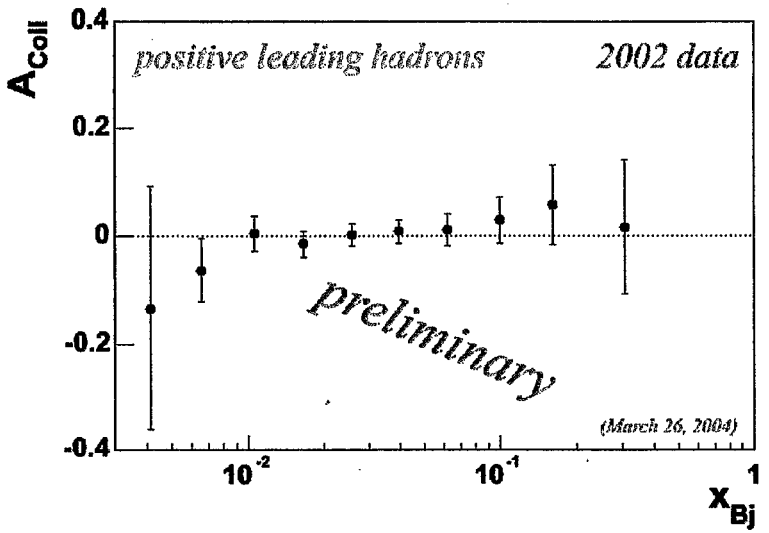

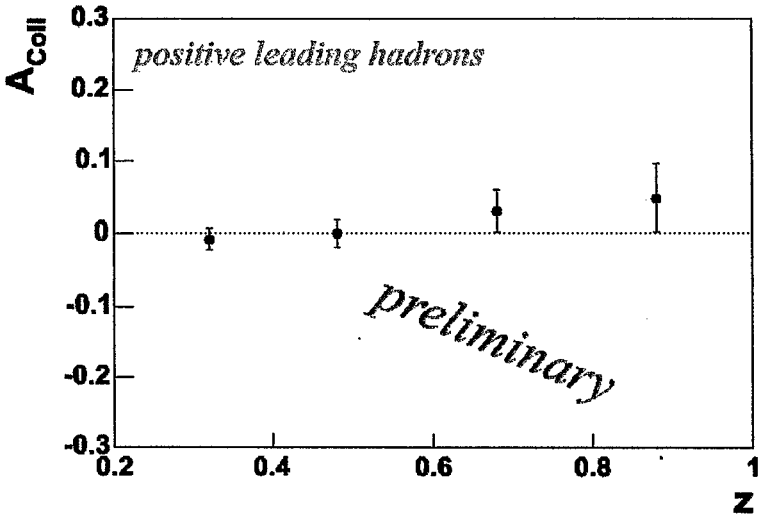

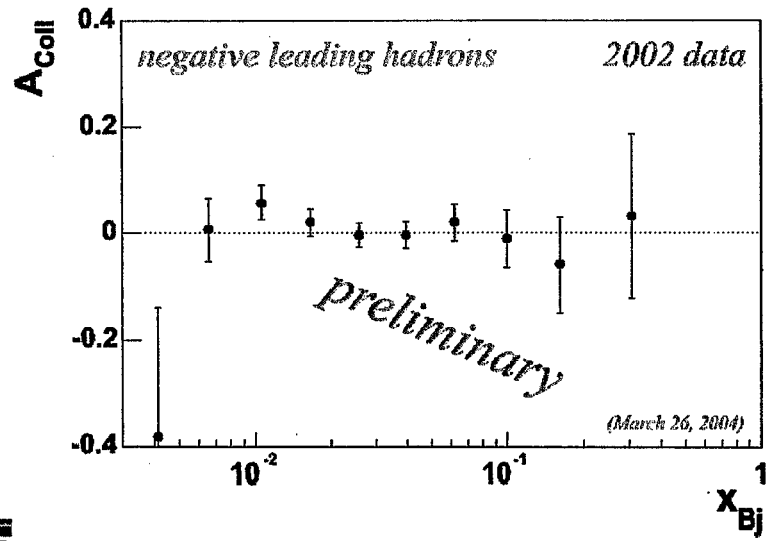

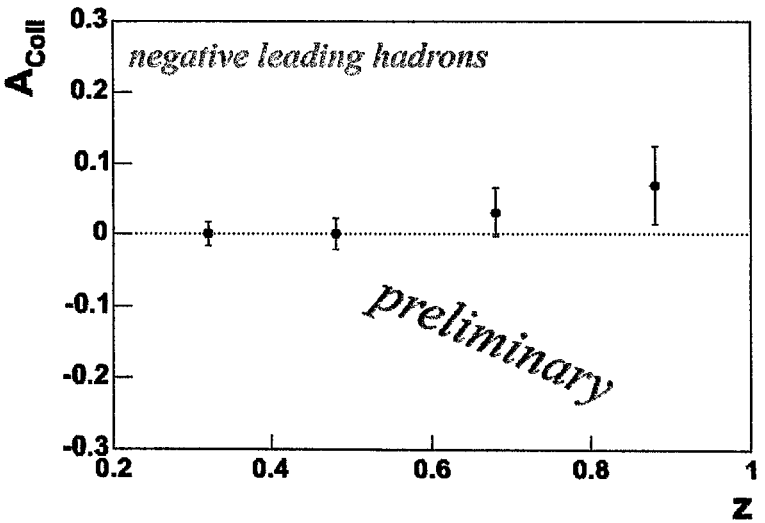

Definitions of Collins angle differ by π from HERMES

Interference Fragmentation

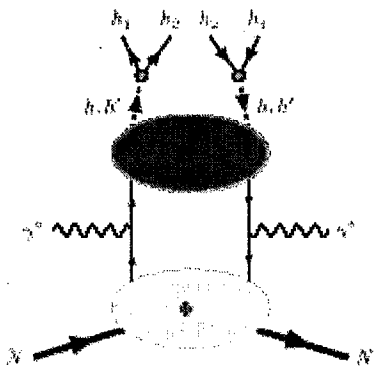

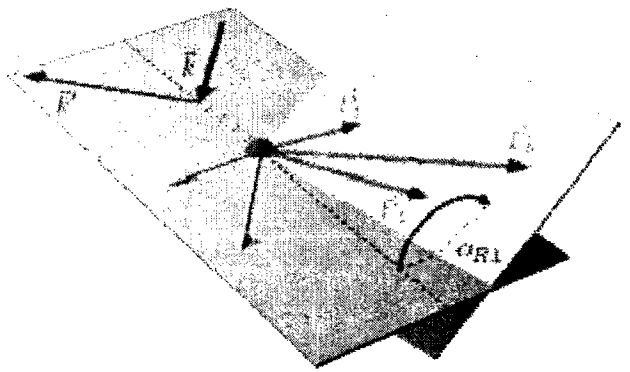

- Production of 2 Mesons around $\rho(\pi^+\pi^-)$, $\phi(K\bar{K})$ or $K^*(K\pi)$ mass region
- Interference of s- und p-waves of 2-meson-system
- different mechanisms proposed with different M_h behaviour

$$\cos\phi_{RT} = \frac{\vec{P}_+ \times \vec{P}_- \cdot \vec{k} \times \vec{k}'}{|\vec{P}_+ \times \vec{P}_-| \cdot |\vec{k} \times \vec{k}'|}$$

$$\frac{d^7\sigma_{UT}}{d\zeta dM^2_{\pi\pi} d\phi_R dz dx dy d\phi_S} = \sum_q \frac{2\alpha^2 e_q^2}{sM^2_{\pi\pi}} |\mathbf{S}_T||R| B(x,y) \sin(\phi_R + \phi_S) \sin\Theta \delta q \left[H^{\sphericalangle q}_{1,UT} + H^{\sphericalangle q}_{1,LT} \cos\Theta \right]$$

First IFF results from HERMES

- Jaffe at al. [Phys. Rev. Lett. **80** (1998)] : inv. mass behavior out of $\pi\pi$-phaseshift analysis⇨sign change at ρ–mass
- Radici et al. [Phys. Rev. **D65** (2002)] : Spectator model in the s-p channel ⇨no sign change

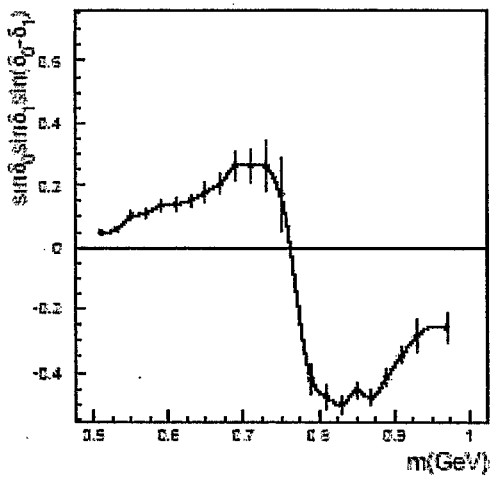

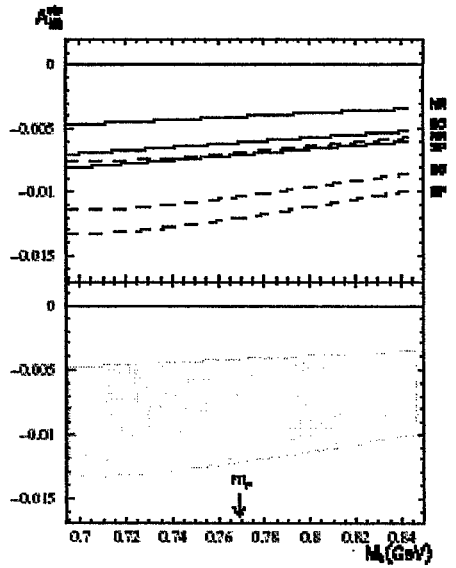

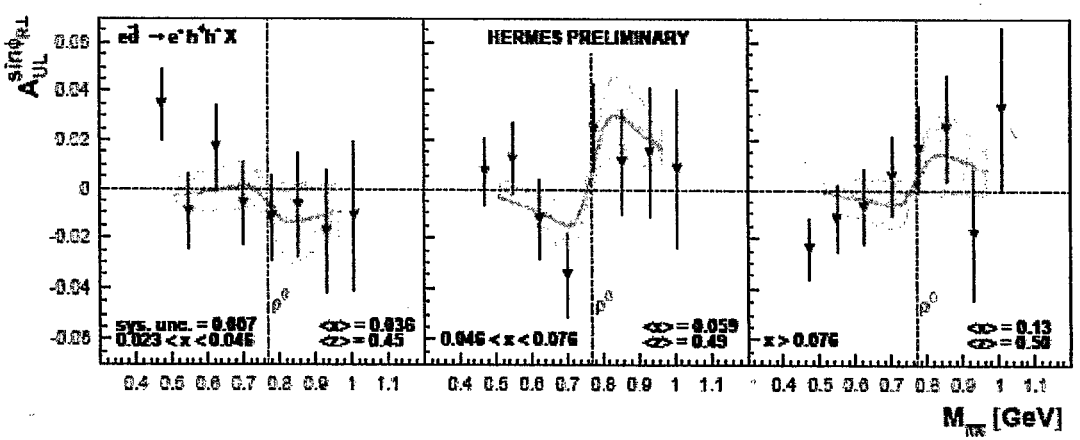

News from COMPASS next week(?)

Transversity extraction

$$A_{UT}^{\sin\phi,h}(x_i) \approx \frac{\sum_q e_q^2 \delta q(x_i) \cdot \int dz H_{1,q}^h(z,Q^2) \mathcal{A}(x_i,Q^2,z)}{\sum_{q'} e_{q'}^2 q(x_i) \cdot \int dz D_{1,q'}^h(z,Q^2) \mathcal{A}(x_i,Q^2,z)}$$

$$= \sum_q \underbrace{\frac{e_q^2 q(x_i) \cdot \mathcal{H}_{1,q}^h(z,Q^2,x_i)}{\sum_{q'} e_{q'}^2 q(x_i) \cdot \mathcal{D}_{1,q'}^h(z,Q^2,x_i)}}_{2P_{q'}^h(x_i)} \cdot \frac{\delta q}{q}(x_i)$$

- purities are completely unpolarized objects → present MC-tunes can be used
- for Transversity extraction Collins FF has to be known ⇒ BELLE e^+e^- Collins Analysis!
- for Sivers extraction everything to generate Purities is known (Analysis ongoing)

Purity method

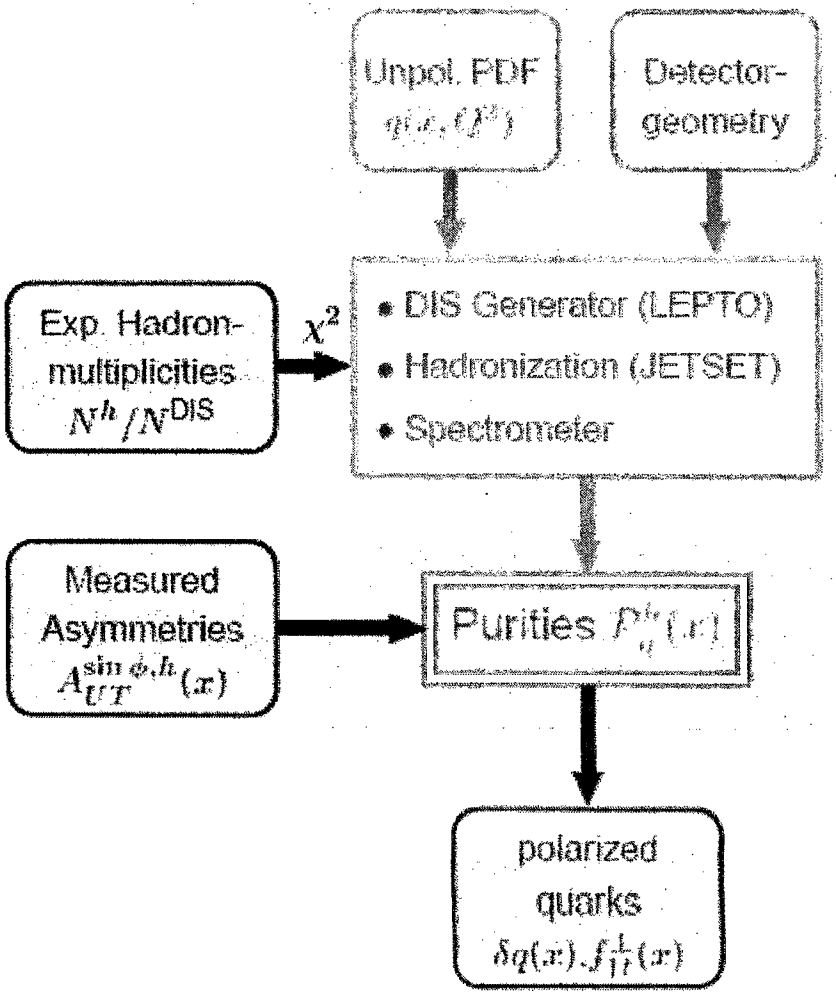

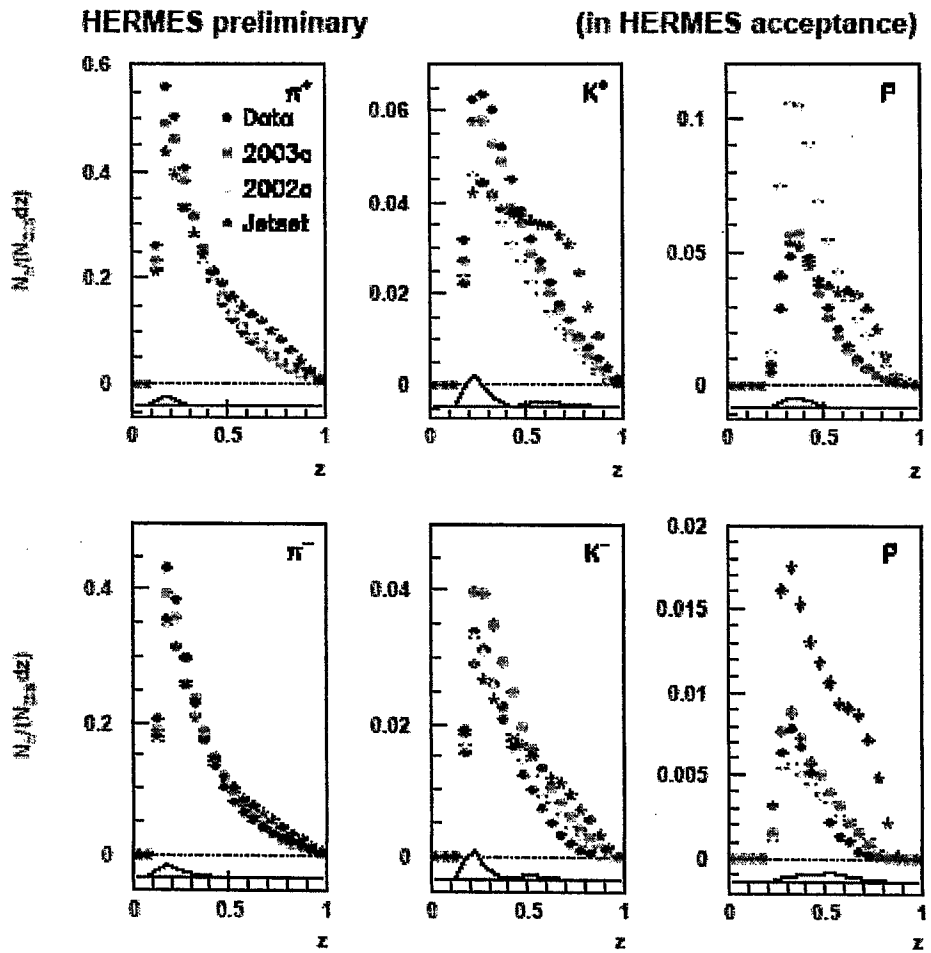

Global Transversity Analysis needed

SIDIS experiments (HERMES and COMPASS) measure $\delta q(x)$ together with either Collins Fragmentation function $H_1^{\perp}(z)$ or Interference Fragmentation function

RHIC measures the same combinations of quark Distribution (DF) and Fragmentation Functions (FF) plus unpolarized DF q(x)

[redacted]

Universality has been proven recently by Collins and Metz: **[hep-ph/0408249]**

[redacted]

Summary and Outlook

- First direct Collins Asymmetries measured in HERMES and COMPASS
- First access to Transversity via Interference Fragmentation functions observed at HERMES
- Indication that disfavored Collins function is large and negative relative to favored Collins function
- Additional input from BELLE spin dependent Fragmentation function analysis needed

- First observation of a nonzero Sivers function at HERMES
- Integrated results from HERMES show sizeable results for light quark Sivers functions → first access to quark's orbital angular momentum
- more results to be expected in the next years

Additional results to come from RHIC and eRHIC

Cuts

- $0.023 < x < 0.4$
- $0.1 < y < 0.85$
- $Q^2 > 1\ GeV^2$
- $W^2 > 10\ GeV^2$
- $\theta_{\gamma h} > 20$ mrad
- $0.2 < z < 0.7$, all hadrons
- $2\ GeV < P_h < 15\ GeV$
- invariant π^0 mass: $0.1\ GeV < m_{\gamma\gamma} < 0.17\ GeV$

Year	Polarization	# event
<2001	L	8.9M (D) 2.4M (P)
2002	T	0.9M (P)
2003-2004	T	1.7M (P)

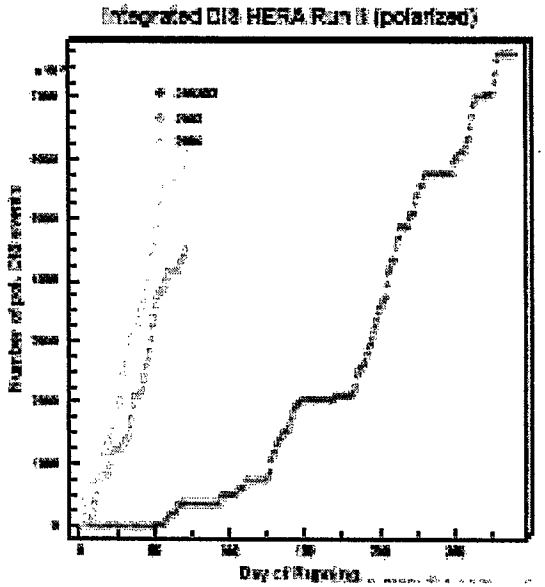

Interpretative uncertainties by exclusive VMs

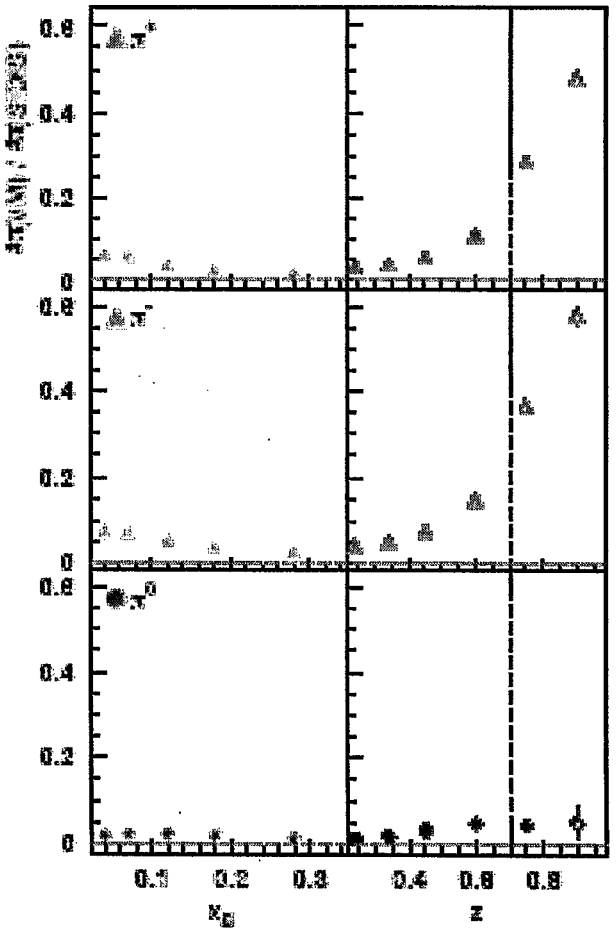

- decay pions of excl. ρ, ω in data sample
- dilutions not negligible
- conservative approach: calculate transfer for maximal ρ asymmetries: $A_{UT}^{Collins,\rho}$ and $A_{UT}^{Sivers,\rho} = \pm 1$
- Positivity limits reduce uncertainties
  ➡ $\sigma(A_{UT}^{Collins,\rho})$ and $\sigma(A_{UT}^{Sivers,\rho}) = \frac{1}{\sqrt{6}}$

Collins interpretation: formulae

Minimal assumptions

- $A_{UT}^{Collins}$ is leading Twist
- Collins FF follows favoured/disfavoured symmetry

$$H_{fav} \equiv H_{1,\perp}^{u\to\pi^+} = H_{1,\perp}^{d\to\pi^-} \ldots$$

$$H_{dis} \equiv H_{1,\perp}^{u\to\pi^-} = H_{1,\perp}^{d\to\pi^+} \ldots$$

$$A^{\pi^+} = k\frac{(4\delta u+\delta d)H_{fav}+(\delta d+4\delta\bar{u})H_{dis}}{(4u+d)D_{fav}+(d+4\bar{u})D_{dis}},$$

$$A^{\pi^-} = k\frac{\cdots}{\cdots}, \text{etc}$$

$$r \equiv \frac{d+4\bar{u}}{u+d/4} \qquad \eta \equiv \frac{D_{dis}}{D_{fav}}$$

$$\delta r \equiv \frac{\delta d+4\delta\bar{u}}{\delta u+\delta d/4} \qquad \eta_H \equiv \frac{H_{dis}}{H_{fav}}$$

Asymmetry ratios $\alpha^- \equiv A^{\pi^-}/A^{\pi^+}$ and $\alpha^0 \equiv A^{\pi^0}/A^{\pi^+}$

$\Rightarrow$ Consistency equation with only unpol. quantities

$$\alpha^- C = \alpha^0(1+C) - 1$$

with $C \equiv \frac{4\eta+r}{4+\eta r}$ $\Rightarrow$ solution space in η_H vs δr can be determined:

$$\eta_H = \frac{\delta r - 4(\alpha^- C)}{(\alpha^- C)\delta r - 4}$$

$$\eta_H = \frac{\delta r - 4(\alpha^0(1+C)-1)}{(\alpha^0(1+C)-1)\delta r - 4}$$

Short comment on HERMES A_{UT}

Makins, Athens'03; Seidl,DIS'04

HERMES (prelim.), Collins A_{UT},

$(E = 26.7\,GeV,\ W > 2\,GeV,\ 1 < Q^2 < 15\,GeV^2,$
$\langle z \rangle \approx 0.4,\ 0.2 < y < 0.85,\ 0.023 < x < 0.4,$
$P_{h\perp} > 0.4\,GeV).$

$$A_{UT}^{\sin(\phi+\phi_s)}(x,z) \propto \frac{\Sigma_a e_a^2\, x\, h_1^a(x)\, H_1^{\perp a/h}(z)}{\Sigma_b e_b^2\, x\, f_1^b(x)\, D_1^{b/h}(z)}$$

Transversally polarized proton target.

A.E., Goeke, Schweitzer EPJC32:337(03)

Our predictions was:

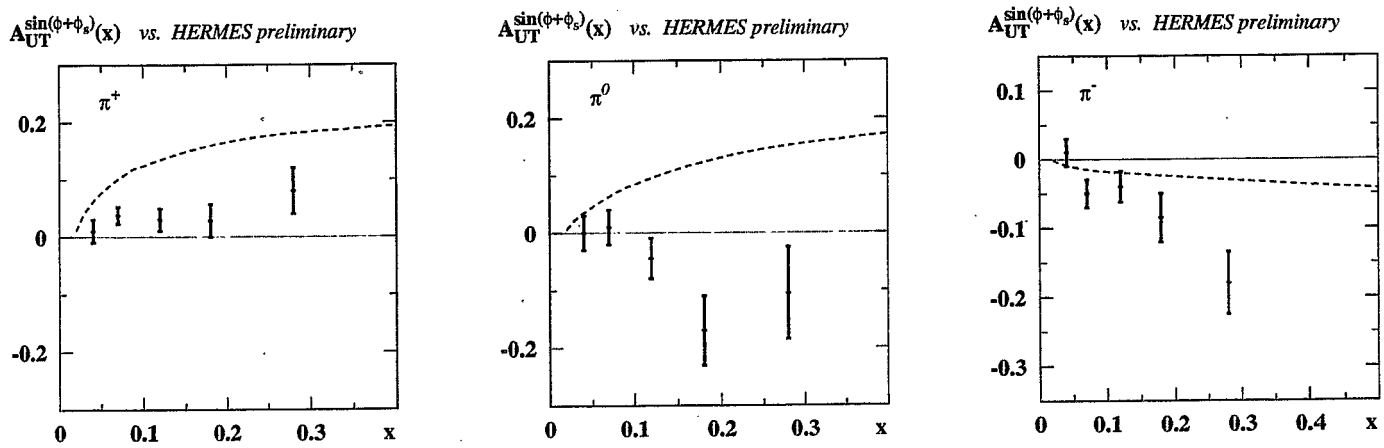

$\Uparrow$

Even sign is wrong for π^0!

New problem in spin physics?
How it could be possible that

$$0 > A(\pi^0) \cong A(\pi^-)\,?$$

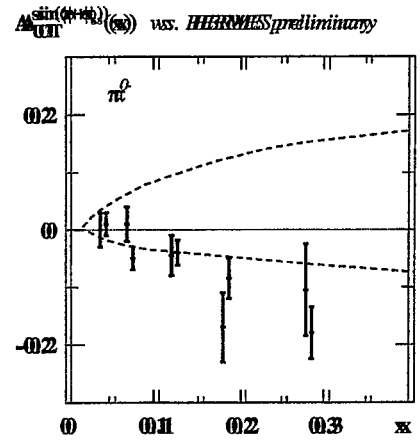

- Charge conjugation and isospin invariance

$$H_1^{\perp u/\pi^+} = H_1^{\perp \bar{u}/\pi^-} = H_1^{\perp d/\pi^-} \ldots \equiv H_1^{\rm fav}\,,$$

$$H_1^{\perp d/\pi^+} = H_1^{\perp \bar{d}/\pi^-} = H_1^{\perp u/\pi^-} \ldots \equiv H_1^{\rm unf}\,,$$

$$H_1^{\perp a/\pi^0} = \frac{1}{2}(H_1^{\perp a/\pi^+} + H_1^{\perp a/\pi^-}) = \frac{1}{2}(H_1^{\rm fav} + H_1^{\rm unf})\,.$$

Same for $D_1(z)$

- x&z-dependence factorization

$$A(\pi^0) = \frac{\sigma(\pi^+)}{\sigma(\pi^+)+\sigma(\pi^-)} A(\pi^+) + \frac{\sigma(\pi^-)}{\sigma(\pi^+)+\sigma(\pi^-)} A(\pi^-)$$

or

$$A(\pi^0) - A(\pi^-) = a[A(\pi^+) - A(\pi^-)] \approx 0\,,$$

$$\Downarrow$$

$$\boxed{a = \frac{\sigma(\pi^+)}{\sigma(\pi^+)+\sigma(\pi^-)} \approx 0}$$ that is nonsense!

x&z factorization is under suspicion and should be carefully checked!

Even without $A(\pi^0)$ the suppression of $A(\pi^+)$ is a problem:

$A(\pi^-) \propto (h_1^d H_1^{\rm fav} + 4h_1^u H_1^{\rm unf})$ should be < 0 (i.e. $H_1^{\rm unf} < 0$),

while

$A(\pi^+) \propto (4h_1^u H_1^{\rm fav} + h_1^d H_1^{\rm unf})$
gain **positive** addition $h_1^d H_1^{\rm unf} > 0$!!

Of course one can take smaller $\frac{H_1^{\rm fav}}{D_1^{\rm fav}}$ (or smaller $\frac{h_1^u}{u}$) but then we miss understanding of A_{UL}!

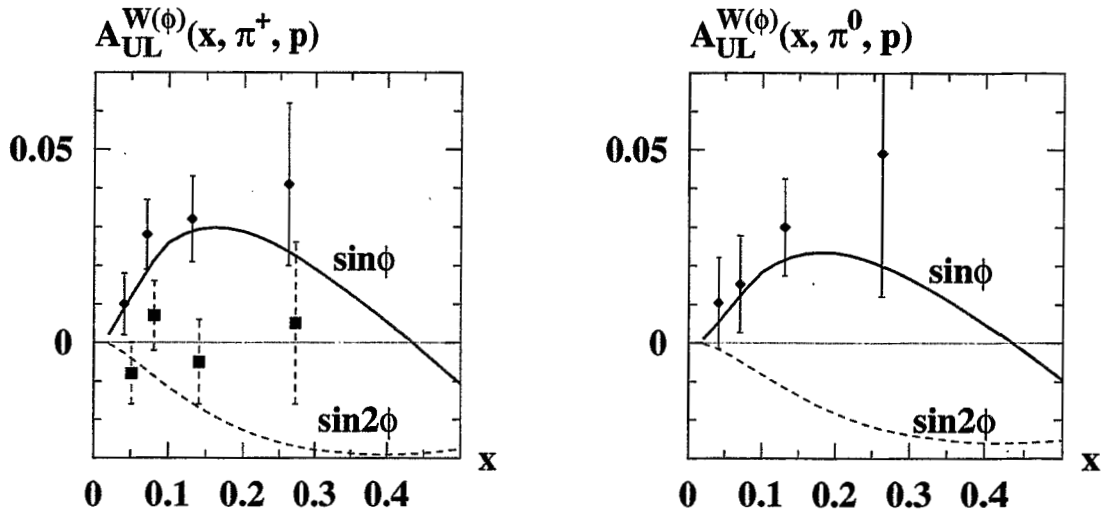

Conclusions

1. We seems understand more complicated A_{UL} asymmetries (Collins, Sivers, A_{UT}-contribution, ...)
2. We do not understand more transparent $A_{UT}^{\sin(\phi+\phi_s)}$ asymmetry!
   (The HERMES data are however PRELIMINARY!)
3. More data are waited from COMPASS, CLAS and HALL-A experiments.

Disentangling the sources of Single Spin Asymmetries

Oleg Teryaev
Joint Institute for Nuclear Research
Dubna 141980, Russia

teryaev@thsun1.jinr.ru

RSC meeting, Torino
8 October 2004

1. Sources of SSA = sources of imaginary phases .
2. Collins vs Sivers; in-jet vs jet asymmetry
3. Collins vs Sivers: how generic is the suppression.
4. RHIC vs E704 - gluonic and fermionic poles
5. Conclusions

SSA - requires imaginary part - due to generalized optical theorem - cut in SOME variable

QCD factorization:

FSI - cuts in jet mass - Collins function

ISI and FSI - cuts in s - twist-3 : fermionic (soft fermion) or gluonic (soft gluon) poles

Some gluonic poles (gluonic exponential) - Sivers function (effective, non-universal) - no variable like the jet mass for initial particle)

Correlated distribution and fragmentation - cuts in s_1 (T-odd) fracture function - may help to resolve the signals for the violation of factorization for transverse SSA at HERMES, discussed at A. Efremov talk.

T-even spin-dependent fracture functions - talk of A. Kotzinian

How to disentangle all this mess?

No complete solution - some hints

(3 for 15 min)

Request for experimentalists

Collins and Sivers do lead to DIFFERENT observables IF hadron in a JET is detected

Sivers - azumuthal ($sin\phi$)asymmetry of the jet itself

Collins - azimuthal asymmetry of the hadrom INSIDE the jet

Averaging of the jet directions - the same observable

Is it possible not to average?

Are the jets directions non-symmetric

Are the jets shaped?

For integration over jets direction - Collins and Sivers contribute together BUT

Recent observation of Cagliari-London-Torino group (talk of U. d'Alesio) -suppression of Collins with respect to Sivers

How generic is it?

(2-nd) Mean value theorem

$$A_h = \frac{\int d\vec{x}\Delta\sigma(\vec{x})}{\int d\vec{x}\sigma(\vec{x})} = \frac{\Delta\sigma(\vec{x}_0)}{\sigma(\vec{x}_0)} = A_p(x_0) \qquad (1)$$

Here $\vec{x}$ includes all transverse momentum and/or momentum fractions, Hadronic asymmetry is equal to partonic one at SOME point x_0 which compromises between maxima of σ and A. Usually they correspond to different regions -suppression of hadronic asymmetry with repect to partonic one EXCEPT $\Delta\sigma$ and σ are similar.

Sivers function case

$$A_h = \frac{\int d\vec{x}[f_T D\hat{\sigma}](\vec{x})}{\int d\vec{x}[f D\hat{\sigma}](\vec{x})} = \frac{f_T(\vec{x}_0)}{f(\vec{x}_0)} \tag{2}$$

In the case Sivers function is modelled similarly to unpolarized one - no reasons for suppression. BUT! maybe quite different because of its effective nature

Compare with Collins function

$$A_h = \frac{\int d\vec{x}[\delta f H \delta\hat{\sigma}](\vec{x})}{\int d\vec{x}[f D\hat{\sigma}](\vec{x})} = \frac{[\delta f H \delta\hat{\sigma}](\vec{x}_0)}{[f D\hat{\sigma}](\vec{x}_0)} \tag{3}$$

Extra generic suppression due to partonic analyzing power!

Complication due to many quark flavours - purities

$$A_h = \frac{\Sigma_i \int d\vec{x} \Delta\sigma_i(\vec{x})}{\Sigma_i \int d\vec{x} \sigma_i(\vec{x})} = \sum_i P_i(\vec{x}_0) \frac{\Delta\sigma_i(\vec{x}_0)}{\sigma_i(\vec{x}_0)} = \sum_i P_i(\vec{x}_0) A_p^i(x_0)$$

$$P_i(\vec{x}_0) = \frac{\sigma_i(\vec{x}_0)}{\Sigma_k \sigma_k(\vec{x}_0)}; \quad \sum_i P_i = 1 \quad (4)$$

For Sivers - purities involve dependence also on fragmentation functions and partonic cross-sections, but not significant unless for some accidental reason large asymmetry is accompaniied by small purity

Imaginary phase (T-odd effects in T-conserving theories) - loops including large and soft distances - genuine twist 3

Soft quarks - fermionic poles (A.V. Efremov, O.T. (85,95)) (DY - no suppression as $1/Q$, still behaves like M/p_T). But consideration of small $P_T \sim M$ - illegitimate - all twists are important.

Soft gluons - gluonic poles - considered to be dominant for large x_F(easier to emit soft gluon than soft quark) - detailed numerics exists (J. Qiu, G. Sterman (91,98))

However

Gluonic poles predictions for large X_F - go above RHIC data.

Gluonic poles - related to genuine twist contribution to $\int dx x^2 g_2$ - small.

Fermionic poles should be reanalyzed.

Another argument - from unpolarized cross-sections

NLO - much better description of RHIC than E704 kinematics ([illegible]) Why (no explicit energy dependence in QCD) ? Possible origin - HT - the typical partonic $x_i \sim p_T/\sqrt{s}$ - larger for E704. HT typically grow with x - less important for RHIC.

Gluonic poles: $\Delta\sigma \sim 1/(1-x)$ - to preserve positivity requires the growing with x spin independent HT term. If it is small, gluonic poles also cannot be large.

Slide 9

1. Experimental detection of jet asymmetry and in-jet asymmetry of hadrons - BEST way to disentangle Collins and Twist-3/Sivers

2. Non-suppression of Sivers - generic unless Sivers functions is very different from unpolarized one; suppression of Collins - generic.

3. Different situation with unpolarized NLO at E704 and RHIC - may be a signal for disentangling fermionic and gluonic poles.

Suppression of the Collins mechanism for SSA in $p^{\uparrow}p \to \pi X$

Umberto D'Alesio
Physics Department and INFN
University of Cagliari, Italy

RHIC SPIN Collaboration Meeting
Torino, Italy, 8-9 October 2004

[In coll. with: *M. Anselmino, M. Boglione, E. Leader, S. Melis, F. Murgia*]

(hep-ph/0408356 + work in progress)

Outline

- Generalized pQCD approach with spin and $k_\perp$-effects in distribution and fragmentation functions and elementary dynamics;
- SSA in $pp \Rightarrow \pi X$: theory - helicity formalism;
- SSA in $pp \Rightarrow \pi X$: phenomenology of the Collins effect;
- Conclusions and outlook

Unpolarized cross sections: $k_\perp$-factorization *ansatz*

- The collinear pQCD factorization formula for $AB \to CX$ reads

$$d\sigma^{AB\to CX} = \sum_{a,b,c,d} f_{a/A}(x_a) \otimes f_{b/B}(x_b) \otimes d\hat{\sigma}^{ab\to cd}(\hat{s},\hat{t}) \otimes D_{C/c}(z)$$

$$\hat{s} = s x_a x_b,\ \hat{t} = t x_a/z,\ \hat{u} = u x_b/z$$

- Including transverse momenta we have:

$$\Rightarrow \sum_{a,b,c,d} \hat{f}_{a/A}(x_a, \boldsymbol{k}_{\perp a}) \otimes \hat{f}_{b/B}(x_b, \boldsymbol{k}_{\perp b}) \otimes d\hat{\sigma}^{ab\to cd}(\hat{s},\hat{t}) \otimes \hat{D}_{C/c}(z, \boldsymbol{k}_{\perp C})$$

$$\hat{s} \to \hat{s}\,\phi_s(\boldsymbol{k}_{\perp a}, \boldsymbol{k}_{\perp b}),\ \hat{t} \to \hat{t}\,\phi_t(\boldsymbol{k}_{\perp a}, \boldsymbol{k}_{\perp C}),\ \hat{u} \to \hat{u}\,\phi_u(\boldsymbol{k}_{\perp b}, \boldsymbol{k}_{\perp C})$$

+ Jacobian in FF + Cahn effect + Gaussian $k_\perp$-depend.; + factoriz. ...

see *U. D., F. Murgia*: hep-ph/0408092, PRD in press

$\boldsymbol{k}_\perp$ - effects

1. $\boldsymbol{k}_\perp$ alters $\langle x \rangle$: small shift but important at large x where PDF are varying rapidly. $\rightarrow$ *enhanced higher-twist* effect (up to a factor of 10 in a cross section);

2. the partonic scattering angle in the pp c.m. frame might be much smaller than the hadronic production angle, thus enhancing the moderately large p_T inclusive production of particles;

3. spin and $\boldsymbol{k}_\perp$-effects generated by soft mechanisms: SSA ($pp \rightarrow hX$)

   (a) Sivers PDF: $\boldsymbol{S} \cdot (\boldsymbol{P} \times \boldsymbol{k}_{\perp q})$

   (b) Collins FF: $\boldsymbol{s}_q \cdot (\boldsymbol{p}_q \times \boldsymbol{k}_{\perp h})$

   (c) Boer-Mulders PDF: $\boldsymbol{s}_q \cdot (\boldsymbol{P} \times \boldsymbol{k}_{\perp q})$

   (d) polarizing FF: $\boldsymbol{S}_h \cdot (\boldsymbol{p}_q \times \boldsymbol{k}_{\perp h})$

Polarized cross sections: Helicity formalism

◇ **Helicity density matrices**, in the $\boldsymbol{k}_\perp$-factorization scheme, to describe parton spin states for a polarized cross section:

$$d\sigma^{A,S_A+B,S_B\to C+X} = \sum_{a,b,c,d,\{\lambda\}} \rho^{a/A,S_A}_{\lambda_a,\lambda'_a}\ \hat{f}_{a/A,S_A}(x_a,\boldsymbol{k}_{\perp a}) \otimes \rho^{b/B,S_B}_{\lambda_b,\lambda'_b}\ \hat{f}_{b/B,S_B}(x_b,\boldsymbol{k}_{\perp b})$$

$$\otimes\ \hat{M}_{\lambda_c,\lambda_d;\lambda_a,\lambda_b}\ \hat{M}^*_{\lambda'_c,\lambda_d;\lambda'_a,\lambda'_b} \otimes \hat{D}^{\lambda_C,\lambda_C}_{\lambda_c,\lambda'_c}(z,\boldsymbol{k}_{\perp C})$$

- $\rho^{a/A,S_A}_{\lambda_a,\lambda'_a}$: helicity density matrix of parton a inside hadron A with polarization S_A
- $\frac{d\hat{\sigma}^{ab\to cd}}{d\hat{t}} \simeq \sum_{\lambda_a,\lambda_b,\lambda_c,\lambda_d} |\hat{M}_{\lambda_c,\lambda_d;\lambda_a,\lambda_b}|^2$ (scattering amplitudes)
- $\hat{D}^{\lambda_C,\lambda'_C}_{\lambda_c,\lambda'_c} \equiv \sum\!\!\!\!\!\!\int_{X,\lambda_X} \hat{\mathcal{D}}_{\lambda_C,\lambda_X;\lambda_c}\ \hat{\mathcal{D}}^*_{\lambda'_C,\lambda_X;\lambda'_c}$

  i.e. the product of *fragmentation amplitudes* for the $c \to C + X$ process

Helicity density matrices: PDF sector

◇ Partonic distribution function at L.O. (and twist two) can be interpreted as the inclusive cross section for the process $A \to a + X$.

Helicity density matrix of parton a $\leftrightarrow$ to the helicity density matrix of hadron A.

$$\rho^{a/A,S_A}_{\lambda_a,\lambda'_a} \quad \hat{f}_{a/A,S_A}(x_a, \boldsymbol{k}_{\perp a}) = \sum_{\lambda_A,\lambda'_A} \rho^{A,S_A}_{\lambda_A,\lambda'_A} \hat{F}^{\lambda_a,\lambda'_a}_{\lambda_A,\lambda'_A}$$

$$\hat{F}^{\lambda_a,\lambda'_a}_{\lambda_A,\lambda'_A} \equiv \sum\!\!\!\!\!\!\int_{X_A,\lambda_X} \hat{\mathcal{F}}_{\lambda_a,\lambda_X;\lambda_A} \hat{\mathcal{F}}^*_{\lambda'_a,\lambda_X;\lambda'_A}$$

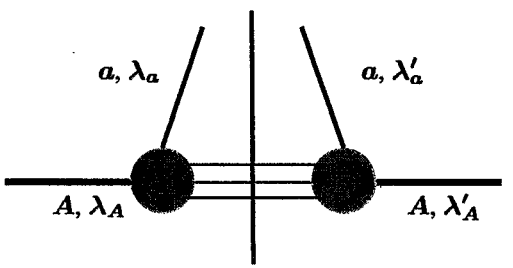

Each helicity density matrix describes the spin orientation of a particle in its own helicity frame.

For a spin-1/2 particle, $\mathrm{Tr}\,(\sigma_i \rho) = P_i$ is the i-component of the spin-polarization vector $\boldsymbol{P}$ in the helicity rest frame of the particle.

The distribution function of parton a inside the polarized (S_A) hadron A is given by

$$\hat{f}_{a/A,S_A}(x_a, \boldsymbol{k}_{\perp a}) = \sum_{\lambda_a,\lambda_A,\lambda'_A} \rho^{A,S_A}_{\lambda_A,\lambda'_A} \hat{F}^{\lambda_a,\lambda_a}_{\lambda_A,\lambda'_A}$$

- We have 16 $\hat{F}^{\lambda_a,\lambda'_a}_{\lambda_A,\lambda'_A}$ which by Parity constraints reduce to 6 independent products.

  4 of them are *Real functions*

  $\Rightarrow$ 8 independent spin-$\boldsymbol{k}_\perp$ PDF.

For instance:

$$\rho^{a/A,S_A}_{\pm,\pm}\, \hat{f}_{a/A,S_A}(x_a, \boldsymbol{k}_{\perp a}) \equiv \hat{f}_{a_\pm/A,S_A}(x_a, \boldsymbol{k}_{\perp a})$$

Partonic interpretation: a few examples

Spin and $k_\perp$-dependent distribution and fragmentation functions of leading twist:
[vs. notation of P.J. Mulders, R.D. Tangerman *Nucl. Phys.* **B461** (1996)]

- $\hat{f}_{q/p} = \hat{F}^{+,+}_{+,+} + \hat{F}^{-,-}_{-,-}$: unpolarized PDF
- $\Delta\hat{f}_{q/p} = \hat{F}^{+,+}_{+,+} - \hat{F}^{-,-}_{-,-}$: long. polariz. PDF
- $\hat{D}_{\pi/q} = \hat{D}^{\pi}_{++}$: unpolarized FF
- $\hat{f}_{q/p^\uparrow} - \hat{f}_{q/p^\downarrow} \equiv \Delta^N f_{q/p^\uparrow} = 4\mathrm{Im}\hat{F}^{+,+}_{+,-} \propto (k_\perp/M) f_{1T}^\perp$: Sivers funct.
- $\hat{f}_{q^\uparrow/p} - \hat{f}_{q^\downarrow/p} \equiv \Delta^N f_{q^\uparrow/p} = 2\mathrm{Im}\hat{F}^{+,-}_{+,+} \propto (k_\perp/M) h_1^\perp$: Boer-Mulders funct.
- $\hat{D}_{h/q^\uparrow} - \hat{D}_{h/q^\downarrow} \equiv \Delta^N D_{h/q^\uparrow} = 2\mathrm{Im}D^h_{+-} \propto (k_\perp/M) H_1^\perp$: Collins funct.
- $\hat{f}_{q_+/p^\uparrow} - \hat{f}_{q_-/p^\uparrow} = 2\mathrm{Re}\hat{F}^{+,+}_{+,-} \propto (k_\perp/M) g_{1T}$
- $\hat{f}_{q^\downarrow/p_+} - \hat{f}_{q^\uparrow/p_+} = 2\mathrm{Re}\hat{F}^{+,+}_{+,-} \propto (k_\perp/M) h_{1L}^\perp$
- $\hat{f}_{q^\uparrow/p^\uparrow} - \hat{f}_{q^\downarrow/p^\uparrow} \Rightarrow \hat{F}^{+,-}_{+,-}; \hat{F}^{-,+}_{+,-} \propto h_1; (k_\perp/M)^2 h_{1T}^\perp$
- and gluons...

see also hep-ph/0410050, ("the Trento conventions")
A. Bacchetta, U.D., M. Diehl, A. Miller

The master formula

$$d\sigma^{A,S_A+B,S_B\to C+X} = \sum_{a,b,c,d,\{\lambda\}} \rho^{A,S_A}_{\lambda_A,\lambda'_A}\, \hat{F}^{\lambda_a,\lambda'_a}_{\lambda_A,\lambda'_A}(\boldsymbol{k}_{\perp a}) \otimes \rho^{B,S_B}_{\lambda_B,\lambda'_B}\, \hat{F}^{\lambda_b,\lambda'_b}_{\lambda_B,\lambda'_B}(\boldsymbol{k}_{\perp b}) \otimes \hat{M}_{\lambda_c,\lambda_d;\lambda_a,\lambda_b}\, \hat{M}^*_{\lambda'_c,\lambda_d;\lambda'_a,\lambda'_b} \otimes \hat{D}^{\lambda_C,\lambda_C}_{\lambda_c,\lambda'_c}$$

On summing over $\{\lambda' s\}$ we get all combinations of spin and $\boldsymbol{k}_\perp$- mechanisms in Single and Double Spin Asymmetries for unpolarized particle production.

Notice: even for $\boldsymbol{S}_A = \boldsymbol{S}_B = 0 \to \rho^{A,S_A}_{\lambda_A,\lambda'_A} = (1/2)\delta_{\lambda_A,\lambda'_A}$ (same for B) the unpolarized cross section would develop Boer-Mulders $\otimes$ Collins effects ($h_1^\perp \otimes H_1^\perp$): negligible (checked numerically!).

[M. Anselmino, M. Boglione, U.D., E. Leader, S. Melis, F. Murgia, in preparation]

Single Spin Asymmetries: $A^{\uparrow}B \to \pi X$, $A_N = (d\sigma^{\uparrow} - d\sigma^{\downarrow})/(d\sigma^{\uparrow} + d\sigma^{\downarrow})$

- Configuration ($AB \equiv pp$):
  AB center of mass frame - A along $+Z$-axis, π in the XZ plane with $\boldsymbol{p}_T$ parallel to $+X$-axis. $S_A = \uparrow$ or $\downarrow$ along Y-axis, $S_B = 0$.

Quantities to be considered (convoluted):

- Numerator of A_N

$$\Sigma(\uparrow,0) - \Sigma(\downarrow,0) = \sum_{\{\lambda\}} \frac{(-i)}{2} \left[\hat{F}^{\lambda_a,\lambda'_a}_{+,-}(k_{\perp a}) - \hat{F}^{\lambda_a,\lambda'_a}_{-,+}(k_{\perp a}) \right] \times \hat{F}^{\lambda_b,\lambda'_b}_{\lambda_B,\lambda_B} \; \hat{M}_{\lambda_c,\lambda_d;\lambda_a,\lambda_b} \; \hat{M}^*_{\lambda'_c,\lambda_d;\lambda'_a,\lambda'_b} \; \hat{D}^{\pi}_{\lambda_c,\lambda'_c}$$

- Denominator of A_N (twice the unpolarized cross section)

$$\Sigma(\uparrow,0) + \Sigma(\downarrow,0) = \sum_{\{\lambda\}} \frac{1}{2} \left[\hat{F}^{\lambda_a,\lambda'_a}_{+,+}(k_{\perp a}) + \hat{F}^{\lambda_a,\lambda'_a}_{-,-}(k_{\perp a}) \right] \times \hat{F}^{\lambda_b,\lambda'_b}_{\lambda_B,\lambda_B} \; \hat{M}_{\lambda_c,\lambda_d;\lambda_a,\lambda_b} \; \hat{M}^*_{\lambda'_c,\lambda_d;\lambda'_a,\lambda'_b} \; \hat{D}^{\pi}_{\lambda_c,\lambda'_c}$$

Helicity scattering amplitudes with full $k_\perp$

- $k_\perp$'s imply: non-planar $ab \to cd$ scattering; different $\perp$ directions.

Parton helicity amplitudes in pp c.o.m frame in terms of hel. amplitudes in partonic c.o.m. frame.

1) Boost along $\boldsymbol{p}_a + \boldsymbol{p}_b$: $S \to S'$

2) Rotation to put $\boldsymbol{p}'_a$ along Z axis: $S' \to S''$

- $\hat{M}_{\lambda_c,\lambda_d;\lambda_a,\lambda_b} = \hat{M}^0_{\lambda_c,\lambda_d;\lambda_a,\lambda_b}(\hat{s},\hat{t})\, \mathrm{e}^{i\sum_m \lambda_m \xi_m}\, \mathrm{e}^{i(\lambda_a-\lambda_b)\phi''_c}$

Notice: various combinations of "T-odd" effects in (un)polarized cross sections but by including proper phases + numerical (VEGAS) integration:

$$d\sigma^{\mathrm{unp}} \simeq f_{a/p} \otimes f_{b/p} \otimes d\hat{\sigma} \otimes D_{\pi/c}$$

$$d\sigma^{\uparrow} - d\sigma^{\downarrow} \simeq \Delta^N f_{a/p^\uparrow} \otimes f_{b/p} \otimes d\hat{\sigma} \otimes D_{\pi/c} \qquad \text{"Sivers effect"}$$

$$+\ h_{1a} \otimes f_{b/p} \otimes d\Delta\hat{\sigma} \otimes \Delta^N D_{\pi/c^\uparrow} \qquad \text{"Collins effect"}$$

$\Rightarrow$ **Let's focus on Collins effect**

On summing over $\{\lambda\}$ $[\,\lambda_a \neq \lambda'_a$ and $\lambda_b = \lambda'_b]$ we get $(b = q, \bar{q}, g)$

$$
\begin{aligned}
[\Sigma(\uparrow,0) - \Sigma(\downarrow,0)]_{qb} \;=\; \Big\{ & F^{+-}_{+-}(x_a, k_{\perp a}) \cos[\phi_a + \phi''_c - \xi_a - \tilde{\xi}_a + \xi_c + \tilde{\xi}_c + \phi^H_\pi] \\
& - F^{+-}_{-+}(x_a, k_{\perp a}) \cos[\phi_a - \phi''_c + \xi_a + \tilde{\xi}_a - \xi_c - \tilde{\xi}_c - \phi^H_\pi] \Big\} \\
& \times\; \hat{f}_{b/B}(x_b, k_{\perp b}) \left[\hat{M}^0_1 \hat{M}^0_2(x_a, x_b, z; \boldsymbol{k}_{\perp a}, \boldsymbol{k}_{\perp b}, \boldsymbol{k}_{\perp \pi})\right]_{qb} \\
& \times\; [2\,\mathrm{Im} D^\pi_{+-}(z, k_{\perp \pi})]
\end{aligned}
$$

$$
(\hat{M}^0_1)_{qb} \equiv \hat{M}^0_{+,+;+,+} = \hat{M}^0_{-,-;-,-} \qquad\qquad (\hat{M}^0_2)_{qb} \equiv \hat{M}^0_{-,+;-,+} = \hat{M}^0_{+,-;+,-}
$$

The product $\hat{M}^0_1 \hat{M}^0_2$, is, for a collinear collision with scattering plane $\equiv XZ$, related to the spin transfer cross section:

$$
\frac{1}{16\pi \hat{s}^2} \left[\hat{M}^0_1 \hat{M}^0_2\right]_{qb} = \frac{d\hat{\sigma}^{q^\uparrow b \to q^\uparrow b}}{d\hat{t}} - \frac{d\hat{\sigma}^{q^\uparrow b \to q^\downarrow b}}{d\hat{t}}
$$

Maximization of the Collins mechanism in $p^\uparrow p \to \pi X$

In the notations of P.J. Mulders, R.D. Tangerman *Nucl. Phys.* **B461** (1996):

$$
\begin{aligned}
F_{+-}^{+-}(x,k_\perp) &= h_1(x,k_\perp) = h_{1T}(x,k_\perp) + \frac{k_\perp^2}{2M_p^2}\, h_{1T}^\perp(x,k_\perp) \\
F_{-+}^{+-}(x,k_\perp) &= \frac{k_\perp^2}{2M_p^2}\, h_{1T}^\perp(x,k_\perp) \\
2\,\mathrm{Im}D_{+-}^{\pi}(z,k_\perp) &= \Delta^N D_{\pi/q^\uparrow}(z,k_\perp) = \frac{2k_\perp}{zM_\pi}\, H_1^{\perp q}(z,k_\perp)
\end{aligned}
$$

The following positivity bounds hold [A. Bacchetta, *et al. Phys. Rev. Lett.* **85** (2000)]:

$$
\begin{aligned}
|h_1(x,k_\perp)| &\leq \frac{1}{2}\left[q(x,k_\perp) + \Delta q(x,k_\perp)\right] = q_+(x,k_\perp) \\
\frac{k_\perp^2}{2M_p^2}\,|h_{1T}^\perp(x,k_\perp)| &\leq \frac{1}{2}\left[q(x,k_\perp) - \Delta q(x,k_\perp)\right] = q_-(x,k_\perp) \\
|\Delta^N D_{\pi/q^\uparrow}(z,k_\perp)| &\leq 2D_{\pi/q}(z,k_\perp)
\end{aligned}
$$

Let's consider $A_N(\pi^+)$: u, d active flavor for h_1 and $h_{1T}^{\perp}$:

$$h_1^u(x,k_\perp) = u_+(x,k_\perp) \qquad h_1^d(x,k_\perp) = -d_+(x,k_\perp)$$

$$\frac{k_\perp^2}{2M_p^2}\, h_{1T}^{\perp u}(x,k_\perp) = -u_-(x,k_\perp) \qquad \frac{k_\perp^2}{2M_p^2}\, h_{1T}^{\perp d}(x,k_\perp) = +d_+(x,k_\perp)$$

being the product of elementary amplitudes $\hat{M}_1^0 \hat{M}_2^0 < 0$, to get $A_N(\pi^+) > 0$

$$\Rightarrow \Delta^N D_{\pi^+/u\uparrow}(z,k_\perp) = -2D_{\pi^+/u}(z,k_\perp)$$

Contribution (maximized) of the sub-leading channel *down* $\rightarrow$ *down* (neglected in former studies); since $h_1^d < 0$, to add in sign, we use

$$\Delta^N D_{\pi^+/d\uparrow}(z,k_\perp) = +2D_{\pi^+/d}(z,k_\perp)$$

A_N for π^-'s is maximized in size (by isospin invariance).

- Pol PDF: LSS01 and LSS-BBS ($\Delta d > 0$ at large $x \rightarrow$ more relaxed bound on h_1^d)
- FF: Kretzer (sea $\simeq (1-z)$ valence) and KKP (sea suppressed)

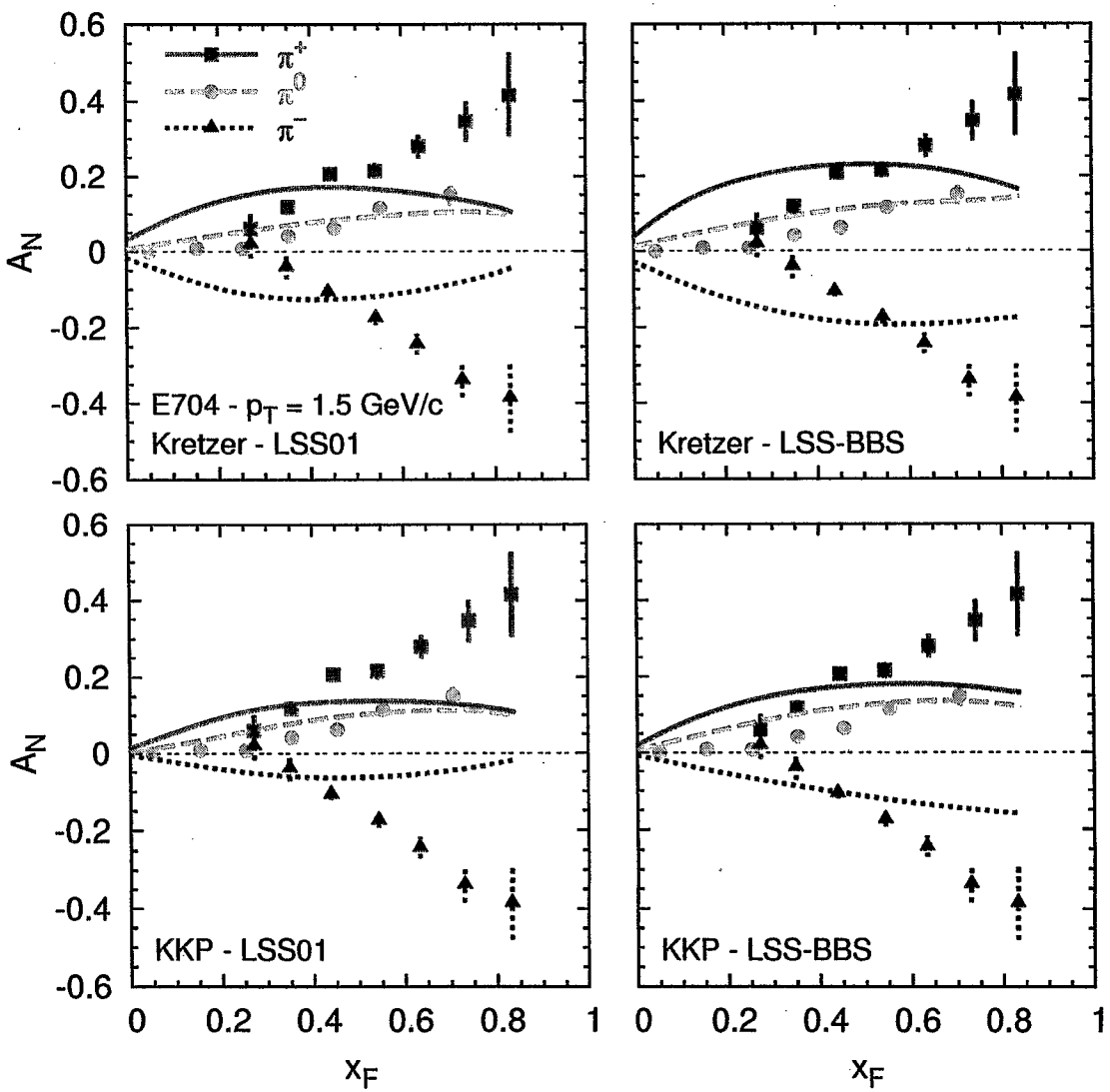

Maximized estimates of $A_N(\pi)$ for $p^\uparrow p \to \pi X$ vs. x_F, at $\langle p_T \rangle = 1.5$ GeV/c and $\sqrt{s} = 20$ GeV. Collins mechanism full saturated. Data are from [E704] D.L. Adams *et al.*, *Phys. Lett.* **B261** (1991) and A. Bravar *et al.*, *Phys. Rev. Lett.* **77** (1996).

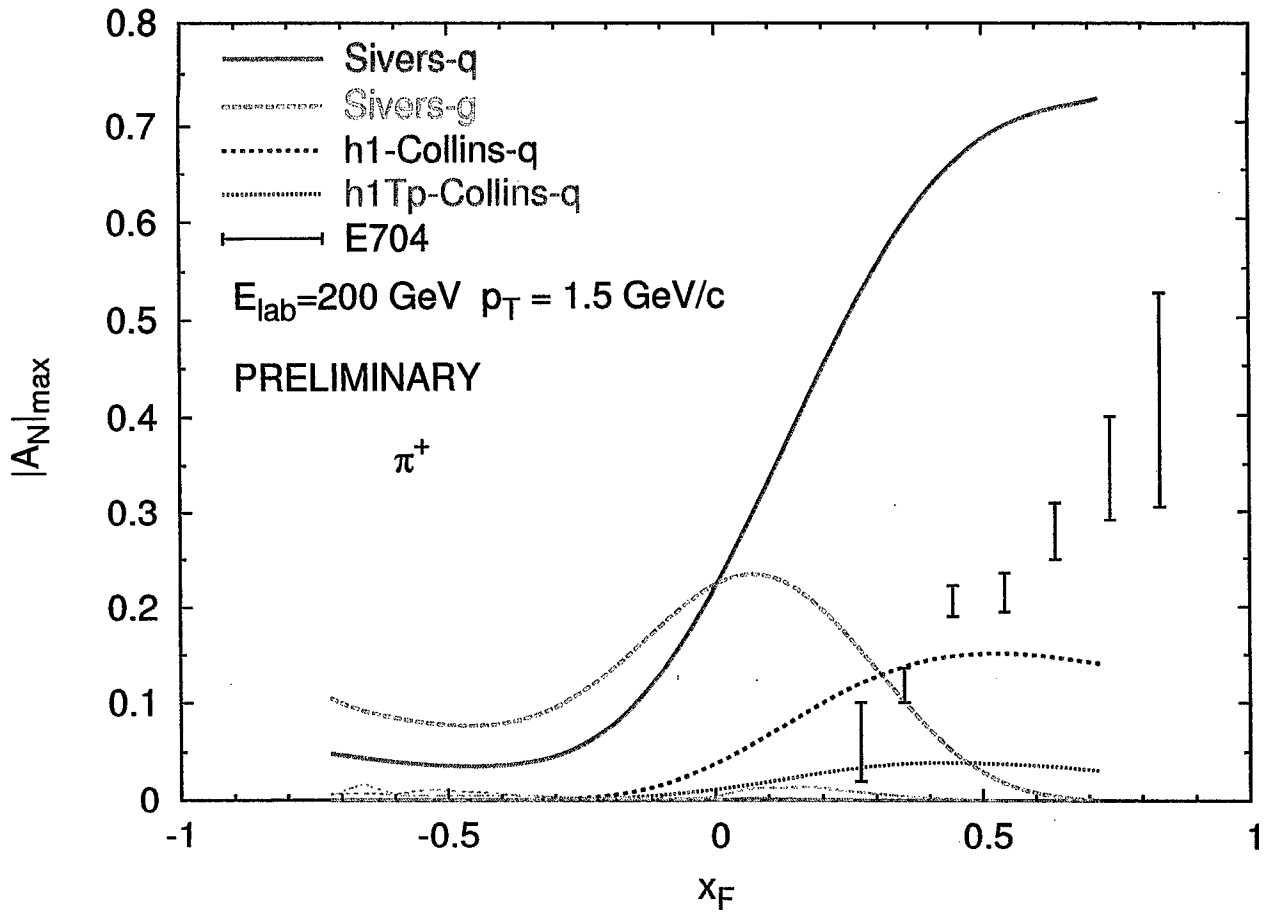

(Over)Maximized estimates of A_N: all possible contributions.

Conclusions and outlook

- A generalized pQCD approach to SSA and unpol. cross sections:
  LO–pQCD + spin and new $k_\perp$-dependent PDF and FF;
- $A_N(p^\uparrow p \to \pi X)$: Complete $\boldsymbol{k}_\perp$-helicity formalism and phenomenology.
  True detailed microscopic dynamics (proper phases) $\Rightarrow$
  Sivers effect results confirmed;
  Collins effect suppressed (against former claims!);
- $p^\uparrow p \to \pi$ jet X: to extract Collins effect (less severe phases cancellations);
- $AB \to CX$ $(C = \pi, \Lambda, \rho)$: Complete $\boldsymbol{k}_\perp$-helicity formalism and phenomenology for A_{LL}, A_{TT}, A_{LT}, P (in progress). Role of "T-odd" effects in $A_{LL}(\pi)$;
- Azimuthal spin asymmetries in SIDIS: role of Collins & Sivers effect
  (+ Kotzinian & Prokudin: detailed $\boldsymbol{k}_\perp$ approach in progress);
- $p^\uparrow p$–data at large energies and at larger p_T, and $ep^\uparrow$–data with transversely polarized target are very welcome.

Current and Future Transverse Spin at the PHENIX Experiment at RHIC

Yousef I. Makdisi
Brookhaven National Laboratory
For
The PHENIX Collaboration

BROOKHAVEN
NATIONAL LABORATORY

Yousef Makdisi
SPIN 2004
October 10-16, 2004

Outline

- A brief experimental review of transverse asymmetries:
  - A symmetries at Large X_T
  - Asymmetries near $X_F = 0$
  - Asymmetries at Large X_F
- Transverse asymmetry measurement in PHENIX at $X_F = 0$
- Near Term upgrades and transverse physics reach
- Longer term upgrades and physics reach
- Summery and outlook

BROOKHAVEN
NATIONAL LABORATORY

Asymmetry in inclusive production at Large X_T

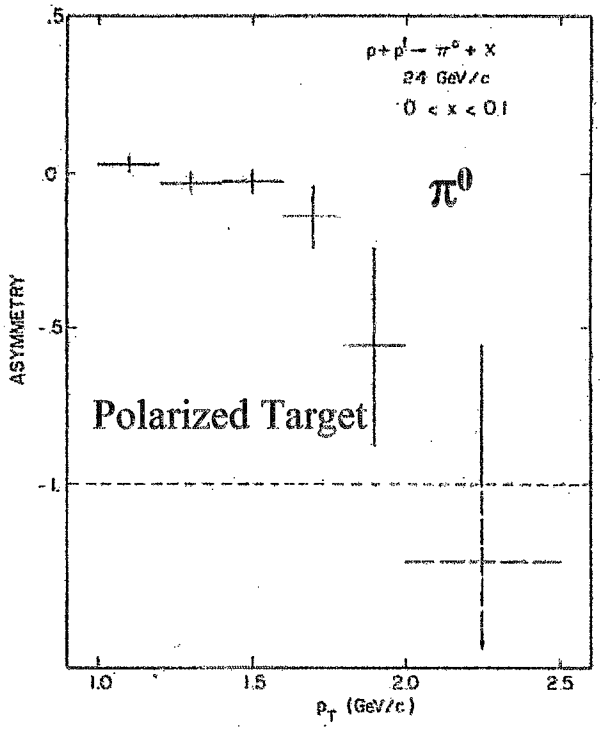

J. Antille et al. Phys.Lett.B94:523,1980

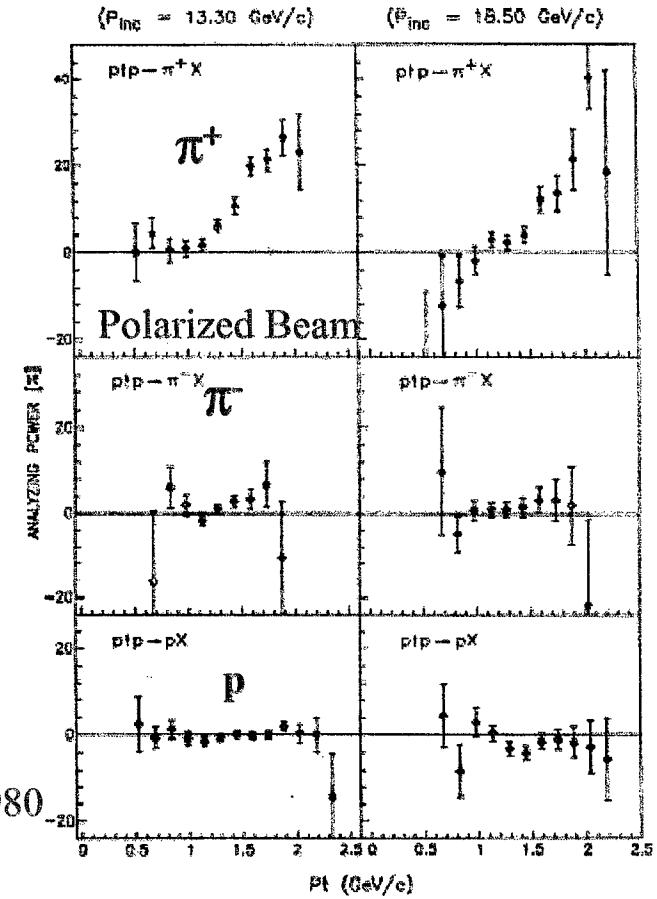

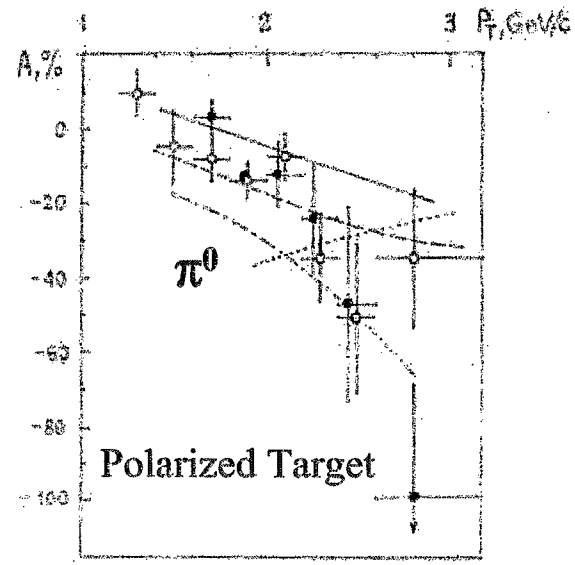

$\pi^- p^\uparrow(d^\uparrow) \rightarrow \pi^0 x$ @ 40 GeV/c
V.D. Apokin et al.,
Phys.Lett.B243:461-464,1990

S. Saroff et al. PRL64,995,1990

Large Asymmetries in π^+ and π^0 production

No asymmetry in π^- and proton production

BROOKHAVEN
NATIONAL LABORATORY

Asymmetry near $X_F = 0$

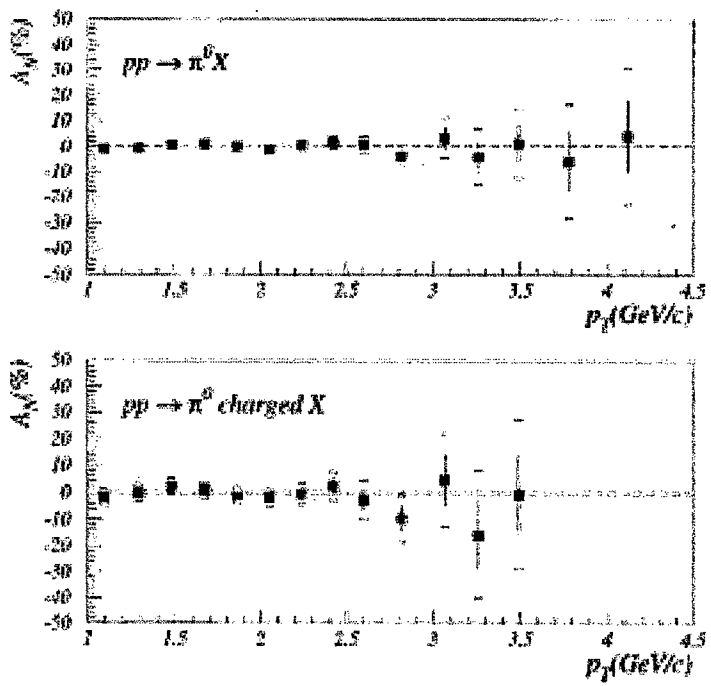

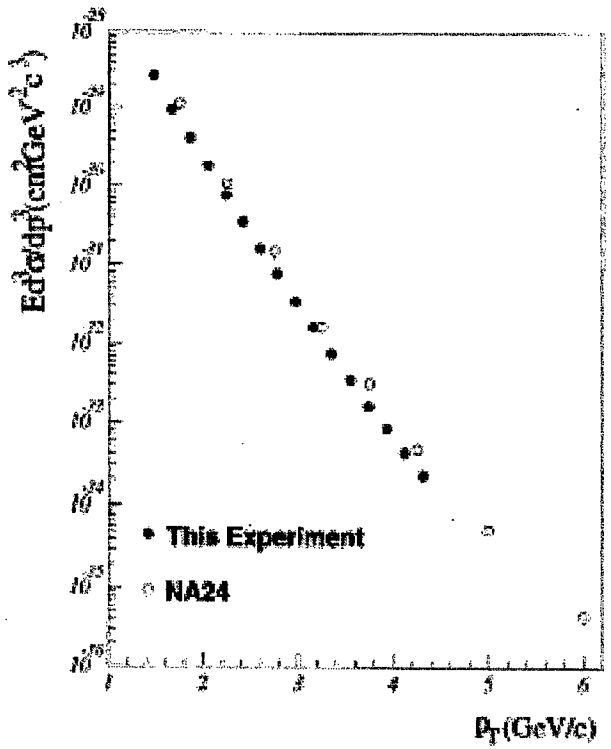

D.L. Adams *et al.* PRD53:4747-4755,1996

Higher $\sqrt{s} = 20$ GeV are we in the partonic regime?

Unlike at lower energy No asymmetry in π^0 production

BROOKHAVEN
NATIONAL LABORATORY

Asymmetry in pion production at large X_F

ZGS (12 GeV)

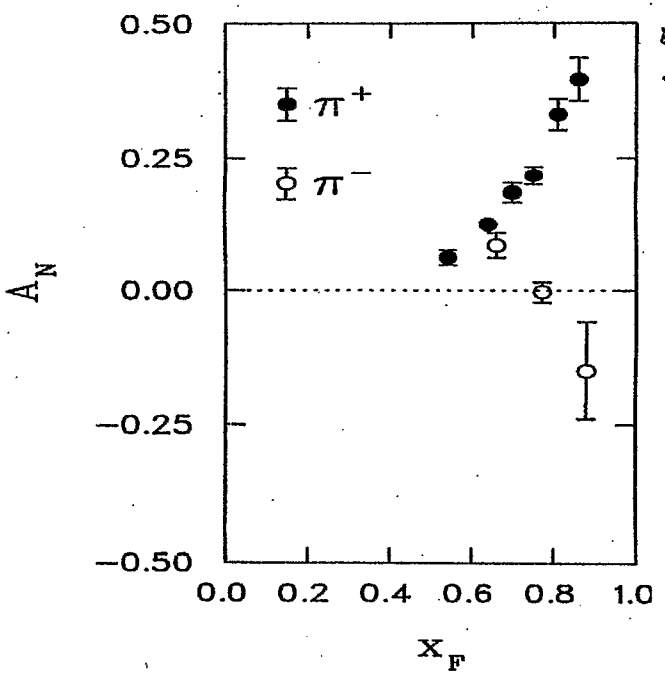

AGS (22 GeV)

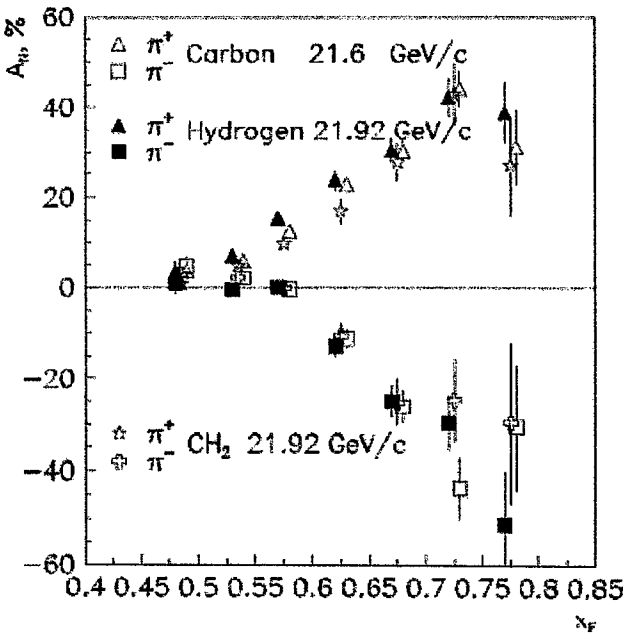

Phys.Rev.D65:092008,2002

FNAL (200 GeV)

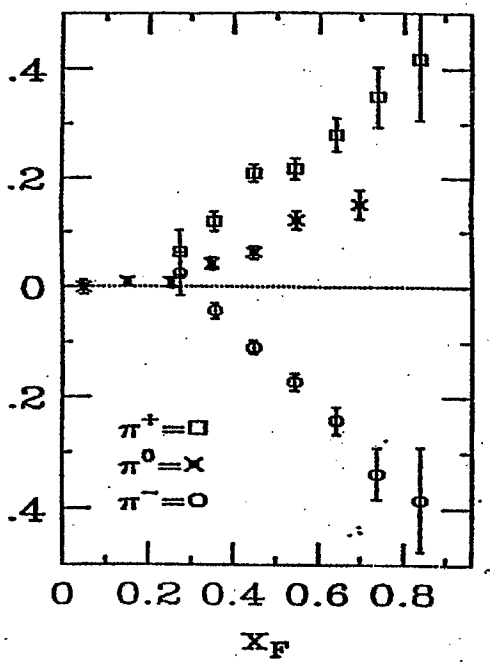

Phys. Lett. B261(1991)201
Phys. Lett. B264(1991)462

BROOKHAVEN NATIONAL LABORATORY

Large asymmetry in pion production

Asymmetry persists to high energy

No asymmetry in proton production at the AGS (not shown)

What should one expect at RHIC energies?

Predictions by different theorists expect non-zero A_N values, attributed to different dynamics, to persist at RHIC energies: $\sqrt{s}$=200 GeV...

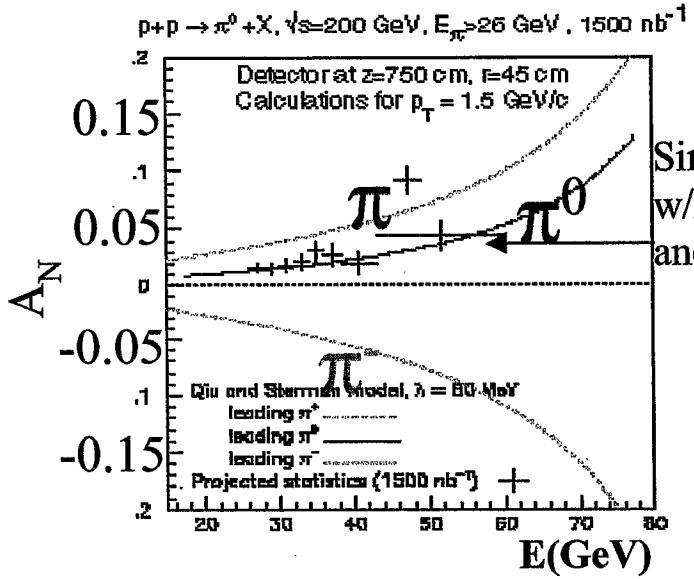

Simulation w/P_b=50% and 1.5pb^{-1}

PRL 92 (2004) 171801

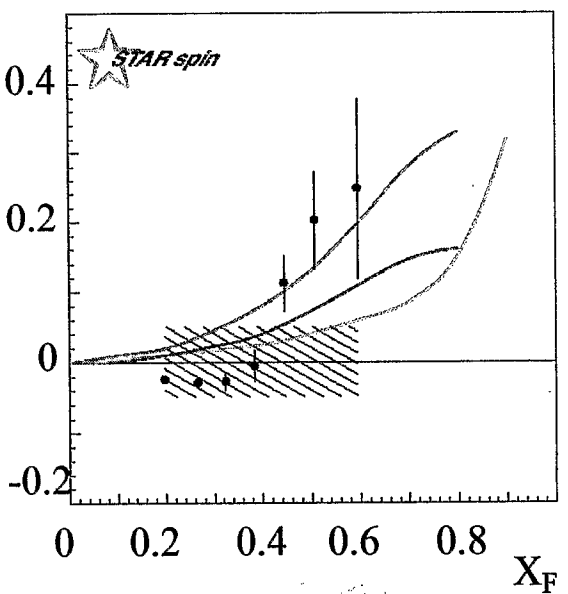

Collins effect
Anselmino, et al.
PRD 60 (1999) 054027.
Sivers effect
Anselmino, et al.
Phys. Lett. B442 (1998) 470.
Twist 3 effect
Qiu and Sterman,
Phys. Rev. D59 (1998) 014004.

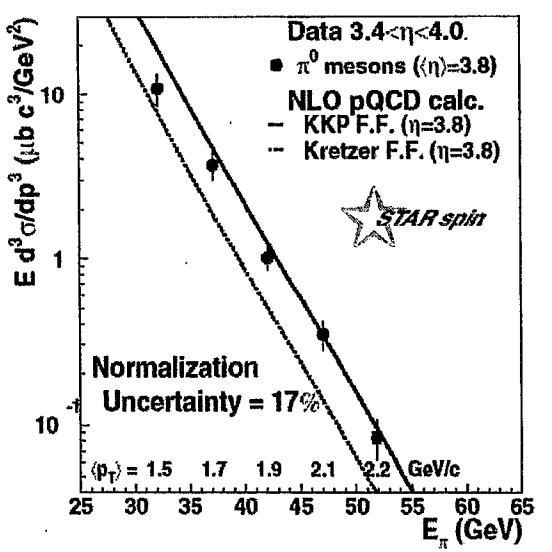

BROOKHAVEN NATIONAL LABORATORY

PRL 92 (2004) 171801

What have we learned so far?

- At large X_F asymmetries persist from low to highest energy measured.
- At large X_T asymmetry is seen in π^+ and π^0 but not in π^-
- Single Spin asymmetry is zero near $X_F = 0$ (not large X_T)
- Sivers and Collins effects apply at low and high energy
- Are we observing partonic effects:
  - polarized quarks interactions at large X_F
  - polarized gluon interaction at $X_F = 0$ and low pt
  - polarized quark-gluon interactions at higher pt
- Or possibly an X_R effect?

- The PHENIX data will probe the gluon-gluon and quark- gluon domain.

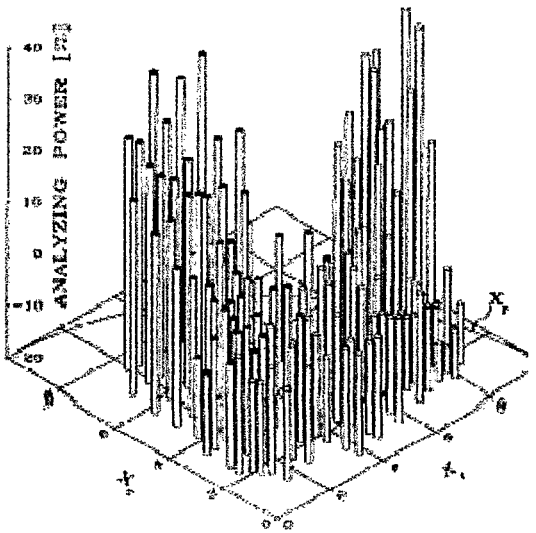

S. Saroff et al. PRL64,995,1990

BROOKHAVEN
NATIONAL LABORATORY

The Phenix Detector for Run 2

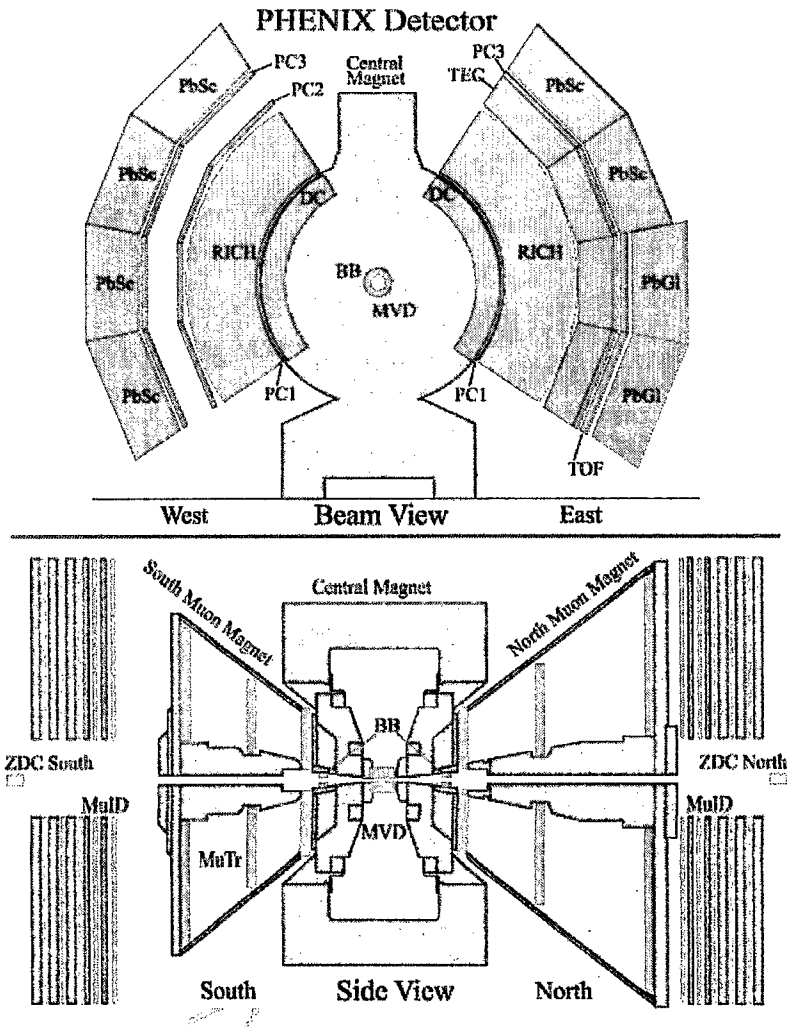

Central arms

Photons, electrons, identified charged hadrons

$|\eta| < 0.35$

$\Delta\phi = 180$ degrees

Forward muon arms

Track and identify muons

$1.2 < |\eta| < 2.4$

$\Delta\phi = 2\pi$

Detector fully operational

BROOKHAVEN
NATIONAL LABORATORY

Midrapidity π^0 and charged hadron Production in Proton-Proton Collisions at $\sqrt{s} = 200$ GeV

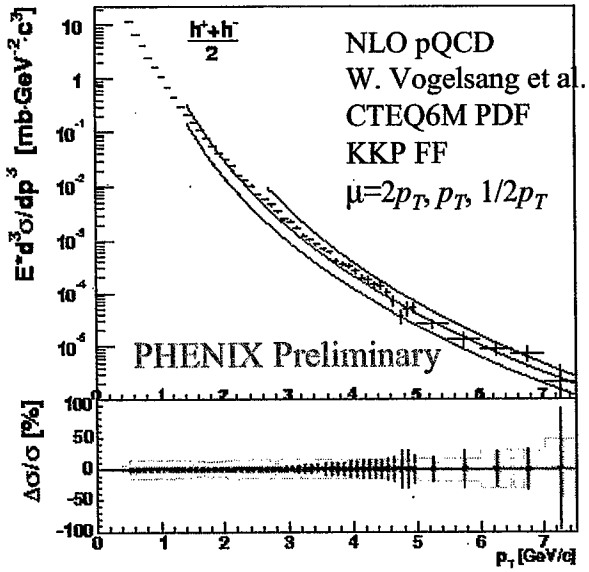

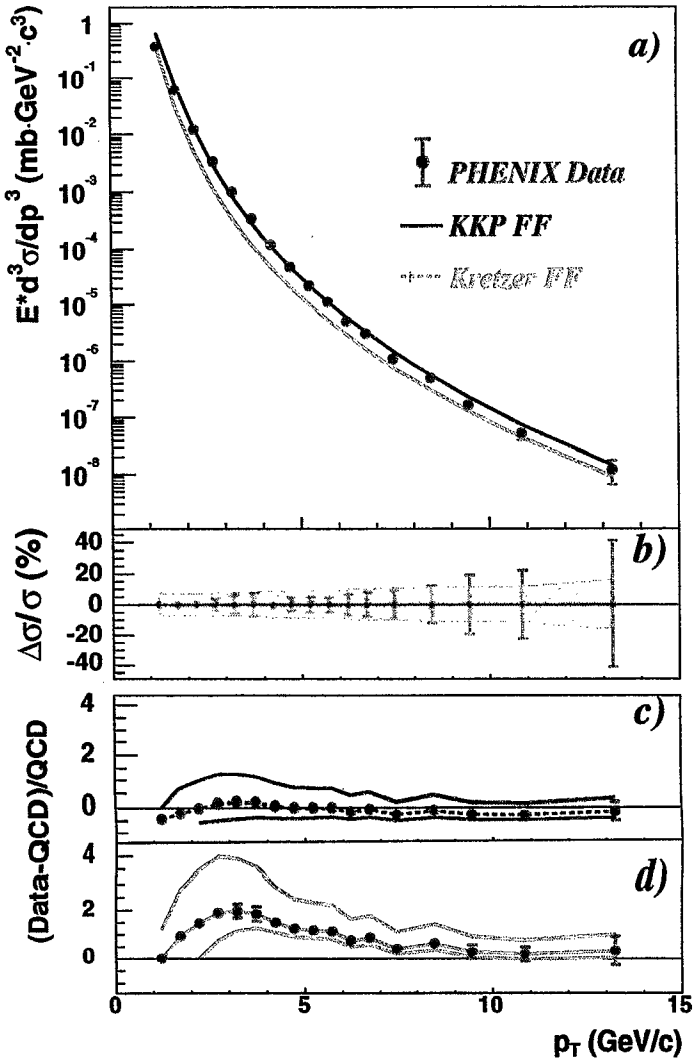

- Results consistent with pQCD calculations and favors a larger gluon-to-pion FF (KKP)
- *Provides confidence to use NLO pQCD analysis to extract spin dependent pdfs. via hadronic channels*

BROOKHAVEN NATIONAL LABORATORY

Phys. Rev. Lett. 91, 241803, 2003

A_N in inclusive charged hadron and π^0 production

- Data were collected in the first polarized proton run at RHIC "Run 2" with 0.15 pb^{-1}. The accelerator ran with vertical polarization only.
- An overall minimum bias trigger was employed using the BBC counters. These counters were also used as relative luminosity monitors between bunches of opposite polarization.
- The EMC photon trigger with an energy threshold @ 0.8 GeV was used to enhance the neutral pion sample.
- The two-photon pizero mass cut was from 0.12 - 0.16 GeV. The Background contribution ranged from 58%-9% from low to high pt and the contribution to the asymmetry was estimated from looking at the both sides of the peak.
- Required no hits in the RICH counter to eliminate electrons < 1% in the charged hadrons sample. No cuts on decays from long lived particles.

BROOKHAVEN
NATIONAL LABORATORY

Inclusive pions analysis cont'd

C. Aidala

- Calculate asymmetry of (signal + background 50 Mev around the peak) in the π^0 mass window

- Calculate the asymmetry of two different background regions
- Subtract the asymmetries

$$A_N^{\pi^0} = \frac{A_N^{\pi^0+bkg} - rA_N^{bkg}}{1-r}$$

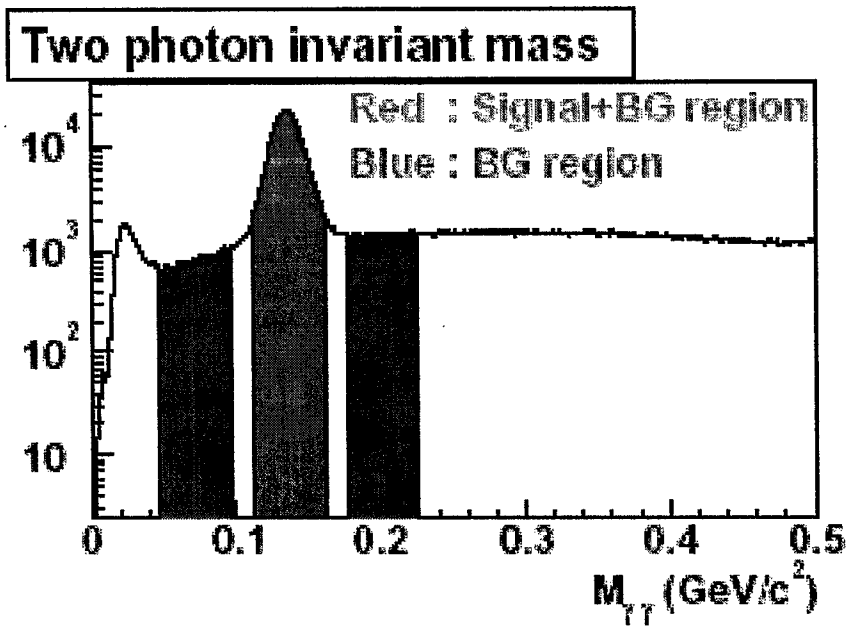

Systematics

C. Aidala and K. Okada

- comparison of independent measurement for two polarized beams
  - both beams ("blue" and "yellow") polarized
- comparison of independent measurement for left and right detectors
- comparison of minimum-bias and high-p_T triggered data samples
- store-by-store consistency of asymmetry values
- "bunch shuffling"
  - randomly reassign the polarization direction for each bunch crossing
  - recalculate the asymmetry
  - repeat many times to produce a shuffled asymmetry distribution centered around zero
  - compare width of "shuffled" distribution to statistical error on the physics asymmetry

A_N in inclusive hadron and pi zero production

C. Aidala and K. Okada

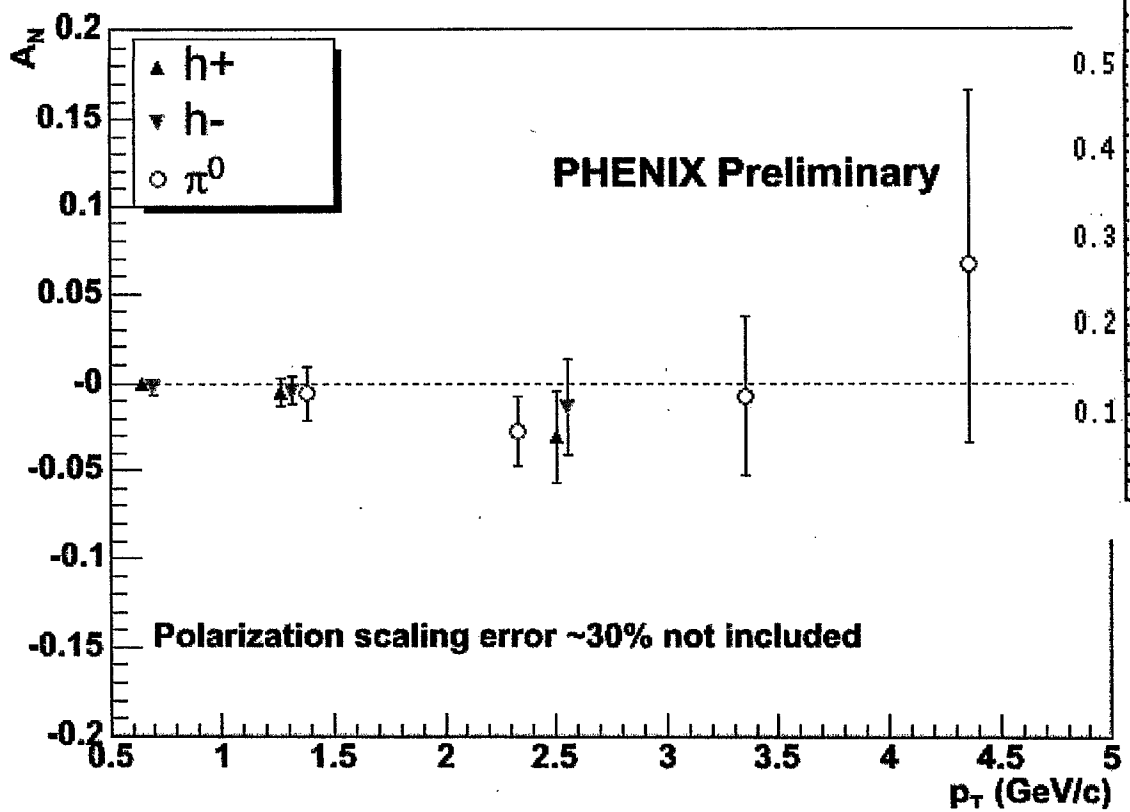

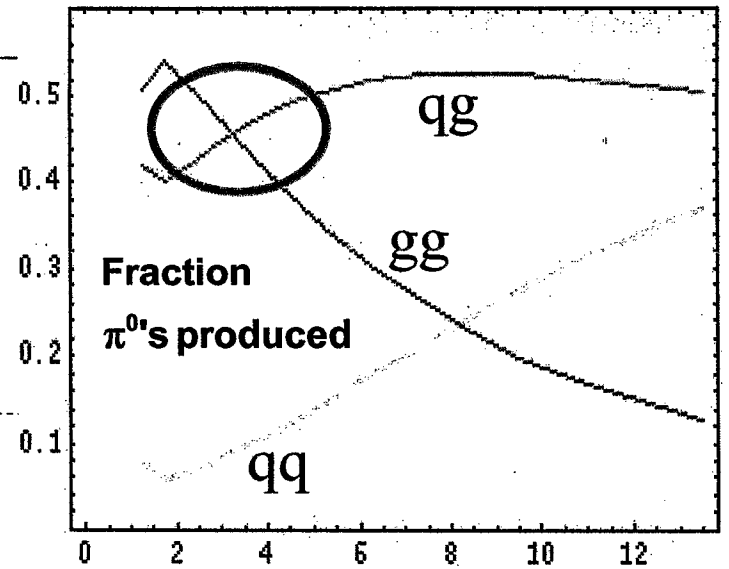

Mainly sensitive to g-g and g-q interactions

Data taken 0.15 pb^{-1} and 15 % beam polarization

A_N is consistent with zero

The difference in p_T reach is due to triggering

BROOKHAVEN NATIONAL LABORATORY

A_N in inclusive forward neutron production

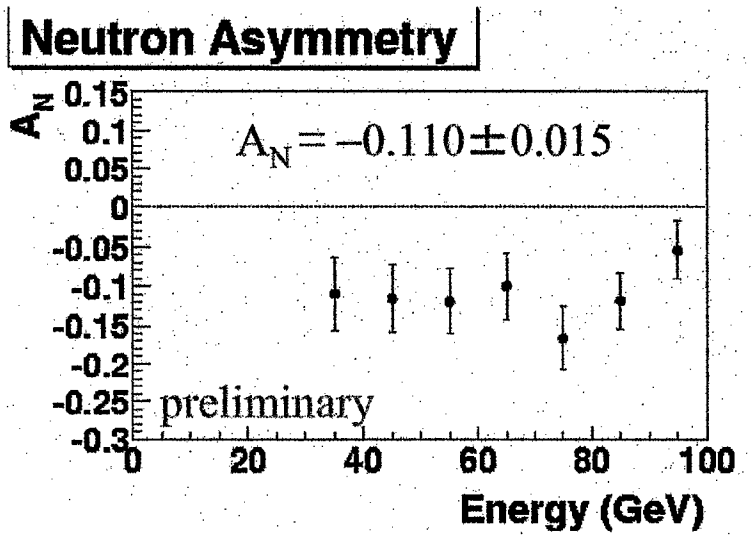

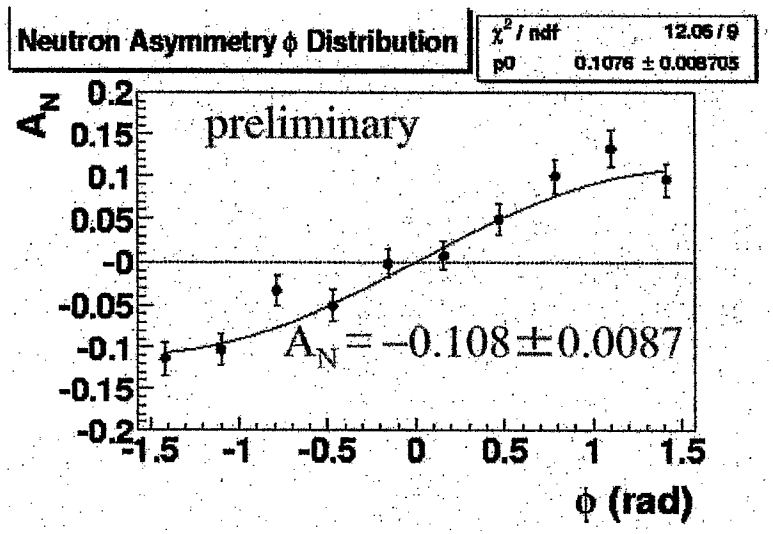

A possible diffractive process

$A_N \sim -12\%$

$x_F > 0.2$

$p_T < 0.3$ GeV/c

BROOKHAVEN
NATIONAL LABORATORY

A_N in inclusive hadron production-near term

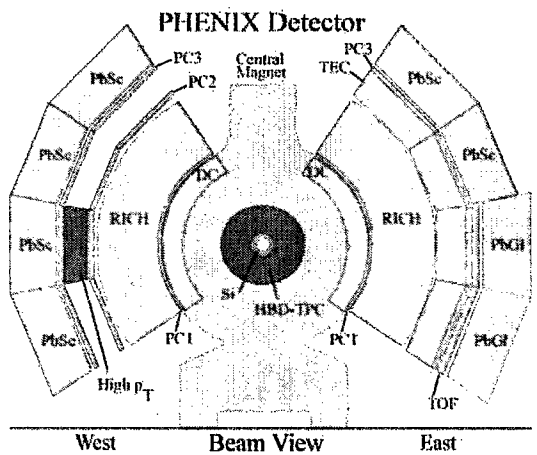

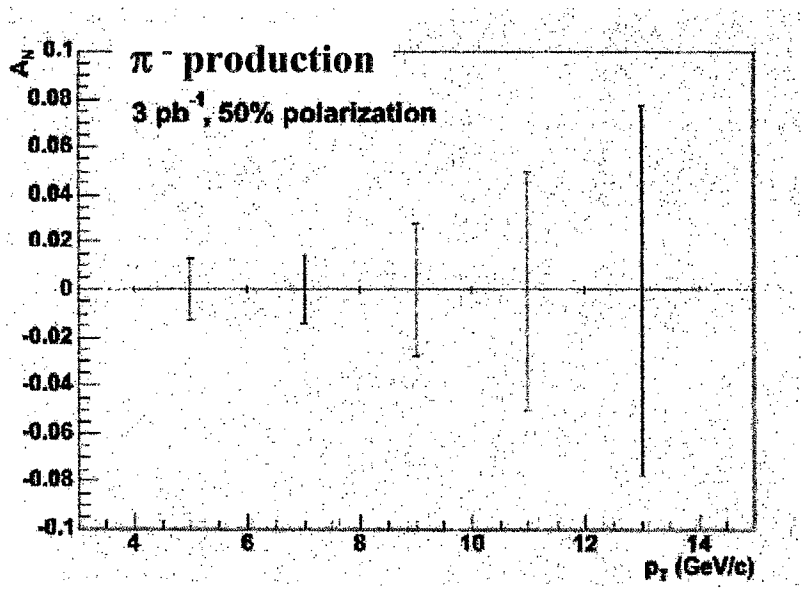

- An aerogel counter was installed to provide PID to 8 GeV/c. For pions above 4 GeV the RICH provides a trigger.
- At ~1 pb-1/week (2006?) with vertical beam polarization one could extend the pt reach to the quark-gluon contribution
- We will attempt to measure the Sivers k_T effect using back-to-back leading hadrons.

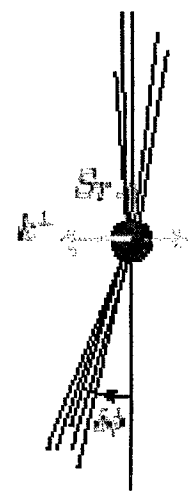

BROOKHAVEN
NATIONAL LABORATORY

Boer and Vegelsang hep-ph/0312320

Transversity measurements-longer term

The proposed PHENIX detector upgrades include the following:

a) A silicon vertex detector with - 1 ⟨η ⟨ +1

b) A Hadron blind detector

c) A nose cone calorimeter

This will provide the capability to:

a) Measure A_N in π^0 production at forward X_F

b) Efficient charged hadron trigger using the HBD/RICH and EMC

c) Reconstruct back to back jets

d) Allow measurement of the Collins effect using ππ interference. Will requires high luminosity 10 pb^{-1}/week

$$A_T(p_\perp \to \pi^+\pi^- + X) \text{ vs } p_T^{\text{pair}}$$

J. Collins, S. Heppelmann, G. Ladinsky, Nucl.Phys. B420 (1994)565

R. Jaffe, X.Jin, J. Tang Phys. Rev. D57 (1999)5920

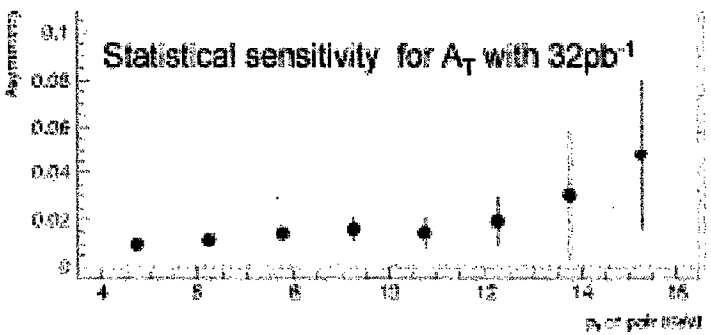

$$\int L dt = 32 pb^{-1}$$

$$E_{\pi_1,\pi_2} > 4 \text{ GeV}$$

$$\sqrt{p_{1T}^2 + p_{2T}^2} > 4 \text{ GeV}$$

$$800 \text{ MeV} < m < 950 \text{ MeV}$$

BROOKHAVEN NATIONAL LABORATORY

Summary

The polarized proton collider at RHIC provides a unique opportunity to study spin physics effects.

RUN II

With 15% beam polarization and low luminosity PHENIX measured the single spin asymmetry A_N in inclusive pi zero and charged hadrons near X_F=0.

- The measured asymmetry is consistent with zero with good statistics.
- The asymmetry is well below that measured by STAR at large X_F
- The measurement is quite sensitive to transverse gluon polarization.

Future RUNS

- The near term upgrades, higher luminosity and beam polarization should allow a higher p_t reach 6-10 GeV/c and access the quark- gluon contribution.
- Attempt a first measurement of the Sivers effect.
- Longer term upgrades of PHENIX and the collider will allow a full compliment of transversity measurements

BROOKHAVEN
NATIONAL LABORATORY

Spin effects in large rapidity neutral pion production at STAR

OGAWA, Akio BROOKHAVEN NATIONAL LABORATORY

For STAR Collaboration

- STAR experiment and Forward Pion Detector
- Forward physics in hadron collider
- Analyzing power with transverse polarized proton beams
- Conclusions and outlook

12 Oct 2004 Spin Trieste Italy

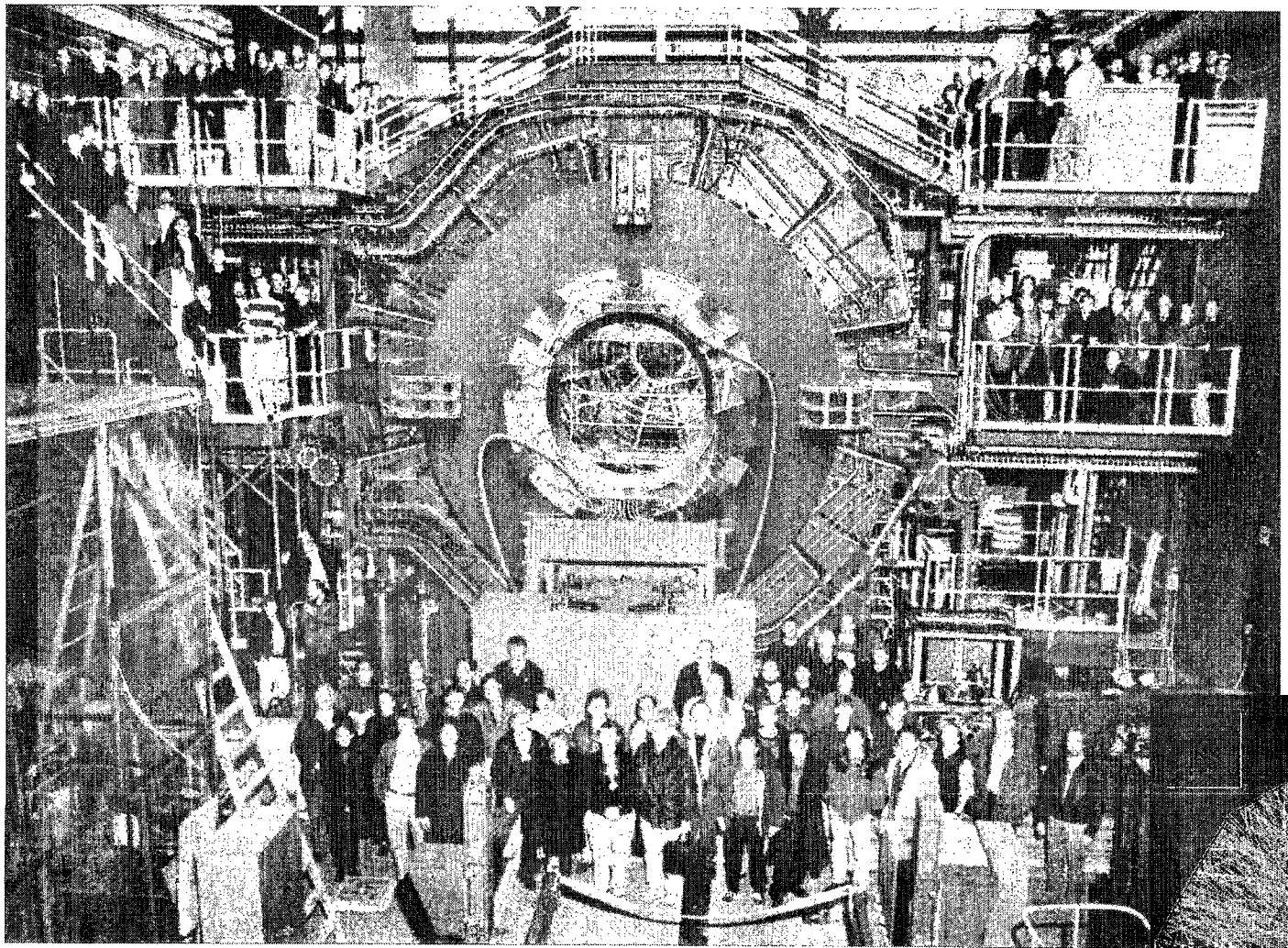

STAR spin

The

STAR

Collaboration

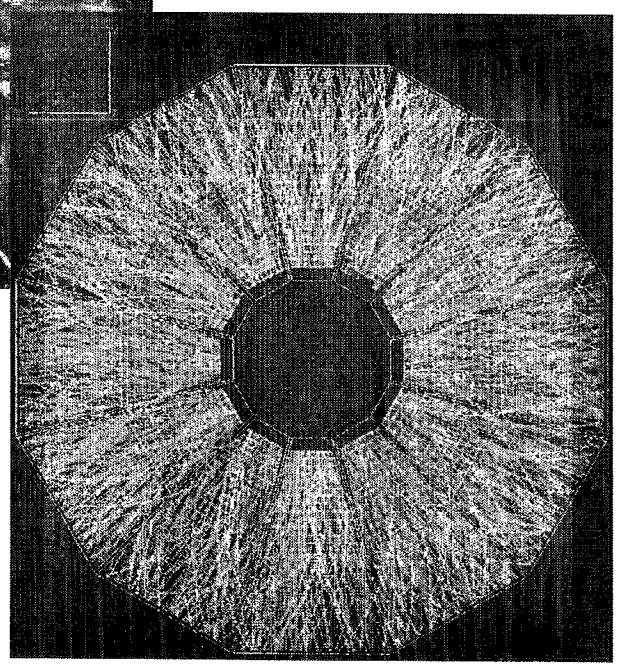

Solenoid Tracker At RHIC

522 collaborators
51 institutions
12 countries

STAR Detector

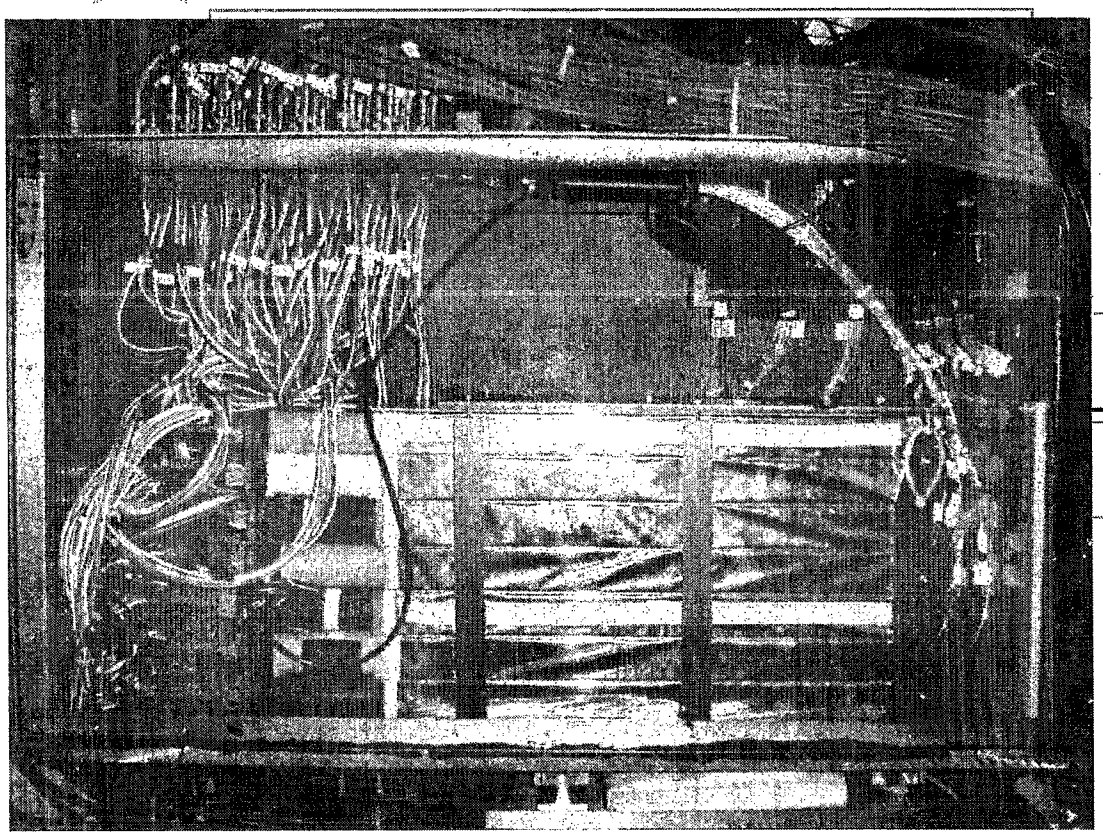

TPC: $-1.0 < \eta < 1.0$

Forward TPC: $2.8 < |\eta| < 3.8$

BBC : $2.2 < |\eta| < 5.0$

FPD: $|\eta| \sim 4.1$ and ~ 3.6

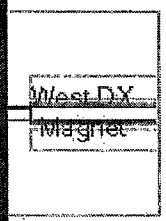

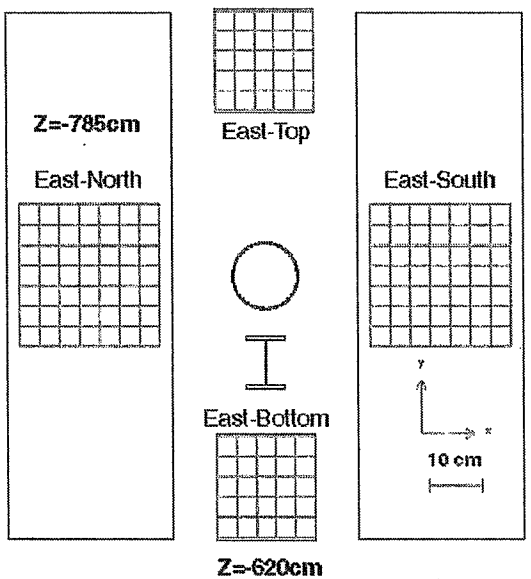

Upgraded Forward π^0 Detector (FPD)

- Pb-glass EM calorimeter
  (from IHEP Protvino, used in E704)
- Shower-Maximum Detector (SMD)
- Preshower

Spin2004, A.Ogawa(BNL)

Forward π^0 production in hadron collider

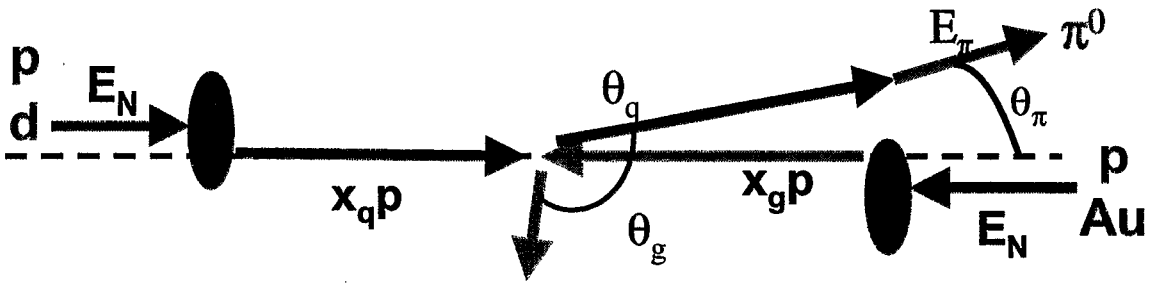

$$Q^2 \sim p_T^2 \qquad x_F \approx \frac{2E_\pi}{\sqrt{s}}$$

$$\sqrt{s} = 2E_N \qquad z = \frac{E_\pi}{E_q}$$

$$\eta = -\ln(\tan(\frac{\theta}{2})) \qquad x_q \approx x_F / \langle z \rangle \qquad x_g \approx \frac{p_T}{\sqrt{s}} e^{-\eta_g}$$

(collinear approx.)

- **Large rapidity π production (η_π~4) probes asymmetric partonic collisions**

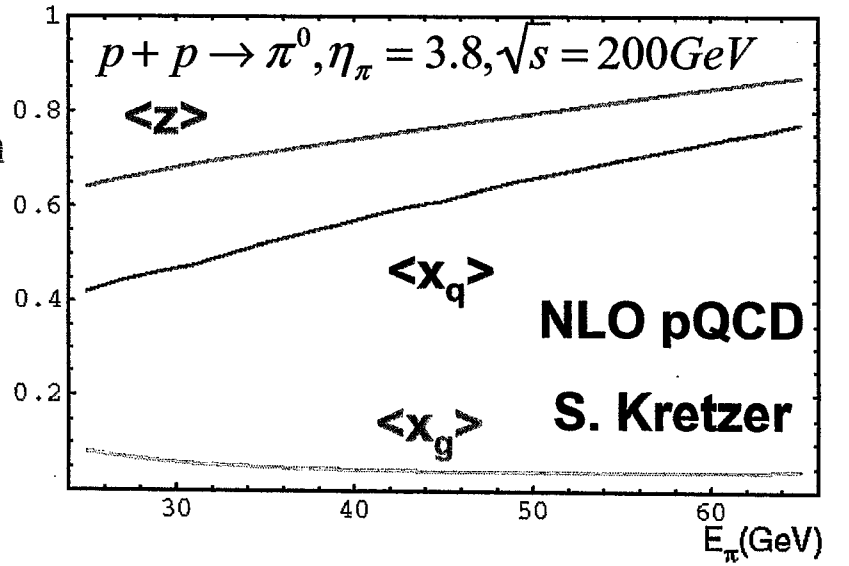

- Mostly **high-x valence quark + low-x gluon**
  - **$0.3 < x_q < 0.7$**
  - **$0.001 < x_g < 0.1$**
- <z> nearly constant and high 0.7 ~ 0.8

- Large-x quark polarization is known to be large from DIS
- Directly couple to gluons = A probe of low x gluons

Spin2004, A.Ogawa(BNL)

But, do we understand forward π^0 production in p + p?

STAR spin

At $\sqrt{s}$ << 200 GeV, not really….

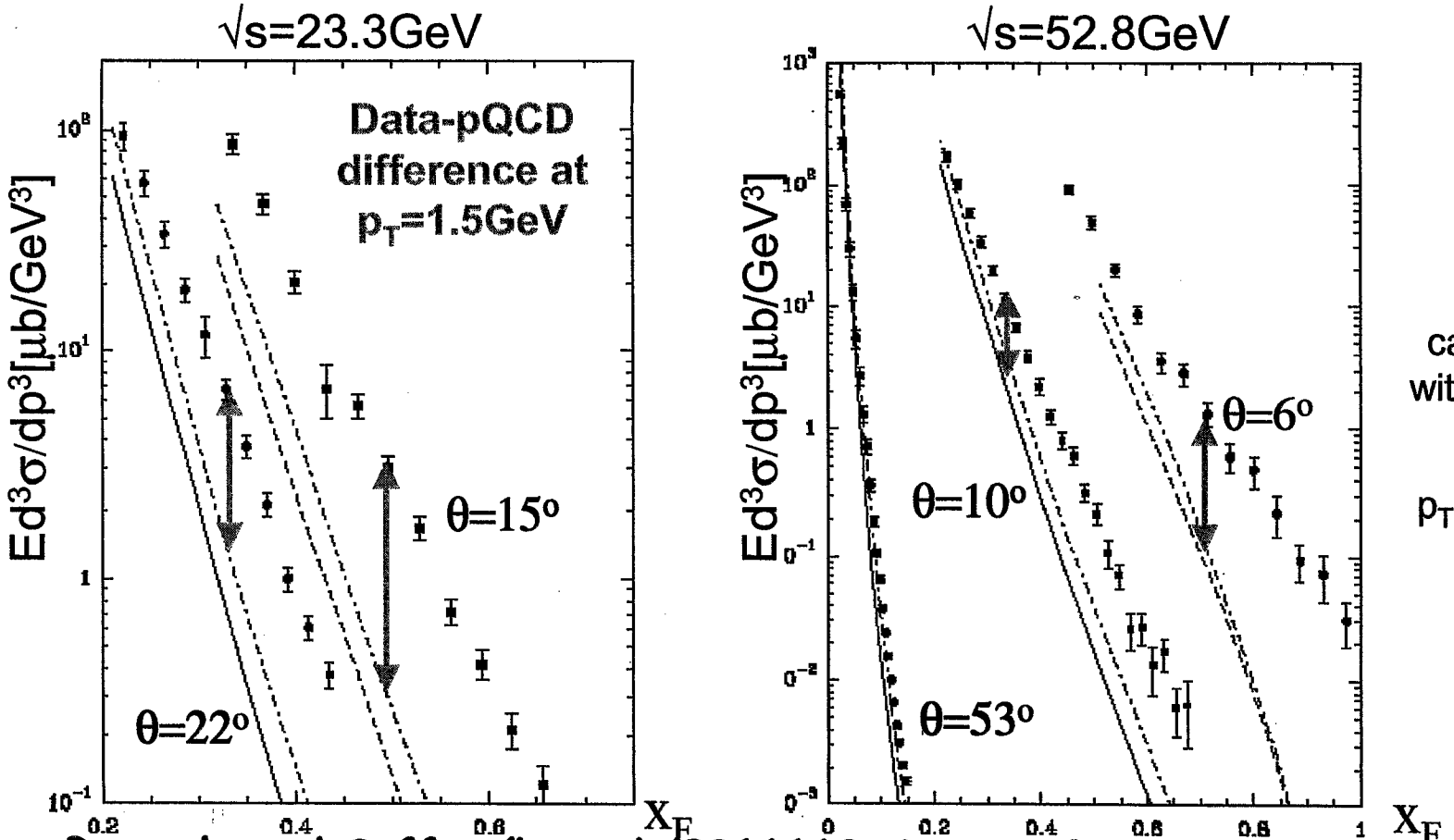

2 NLO calculation with different scale:

p_T and $p_T/2$

Bourrely and Soffer (hep-ph/0311110, Data references therein):

NLO pQCD calculations underpredict the data at low $\sqrt{s}$ from ISR

$\sigma_{data}/\sigma_{pQCD}$ appears to be function of θ, $\sqrt{s}$ in addition to p_T

Forward π^0 Inclusive Cross Section

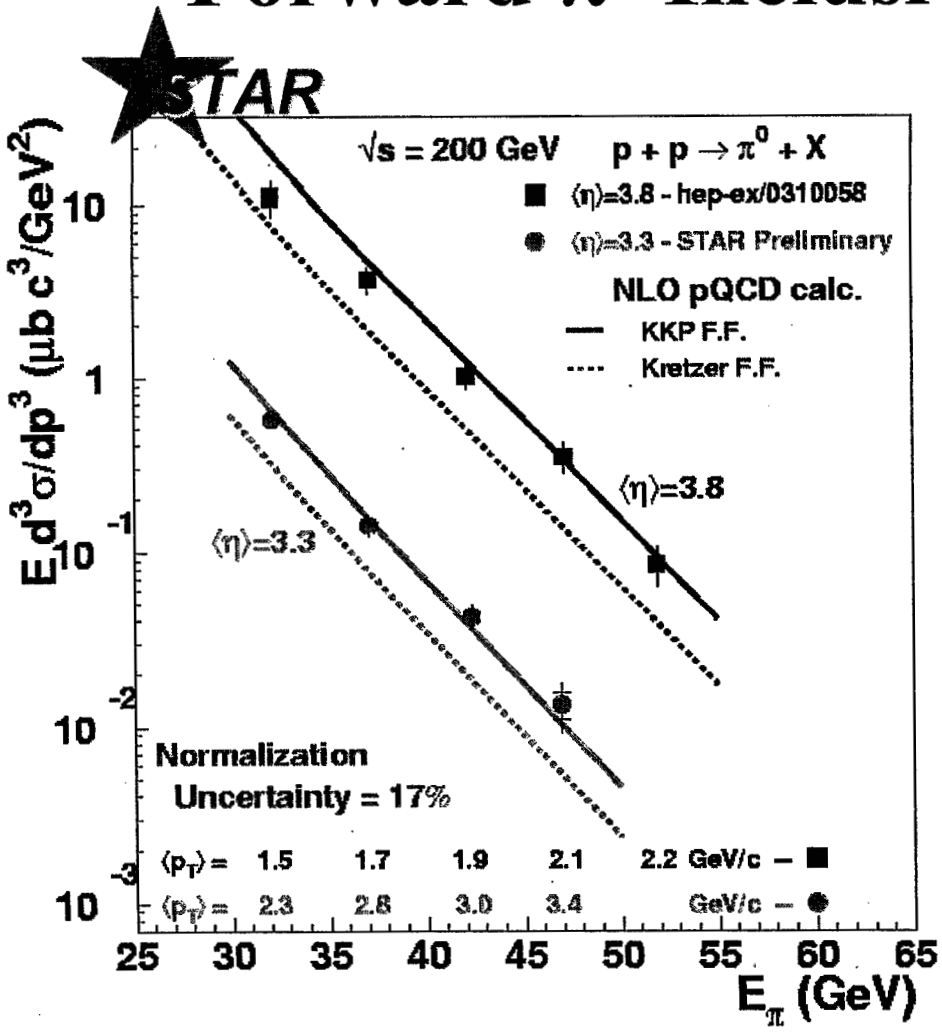

- STAR data at
  - $\langle\eta\rangle$= 3.8 (hep-ex/0310058, Phys. Rev. Lett. **92** (2004) 171801)
  - $\langle\eta\rangle$= 3.3 (hep-ex/0403012, Preliminary)
- NLO pQCD calculations at fixed η with equal factorization and renormalization scales = p_T
- Solid and dashed curves differ primarily in the $g \rightarrow \pi$ fragmentation function

STAR data consistent with Next-to-Leading Order pQCD calculations

in contrast to data at lower √s (Bourelly and Soffer, Eur.Phys.J. C36 (2004) 371-374)

$p + p \rightarrow \pi^0 + h^{\pm}$, $\sqrt{s} = 200$ GeV

$|\langle\eta_\pi\rangle| = 4.0$, $|\eta_h| < 0.75$

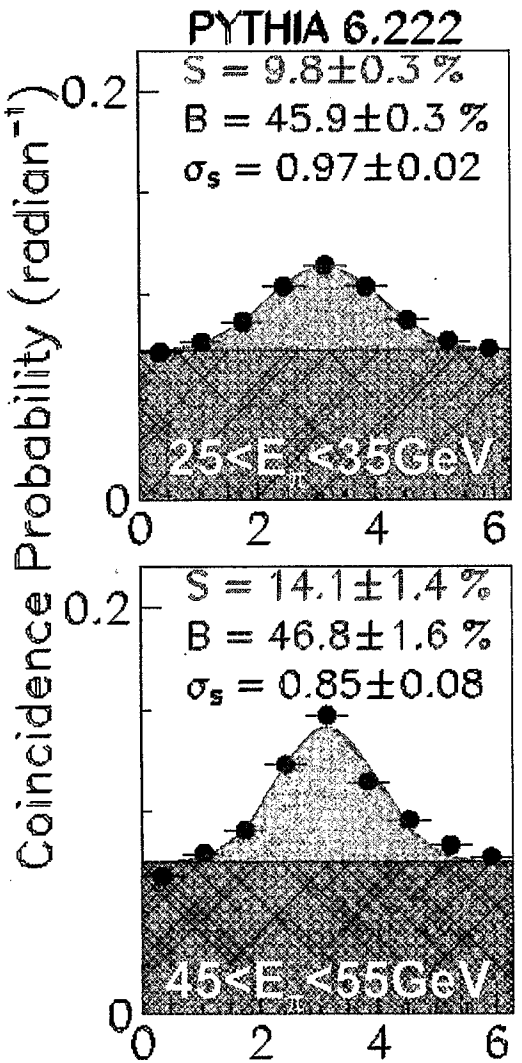

nucl-ex/0408004 $\varphi_\pi - \varphi_{LCP}$

Statistical errors only

Azimuthal di-hadron correlation with large rapidity interval

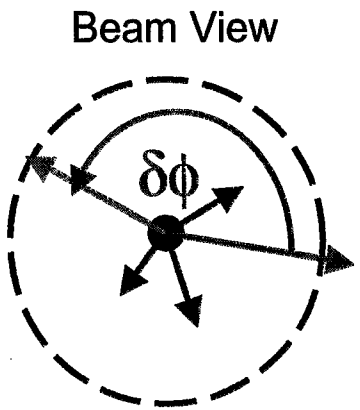

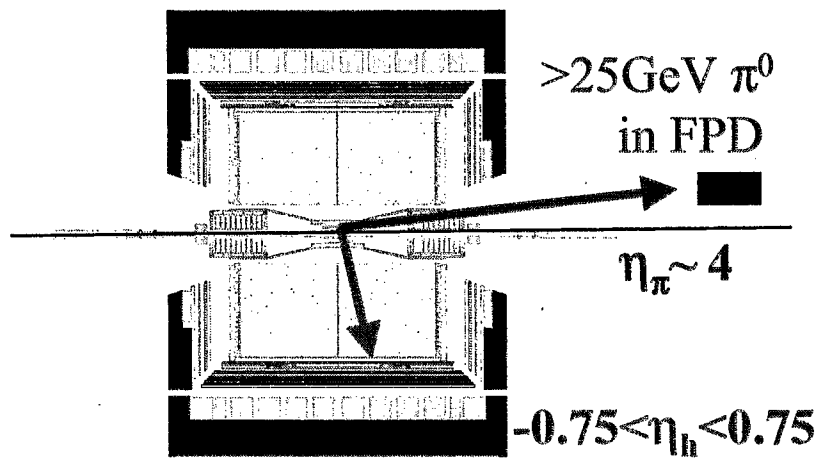

Leading charged particles (LCP) of p_T>0.5GeV in mid rapidity TPC

Large Analyzing Powers at RHIC

First measurement of A_N for forward π^0 production at $\sqrt{s}$=200GeV

STAR collaboration, hep-ex/0310058,
Phys. Rev. Lett. **92** (2004) 171801

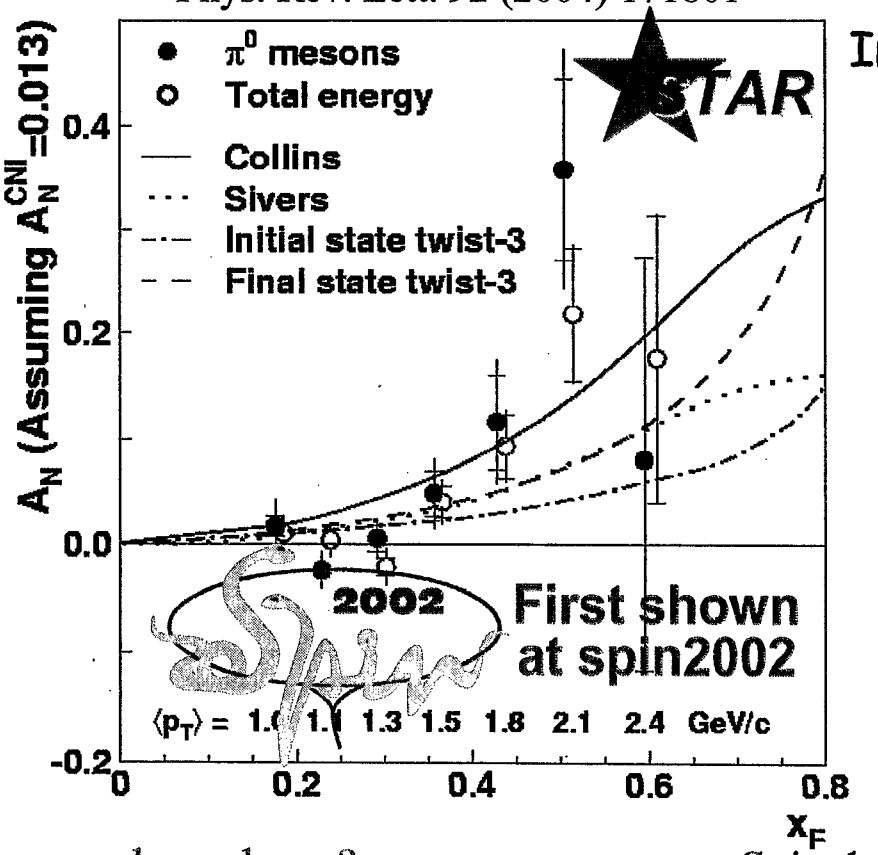

Similar to **FNAL E704** result at $\sqrt{s}$ = 20 GeV

In agreement with several models including different dynamics:

- Sivers: spin and $k_\perp$ correlation in initial state (related to orbital angular momentum?)
- Collins: Transversity distribution function & spin-dependent fragmentation function

  → suppressed? (hep-ph/0408356)
- Qiu and Sterman (initial-state) / Koike (final-state) twist-3 pQCD calculations

- p_T dependence?
- x_F<0?
- A_N with mid-rapidity correlation?
- Spin dependence in jet?
- Heavy flavors??
- Related to "gluon saturation"???

Time/luminosity dependent

d calibration

FTPC-FPD matching

Photon conversion in beam pipe

$\rightarrow \pi^0 (+ X) \rightarrow \gamma (+ \gamma) \rightarrow e^+ e^-$

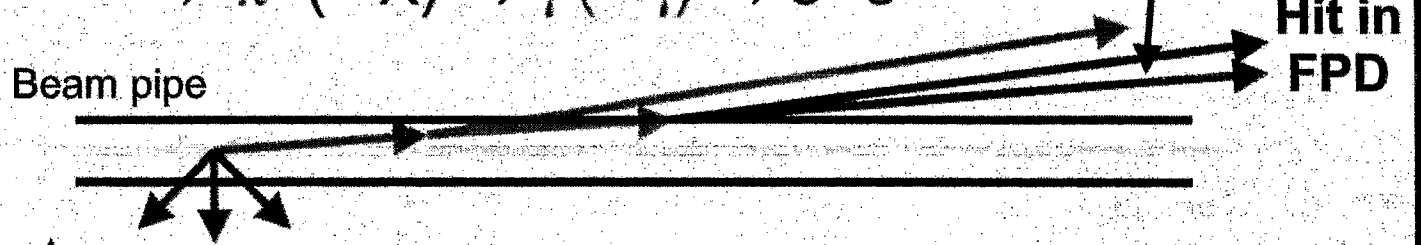

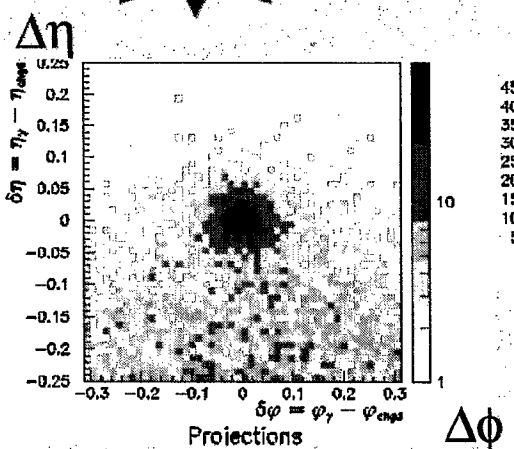

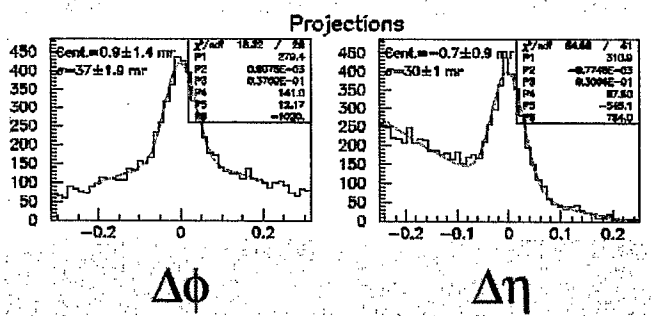

⇒ FPD position known relative to STAR

(Recon. Eff.)(Frac. of 2 contained γ)

config=dau03close4

2nd mom

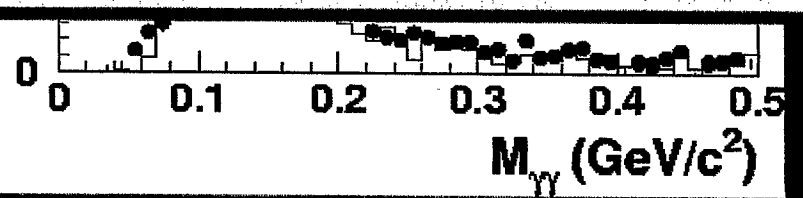

RHIC Run3 data analysis for FPD

STAR spin

RHIC-Run3 (2003 May)

Polarization ~ 30%

0.5/pb with transverse pol. in 2 weeks

(0.4/pb with longitudinal pol. In 2 weeks)

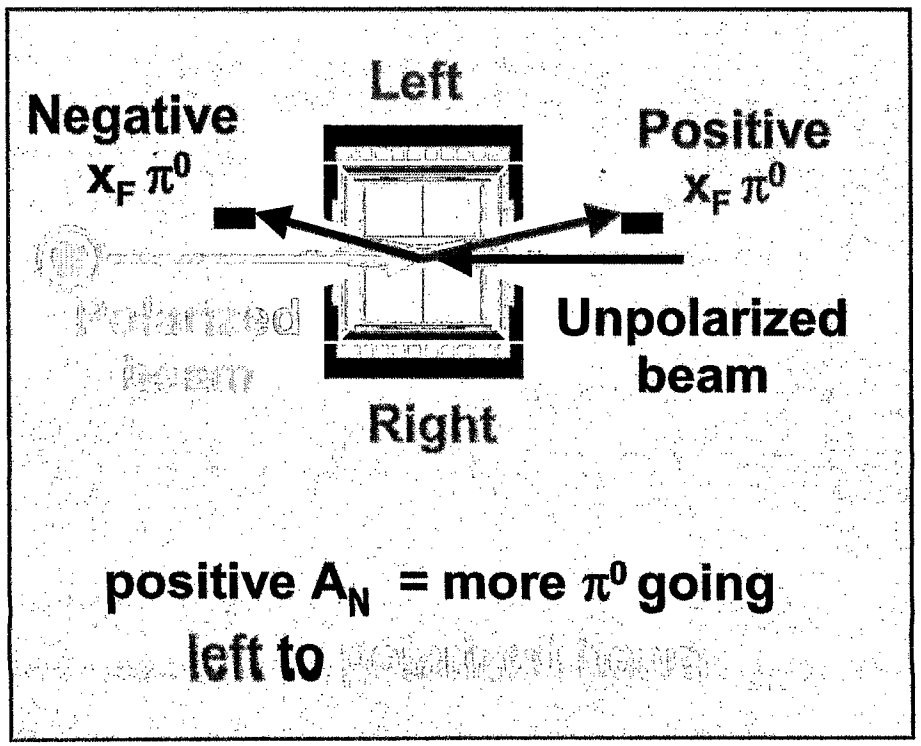

Polarization is measured by RHIC pC CNI polarimeter

FPD East North & South

"Cross ratio" method

$$A = \frac{1}{P}\left(\frac{\sqrt{N_L^{\uparrow}\cdot N_R^{\downarrow}}-\sqrt{N_R^{\uparrow}\cdot N_L^{\downarrow}}}{\sqrt{N_L^{\uparrow}\cdot N_R^{\downarrow}}+\sqrt{N_R^{\uparrow}\cdot N_L^{\downarrow}}}\right)$$

FPD West South

Single arm measurement

$$A = \frac{1}{P}\left(\frac{N^{\uparrow}-RN^{\downarrow}}{N^{\uparrow}+RN^{\downarrow}}\right) \qquad R = \frac{L^{\uparrow}}{L^{\downarrow}}$$

Relative luminosity R is measured by BBC

→ J. Kiryluk's talk

2 measurements are consistent

→ averaged

A_N at negative x_F

Will it be really zero? Or will we see twist-3 gluon correlations?

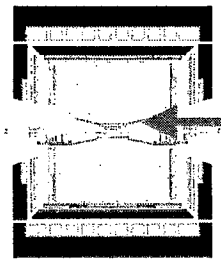

FPD

Blue beam

Sort by blue beam spin

Sort by yellow beam spin

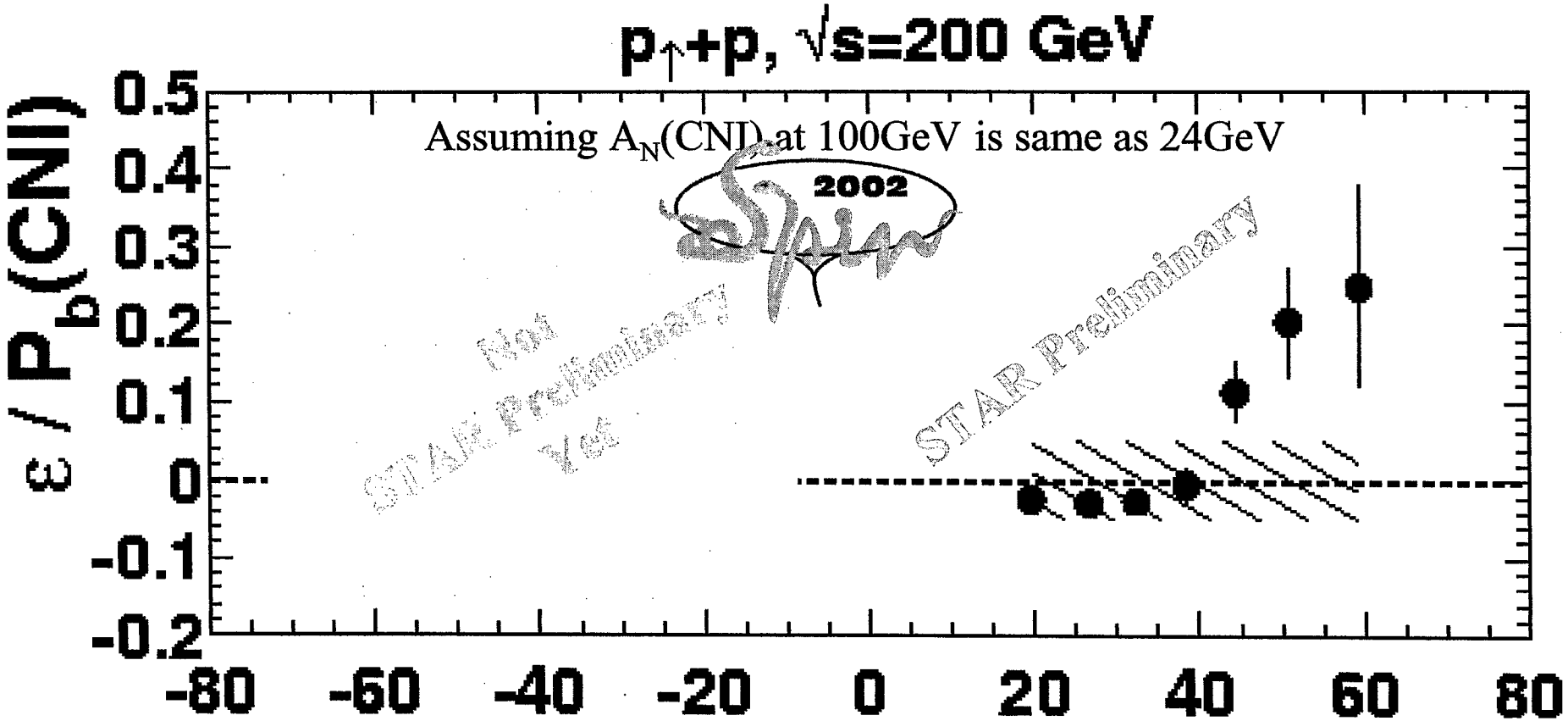

Last call for PRE-dictions

$\sim x_F * 100$ Via(BNL)

Measurement of A_N

for fo … 200GeV

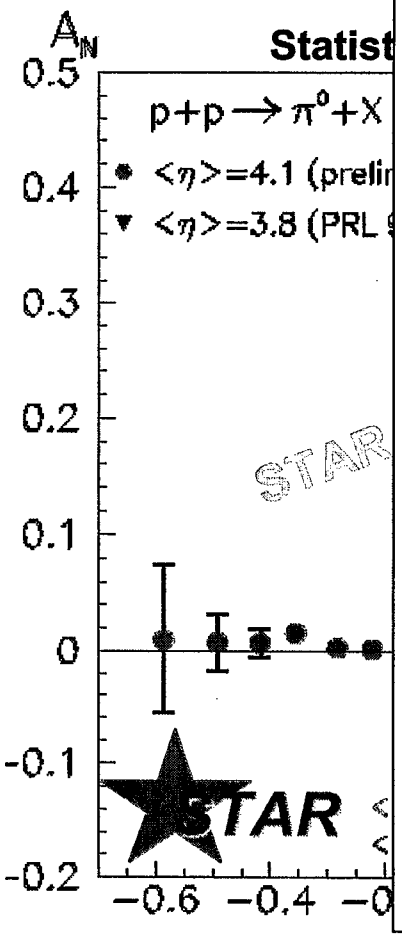

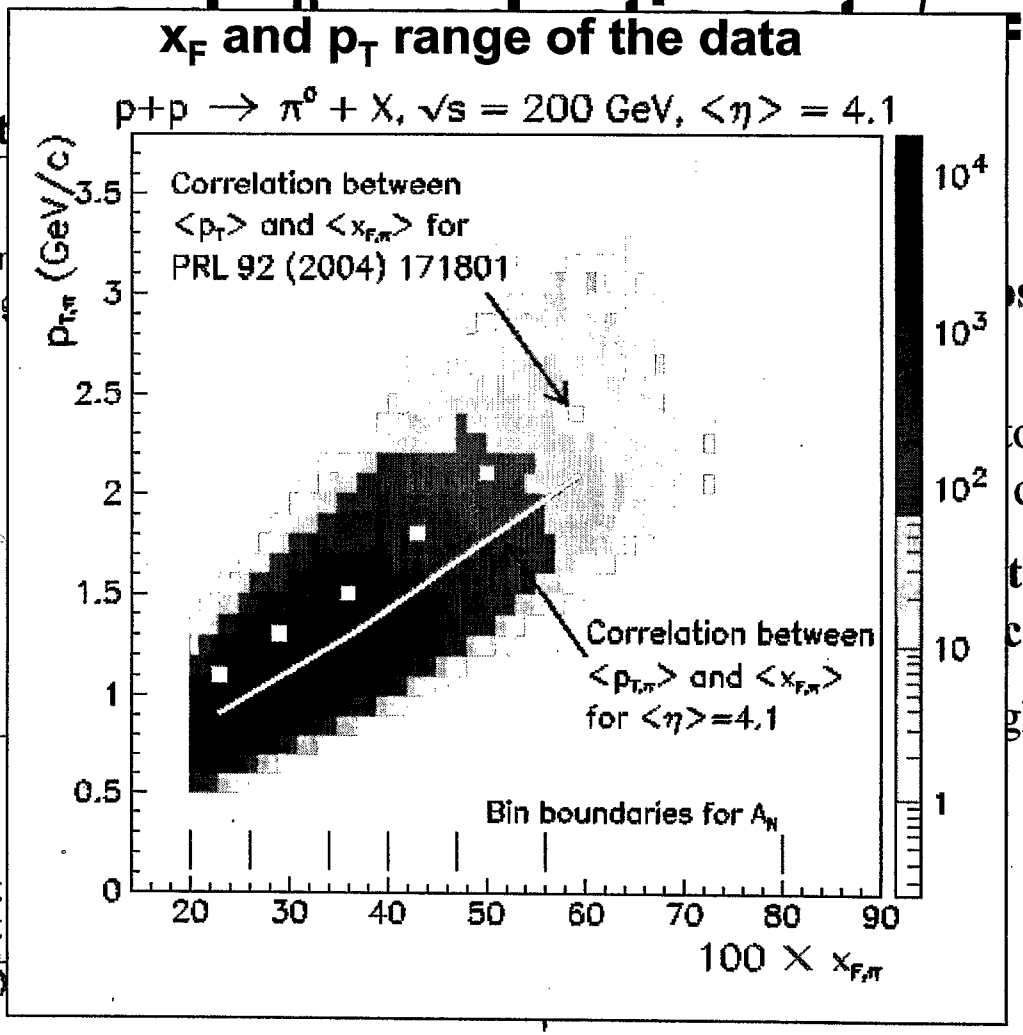

…sitive x_F has been

…o be non-zero &
…data

…t of negative x_F A_N
…consistent with zero

…gluon-gluon

Mapping of A_N in x_F and p_T plane has begun !

Beam Beam Counters at STAR

- 1cm thick scintillator annulus installed around the beam pipe, on the east and west poletips of STAR magnet at ±3.74m from IR for detection of <u>charged particles</u> (no identification) in $2 < |\eta| < 5$

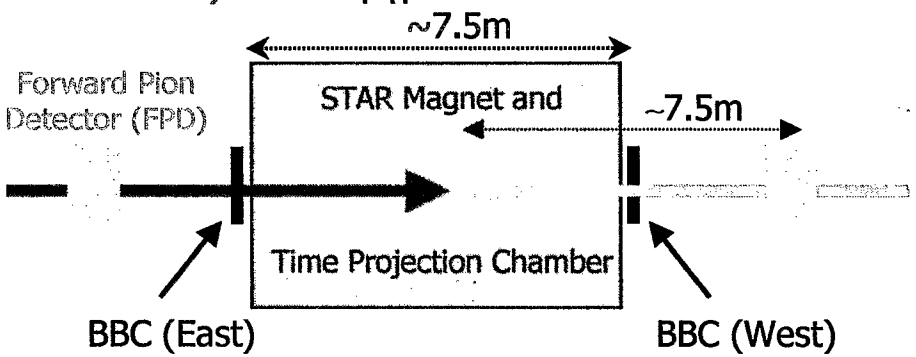

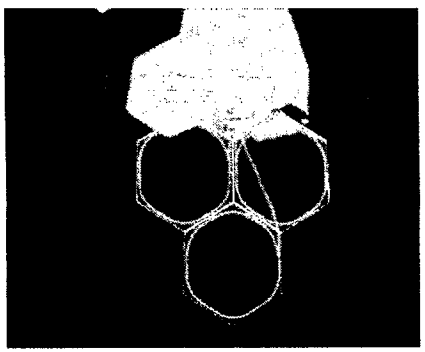

- <u>Small hexagonal annulus:</u>
- Inner (outer) diameter 9.6cm (48cm);
- Covering $3.3<|\eta|< 5.0$ and $0<\phi<2\pi$
- 16 PMT - feasible segmentation
  - two bins in η
  - azimuthal

Top/Bottom/Left/Right

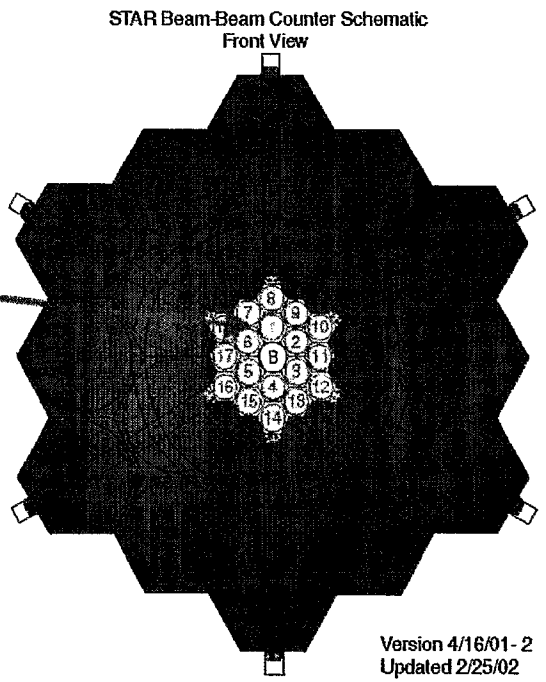

Transverse Single Spin Asymmetries at BBC
(A_N for forward unidentified charged particles)

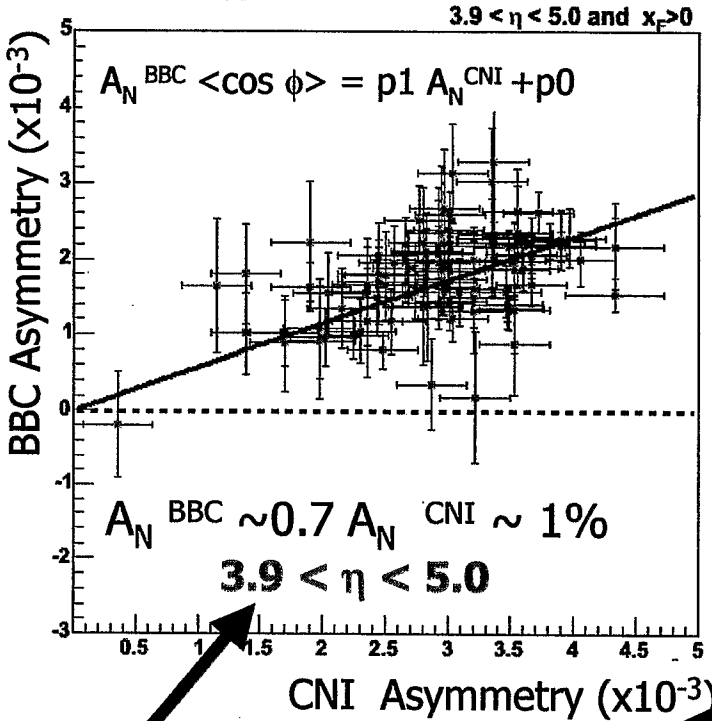

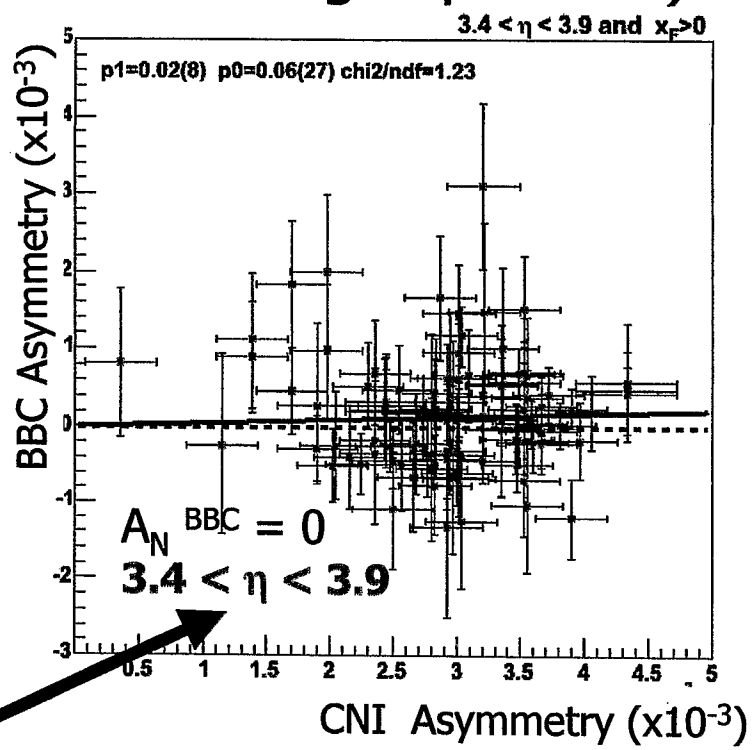

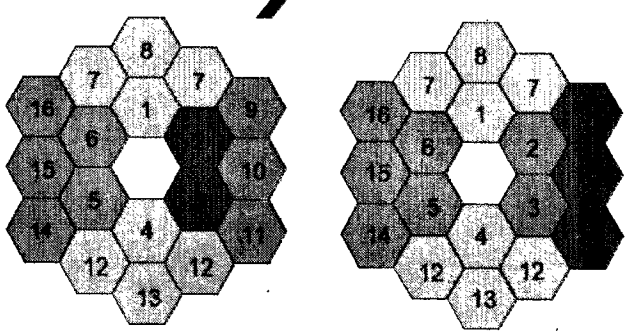

Red=Have hit
Green=No hit Blue=Don't care

- Unexpected A_N of unknown origin measured with the BBC
- Strong pseudorapidity dependence of A_N for $x_F>0$ and $A_N = 0$ for $x_F<0$
- $\delta\varepsilon(syst) < \delta\varepsilon(stat)$

Spin2004, A.Ogawa(BNL)

Conclusions

- Forward hadron production at hadron-hadron collider selects high-x (thus high polarization) quark + low-x gluon scatterings
- Inclusive cross section is consistent with NLO pQCD calculations and PYTHIA(LO pQCD + parton showers)
- Di-hadron correlation with large rapidity interval in p+p agree with PYTHIA prediction
- Analyzing power for forward π^0 mesons at large positive x_F was found to be positive
  - The first measurement of negative x_F A_N has been done, and is consistent with zero
- More (Cross section at $\langle\eta\rangle=4.1$, A_{TT}, A_{LL}, correlations with other detectors) on the way

Outlook

- **Disentangling the dynamics of A_N via**
  - Higher precision A_N measurement vs x_F and p_T
  - A_N with mid rapidity correlation
  - Forward jets (FPD + BBC/FTPC)
- Proposal for forward calorimeter upgrade →
  - Heavy mesons and direct photons
  - Low x gluons in nuclei
- **Mid rapidity jets**
  - Di-jet k_T balance → gluon Sivers function
  - Inside jet particle correlation → Collins function * Transversity
- **A_{LL} for forward π^0 = gluon polarization at low x**

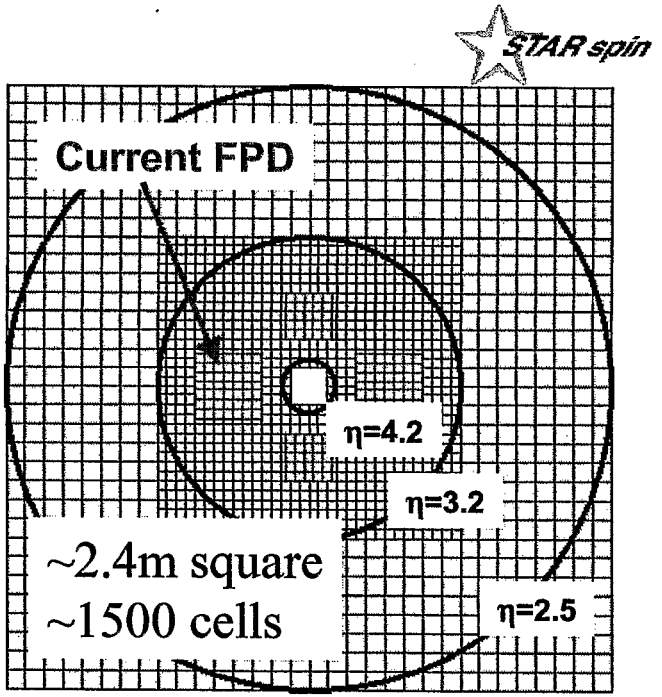

→**Tomorrow L. Bland's Talk**

RHIC run for 2005 starts in November (next month)

First long physics run for p+p, with P~50%, starting 2005 Jan

Plans for some data taking with transverse spin @ STAR after longitudinal spin data taking

Transversity Properties of Quarks and Nucleons in SIDIS and Drell Yan

Leonard Gamberg*
Division of Science, Penn State Berks

RHIC SPIN Collaboration Meeting *INFN, Turin*

297

- Remarks on Transversity and Spin Structure of Nucleon
  - ⋆ Minining Transversity Through Hard Scattering
- Transversity in Azimuthal Asymmetries
  - ⋆ Reaction Mechanism-Rescattering in T-odd Structure and Fragmentation Functions
  - ⋆ Estimates of the Collins and Sivers Asymmetries
  - ⋆ Novel Transversity Properties in Hard Scattering
  - ⋆ Double T-odd $\cos 2\phi$ asymmetry & higher twist
  - ⋆ Beam Asymmetry
- Conclusions

*Gary R. Goldstein, Tufts Univ. & Karo Oganessyan formerly *INFN-LNF* Frascati & Now undisclosed Financial Co., NYC

Introductory Remarks: Transversity

- Transversity "δq" as combinations of helicity states

$$|\perp/\top>=\frac{1}{\sqrt{2}}(|+> \quad \pm \quad |->)$$

Goldstein & Moravcsik, Ann. Phys. 1976 introduced reveal underlying simplicity spin-dependent nucleon-nucleon scattering amps, $f_{a,b;c,d}(s,t)$

- Connection with spin structure of nucleon revealed through the quark distribution $h_1^a(x) = \delta q^a(x)$

- First moment, tensor charge Jaffe & Ji, PRL:1991 $\int_0^1 (\delta q^a(x) - \delta \overline{q}^a(x))\, dx = \delta q^a$

- LO anomalous dimensions Baldracchini *et al* Fortsch. Phys. 1981, Artru & Mekhfi, ZPC:1990

TRANSVERSITY:
Understood Context Parton Model in IMF

- Light Cone Rep. of "Good" Dirac Spinors (Kogut, Soper PRD:1970)

$$\psi_+(\xi^-) = \int d^2k_\perp dk^+ \sum_{s=1,2} \left\{ b_s(k)u(s)\mathrm{e}^{-ik^+\xi^-} + d_s^\dagger(k)v(s)\mathrm{e}^{ik^+\xi^-} \right\}$$

$P_\pm \psi = \psi_\pm$
projector of *good* $+$ (indept.) and bad - (dept.) light cone spinors

- Instead of diagonalizing free Hamiltonian w/r to HELICITY eigenstates: use $\perp/\top$ TRANSVERSITY eigenstates: $Q_{\top/\perp} = \frac{1}{2}\left(\mathbf{1} \mp \gamma_5 \not{S}_\perp\right)$

  ⋆ Projector $Q_{\top/\perp}$ commutes with the free-quark Hamiltonian and with $P_\pm$, is a *good* light cone operator

TRANSVERSITY BASIS

- Transverse Basis: $Q_{\top/\perp} = \frac{1}{2}\left(\mathbf{1} \mp \gamma_5 \gamma^{\perp}\right)$

While $g_1(x)$ meaning is obscure

$$g_1(x) \;=\; \mathrm{Re}\frac{2}{x}\langle P\hat{\mathbf{e}}_3|b_{\perp}^{\dagger}(xP)b_{\top}(xP)|P\hat{\mathbf{e}}_3\rangle$$

in transversity basis

300

$$h_1(x) \;=\; \frac{1}{x}\langle P\hat{\mathbf{e}}_{\perp}|b_{\perp}^{\dagger}(xP)b_{\perp}(xP) - b_{\top}^{\dagger}(xP)b_{\top}(xP)|P\hat{\mathbf{e}}_{\perp}\rangle$$

$h_1(x)$ is clearly defined as the probability to find quark with spin polarized along transverse spin direction minus oppositely polarized case

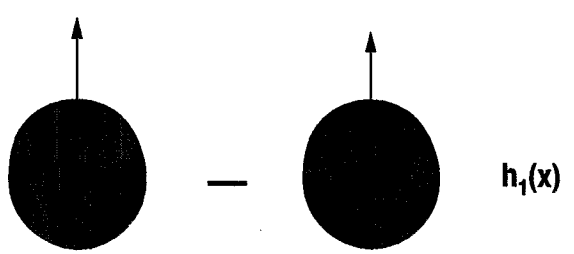

Theoretically among other things:

⋆ Soffer's inequality (Soffer, PRL:1995) & possible saturation/violation (Goldstein Jaffe Ji, PRD:1995) places bounds on leading twist distributions
$\left|2\delta q^a(x,Q^2)\right| \leq q^a(x,Q^2) + \Delta q^a(x,Q^2)$

⋆ NLO analysis Martin & Vogelsang *et al*, PRD: 1998; indicates bound respected under evolution

301

- Decouples leading twist DIS: Helicity of struck quark must flip to probe transversity chiral-odd
  ⇒require chiral-odd partner
  ⇒ and one or more hadrons
  involved in process probe transversity

Hard scattering conserves chirality
thus hadron helicity flip suppressed in DIS by m/Q

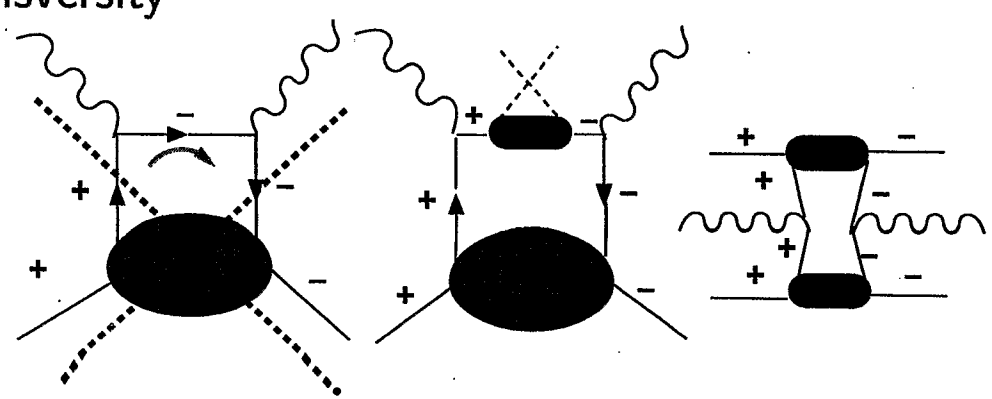

Mining Transversity thru Hard Scattering

Drell-Yan $p_\perp\, p_\perp \Rightarrow l^+ l^- \; X$ (2 in the initial state)
SIDIS $l\; p_\perp \Rightarrow l'\, h \; X$ (1 in the initial 1 in the final)

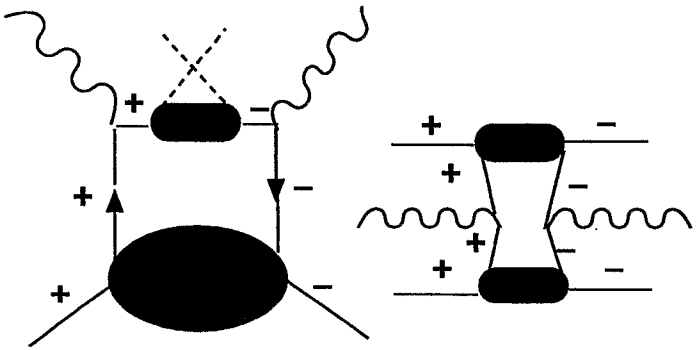

★ DY:Ralston and Soper NPB:1979 encountered double transverse spin asymmetry

302

$$A_{TT}^{DY} = \frac{2\sin^2\theta\cos(\phi_1+\phi_2)}{1+\cos^2\theta}\frac{\sum_a e_a^2 h_1^a(x)\overline{h}_1^a(x)}{\sum_a e_a^2 f_1^a(x)\overline{f}_1^a(x)}$$

★ SIDIS:Jaffe and Ji PRL:1993 encountered at twist three level Estimate, Gamberg, Hwang, Oganessyan PLB:2004

$$A_{LT} = \frac{\lambda_e |\boldsymbol{S}_T| \sqrt{1-y}\,\frac{4}{Q}\left[M\, x\, g_T(x) D_1(z) + M_h\, h_1(x)\frac{E(z)}{z}\right]}{\frac{[1+(1-y)^2]}{y}\, f_1(x) D_1(z)}$$

SIDIS and Transversity: Leading Twist

- Collins NPB:1993, Kotzinian NPB:1995, Mulders, Tangermann PLB:1995

  Transversity can be measured via azimuthal asymmetry in the fragmenting hadron's momentum, Collins effect:

  $P_{h\perp}$ - hadron transverse momentum

  ϕ, azimuth between $[k\, q]$ and $[P_h\, q]$ planes

  ϕ_S, azimuth of the target spin vector

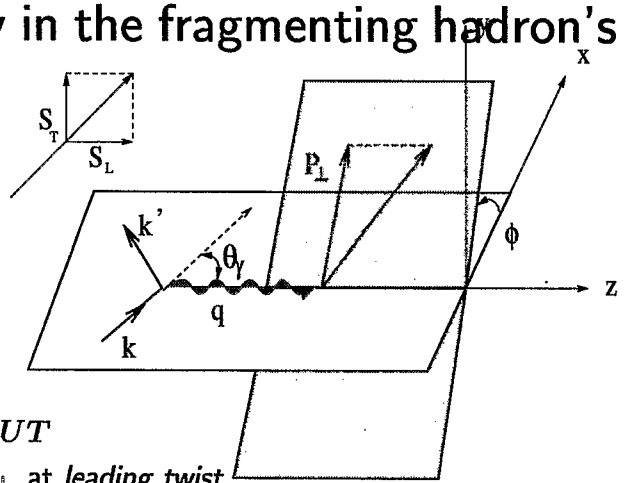

Here one considers cross sections differential in transverse momentum: SSA is not surpressed by inverse powers of the hard scale, ie in A_{UT} quarks in target, and current fragmentation region possess transverse momentum $p_\perp$, $k_\perp$ at *leading twist*

Beyond Colinearity

The hadron helicity flip generated by quark orbital angular momentum, quarks have transverse momentum k_T in hadrons. Hadron helicity flip occurs by addition of quark orbital angular

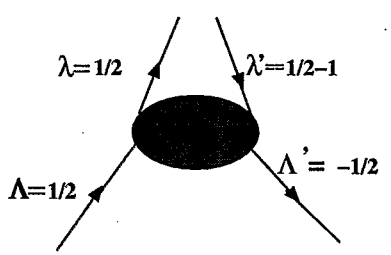

$$\langle \frac{P_{h\perp}}{M_\pi} \sin(\phi + \phi_s) \rangle_{UT}$$

$$= \frac{\int d\phi_s \int d^2 P_{h\perp} \frac{P_{h\perp}}{M_\pi} \sin(\phi + \phi_s) \left(d\sigma^\uparrow - d\sigma^\downarrow\right)}{\int d\phi_s \int d^2 P_{h\perp} \left(d\sigma^\uparrow + d\sigma^\downarrow\right)}$$

$$= |S_T| \frac{2(1-y) \sum_q e_q^2 h_1(x) z H_1^{\perp(1)}(z)}{(1 + (1-y)^2) \sum_q e_q^2 f_1(x) D_1(z)}$$

Color Gauge Invariance & Novel Transversity Properties of Quarks and Nucleons

Employ Factorized Description

Levelt & Mulders, Mulders & Tangerman, NPB: 1994, 1996, See new work of Ji, Ma, Yuan: 2004

$$\frac{d\sigma^{\ell+N\to\ell'+h+X}}{dxdydzd^2P_{h\perp}} = \frac{M\pi\alpha^2 y}{2Q^4 z} L_{\mu\nu}\mathcal{W}^{\mu\nu}$$

304 Hadronic Tensor

$$2M\mathcal{W}^{\mu\nu}(q,P,P_h) = \int d^2\boldsymbol{p}_T d^2\boldsymbol{k}_T \delta^2(\boldsymbol{p}_T+\boldsymbol{q}_T-\boldsymbol{k}_T)$$
$$\mathrm{Tr}[\Phi(x_B,\boldsymbol{p}_T)\gamma^\mu\Delta(z_h,\boldsymbol{k}_T)\gamma^\nu] + (q\leftrightarrow -q\ ,\ \mu\leftrightarrow\nu)\ ,$$

where

$$\Phi(p,P) = \int \frac{d^3\xi}{2(2\pi)^3} e^{ip\cdot\xi}\langle P|\overline{\psi}(\xi^-,\xi_\perp)\mathcal{G}^\dagger_{[\xi^-,\infty]}|x\rangle\langle x|\mathcal{G}_{[0,\infty]}\psi(0)|P\rangle|_{\xi^+=0}$$

$$\Delta(k,P_h) = \int \frac{d^3\xi}{4z(2\pi)^3}\ e^{ik\cdot\xi}\ \langle 0\ |\mathcal{G}_{[\xi^+,-\infty]}\psi(\xi)|x;P_h\rangle\langle x;P_h|\overline{\psi}(0)\mathcal{G}^\dagger_{[0,-\infty]}|0\rangle|_{\xi^-=0}$$

- Gauge Invariant Distribution and Fragmentation Functions Ji, Yuan & Belitsky PLB: 2002, NPB 2003, Boer, Mulder, Pijlman NPB 2003

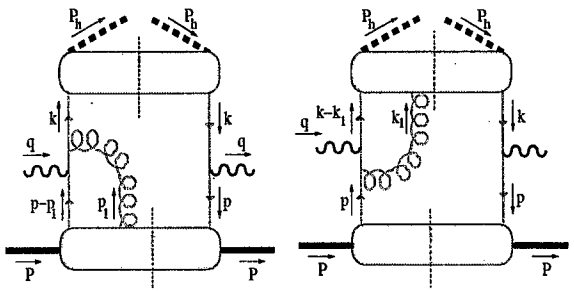

- **T-odd Distribution Functions: Transversity Properties of quarks in Hadrons**
  Boer, Mulder, PRD 1998

$$
\begin{aligned}
\Delta(z, \boldsymbol{k}_T) &= \frac{1}{4}\{D_1(z, z\boldsymbol{k}_T)\,\not{n}_- + H_1^{\perp}(z, z\boldsymbol{k}_T)\frac{\sigma^{\alpha\beta}k_{T\alpha}n_{-\beta}}{M_h} \\
&+ \frac{M_h}{P_h^-}E(z, z\boldsymbol{k}_T) + \cdots\}. \\
\Phi(x, \boldsymbol{p}_T) &= \frac{1}{2}\{f_1(x, \boldsymbol{p}_T)\,\not{n}_+ + h_1^{\perp}(x, \boldsymbol{p}_T)\frac{\sigma^{\alpha\beta}p_{T\alpha}n_{+\beta}}{M} \\
&+ \frac{M}{P^+}e(x, \boldsymbol{p}_T) + f_{1T}^{\perp}(x, \boldsymbol{p}_T)\frac{\epsilon^{\mu\nu\rho\sigma}\gamma^{\mu}n_+^{\nu}p_T^{\rho}S_T^{\sigma}}{M}\cdots\}\ ,
\end{aligned}
$$

Experimental status of SSAs

⋆ Dedicated transversity programs:

- $\ell \vec{p} \to \ell' \pi X$ DESY( ), (1999, 2003....) See talk of Ralf Seidl
- $p^{\uparrow} p \to \pi X$ *RHIC* BNL(⋆STAR). See Talks of A. Ogawa and Les Bland
- CERN(COMPASS). See Talks at SPIN 2004
- JLAB-Hall A, B, C $\vec{\ell} \vec{p} \to \ell' \pi X$. See Talks at SPIN 2004

306 • Also, large SSA are observed in $P P^{\uparrow} \to \pi X$
E704 Collaboration (1991)

NON-ZERO AZIMUTHAL ASYMMETRIES

- Origins/Mechanisms

  ⋆ In the naive parton model all azimuthal asymmetries are zero at leading order

  ⋆ However, both intrinsic k_T dependence & higher order in α_s PQCD generate azimuthal asymmetries

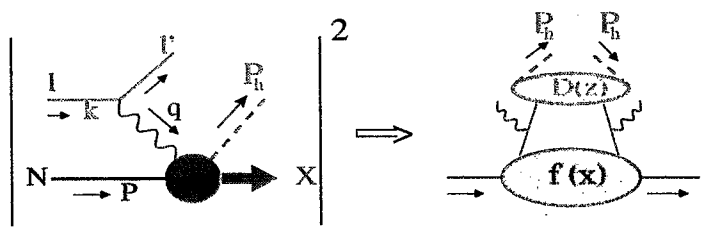

may arise from different mechanisms containing ordinary T-even soft parts:

⋆ H. Georgi, H.D. Politzer, PRL:1978: pQCD first order α_s

⋆ R.N. Cahn, PLB: 1978; PRD: 1989; Chay, Ellis, Stirling, PRD: 1991, Oganessyan *et al.*, ZPC: 1998

Intrinsic $k_\perp$ & pQCD expansion in α_s

PLB: 2002 Brodsky, Hwang, and Schmidt demonstrate rescattering of a gluon could produce the necessary phase leading to nonzero SSAs at *Leading Twist*

Rescattering-Mechanism: T-Odd Contributions to Asymmetries

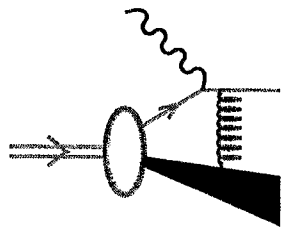

- Ji, Yuan & Belitsky PLB: 2002, NPB 2003 describe effect in terms of gauge invariant distribution functions (Collins,Soper NPB: 1982)

$$\Rightarrow \quad \langle P|\overline{\psi}(\xi^-,\xi_\perp)\mathcal{G}^\dagger_{[\xi,\infty]}|X\rangle\langle X|\mathcal{G}_{[0,\infty]}\psi(0)|P\rangle|_{\xi^+=0}$$

$$\mathcal{G}_{[\xi,\infty]} = \mathcal{G}_{[\xi_T,\infty]}\mathcal{G}_{[\xi^-,\infty]}, \quad \text{where} \quad \mathcal{G}_{[\xi^-,\infty]} = \mathcal{P}exp(-ig\int_{\xi^-}^{\infty} d\xi^- A^+)$$

- Demnstrates that BHS calculated Sivers Function, $f_{1T}^\perp(x,k_\perp)|_{\rm SDIS}$
  In Singular gauge, $A^+ = 0$, effect remains

- Collins, PLB: 2002, modifies earlier claim of trivial Sivers Effect
  $f_{1T}^\perp(x,k_\perp)|_{\rm SDIS} = -f_{1T}^\perp(x,k_\perp)|_{\rm DY}$

Sivers Asymmetry in SIDIS

- Probes the probability that for a transversely polarized target, pions are produced asymmetrically about the transverse spin vector:

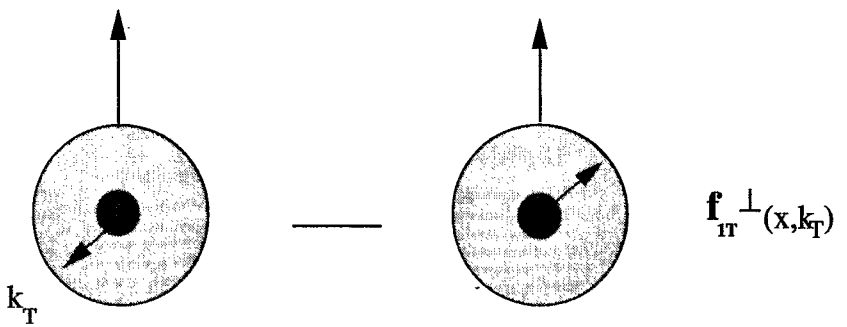

$$\langle \frac{|P_{h\perp}|}{M} \sin(\phi - \phi_S) \rangle_{UT} = |\boldsymbol{S}_T| \frac{(1+(1-y)^2) \sum_q e_q^2 f_{1T}^{\perp(1)}(x) z D_1^q(z)}{(1+(1-y)^2) \sum_q e_q^2 f_1(x) D_1(z)},$$

Reaction Mechanism explained as FSI

⋆ See Star and HERMES Data

T-Odd Contributions to Asymmetries

- $T-$odd quark distribution functions, *e.g.* $f_{1T}^{\perp}(x, k_{\perp})$, $h_1^{\perp}(x, k_{\perp})$, (Sivers PRD: 1990, Anselmino & Murgia PLB: 1995 ...) may exist as leading or higher twist effects due to initial/final state interactions or ...

- PRD: 1998 Boer and Mulders considered asymmetries, due to the presence of leading twist T-odd distribution functions, $f_{1T}^{\perp}, h_1^{\perp}$

$$
\begin{aligned}
d\sigma_{\lambda,S} \quad \propto \quad & f_1 \otimes D_1 + \frac{k_T}{Q} f_1 \otimes D_1 \cdot \cos\phi \\
+ \quad & \left[\frac{k_T^2}{Q^2} f_1 \otimes D_1 + h_1^{\perp} \otimes H_1^{\perp} \right] \cdot \cos 2\phi \\
+ \quad & |S_T| \cdot h_1 \otimes H_1^{\perp} \cdot \sin(\phi + \phi_S) \quad \textbf{Collins} \\
+ \quad & |S_T| \cdot f_{1T}^{\perp} \otimes D_1 \cdot \sin(\phi - \phi_S) \quad \textbf{Sivers} \\
+ \quad & \cdots
\end{aligned}
$$

- Also the case in Drell Yan ... in progress. See talk of Goldstein Trento June 2004, Gamberg Marseille HiX Workshop leading and higher twist analysis. Also Boer PRD 1999 for leading twist T-odd contribution.

Rescattering Mechanism to Generate T-Odd Function $h_1^\perp$

Goldstein, Gamberg–ICHEP-proc., Amsterdam: 2002, hep-ph/0209085

- $h_1^\perp$ Naturally defined from gauge invariant TMPDF(s)
- Apply "eikonal Feynman rules", (Collins, Soper, NPB: 1982)

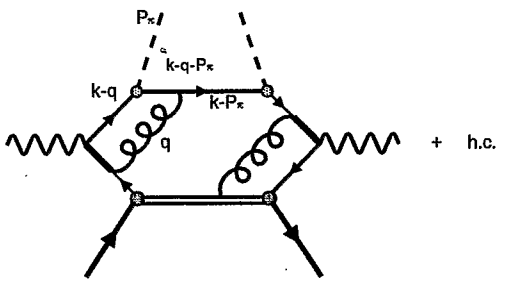

- $h_1^\perp(x, k_\perp)$, represents, number density transversely polarized quarks in an unpolarized nucleons nucleons-complementary to $f_{1T}^\perp(x, k_\perp)$,

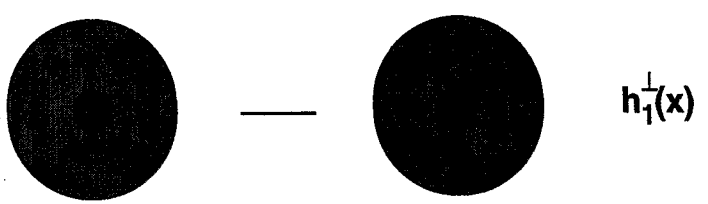

311

Estimates of T-odd Contributions to Azimuthal Asymmetries at Leading Twist

$\cos 2\phi$ Asymmetry

⋆ The quark-nucleon-spectator model used in previous rescattering calculations assumes point-like nucleon-quark-diquark vertex, leads to logarithmically divergent, asymmetries
Brodsky, Hwang, Schmidt, PLB: 2002;
Goldstein, L. Gamberg, ICHEP 2002;
Boer, Brodsky, Hwang, PRD: 2003

312

$$\begin{aligned} h_1^{\perp}(x,k_\perp) &= f_{1T}^{\perp}(x,k_\perp) \\ &= \frac{g^2 e_1 e_2}{(2\pi)^4}\frac{(1-x)(m+xM)}{4\Lambda(k_\perp^2)}\frac{M}{k_\perp^2}\ln\frac{\Lambda(k_\perp^2)}{\Lambda(0)} \end{aligned}$$

$\Lambda(k_\perp^2) = k_\perp^2 + x(1-x)\left(-M^2 + \frac{m^2}{x} + \frac{\lambda^2}{1-x}\right)$

- Asymmetry involves weighted function

$$h_1^{(1)\perp}(x) \equiv \int d^2k_\perp \frac{k_\perp^2}{2M^2} h_1^{\perp}(x,k_\perp^2) \quad diverges$$

Gaussian Distribution in $k_\perp$

Log divergence addressed by approximating the transverse momentum dependence of the quark-nucleon-vertex by a Gaussian distribution in $k_\perp^2$,

Gamberg, Goldstein, Oganessyan, PRD 67 (2003)

$$\langle n|\psi(0)|P\rangle = \left(\frac{i}{\not{k} - m}\right)\frac{b}{\pi}e^{-bk_\perp^2}U(P,S), \quad b \equiv \frac{1}{\langle k_\perp^2\rangle}$$

313 $U(P,S)$ nucleon spinor, and quark propagator comes from untruncated quark line

$$\begin{aligned} h_1^\perp(x,k_\perp) &= \frac{e_1 e_2 g^2}{2(2\pi)^4}\frac{b^2}{\pi^2}\frac{(m+xM)(1-x)}{\Lambda(k_\perp^2)}\frac{1}{k_\perp^2} \\ &\quad \times e^{-b\left(k_\perp^2-\Lambda(0)\right)}\left[\Gamma(0,b\Lambda(0)) - \Gamma(0,b\Lambda(k_\perp^2))\right] \end{aligned}$$

$\Gamma(0,z) \equiv$ incomplete gamma function:

- Check approach: $\lim < k_\perp^2 > \to \infty$ Gaussian width goes to infinity, regain *log divergent* result

Unpolarized Structure Function

$$f(x) = \frac{g^2}{(2\pi)^2}\frac{b^2}{\pi^2}(1-x)$$

$$\cdot\left\{\frac{(m+xM)^2-\Lambda(0)}{\Lambda(0)} - \left[2b\left((m+xM)^2-\Lambda(0)\right)-1\right]e^{2b\Lambda(0)}\Gamma(0,2b\Lambda(0))\right\}$$

- ⋆ Normalization, $\int_0^1 u(x) = 2$
- Black curve- $xu(x)$
- Purple curve - $xu(x)$ from GRV
- Pink curve $xh_1^{\perp(u)}$

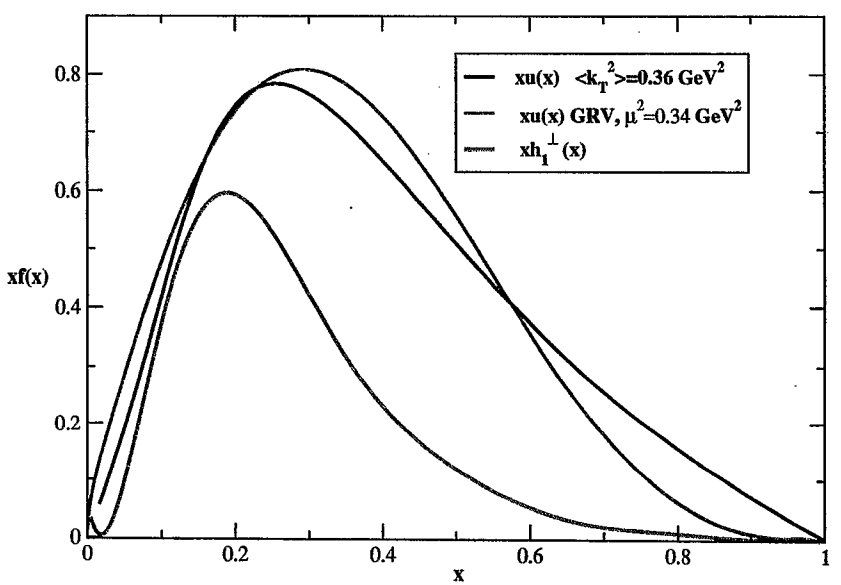

Pion Fragmentation Function

$$D_1(z) = \frac{N'^2 f_{qq\pi}^2}{4(2\pi)^2}\frac{1}{z}\frac{(1-z)}{z}\Big\{\frac{m^2-\Lambda'(0)}{\Lambda'(0)} - \left[2b'\left(m^2-\Lambda'(0)\right)-1\right]e^{2b'\Lambda'(0)}\Gamma(0,2b'\Lambda'(0))\Big\},$$

which, multiplied by z at $< k_\perp^2 >= (0.5)^2$ GeV^2 and $\mu = m$, estimates the distribution of Kretzer, PRD: 2000

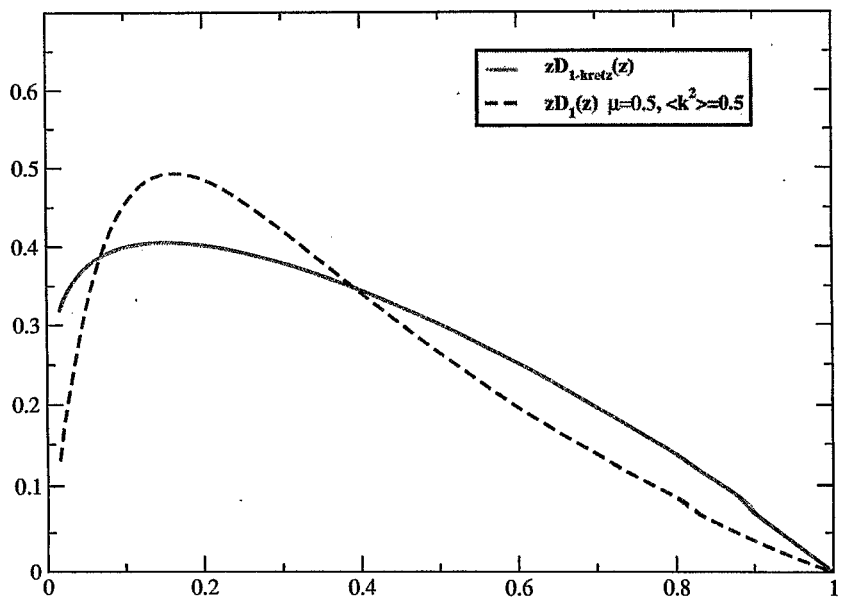

Rescattering Mechanism for T-Odd Collins Function

Gamberg,Goldstein,Oganessyan hep-ph/0307139, PRD68,2003

- Gauge-link contribution to the Collins Function:

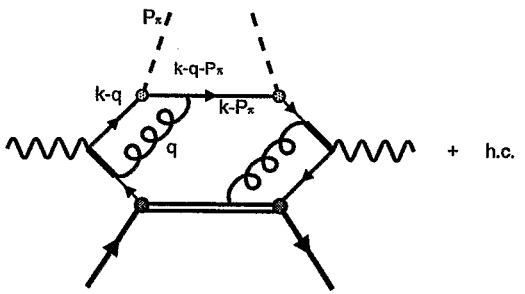

Figure depicts $h_1^\perp \star H_1^\perp \cos 2\phi$ asymmetry. The momenta flow to the quark-pion vertex is shown. The momentum q is the loop integration variable.

We evaluate the projection $\Delta^{[i\sigma^{\perp -}\gamma_5]}$, which results in the leading twist, contribution to T-odd pion fragmentation

$$H_1^\perp(z,k_\perp) = \frac{N'^2 f^2 g^2}{(2\pi)^4}\frac{1}{4z}\frac{(1-z)}{z}\frac{m}{\Lambda'(k_\perp^2)}\frac{M_\pi}{k_\perp^2}e^{-b'\left(k_\perp^2-\Lambda'(0)\right)}\left[\Gamma(0,b\Lambda'(0))-\Gamma(0,b'\Lambda'(k_\perp^2))\right],$$

where, $\Lambda'(k_\perp^2) = k_\perp^2 + \frac{1-z}{z^2}M_\pi^2 + \frac{\mu^2}{z} - \frac{1-z}{z}m^2$

Collins Asymmetry

- Convolution of two chiral-odd (both T-odd and T-even) structures,

$$\langle \frac{P_{h\perp}}{M_\pi} \sin(\phi+\phi_s)\rangle_{UT} = \frac{\int d\phi_s \int d^2P_{h\perp} \frac{P_{h\perp}}{M_\pi} \sin(\phi+\phi_s) \left(d\sigma^\uparrow - d\sigma^\downarrow\right)}{\int d\phi_s \int d^2P_{h\perp} \left(d\sigma^\uparrow + d\sigma^\downarrow\right)}$$

$$= |S_T| \frac{2(1-y)\sum_q e_q^2 h_1(x) z H_1^{\perp(1)}(z)}{(1+(1-y)^2)\sum_q e_q^2 f_1(x) D_1(z)}.$$

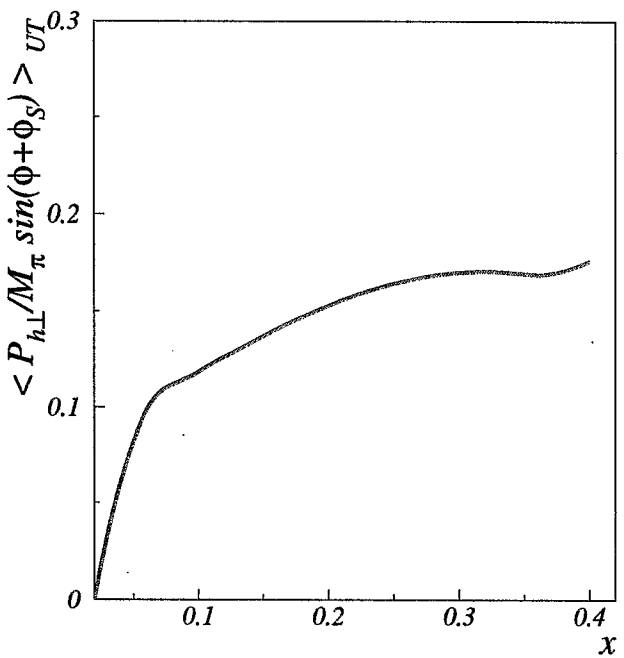

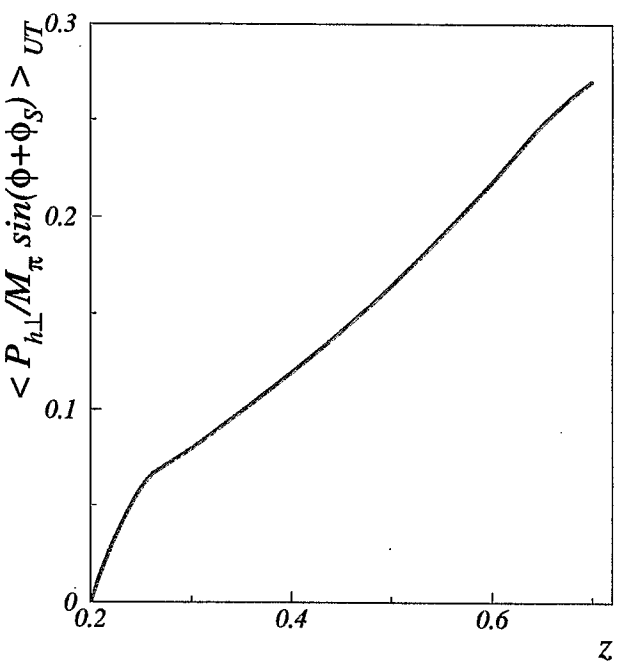

317

Double T-odd $\cos 2\phi$ asymmetry

Transversity of quarks inside an unpolarized hadron, and $\cos 2\phi$ asymmetries in unpolarized semi-inclusive DIS

Gamberg, Goldstein, Oganessyan PRD 2003

For the HERMES kinematics

$1\ \text{GeV}^2 \leq Q^2 \leq 15\ \text{GeV}^2$, $4.5\ \text{GeV} \leq E_\pi \leq 13.5\ \text{GeV}$,

$0.2 \leq z \leq 0.7$, $0.2 \leq y \leq 0.8$, $< P_{h\perp}^2 >= 0.25\ \text{GeV}^2$ and $< P_{h\perp} >= 0.4\ \text{GeV}$

$$\langle \frac{|P_{h\perp}^2|}{MM_h} \cos 2\phi \rangle_{UU} = \frac{\int d^2P_{h\perp} \frac{|P_{h\perp}^2|}{MM_h} \cos 2\phi \, d\sigma}{\int d^2P_{h\perp} \, d\sigma} = \frac{8(1-y)\sum_q e_q^2 h_1^{\perp(1)}(x) z^2 H_1^{\perp(1)}(z)}{(1+(1-y)^2)\sum_q e_q^2 f_1(x) D_1(z)}$$

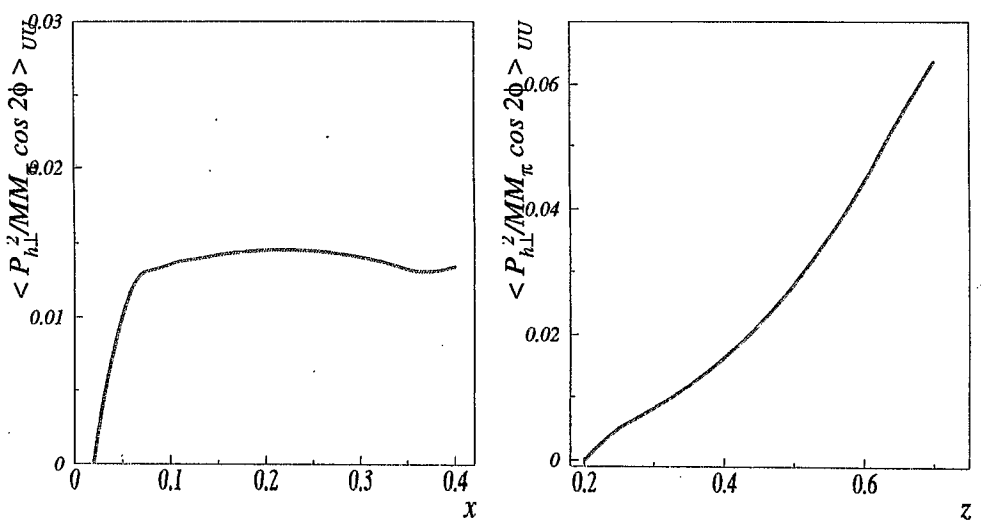

The T-odd $\cos 2\phi$ *vs* Sivers SSA

$$A = \frac{\langle \cos 2\phi \rangle_{UU}}{A_{UT}^{\sin(\phi-\phi_S)}} \sim z \cdot \frac{H_1^{\perp(1)}(z)}{D_1(z)},$$

Reflected in equality of $h_1^\perp$ and $f_{1T}^\perp$ functions in diquark model. Supports suggestion that the single-spin $\sin(\phi - \phi_S)$ Sivers and spin-independent $\cos 2\phi$ asymmetries are closely related in hard scattering processes

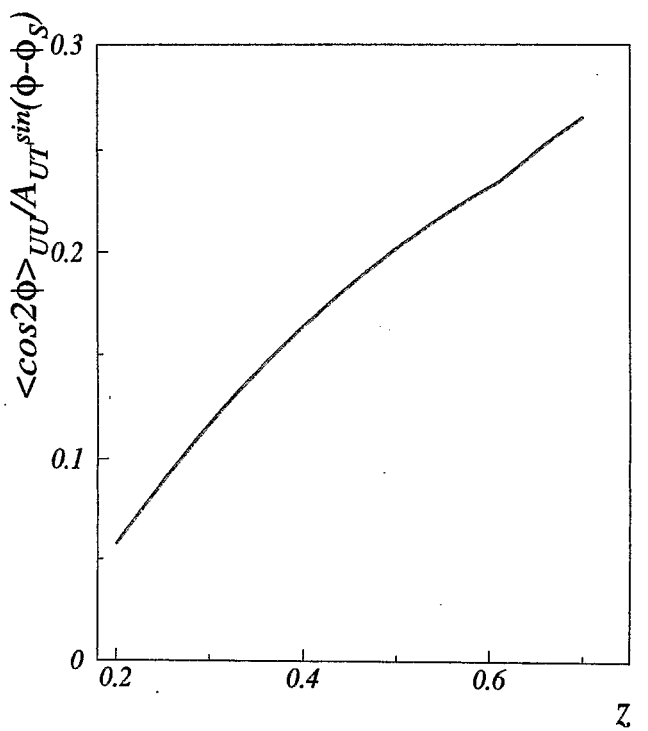

Estimates for Sivers Asymmetry

$$\langle \frac{|P_{h\perp}|}{M} \sin(\phi - \phi_S) \rangle_{UT} = \frac{\int d^2 P_{h\perp} \frac{|P_{h\perp}|}{M} \sin(\phi - \phi_S)\, d\sigma}{\int d^2 P_{h\perp}\, d\sigma}$$

$$= \frac{(1 + (1-y)^2) \sum_q e_q^2 f_{1T}^{\perp(1)}(x) z D_1^q(z)}{(1 + (1-y)^2) \sum_q e_q^2 f_1(x) D_1(z)},$$

where $A_{UT}^{\sin(\phi-\phi_S)} \approx \frac{M}{\langle P_{h\perp} \rangle} \langle \frac{|P_{h\perp}|}{M} \sin(\phi - \phi_S) \rangle_{UT}$

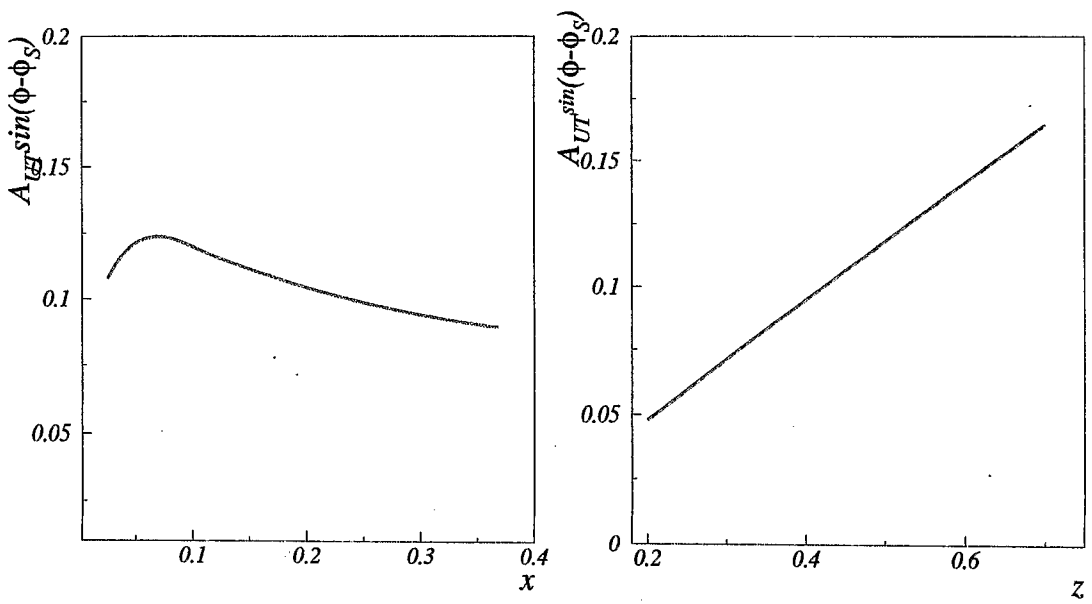

Combined $\cos 2\phi$ asymmetry

Effects that vanish as $k_\perp^2/Q^2$ important at small and moderate values of $Q^2 \Rightarrow \langle \cos 2\phi \rangle_{UU}$ results from the ordinary kinematic twist-4 T-even and leading double T-odd effects,

Gamberg, Goldstein, Oganessyan:DIS-2003-hep/ph-arXiv

$$\langle \cos 2\phi \rangle_{UU} = \frac{2\frac{\langle k_\perp^2 \rangle}{Q^2}(1-y) f_1(x) D_1(z) + 8(1-y) h_1^{\perp(1)}(x) H_1^{\perp(1)}(z)}{\left[1 + (1-y)^2 + 2\frac{\langle k_\perp^2 \rangle}{Q^2}(1-y)\right] f_1(x) D_1(z)}$$

321

The z-dependences of the asymmetry The full and dashed curves correspond to the asymmetry with and without $k_\perp^2/Q^2$ term in the denominator, respectively.

Red $\Rightarrow$ T-odd term.

Green $\Rightarrow$ T-even term

Blue $\Rightarrow$ sum of them

Magenta $\Rightarrow$ difference

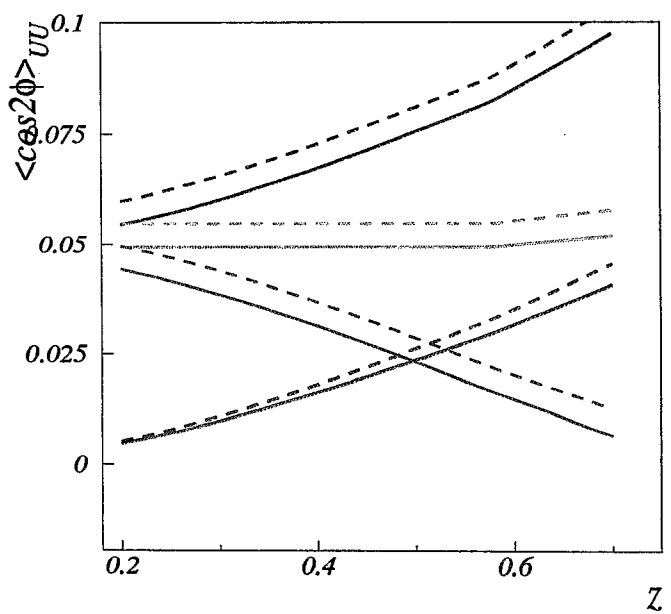

Unpolarized DRELL YAN $cos2\phi$

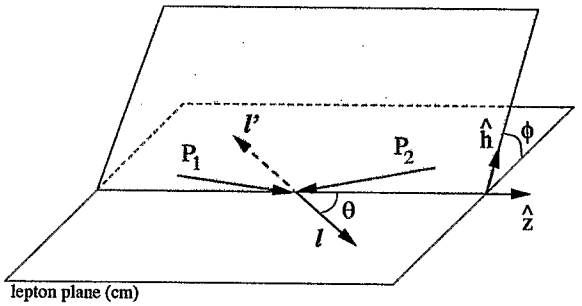

$$\bar{p} + p \to \mu^- \mu^+ + X$$

$$\frac{1}{\sigma}\frac{d\sigma}{d\Omega} = \frac{3}{4\pi}\frac{1}{\lambda+3}\left(1 + \lambda\cos^2\theta + \mu\sin^2\theta\cos\phi + \frac{\nu}{2}\sin^2\theta\cos 2\phi\right) \tag{1}$$

The angles refer to the lepton pair orientation in their rest frame relative to the boost direction and the initial hadron's plane. Asymmetry parameters, λ, μ, ν, depend on $s, x, m^2_{\mu\mu}, q_T$

BoerPRD: 1999, Collins SoperPRD: 1977

- Interesting that the $\cos 2\phi$ azimuthal asymmetry depends on the T-odd distribution $h_1^\perp$.

$$\nu = \frac{2\sum_a e_a^2 \mathcal{F}\left[(2\boldsymbol{p}_\perp \cdot \boldsymbol{k}_\perp - \boldsymbol{p}_\perp \cdot \boldsymbol{k}_\perp)\frac{h_1^\perp(x,\boldsymbol{k}_T)\bar{h}_1^\perp(\bar{x},\boldsymbol{p}_T)}{M_1 M_2}\right]}{\sum_{a,\bar{a}} e_a^2 \mathcal{F}[f_1 \bar{f}_1]} \tag{2}$$

with the convolution integral

$$\mathcal{F} \equiv \int d^2\boldsymbol{p}_\perp d^2\boldsymbol{k}_\perp \delta^2(\boldsymbol{p}_\perp + \boldsymbol{k}_\perp - \boldsymbol{q}_\perp) f^a(x,\boldsymbol{p}_\perp)\bar{f}^a(\bar{x},\boldsymbol{k}_\perp). \tag{3}$$

Higer twist comes in

$$\nu = \frac{2\sum_a e_a^2 \mathcal{F}\left[(2\boldsymbol{p}_\perp \cdot \boldsymbol{k}_\perp - \boldsymbol{p}_\perp \cdot \boldsymbol{k}_\perp)\frac{h_1^\perp(x,\boldsymbol{k}_T^2)\bar{h}_1^\perp(\bar{x},\boldsymbol{p}_T)}{M_1 M_2} + T_4(x,\bar{x},\boldsymbol{k}_T,\boldsymbol{p}_T;[f_1\bar{f}_1])\right]}{\sum_{a,\bar{a}} e_a^2 \mathcal{F}[f_1\bar{f}_1]} \quad (4)$$

- Gamberg Goldstein higher twist... In prep
- $s = 500GeV^2$, $x = 0.2 - 1.0$, and $q = 4.0 - 8.6\ GeV$ and $s = 50\ GeV^2$ ...

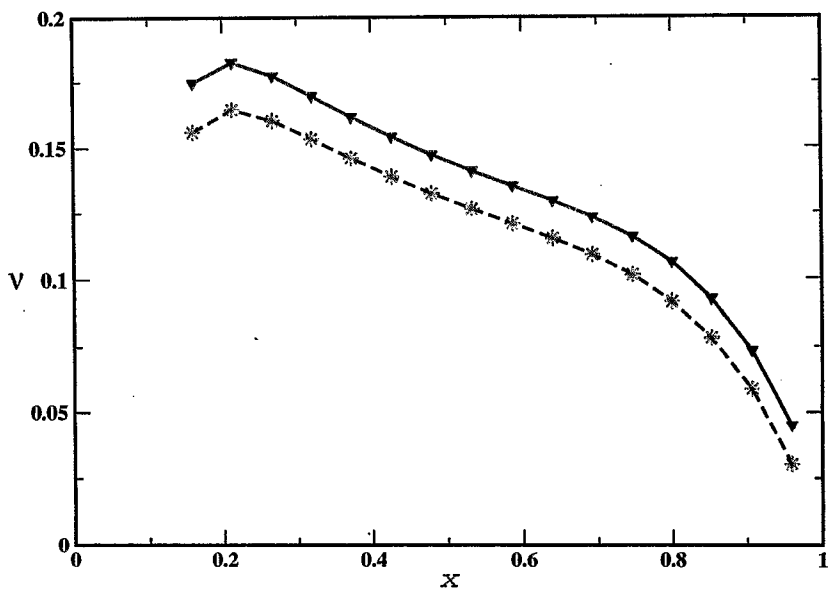

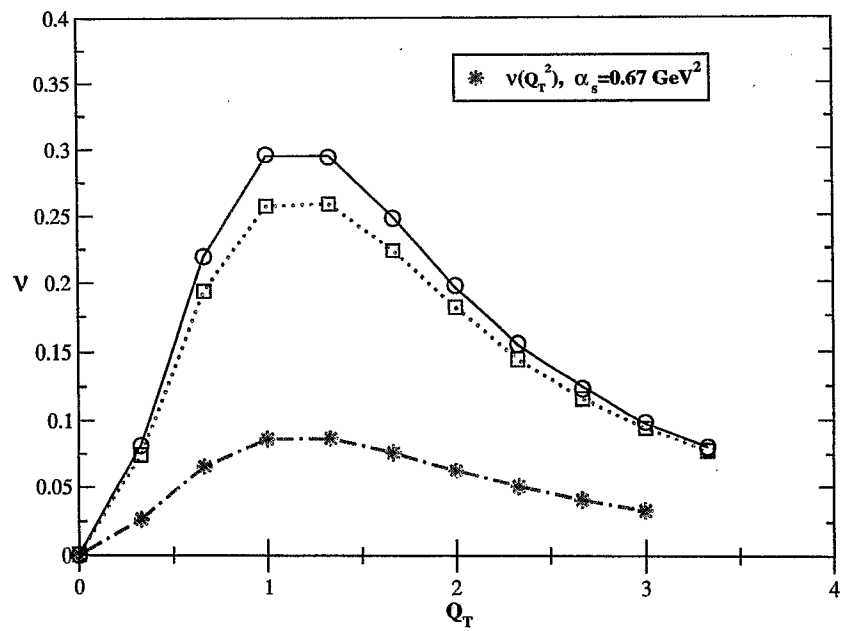

On the Subject of other approachs see Bacchetta, Metz, Yang PLB2004

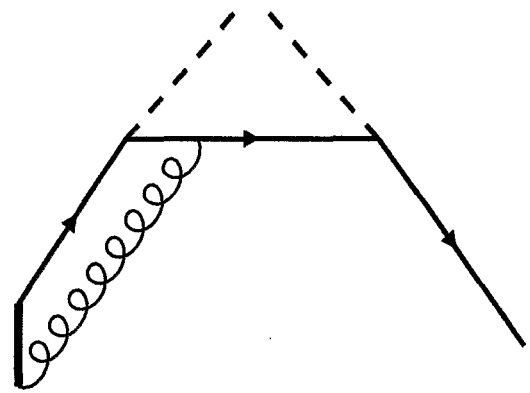

- Can mass corrections generate necessary phases?
- Must be careful about scales off shellness goes to on shell in deriving mass singularities or colinear singularities.
- Here we confront the "boundary" of non-perturbative physics with PQCD....

$$\log \frac{Q^2}{\mu^2}$$

See new work of Ji, Ma, Yuan hep-ph/0404183 and Collins and Metz ....

★ SIDIS:Jaffe and Ji PRL:1993 encountered at twist three level Estimate of this effect, Gamberg, Hwang, Oganessyan PLB:2004

$$A_{LT} = \frac{\lambda_e |\boldsymbol{S}_T| \sqrt{1-y}\, \frac{4}{Q} \left[M\, x\, g_T(x) D_1(z) + M_h\, h_1(x) \frac{E(z)}{z} \right]}{\frac{[1+(1-y)^2]}{y}\, f_1(x) D_1(z)}$$

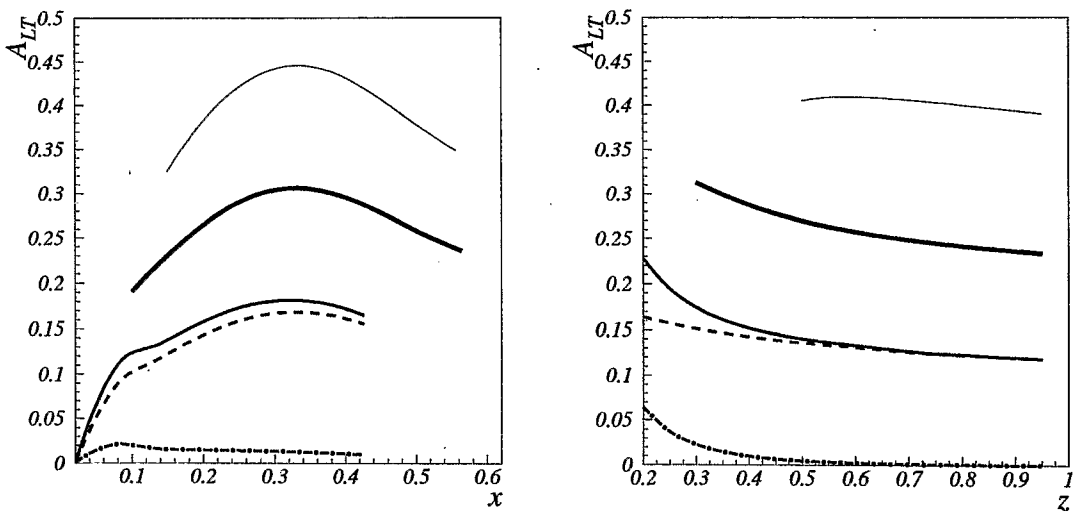

A_{LT} for π^+ production function of x and z at 27.5 GeV energy. The dashed and dot-dashed curves correspond contributions of the two terms of above respectively, and the full curve is the sum. The thin curve corresponds to 6 GeV and the thick curve to 12 GeV energies respectively.

★ **Bean Asymmetry** Estimate of this effect, Gamberg, Hwang, Oganessyan PLB:2004

$$\langle |P_{h\perp}| \sin\phi \rangle_{LU} = \lambda_e \sqrt{1-y}\,\frac{4}{Q}\,M M_h \Big[x\, e(x) z H_1^{\perp\,(1)}(z) + h_1^{\perp\,(1)}(x)\, E(z) \Big],$$

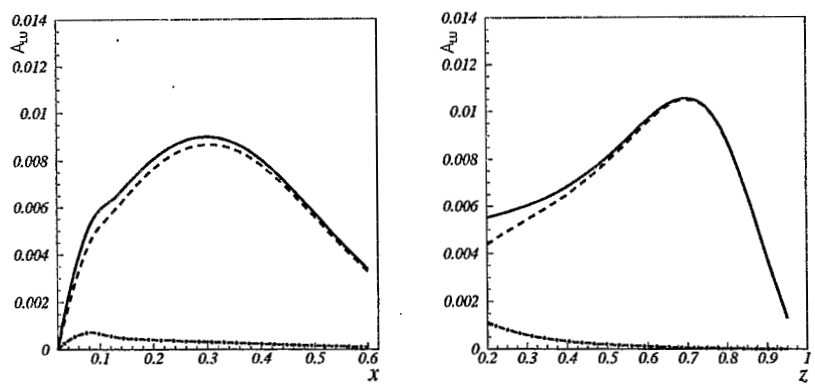

A_{LU} for π^+ production as a function of x and z at 27.5 GeV energy. The dashed and dot-dashed curves correspond to contribution of the first and second terms of above equation respectively, and the full curve is the sum of the two

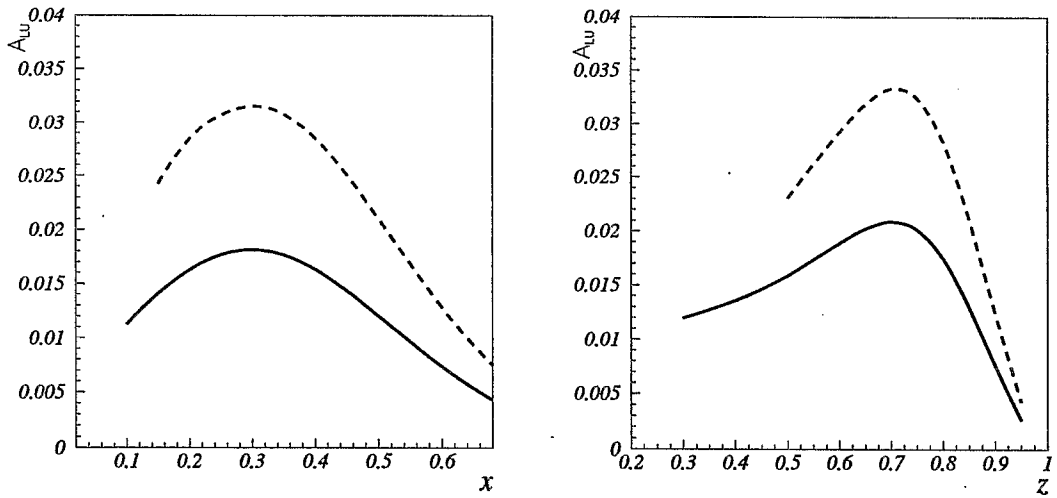

327 Also F. Yuan, PLB: 2004. Metz and Schleigel, hep-ph/0403182, Bacchetta *et al* hep-ph/0405154.

SUMMARY

- The angular correlations in semi-inclusive DIS are considered from the stanpoint of "rescattering" mechanism which generate T-odd, intrinsic transverse momentum, $k_\perp$, dependent *distribution and fragmentation* functions at leading twist

- We have evaluated these functions by modeling the quark, spectator hadron verticies in a quark-diquark-hadron framework
- We have evaluated azimuthal and SSA with Gaussian "regularization" in $\langle k_\perp \rangle$ and addressed the Log divergence problem

- Analyzed the leading twist contribution to the $\cos 2\phi$ azimuthal asymmetries . We considered the impact that novel T-odd distribution and fragmentation functions have on transversity of quarks within unpolarized nucleon

- We consider the implications that these T-odd distribution and fragmentation functions have in Sivers and Collins asymmetries

⋆ Azimuthal asymmetries and SSA measured at HERMES and COMPASS and in future JLAB *may* reveal the extent to which these leading twist T-odd effects are generating the data

- These experiments may point to the essential role played by quark transverse momentum and $T-$odd quark distributions and effects of higher twist

Sivers gluon distribution in $p^{\uparrow}p \to DX$ at RHIC

M. Boglione

M. Anselmino *U. D'Alesio*

E. Leader *F. Murgia*

INFN Istituto Nazionale di Fisica Nucleare

Università di Torino

Trieste, 11-16/10/2004

The Sivers Mechanism

The pdf's and the ff's are phenomenological quantities which have to be obtained from experimental observation and cannot be theoretically predicted. The pdf's of unpolarized nucleons are now remarkably well known; their $k_\perp$ dependence is usually assumed to be of a gaussian form, and the average $k_\perp$ value can be fixed so that it agrees with experimental data.

When considering polarized nucleons the number of pdf's involved grows and dedicated polarized experiments have to be performed in order to isolate and measure these functions. We have by now good data on the pdf's of longitudinally polarized protons, but nothing is experimentally known on the transverse spin distribution. When parton intrinsic transverse momenta are taken into account, many more distribution and fragmentation functions arise, like the Sivers function $\Delta^N f(x, \boldsymbol{k}_\perp) \propto f_{1T}^{\perp}(x, k_\perp)$, which describes the probability density of finding unpolarized partons inside a transversely polarized proton.

One of the difficulties in gathering experimental information on these new spin and $\boldsymbol{k}_\perp$ dependent pdf's and ff's is that most often two or more of them contribute to the same physical observable, making it impossible to disentangle them.

$p^{\uparrow}p \to DX$ allows a clear measurement of the Sivers gluon distribution function

D mesons originate from c or $\bar{c}$ quarks, which at LO can be created either via $q\bar{q} \to c\bar{c}$, or via $gg \to c\bar{c}$. The elementary cross section for the gluon fusion process includes contributions from s, t and u-channels, and turns out to be much larger than the $q\bar{q}$ annihilation cross section, which receives contribution from the s-channel alone. Therefore, $gg \to c\bar{c}$ dominates the whole $p^{\uparrow}p \to DX$ process up to $x_F \simeq 0.6$. Beyond this, the $q\bar{q} \to c\bar{c}$ contribution to the total cross section becomes slightly larger than the $gg \to c\bar{c}$ contribution, due to the much smaller values, at large x, of the gluon pdf, as compared to the quark ones.

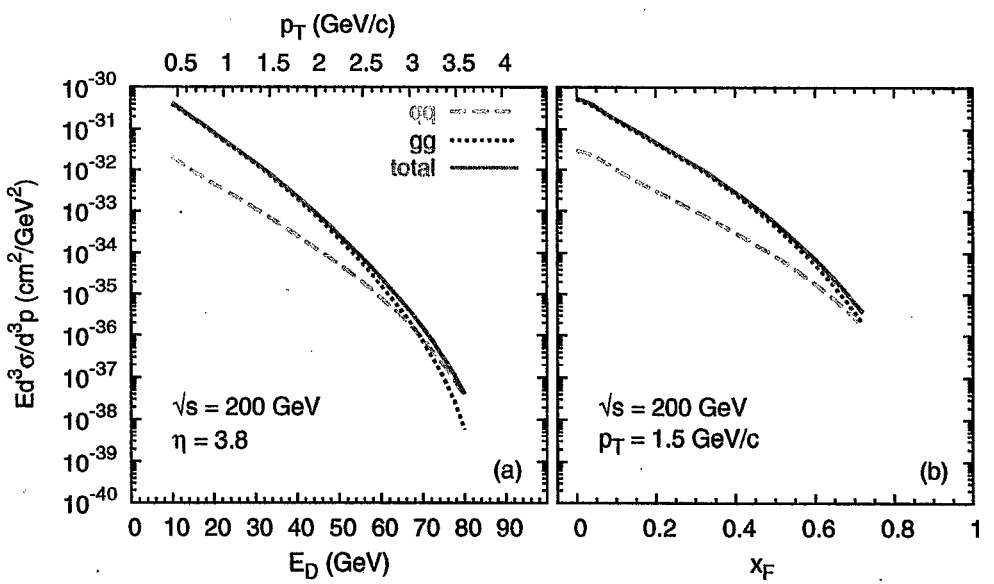

As the gluons cannot carry any transverse spin, the elementary process $gg \to c\bar{c}$ results in unpolarized final quarks. In the $q\bar{q} \to c\bar{c}$ process one of the initial partons (that inside the transversely polarized proton) can be polarized; however, there is no single spin transfer in this s-channel interaction so that the final c and $\bar{c}$ are again not polarized. One might invoke the possibility that also the quark inside the unpolarized proton is polarized, so that both initial q and $\bar{q}$ are polarized: even in this case the s-channel annihilation does not create a polarized final c or $\bar{c}$. Consequently, the charmed quarks fragmenting into the observed D cannot be polarized, and there cannot be any Collins fragmentation effect.

Therefore, transverse single spin asymmetries in $p^{\uparrow}p \to DX$ can only be generated by the Sivers mechanism, namely a spin-$\boldsymbol{k}_{\perp}$ asymmetry in the distribution of the unpolarized quarks and gluons inside the polarized proton, coupled respectively to the unpolarized interaction process $q\bar{q} \to c\bar{c}$ and $gg \to c\bar{c}$, and the unpolarized fragmentation function of either the c or the $\bar{c}$ quark into the final observed D meson.

$$A_N = \frac{d\sigma^{\uparrow} - d\sigma^{\downarrow}}{d\sigma^{\uparrow} + d\sigma^{\downarrow}}$$

$$\begin{aligned}
d\sigma^{\uparrow} - d\sigma^{\downarrow} &= \frac{E_D\, d\sigma^{p^{\uparrow} p \to DX}}{d^3\boldsymbol{p}_D} - \frac{E_D\, d\sigma^{p^{\downarrow} p \to DX}}{d^3\boldsymbol{p}_D} \\
&= \int dx_a\, dx_b\, dz\, d^2\boldsymbol{k}_{\perp a}\, d^2\boldsymbol{k}_{\perp b}\, d^3\boldsymbol{k}_D\, \delta(\boldsymbol{k}_D \cdot \hat{\boldsymbol{p}}_c)\, \delta(\hat{s} + \hat{t} + \hat{u} - 2m_Q^2)\, \mathcal{C}(x_a, x_b, z, \boldsymbol{k}_D) \\
&\times \left\{ \sum_q \left[\Delta^N f_{q/p^{\uparrow}}(x_a, \boldsymbol{k}_{\perp a})\, \hat{f}_{\bar{q}/p}(x_b, \boldsymbol{k}_{\perp b})\, \frac{d\hat{\sigma}^{q\bar{q} \to Q\bar{Q}}}{d\hat{t}}(x_a, x_b, \boldsymbol{k}_{\perp a}, \boldsymbol{k}_{\perp b}, \boldsymbol{k}_D)\, \hat{D}_{D/Q}(z, \boldsymbol{k}_D \right. \right. \\
&+ \left. \left. \left[\Delta^N f_{g/p^{\uparrow}}(x_a, \boldsymbol{k}_{\perp a})\, \hat{f}_{g/p}(x_b, \boldsymbol{k}_{\perp b})\, \frac{d\hat{\sigma}^{gg \to Q\bar{Q}}}{d\hat{t}}(x_a, x_b, \boldsymbol{k}_{\perp a}, \boldsymbol{k}_{\perp b}, \boldsymbol{k}_D)\, \hat{D}_{D/Q}(z, \boldsymbol{k}_D) \right] \right\}
\end{aligned}$$

Numerical Estimates

So far, all analyses and fits of the single spin asymmetry data were based on the assumption that the gluon Sivers function $\Delta^N f_{g/p^\uparrow}$ is zero. RHIC data on A_N in $p^\uparrow p \to DX$ will enable us to test the validity of this assumption.

Since we have no information about the gluon Sivers function from other experiments, we are unable to give predictions for the size of the A_N one can expect to measure at RHIC. Instead, we show what asymmetry one can find in two opposite extreme scenarios: the first being the case in which the gluon Sivers function is set to zero, $\Delta^N f_{g/p^\uparrow}(x_a, \boldsymbol{k}_{\perp a}) = 0$, and the quark Sivers function $\Delta^N f_{q/p^\uparrow}(x_a, \boldsymbol{k}_{\perp a})$ is taken to be at its maximum allowed value at any x_a; the second given by the opposite situation, where $\Delta^N f_{q/p^\uparrow} = 0$ and $\Delta^N f_{g/p^\uparrow}$ is maximized in x_a.

Model for pdf's and FF's

$$\hat{f}(x, \boldsymbol{k}_\perp) = f(x)\, \frac{1}{\pi\langle k_\perp^2\rangle}\, e^{-k_\perp^2/\langle k_\perp^2\rangle}\,,$$

$$\Delta^N f(x, \boldsymbol{k}_\perp) = \Delta^N f(x)\, \frac{1}{\pi\langle k_\perp^2\rangle}\, e^{-k_\perp^2/\langle k_\perp^2\rangle}\, \frac{2k_\perp M}{k_\perp^2 + M^2}\, \cos(\phi_{k_\perp})\,,$$

$$\Delta^N f_{a/p\uparrow}(x_a) \leq 2\, f_{a/p}(x_a)\,.$$

$$\hat{D}_{D/Q}(z, \boldsymbol{k}_{\perp D}) = D_{D/Q}(z)\, g(\boldsymbol{k}_{\perp D})\,,$$

$$\int d^3\boldsymbol{k}_D\, \delta(\boldsymbol{k}_D \cdot \hat{\boldsymbol{p}}_C)\, \hat{D}_{D/Q}(z, \boldsymbol{k}_D) = D_{D/Q}(z)\,.$$

Results

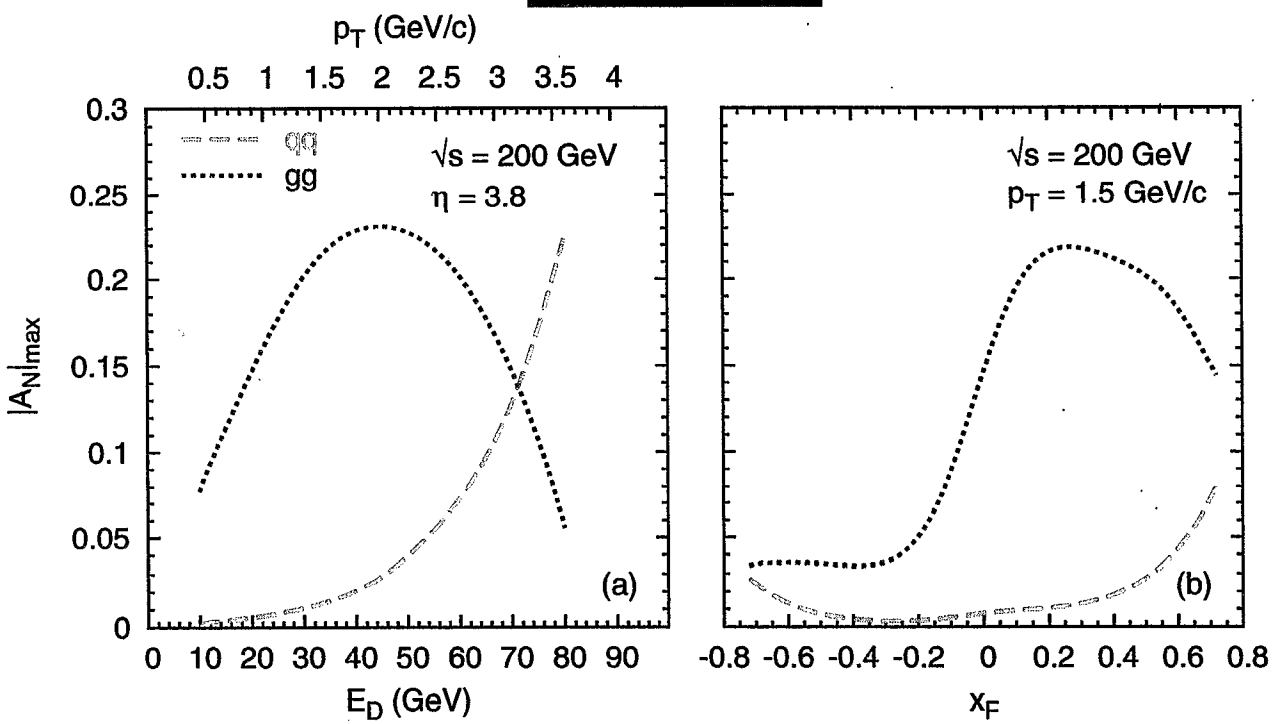
p_T (GeV/c)
0.5 1 1.5 2 2.5 3 3.5 4
0.3
0.25
0.2
0.15
0.1
0.05
0
$|A_N|_{max}$
qq
gg
√s = 200 GeV
η = 3.8
(a)
0 10 20 30 40 50 60 70 80 90
E_D (GeV)
√s = 200 GeV
p_T = 1.5 GeV/c
(b)
-0.8 -0.6 -0.4 -0.2 0 0.2 0.4 0.6 0.8
x_F

Comments and Conclusions

* The observation of the transverse single spin asymmetry A_N for D mesons generated in $p^{\uparrow}p$ scattering offers a great chance to study the Sivers distribution functions.

* This channel allows a direct, uncontaminated access to this function since the underlying elementary processes guarantee the absence of any polarization in the final partonic state; consequently, contributions from Collins-like terms cannot be present to influence the measurement.

* The large dominance of the $gg \to c\bar{c}$ process at low and intermediate x_F offers a unique opportunity to measure the gluon Sivers distribution function $\Delta^N f_{g/p^{\uparrow}}$.

* Intrinsic parton motions play a crucial role and have to be properly taken into account. Adopting a simple model to parameterize the $k_\perp$ dependence we have given some estimates of the unpolarized cross section for D meson production, together with some upper estimate of the SSA in the two opposite scenarios in which either $\Delta^N f_{g/p^\uparrow}$ is maximal and $\Delta^N f_{q/p^\uparrow} = 0$ or $\Delta^N f_{g/p^\uparrow} = 0$ and $\Delta^N f_{q/p^\uparrow}$ is maximal. Our results hold for $D = D^+, D^-, D^0, \overline{D}^0$.

* Both the cross section and A_N could soon be measured at RHIC.

* It clearly turns out that any sizeable contributions to the $p^\uparrow p \to DX$ single spin asymmetry at low to intermediate E_D's or x_F's would be a most direct indication of a non zero gluon Sivers function.

A CRITIQUE OF THE ANGULAR MOMENTUM SUM RULES AND A NEW ANGULAR MOMENTUM SUM RULE

B.L.G.BAKKER
Vrije Universiteit, Amsterdam

E.LEADER
Imperial College London

T.L.TRUEMAN
Brookhaven National Laboratory

hep-ph/0406139 v2
to appear in Phys. Rev. D
(results in v1 and v2 are the same, but v2 is much more 'reader friendly')

Presented by E.Leader
at the
RHIC Spin Collaboration Meeting
Turin, October 2004

1 INTRODUCTION

Sum rules, relating the total angular momentum of a nucleon to the spin and orbital angular momentum carried by its constituents, are interesting and important in understanding the internal structure of the nucleon. Indeed it is arguable that the main stimulus for the tremendous present day experimental activity in the field of spin-dependent structure functions was the surprising result of the European Muon Collaborations polarized DIS experiment in 1988, which, via such sum rules, led to what was called a "spin crisis in the parton model", namely the discovery that the spins of its quarks provide a very small contribution to the angular momentum of the proton.

In a much cited paper, Jaffe and Manohar stressed the subtleties involved in deriving general angular momentum sum rules. As they point out, too naive an approach leads immediately to highly ambiguous divergent integrals, and a careful limiting procedure has to be introduced in order to obtain physically meaningful results. In this it is essential to work with non-diagonal matrix elements $\langle p', \sigma | \boldsymbol{J} \; | p, \sigma \rangle$ and, this can have some unexpected consequences. Jaffe and Manohar comment that to justify rigorously the steps in such a procedure requires the use of normalizable wave packets, though they do *not* do this explicitly in their paper.

We show that the results in the literature are incorrect, and we have taken pains to derive the correct expressions in three different ways, two involving explicit physical wave packets and the third, totally independent, based upon the rotational properties of the state vectors. Surprisingly it turns out that the results are very sensitive to the type of relativistic spin state used to describe the motion of the particle i.e. whether a standard canonical (i.e. boost, as in e.g. Bjorken -Drell) state or a helicity state is utilized.

We present results for the matrix elements of the angular momentum operators, valid in an arbitrary Lorentz frame, both for helicity states and canonical states.

We present a new sum rule for transversely polarized nucleons.

2 CONTENTS

We shall discuss:

1) The origin of the problem

2) The source of errors in the literature

3) Brief summary of our calculations

4) Comparison of our results with those in the literature

5) The new sum rule for transversely polarized nucleons

3 THE ORIGIN OF THE PROBLEM

In the standard approach one relates the matrix elements of the angular momentum operators to those of the energy-momentum tensor $T^{\mu\nu}(x)$, which is conserved. Typically one deals with expressions like

$$M^{\mu\nu\lambda}(x) \equiv x^\nu T^{\mu\lambda}(x) - x^\lambda T^{\mu\nu}(x) \tag{1}$$

The angular momentum operators are space integrals of the spatial components of these, so we would like to know the structure of the forward matrix elements

$$\mathcal{M}^{0ij}(p,s) \equiv \langle p,s| \int d^3x M^{0ij}(\boldsymbol{x},0)|p,s\rangle \tag{2}$$

i.e. what is the functional dependence on the momentum and spin label of the nucleon.

We have:

$$\begin{aligned} \mathcal{M}^{0ij}(p,s) &= \int d^3x \langle p,s|x^i T^{0j}(x) - x^j T^{0i}(x)|p,s\rangle \\ &= \int d^3x\, x^i \langle p,s|e^{iP\cdot x}T^{0j}(0)e^{-iP\cdot x}|p,s\rangle \\ -(i\leftrightarrow j) & \\ &= \int d^3x\, x^i \langle p,s|T^{0j}|p,s\rangle - (i\leftrightarrow j). \end{aligned} \tag{3}$$

The integral in Eq. (3) is *totally ambiguous*, being either infinite or, by symmetry, zero.

The essential problem is to obtain a sensible physical expression, in terms of p and $\boldsymbol{s}$, for the above matrix element. The fundamental idea is to work with a *non-forward* matrix element and then to try to approach the forward limit. This is similar to what is usually done when dealing with non-normalizable plane wave states and it requires the use of wave packets for a rigorous justification.

4 THE SOURCE OF ERRORS IN THE LITERATURE

The spin state of the nucleon is labelled by the momentum and the *covariant* spin vector $\mathcal{S}$.

1) The most crucial error in these treatments is the mishandling of the matrix elements of a covariant tensor operator. If $T^{\mu\lambda}$ transforms as a second-rank tensor its *non-forward* matrix elements do *not* transform covariantly. This was the motivation, decades ago, for Stapp to introduce M-functions.

Namely, the covariance is spoilt, for canonical spin states by the Wigner rotation, and, for helicity states by the analogous Wick helicity rotation.

Only by first factoring out the wave-functions (in our case Dirac spinors) i.e. by writing

$$\langle p', \mathcal{S}'|T^{\mu\lambda}|p, \mathcal{S}\rangle = \bar{u}(p', \mathcal{S}')\mathcal{T}^{\mu\nu}(p', p)u(p, \mathcal{S}). \tag{4}$$

does the remaining M-function, in this case $\mathcal{T}^{\mu\nu}(p', p)$, transform covariantly.

2) For simplicity $\mathcal{S}'$ is chosen equal to $\mathcal{S}$.

A wave packet is constructed

$$|\Psi_{p,\mathcal{S}}\rangle = \frac{N}{\sqrt{(2\pi^3)}} \int d^3q e^{-\lambda^2(q-p)^2}|q, \mathcal{S}\rangle \tag{5}$$

But for physical states $q^2 = M^2$ and $\mathcal{S}.q = 0$, so for a superposition of physical nucleon states the integration over $\boldsymbol{q}$ is restricted, and this fact is ignored.

The correct way to do it is to build the packet as a superposition of physical plane waves all with the same *rest frame spin vector* $\boldsymbol{s}$

$$|\Psi_{p,s}\rangle = \frac{N}{\sqrt{(2\pi^3)}} \int d^3q e^{-\lambda^2(q-p)^2}|q, s\rangle \tag{6}$$

5 OUR CALCULATIONS

We have used THREE different approaches, all giving the same answer:

1) Relativistic Quantum-Mechanical Dirac particle.

We construct a wave-function corresponding to a superposition of plane wave physical states centered around momentum $\boldsymbol{p}$, all of which have rest-frame spin vector $\boldsymbol{s}$:

$$\psi_{p,s}(\boldsymbol{x}, t) = \frac{\bar{N}}{(2\pi)^3} \int \frac{d^3q}{q^0} e^{-\lambda^2(q-p)^2} e^{i(q\cdot x - q^0 t)} u(q, s), \tag{7}$$

where $q^0 = \sqrt{\boldsymbol{q}^2 + M^2}$, and $u(q, s)$ is a standard Dirac spinor.

2) Field Theoretic State

We construct a wave-packet state

$$|\Psi_{p,s}\rangle = \frac{N}{\sqrt{(2\pi^3)}} \int d^3q e^{-\lambda^2(q-p)^2}|q, s\rangle \tag{8}$$

3) A Totally Independent Method Based On The Rotational Properties Of States

This is the simplest most direct approach.

a) It does not need wave packets because it does not use the energy momentum tensor.

b) It works for arbitrary spin, and equally well for *helicity states* or standard *canonical or boost states*.

Let $|p, m\rangle$ be a state with momemtum p which has spin projection m in the rest system.

Under a rotation about axis-i through an angle β:

$$U[R_i(\beta)]\,|p, m\rangle = |R_i(\beta)p, n\rangle \mathcal{D}^s_{nm}(R_W(p, \beta)). \tag{9}$$

where $U[R_i(\beta)]$ is the unitary operator effecting the rotation and $R_W(p, \beta)$ is the Wigner rotation.

Since the angular momentum operators are the generators of rotations

$$U[R_i(\beta)] = \exp(-i\beta J_i) \tag{10}$$

it is relatively straightforward to derive the matrix elements of the J_i from Eq. (9).

(For helicity states the Wigner rotation is replaced by the Wick helicity rotation)

6 COMPARISON OF OUR RESULTS WITH THOSE IN THE LITERATURE

The nicely covariant looking, but alas wrong, form of the expectation value of the angular momentum operators given by Jaffe-Manohar is:

$\langle p, \mathcal{S}| \int d^3x M^{0ij}(x) |p, \mathcal{S}\rangle|_{\rm JM}$

$= \frac{1}{4Mp_0}\left[2p^0\epsilon^{ji\beta\sigma} - p^i\epsilon^{0j\beta\sigma} + p^j\epsilon^{0i\beta\sigma}\right] p_\beta \mathcal{S}_\sigma$

In terms of $\boldsymbol{p}$ and $\boldsymbol{s}$ this leads to

For standard (e.g. Bjorken-Drell) canonical spin states:

$$\langle J_i\rangle_{JM} = \frac{1}{4Mp^0}\left\{(3p_0^2 - M^2)s_i - \frac{3p_0 + M}{p_0 + M}(\boldsymbol{p}\cdot\boldsymbol{s})p_i\right\} \tag{11}$$

to be compared with our result

$$\langle J_i\rangle = \tfrac{1}{2}s_i \tag{12}$$

Note: In the above we have left out terms involving the derivative of a delta-function, which vanish for a symmetrical wave-packet.

In general these are different. However, one may easily check that if $\boldsymbol{s} = \hat{\boldsymbol{p}}$ the Jaffe-Manohar value agrees with Eq.(12), while if $\boldsymbol{s} \perp \hat{\boldsymbol{p}}$ they are not the same.

Because our result Eq. (12) does not look manifestly covariant, we have shown in detail that it does in fact respect Lorentz invariance.

7 SUM RULES

Sum rules, relating the total angular momentum of a nucleon to the spin and orbital angular momentum carried by its constituents, are interesting and important in understanding the internal structure of the nucleon.

In order to deal with the massless gluons we need the analogue of Eq. (12) for helicity states for which we find a surprisingly different result:

$$\langle p', \lambda' | J_i | p, \lambda \rangle = (2\pi)^3 2p_0 \left[\lambda \eta_i(\boldsymbol{p}) \delta_{\lambda\lambda'}\right] \tag{13}$$

where

$$\begin{aligned} \eta_x &= \cos(\phi)\tan(\theta/2), \qquad \eta_y = \sin(\phi)\tan(\theta/2), \\ \eta_z &= 1. \end{aligned} \tag{14}$$

and (θ, ϕ) are the polar angles of $\boldsymbol{p}$.

The agreement between our results and those of J-M for canonical spin states when $\boldsymbol{s} = \hat{\boldsymbol{p}}$ is consistent with the much used and intuitive sum rule

$$\tfrac{1}{2} = \tfrac{1}{2}\Delta\Sigma + \Delta G + \langle L^q \rangle + \langle L^G \rangle \tag{15}$$

In the case that $\boldsymbol{s} \perp \hat{\boldsymbol{p}}$ we find a new sum rule. For a proton with transverse spin vector $\boldsymbol{s}_T$ we find

$$\tfrac{1}{2} = \tfrac{1}{2} \sum_{q,\bar{q}} \int dx\, \Delta_T q^a(x) + \sum_{q,\bar{q},G} \langle L_{s_T} \rangle^a \tag{16}$$

where L_{s_T} is the component of $\boldsymbol{L}$ along $\boldsymbol{s}_T$. The structure functions $\Delta_T q^a(x) \equiv h_1^q(x)$ are known as the quark transversity or transverse spin distributions in the nucleon. Note that no such parton model sum rule is possible with the Jaffe-Manohar formula because, as $p \to \infty$, Eq. (11) for $i = x, y$ diverges.

The result Eq. (16) has a very intuitive appearance, very similar to Eq. (15).

Note that the RHS of Eq. (16) is different from the expression for the *tensor charge* (that expression should not be called a sum rule since the LHS is not known *a priori*), which involves the difference of the contributions of quarks and antiquarks. In Eq. (16) they are added.

The structure functions $\Delta_T q^a(x) \equiv h_1^q(x)$ are most directly measured in doubly polarized Drell-Yan reactions where the asymmetry is proportional to

$$\sum_a e_a^2 [\Delta_T q^a(x_1) \Delta_T \bar{q}^a(x_2) + (1 \leftrightarrow 2)]. \tag{17}$$

They can also be determined from the asymmetry in semi-inclusive hadronic interactions like

$$p + p(\boldsymbol{s}_T) \to H + X$$

where H is a detected hadron, typically a pion, and in SIDIS reactions with a transversely polarized target

$$\ell + p(\boldsymbol{s}_T) \to \ell + H + X.$$

The problem is that in these semi-inclusive reactions $\Delta_T q^a(x)$ always occurs multiplied by the largely unknown Collins fragmentation function.

8 SUMMARY

1) The standard derivation of the tensorial structure of the expectation value of the angular momentum $\boldsymbol{J}$, for a relativistic spin-s particle, in which the matrix elements of the angular momentum operators are related to the matrix elements of the energy-momentum tensor, is rendered difficult by the singular nature of the operators involved.

We have shown that the results in the literature are incorrect, and have derived the correct expressions in three different ways, two of them based on a careful wave-packet treatment of the standard approach, and the third, quite independent, based on the known rotational properties of the spin states, which circumvents the use of the energy-momentum tensor. All three methods yield the same results.

2) We have shown that, surprisingly, the results for helicity states are very different from those for standard canonical spin states.

3) Using a Fock-space picture of the proton, we have used our results to obtain a new sum rule for a transversely polarized nucleon, which involves the transverse spin or transversity distribution $\Delta_T q(x) \equiv h_1(x)$, and which is similar in form to the classic longitudinal spin sum rule.

Discussion: Sivers and Collins Mechanisms

M. Anselmino, INFN

for
RHIC Spin Collaboration Meeting XXIX
October 8-9, 2004
Torino, Italy

Sivers and Collins mechanisms

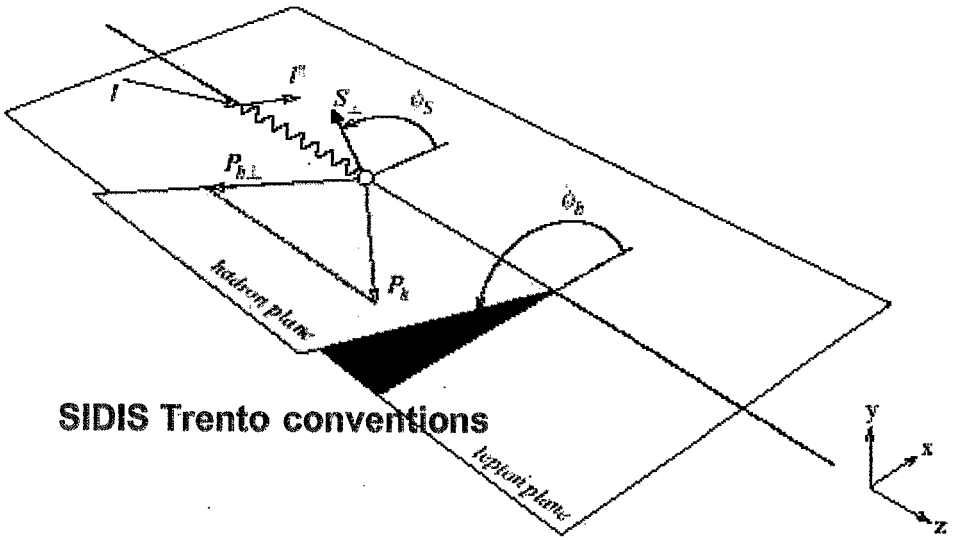

SIDIS Trento conventions

lp→lhX : 2 planes + polarization vector ⇨

Possible disentangling of different contributions:

Sivers ~ sin $(\Phi_s - \Phi_h)$
Collins ~ sin $(\Phi_s + \Phi_h)$

(is this really true?)

$S_\perp \cdot (l \times q)$ $S_\perp \cdot (l \times p_h)$ $S_\perp \cdot (q \times p_h)$ (3 scalars)

pp → πX: 1 plane + polarization vector $S_\perp \cdot (p \times p_h)$ (1 scalar)

➡ Look for less inclusive cross sections

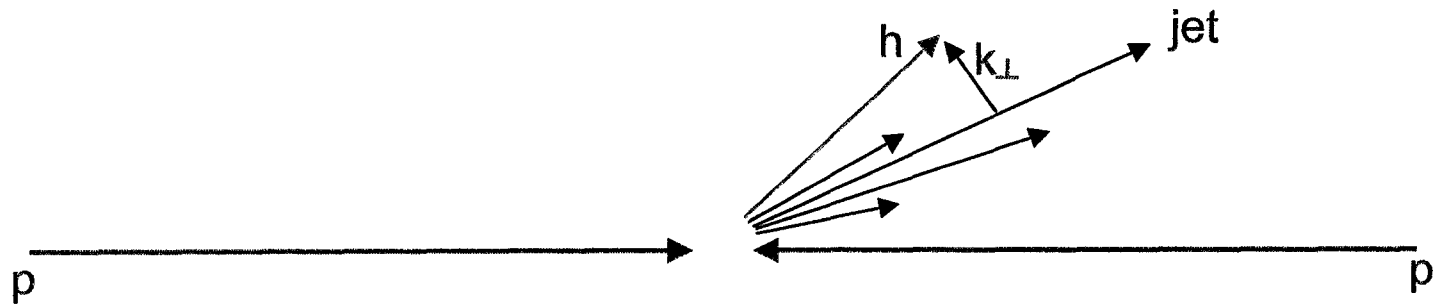

Look for azimuthal distribution of h in jet

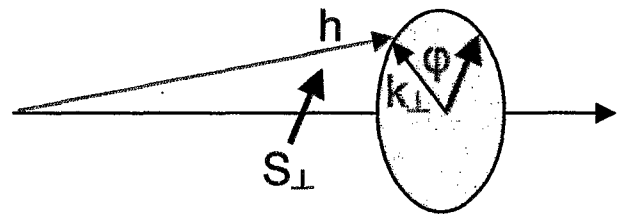

$$\frac{d^5\sigma}{d^3p_h\, d^2k_\perp}$$

would give access to Collins function

can it be measured?

$$d^5\sigma^{\uparrow,\downarrow} \sim d^5\sigma^{unp} \pm (1/2) \int d_2k_{\perp a}\, d^2k_{\perp b}\, h_1\, \Delta\sigma\, \hat{\Delta}^N D_{h/q}$$

transversity

One integration less might give less suppression to Collins mechanism

Extracting Sivers function:

A_N in Drell-Yan processes, $p^{\uparrow}p \rightarrow l^+ l^-$

A_N in $p^{\uparrow}p \rightarrow D\ X$, 2 jets, ...

Extracting h_1:

A_{TT} in Drell-Yan processes

$$A_{TT} = \hat{a}_{tt} \frac{\sum_q e_q^2 [\, h_{1q}(x_1)\, h_{1\bar{q}}(x_2) + h_{1\bar{q}}(x_1)\, h_{1q}(x_2) \,]}{\sum_{\bar{q}} e_q^2 [\, q(x_1)\, \bar{q}(x_2) + \bar{q}(x_1)\, q(x_2) \,]}$$

$$\frac{d\hat{\sigma}^{\uparrow\uparrow} - d\hat{\sigma}^{\uparrow\downarrow}}{d\hat{\sigma}^{\uparrow\uparrow} + d\hat{\sigma}^{\uparrow\downarrow}} = \frac{\sin^2\theta}{1 + \cos^2\theta} \cos 2\varphi$$

$\sqrt{s} = 200$ GeV $\quad M^2 \leq 100$ $\Rightarrow$ $M^2/s = x_1 x_2 \leq 2 \cdot 10^{-3}$ small x_1 and/or x_2

A_{TT} small due to $h_{1\bar{q}}$ and x, M^2 region: could smaller $\sqrt{s}$ or bigger M^2 help?

Discussion: Near-Term (<2 years) Experimental Opportunities

L. Bland, BNL

for
RHIC Spin Collaboration Meeting XXIX
October 8-9, 2004
Torino, Italy

Near-Term (<2 years) Experimental Opportunities

Transverse Spin Measurements at RHIC

- increase statistics for mid-rapidity π^0, $h^\pm$ A_N for p+p at $\sqrt{s}$=200 GeV
- measure A_N for $p+p \rightarrow \pi^\pm + X$ at BRAHMS at $\sqrt{s}$=200 GeV.
- di-jet correlations $\Rightarrow$ spin-correlated k_T measurements.
- begin determination of p_T dependence of A_N at fixed x_F.
- measure A_N for 'near-side' π^0-$h^\pm$ azimuthal correlations.

Following the recording of 7 pb^{-1} with P_{beam}>0.4 for A_{LL} measurements, STAR requested 4 pb^{-1} of p+p collisions at $\sqrt{s}$=200 GeV with transverse polarization for run 5.

- possibility of 1-2 day measurements of p+p collisions with $\sqrt{s} \geq 400$ GeV during run 5.

RSC Meeting (Torino)
October, 2004
L.C. Bland

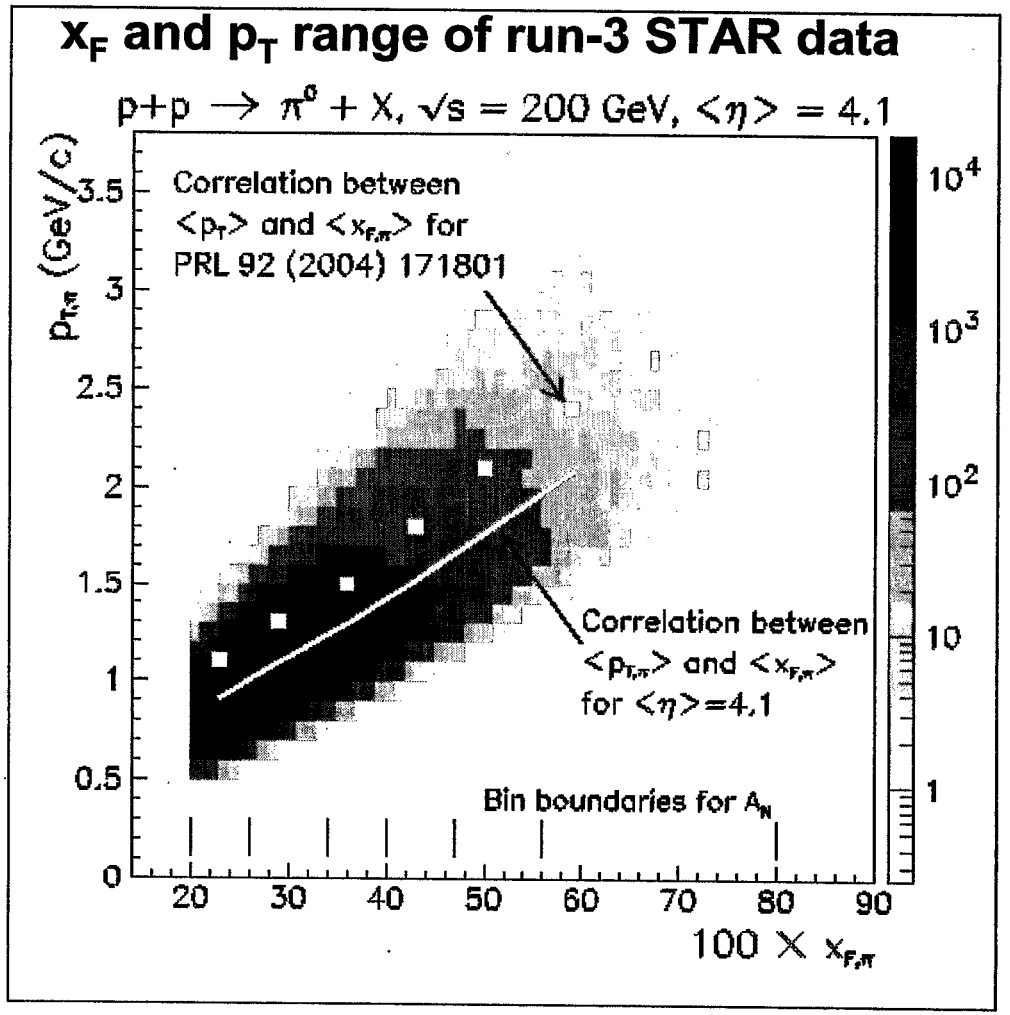

RSC Meeting (Torino)
October, 2004
Akio Ogawa

STAR Detector

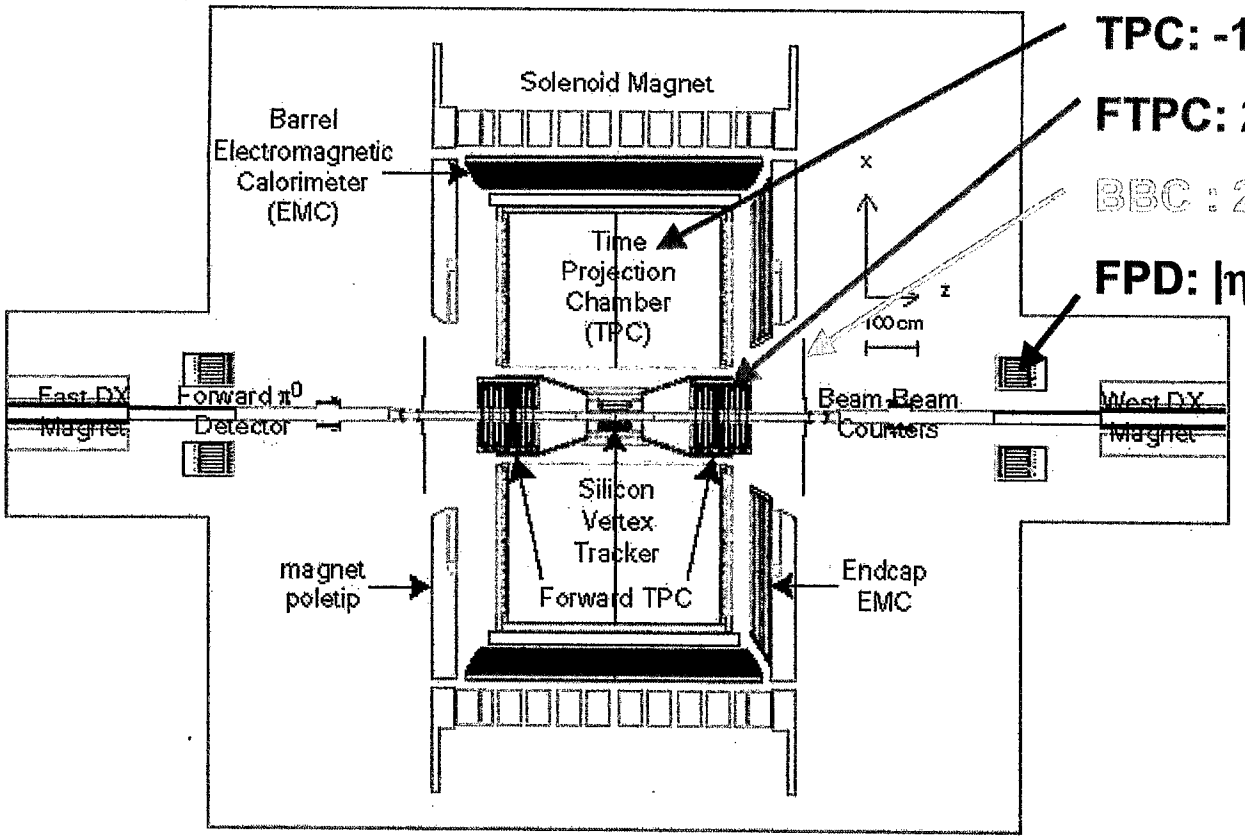

TPC: $-1.0 < \eta < 1.0$

FTPC: $2.8 < |\eta| < 3.8$

BBC : $2.2 < |\eta| < 5.0$

FPD: $|\eta| \sim 4.1$ and ~ 3.6

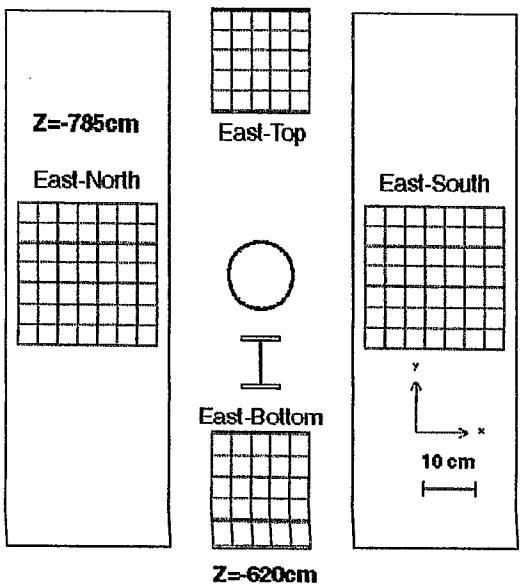

Upgraded Forward π^0 Detector (FPD)

- **Pb-glass EM calorimeter**
- **Shower-Maximum Detector (SMD)**
- **Preshower**

RSC Meeting (Torino)

October, 2004

Akio Ogawa

Transverse Single-Spin Asymmetries

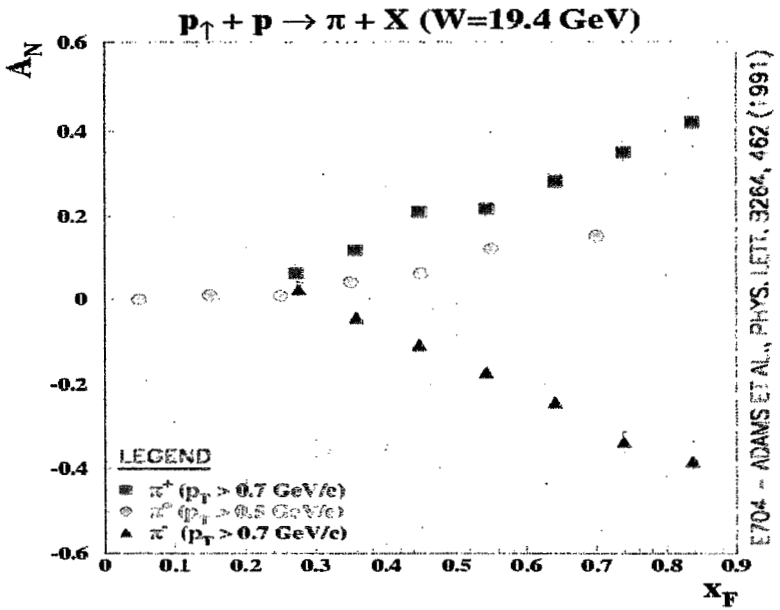

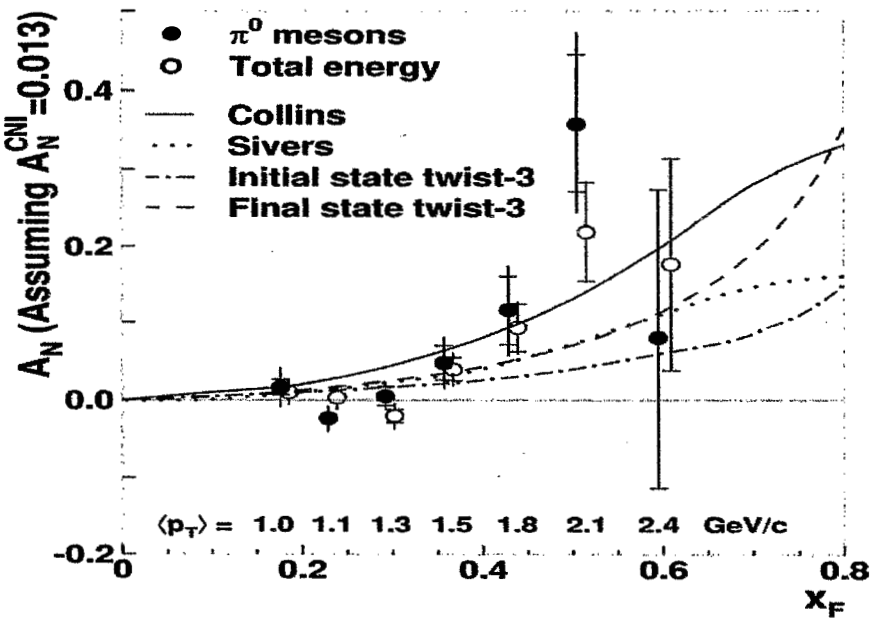

STAR PRL 92,06230(2004)

Low energy data (FNAL) show clear differences between π^{+-} and π^0. At higher energies the models used to describe the data differ.
Large spin effects reported for π^0 by STAR for $\sqrt{s}$ = 200 GeV *pp* collisions

Analysis Status

Data are from ~5 shifts of pp during run-4.

Normalization accuracy ~0.3%. So far I believe to be at ~0.6% based on various tests. This sample will give stat. accuracy of ~ 1% at x_F=.25. 10-20* statistics will be sufficient for a measurement of π+ an π- up to ~.35; Data from Run-4 should be available at DNP meeting.

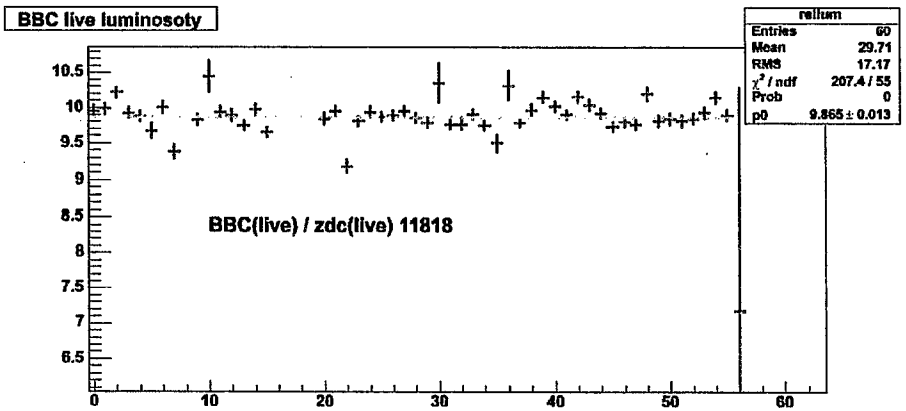

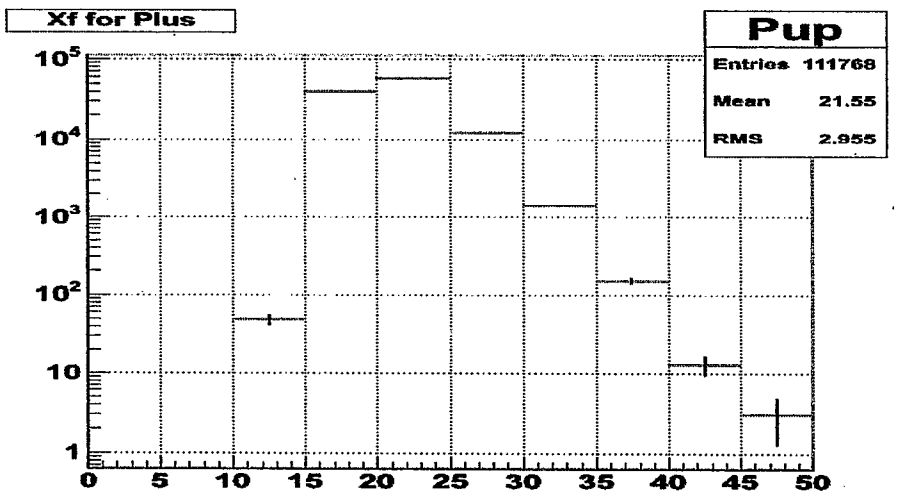

Other considerations

- The request for Run-5 is 2 pb-1 which will give the factor 10 advocated in slide before.
- Jaffe pointed out at the PAC that going to a lower energy could be of interest in disentangling the different effects.
- In addition e.g. running at 50+50 or 62+62 would give a nominal coverage up to xF of ~ 0.6 where asymmetries are expected to be Large.

Acceptance of Brahms

Nominal coverage for 2.3,4 and 4 deg in x_F-p_T space.

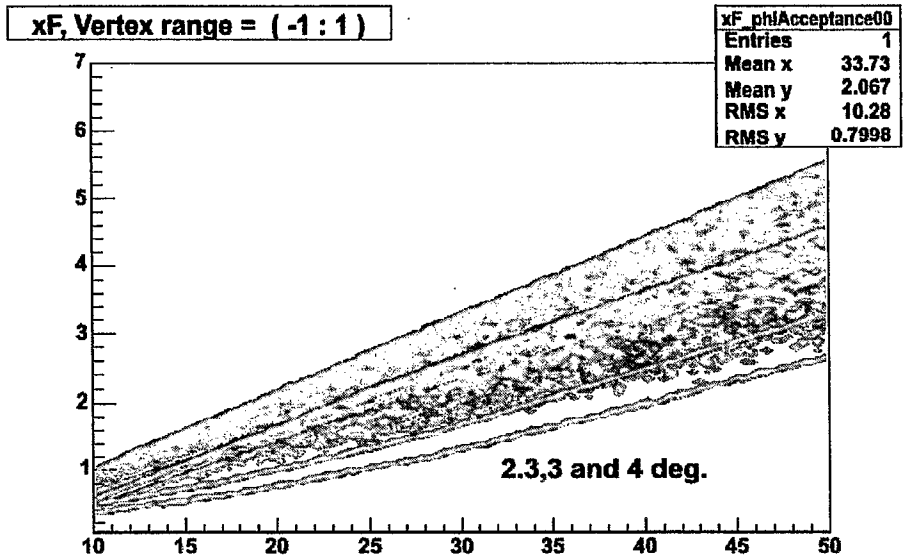

Actual population at 2.3 deg during run-4

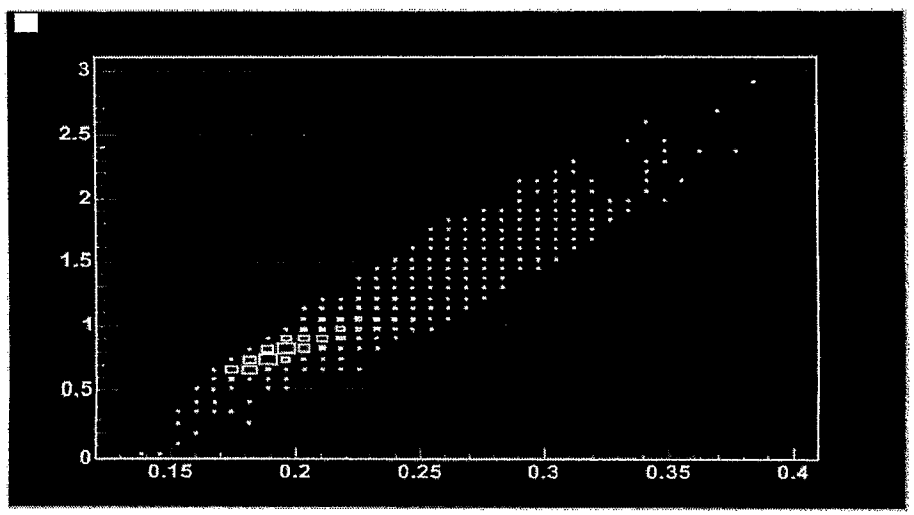

Yields that can be used for analysis

	positive	negative
pion	219K	216K
kaon	46K	26K
proton	165K	17K

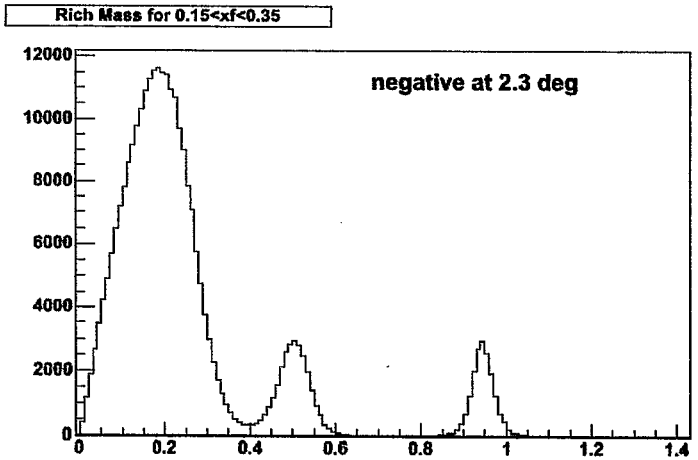

Integrated yields of π, K and proton in x_F range 0.15-0.35

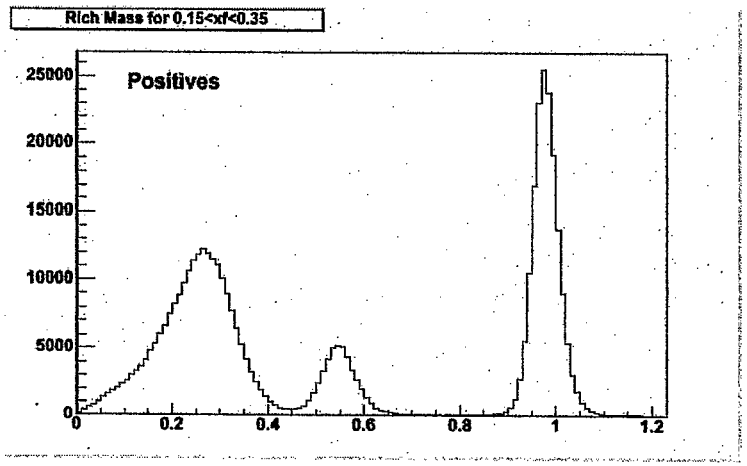

Physics at Hermes

Delia Hasch

INFN Frascati

RHIC-SPIN collaboration meeting
October 8/9, 2004; Torino (Italy)

→ "longitudinal" spin observables ←

nucleon quark structure

$$\Phi^{\mathrm{Tw2}}_{\mathrm{Corr}}(x) = \frac{1}{2}\left\{f_1(x) + \mathrm{S_L}\, g_1(x)\gamma_5 + h_1(x)\gamma_5\gamma^1\mathrm{S_T}\right\} n^+$$

$f_1^q =$ 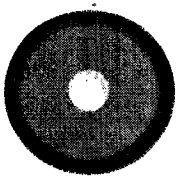

$g_1^q =$ 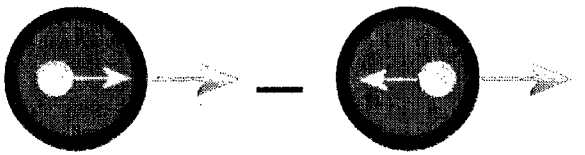

$h_1^q =$ 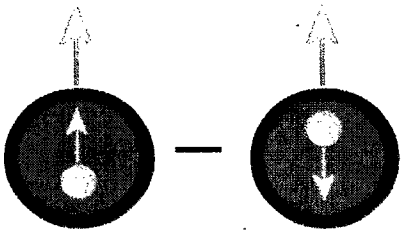

unpolarised quarks and nucleons	longitudinally polarised quarks and nucleons	transversely polarised quarks and nucleons
q(x): spin averaged	Δq(x): helicity difference	δq(x): *helicity flip*
→vector charge	→axial charge	→tensor charge
well known	known	*unmeasured !*

nucleon quark structure

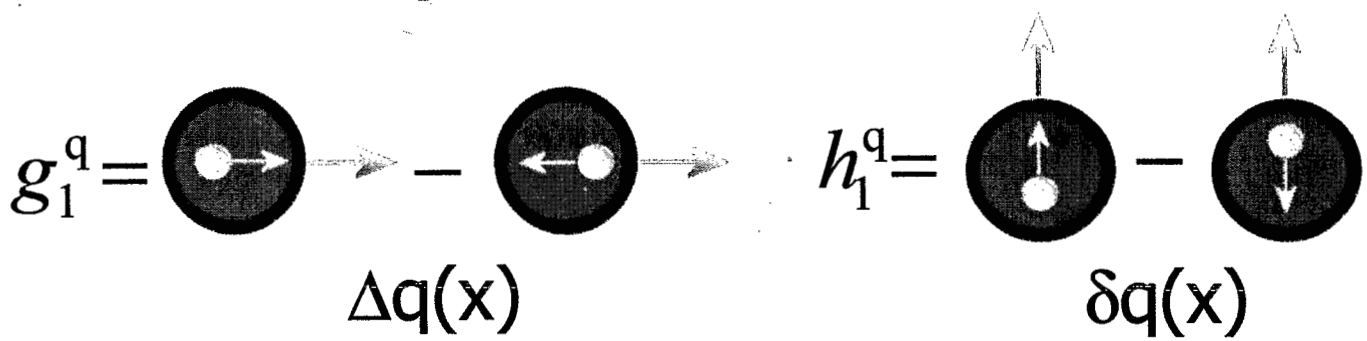

<u>Outline:</u>

- the Hermes experiment
- final result on g_1 for the proton and deuteron
- first direct flavour decomposition of Δq
- single target+beam-spin asymmetries (longitudinal)

nucleon spin structure

$$\langle S_z^N \rangle = \frac{1}{2} = \frac{1}{2}\Delta\Sigma + L_q + J_g$$

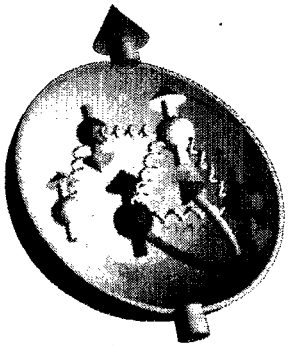

<u>Outline:</u>

- the Hermes experiment
- final result on g_1 for the proton and deuteron
- first direct flavour decomposition of Δq
- single target+beam-spin asymmetries (longitudinal)
- news on exclusive meson production and DVCS

Hermes @ DESY

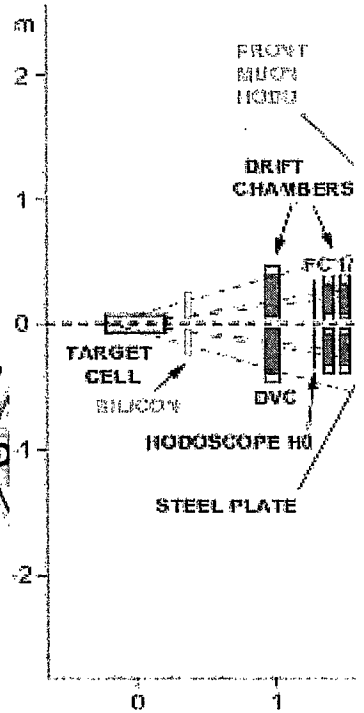

27

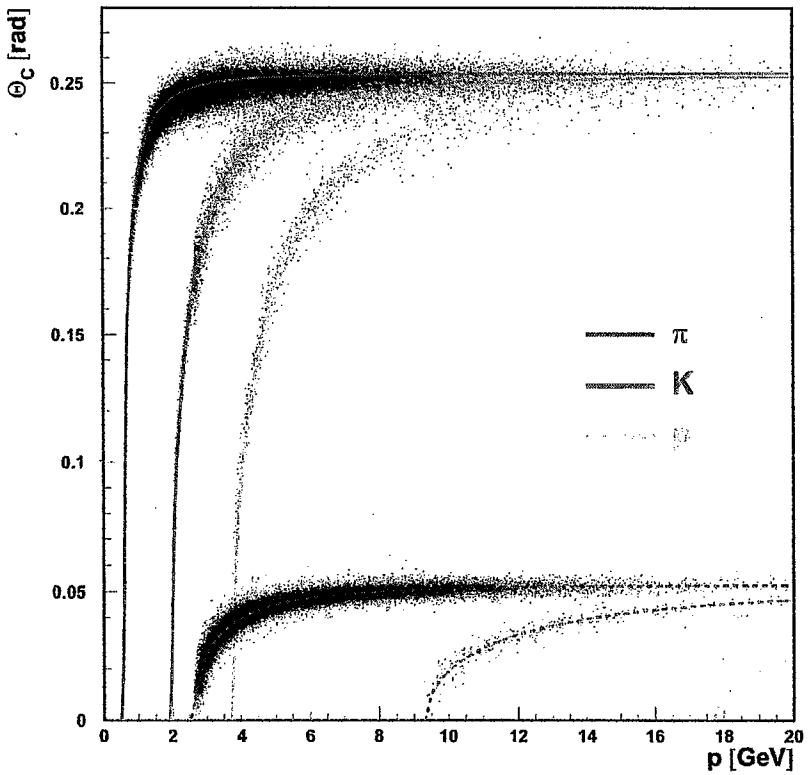

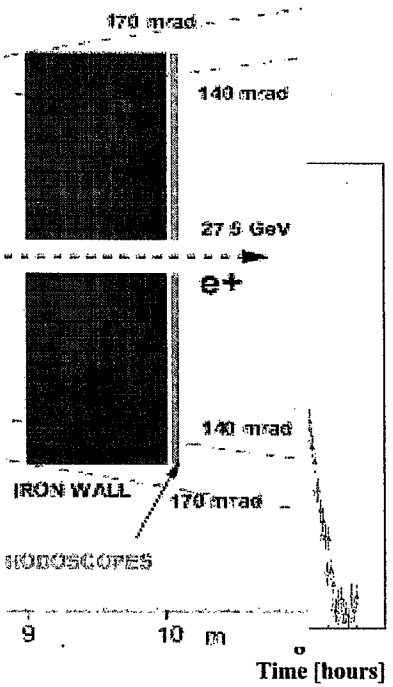

- resolution
- particle ID

1%

RICH: π, K, p ID within $2<E_h<15$ GeV

Hermes @ DESY

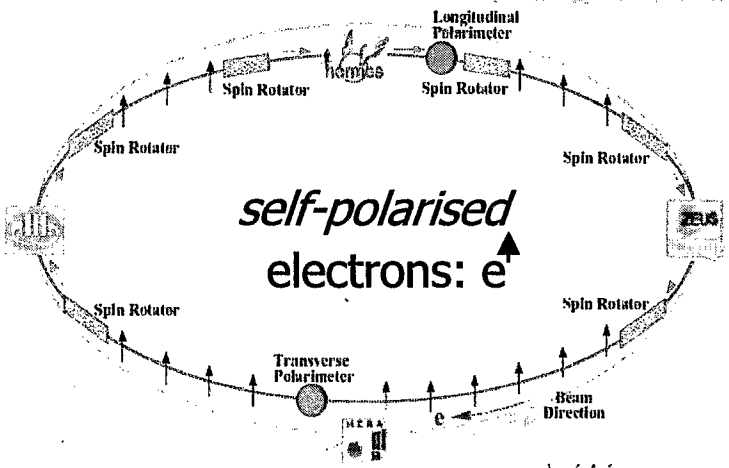

self-polarised electrons: e↑

27.5 GeV (e^+/e^-) →

$\langle P_b \rangle \sim 53 \pm 2.5$ %

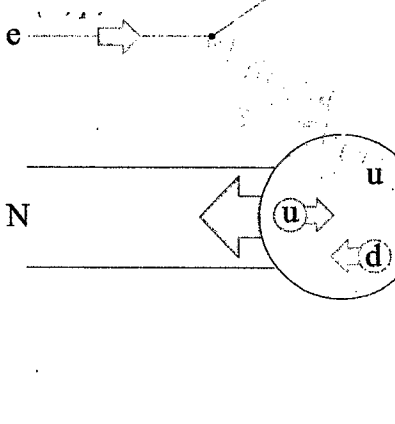

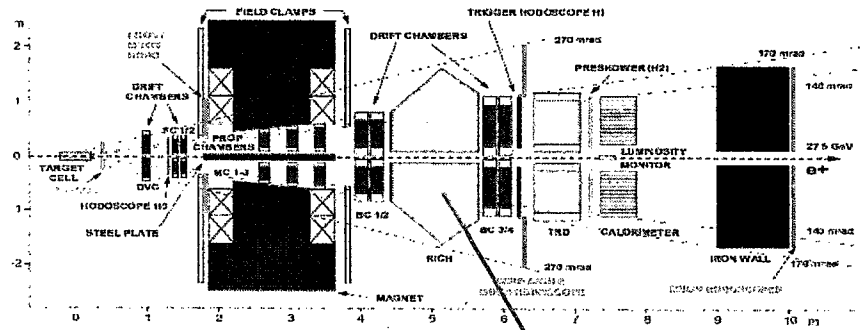

Stern-Gerlach separation

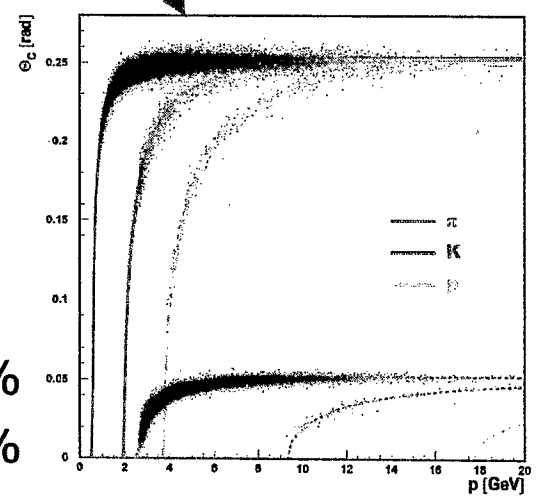

$^1H\rightarrow$ $\langle |Pt| \rangle \sim 85 \pm 3.8$ %

$^2H\rightarrow$ $\langle |Pt| \rangle \sim 84 \pm 3.5$ %

$^1H\uparrow$ $\langle |Pt| \rangle \sim 74 \pm 4.2$ %

pure nuclear polarised gas; flipped at 90s time intervals

Hermes @ DESY

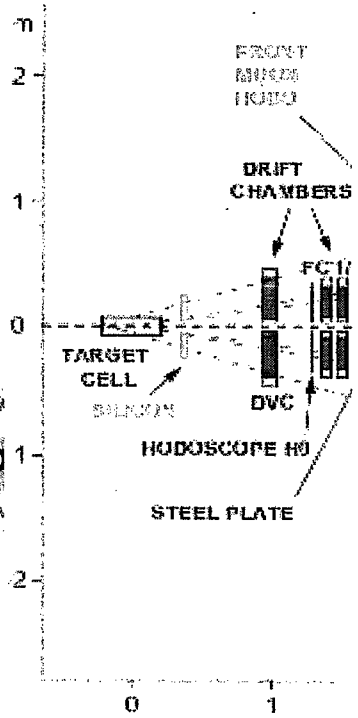

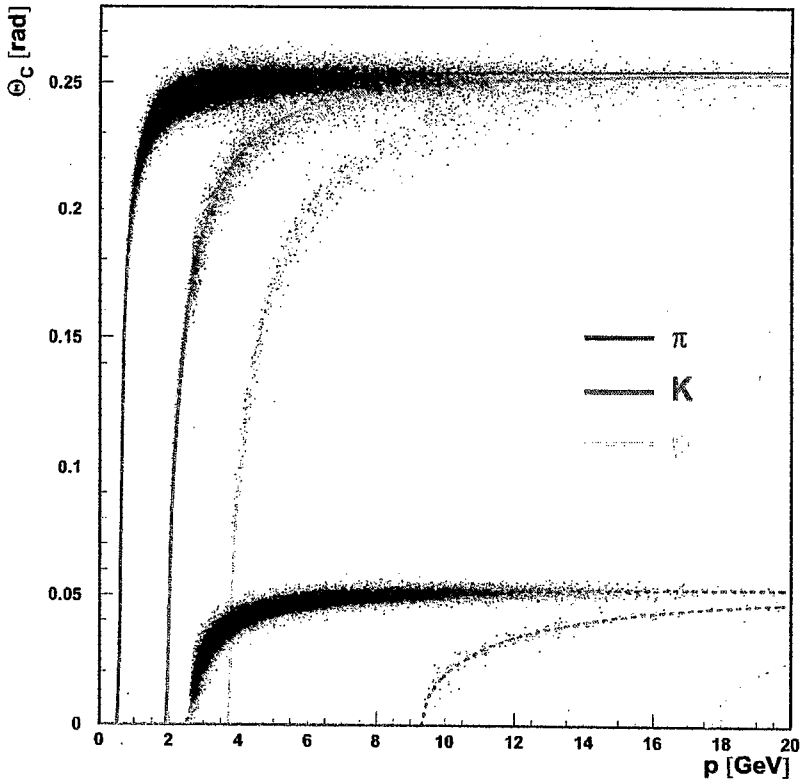

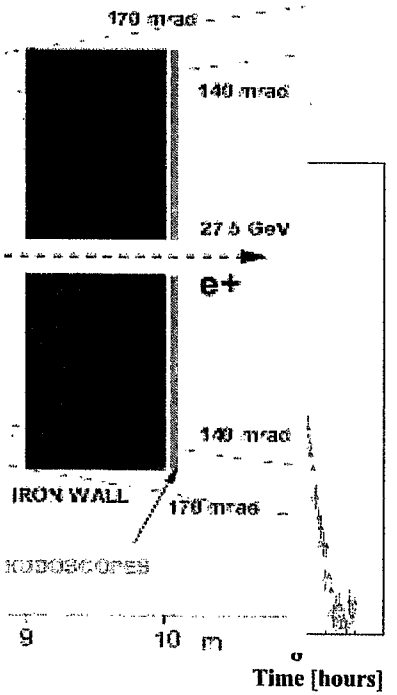

27

<P

- resolution
- particle ID

1%

RICH: π, K, p ID within $2<E_h<15$ GeV

Hermes kinematics

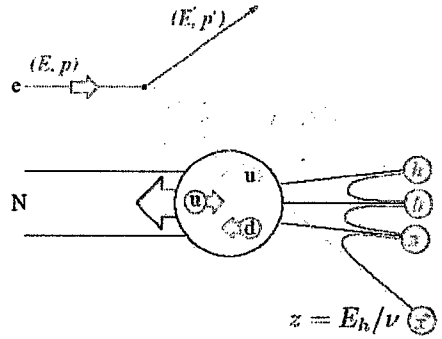

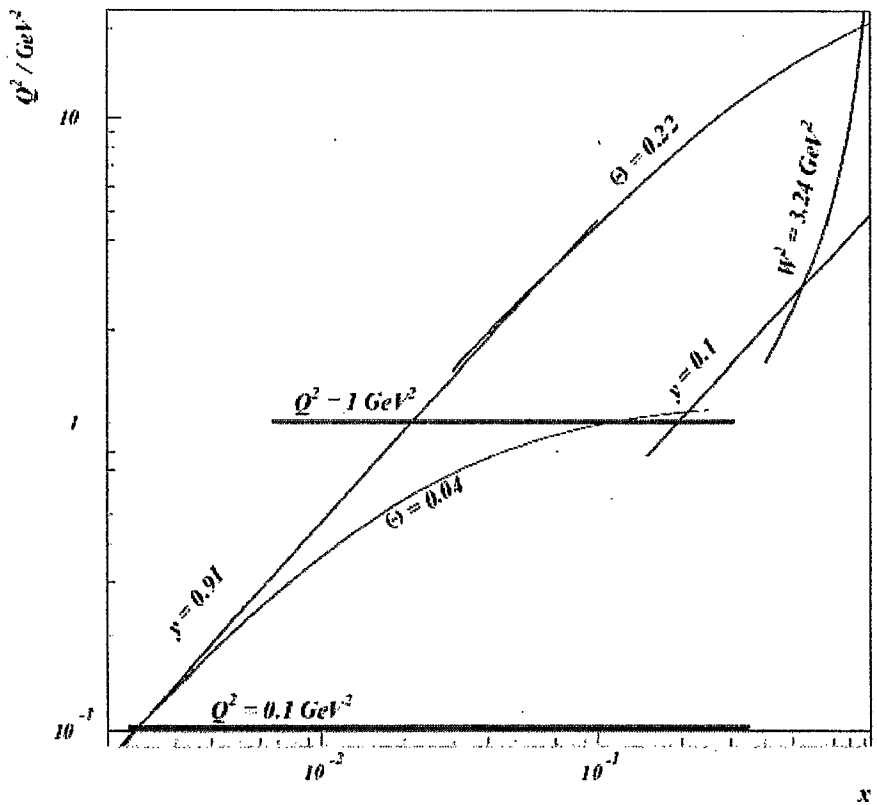

inclusive:

$Q^2 > 0.1\ GeV^2$:

$0.002 < x < 0.9$

with $y<0.91$

$W^2>3.24\ GeV^2$

semi-inclusive:

$Q^2 > 1.0\ GeV^2$:

$0.02 < x < 0.6$

with $y<0.85$, $W^2>10\ GeV^2$

$0.2<z<0.8$

model-independent unfolding

→ detector smearing
→ QED radiative effects

$$S_{ij} = \frac{\partial\sigma^{meas}}{\partial\sigma^{born}} = \frac{\partial N^{meas}}{\partial N^{born}}$$

$$= \frac{N(i,j)}{N^{born}(j)}$$

→ kinematic migration inside acceptance for each spin state

smearing within acceptance

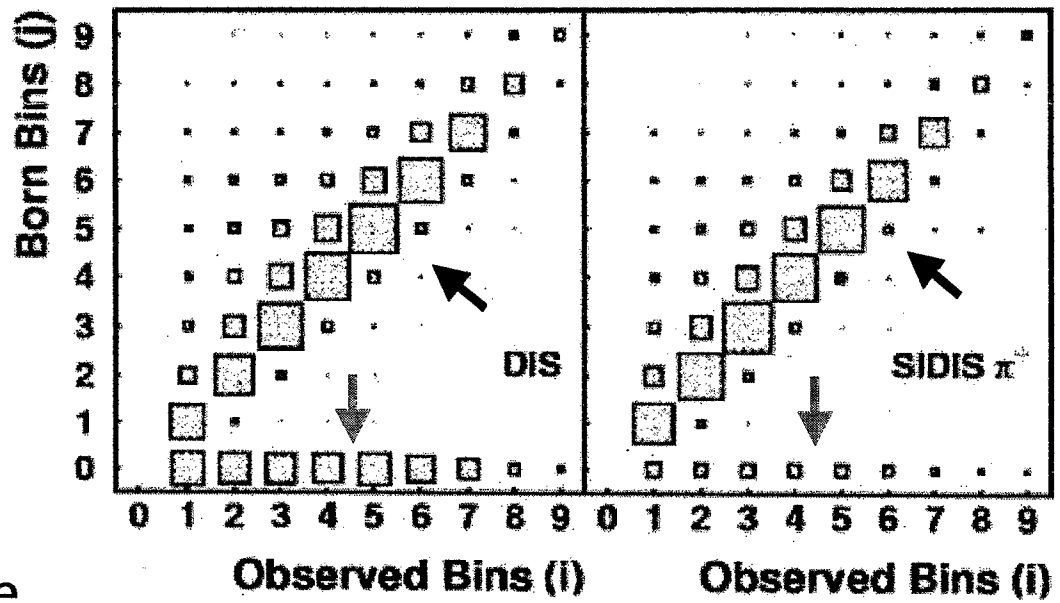

radiative effects detector smearing

→ systematic correlations between bins fully unfolded
→ resulting (small) statistical correlations *known*

quark helicity distributions

$$g_1(x) = \frac{1}{2}\sum_q e_q^2\,\Delta q = \frac{1}{2}\sum_q e_q{}^2\left(q^+(x) - q^-(x)\right)$$

$$g_1(x) \propto \sigma_{1/2} - \sigma_{3/2}$$

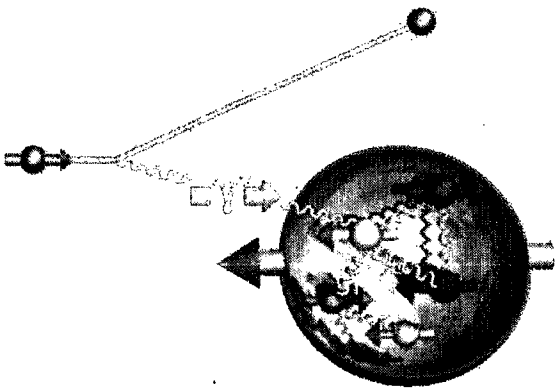

$$\sigma_{1/2} \approx q^+(x)$$

$$S_\gamma + S_N = \frac{1}{2}$$

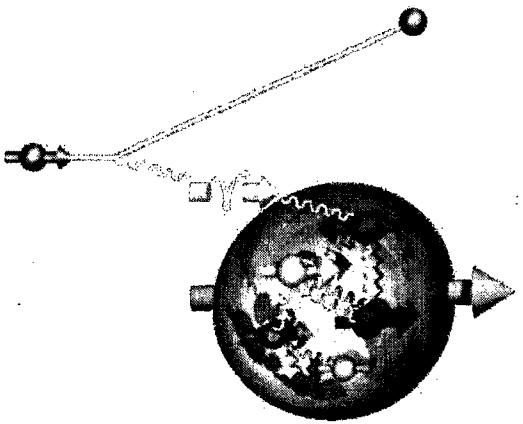

$$\sigma_{3/2} \approx q^-(x)$$

$$S_\gamma + S_N = \frac{3}{2}$$

virtual photon asymmetry

$$A_1 = \frac{\sigma_{1/2} - \sigma_{3/2}}{\sigma_{1/2} + \sigma_{3/2}} = \frac{g_1 - \gamma^2 g_2}{F_1} \approx \frac{g_1(x, Q^2)}{F_1(x, Q^2)}$$

$$= \frac{1}{(1+\gamma^2)} \left(\frac{A_\parallel}{D} + (\gamma - \eta) A_2 \right)$$

$$A_\parallel(\Delta x, \Delta Q^2) = \frac{1}{|P_t P_b|} \frac{N^{\rightarrow\Leftarrow} - N^{\rightarrow\Rightarrow}}{N^{\rightarrow\Leftarrow} + N^{\rightarrow\Rightarrow}}$$

- A2 parameterised from SLAC data
- F2 ALLM parametrisation

g_1/F_1 of the proton and deuteron

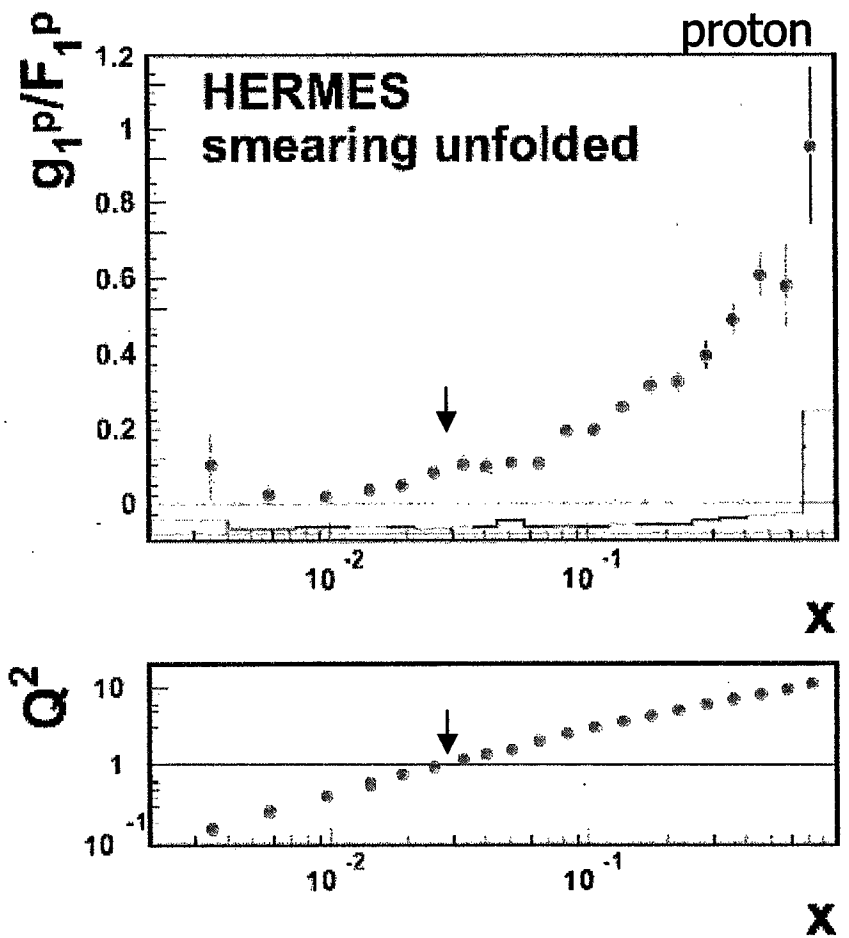

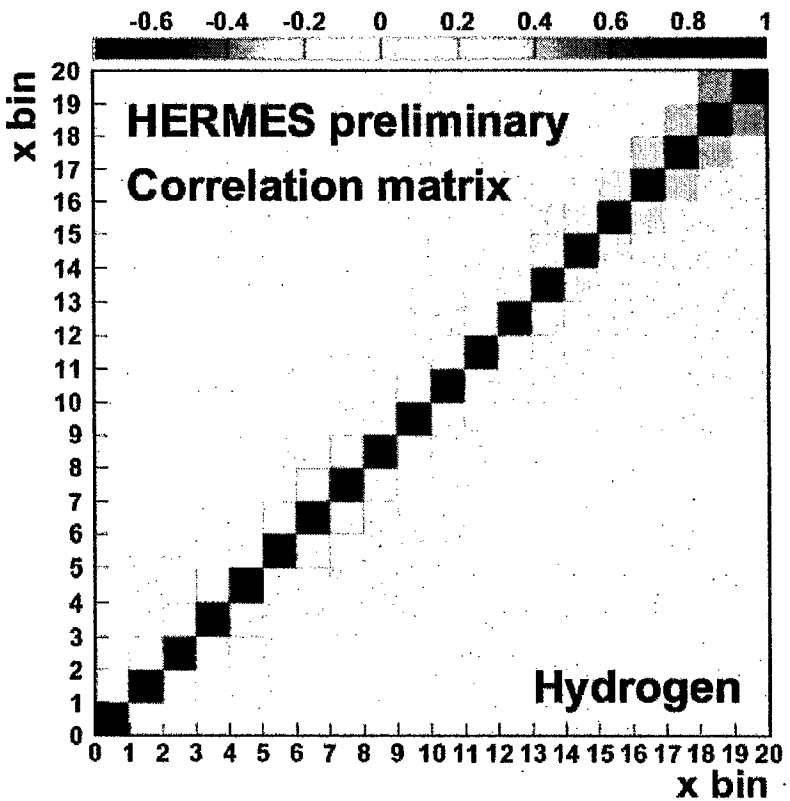

structure function $g_1(x)$

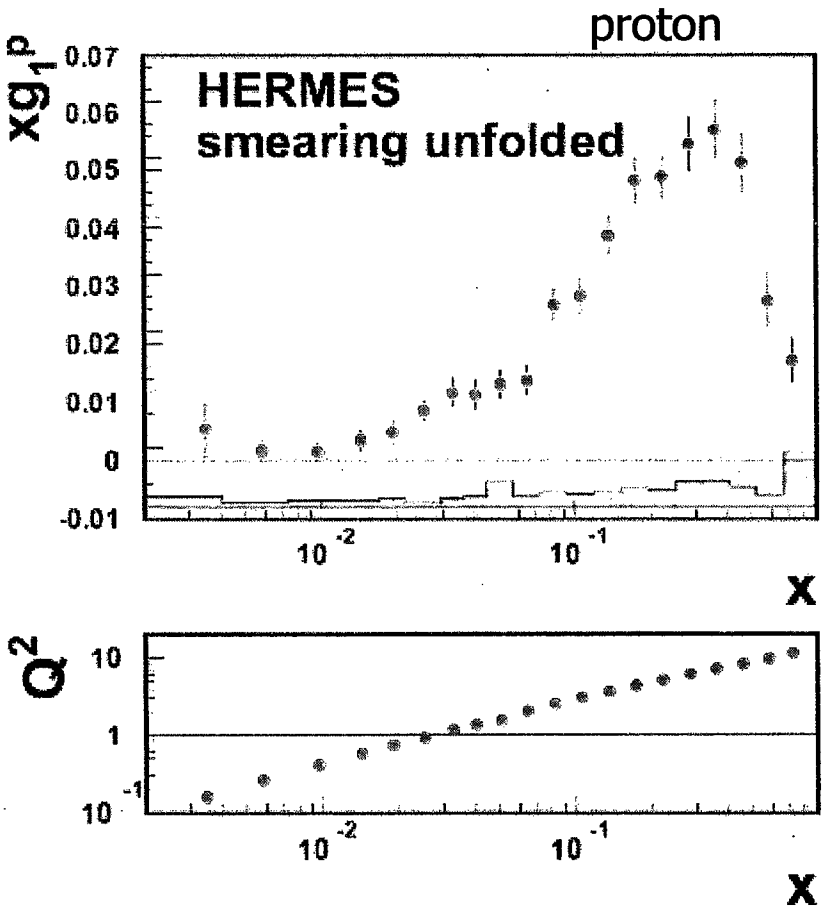

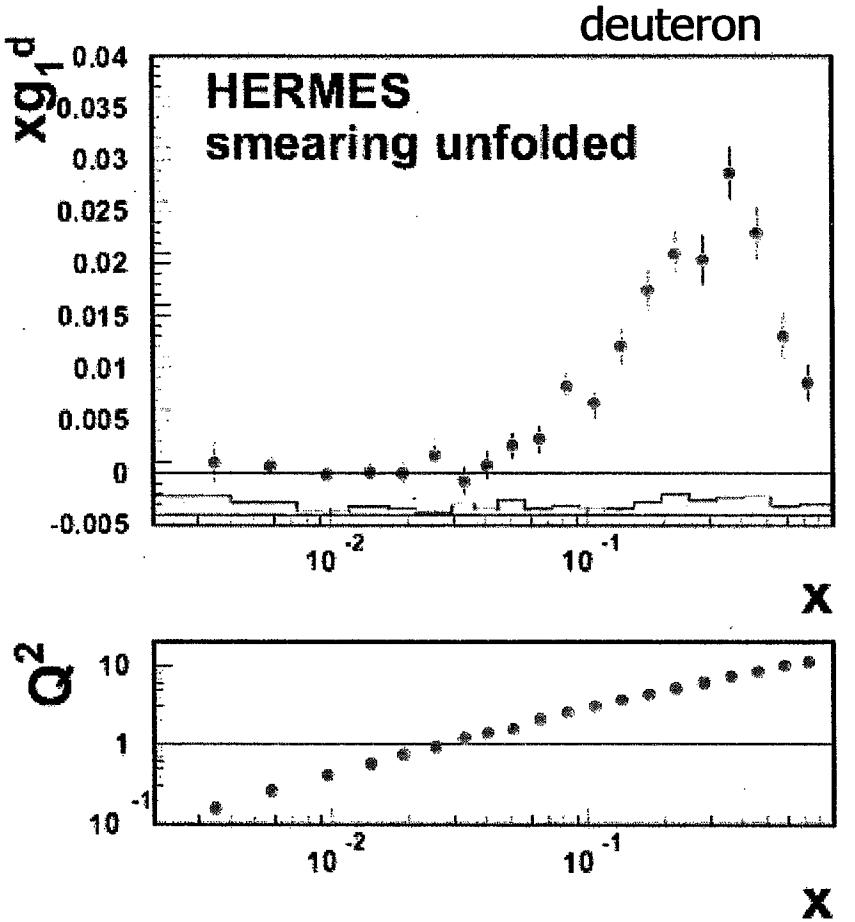

Δq from inclusive data

$$g_1^{\mathrm{NLO}}(x) = g_1^{\mathrm{LO}} + \frac{\alpha_s}{2\pi}\frac{1}{2}\sum_q e_q^2\left[\Delta q(x,Q^2)\otimes C_q + \Delta G(x,Q^2)\otimes C_g\right]$$

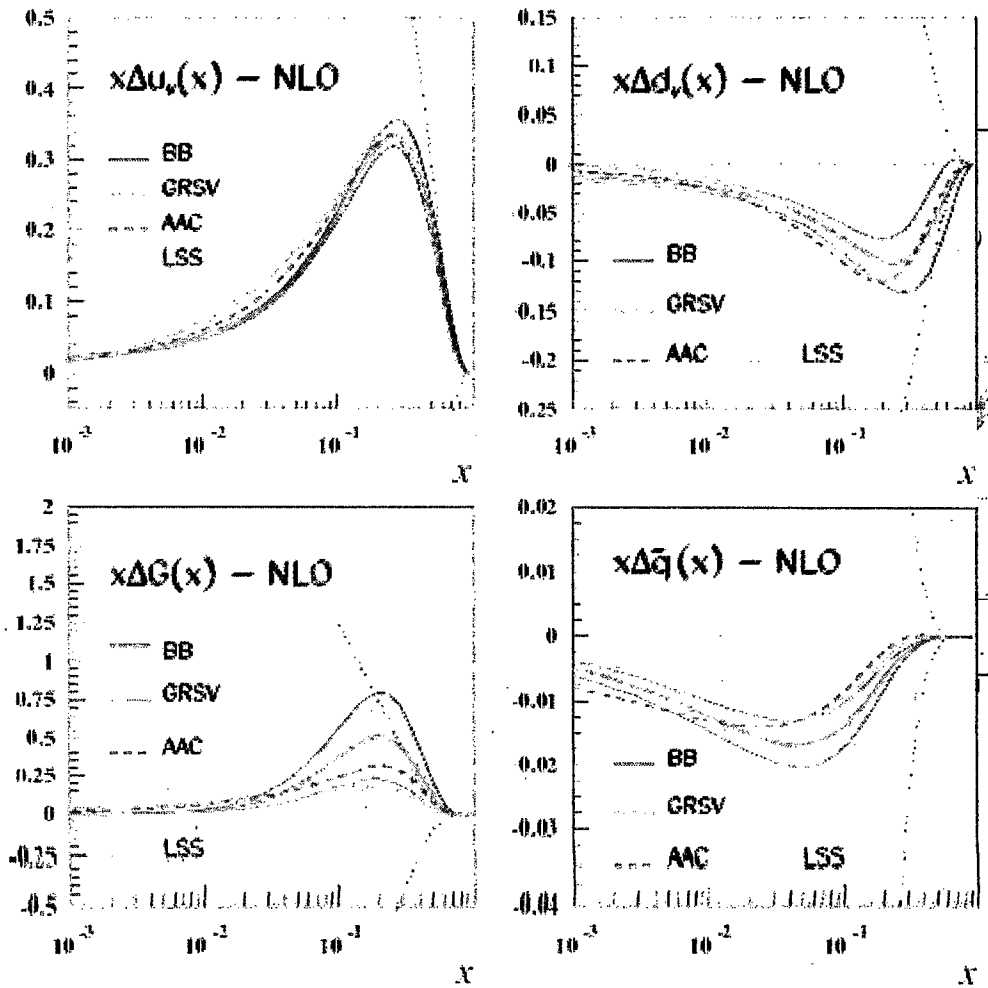

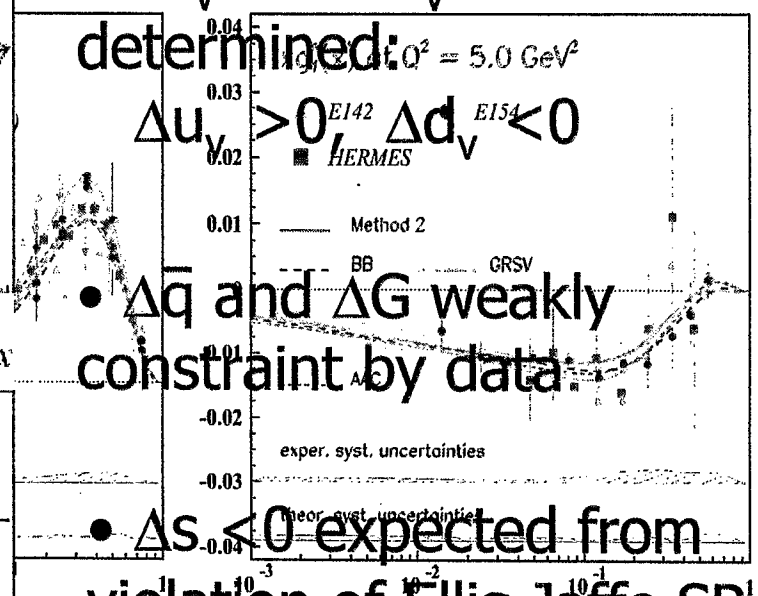

- Δu_v and Δd_v well determined: $\Delta u_v > 0$, $\Delta d_v < 0$
- $\Delta\bar{q}$ and ΔG weakly constraint by data
- $\Delta s < 0$ expected from violation of Ellis-Jaffe SR

→more, direct probes needed

polarised quark distributions

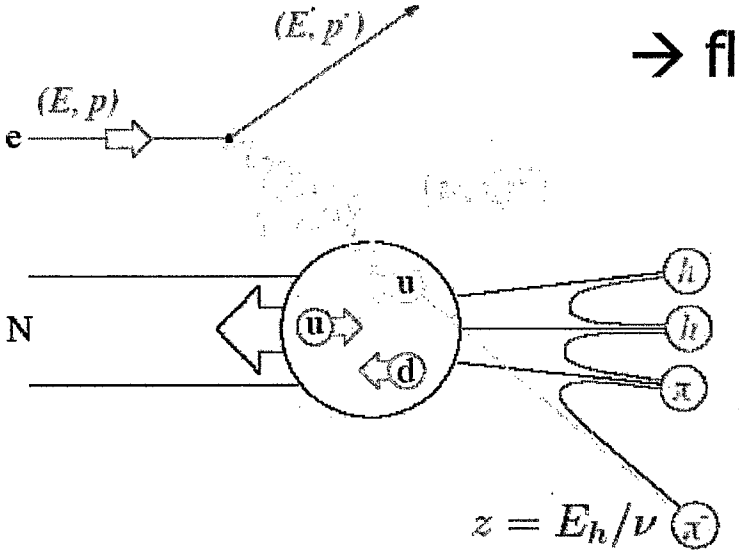

→ flavour separation by flavour tagging

flavour content of final state hadrons related to flavour of struck quark via fragmentation functions

$$A_1^h(x,Q^2) \approx \frac{\sigma_{1/2}^h}{\sigma_{1/2}^{hq}} \approx \frac{\sum_q e_q^2 \Delta q(x,Q^2) \int dz\, D_q^h(z,Q^2)}{\sum_q e_q^2 q(x,Q^2) \int dz\, D_q^h(z,Q^2)}$$

$$A = PQ$$

$$Q = \left(\frac{\Delta u}{u}, \frac{\Delta d}{d}, \frac{\Delta \bar{u}}{\bar{u}}, \frac{\Delta \bar{d}}{\bar{d}}, \frac{\Delta s}{s}, \frac{\Delta \bar{s}}{\bar{s}} = 0 \right)$$

measured asymmetries

$$\vec{A} = \left(A_{1,p}, A_{1,d}, A_{1,p}^{\pi^\pm}, A_{1,d}^{\pi^\pm}, A_{1,d}^{K^\pm} \right)$$

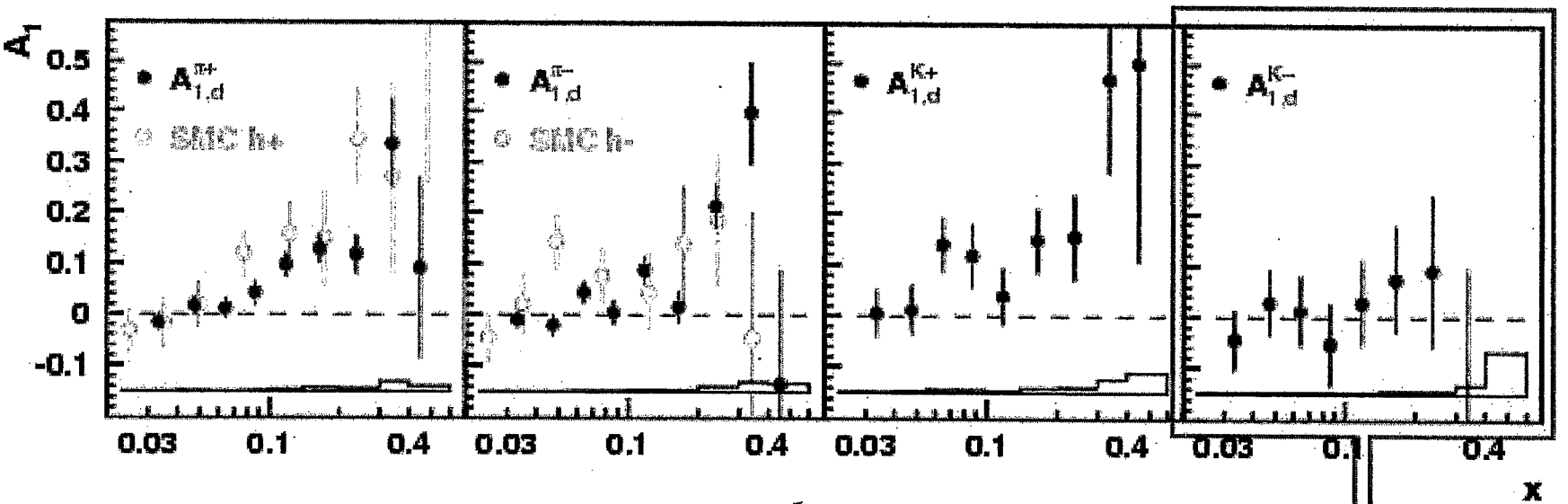

K^- $(\bar{u}s)$ all sea objects

purity analysis @ HERMES

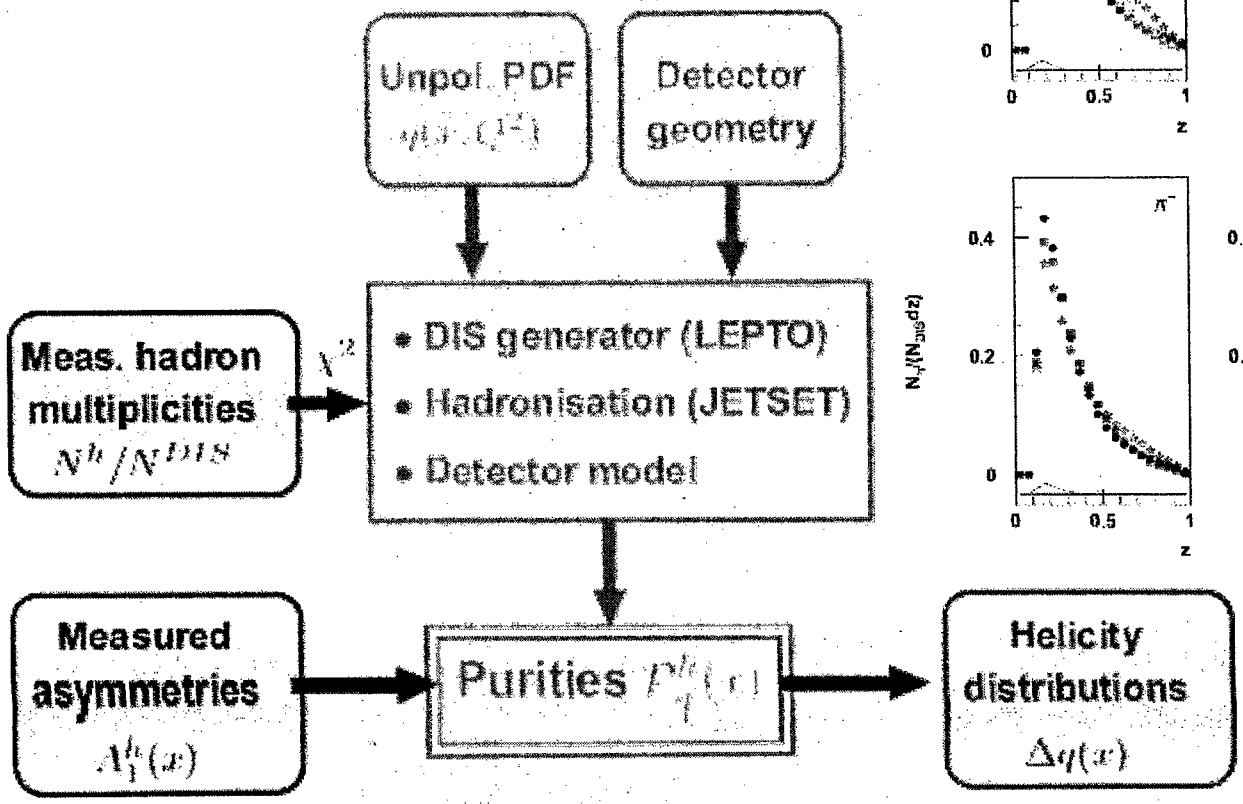

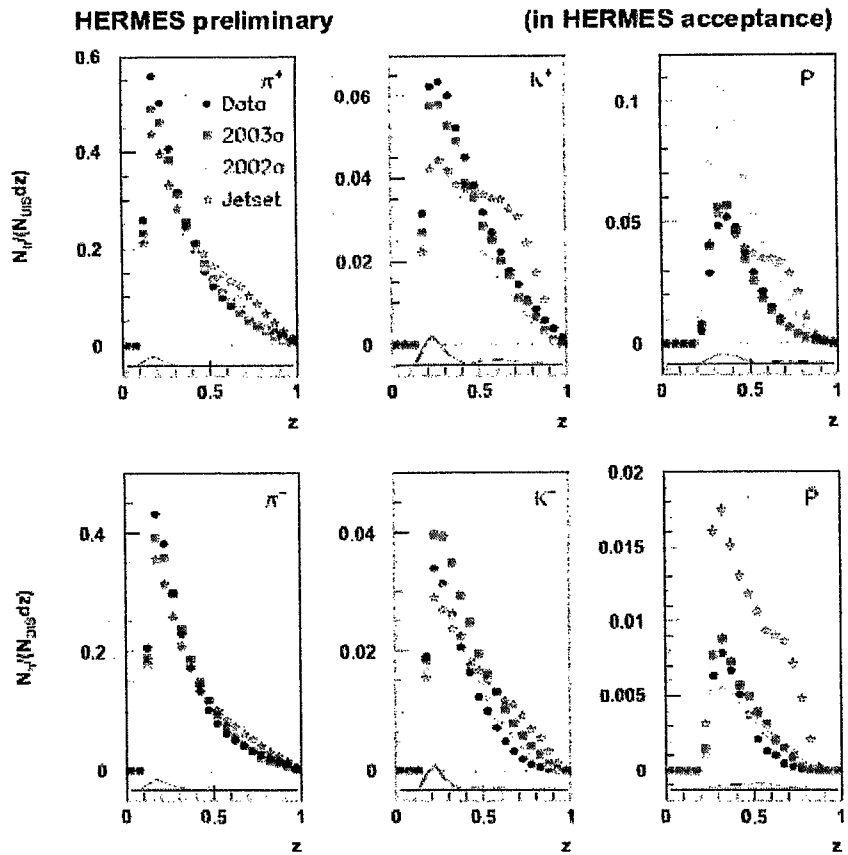

purities @Hermes

probability that γ^* hit a quark of flavour q when hadron of type h was detected

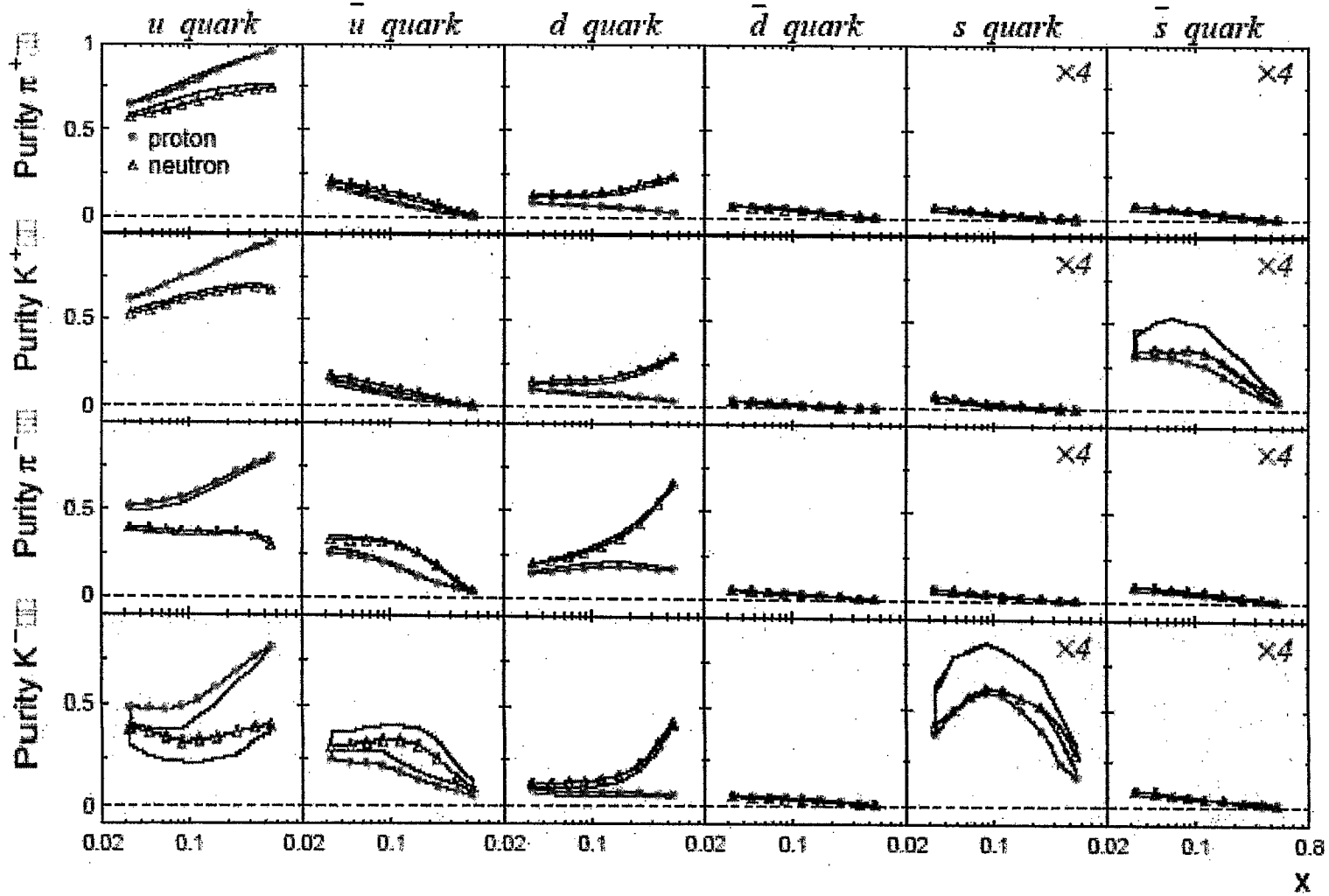

[PRL92,2004; hep-ex/0407032, submitted to PRD]

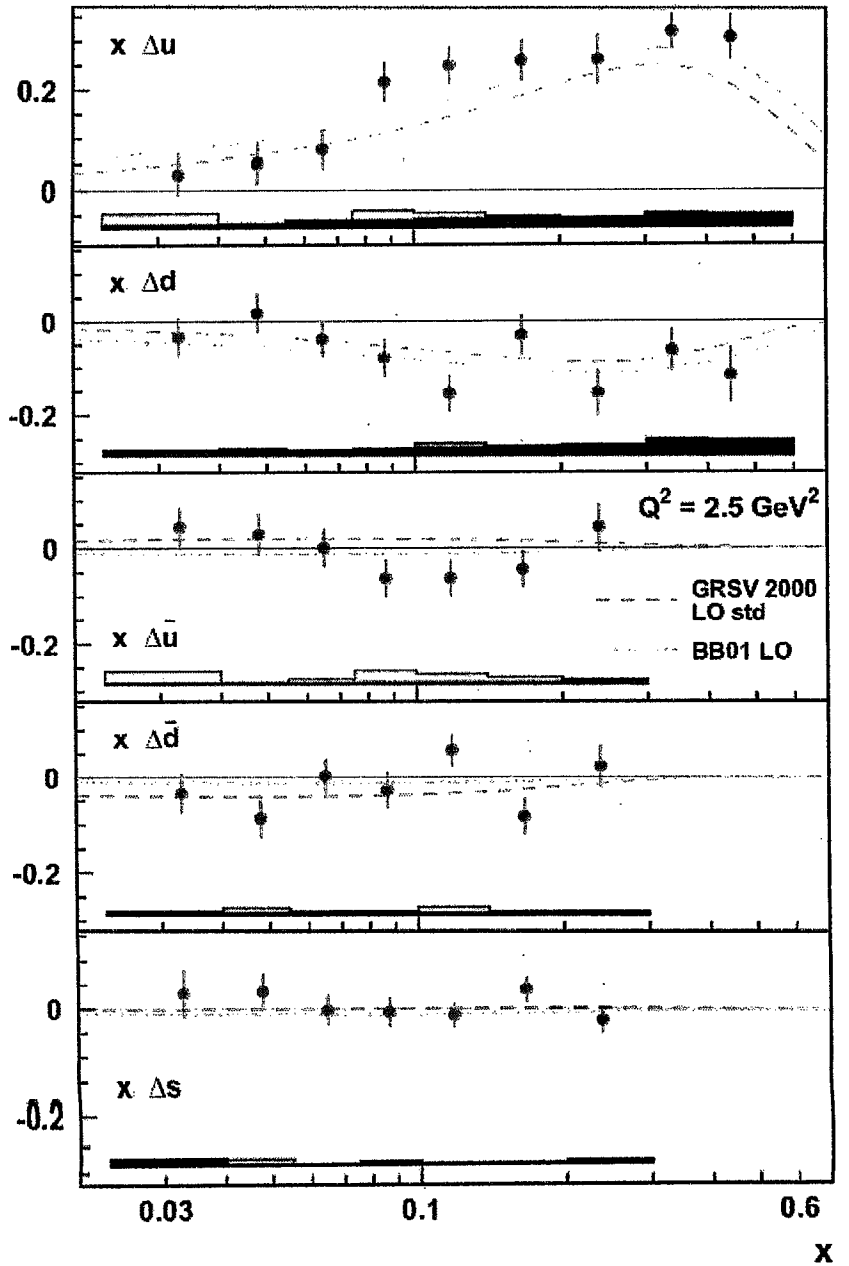

quark polarisations

first 5-flavour fit to Δq

- no significant $\bar{q}$ polarisation

→ results perfectly consistent with incl. fits: χ^2/dof =0.6...1.6 for BB(SU3-sym) and GRSV-valence

- in measured range (0.023-0.6):

$$\int \Delta\bar{u} = -0.002 \pm 0.043$$

$$\int \Delta\bar{d} = -0.054 \pm 0.035$$

$$\int \Delta s = +0.028 \pm 0.034$$

light sea flavour asymmetry

$$\vec{Q} = \left(\frac{\Delta u}{u}, \frac{\Delta d}{d}, \frac{\Delta\bar{u} - \Delta\bar{d}}{\bar{u} - \bar{d}}, \frac{\Delta\bar{d}}{\bar{d}}, \frac{\Delta s}{s} \right)$$

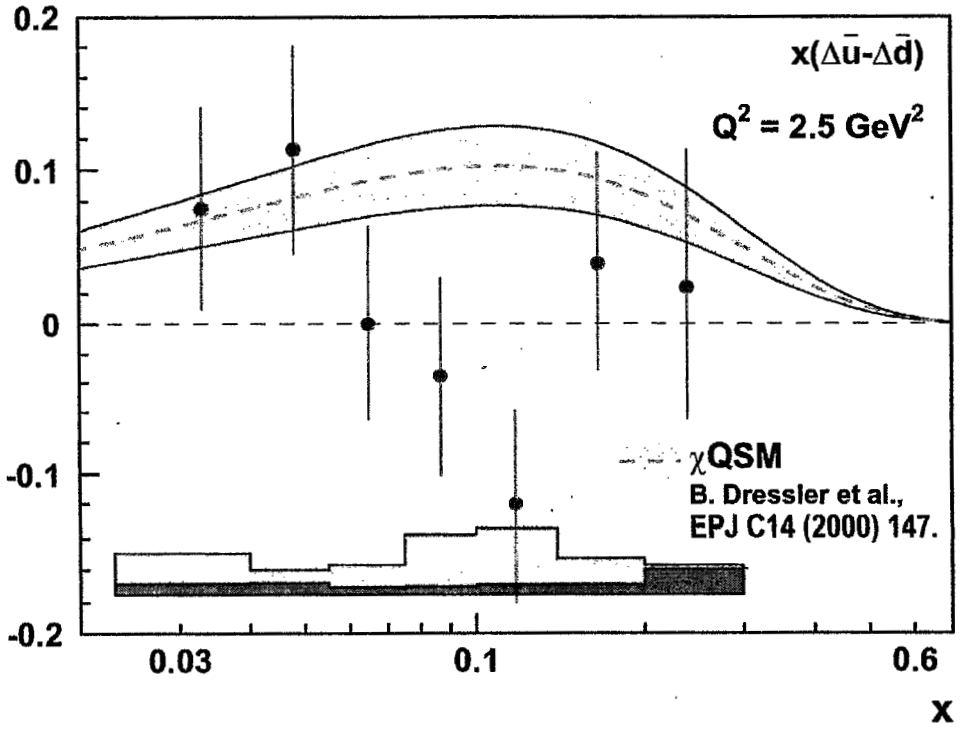

- no significant breaking of polarised SU(2)-flavour symmetry
- χQSM asymmetric sea disfavoured: χ^2/dof=17.6/7

single-spin asymmetries

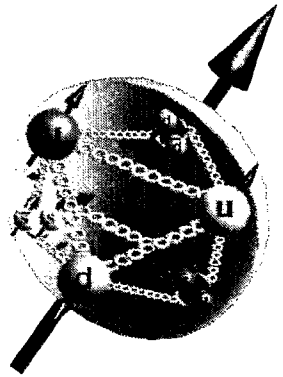

$$d\sigma = d\sigma_{UU} + \cos 2\phi\, d\sigma_{UU} + \frac{1}{Q}\cos\phi\, d\sigma_{UU} + \lambda \frac{1}{Q}\sin\phi\, d\sigma_{LU}$$

f_1 $\quad h_1^{\perp} \otimes H_1^{\perp} + \ldots \quad e \otimes H_1^{\perp} + \ldots$

$$+ S_L\left[\sin 2\phi\, d\sigma_{UL} + \frac{1}{Q}\sin\phi\, d\sigma_{UL}\right] + \lambda S_L\, d\sigma_{LL} + \frac{1}{Q}\cos\phi\, d\sigma_{LL}\Big]$$

$h_1 \otimes H_1^{\perp} + f_{1T}^{\perp} \otimes D_1 + h_L \ldots \quad g_1$

$$+ S_T\left[\sin(\phi+\phi_S)d\sigma_{UT} + \sin(\phi-\phi_S)d\sigma_{UT} + \sin(3\phi-\phi_S)d\sigma_{UT} + \frac{1}{Q}\ldots\right]$$

$h_1 \otimes H_1^{\perp} \quad f_{1T}^{\perp} \otimes D_1$

$$+ \lambda S_T \cos(\phi-\phi_S) + \frac{1}{Q}\ldots\Big]$$

A_{UL} on proton and deuteron

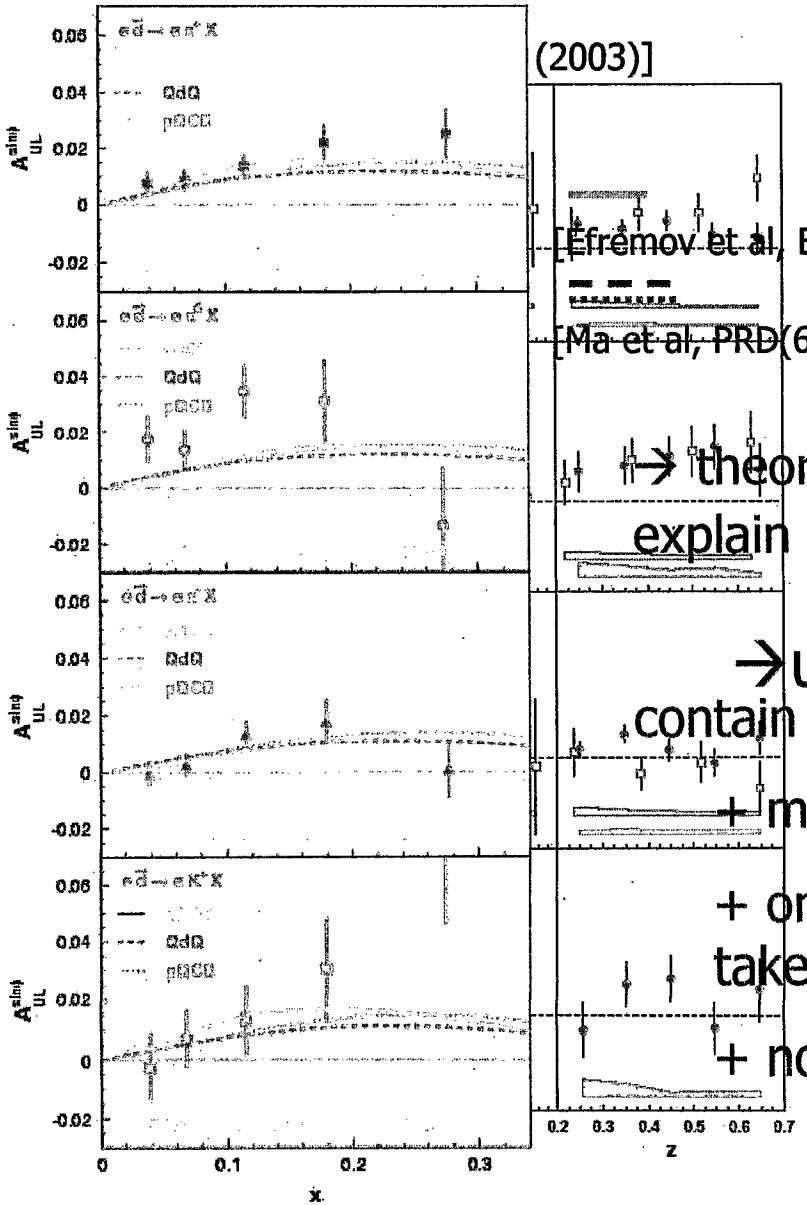

(2003)]

[Efremov et al, EPJC(24),2002]

[Ma et al, PRD(66),2002]

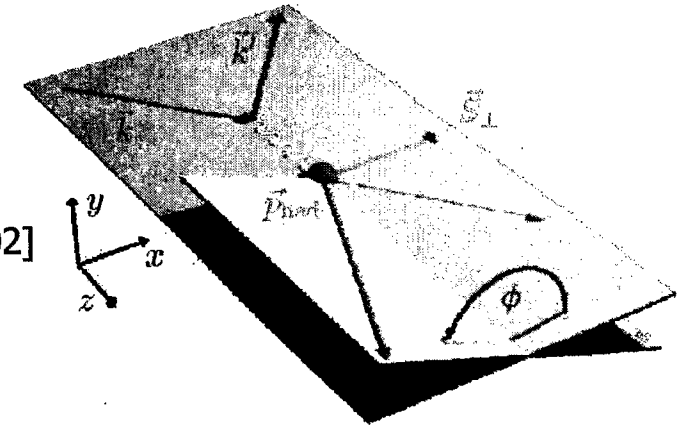

→ theory predictions seem to explain well the data

$$A_{UL}^{h}(\phi) = \frac{1}{|P_t|}\frac{N_h^{\leftarrow}(\phi) - N_h^{\rightarrow}(\phi)}{N_h^{\leftarrow}(\phi) + N_h^{\rightarrow}(\phi)}$$

→ BUT ←

→use data on A_{UT} to extract twist-3 part in A_{UL}

contain a lot of assumptions:

+ magnitude of $H_1^{\perp}/D_1 \approx 4 \ldots 12\%$

+ only part of twist-3 contribution taken into account

+ no Sivers contrib. considers

single beam-spin asymmetry

$$A_{LU}^{h}(\phi) = \frac{1}{|P_b|}\frac{N_h^{\leftarrow}(\phi) - N_h^{\rightarrow}(\phi)}{N_h^{\leftarrow}(\phi) + N_h^{\rightarrow}(\phi)}$$

$$\propto \lambda_e \sin(\phi)\ y\sqrt{1-y}\ \frac{M}{Q}\sum_q e_q^2\, x^2$$

$$\cdot\left[\, e^q(x)H_1^{\perp q}(z) + h_1^{\perp q}(x)E^q(z)\right]$$

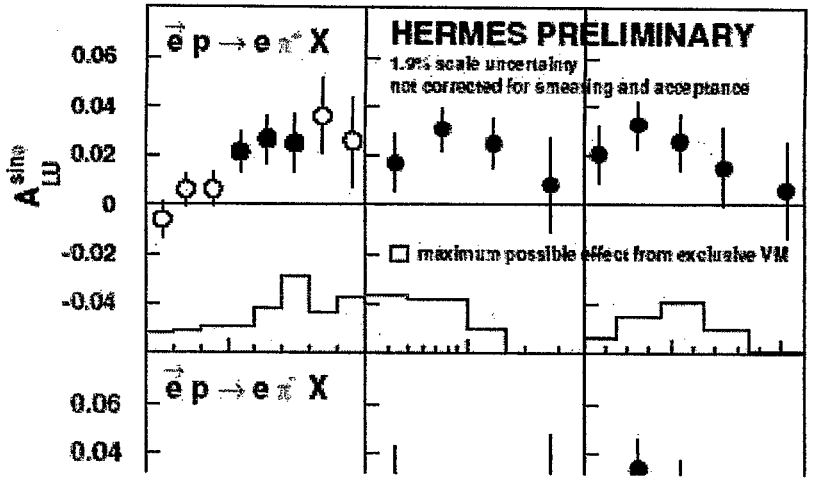

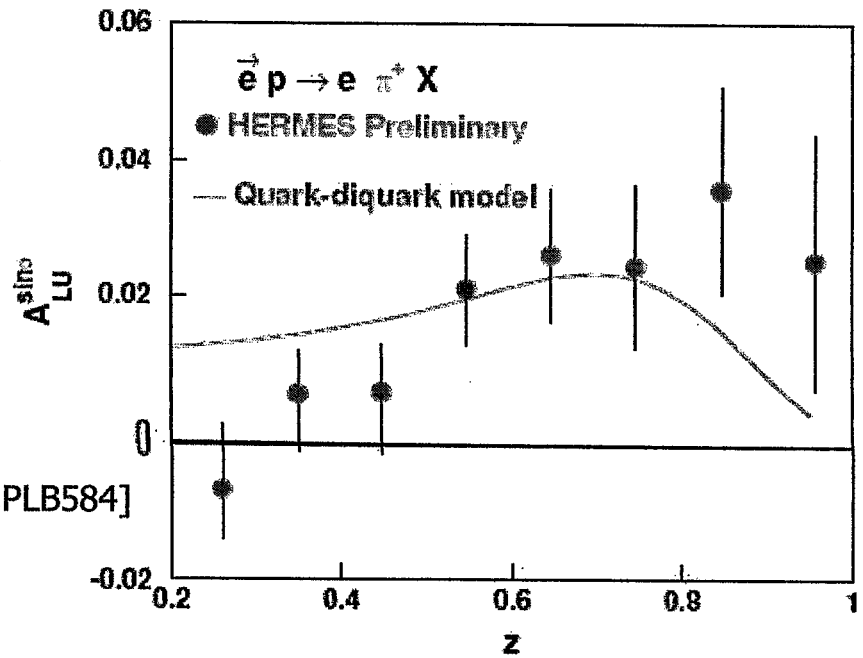

→ QdQ-model prediction of z-dependence [Gamberg,Hwang,Oganessyan,PLB584]

hunting for L_q

factorisation theorem for *hard exclusive processes:*

Müller (1994)

Ji & Radyushkin (1996)

Generalised **P**arton **D**istributions

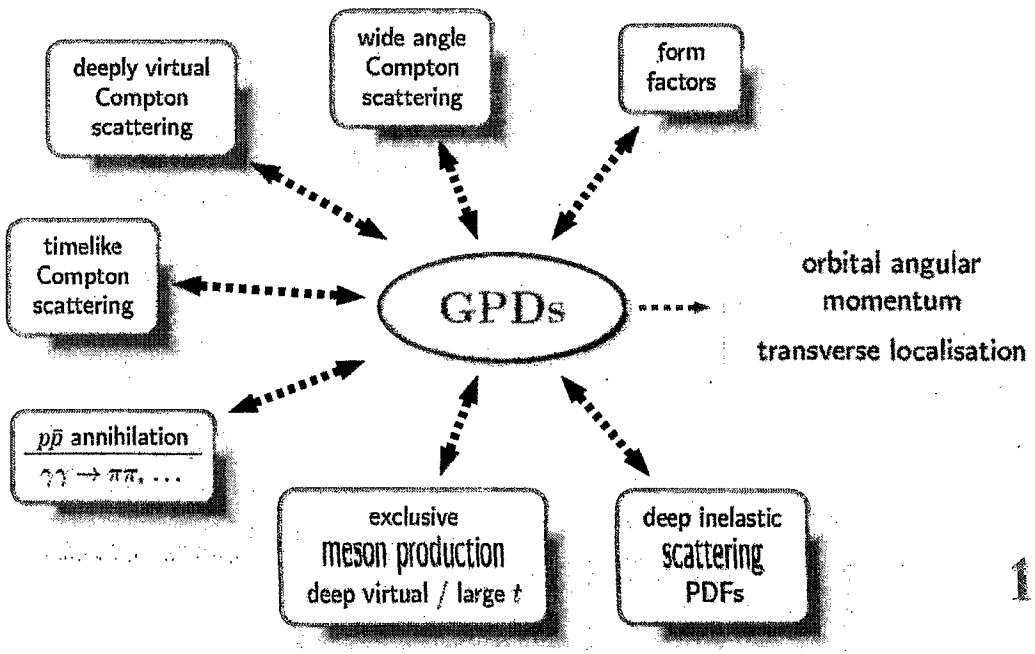

$$\int (H + E)\, x\, dx = J_q$$

$$= 1/2\, \Delta\Sigma + L_z$$

10-30%(DIS)

Generalised Parton Distributions

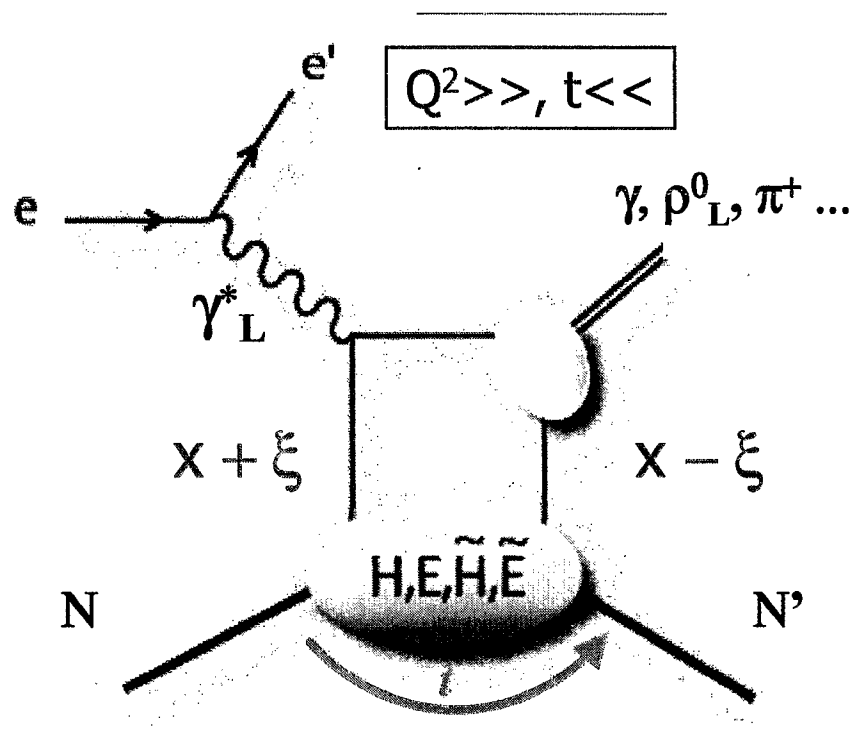

GPDs @twist-2:

H, E $\tilde{H}, \tilde{E}$

quantum number of final state selects different GPDs:

→ DVCS ←

vector mesons pseudoscalar mesons

exclusivity for ep → e′π⁺(n)

Missing Mass^2 = $(\gamma+p-\pi^+)^2$

use π^- yield (ep $\not\rightarrow$ e′π^-n) to subtract non-exclusive background

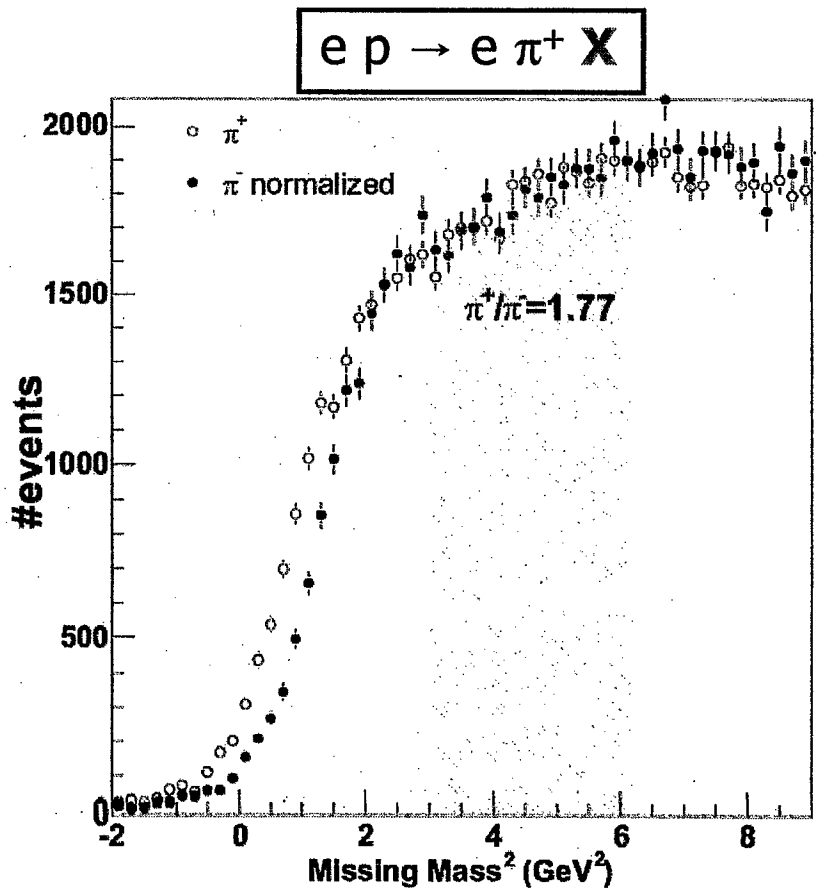

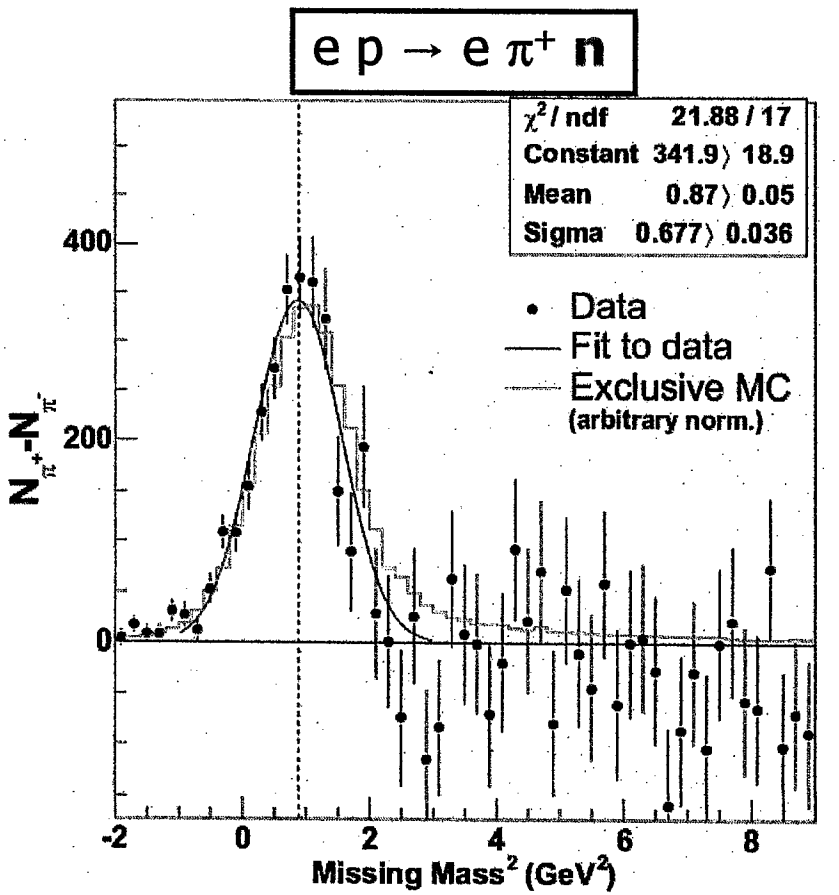

cross section for ep → e′π⁺n

- data distributions background subtracted
- Monte Carlo - arbitrary normalization [Vanderhaegen,Guichon,Guidal(1999)]

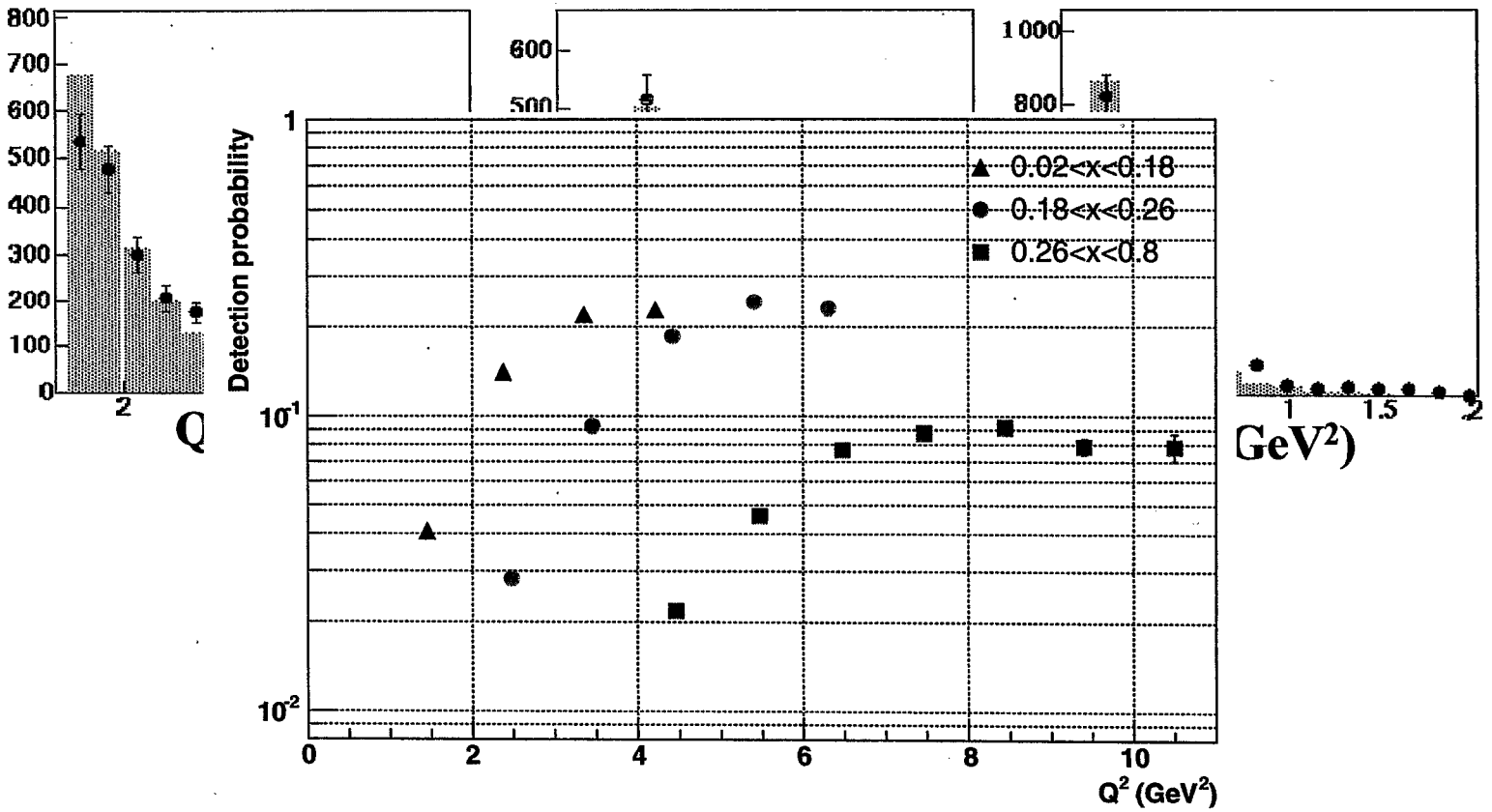

probability to detect e and π+ (generated in 4π) with the Hermes detector

cross section for ep → e′π⁺n

no L/T separation but σ_T suppressed by $1/Q^2$ and $\varepsilon > 0.8$

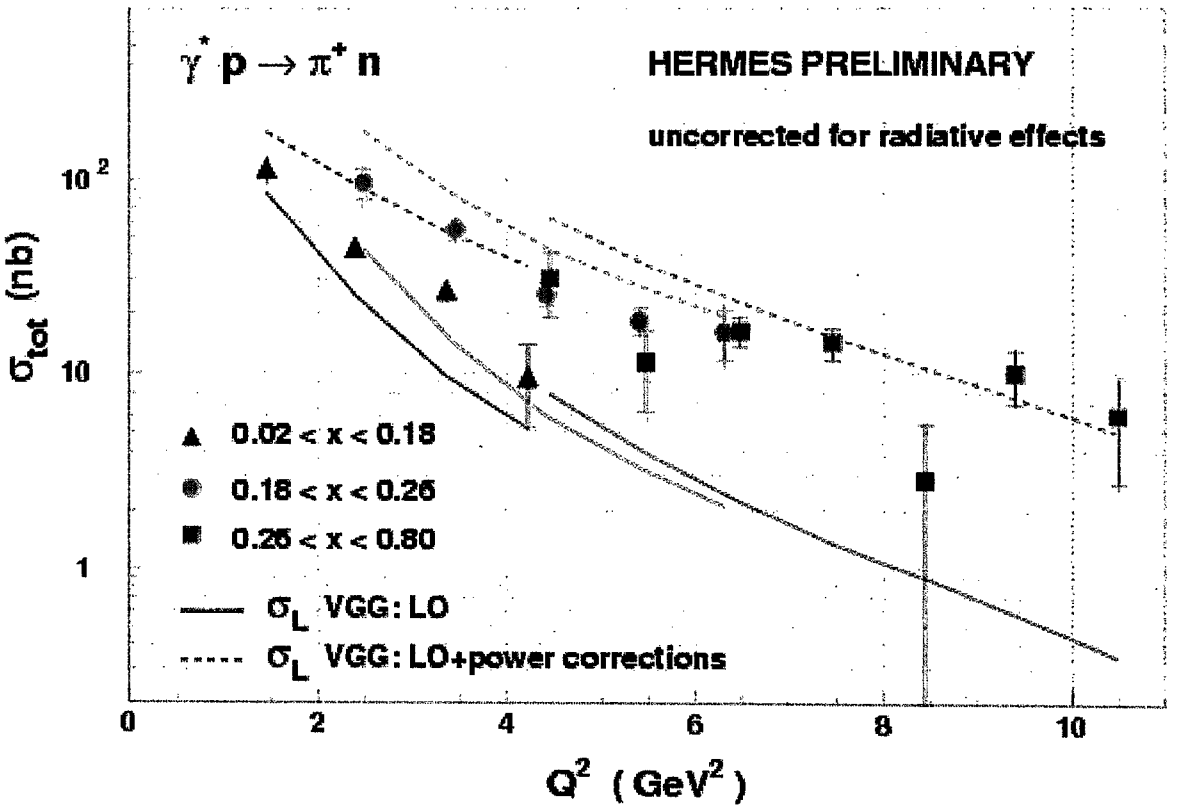

[Vanderhaeghen, Guichon & Guidal (1999)]

π production:

$\tilde{H}$ pseudovector contrib.

$\tilde{E}$ pseudoscalar contrib.

(pion pole related to F_π)

→ LO calculations underestimate the data

→ evaluation of the *power correction* appears too large

Q^2 dependence

factorisation theorem: $\sigma_L \xrightarrow[\text{for fixed } x_B \text{ and } t]{\text{asymptotically}} \frac{1}{Q^6}$

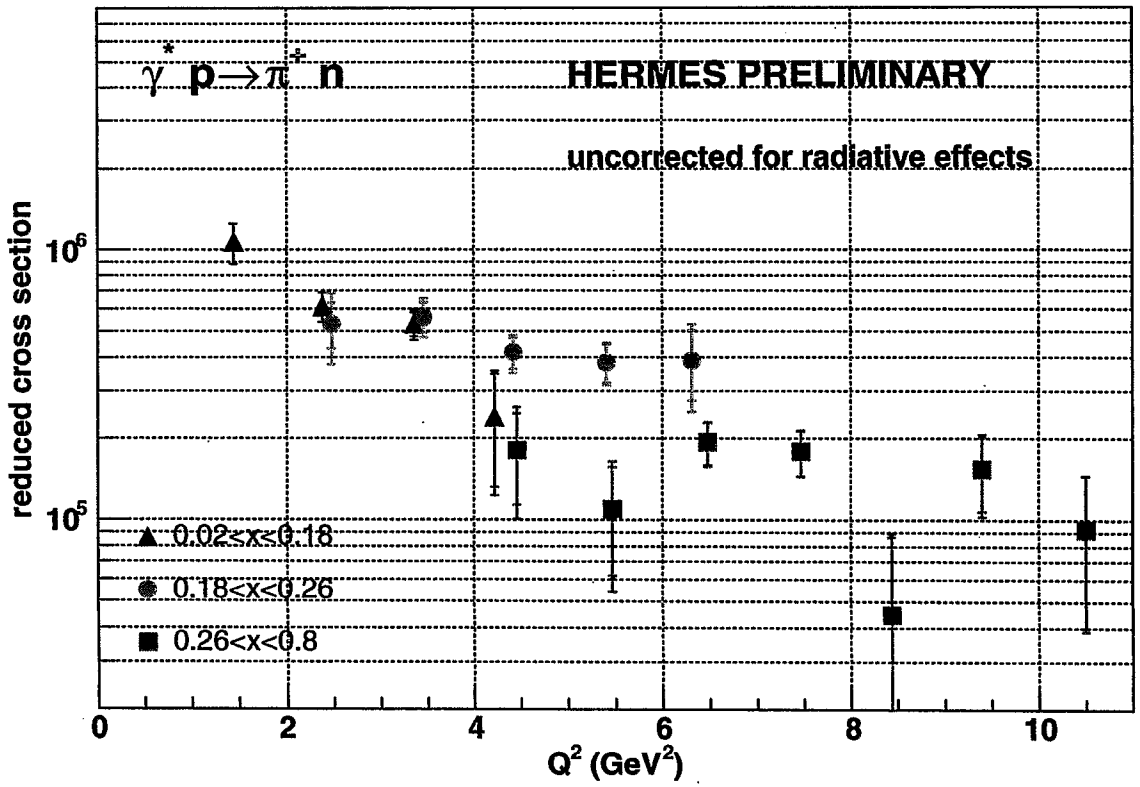

$$\sigma_L = \text{kine factor} * \sum_{\text{spins}} |M|^2$$

$\frac{1}{Q^4}$ $\frac{1}{Q^2}$

<u>fit: $1/Q^p$</u>

p=1.9±0.5

p=1.7±0.6

p=1.5±1.0

→ Q^2 dependence in agreement with theoretical expectation

deeply virtual Compton scattering

$$e\,p \rightarrow e'\,p'\,\gamma$$

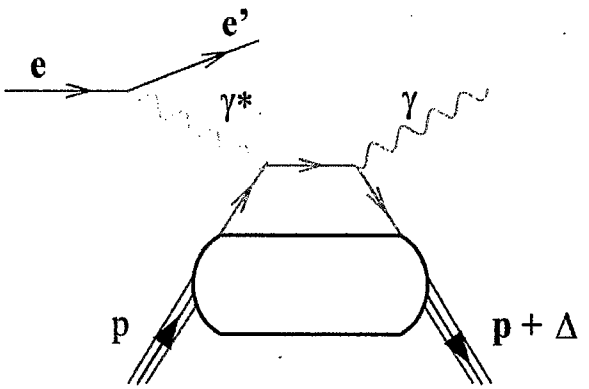

Bethe-Heitler

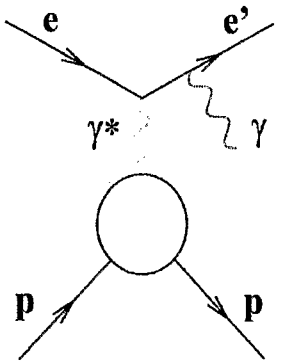

@HERMES kinematics:
DVCS << Bethe-Heitler

$$d\sigma \propto |\tau_{BH}|^2 + |\tau_{DVCS}|^2 + (\tau^*_{BH}\tau_{DVCS} + \tau^*_{DVCS}\tau_{BH})$$

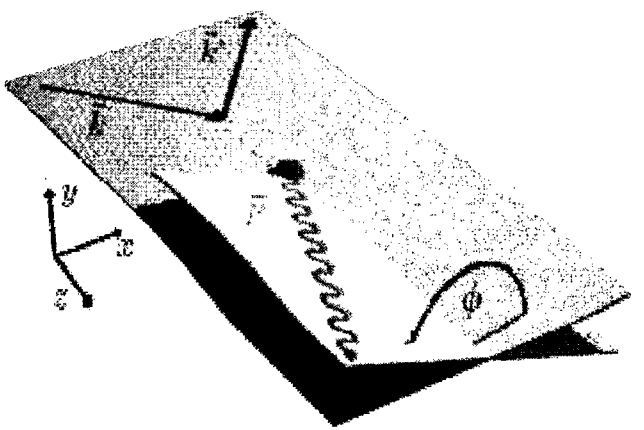

DVCS-BH interference leads to non-zero azimuthal asymmetry

$$A_{C,LU}(\varphi) = \frac{N^+(\phi) - N^-(\phi)}{N^+(\phi) + N^-(\phi)}$$

exclusivity for ep → e'p'γ

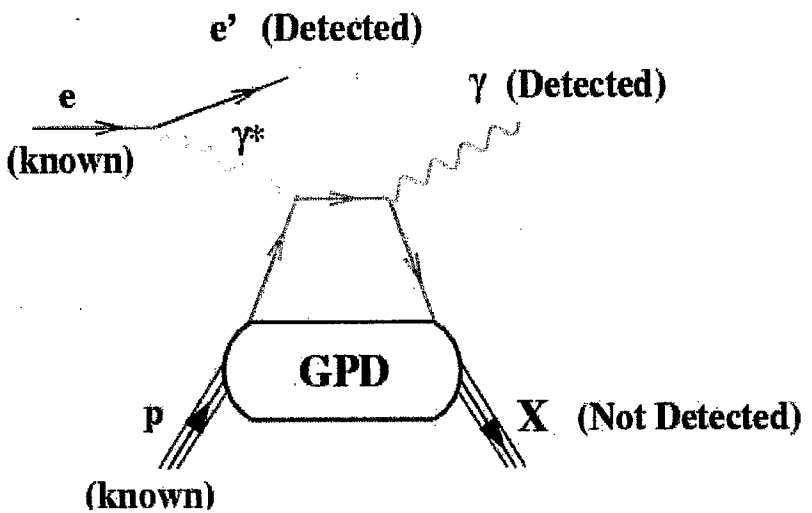

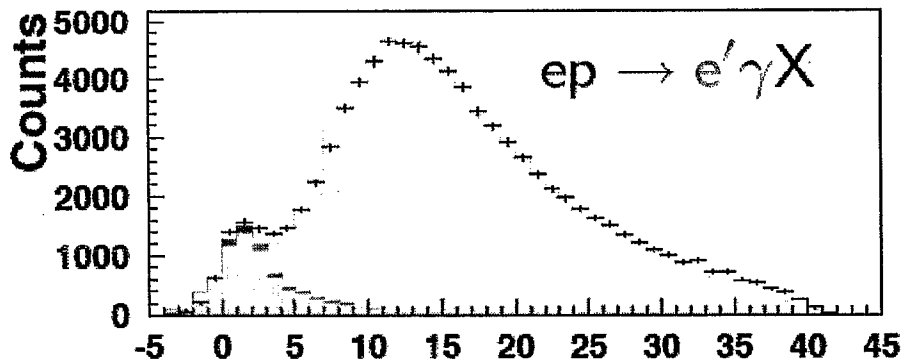

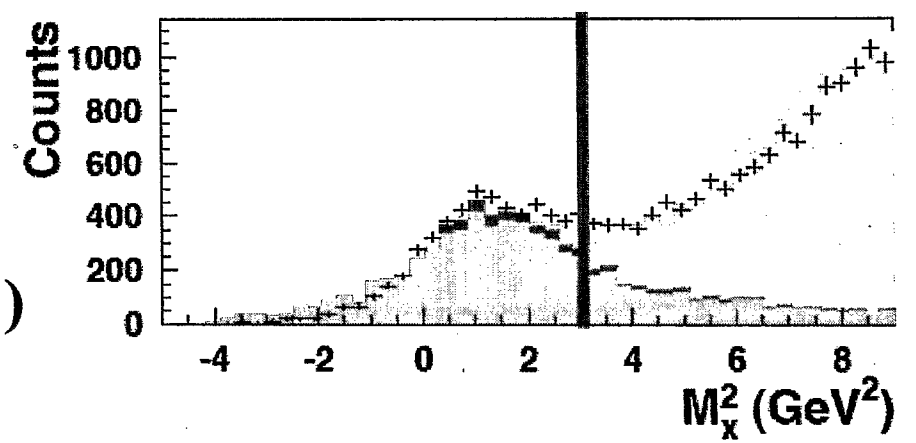

→ no recoil detection:
exclusivity via $M_X = (p + \gamma^* - \gamma)$

→ good agreement between data and MC (*absolute* normalisation)

→ exclusive region: $M_X^2 < 3$ GeV^2

DVCS asymmetries

Beam Spin Asymmetry

$$\vec{e}\,p \rightarrow e'p'\gamma$$

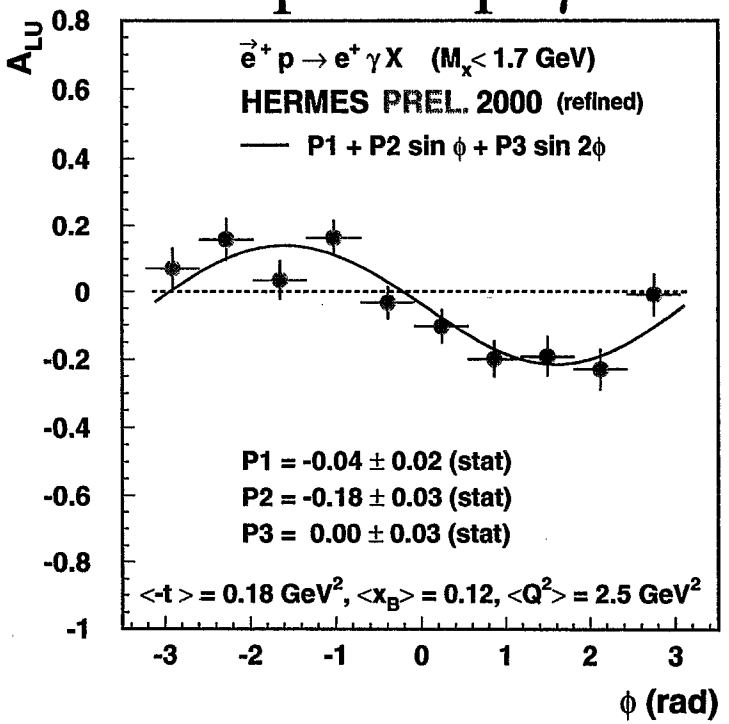

$$\mathrm{BSA} \sim \mathrm{Im}(\tau_{BH}\tau_{DVCS})$$

Beam Charge Asymmetry

$$e^{+/-}\,p \rightarrow e'p'\gamma$$

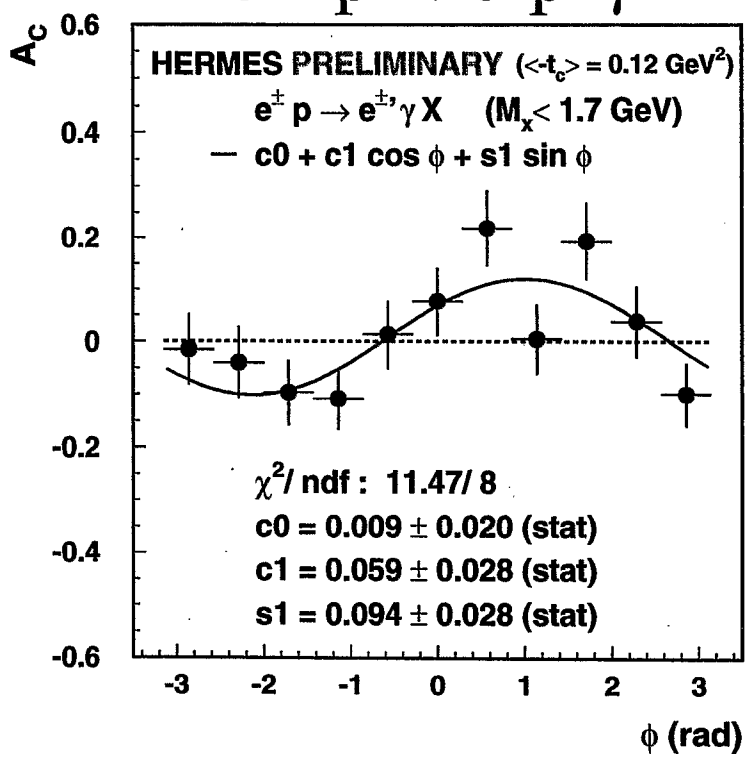

$$\mathrm{BCA} \sim \mathrm{Re}(\tau_{BH}\tau_{DVCS})$$

latest news: BCA vs *t*

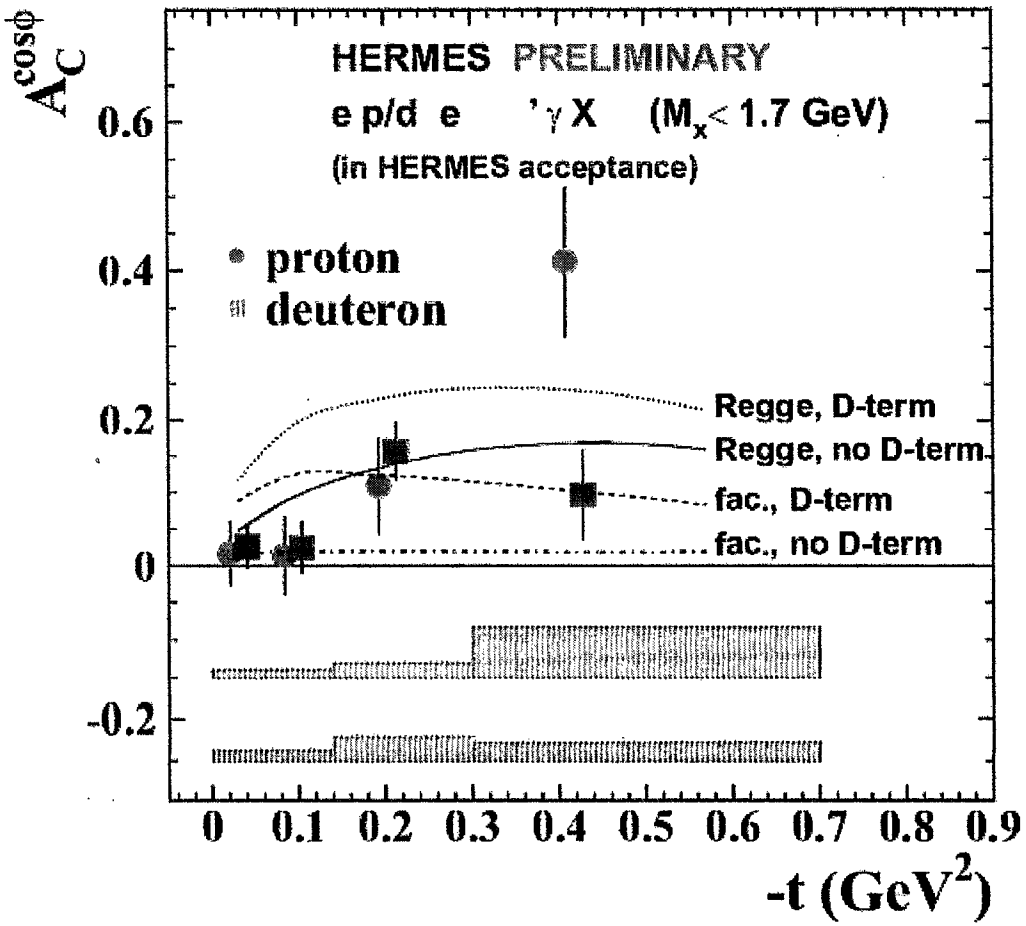

GPD calculations:

- Vanderhaeghen (1999/02) –

different parametrisations for H

→ t-dependence of BCA: high sensitivity to model assumptions

tiny e^-p sample ($L \sim 10 pb^{-1}$)

...BUT...

HERA: >2005 e^-

improvement of exclusivity

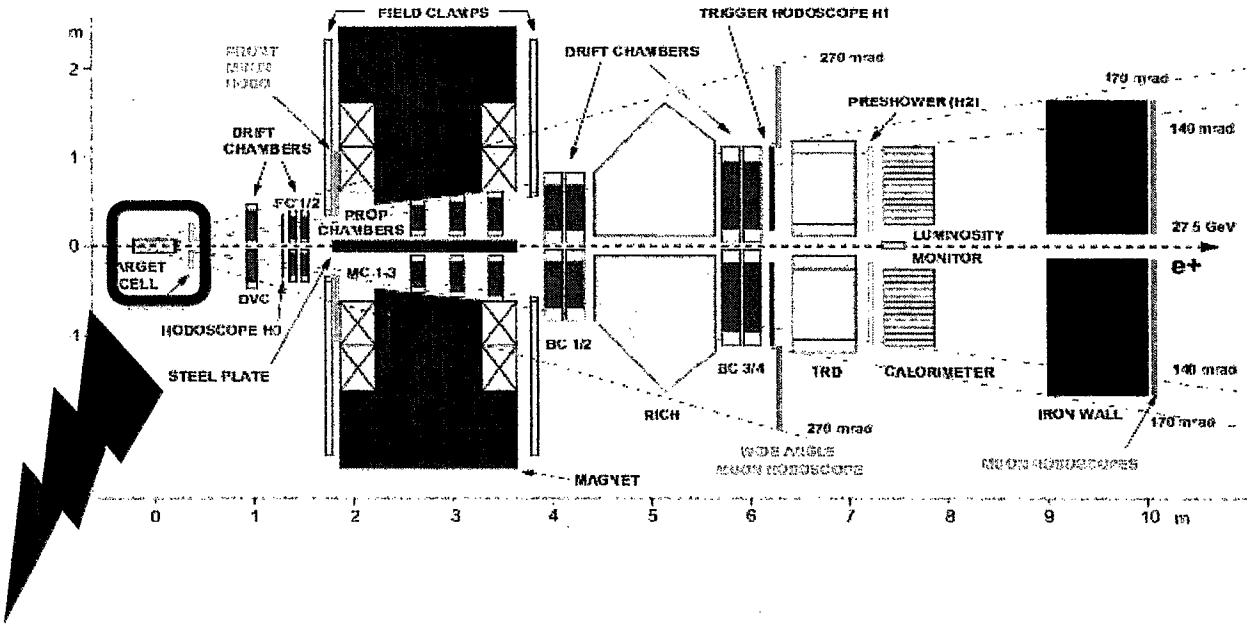

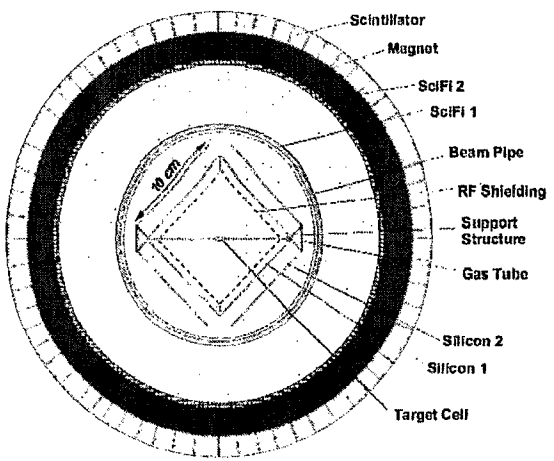

> mid 2005:

→full reconstruction of exclusive events with recoiling *proton*

- **DVCS**: HERA switches to e^- !

exclusive meson production: A_{UT}

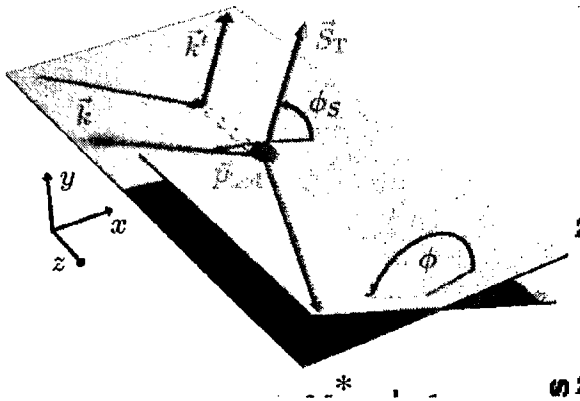

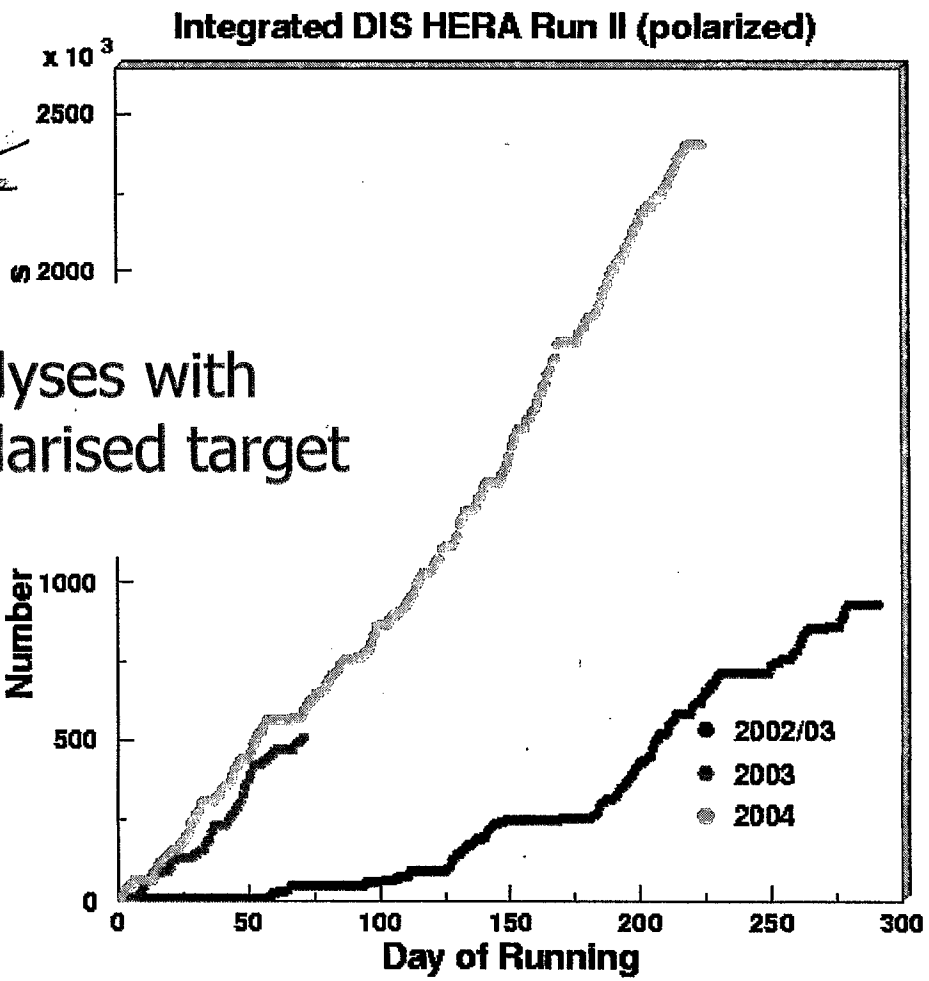

→ ongoing analyses with transversely polarised target

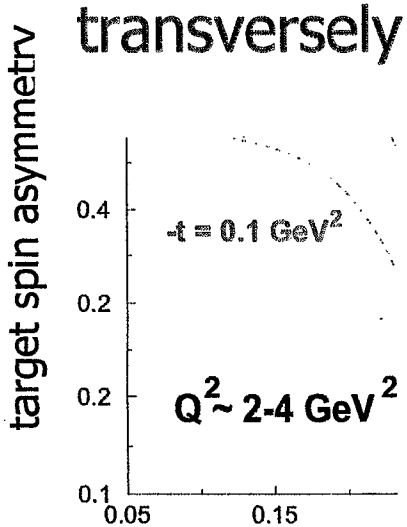

conclusion

- longitudinally polarised protons and deuterons:
  - final data set on g_1 and Δq
  - final data set on A_{UL}

→high P_T pair and single hadron analysis going on → ΔG
tuned Pythia-6

- transversely polarised protons:
  - A_{UT} analysis going on
  - A_{LT} just started

HERMES >mid 2005: exclusive processes

LEPTO & Polarized SIDIS

Aram Kotzinian

Torino University & INFN

On leave of absence from YerPhI, Armenia and JINR, Russia

- (polarized) SIDIS
  - Independent fragmentation
    - ***Purity*** method for polarized quark DF extraction
  - LEPTO
    - ***New*** "Lund Hadronization Functions" (LHF)
- Discussion & Conclusions

SIDIS

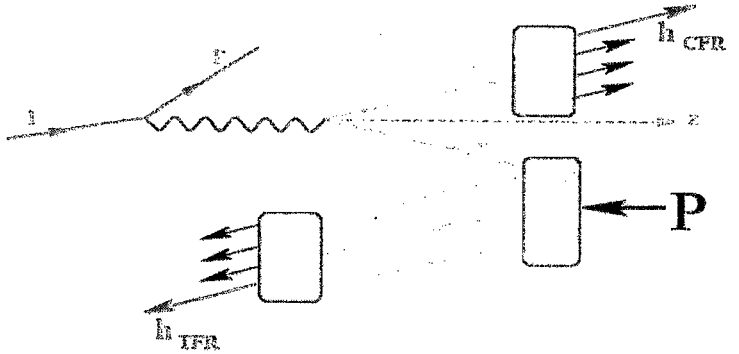

$x_F > 0$ – current fragmentation (CFR)

$x_F < 0$ – target fragmentation (TFR)

Commonly used framework: for hadrons with z>0.2 ⟹ the parton model with independent quark fragmentation

Virtual boson – nucleon CMS:

$$\sigma^h(x,Q^2,z) \propto (1+(1-y)^2)\sum_q e_q^2\, q(x,Q^2)\, D_q^h(z,Q^2)$$

$$\Delta\sigma^h(x,Q^2,z) \propto (1-(1-y)^2)\sum_q e_q^2\, \Delta q(x,Q^2)\, D_q^h(z,Q^2)$$

$$A_1^h(x,Q^2,z) = \frac{\sum_q e_q^2\, \Delta q(x,Q^2)\, D_q^h(z,Q^2)}{\sum_q e_q^2\, q(x,Q^2)\, D_q^h(z,Q^2)}$$

Purities:

$$A_1^h(x,Q^2,z) = \sum_q P_q^h(x,Q^2,z)\,\frac{\Delta q(x,Q^2)}{q(x,Q^2)} \qquad P_q^h(x,Q^2,z) = \frac{e_q^2\, q(x,Q^2)\, D_q^h(z,Q^2)}{\sum_q e_q^2\, q(x,Q^2)\, D_q^h(z,Q^2)}$$

LO SIDIS in LEPTO

- Before

- After Target remnant quark

-Example: valence struck quark

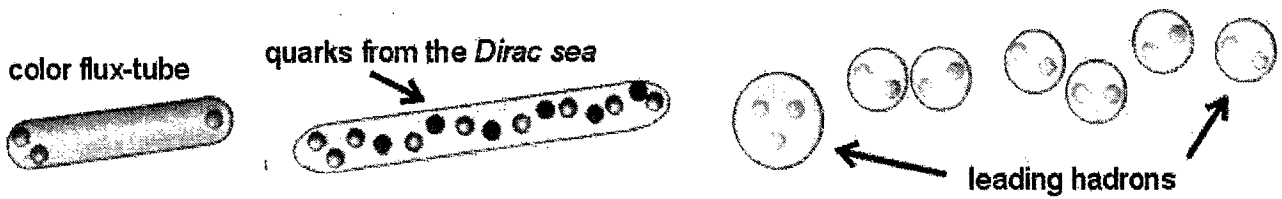

Natural question: does Lund hadronization exactly correspond to independent quark fragmentation in the CFR with z>0.2?

The important property of FF's is universality: independence of energy and of process type

1. Independence of Bjorken variable x
2. Target type independence

Bjorken variable dependence of "FFs" in LEPTO

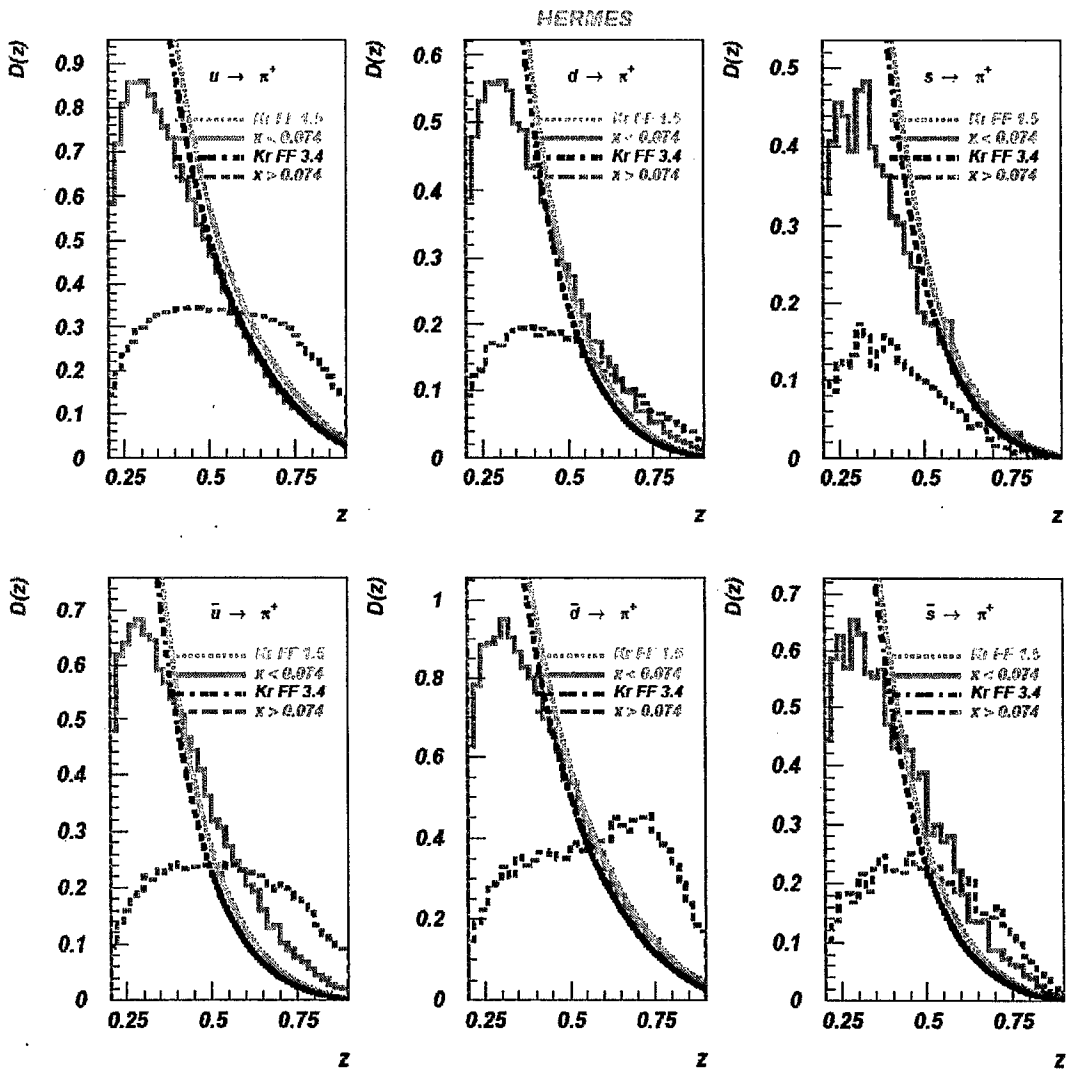

Target type dependence of "FFs" in LEPTO

p-*u*=*(ud)*

n-*u*=*(dd)*

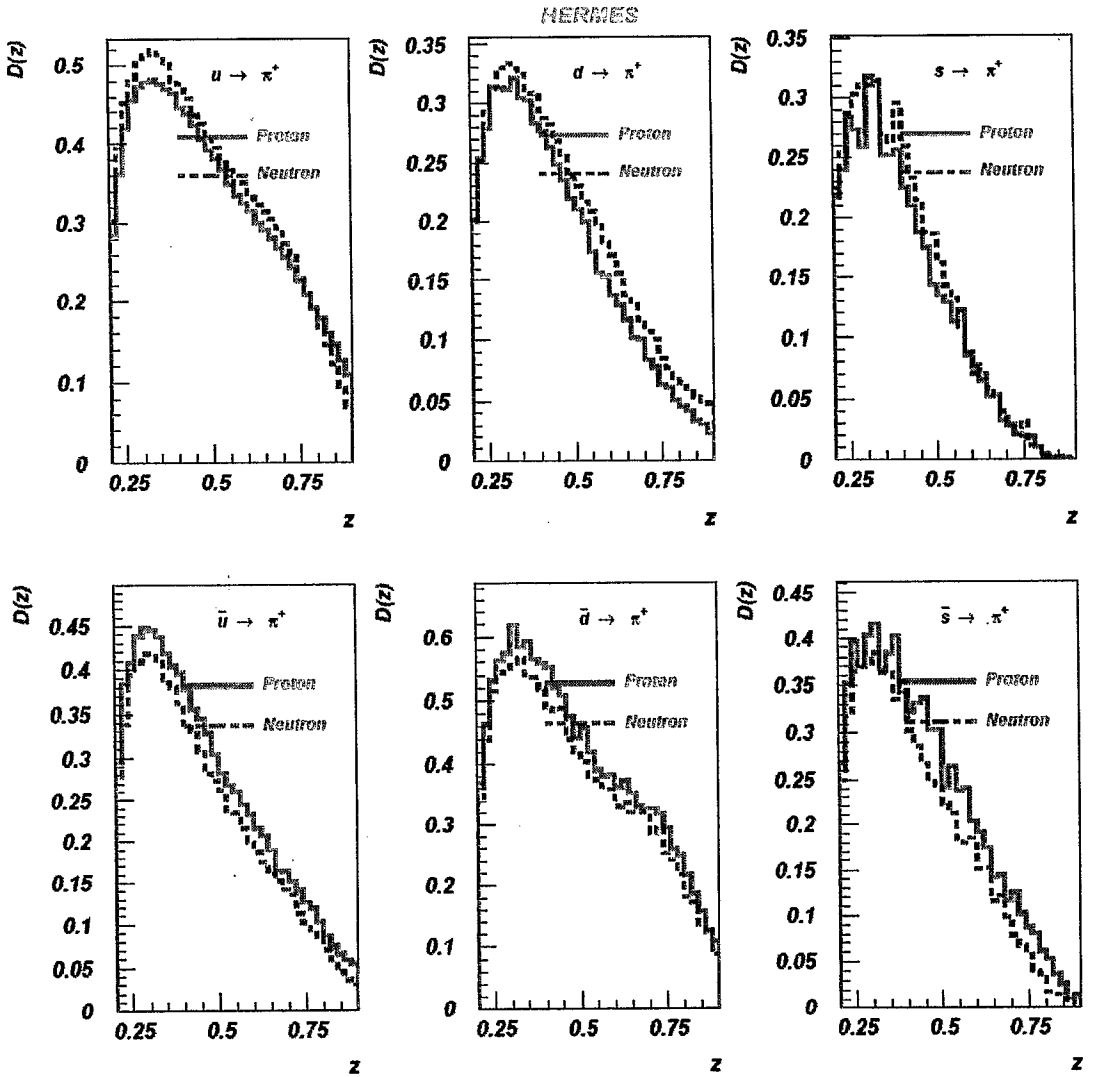

LUND string fragmentation

The primary hadrons produced in string fragmentation come from the string as a whole, rather than from an individual parton.

PYTHIA 6.2

Physics and Manual

Torbjörn Sjöstrand,[1] Leif Lönnblad,[1]
Stephen Mrenna,[2] Peter Skands[1]

[1]Department of Theoretical Physics,
Lund University, Sölvegatan 14A,
S-223 62 LUND, SWEDEN

LUND Hadronization Functions (LHF)

Even for meson production in the CFR LEPTO does not correspond to SIDIS description within FF's $D_q^h(z, Q^2)$ framework

We are dealing with LUND hadronization functions: $H_{q/N}^h(x, z, Q^2)$

$$\sigma_N^h(x, z, Q^2) \propto (1 + (1-y)^2) \sum_q e_q^2 \, q(x, Q^2) \, H_{q/N}^h(x, z, Q^2)$$

More general framework -- Fracture Functions:

$$M_{q/N}^h(x, x_F, Q^2)$$

LEPTO is a model for Fracture Functions:

$$M_{q/N}^h(x, x_F, Q^2) = q(x, Q^2) H_{q/N}^h(x, x_F, Q^2)$$

Violation of naïve *x-z* factorization and isotope invariance

The dependence on target flavor is due to dependence on target remnant flavor quantum numbers. What about spin quantum numbers?

Dependence on target remnant spin state (unpolarized LEPTO)

Example: valence u-quark is removed from proton. Default LEPTO: the remnant (***ud***) diquark is in 75% (25%) of cases scalar (vector)

$\{(ud)_0 \cdots u\}, \quad w = 1,$

$\{(ud)_1 \cdots u\}, \quad w = 1.$

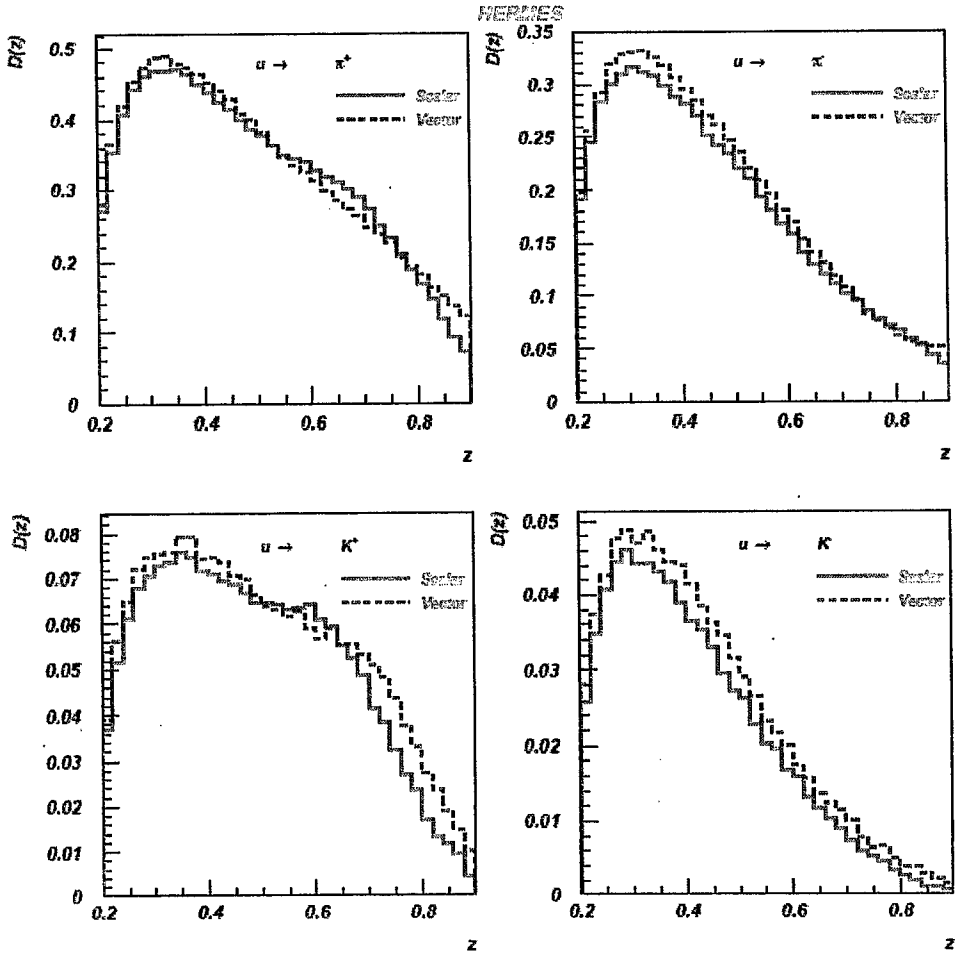

Even in unpolarized LEPTO there is a dependence on target remnant spin state

Target remnant in Polarized SIDIS

JETSET is based on SU(6) quark-diquark model

$$p^+ = \frac{1}{\sqrt{18}}\{u^+[3(ud)_{0,0} + (ud)_{1,0}] - \sqrt{2}u^-(ud)_{1,1} - \sqrt{2}d^+(uu)_{1,0} + 2d^-(uu)_{1,1}\}$$

$$n^+ = \frac{1}{\sqrt{18}}\{d^+[3(ud)_{0,0} + (ud)_{1,0}] - \sqrt{2}d^-(ud)_{1,1} - \sqrt{2}u^+(dd)_{1,0} + 2u^-(dd)_{1,1}\}$$

$$p^+ \ominus u^+ \Longrightarrow \begin{cases} \{(ud)_{0,0} \cdot \cdot \cdot \cdot \cdot u^+\}, & w = 0.9 \\ \{(ud)_{1,0} \cdot \cdot \cdot \cdot \cdot u^+\}, & w = 0.1 \end{cases}$$

$$p^- \ominus u^+ \Longrightarrow \{(ud)_{1,-1} \cdot \cdot \cdot \cdot \cdot u^+\}, \qquad w = 1$$

$$n^+ \ominus u^+ \Longrightarrow \{(dd)_{1,0} \cdot \cdot \cdot \cdot \cdot u^+\}, \qquad w = 1$$

$$n^- \ominus u^+ \Longrightarrow \{(dd)_{1,-1} \cdot \cdot \cdot \cdot \cdot u^+\}, \qquad w = 1$$

Probabilities of different target remnant spin states depend on quark and target polarizations and types!

Polarized SIDIS & LHF

$\sigma^h_{N\lambda_l\lambda_N}$ -- spin dependent cross section

$$\sigma^h_{N++} \propto \sum e_q^2 \{q^+ H^h_{q/N++} + (1-y)^2 q^- H^h_{q/N-+}\}$$

$$\sigma^h_{N+-} \propto \sum_q e_q^2 \{q^- H^h_{q/N+-} + (1-y)^2 q^+ H^h_{q/N--}\}$$

$$H^h_{q/N} = H^h_{q/N++} + H^h_{q/N+-}$$

$$\Delta H^h_{q/N} = H^h_{q/N++} - H^h_{q/N+-}$$

$$\sigma^h_{N\lambda_l\lambda_N} \propto [1+(1-y)^2] \sum_q e_q^2 \{q H^h_{q/N} + \Delta q \Delta H^h_{q/N}\} +$$

$$\lambda_l \lambda_N [1-(1-y)^2] \sum_q e_q^2 \{\Delta q H^h_{q/N} + q \Delta H^h_{q/N}\}.$$

Sum rule:

$$\int dx_F H^h_{q/N} = \langle n^h \rangle$$

$$\int dx_F \Delta H^h_{q/N} = 0$$

$$A_1^h(x, Q^2, z) = \frac{\sum_q e_q^2 [\Delta q(x, Q^2) H^h_{q/N}(x, z, Q^2) + q(x, Q^2) \Delta H^h_{q/N}(x, z, Q^2)]}{\sum_q e_q^2 [q(x, Q^2) H^h_{q/N}(x, z, Q^2) + \Delta q(x, Q^2) \Delta H^h_{q/N}(x, z, Q^2)]}$$

These Eqs. coincide with those proposed by Gluk&Reya (polarized FF's)

LHFs in addition to z depend on ***x and target type:***

non-universality

Energy Dependence

The standard expression for SIDIS asymmetry is obtained when

$$H^h_{q/N}(x,z,Q^2) \to D^h_q(z,Q^2)$$

$$\Delta H^h_{q/N}(x,z,Q^2) \to 0.$$

For validity of purity method most important is the second relation

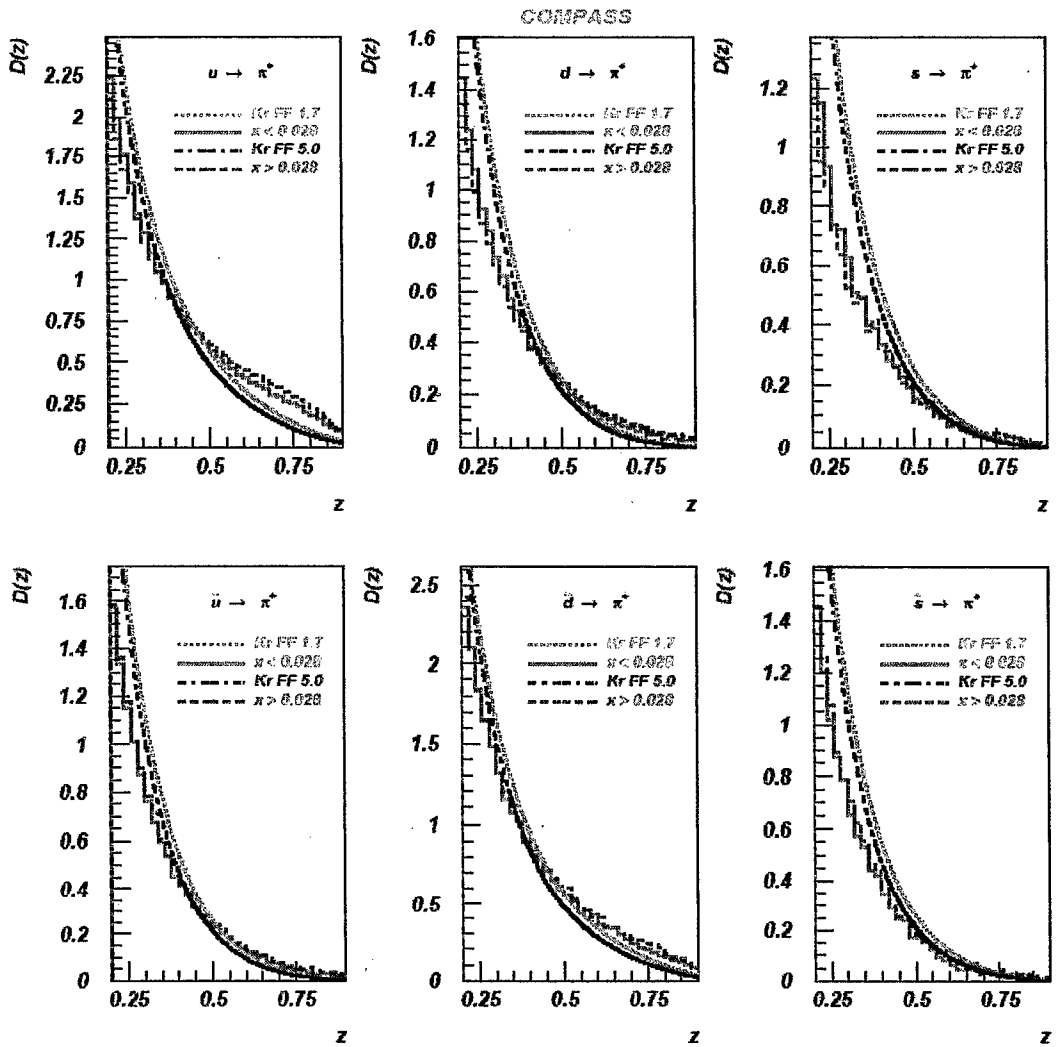

Some conclusions

- "FFs" calculated in LEPTO do not exactly correspond to simple LO ***x-z factorized*** picture for SIDIS.
  - Situation seems better for higher (COMPASS) energies:
    - the dependencies of "FFs" on ***x, target type and target remnant quantum numbers*** are weaker
- There is no reason to believe that polarized LHFs =0 at moderate energies
  - Purity method of HERMES is based on misleading identification of physics included in LEPTO MC code with naive parton model picture of SIDIS.
    - The results on polarized DFs obtained with this method can not be considered precise.
  - Validity of the MC based approach for ΔG extraction may also be questionable at moderate energies.
- More studies on the accuracy of different methods of the polarized quark DF extraction using SIDIS asymmetries are needed.
- Alternative measurements are highly desirable
  - W production in polarized $p+p$ collisions
  - ***(Anti)neutrino*** DIS on ***polarized targets*** (neutrino factory)

Spin Asymmetries for High-p_T Pions and Jets

Marco Stratmann
University of Regensburg

- *brief tour: QCD framework*
- *results: pions and jets at mid and forward rapidities*
- *outlook: calculations in the pipeline*

Cross sections relevant for RHIC spin

main goal of RHIC spin program with longitudinal polarization:

pin down all aspects of helicity pdfs, in particular the poorly known Δg

$\longrightarrow$ study processes with a *dominant* gluon contribution in LO:

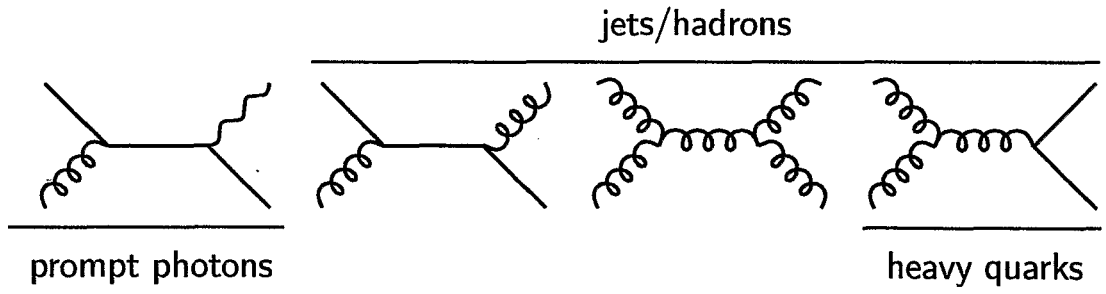

reaction	LO subprocesses	partons probed	x-range ($\eta = 0$)
$pp \longrightarrow$ jets X	$q\bar{q}, qq, qg, gg \longrightarrow$ jet X	Δq, Δg	$x \gtrsim 0.03$
$pp \longrightarrow \pi X$	$q\bar{q}, qq, qg, gg \longrightarrow \pi X$	Δq, Δg	$x \gtrsim 0.03$
$pp \longrightarrow \gamma X$	$qg \longrightarrow q\gamma$, $q\bar{q} \longrightarrow g\gamma$	Δg	$x \gtrsim 0.03$
$pp \longrightarrow Q\bar{Q}X$	$gg \longrightarrow Q\bar{Q}$, $q\bar{q} \longrightarrow Q\bar{Q}$	Δg	$x \gtrsim 0.01$
$pp \longrightarrow W^{\pm}X$	$q\bar{q}' \longrightarrow W^{\pm}$	Δu, $\Delta\bar{u}$, Δd, $\Delta\bar{d}$	$x \gtrsim 0.06$

Perturbative QCD approach for hadron-hadron cross sections

starting point: • exploit universality of pdf's

• invoke *factorization* Libby, Sterman; Ellis et al.; Amati et al.; Collins et al.; . .

$\longrightarrow$ way to separate long-distance (= non-perturbative) from short-distance (= perturbative) phenomena

example: (un)polarized high-p_T single-inclusive hadron production

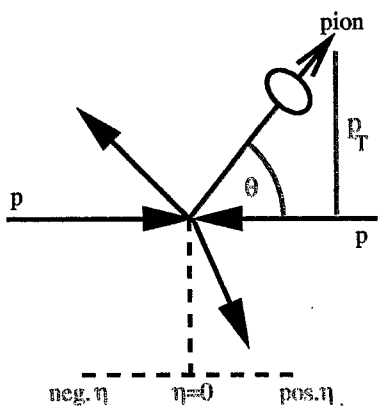

factorization
$\longrightarrow$
theorem

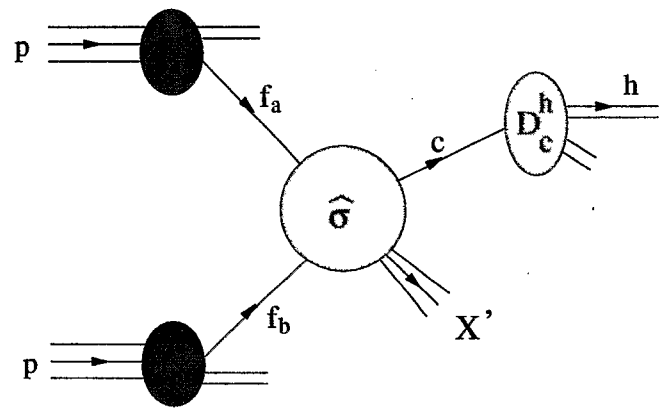

ingredients: parton densities $f_a(x_a)$, $f_b(x_b)$, fragmentation fcts. $D_c^h(z)$,

hard partonic cross section $\hat{\sigma}$

Factorized $\vec{p}\vec{p}$ cross sections

long-distance

from exp.; μ-dep.: $d\sigma/d\mu = 0$ (pQCD)

$$\frac{d\Delta\sigma^{\vec{p}\vec{p}\to\pi X}}{dp_T d\eta} = \sum_{abc}\int dx_a\, dx_b\, dz_c\, \Delta f_a(x_a,\mu_f)\, \Delta f_b(x_b,\mu_f)\, D_c^{\pi}(z_c,\mu'_f) \times \frac{d\Delta\hat{\sigma}^{ab\to cX'}}{dp_T d\eta}(x_aP_a, x_bP_b, P^{\pi}/z_c, \mu_f, \mu'_f, \mu_r) + \mathcal{O}(\frac{\lambda}{p_T})^n$$

short-distance

calculable in pQCD: power series in α_s

power corrections

neglected

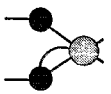

- separation of long- ($\Delta f_{a,b}$, D_c^h) and short-distance ($d\Delta\hat{\sigma}$) physics not unique
  - controlled by arbitrary *factorization scales* μ_f and $\mu'_f \simeq \mathcal{O}(p_T)$

    [amount of "parton radiation" 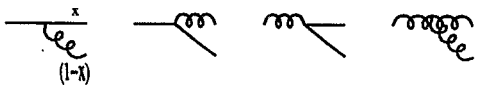 included in $\Delta f_{a,b}$, D_c^h]
  - another arbitrary scale controls the running of α_s: *renormalization scale* μ_r

Factorized $\vec{p}\vec{p}$ cross sections (cont.)

measured cross section *must not* depend on theoretical scales: $\mu_f \frac{d\Delta\sigma}{d\mu_f} = 0$

$\leftrightarrow d\Delta\hat{\sigma}(\mu_f \to \mu_f + d\mu_f, \mu'_f)$ canceled by scale behavior of $\Delta f_{a,b}(x_{a,b}, \mu_f)$

catch: . . . we work with a perturbative expansion in α_s:

$$d\Delta\hat{\sigma} = \overset{\text{LO}}{d\Delta\hat{\sigma}^{(0)}} + \overset{\text{NLO}}{\alpha_s\, d\Delta\hat{\sigma}^{(1)}} + \overset{\text{NNLO}}{\alpha_s^2\, d\Delta\hat{\sigma}^{(2)}} + \ldots$$

μ_f cancellation only happens to all orders

LO	:	no cancellation whatsoever
NLO	:	cancellation starts to work
NNLO	:	better and better
. . .		

$\longrightarrow$ higher order calculations mandatory

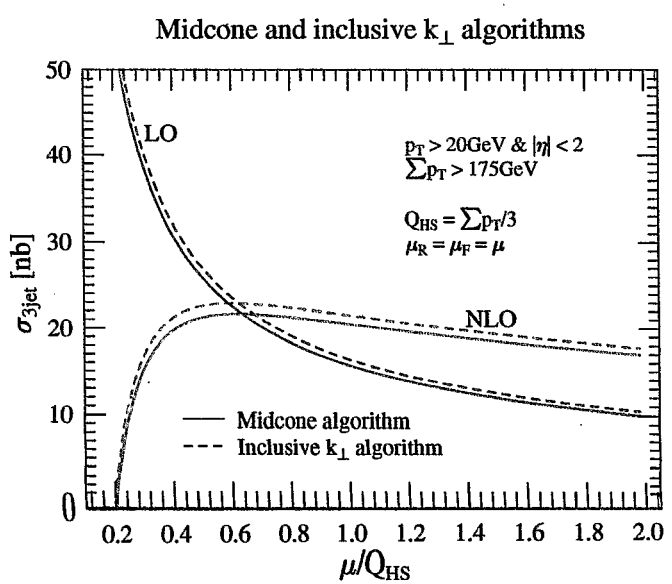

typical example: 3-jets @ TeVatron (Z. Nagy)

NLO corrections in a nutshell

going beyond the LO is in every respect a major enterprise . . .

$$d\Delta\hat{\sigma} = \overset{\text{LO}}{d\Delta\hat{\sigma}^{(0)}} + \overset{\text{NLO}}{\alpha_s\, d\Delta\hat{\sigma}^{(1)}} + \overset{\text{NNLO}}{\alpha_s^2\, d\Delta\hat{\sigma}^{(2)}} + \ldots$$

number of partons → complexity of calculation

- NLO techniques are well established and most cross sections are available
- NNLO still far from being standard, a lot of progress though

recent example: the NNLO DGLAP evolution kernels P_{ij} Moch, Vermaseren, Vog

$\longrightarrow$ NNLO = pushing computer algebra programs to their limits

	# diagrams	# integrals
LO	18	a few
NLO	350	some more
NNLO	9607	$\sim 10^5$

NLO corrections in a nutshell (cont.)

at $\mathcal{O}(\alpha_s^3)$ (NLO) one has to consider:

- one-loop (virtual) corrections to all LO $2 \to 2$ 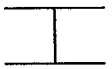 processes

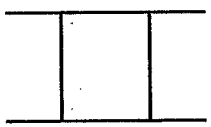

"box"

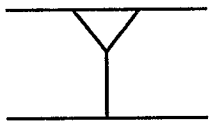

"vertex"

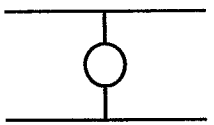

"selfenergy"

- all conceivable $2 \to 3$ parton-parton scattering processes

  this includes additional gluon emission to existing LO processes

$$qq' \to qq'g,\ q\bar{q} \to ggg,\ gg \to ggg, \text{ etc.}$$

  as well as genuine NLO processes not possible at $\mathcal{O}(\alpha_s^2)$

$$qg \to qq'\bar{q}',\ qg \to qq\bar{q}, \text{ etc.}$$

NLO corrections in a nutshell (cont.)

good news: steady progress – list of results relevant for RHIC spin:

evol. kernels	ΔP_{ij}	NLO	Mertig, van Neerven; Vogelsang
hadrons	$\vec{p}\vec{p} \to H + X$	NLO	De Florian; Jäger, Schäfer, MS, Vogelsang
	$\vec{p}\vec{p} \to H_1 + H_2 + X$	NLO	Jäger, Owens, MS, Vogelsang (very soon)
	$p\vec{p} \to \vec{H} + X$	NLO	Jäger, MS, Vogelsang (in preparation)
jets	$\vec{p}\vec{p} \to \text{jet(s)} + X$	NLO	De Florian et al.; Jäger, MS, Vogelsang
prompt γ	$\vec{p}\vec{p} \to \gamma + X$	NLO	Gordon, Vogelsang; Contogouris et al.
	$\vec{p}\vec{p} \to \gamma\gamma + X$	NLO	Coriano, Gordon
	$p\vec{p} \to \vec{\gamma} + X$	NLO	Vogelsang
γ **+ jet**	$\vec{p}\vec{p} \to \gamma + \text{jet} + X$	NLO	Gordon
γ **+ charm**	$\vec{p}\vec{p} \to \gamma + c + X$	NLO	Berger et al. ($m_c = 0$)
heavy quarks	$\vec{p}\vec{p} \to Q\bar{Q}X$	NLO	Bojak, MS
Drell-Yan	$\vec{p}\vec{p} \to (\gamma^*)X$	NLO	Weber; Gehrmann;
		NNLO	Smith et al.
vector bosons	$\vec{p}\vec{p} \to (Z^0, W^\pm)X$	NLO	Weber; Gehrmann
	$p\vec{p} \to (Z^0, W^\pm)X$	NLO	Weber; Gehrmann

High-p_T Hadron Production at RHIC

high-p_T pions:

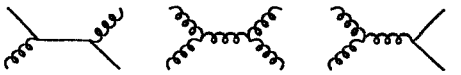

NLO: Jäger, MS, Vogelsang; de Floria

recall: 1st *unpolarized* measurements at RHIC agree well with pQCD

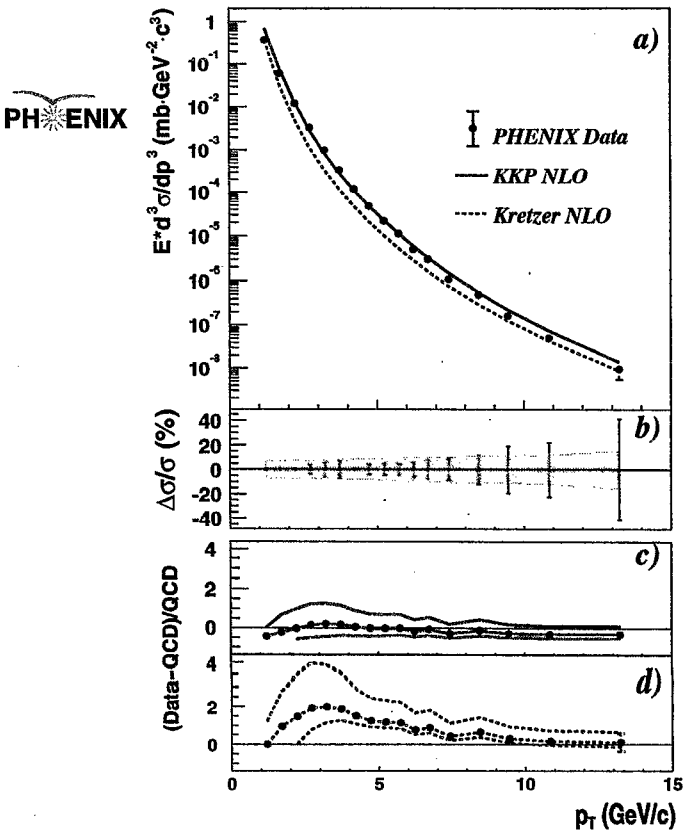

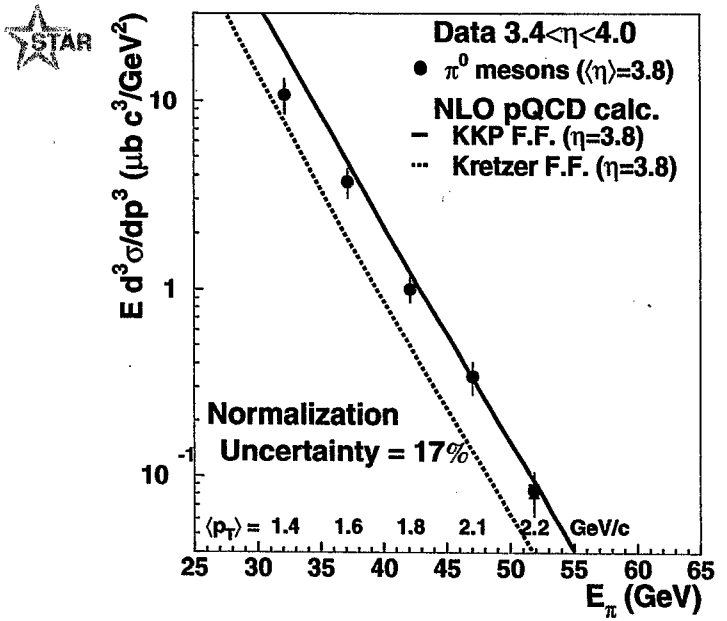

- $D^{\pi}(z)$ set of KKP favored by data

$\longrightarrow$ foundation for similar measurements with polarization

Interlude: importance of unpolarized cross sections

unpolarized measurements should always precede an A_{LL} measurement:

- demonstrate applicability of standard perturbative QCD methods
  - not a priori known where power corrections 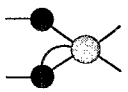 , etc. set in
- measurements at $\sqrt{S} = 200\,\mathrm{GeV}$ never done before
  - allows us to study energy dependence of cross sections at a given p_T

    (fixed target) $\longrightarrow$ RHIC $\longrightarrow$ SPS $\longrightarrow$ Tevatron $\longrightarrow$ LHC
- valuable source of information about non-perturbative functions
  - e.g. to improve our understanding of hadronization (fragmentation functions)

    $\longrightarrow$ reduces theoretical uncertainties of subsequent extractions of, e.g., Δg!

High-p_T Hadron Production at RHIC (cont.)

a closer look at pQCD results for π^0-production at $\sqrt{S} = 200\,\mathrm{GeV}$, $|\eta| \leq 0.38$:

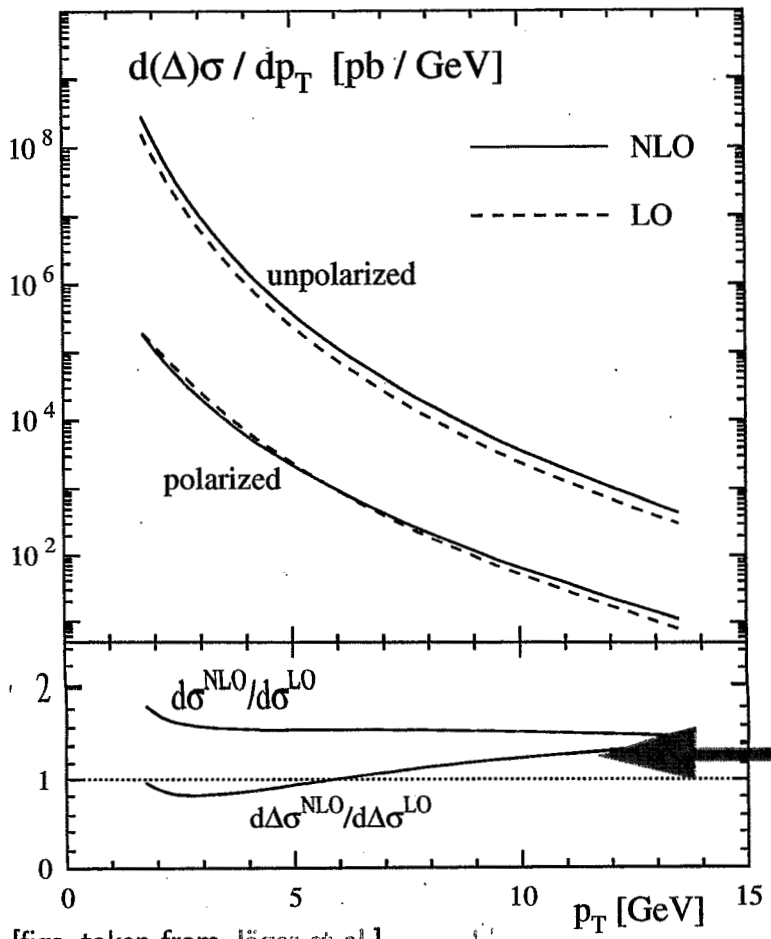

[figs. taken from Jäger et al.]

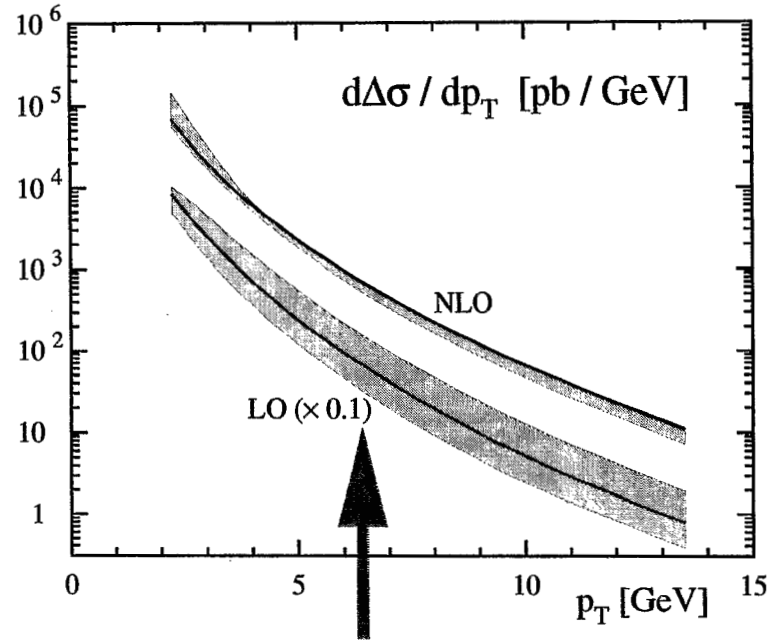

μ_f dependence much reduced in NLO

NLO corrections different for $d\Delta\sigma$ and $d\sigma$
$\rightarrow$ do not cancel in $A_{\mathrm{LL}} = d\Delta\sigma/d\sigma$

High-p_T Hadron Production at RHIC (cont.)

Is the spin asymmetry A_{LL} sensitive to unknown gluon polarization Δg ?

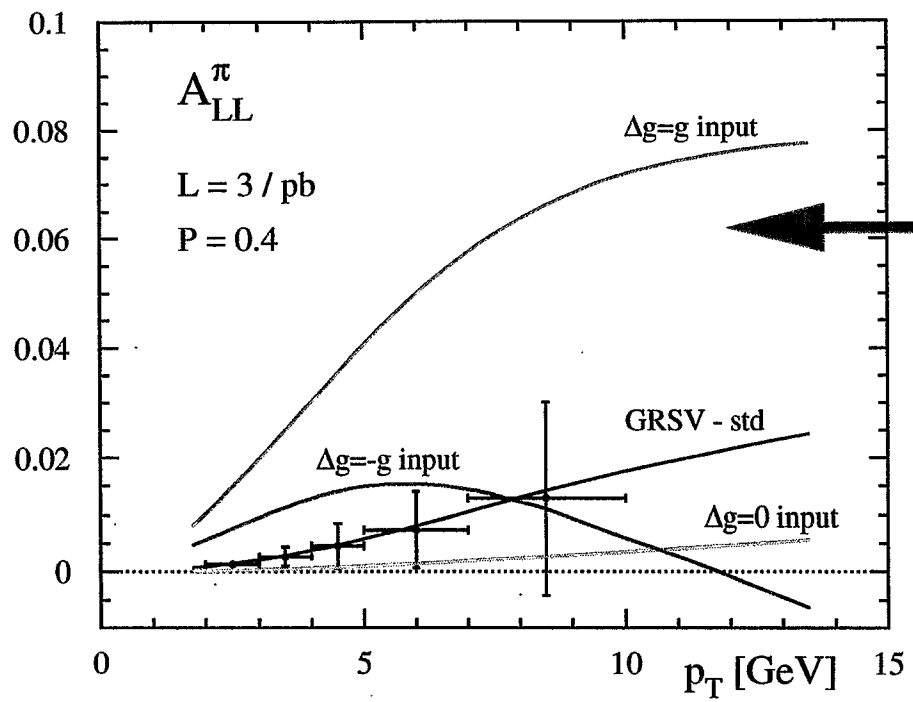

predictions for very different Δg

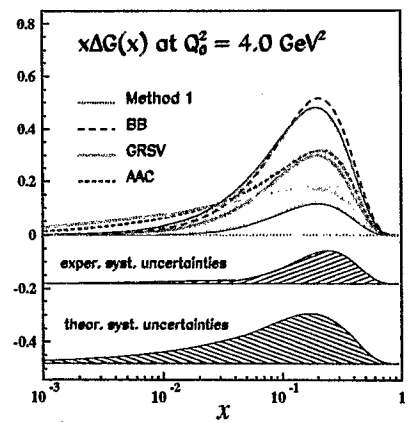

all compatible with current DIS data

estimate of statistical precision:

$$\delta A_{LL} \simeq \frac{1}{\mathcal{P}^2} \frac{1}{(\mathcal{L} d\sigma_{\rm bin})^{1/2}}$$

$\mathcal{P}$: beam polarization; $\mathcal{L}$: integrated luminosity

note:

(1) for $p_T \leq 10\,\mathrm{GeV}$: $A_{LL} > 0$

(2) $\mathcal{L} = 3\,\mathrm{pb}^{-1}$ assumed

High-p_T Hadron Production at RHIC (cont.)

discussion of first results on A_{LL}:

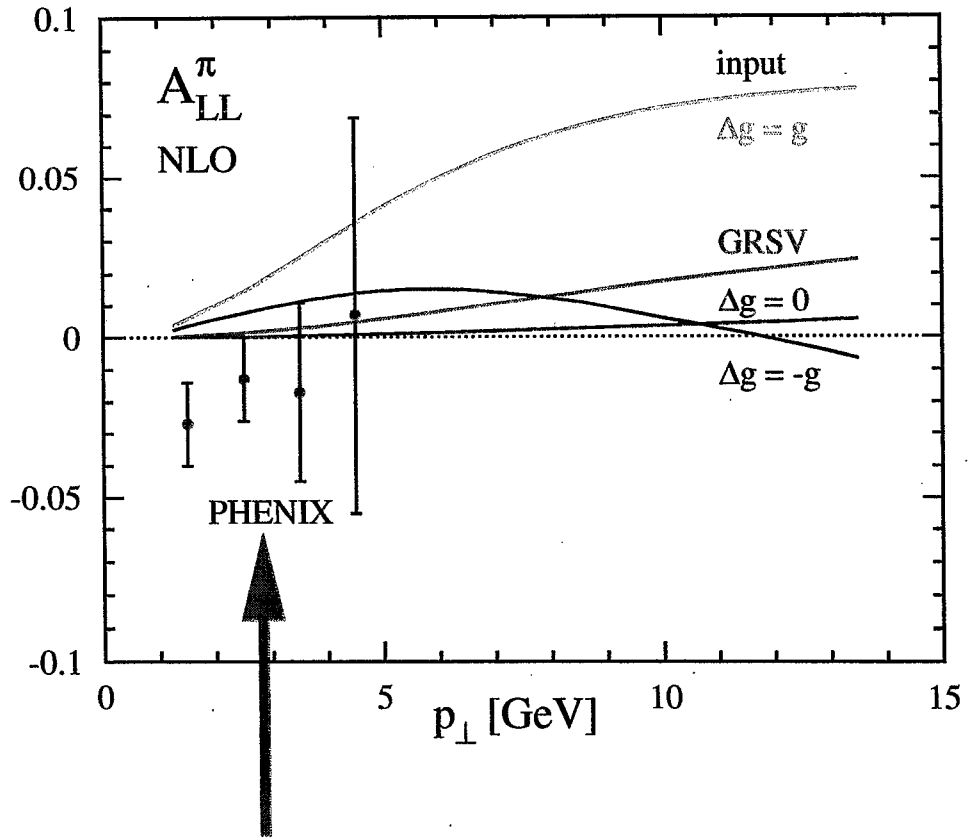

trend for $A_{LL} < 0$ at small p_T contrary to expectations

High-p_T Hadron Production at RHIC (cont.)

How can *that* be?

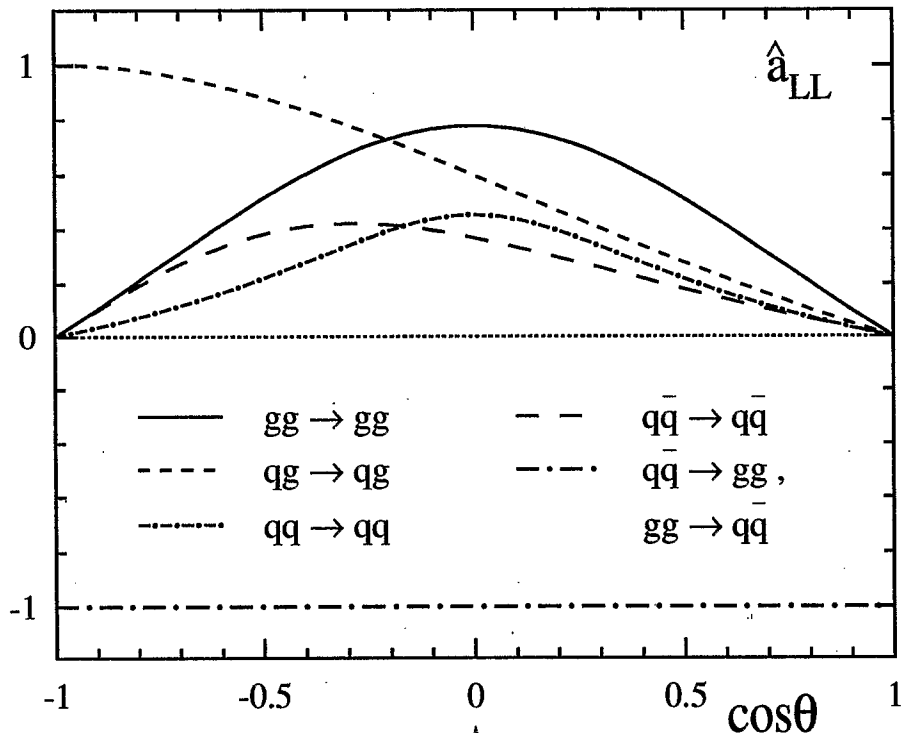

PHENIX measures at central rapidities

Naive analysis:

need process with $\hat{a}_{LL} < 0$

recall partonic asymmetries

$$gg \to gg \quad \hat{a}_{LL} > 0$$
$$gg \to q\bar{q} \quad \hat{a}_{LL} = -1$$
$$gq \to gq \quad \hat{a}_{LL} > 0$$

conclude:

$gg \to q\bar{q}$ resp. for neg. A^{π}_{LL}

NO!

$$\Delta\hat{\sigma}_{gg\to gg} \underset{(\eta \simeq 0)}{\simeq} 160\, \Delta\hat{\sigma}_{gg\to q\bar{q}}$$

High-p_T Hadron Production at RHIC (cont.)

So - can A_{LL}^{π} be negative?

Jäger, Kretzer, MS, Vogelsan

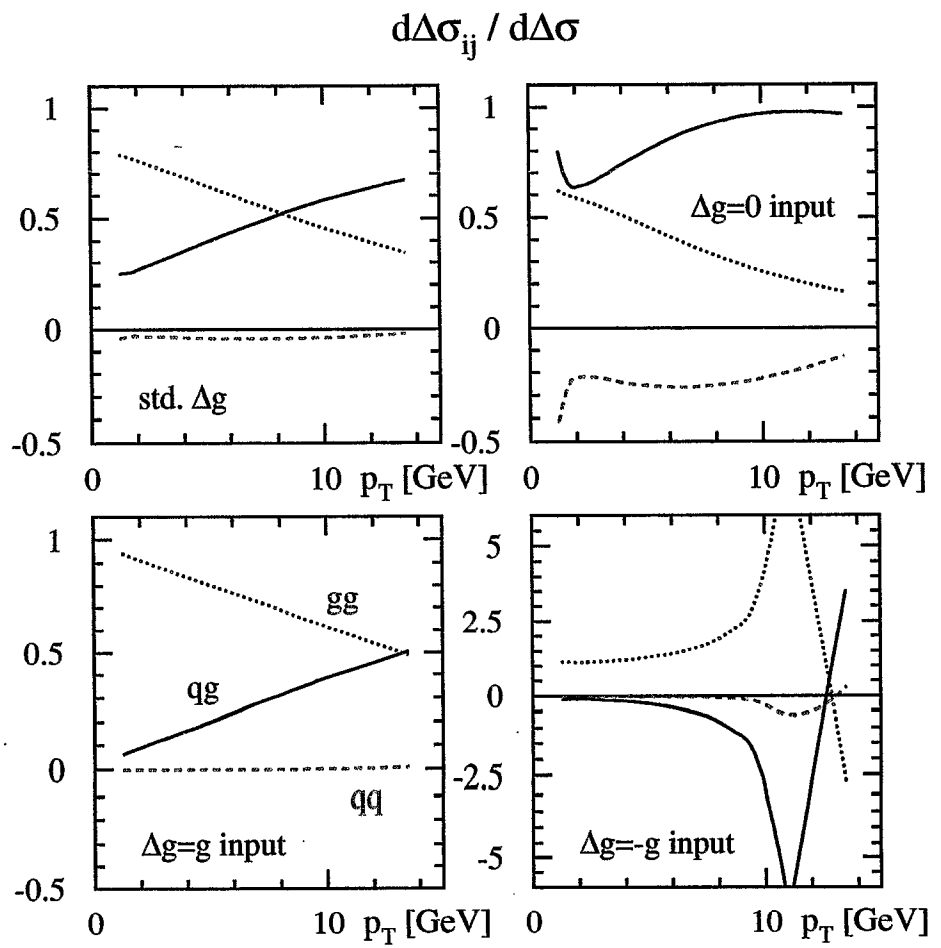

subprocess contributions:

fairly independent on what one assumes about Δg:

gg processes:
dominate for $p_T \lesssim 10\,\mathrm{GeV}$

qg processes:
take over for $p_T \gtrsim 10\,\mathrm{GeV}$

qq processes:
always small unless p_T very large

High-p_T Hadron Production at RHIC (cont.)

not yet taken into account:

both partons are not probed at the same momentum fraction x

$\longrightarrow$ even for $\hat{a}_{\rm LL} > 0$ we can have $A_{\rm LL} < 0$ *if* $\Delta f_a(x_a)\Delta f_b(x_b) < 0$

we can even *analytically* derive a lower bound on $A_{\rm LL}$:

$$\frac{d\Delta\sigma}{dp_T} = \sum_{a,b,c} \Delta f_a(x_a) \otimes \Delta f_b(x_b) \otimes \frac{d\Delta\hat{\sigma}_{ab}(x_a, x_b, z_c)}{dp_T} \otimes D_c^h(z_c)$$

take $x_T^2 \equiv 4p_T^2/S$ moments $\int dx_T^2 (x_T^2)^{N-1} \ldots \longrightarrow$ convolutions turn into products

$$\Delta\sigma^\pi(N) = \left(\Delta g^{N+1}\right)^2 \underset{gg}{\underset{\updownarrow}{\mathcal{A}^N}} + 2\Delta g^{N+1} \underset{qg}{\underset{\updownarrow}{\mathcal{B}^N}} + \underset{qq}{\underset{\updownarrow}{\mathcal{C}^N}}$$

this is a parabola in $\Delta g^N \longrightarrow$ minimize!

High-p_T Hadron Production at RHIC (cont.)

minimization yields: $\Delta\sigma^\pi(N)\Big|_{\rm min} = -\frac{(\mathcal{B}^N)^2}{\mathcal{A}^N} + \mathcal{C}^N$

$\longrightarrow$ negative, but tiny *lower bound* $A^\pi_{\rm LL}\Big|_{\rm min} \simeq \mathcal{O}(-10^{-3}) \ggg$ indications from data

as expected:

the resulting Δg has a node

i.e., $\Delta g(x_a)\Delta g(x_b) < 0$

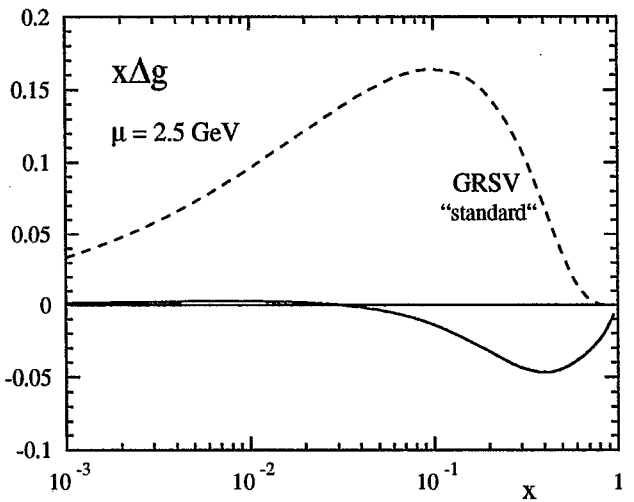

but still way too early to cry!

- "problem" only in lowest p_T bin where uncertainties are large
- p_T perhaps too small to apply pQCD [it works for $d\sigma/dp_T$ though!]

we need much more data to call this a new "spin surprise"

High-p_T Hadron Production at RHIC (cont.)

another lesson: around mid-rapidity and for $p_T \lesssim 10\,\mathrm{GeV}$ it is difficult to even pin down the sign of Δg

reason: gg dominance and $\eta \simeq 0 \leftrightarrow x_a \simeq x_b$

What about A_{LL}^{π} measurements away from $\eta \simeq 0$?

idea: $|\eta| \gg 0$: partonic system boosted

$\longrightarrow$ probes highly asymmetric x_a, x_b

expect: dominance of qg sets in earlier

$\longrightarrow$ sign/size of A_{LL}^{π} tied to sign/size of Δg

error estimates for $\mathcal{L} = 7\,\mathrm{pb}^{-1}$, $\mathcal{P} = 0.4$

[more plots on Bernd Surrow's homepage]

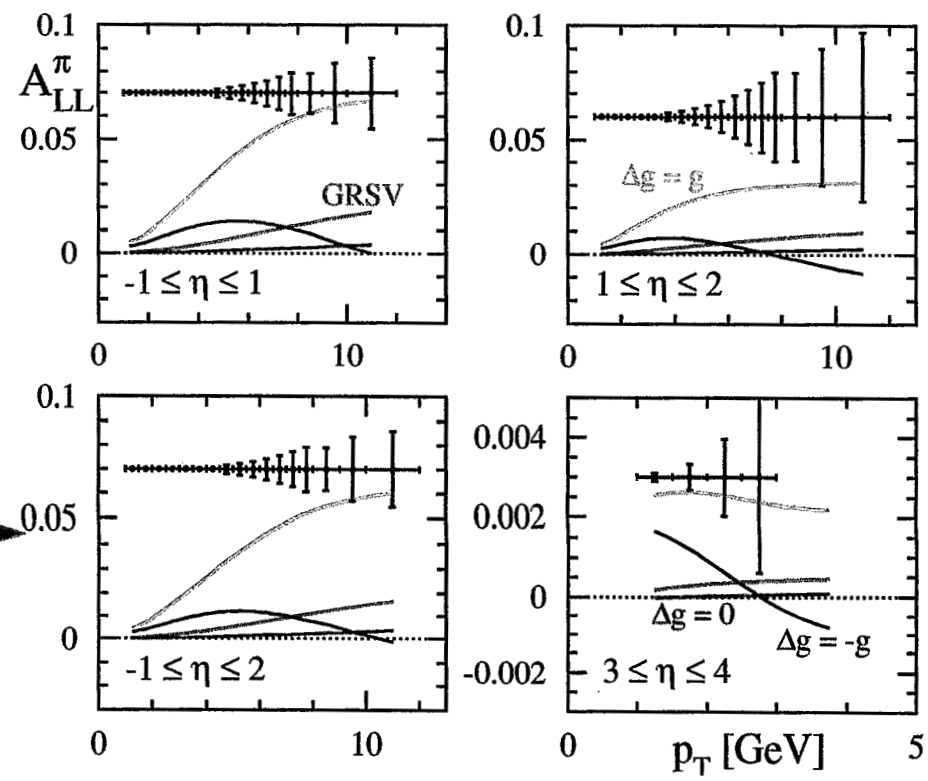

High-p_T Hadron Production at RHIC (cont.)

with more luminosity one can go to higher p_T at $\langle\eta\rangle \simeq 0$ *plus* $A_{LL}^{\pi^\pm}$ vs. $A_{LL}^{\pi^0}$

π^- 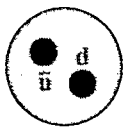

π^0

π^+ 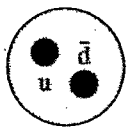

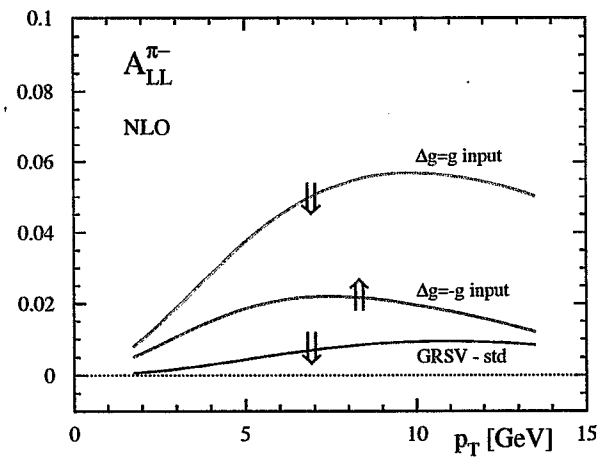

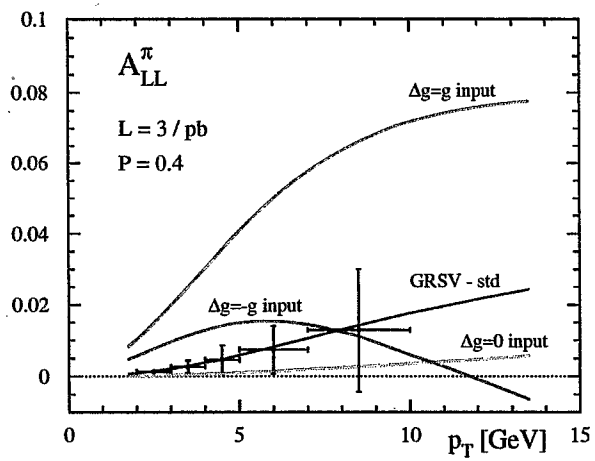

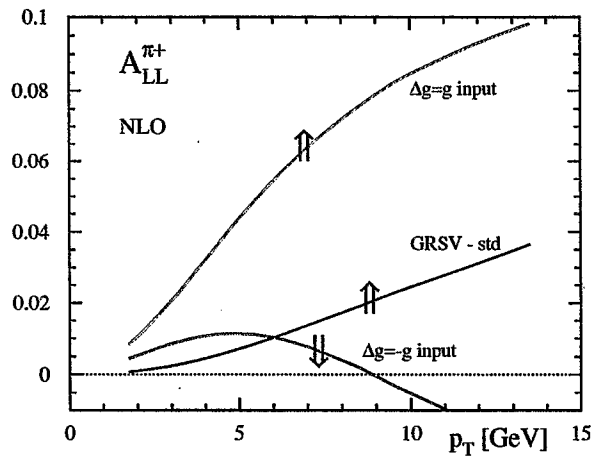

idea: qg starts to dominate for $p_T \gtrsim 5\,\mathrm{GeV}$ and $D_u^{\pi^+} > D_u^{\pi^0} > D_u^{\pi^-}$, $D_g^{\pi^+} = D_g^{\pi^-}$

expect: sensitivity to sign of Δg, e.g., positive Δg: $A_{LL}^{\pi^+} > A_{LL}^{\pi^0} > A_{LL}^{\pi^-}$

High-p_T Jet Production at RHIC

single-incl. jet production:

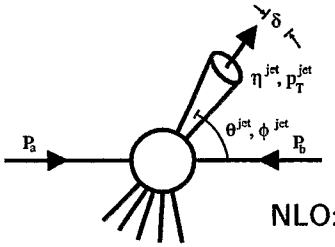

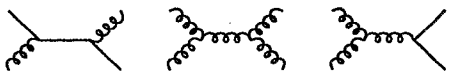

NLO: Jäger, MS, Vogelsang; de Florian, Frixione, Signer, Vogelsar

jet = bunch of particles in a small pencil-like cone; all final-state sing. cancel

jet production proceeds through the same partonic subprocesses as π-production:

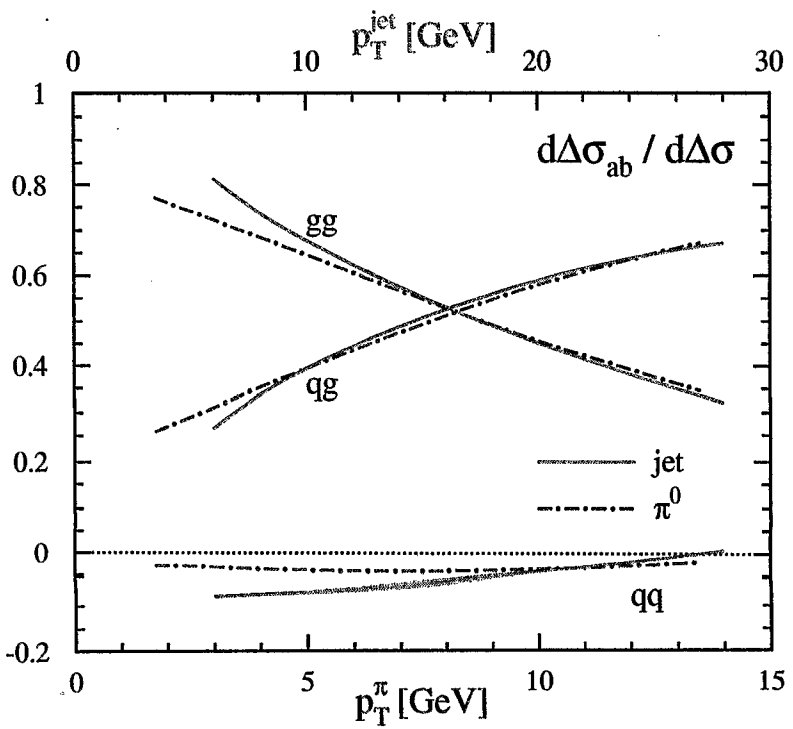

π's have roughly $\langle z \rangle \simeq 0.5$:

$\rightarrow$ π with $p_T \simeq$ jet with $2p_T$

comparison to hadrons:

✓ higher rates

✓ no uncertainties from $D(z)$

✗ dependence on precise definition of jet

High-p_T Jet Production at RHIC (cont.)

pQCD results for jet-production at $\sqrt{S} = 200\,\mathrm{GeV}$, $R_{\mathrm{cone}} = 0.4$ (SCA), $|\eta| \leq 1$:

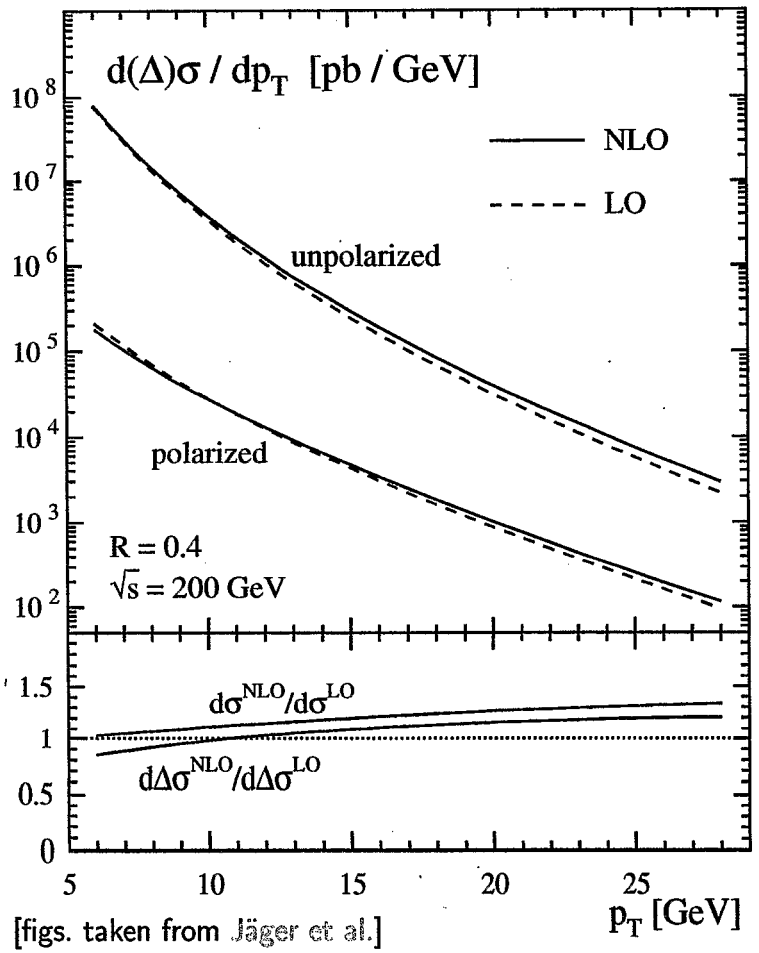

[figs. taken from Jäger et al.]

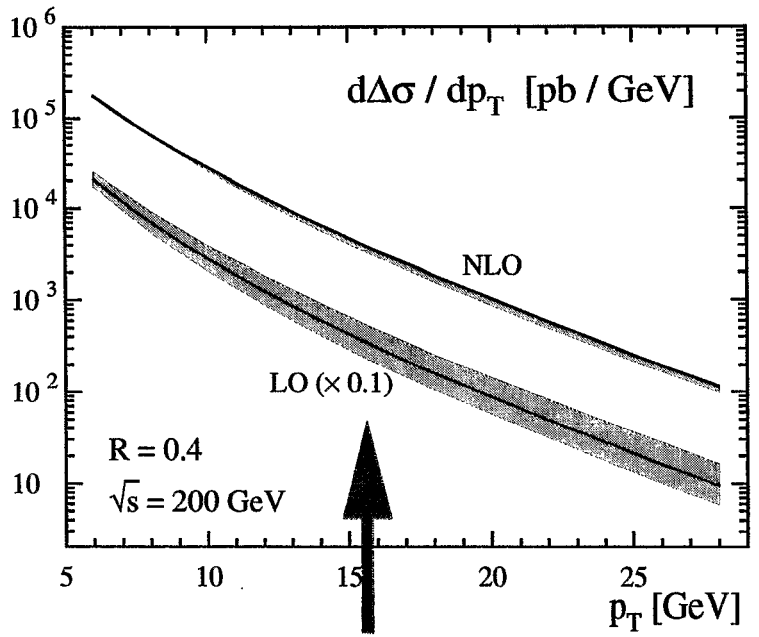

μ_f dependence much reduced in NLO

theoretical uncertainties even smaller than for hadrons

High-p_T Jet Production at RHIC (cont.)

not surprisingly, A_{LL}^{jet} is sensitive to gluon polarization Δg: [fig. taken from Jäger, MS, Vogelsang

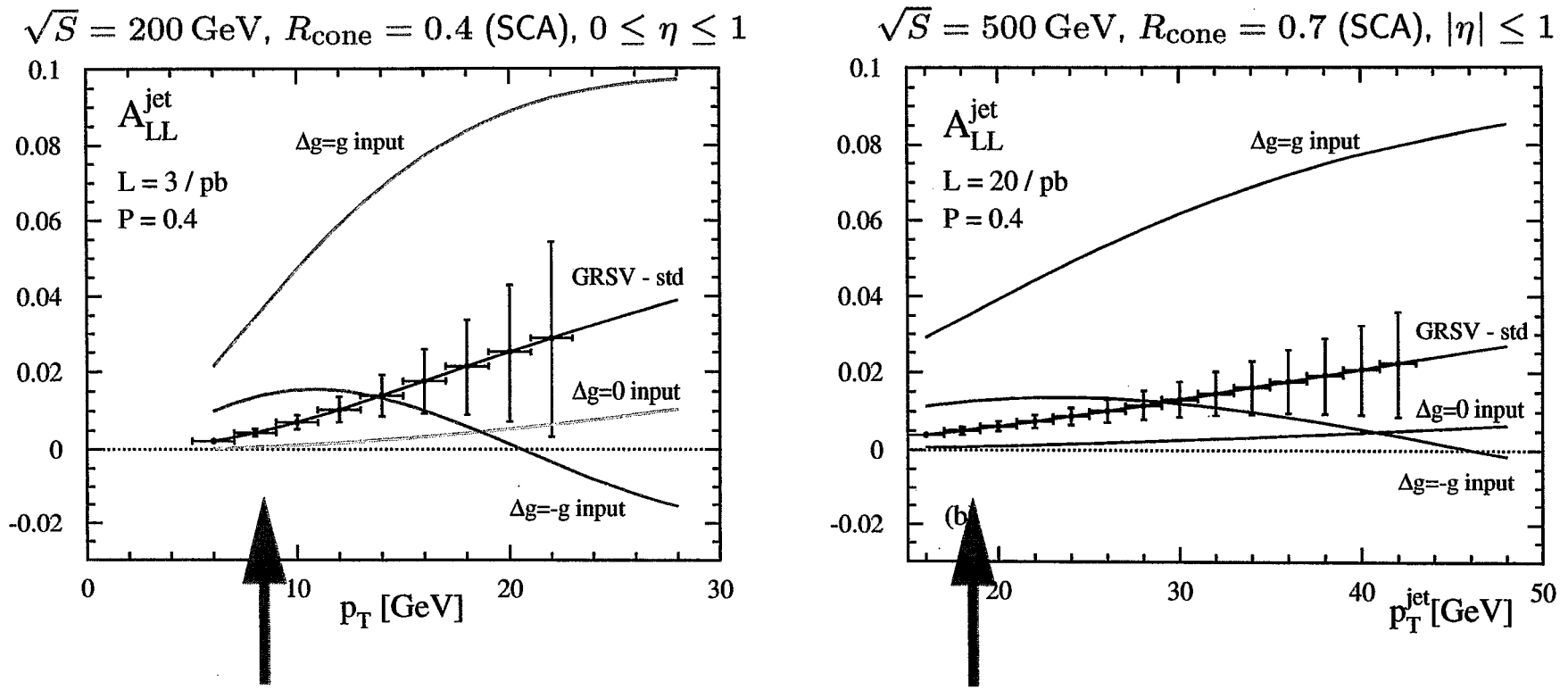

again: at small p_T no sensitivity to sign of Δg

High-p_T Jet Production at RHIC (cont.)

subprocess contributions for different Δg:

very similar to pion production (as expected)

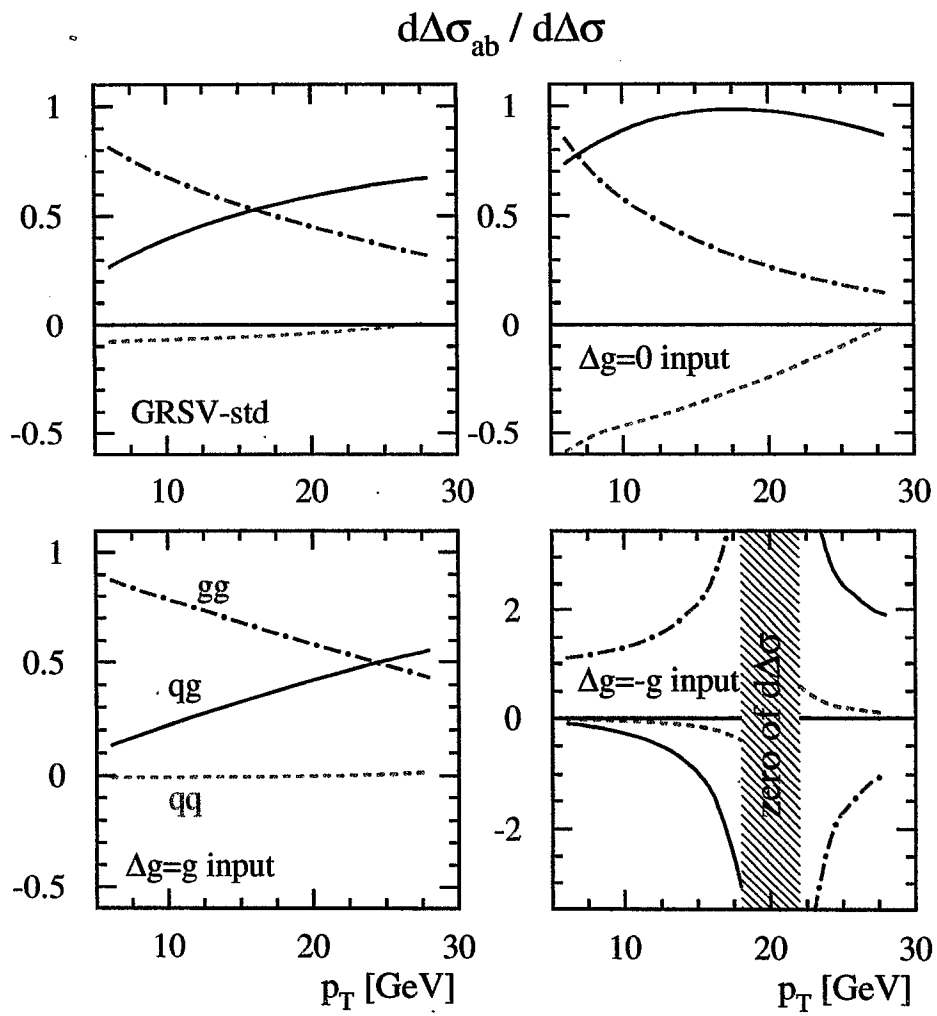

Outlook: calculations in the pipeline

- **high-p_T hadron pairs** Jäger, Owens, MS, Vogelsan

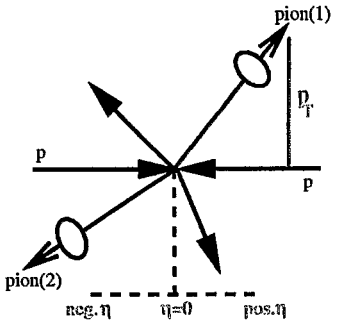

status: Monte-Carlo code almost ready

feedback: at which observables ($p_{T,1}$, $p_{T,2}$, $M_{\rm pair}, \ldots$) would you like to look at?

- **A_{TT} for single inclusive high-p_T hadrons** Mukherjee, MS, Vogelsan

status: almost done (have to put everything together and produce a code)

- **heavy flavor pair production** MS, volunteer

status: some homework to be done (matrix elements known from Bojak, MS)

have to setup a MC code to study exp. relevant observables

$\pi 0$ A_{LL} results from PHENIX

RHIC Spin Collaboration Meeting
Torino, Italy, October 8-9, 2004

A.Bazilevsky,
Brookhaven National Laboratory
For PHENIX Collaboration

To be reported at SPIN2004 by Yoshi Fukao

A_{LL}

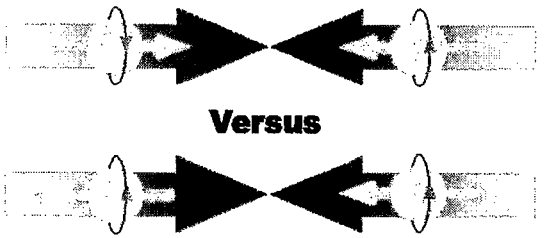

$$A_{LL} = \frac{\sigma_{++} - \sigma_{+-}}{\sigma_{++} + \sigma_{+-}} = \frac{1}{|P_B P_Y|} \frac{N_{++} - RN_{+-}}{N_{++} - RN_{+-}}; \qquad R = \frac{L_{++}}{L_{+-}}$$

++ same helicity
+– opposite helicity

(P) Polarization
(R) Relative Luminosity
(N) Number of pi0s

PHENIX

PHENIX Detector

Philosophy:

- ✓ High rate capability & granularity
- ✓ Good mass resolution and particle ID
- ➢ Sacrifice acceptance

$\pi 0$ reconstruction and high p_T photon trigger:

EMCal: $|\eta|<0.35$, $\Delta\varphi=\pi$

Granularity $\Delta\eta\times\Delta\varphi = 0.01\times0.01$

Minimum Bias trigger and Relative Luminosity:

Beam-Beam Counter (BBC):

$3.0<|\eta|<3.9$, $\Delta\varphi=2\pi$

Local Polarimeter

Zero-Degree Calorimeter (ZDC):

$|\eta|>6$

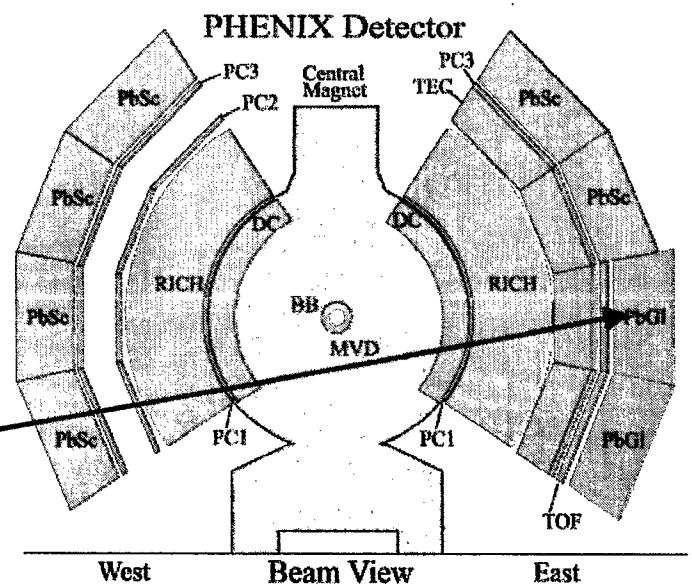

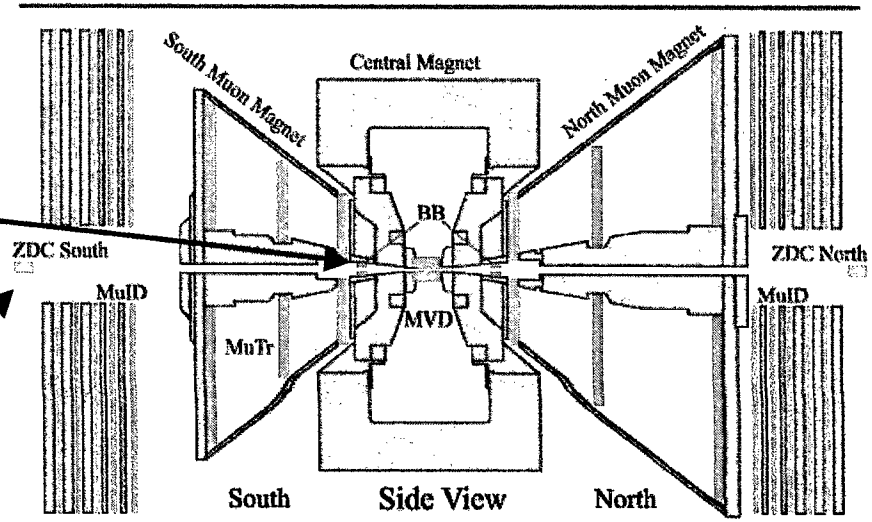

PHENIX

Beam Polarization (in PHENIX)

Absolute polarization scale (see O.Jinnouchi talk)

- ✓ With RHIC CNI Polarimeter
- ✓ Relative uncertainty ~32% (will be decreased soon)
- ✓ This error does not change the significance of non-zero A_{LL}, because it scales both value and error in the same way (but it does change the comparison to theory)

Long. component of the spin direction

- ✓ PHENIX Local Polarimeter vs RHIC CNI Polarimeter

PHENIX

PHENIX Local Polarimeter

- ✓ Forward neutron transverse asymmetry (A_N) measurements
- ✓ SMD (position) + ZDC (energy)

ϕ distribution

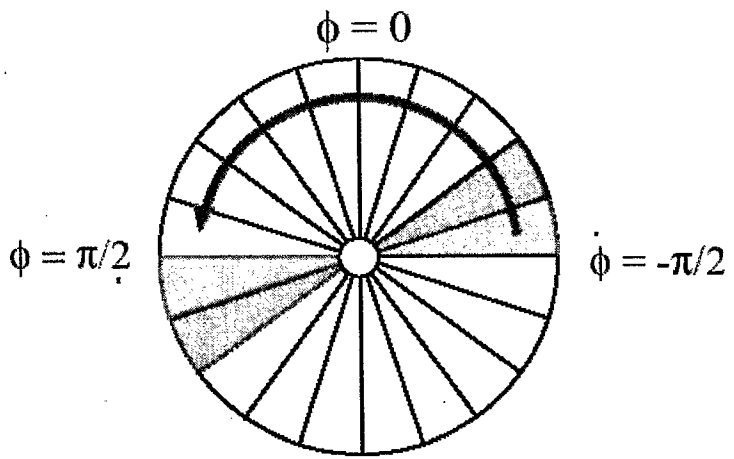

Vertical → $\phi \sim \pm\pi/2$
Radial → $\phi \sim 0$
Longitudinal → no asymmetry

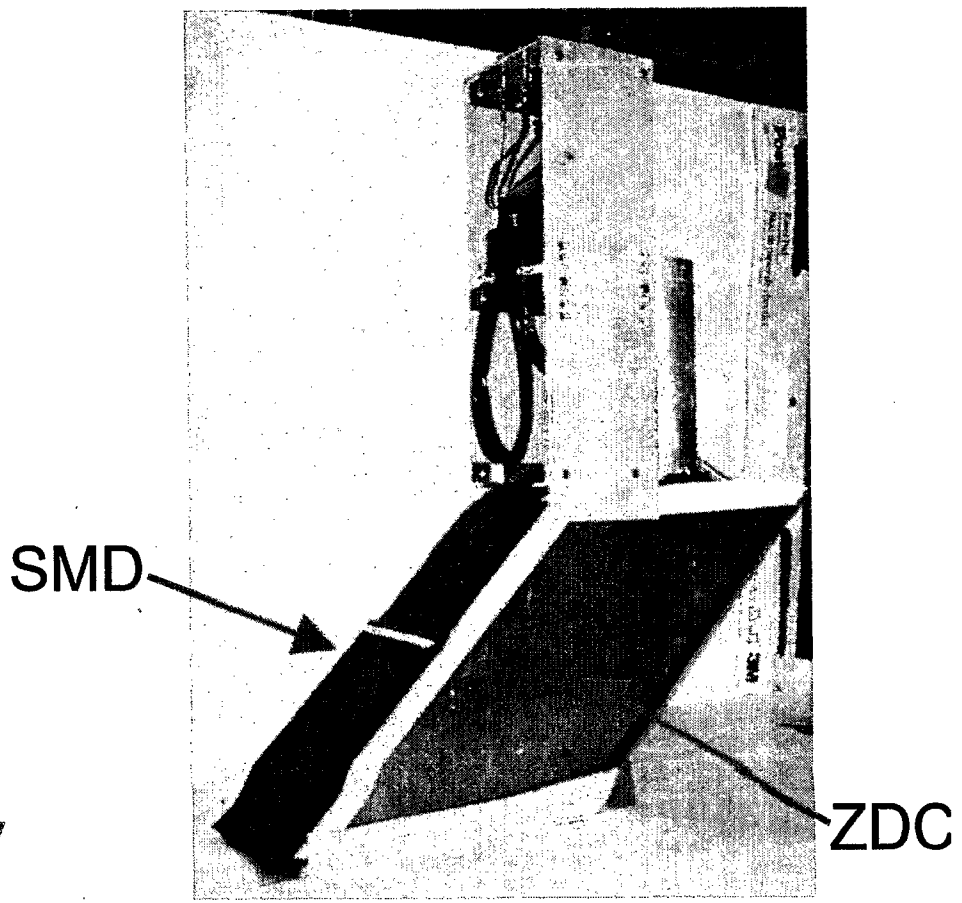

PHENIX

Spin Long. Component

$$S_L = \sqrt{1 - S_T^2}, \qquad S_T = \sqrt{S_{T-vertical}^2 + S_{T-radial}^2}$$

S_T is measured with PHENIX Local Polarimeter

Left-Right asymmetry Up-Down asymmetry

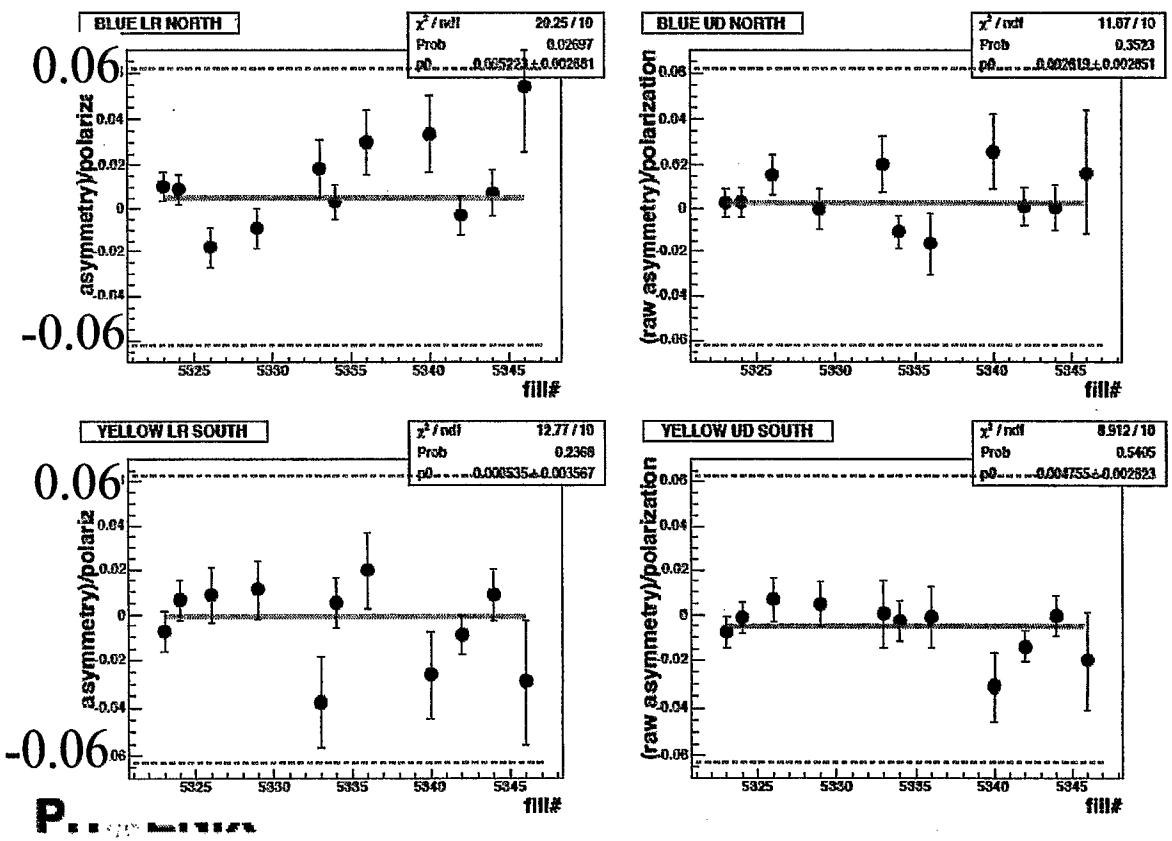

$$S_L(blue) = 99.68^{+0.25}_{-0.66}$$

$$S_L(yellow) = 99.82^{+0.16}_{-0.65}$$

Beam Polarization is pure longitudinal

Relative Luminosity

$$R = \frac{L_{++}}{L_{+-}}$$

Beam-Beam-Counter (BBC) used as Relative Luminosity Monitor

- $\eta = \pm 3.0\text{-}3.9$
- Low background
- High statistics: $\sigma_{BBC} \approx 0.5 \cdot \sigma_{pp}^{inel}$

Zero Degree Calorimeter (ZDC) used as a cross check

- Different kinematics & acceptances ($|\eta|>6$)

Bunch-by-bunch comparison of the number of hits in BBC and ZDC

- ✓ The same vertex cut $|z|<30$cm as in offline analysis is used
- ✓ BBC and ZDC have different position resolution → systematics due to variation of the z-vertex distribution
- ✓ After correction for the vertex width some residual systematics left (χ^2/NDF~1.8)

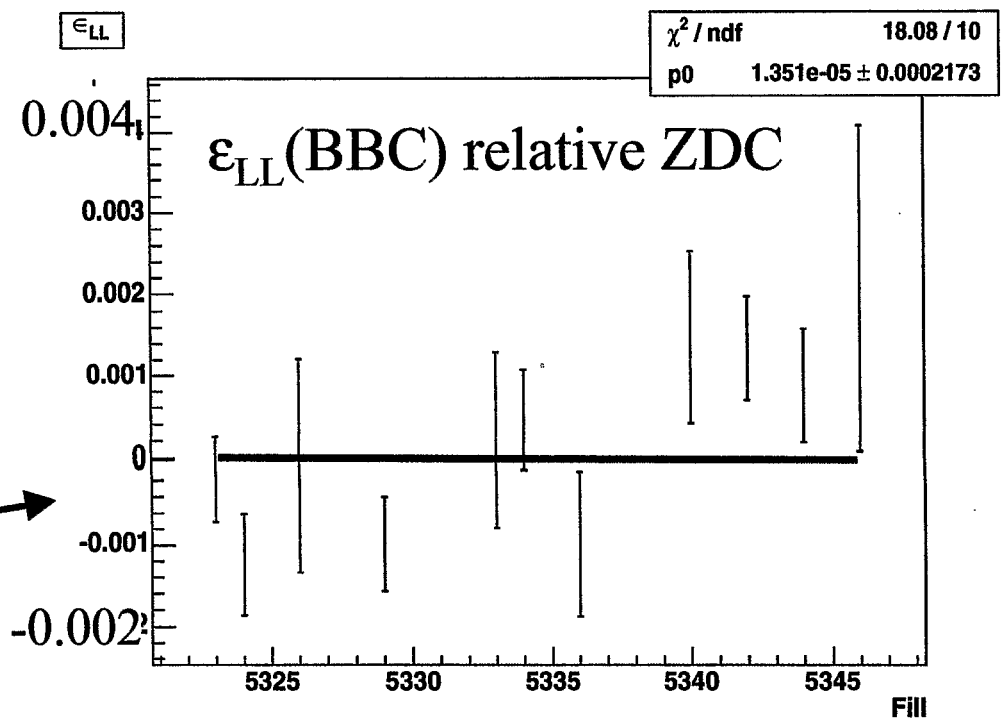

-0.06

PHENIX

Relative Luminosity: Results

Achieved relative luminosity precision $\delta R = 5.8 \cdot 10^{-4}$

Rel. Lum. contribution for pi0 A_{LL} less than 0.2%

For average beam polarizations of 40%

A_{LL} of BBC relative to ZDC consistent with 0 (<0.2%)

Strong indication that both A_{LL}s are zero (very different kinematical regions, different physics signals)

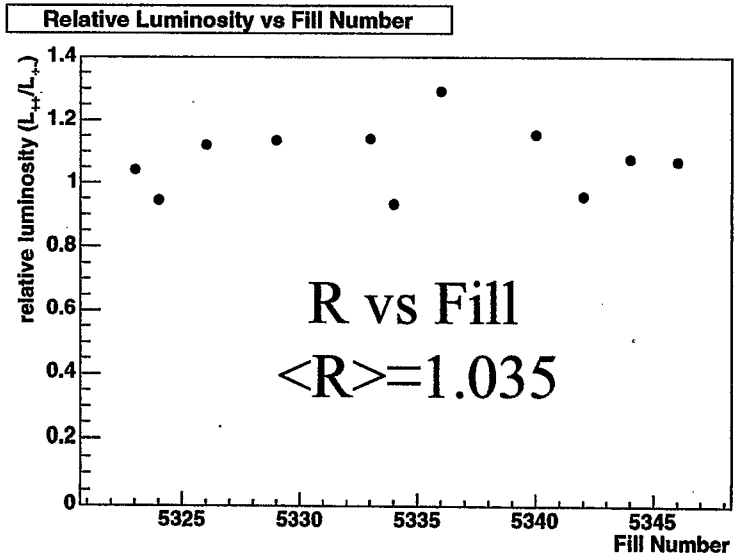

PHENIX

Data set from Run4

Data collected with high p_T photon trigger

- Based on EMCal; Threshold ~1.6 GeV/c
- Rejection factor ~80
- Analyzed data sample: **21.4M events (~75 nb^{-1})**
  sqrt(<$P_b P_y$>)~40%

Minimum Bias data

- To obtain "unbiased" $\pi 0$ cross section at low p_T
- For high p_T photon trigger efficiency study

PHENIX

Photon trigger efficiency for π0

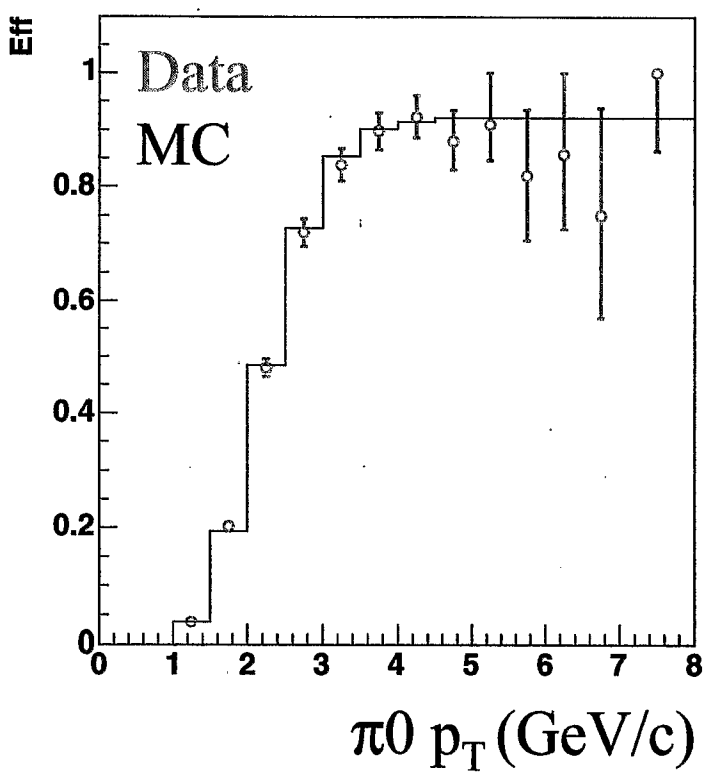

- ✓ Pi0 efficiency plateaus for p_T>4 GeV/c
- ✓ Limited efficiency at p_T<4 GeV/c:
  - 1-2 GeV/c: 10%
  - 2-3 GeV/c: 57%
  - 3-4 GeV/c: 86%
  - 4-5 GeV/c: 90%
- ✓ Monte Carlo reproduces Data well

PHENIX

π^0 A_{LL} measurements

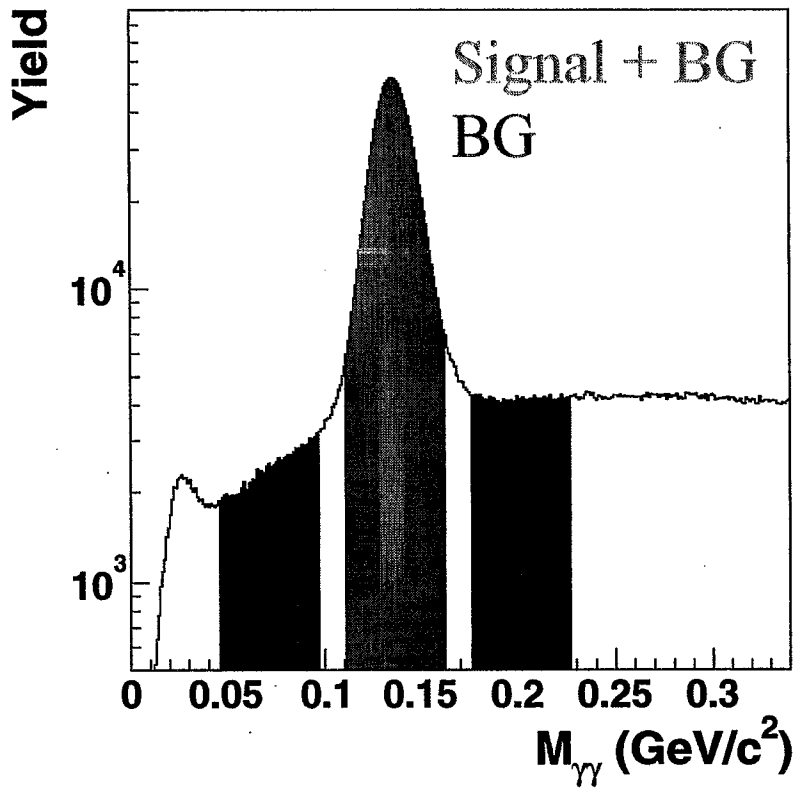

- Photons in PHENIX EMCal: $|\eta|<0.35$, $\Delta\varphi=180^0$
- Done in four p_T bins from 1 to 5 GeV/c; collected statistics 1.8M
- Blue area used to estimate A_{LL} of background under π^0 peak
- Background contribution (r) under π^0 peak varies from 31% in 1-2 GeV/c bin to 5% in 4-5 GeV/c bin

$$A_{LL}^{\pi 0} = \frac{A_{LL}^{\pi 0+BG} - rA_{LL}^{BG}}{1-r}$$

$$\sigma_{A_{LL}^{\pi 0}} = \frac{\sqrt{\sigma^2_{A_{LL}^{\pi 0+BG}} + r^2\sigma^2_{A_{LL}^{BG}}}}{1-r}$$

PHENIX

A_{LL} measurements

$$A_{LL} = \frac{\sigma_{++} - \sigma_{+-}}{\sigma_{++} + \sigma_{+-}} = \frac{1}{|P_B P_Y|} \frac{N_{++}/L_{++} - N_{+-}/L_{+-}}{N_{++}/L_{++} + N_{+-}/L_{+-}}, \quad \delta_{A_{LL}} = \frac{1}{|P_B P_Y|} \frac{1}{\sqrt{N_{++} + N_{+-}}}$$

++ same helicity
+– opposite helicity

Procedure

1. Collect N and L for ++ and +– configurations (sum over all crossings) and calculate A_{LL} for each fill
2. Average A_{LL} over fills; use χ^2/NDF to control fit quality; use "bunch shuffling" to check syst. errors

PHENIX

A_{LL} Calculations

A_{LL} averaged over fills for pi0+BG

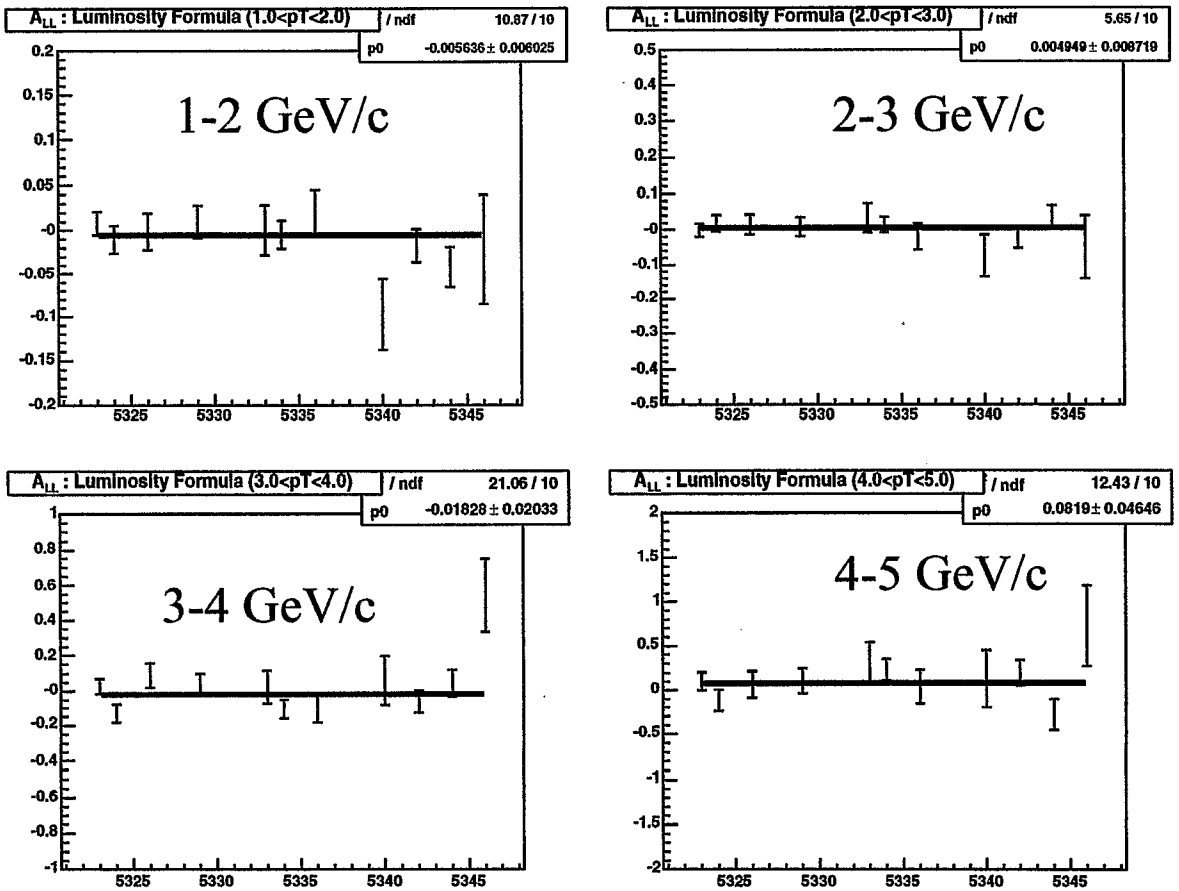

1-2 GeV/c

A_{LL} = -0.6%±0.6%

χ^2/ndf = 11/10

2-3 GeV/c

A_{LL} = 0.5%±0.9%

χ^2/ndf = 6/10

3-4 GeV/c

A_{LL} = -1.8%±2.0%

χ^2/ndf = 21/10

4-5 GeV/c

A_{LL} = 8.2%±4.6%

χ^2/ndf = 12/10

PHENIX

Bunch shuffling

to check for syst. errors

Bunch shuffling = Randomly assigns helicity for each crossing

χ^2/NDF

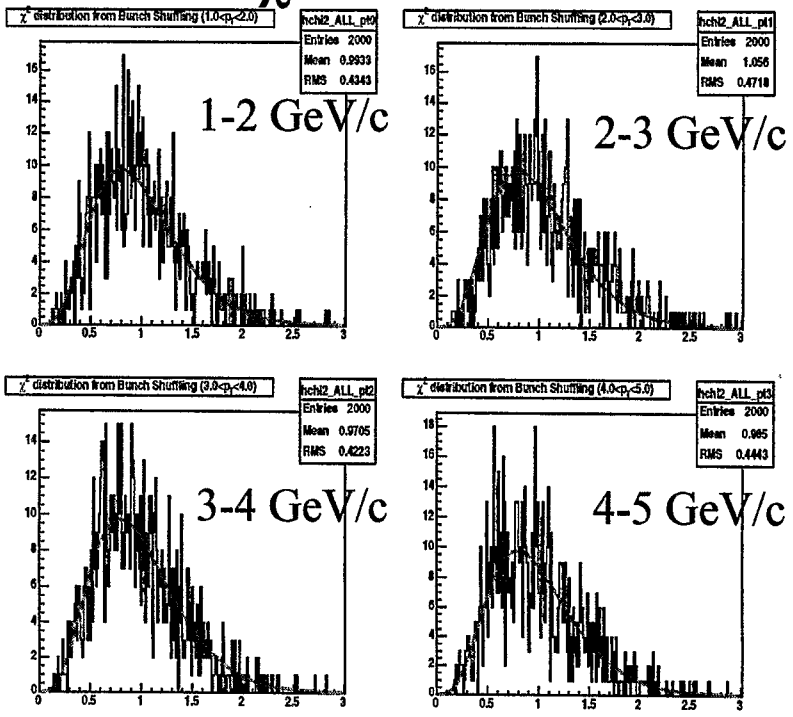

All <χ^2/NDF> are ~1

Consistent with stat. distribution of χ^2/NDF (red)

A_{LL}

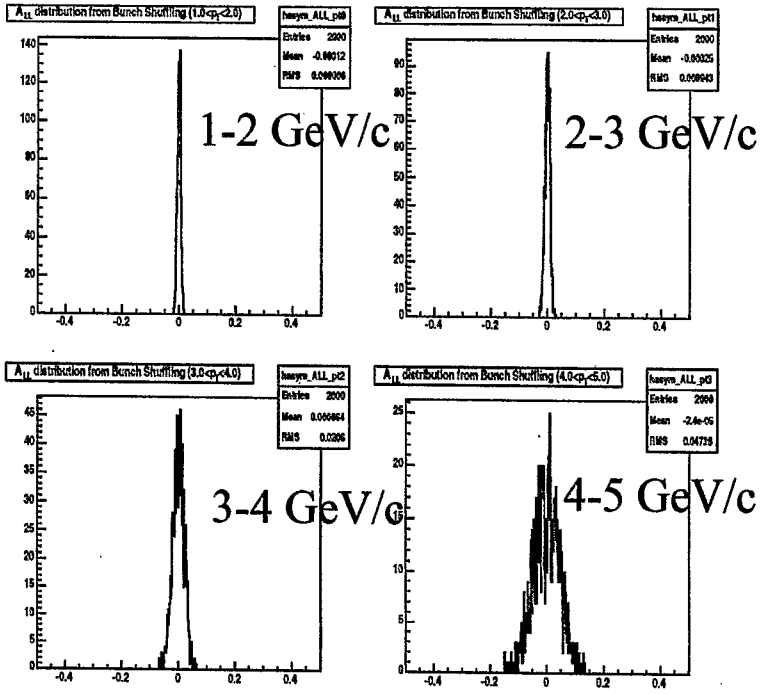

Widths are consistent with obtained errors $\delta(A_{LL})$

PHENIX

Other checks

- ✓ Different photon PID and $\pi 0$ reconstruction cut
- ✓ Various mass range for $\pi 0$ and BG

  Results are consistent

- ✓ Single asymmetry A_L
- ✓ Parity violating double asymmetries: $\sigma(++)$ vs $\sigma(--)$ and $\sigma(+-)$ vs $\sigma(-+)$

  Consistent with 0 as expected

PHENIX

π^0 A_{LL} from pp at 200 GeV

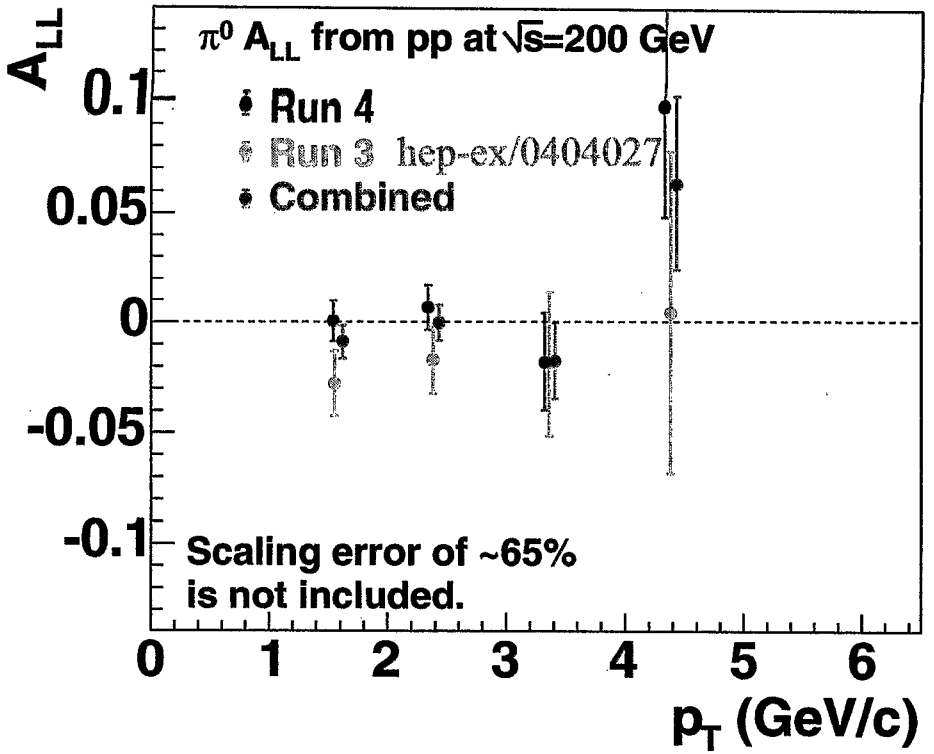

Run3 and Run4 results are consistent: χ^2=5.7, CL=22%

p_T GeV/c	$A_{LL}^{\pi 0+bck}$	A_{LL}^{bck}	$A_{LL}^{\pi 0}$(Run-4)	$A_{LL}^{\pi 0}$(Run-3)	$A_{LL}^{\pi 0}$ (Comb)
1-2	-0.6±0.6	-1.9±0.9	0.0±0.9	-2.7±1.3	-0.9 ±0.7
2-3	0.5±0.9	-0.7±1.9	0.9±1.0	-1.3±1.3	0.0 ±0.8
3-4	-1.8±2.0	-2.3±6.5	-1.8±2.2	-1.7±2.8	-1.8 ±1.7
4-5	8.2±4.6	-18±17	9.7±4.9	0.7±6.2	6.2 ±3.8

PHENIX

Comparison to theory

B.Jager et al., PRD67, 054005 (2003)

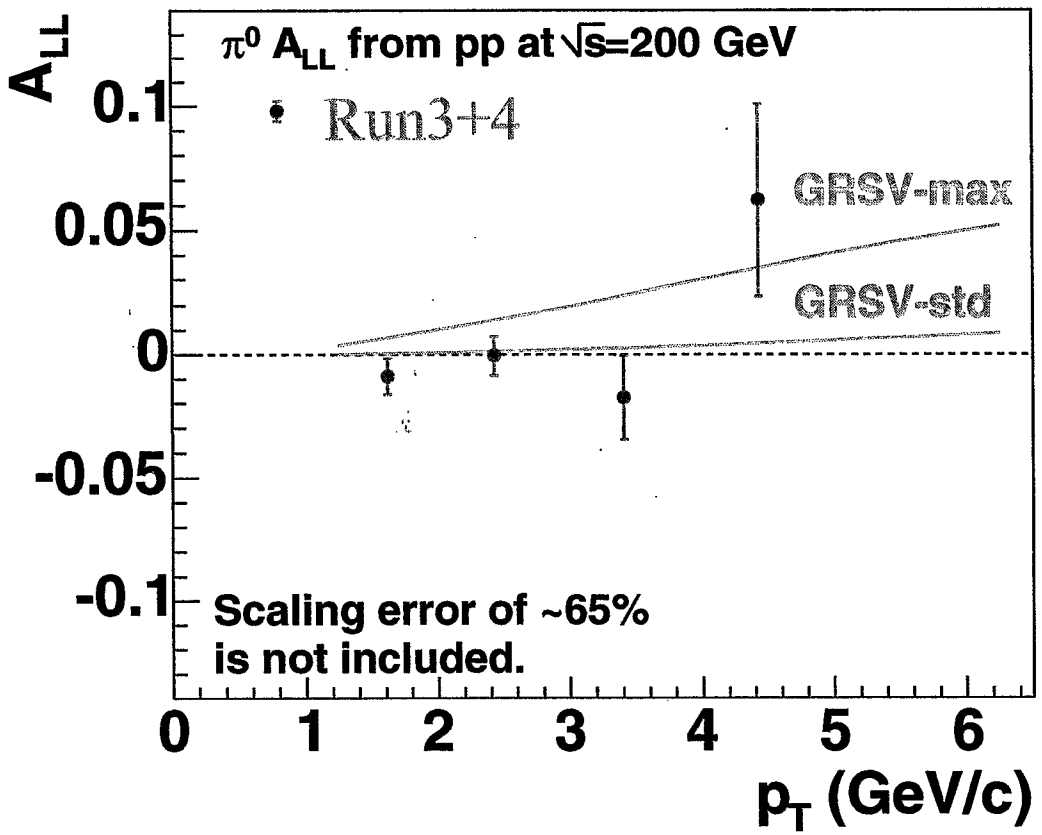

- Note considerable contribution of soft physics in the lowest p_T point (~50%)

Comparison of Run3+4 with theory:

✓ GRSV-std
21-24% (p_T>1 GeV/c)
27-29% (p_T>2 GeV/c)

✓ GRSV-max
0.00-6% (p_T>1 GeV/c)
0.01-13% (p_T>2 GeV/c)

Consistent with GRSV-std
Less consistent with GRSV-max

PHENIX

Summary

- ✓ PHENIX obtained results on A_{LL} in $\pi 0$ production from Run4 with average beam polarization ~40%
- ✓ Run3 and Run4 results are consistent
- ✓ Stat. errors in Run3+4 combined results are ×1.6 smaller than Run3
- ✓ The same conclusion as from Run3 (paper accepted by PRL): data consistent with GRSV-std and less consistent with GRSV-max

Soon, expect to have considerably smaller scale uncertainty due to beam polarization

PHENIX

Backup slides

PHENIX

RHIC as polarized proton collider

"Blue" and "yellow" rings

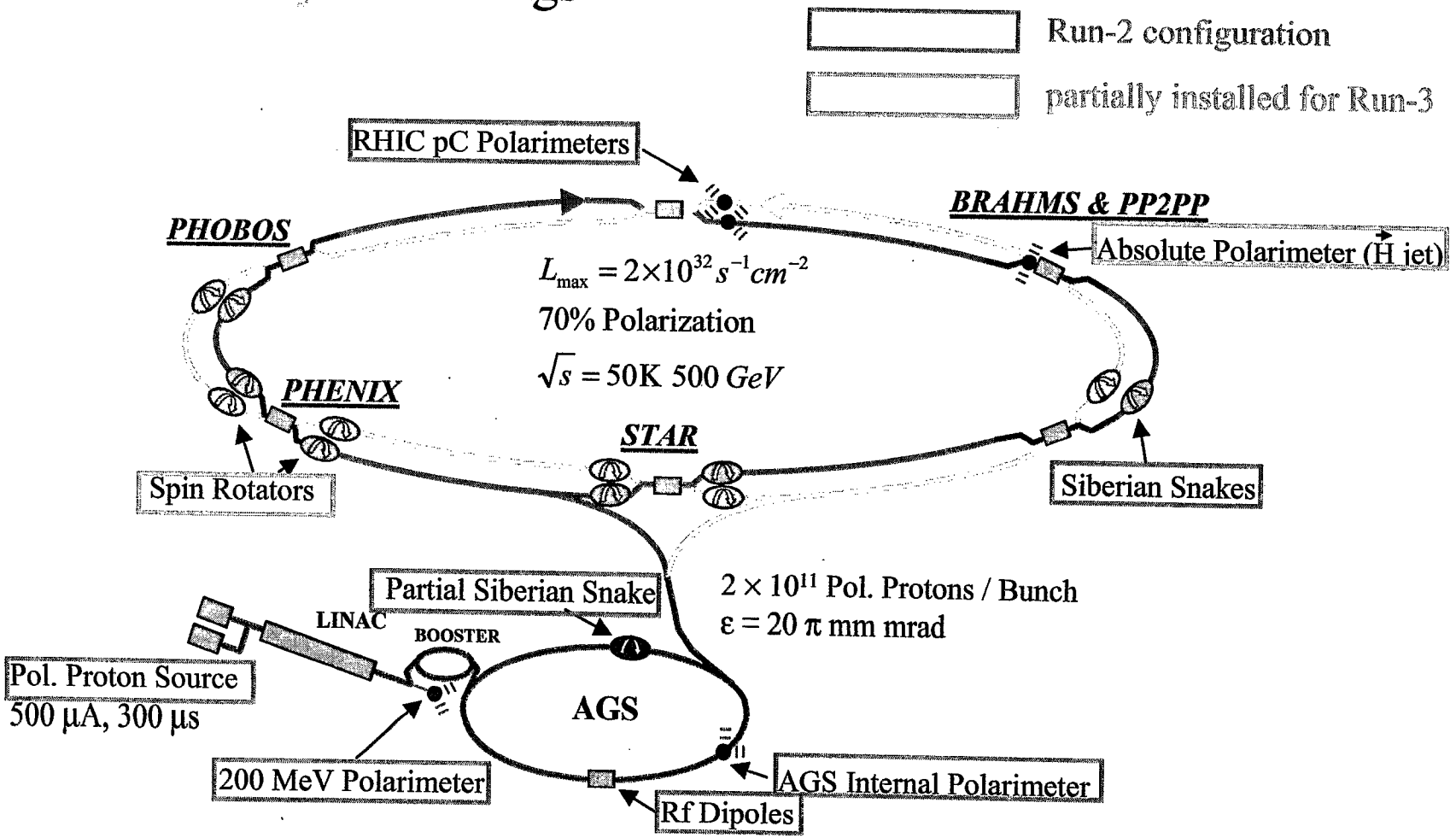

PHENIX

Loc. Pol. Asymmetry (Transverse RUN)

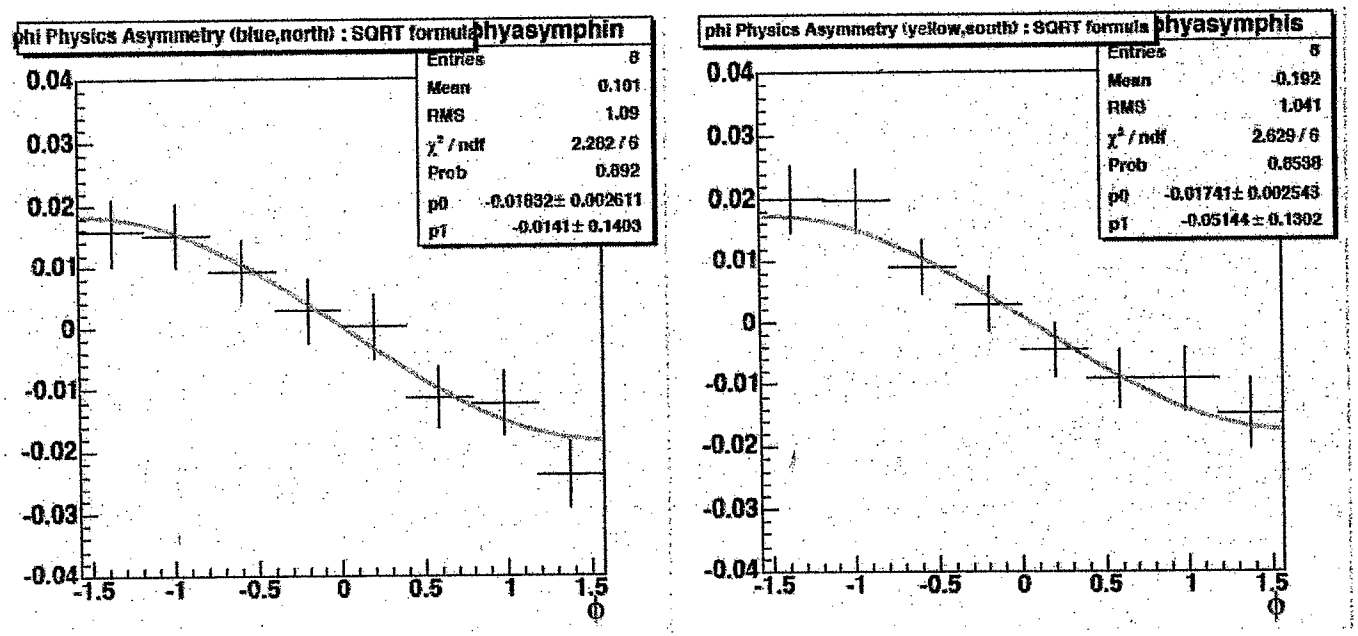

- This picture is raw asymmetry of blue (left) and yellow beam (right) in transverse run period (just 1 run period).
- In this period, we have 30.8 +- 2.5% and 25.9 +- 1.9% polarization for blue and yellow beam respectively. For estimate effective analyzing power at RUN4, I use

  Effective A_N = (raw asymmetry) / polarization @ transverse run

- Though All transverse period, we got Effective A_N as,

Blue : 6.21 +- 0.50% **Yellow : 6.39 +- 0.55%**

PHENIX

π^0 Cross Section in *pp*

Run2

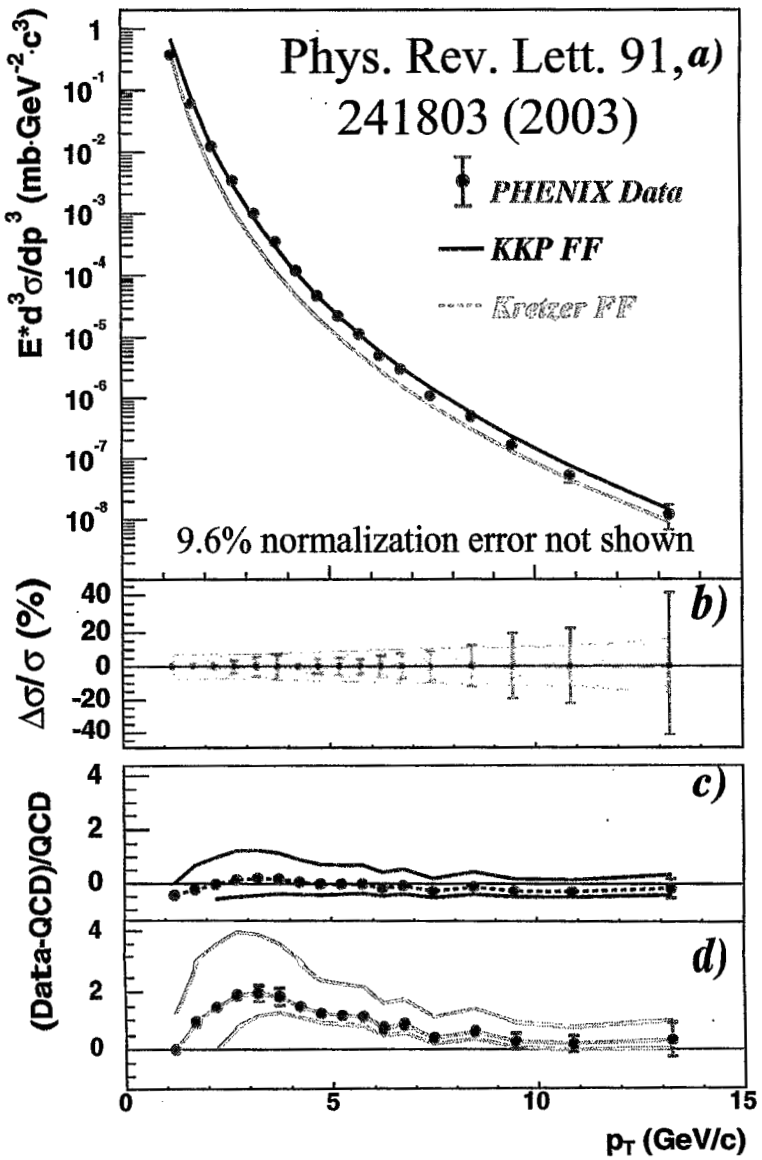

- NLO pQCD consistent with data within theoretical uncertainties
  - PDF: CTEQ5M
  - Fragmentation functions:
    - Kniehl-Kramer-Potter (KKP)
    - Kretzer
  - Spectrum constrains D(gluon→π) fragmentation function
- Important confirmation of theoretical foundation for spin program
- Data from Run4 reproduce Run2 results

Pi0 reconstruction for A_{LL}

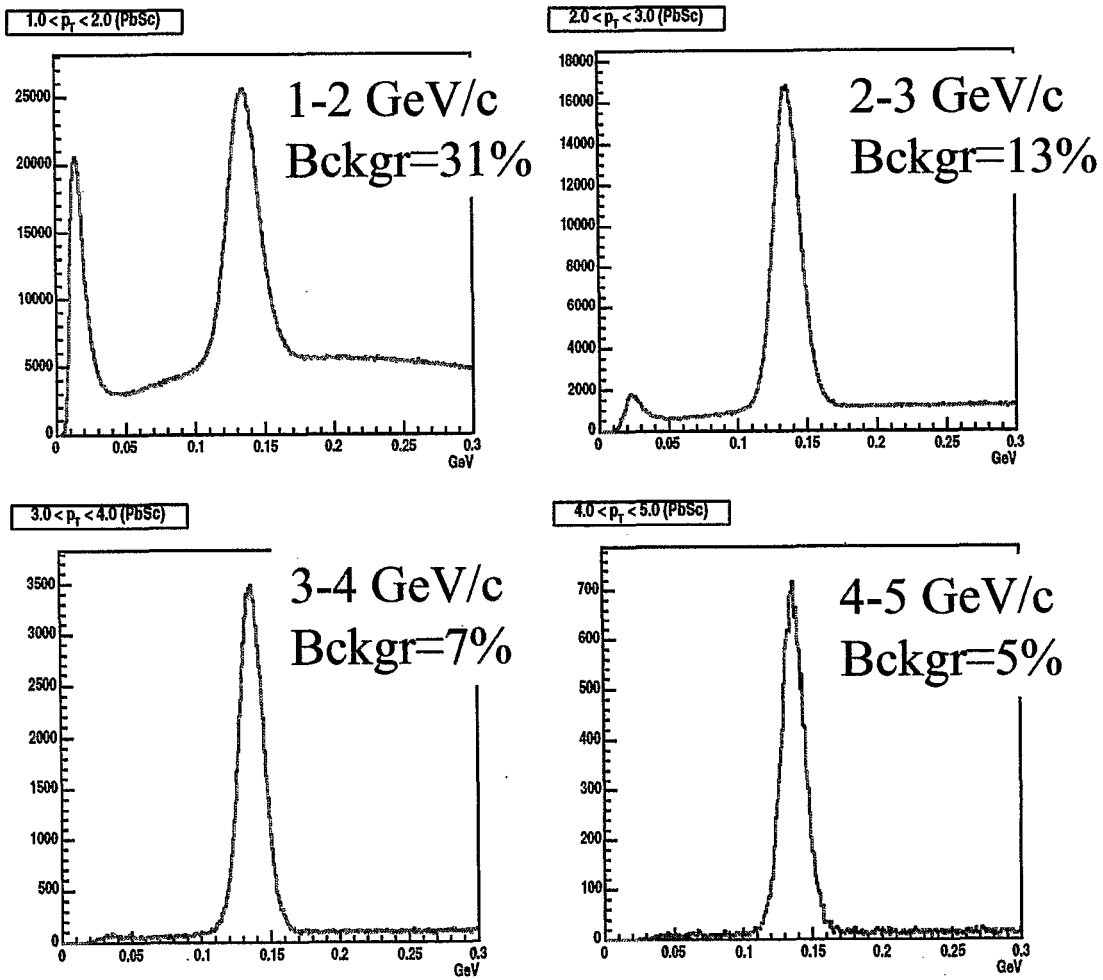

Results obtained for four pt bins from 1 to 5 GeV/c

Pi0 peak width varies from 12 to 9 MeV/c^2 from lowest to highest pt bins

Background contribution under pi0 peak for ±25 MeV/c^2 mass cut varies from 31% to 5% from lowest to highest pt bins

PHENIX

Alpha

Data

MC vs Data

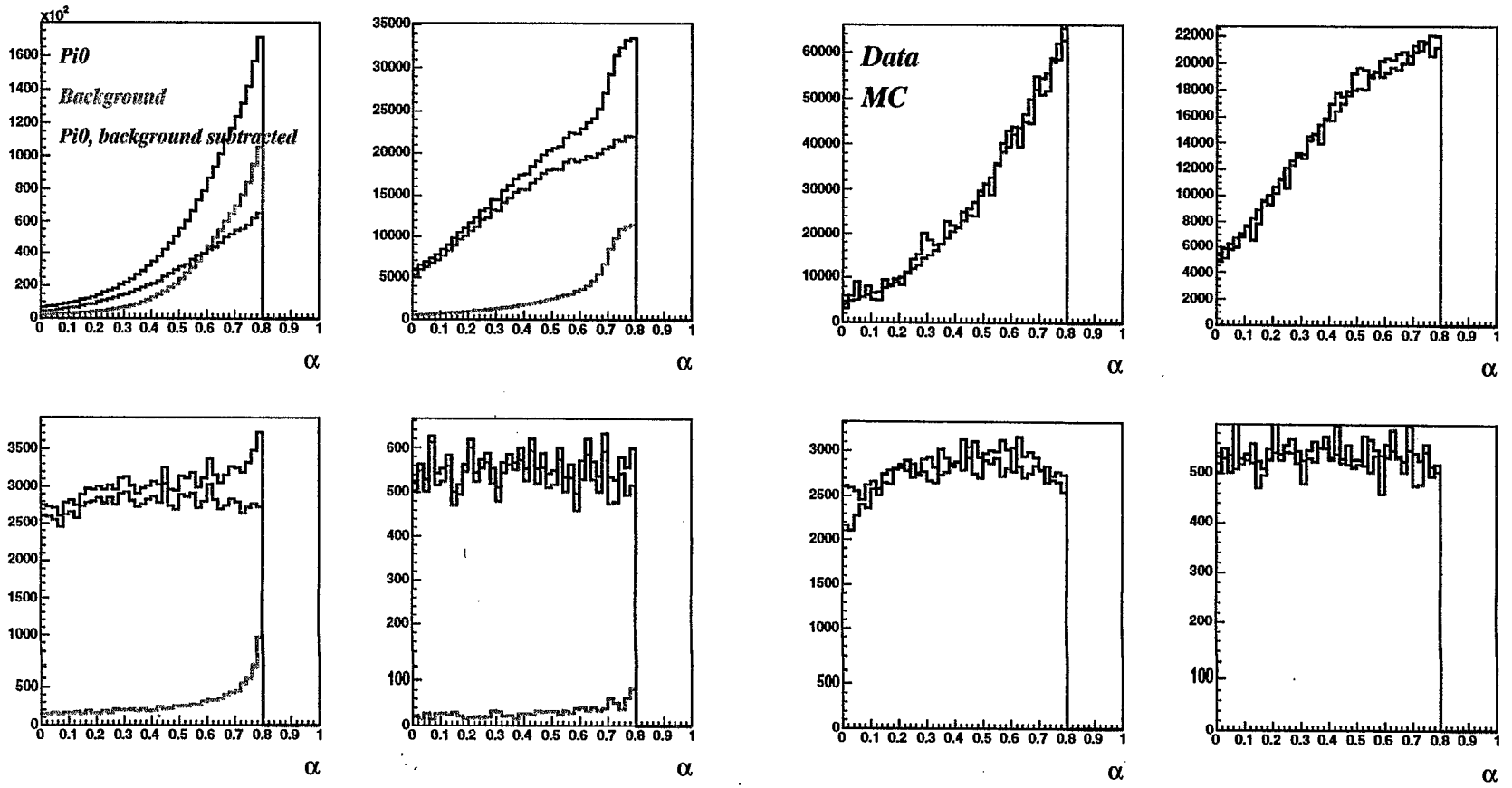

PHENIX

ΔG: other experiments

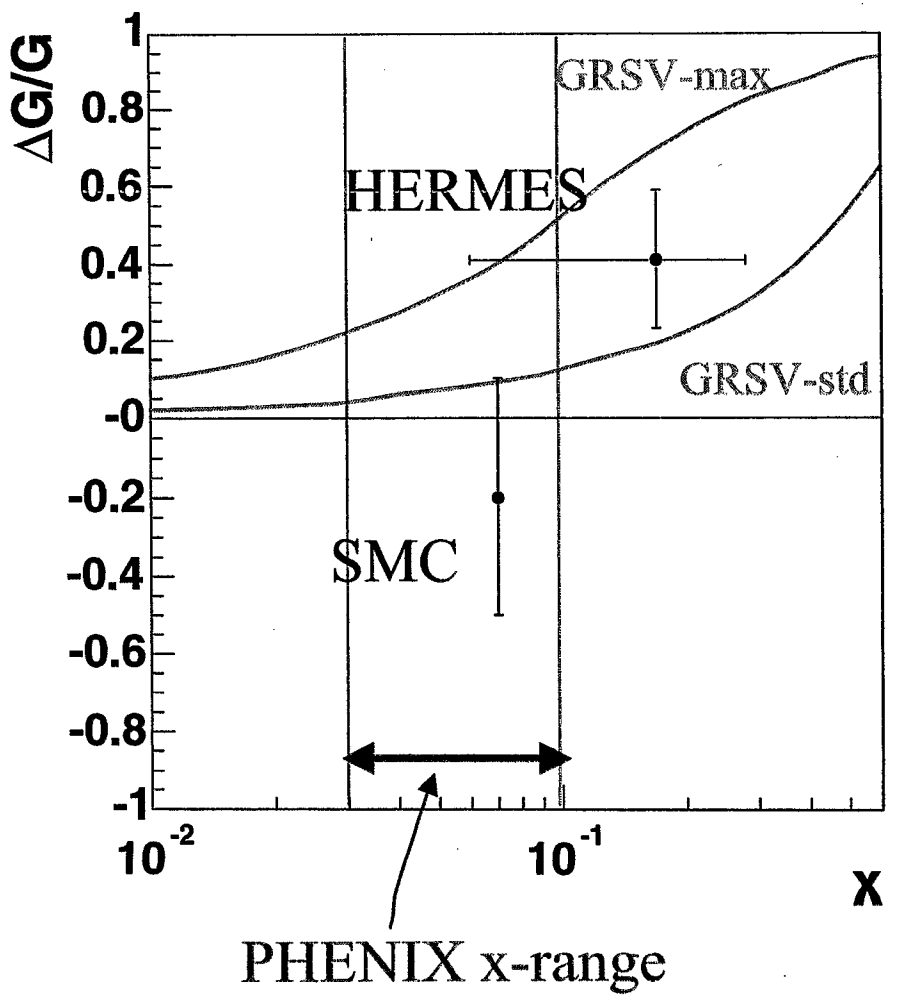

- Theory curves from W.Vogelsang
- HERMES: high pt hadron pairs (PRL84, 2584, 2000)
  Consistent with both GRSV-max and GRSV-std
- SMC: high pt hadron pairs (PRD70, 012002, 2004)
  Consistent with GRSV-std
- PHENIX: π^0 A_{LL}
  Consistent with GRSV-std

So far all results are consistent with GRSV-std

PHENIX

Measurement of prompt photon in $\sqrt{s}$=200GeV pp collisions

Kensuke Okada
(RIKEN-BNL Research Center)
For the PHENIX collaboration

Motivations

- Physics meaning of prompt photon
  - Is a good probe of parton structure in nucleon.
  - One of simple processes at hadron collisions.

- At RHIC (a polarized proton collider capable of $\sqrt{s}$ up to 500GeV)
  - The highest energy available for pp→gamma+"X"
  - Prompt photon production can probe the gluon polarization in proton.

460

Data

RHIC run3 p+p

2003 April-May
$\sqrt{s}$=200GeV Proton-proton collisions
Luminosity= 266nb^{-1}

RHIC-PHENIX detector

Central Arm (West)
(Rapidity |y|<0.35)
Electromagnetic Calorimeter (EMCal)
Photon detection
High granularity (~10*10mrad^2)
Drift chamber (DC)
Charged hadron veto
Beam forward / backward
(Rapidity 3.1<|y|<3.9)
Beam-beam counter (BBC)
Triggering and vertex determination

BBC and EMCal Trigger for the data taking

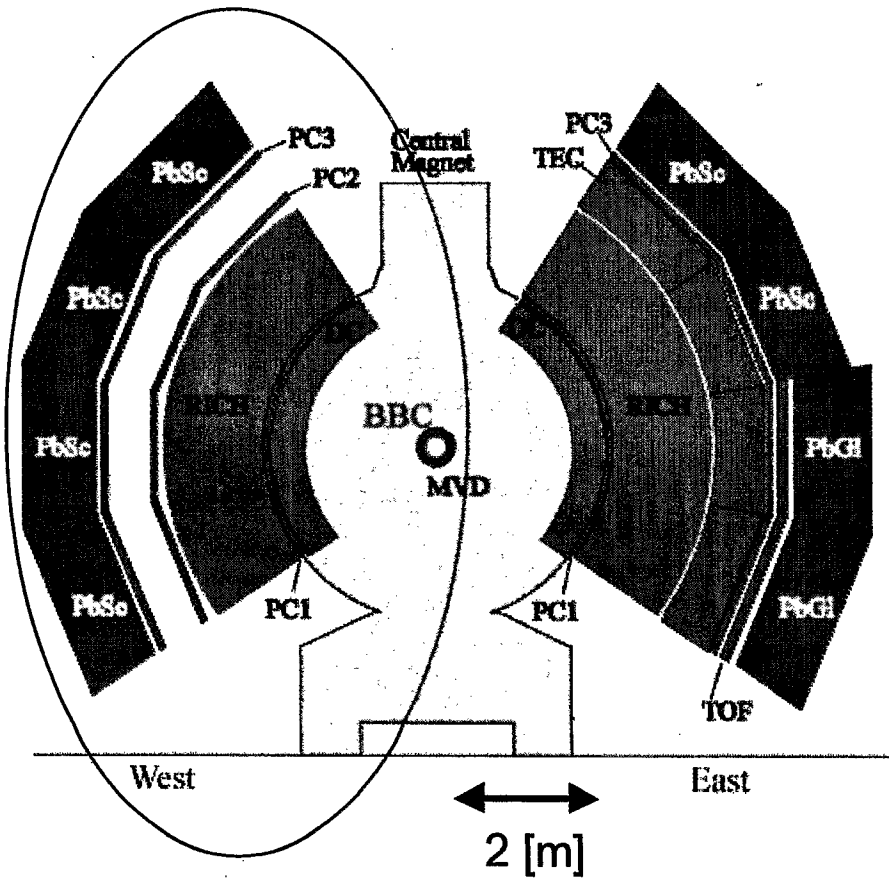

Analysis procedure (1)

Prompt photon signal = All EMCal clusters – known contributions
Signal / Noise = 0.2~1 (pT 5~17GeV/c) without π^0 tag

Non photon contributions (hadronic shower)

Electromagnetic shower shape requirement
Charged hadron veto with drift chamber tracking

Photon contributions

π^0 with both photons seen in detector
—Eliminate using a π^0 tag.
π^0 with only on photon seen in detector
—Estimate based on photon tagged as π^0
Photonic decay of η,ω etc.
—Estimate to be 23±5% of the total π^0 contributions
(=Production * Br($h \rightarrow \gamma$))

Analysis procedure (2)

Isolation cut in this analysis

$$R = \sqrt{\Delta\eta^2 + \Delta\phi^2} < 0.5$$

$$E_{sum}(R < 0.5) < E_\gamma \times 0.1$$

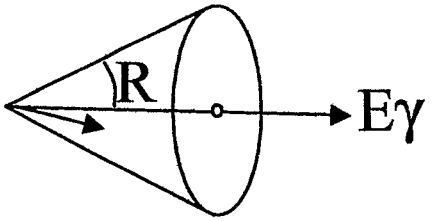

We expect that the isolation cut around well-identified high-pT photons reduces the background from hadronic decays (π^0, η, ω ...)

In addition, the isolation cut could separate photon production processes.

Total prompt photons
= photons (gluon Compton scattering) + photons (fragmentation)

Obtained by the subtraction method

Pass the isolation cut

Mostly eliminated by the isolation cut

Yes, it's not so simple. (cancellation of infrared divergences, underlying parton picture)

In this analysis, we compare with/without the isolation cut <u>without efficiency correction</u>.

π^0 tag

Reason to miss the partner	Our efforts to recover them
—Out of EMCal Arm →	Assign edges only for partner search (guard veto region)
—EMCal bad area →	Careful definition
—Less than the minimum E →	Set E_{min} at 150MeV (as low as possible).
—Photon conversions →	Charged veto with DC tracks, not with a detector in front of the EMCal
—Photon merging →	In our pT region, those are rejected by the EM shower shape cut.

From MC,
γ from missed π^0 / from tagged π^0
= 40% @ pT=5GeV/c
= 20% @ pT=10GeV/c

Now we are ready to obtain prompt photon yield.

S/N ratio

S: signal
= all – (π^0,η, etc. contributions)
N: noise
= all – signal – (tagged π^0)

With the isolation cut,
The signal is enhanced.

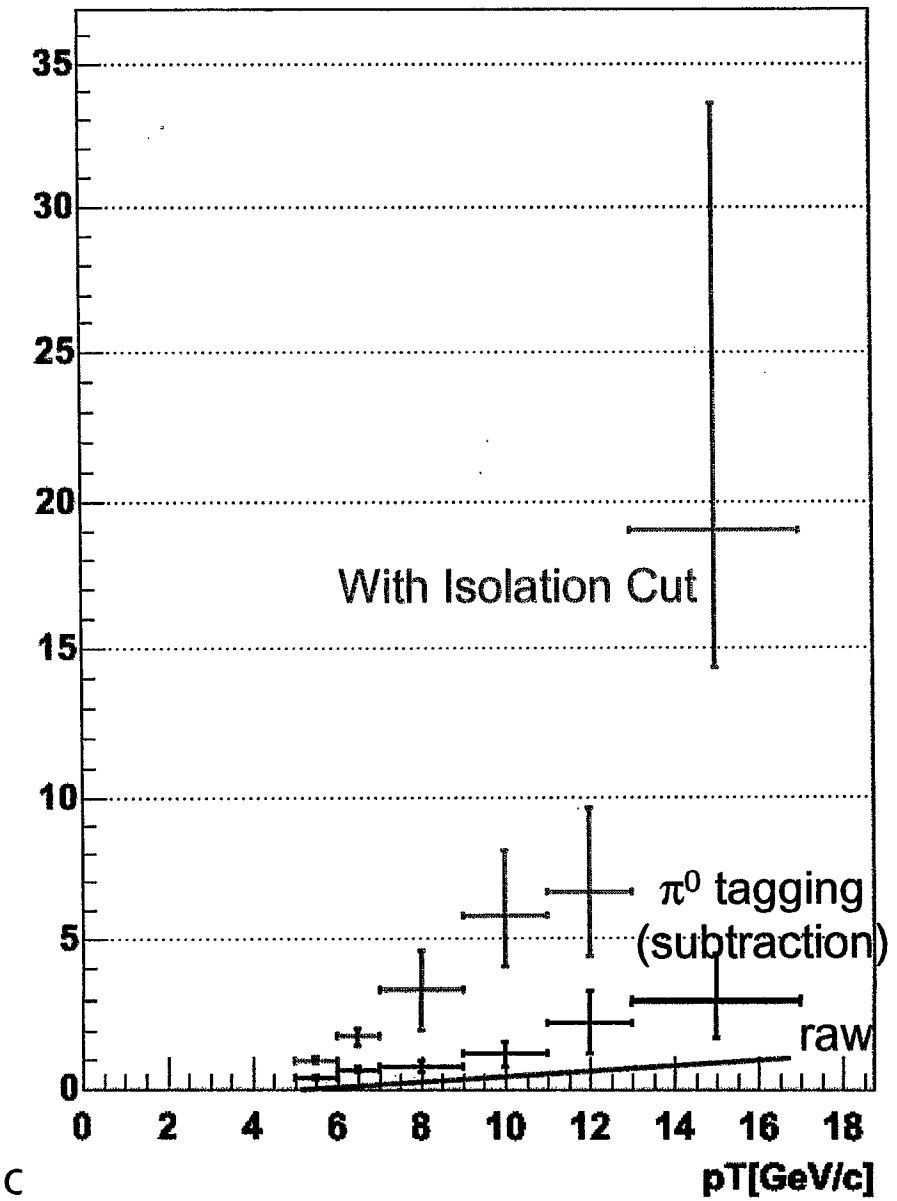

Cross section calculation

Factors

1/Luminosity: 1/266nb^{-1} (=5.450e9 events/20.5mb)
1/bbc_bias: 1/0.785
1/(acceptance+smearing): 1/0.0982
1/(shower shape cut efficiency): 1/0.98
1/(Conversion probability): 1/0.97

Systematic error sources

For π^0 tagging (subtraction) method	Lowest 5-5.5 [GeV/c]	Highest 15-17 [GeV/c]	
Pi0 photon estimation	30%	5	Point to point
Non pi0 hadron contribution	27	6	
Photon acceptance and smearing	10	10	
Photon conversion effect	1	1	
Luminosity measurement	12	12	global
BBC trigger bias	3	3	
Total (quadratic sum)	43%	18	

* Errors on the backgrounds result in enlarged errors on the signal, especially at low-pT region.

* With the isolation cut, those are less thanks to high S/N ratio.

Result

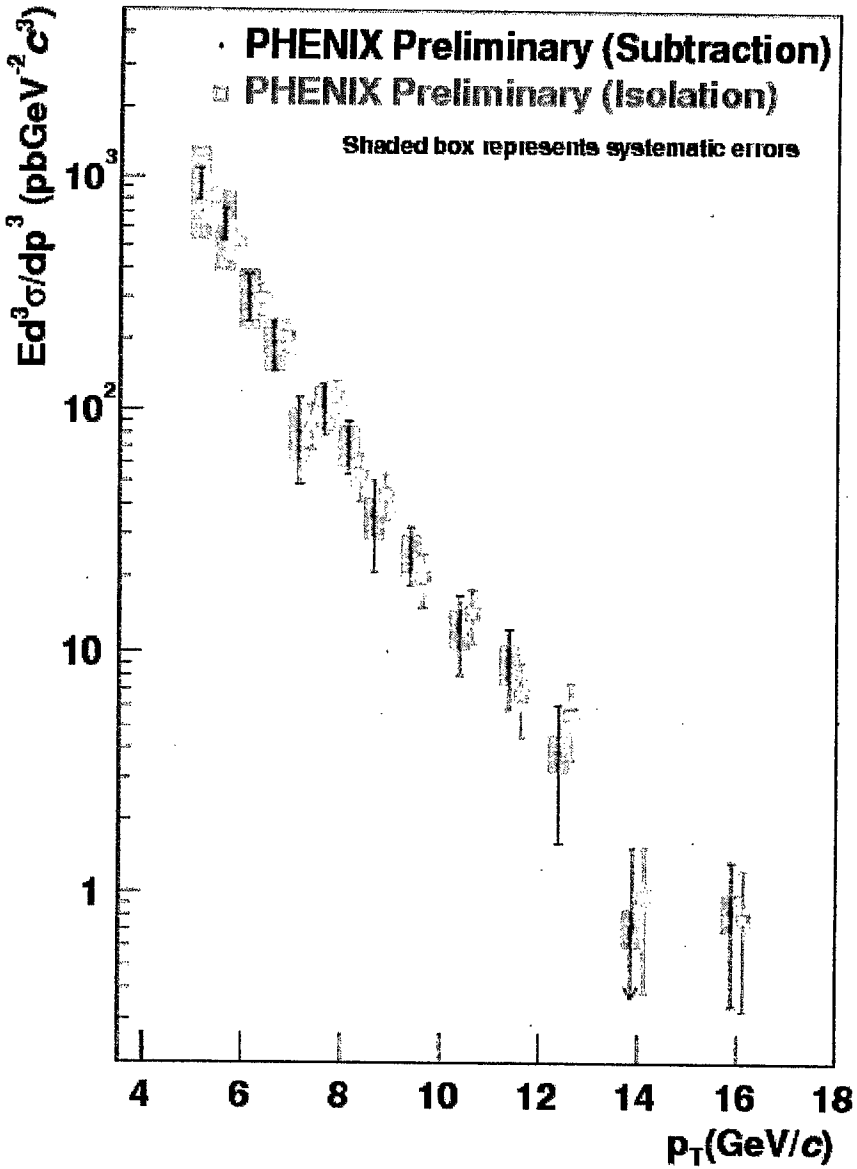

Two methods don't have a large difference.

It suggests
— low rejection power for the fragmentation photon contributions
or/and
— a large contribution from gluon Compton scattering

Comparison to NLO pQCD calculation

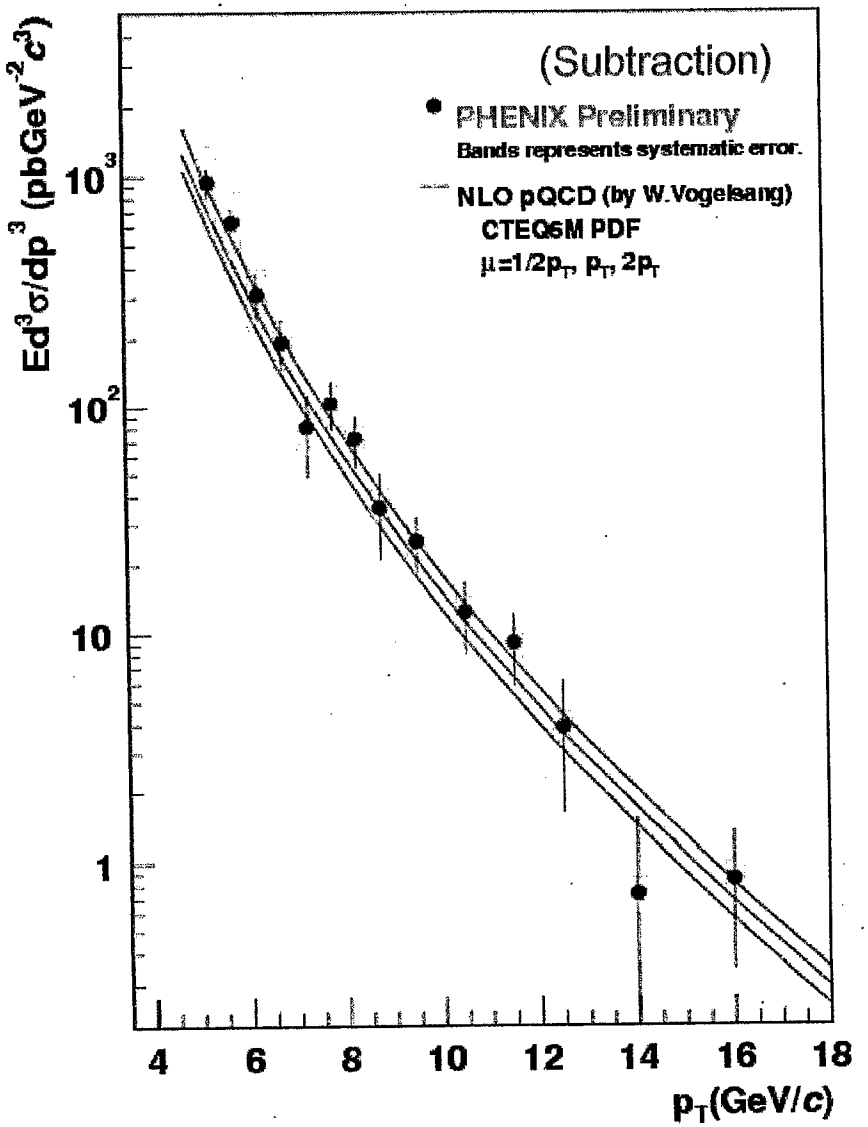

- NLO-pQCD calculation
  - Private communication with W.Vogelsang
  - CTEQ6M PDF.
  - Gluon compton scattering + fragmentation photon
  - Set Renormalization scale and factorization scale pT/2,pT,2pT

The theory calculation shows a good agreement with our result.

Summary

— The prompt photon cross section for 200GeV p+p collisions has been measured at PHENIX.

—In the analysis, it is important to tag π^0.

—The isolation cut improves the signal-to-noise ratio (important for future spin asymmetry measurement) without significantly reducing the signal.

—NLO pQCD calculation agrees well with our measurement.

Backup slides

EMCal (PbSc)

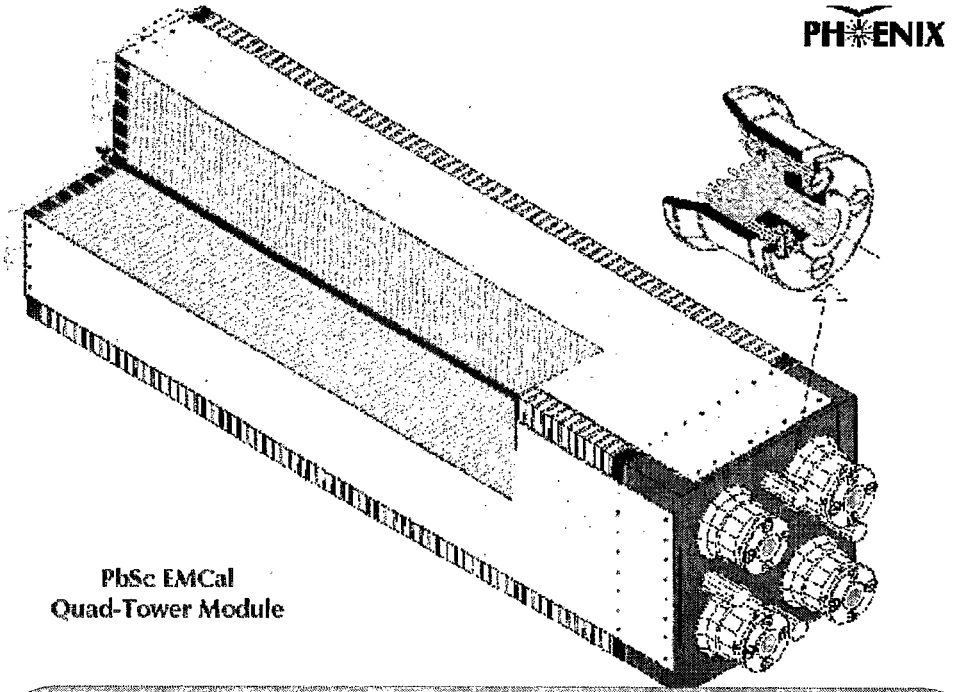

	PbSc
Size(cm x cm)	5.52 x 5.52
Depth(cm)	37.5
Number of towers	15552
Sampling fraction	~20%
η cov.	0.7
φ cov.	90+45deg
η/mod	0.011
φ/mod	0.011
X_0	18
Molière Radius	~3cm

Sandwich type calorimeter
- Lead plates 55.2x55.2x1.5mm
- Scintillator plates 110.4x110.4x4mm

Shish-kebab geometry wave shifter fiber readout
- 6x6 fibers → 1 PMT = 1 tower
- 2 x 2 towers = 1 module
- 6 x 6 module = 1 super module
- 6 x 3 super module = 1 sector

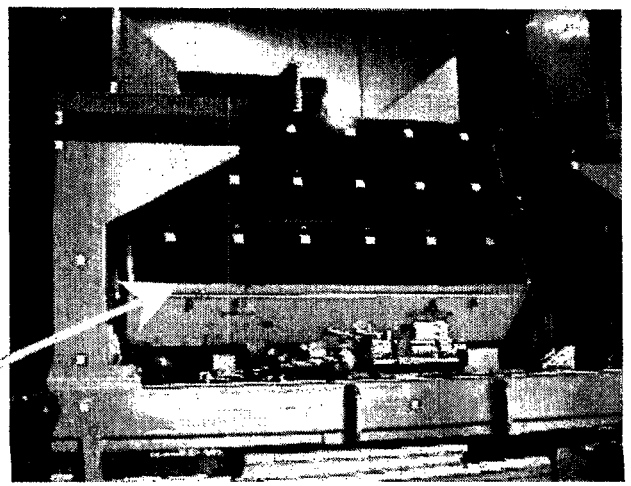

PbSc sector 2.0m x 4.0m

EMCal Trigger

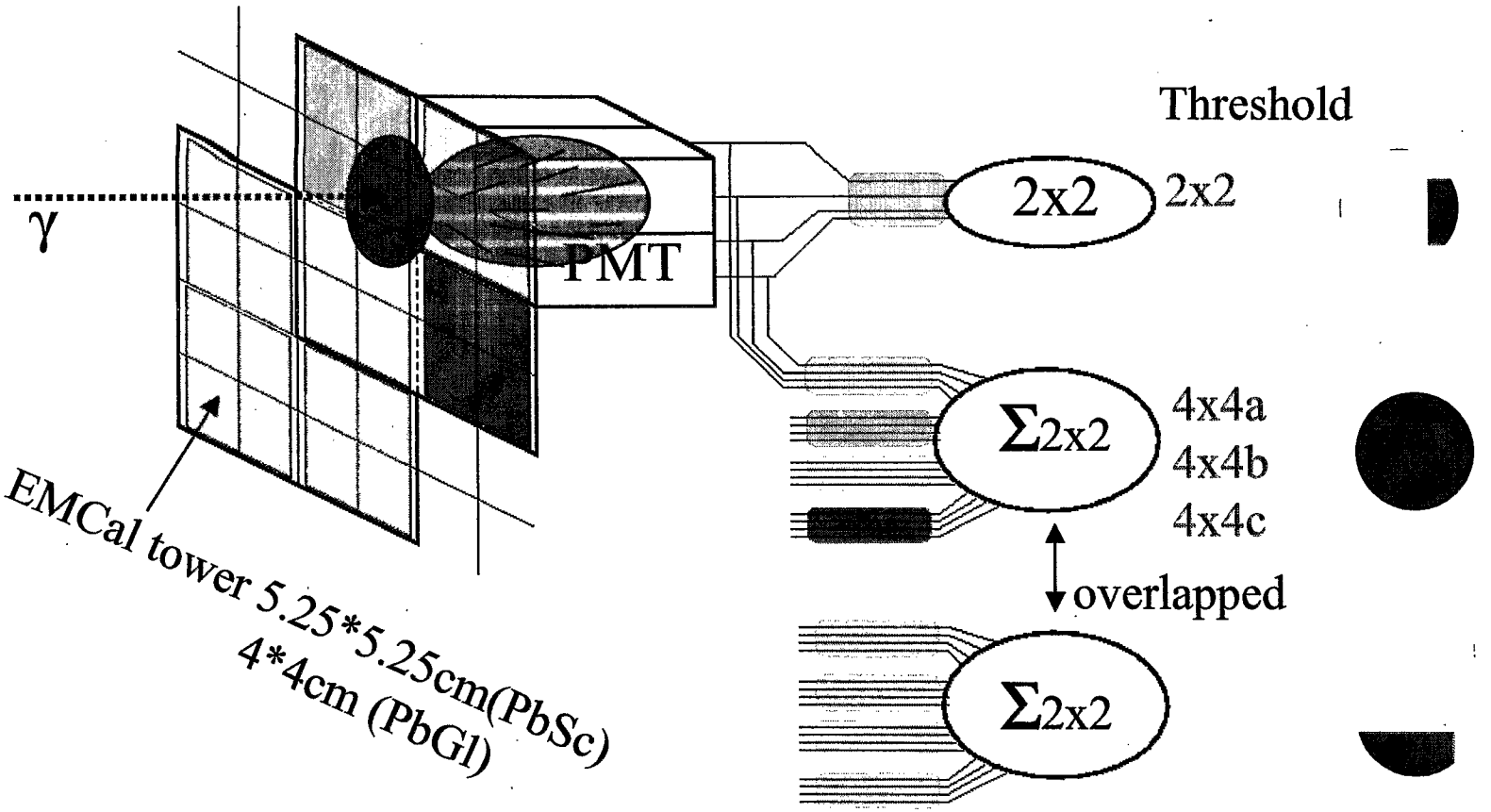

EMCal = 172 Super modules (SM)

36 tiles (~60*60cm)

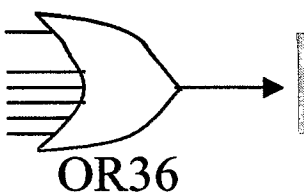

1 trigger bit

EMCal Trigger

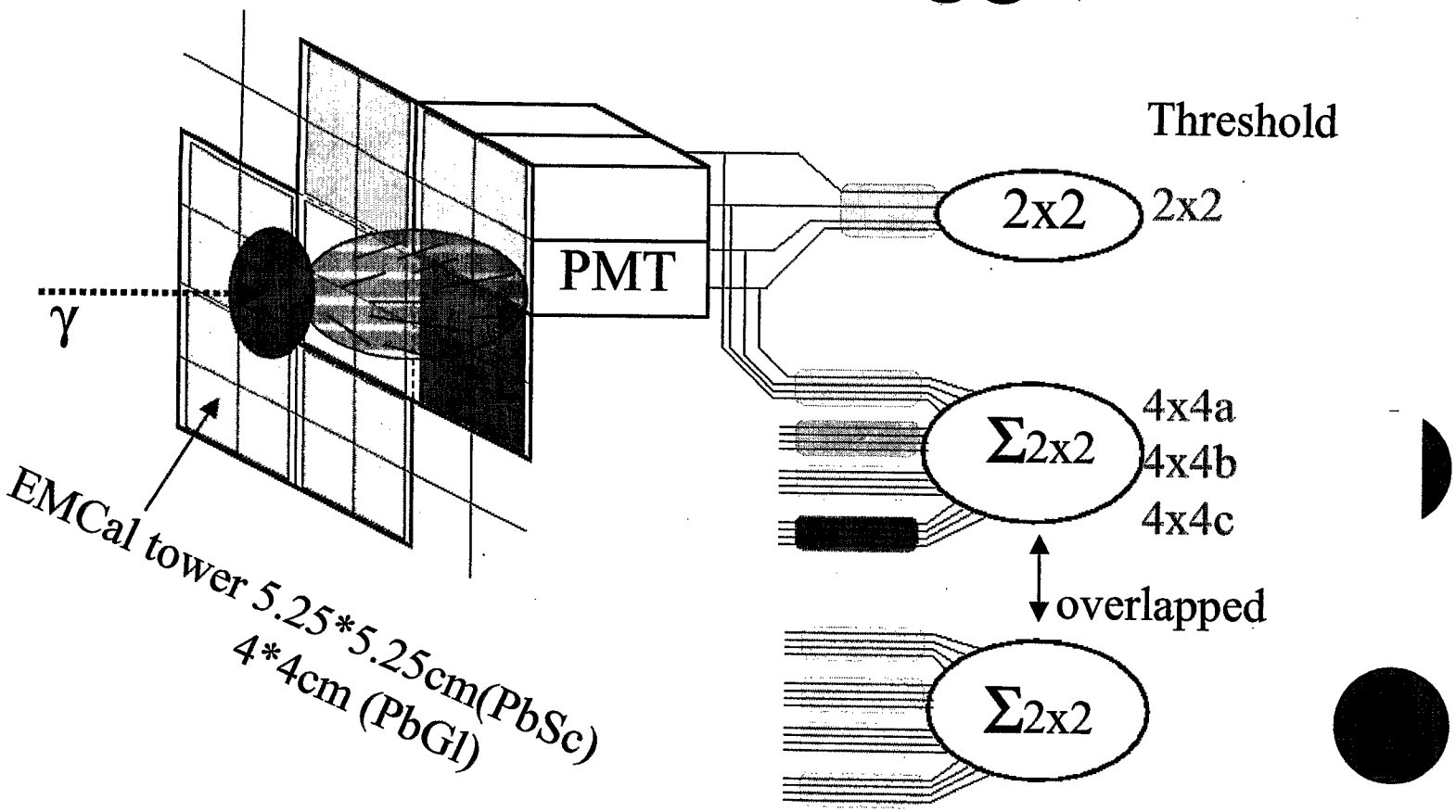

EMCal = 172 Super modules (SM)

36 tiles (~60*60cm)

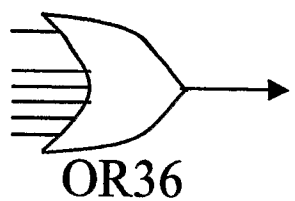

1 trigger bit

EMCal Trigger performance

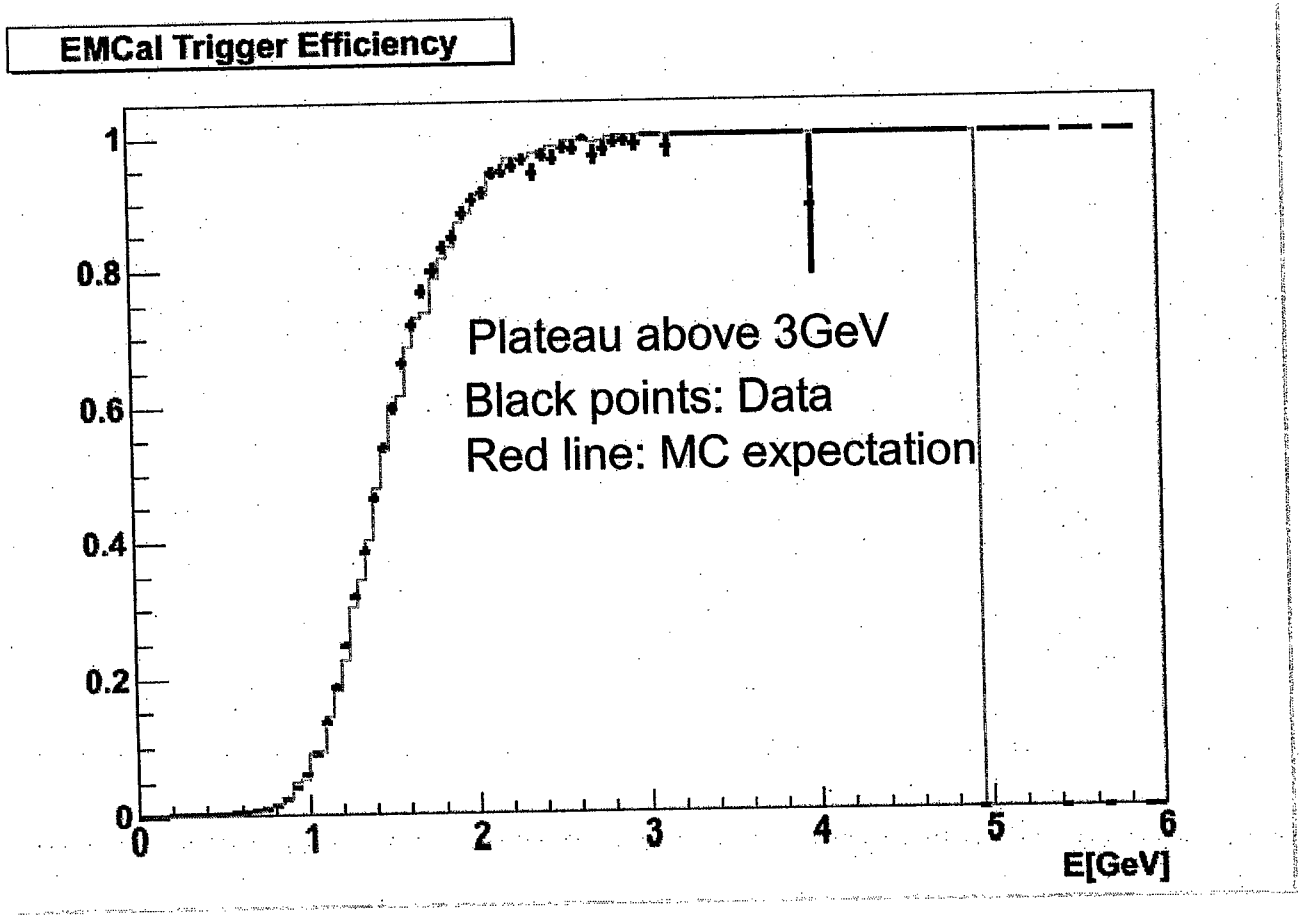

Electromagnetic shower shape cut

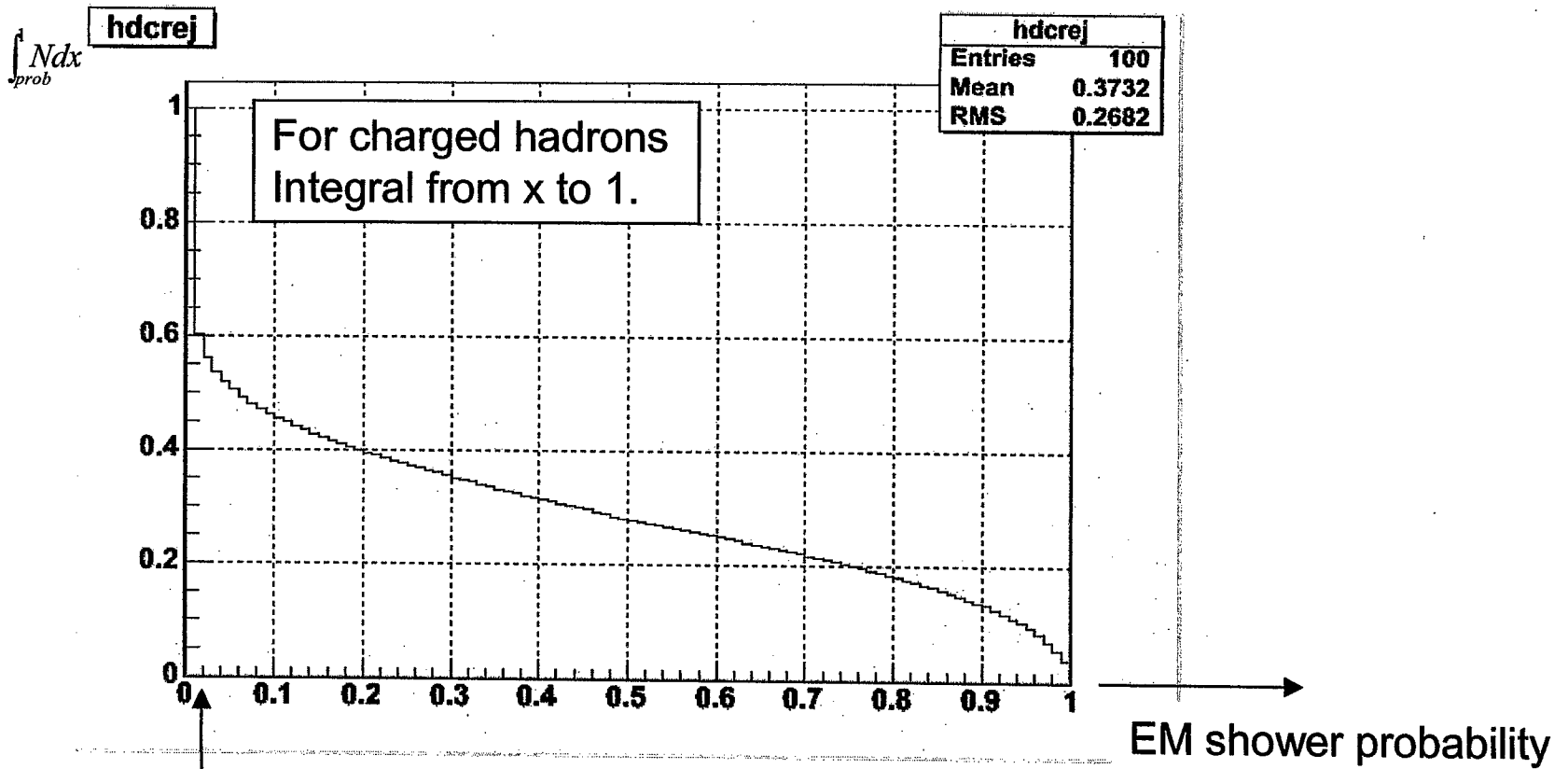

With Prob>0.02 cut

40% of hadronic shower hits are rejected

98% of photons are remained

EM shower cut (photon)

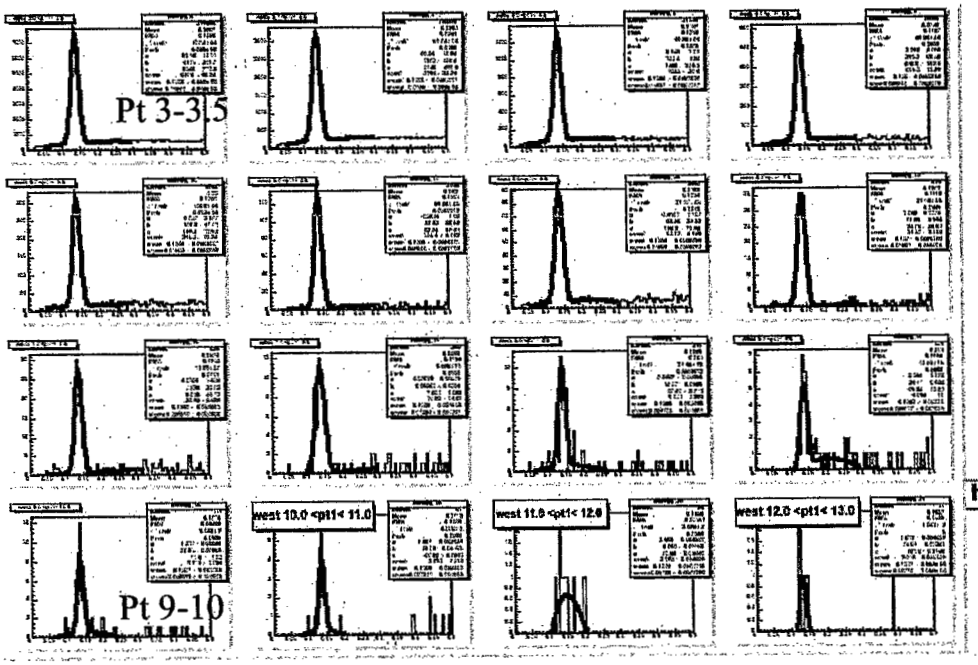

Photons are selected from pi0 mass window

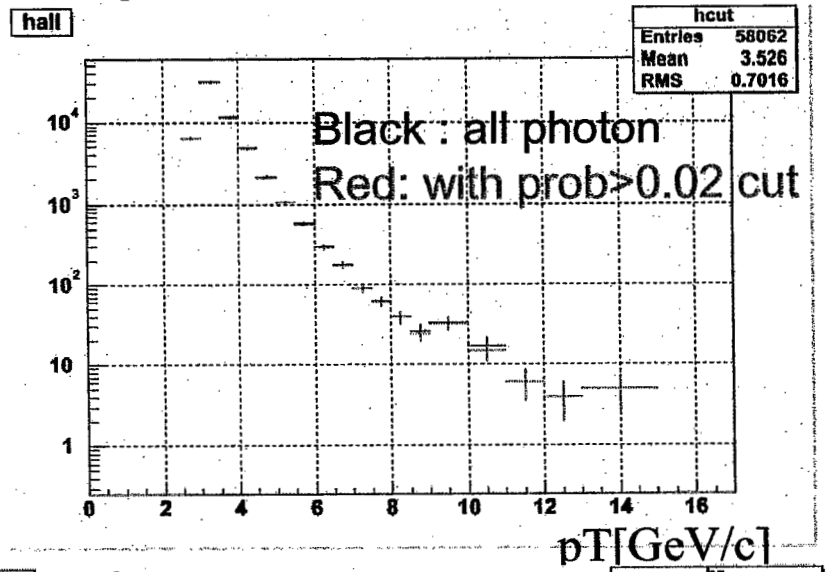

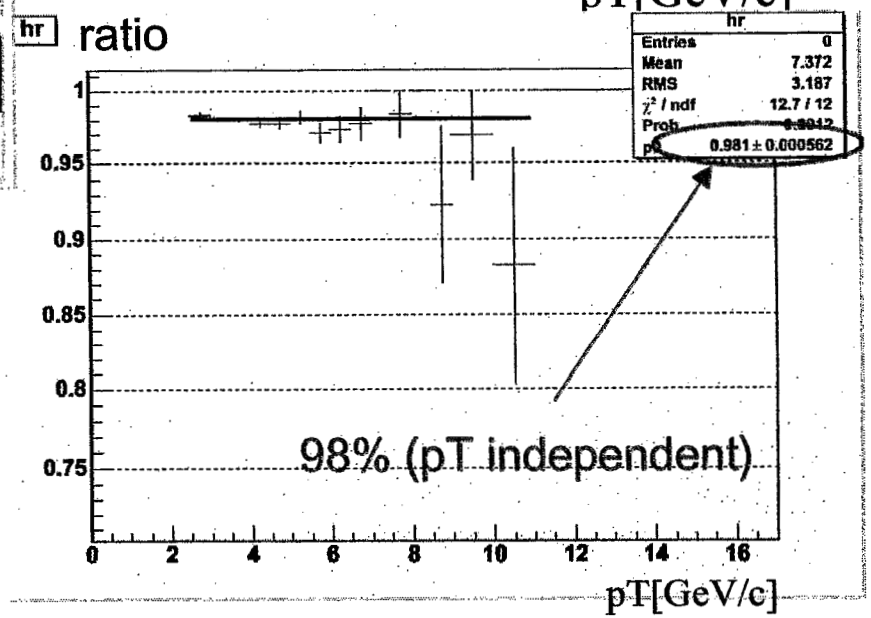

Counts (PbSc west)

ecore>3GeV
PC3 dead area is masked off.

The difference of 3 converter runs is consistent to electron group's study.

no_cut tof prob			
all	1_1	1_2	1_3
pc3match	2_1	2_2	2_3
dcmatch	3_1	3_2	3_3
dcmatch(n0>0)	4_1	4_2	4_3
dcmatch(n0>1)	5_1	5_2	5_3

run87618-88006 40mil
#event 395M
14618 14493 13545 (92%) =1_3/1_1
2510 2491 1926 (77%) =2_3/2_1
1254 1244 770 (61%) =3_3/3_1
405 403 314 (78%) =4_3/4_1
362 361 296 (82%) =5_3/5_1

pc3match ratio : 14% =2_3/1_3
dcmatch ratio : 5.6% =3_3/1_3
electron ratio(n0>0) : 2.3% =4_3/1_3
electron ratio(n0>1) : 2.2% =5_3/1_3

electron/dcmatch(org) : 29% =5_1/3_1
electron/dcmatch : 38% =5_3/3_3
Electron/1M events : 0.75

run88825-89211 10mil
#event 841M
33879 33452 31270 (92%)
5542 5491 4238 (76%)
2630 2618 1533 (58%)
663 659 437 (66%)
565 562 403 (71%)

pc3match ratio : 14%
dcmatch ratio : 4.9%
electron ratio(n0>0) : 1.4%
electron ratio(n0>1) : 1.3%

electron/dcmatch(org) : 21%
electron/dcmatch : 26%
Electron/1M events : 0.48

Run88007-88824, 89212-92466
#event 4315M
170922 168940 157748 (92%)
26880 26666 20221 (75%)
12695 12632 7002 (55%)
2972 2960 1858 (62%)
2488 2477 1678 (67%)

pc3match ratio : 13%
dcmatch ratio : 4.4%
electron ratio(n0>0) : 1.2%
electron ratio(n0>1) : 1.1%

electron/dcmatch(org) : 20%
electron/dcmatch : 24%
Electron/1M events : 0.39

9% conversion

Counts (energy dependence)

Ecore>3GeV	Ecore>5GeV	Ecore>7GeV
Run88007-88824, 89212-92466	Run88007-88824, 89212-92466	Run88007-88824, 89212-92466
#event 4315M	#event 4315M	#event 4315M
170922 168940 157748 (92%) photon 97%	8660 8372 7868 (91%) photon 97%	1279 1177 1080 (84%) photon 95%
26880 26666 20221 (75%)	1358 1330 1048 (77%)	188 181 141 (75%)
12695 12632 7002 (55%)	577 572 341 (59%)	81 79 45 (56%)
2972 2960 1858 (62%)		
2488 2477 1678 (67%)	267 265 153 (57%)	54 53 34 (63%)
pc3match ratio : 13%	pc3match ratio : 13%	pc3match ratio : 13%
dcmatch ratio : 4.4%	dcmatch ratio : 4.3%	dcmatch ratio : 4.2%
electron ratio(n0>0) : 1.2%	electron ratio(n0>0) :	electron ratio(n0>0) :
electron ratio(n0>1) : 1.1%	electron ratio(n0>1) : 1.9%	electron ratio(n0>1) : 3.1%
electron/dcmatch(org) : 20%	electron/dcmatch(org) : 46%	electron/dcmatch(org) : 67%
electron/dcmatch : 24%	electron/dcmatch : 45%	electron/dcmatch : 76%
Electron/1M events : 0.39	Electron/1M events : 0.035	Electron/1M events : 0.0079

High pT charged pion contamination can be seen in electron/dcmatch ratio.
Matching behavior looks the same.

Isolation cut cone size

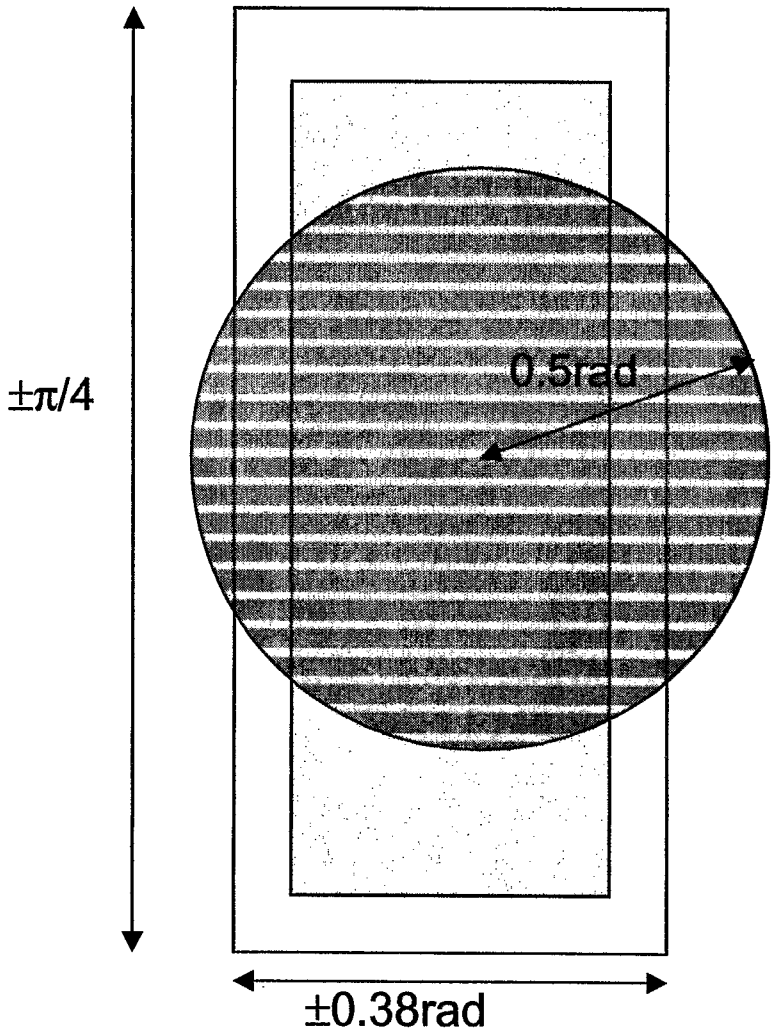

Invariant mass of two photons

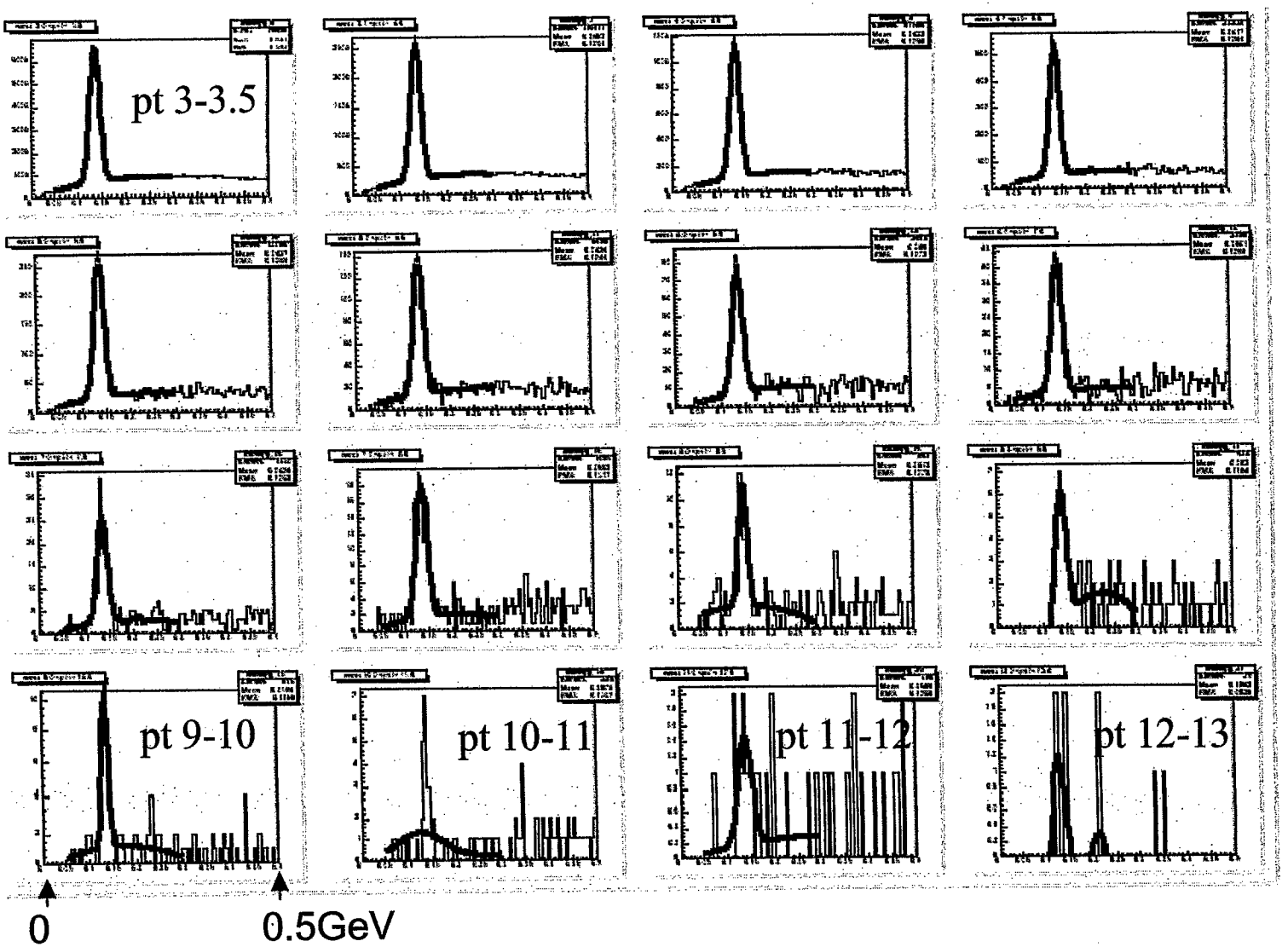

481

Invariant mass of two photons

With the isolation cut

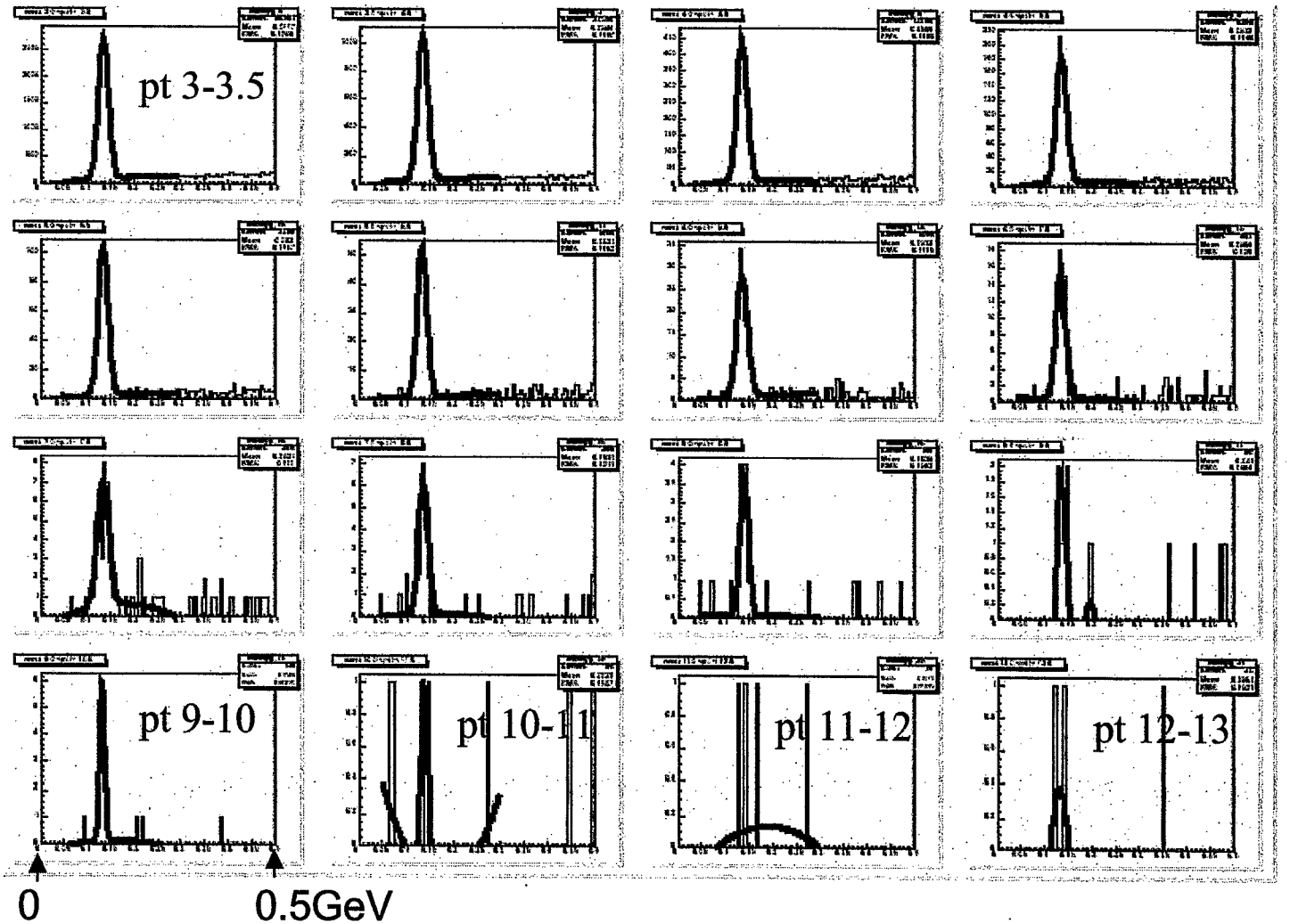

pi0 photon merging

MC tuned with the test beam result

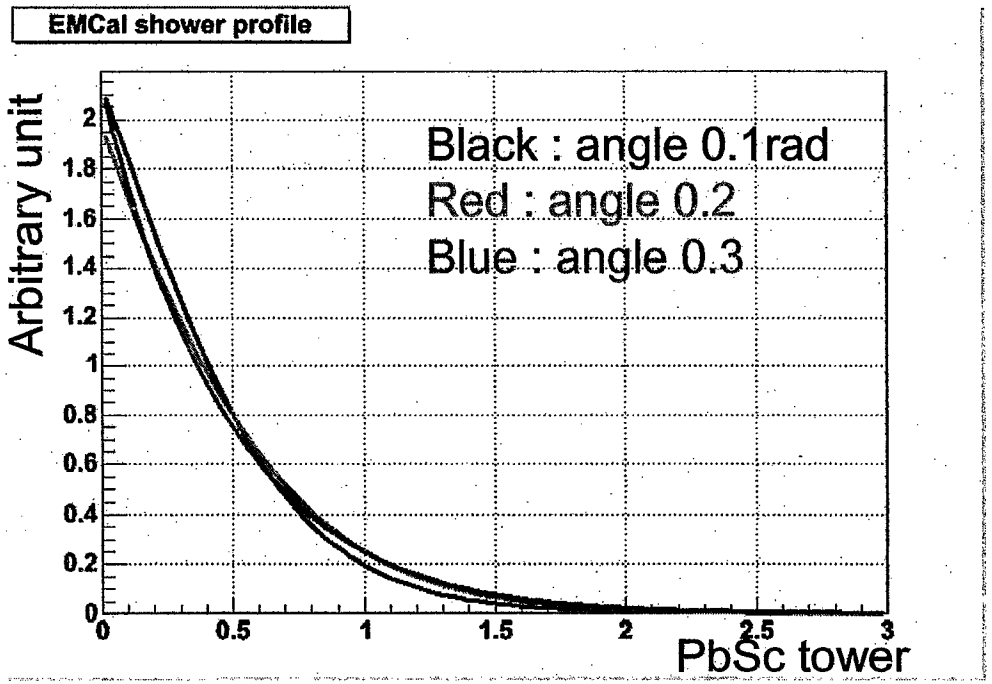

(second tower) / (first tower)

0.2/2 = 10% (tower center)

0.5/1.25=40% (center + 0.3unit)

Pi0 photon merging

At 5m away, distance of 2 photons is

140cm / E_pi0[GeV]
= 25.4 towers / E_pi0[GeV]

For example, 20GeV pi0 makes 10GeV photons with 1.27towers distance.

Numbers show the deposit energy [%] of these two photon in 5x5 towers.

These are merged and is 20GeV cluster, but it can't pass the EMCal shower shape criteria.

---1--- (0,0)

0.0	0.1	0.3	0.1	0.0
0.1	1.6	6.1	1.6	0.1
0.3	6.1	**66.5**	6.1	0.3
0.1	1.6	6.1	1.6	0.1
0.0	0.1	0.3	0.1	0.0

---2--- (0,1.27273)

0.0	0.0	0.1	0.3	0.2
0.0	0.1	1.1	7.0	3.7
0.0	0.2	3.3	**53.8**	17.5
0.0	0.1	1.1	7.0	3.7
0.0	0.0	0.1	0.3	0.2

---1--- (-0.5,0)

0.1	0.7	1.7	0.7	0.1
0.3	5.8	**34.4**	5.8	0.3
0.3	5.8	**34.4**	5.8	0.3
0.1	0.7	1.7	0.7	0.1
0.0	0.1	0.1	0.1	0.0

---2--- (-0.5,1.27273)

0.0	0.1	0.4	1.7	1.1
0.0	0.2	2.8	**30.8**	12.8
0.0	0.2	2.8	**30.8**	12.8
0.0	0.1	0.4	1.7	1.1
0.0	0.0	0.1	0.1	0.1

---1--- (0,-0.5)

0.1	0.3	0.3	0.1	0.0
0.7	5.8	5.8	0.7	0.1
1.7	**34.4**	**34.4**	1.7	0.1
0.7	5.8	5.8	0.7	0.1
0.1	0.3	0.3	0.1	0.0

---2--- (0,0.772727)

0.0	0.1	0.2	0.3	0.1
0.0	0.3	3.2	6.9	1.2
0.0	0.7	14.7	**56.2**	3.6
0.0	0.3	3.2	6.9	1.2
0.0	0.1	0.2	0.3	0.1

---1--- (-0.5,-0.5)

0.3	1.4	1.4	0.3	0.0
1.4	**21.7**	**21.7**	1.4	0.1
1.4	**21.7**	**21.7**	1.4	0.1
0.3	1.4	1.4	0.3	0.0
0.0	0.1	0.1	0.0	0.0

---2--- (-0.5,0.772727)

0.0	0.2	1.0	1.7	0.5
0.0	0.6	11.1	**31.6**	3.1
0.0	0.6	11.1	**31.6**	3.1
0.0	0.2	1.0	1.7	0.5
0.0	0.0	0.1	0.1	0.1

pi0 photon missing ratio (with MC)

Input: pi0 spectra, Energy resolution, Shower size from measurements
The same MC used in pi0 cross section measurement.

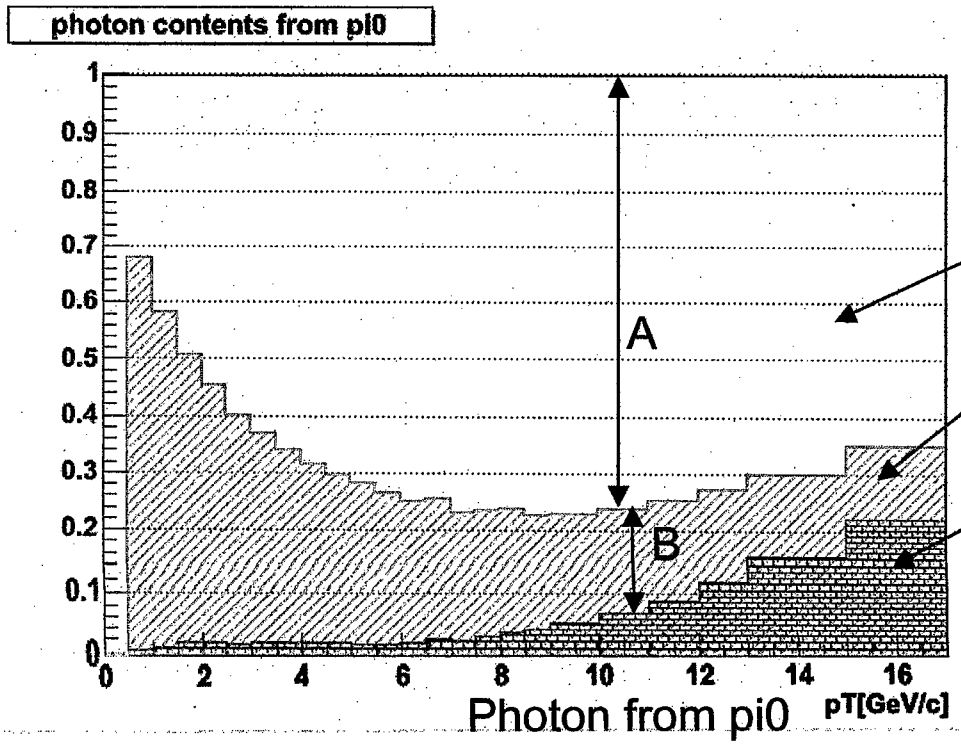

This figure shows components of photon from pi0.

(A) 2 photons tagged as pi0

(B) 1photon (the partner missing)

Merged photons
(to be discarded by the shower shape cut
And those have almost double energy)

Miss/ tag (=B/A)
40% at 5GeV/c
20% at 10GeV/c

Eta/pi0 ratio

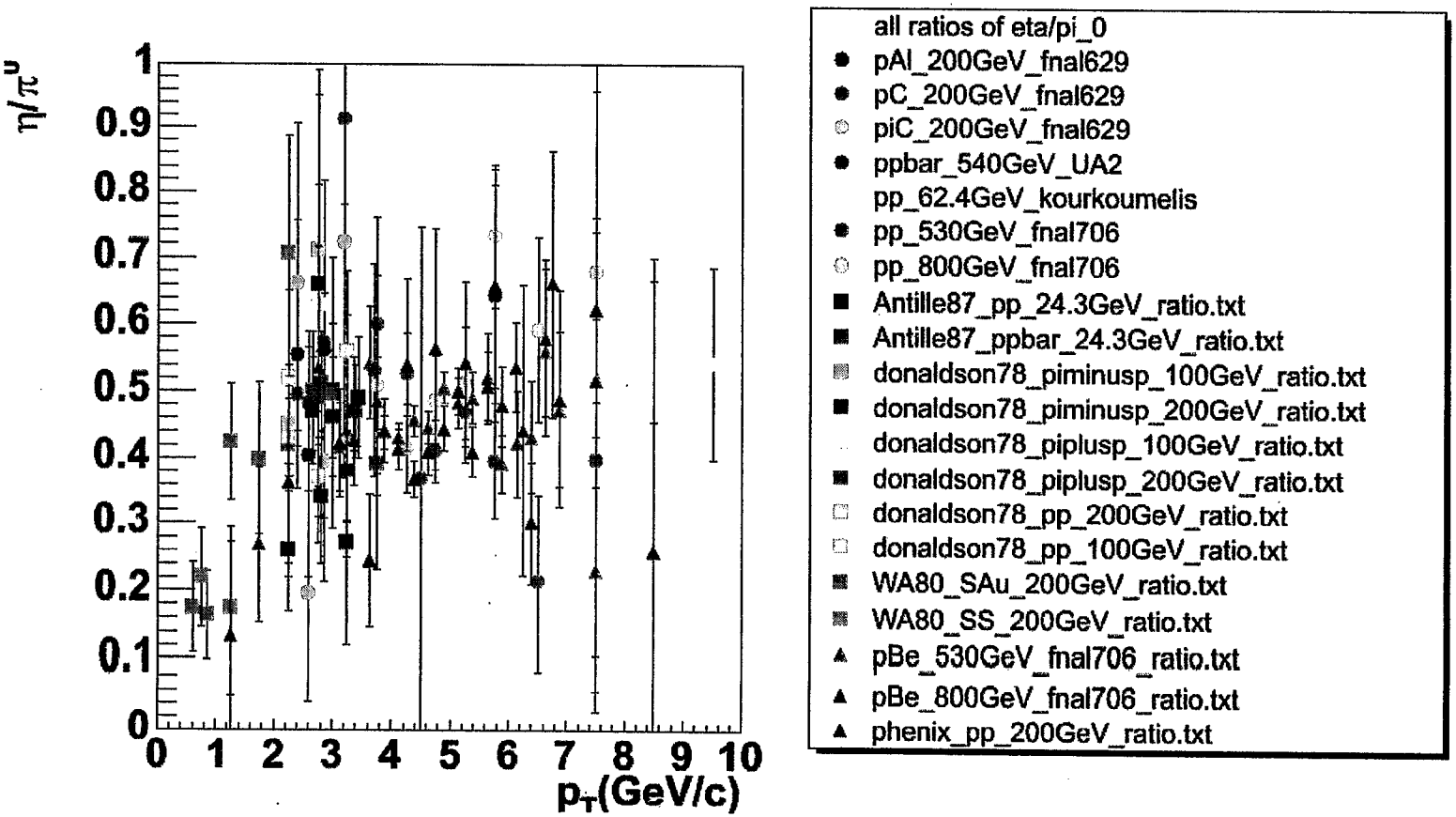

Yields (West arm)

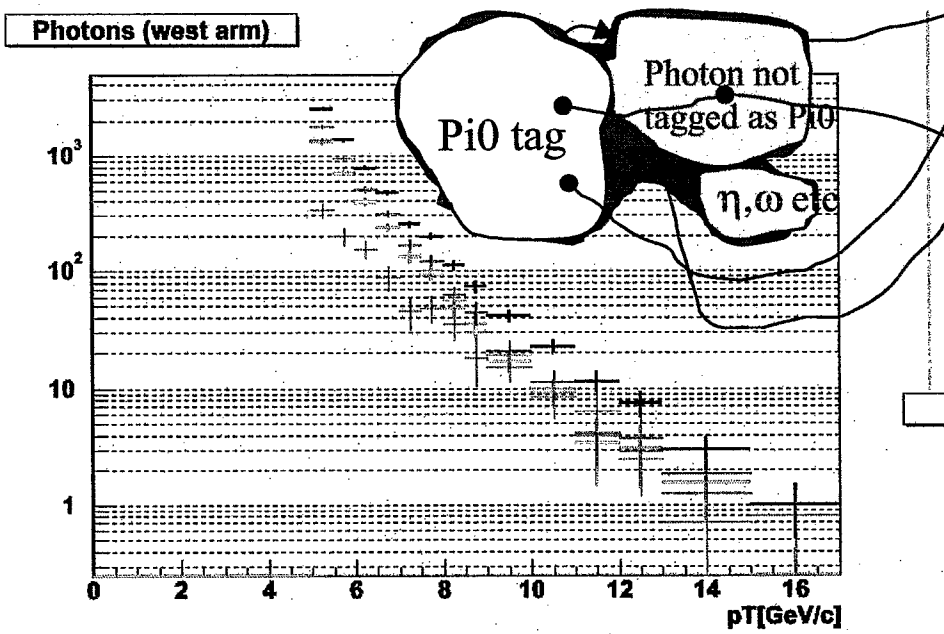

black : all photons
red : photons tagged as pi0
green : applied a combinatorial bg correction to (red)
blue : all pi0 contributions (green *(1+missing ratio))
magenta : (black)−(blue)*1.23

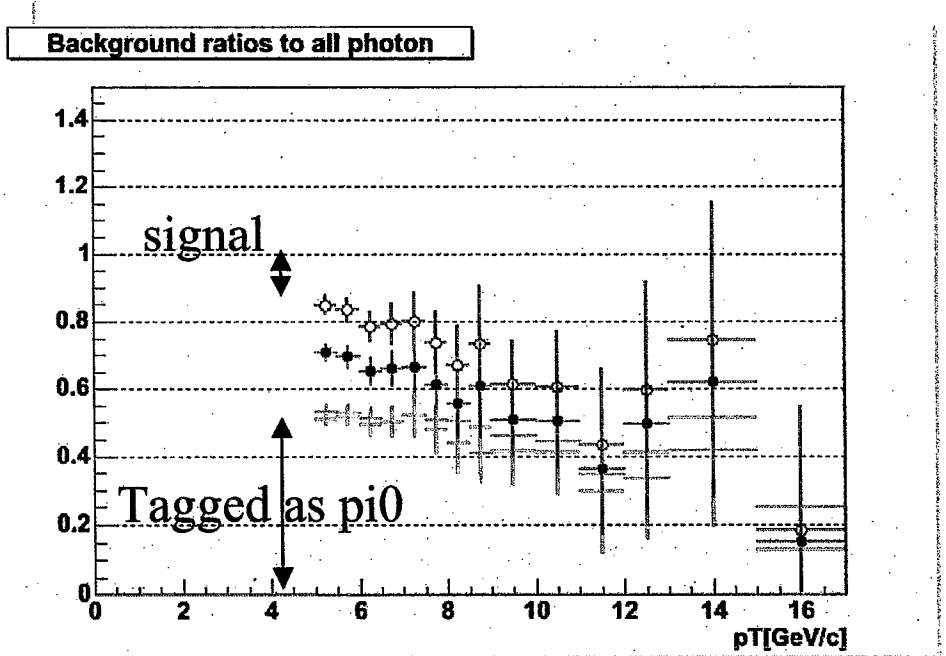

bg ratios to the total
red :
green :
blue :
magenta : all hadron contributions (blue)*1.23

Yields (west arm)
(with an isolation cut)

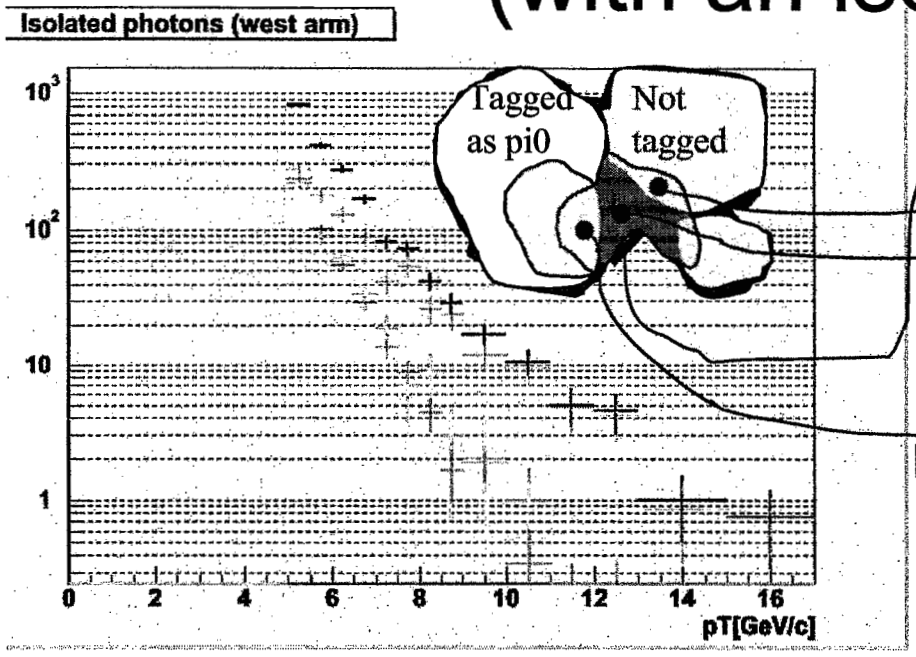

black : all isolated photons
red : isolated photon tagged as pi0
green : applied a combinatorial bg correction to (red)
blue : isolated photon estimated from isolated pi0s
magenta : (black)−(green+blue)*1.23

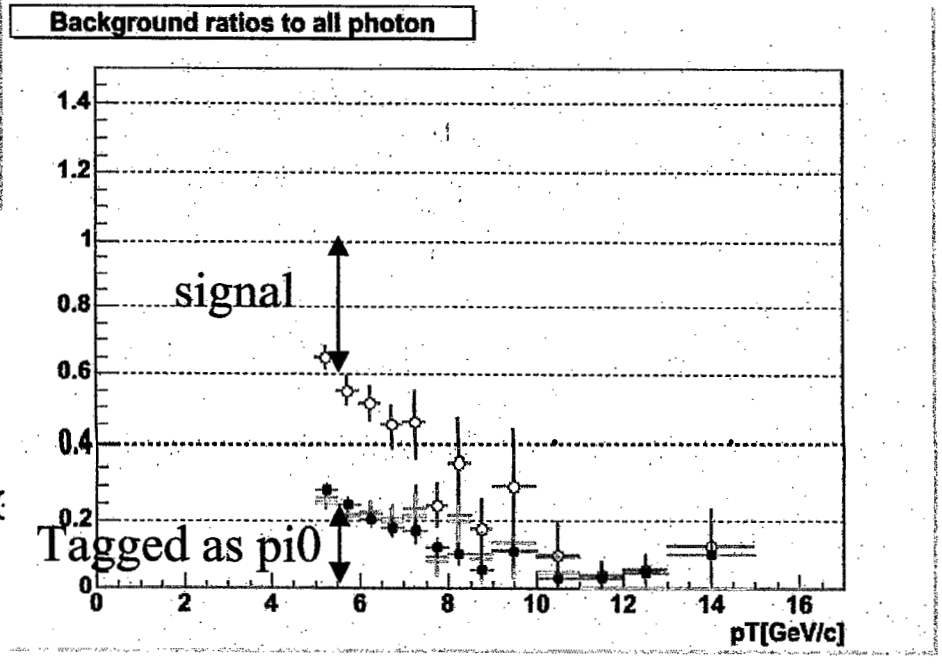

bg ratios to the total
red:
green:
blue:
magenta: all hadron contribution (green+blue)*1.23

Systematic error sources

For isolation cut method	Lowest 5-5.5 [GeV/c]	Highest 15-17 [GeV/c]	
Pi0 photon estimation	16%	2	Point to point
Non pi0 contribution	8	1	
Photon acceptance and smearing	10	10	
Photon conversion effect	1	1	
Luminosity measurement	12	12	global
BBC trigger bias	3	3	
Total (quadratic sum)	24%	16	

Comparison to NLO pQCD calculation

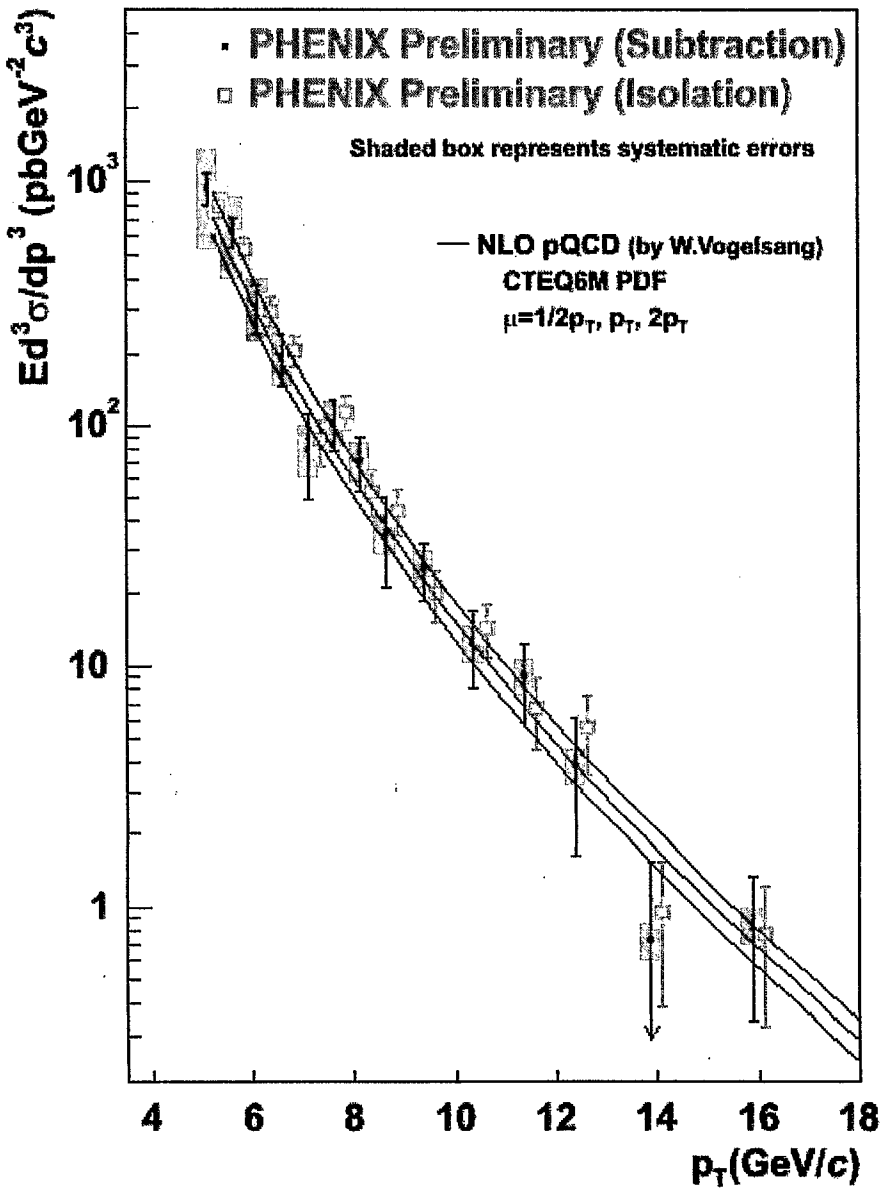

- NLO-pQCD calculation
  - Private communication with W.Vogelsang
  - CTEQ6M PDF.
  - direct photon + fragmentation photon
  - Set Renormalization scale and factorization scale pT/2,pT,2pT

The theory calculation shows a good agreement with our result.

(RBRC)

Results (gamma/pi0 ratio)

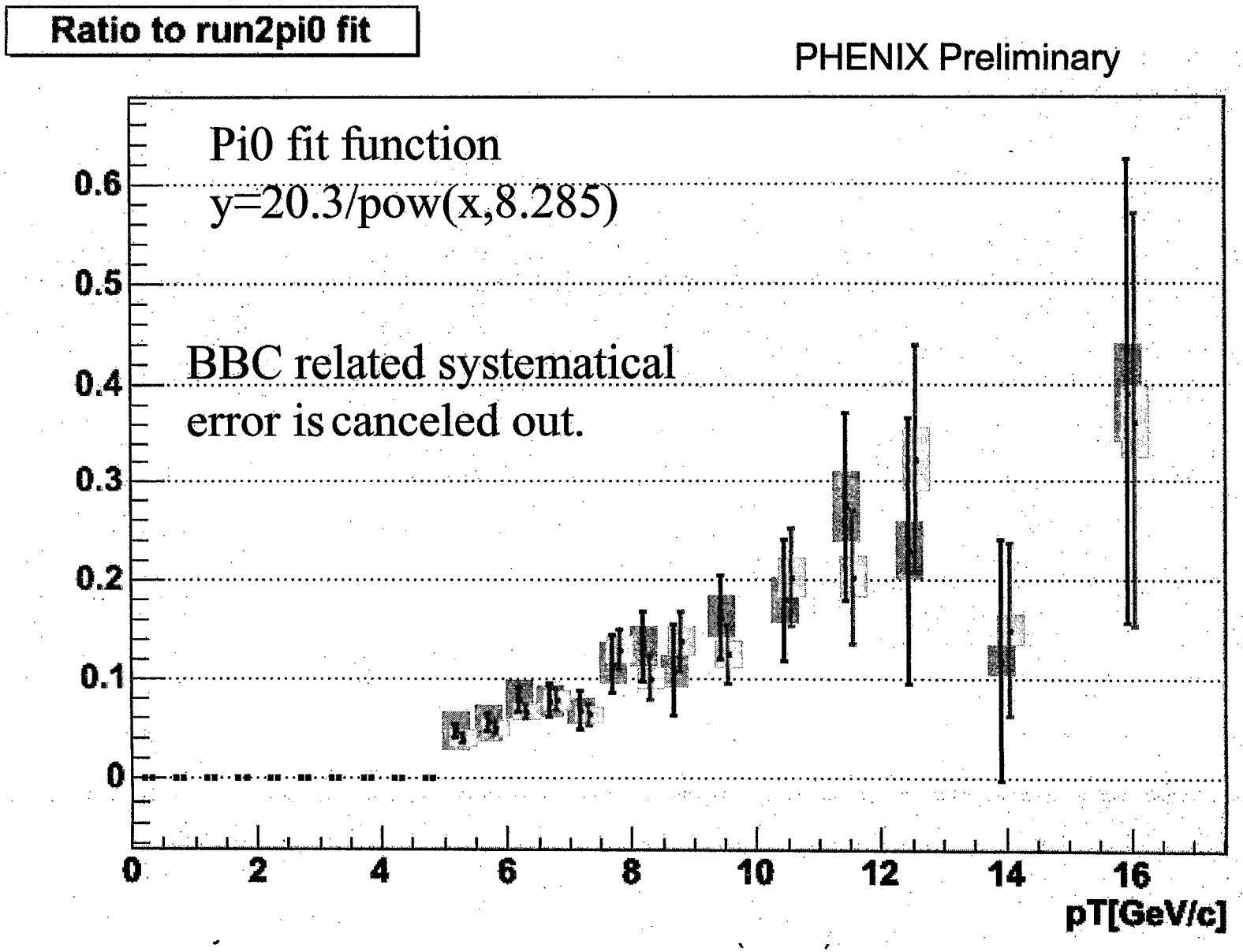

Comparison

- Comparison with existing data from p+p and p+pbar collisions
  - The cross section increases systematically as the energy increases.

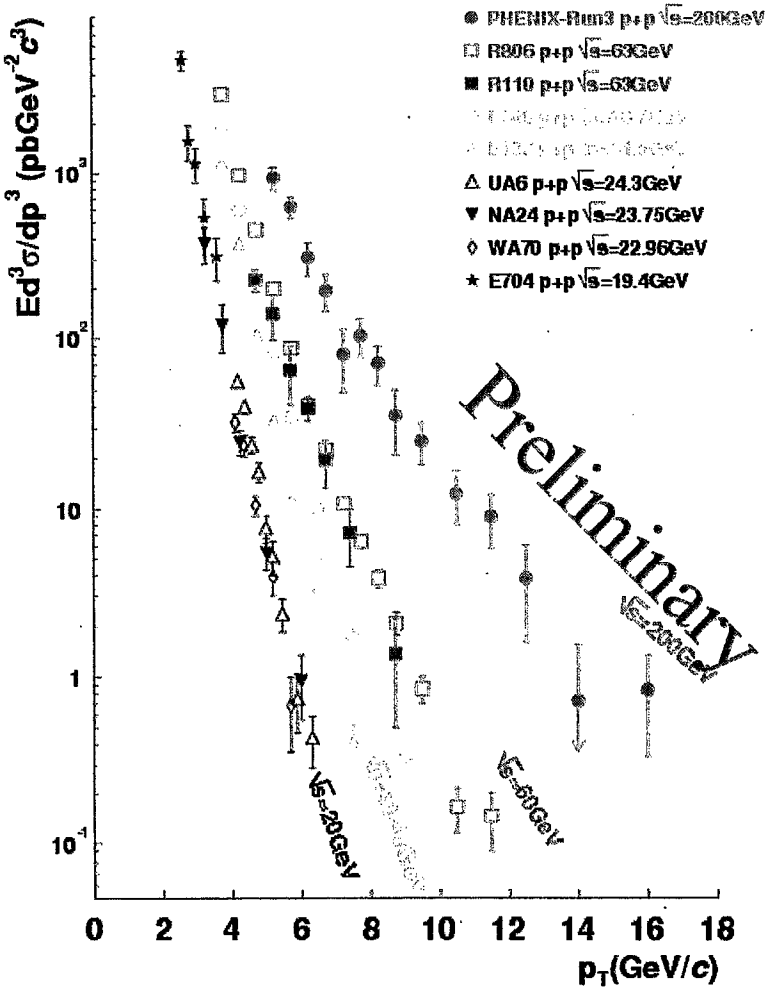

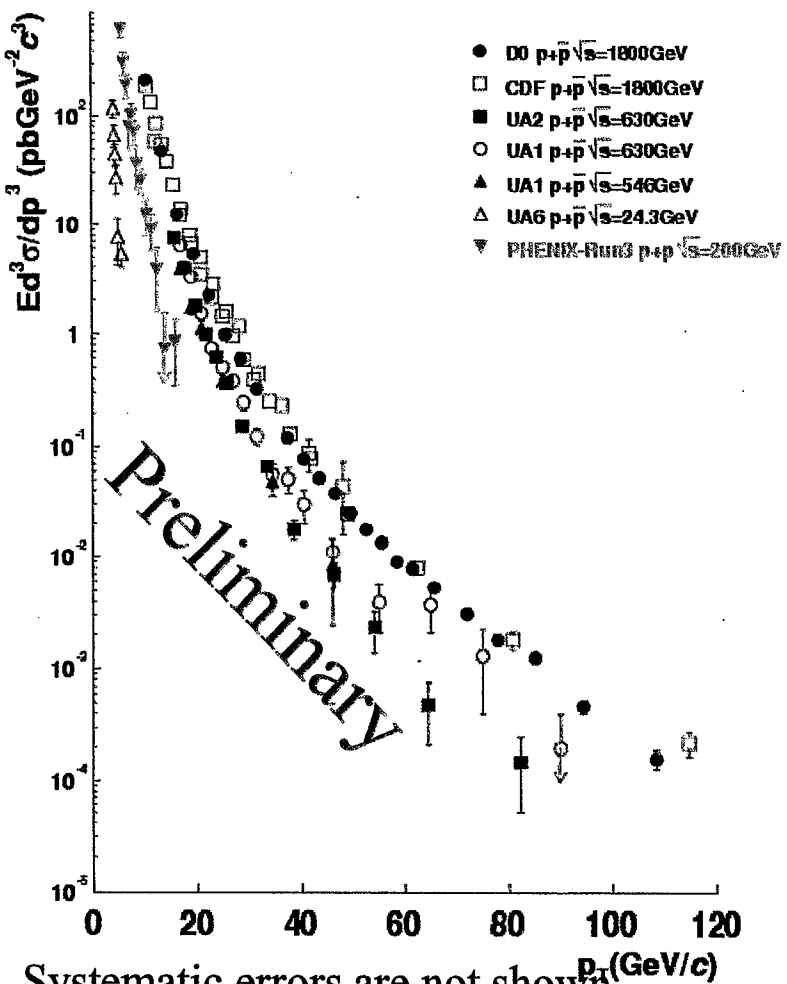

Systematic errors are not shown

x_T scaling

- QCD理論によると、以下の仮定
  - PDFとFFのQ^2スケーリング
  - Coupling constant(α_s)がQ^2に非依存。

$$\sigma = \left(\sqrt{s}\right)^{-n} \times F\left(x_T\right)$$

n=定数。$x_T=2p_T/\sqrt{s}$

  - 相互作用項と構造を表す項に分離

    ➔x_Tスケーリング
  - 定数nに対する予想
    - Leading order n=4
    - Next-to-leading order: n=4+α

x_Tスケーリング則n=5付近で成立

今回得られたデータを過去のデータ($\sqrt{s}$>20GeV)と比較して、x_Tスケーリング則がn=5付近で成り立つ

X-T scaling shows a point like interaction of the measurement.

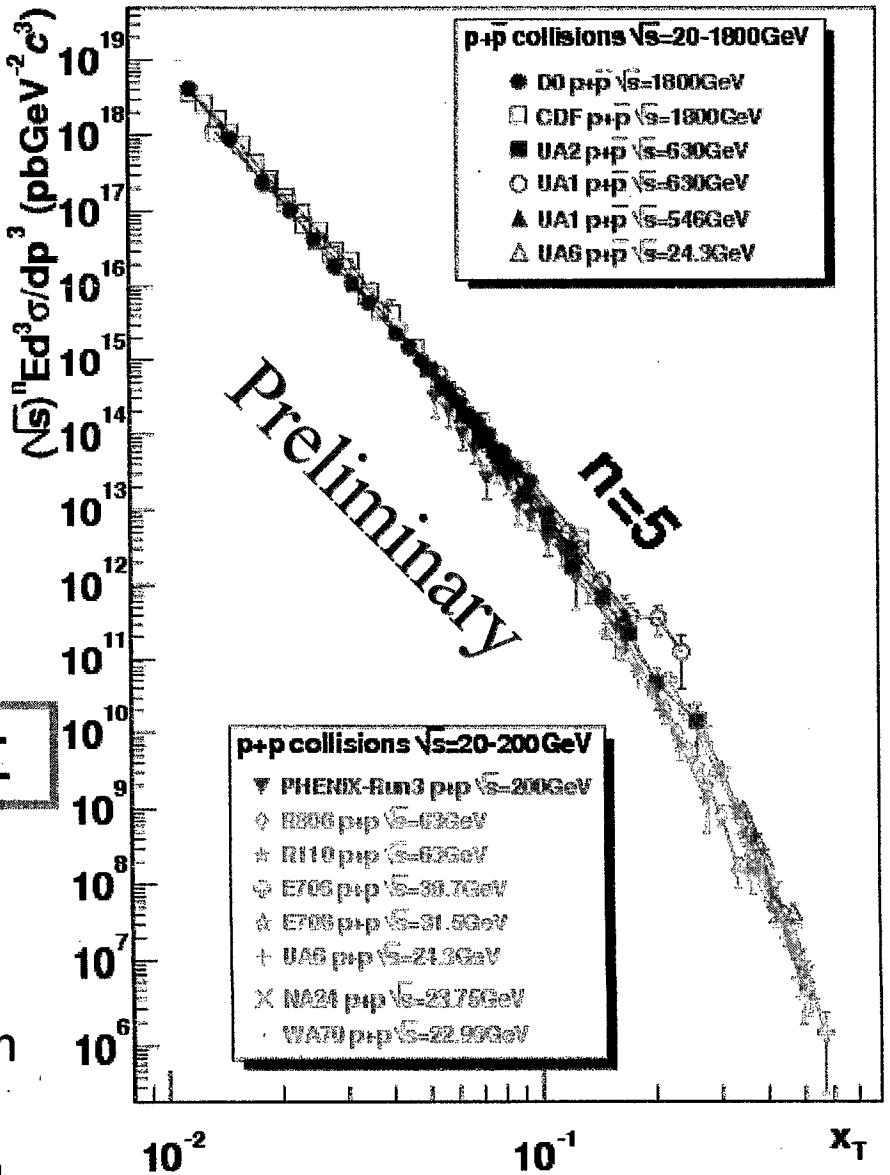

Bias on Physics Process

- Two processes
  - Direct
  - Fragmentation

- Direct photon measurement at pT>5GeV/c is dominated by direct process.
  - The difference between two methods is small.

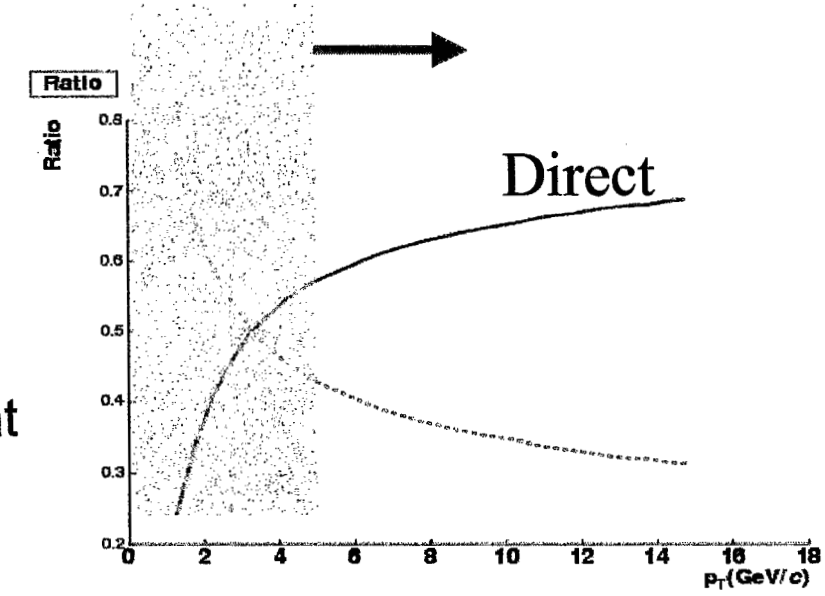

Private communication with W.Vogelsang

Fragmentation

Longitudinal Progress at STAR

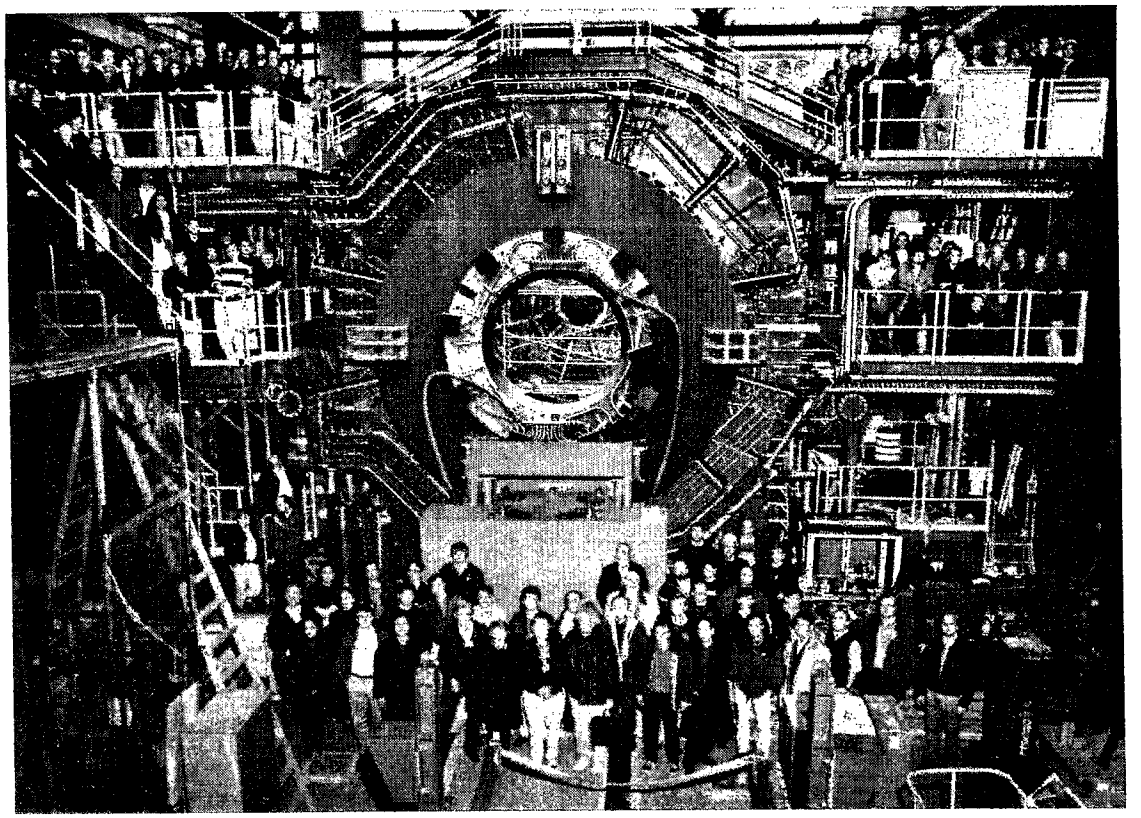

J. Sowinski
for the
STAR
Collaboration

- Spin related hardware improvements to STAR
- Jets and π^0s in '04 and '05 runs
- Sivers Functions from jets at mid-rapidity

STAR Detector

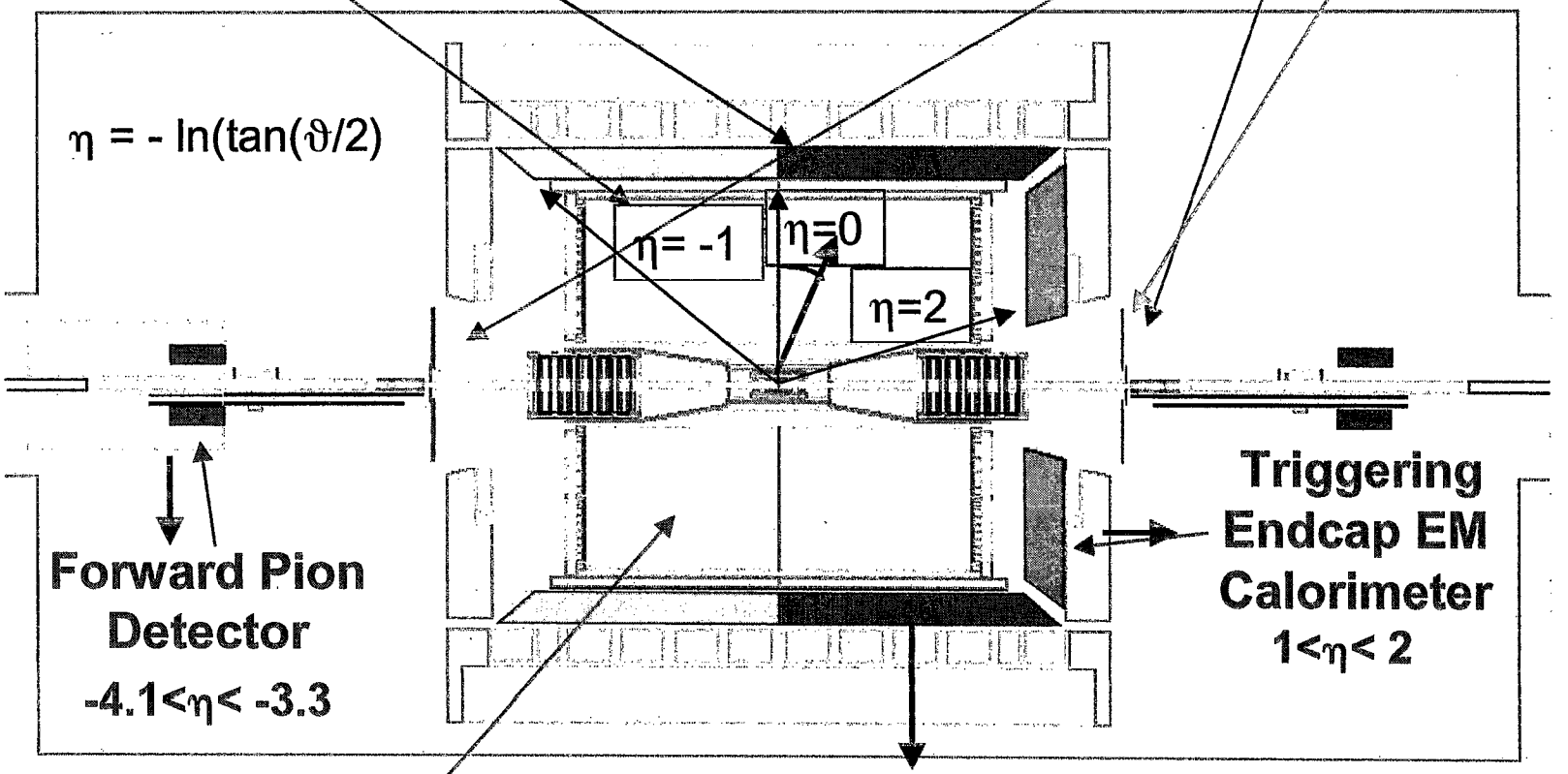

2005

Endcap ElectroMagnetic Calorimeter

2003 1/3 Towers
2004 All Towers
1/3 SMD
2005 Fully Instr.

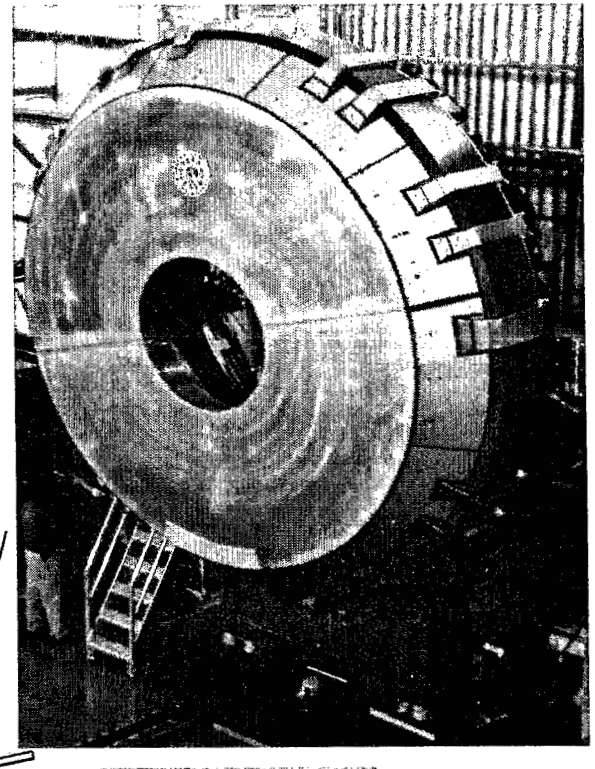

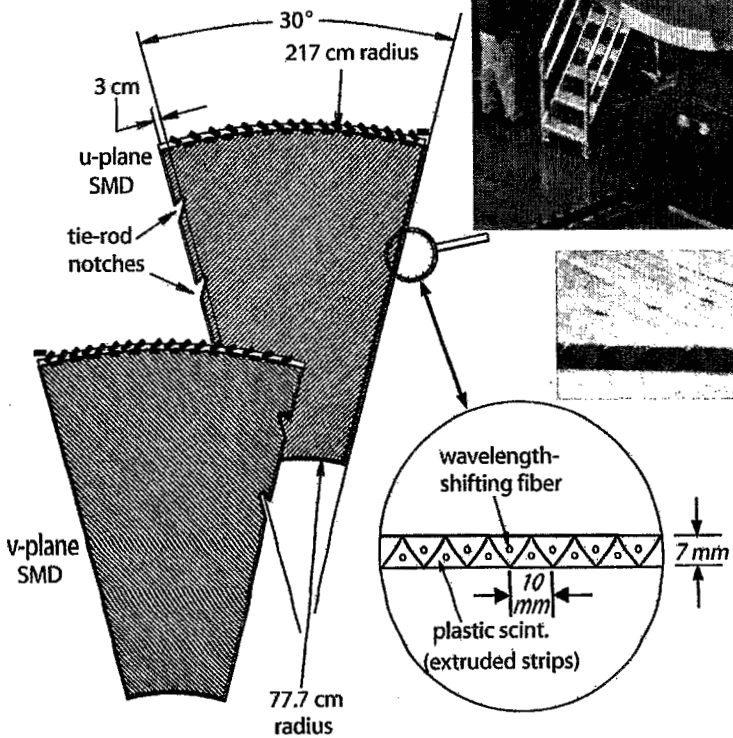

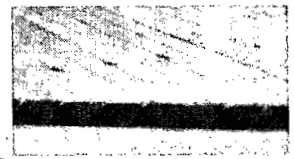

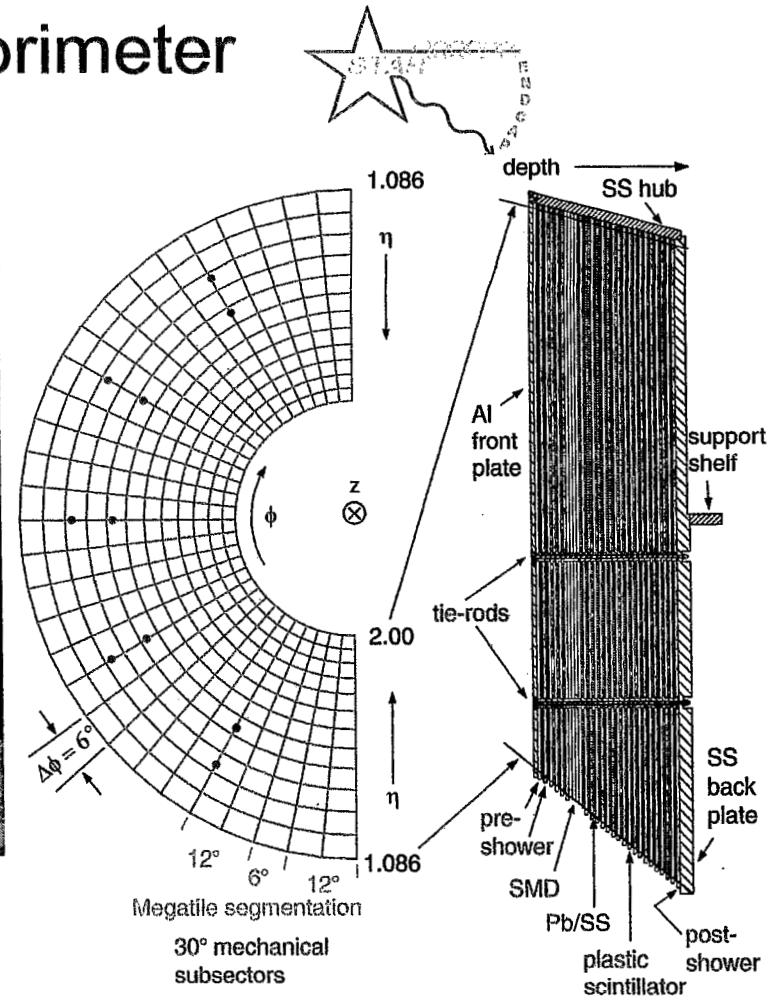

- Pb Scintillator sampling calorimeter – 21 rad. lengths
- 720 Towers give EM energy
- Shower Max. Detector for π^0/γ discrimination
- Pre- and post-shower det's for e/h discrimination
- 9,792 channels read out
- High Tower and Jet Patch triggers

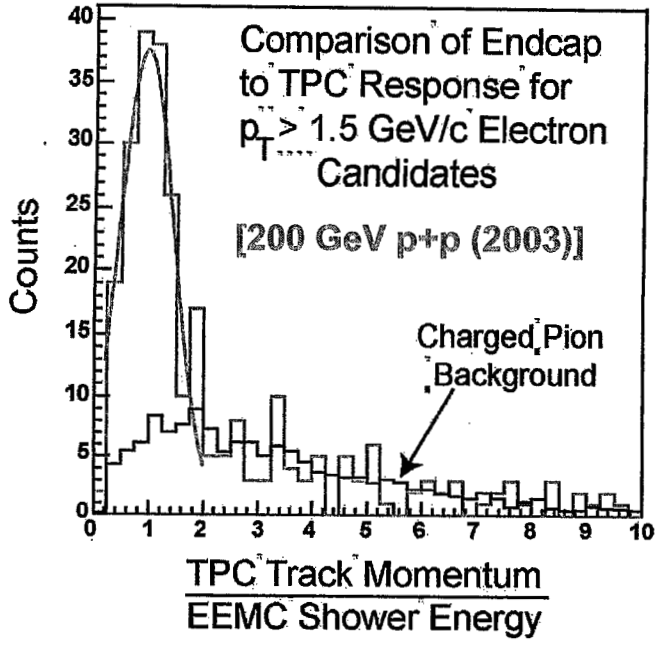

SMD profiles for a 9 GeV π^0 candidate

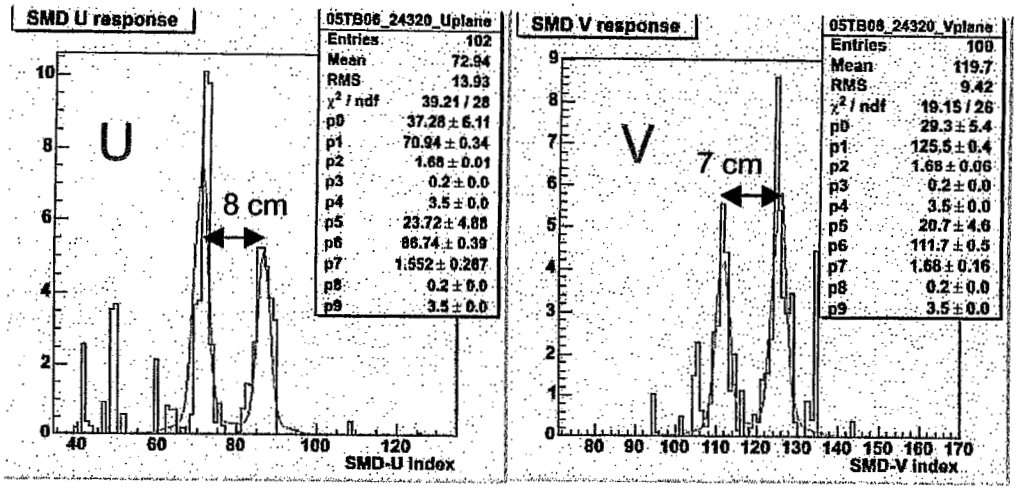

Online tower-only π^0 reconstruction, 200 GeV Au+Au

Charged tracks matched to fired EEMC towers for a 62 GeV Au+Au event. 2004 Data MIPs ~ 0.3GeV γ

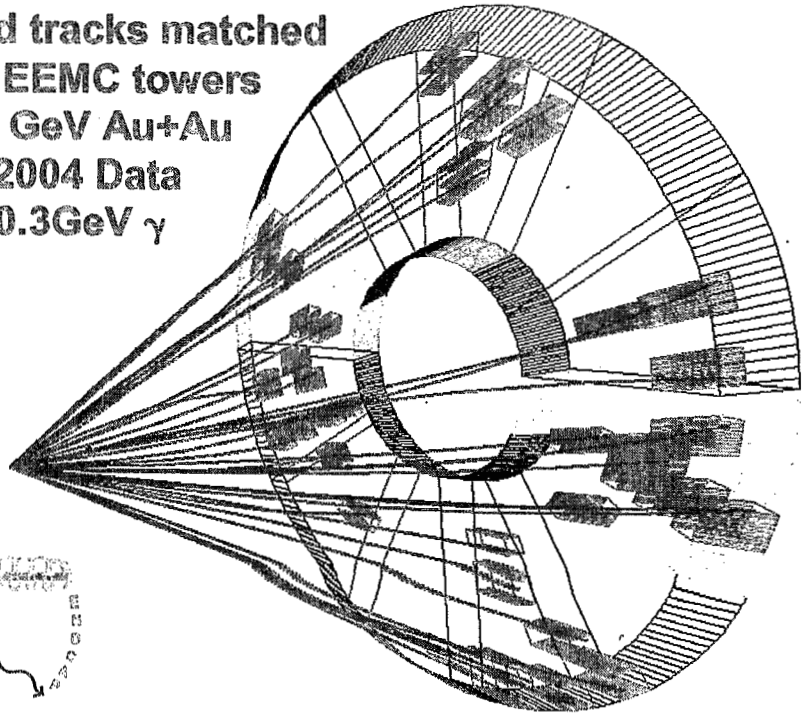

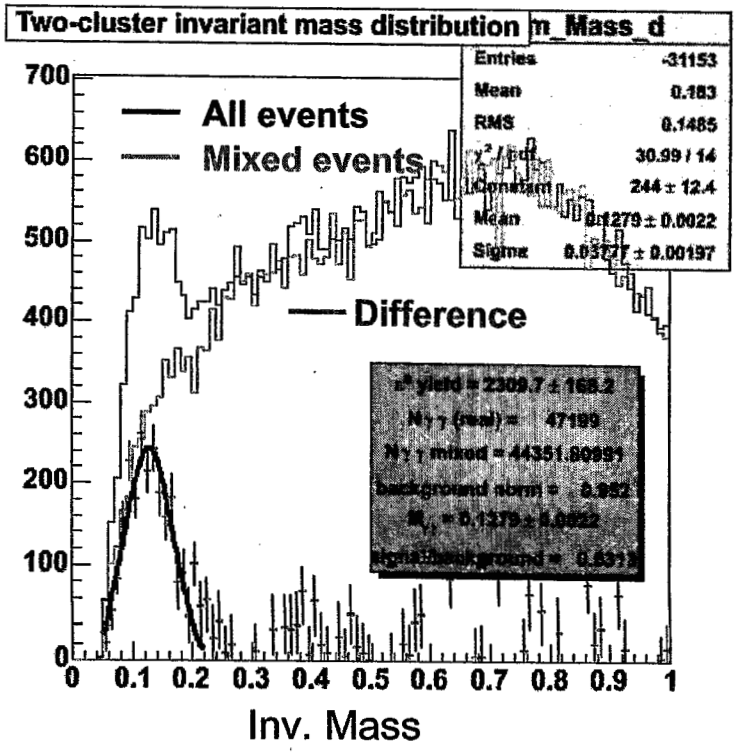

Barrel ElectroMagnetic Calorimeter

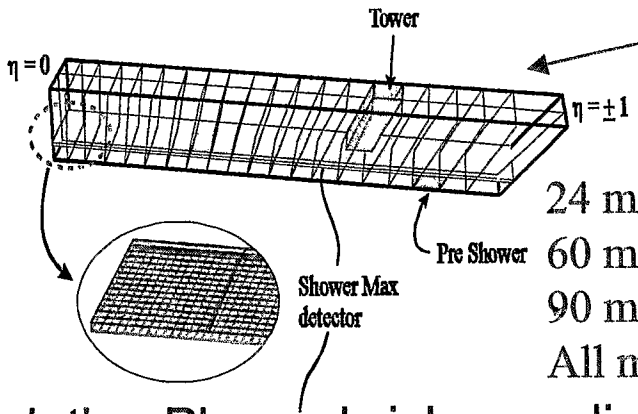

One module = 40 towers

24 modules	FY02
60 modules	FY03
90 modules	FY04
All modules (plan all elect.)	FY05

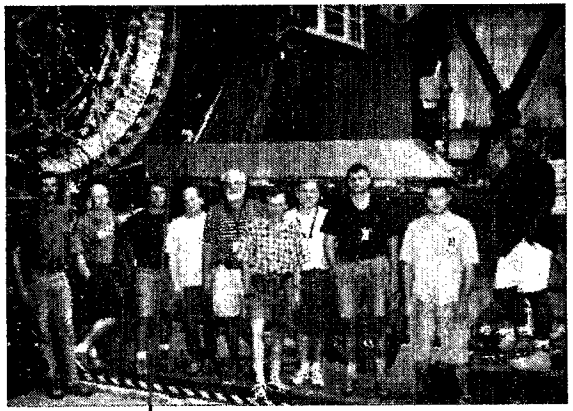

#120 – the last one!
August 2004

Scinti. + Pb sandwich sampling EMC

- 4800 projective towers (2π in ϕ, $-1<\eta<1$)
- Shower Max Detector-gas detector-18K strips
- Pre Shower Detector (first 2 layers)
- High tower trigger & 1x1 (η, φ) jet trigger

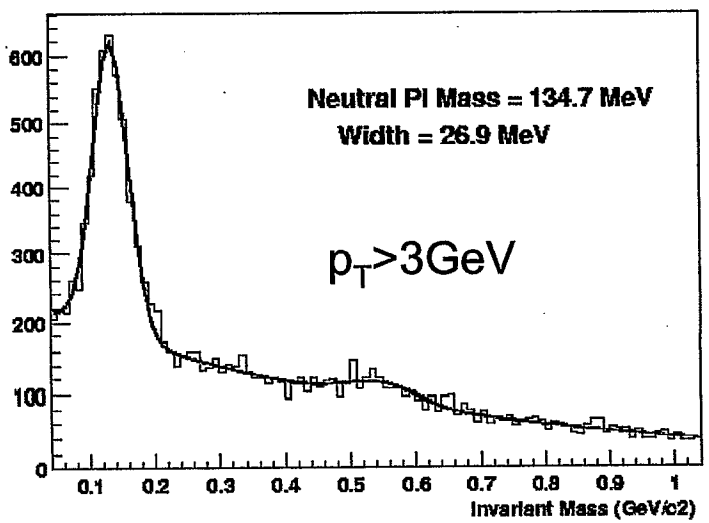

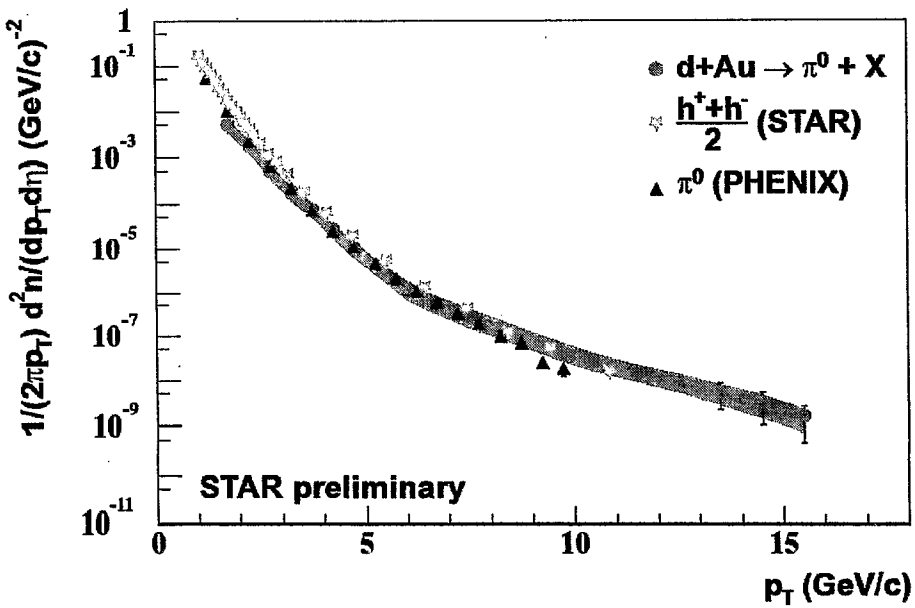

Triggering in STAR

DAC 100 in place

- Up to 100 Hz full detector readout and tape writing
- Really means 50% dead at 50Hz
- Selective triggers important to STAR
  - Minbias based on BBCs
  - Increasingly, important spin triggers primarily calorimeter based
  - High tower triggers – 3 thresholds
  - Jet patch triggers – 3 thresholds
  - Adjacent jet patch triggers
  - Opposed jet patch triggers – $\Delta\phi=180^0$
  - All tested in '04 run – evaluate for '05
- Can also take higher rates of "Fast" detector only – primarily EM calorimeters – π^0 stats
  - Fast detector only runs while slow detectors turning on or off – few 100 Hz
  - In background while slow detectors read out in normal runs - <100 Hz

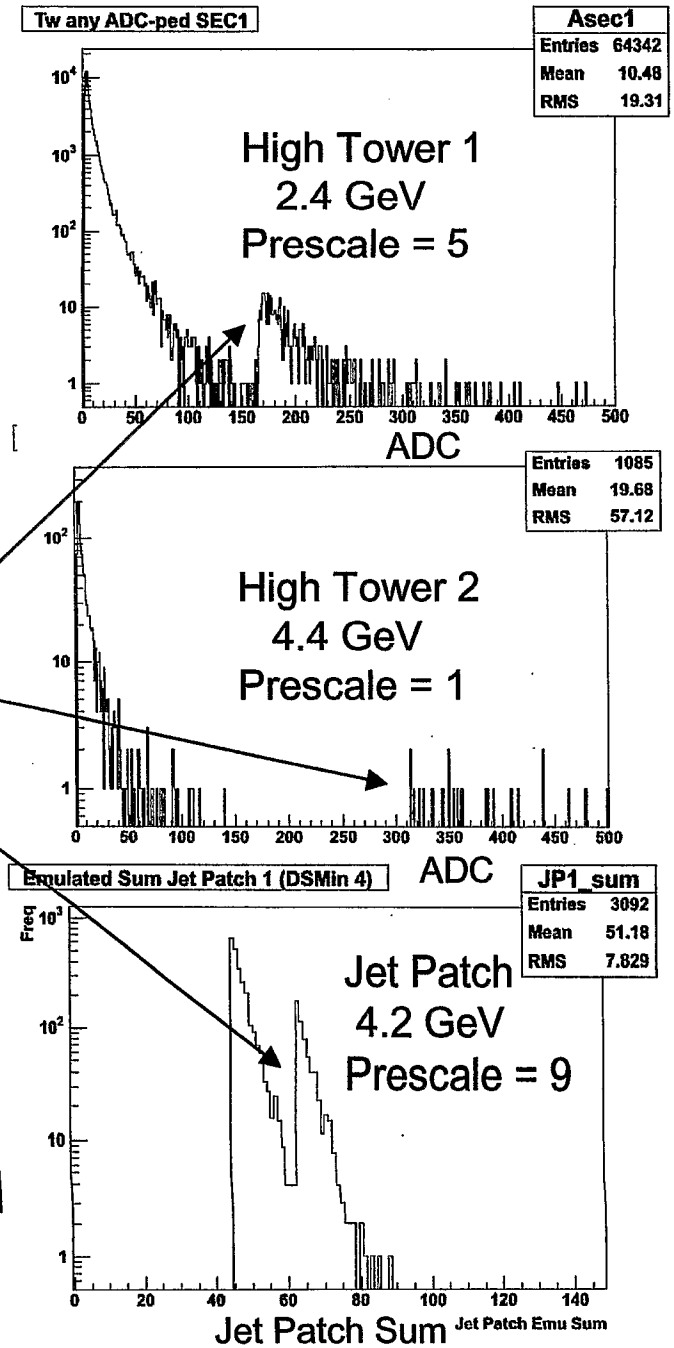

How do we (know we) get longitudinal polarization?

J. Kiryluk

STAR

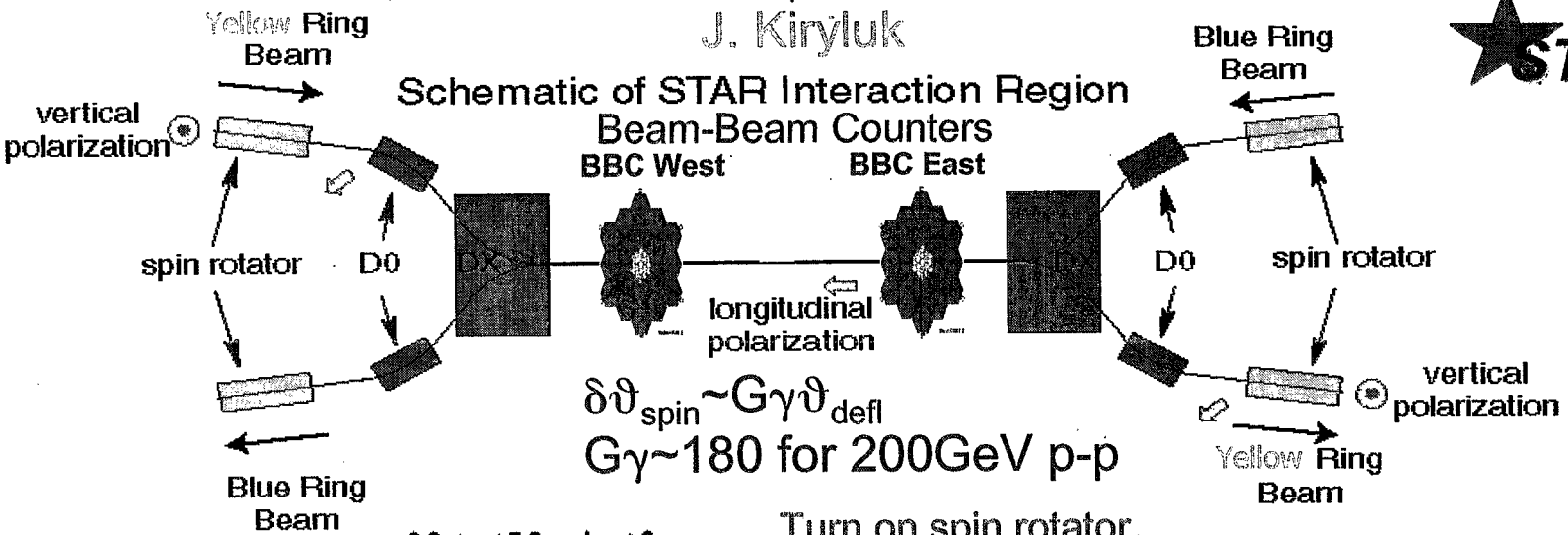

$\delta\vartheta_{spin} \sim G\gamma\vartheta_{defl}$

$G\gamma \sim 180$ for 200GeV p-p

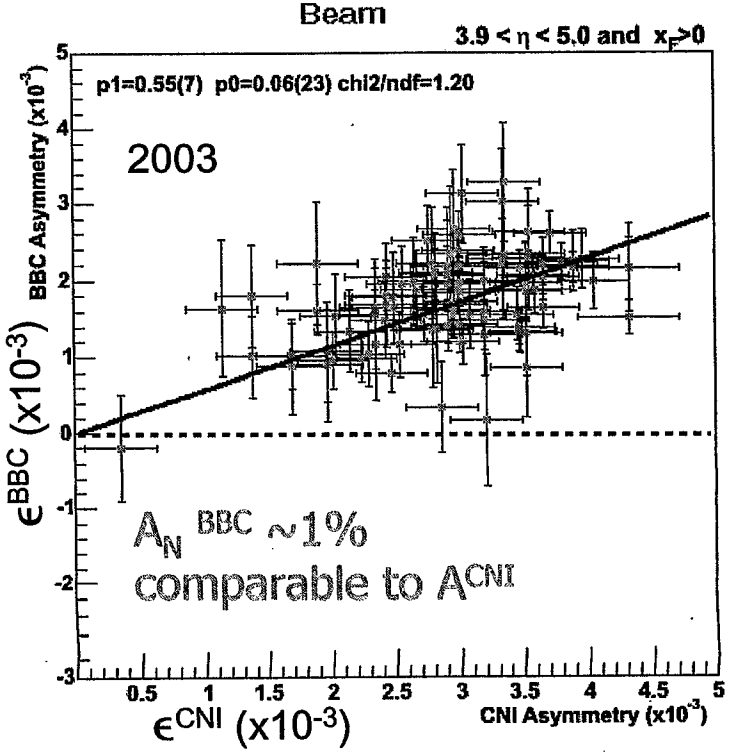

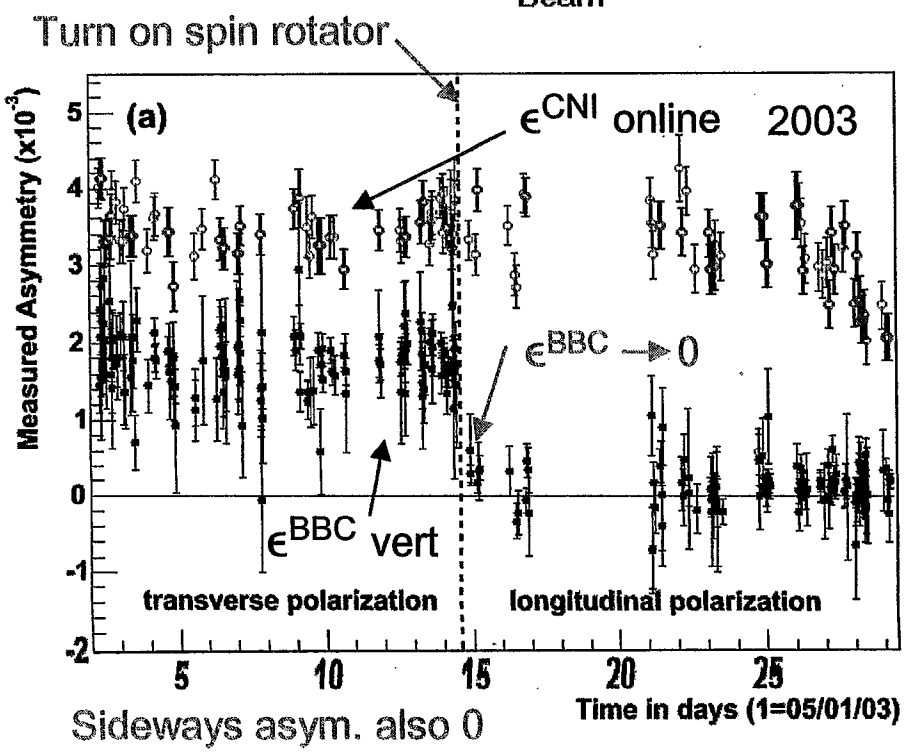

Transverse Single Spin Asymmetries at BBC – η Dependence

STAR Spin (A_N for forward unidentified charged particles)

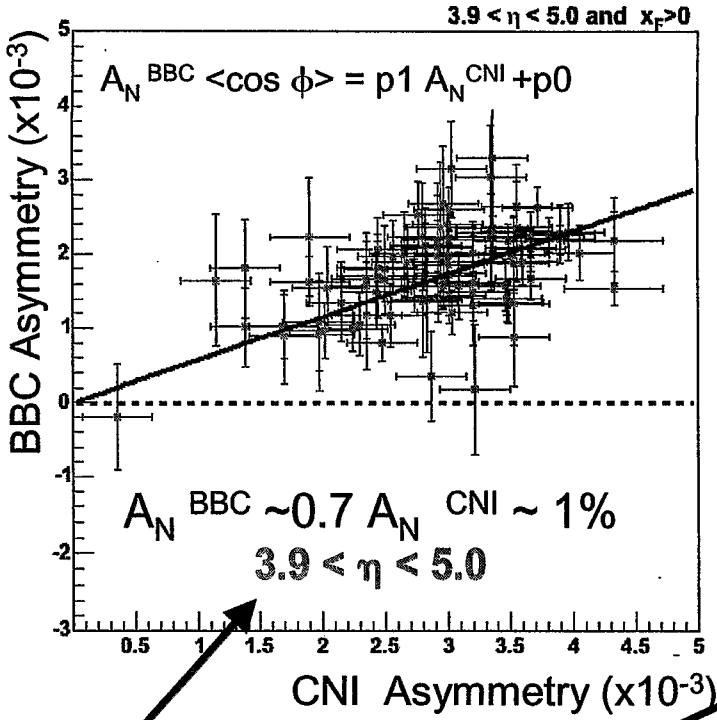

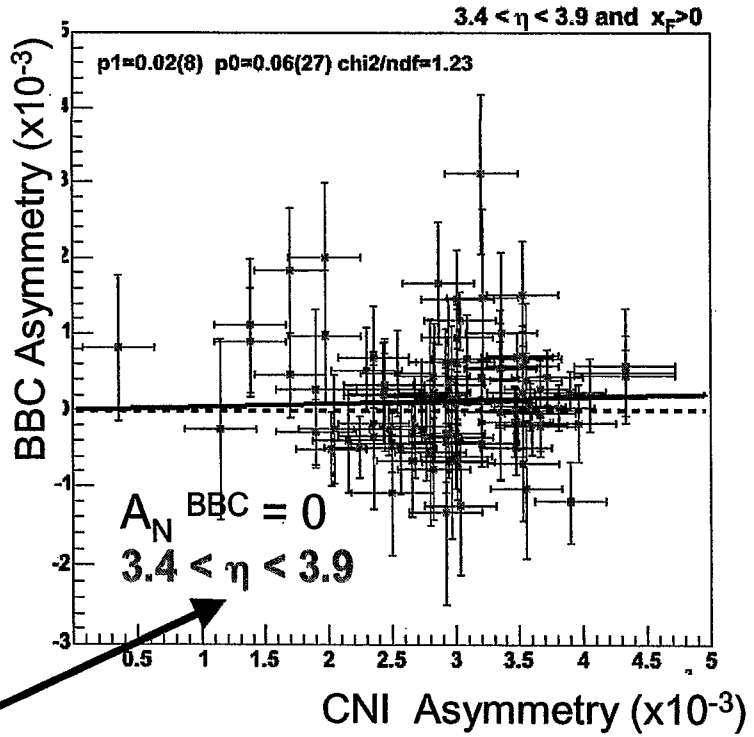

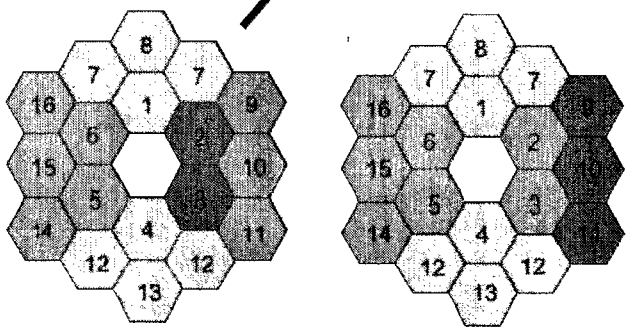

Red=Have hit

Green=No hit Blue=Don't care

- Unexpected A_N of unknown origin measured with the BBC
- Strong pseudorapidity dependence of A_N for x_F>0 and A_N = 0 for x_F<0
- $\delta\epsilon$(syst) < $\delta\epsilon$(stat)

J. Kiryluk

ΔG from jets with STAR

Sees and reconstructs jets
Large solid angle is crucial

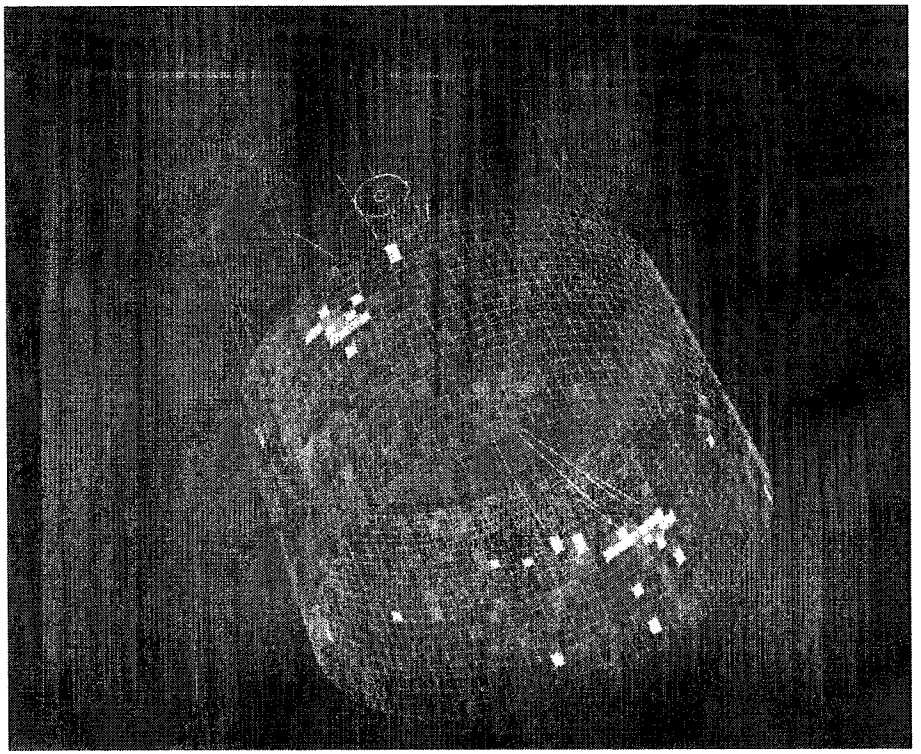

But signal is mixture of multiple partonic subprocesses

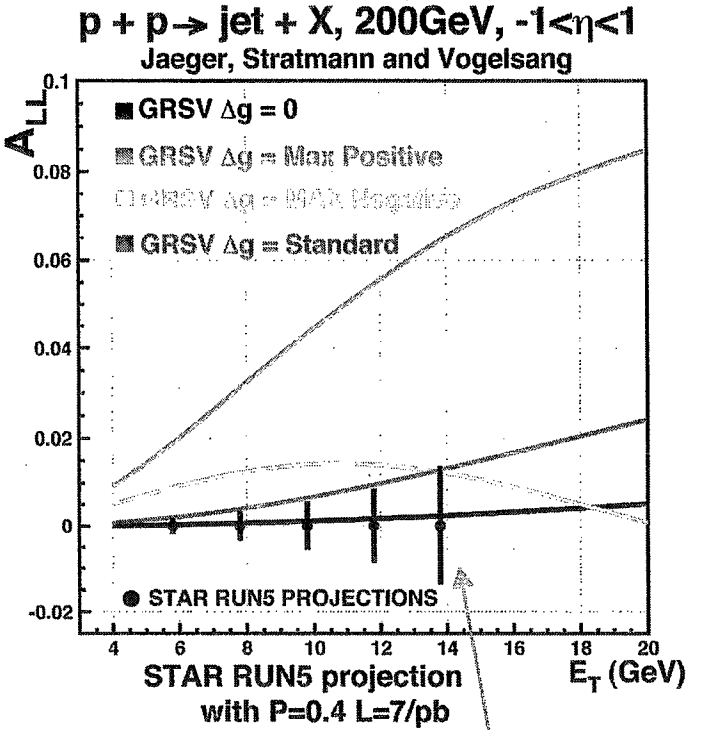

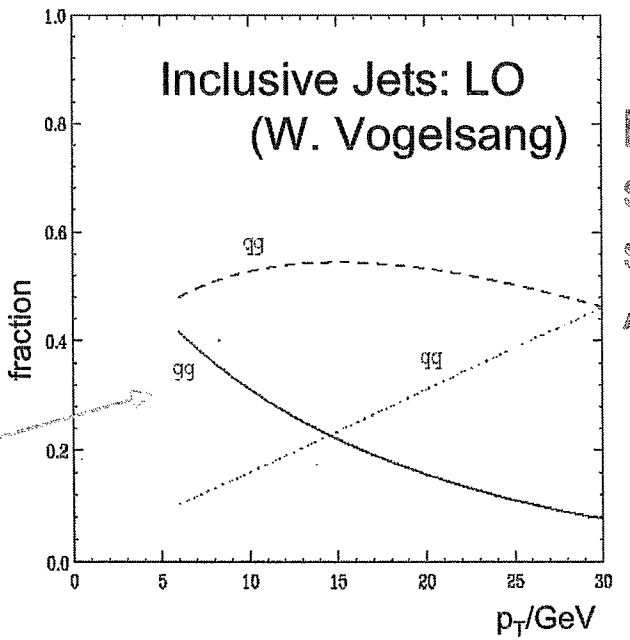

Leads to small but significant A_{LL} in 2005

(~1/10 of these stats from 2004 currently being processed)

~1/3 of the jet energy is EM

Use EM cals for triggering jets

π^0s carry ~same physics

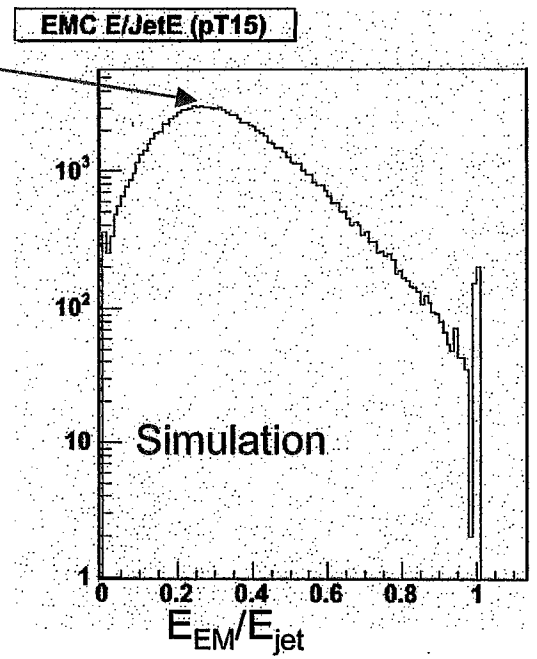

Jager, Stratmann, Vogelsang NLO pQCD calculations

hep-ph/0404057

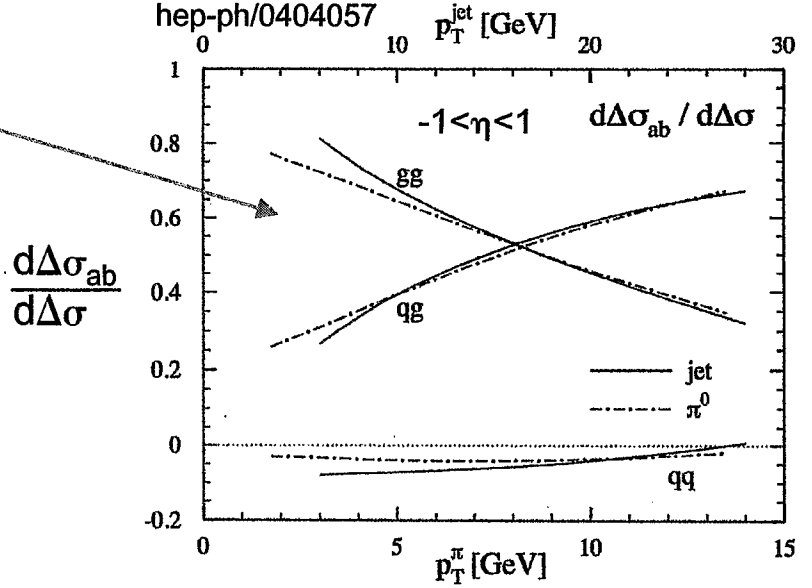

Significant const. on ΔG expected in 2005 data (~1/10 stats. from '04 being analyzed)

(error bar estimates too small pT<6 GeV)

STAR A_{LL} projection (P=0.4 L=7pb^{-1}): Inclusive π^0 production

(Calculations provided by Jaeger, Stratmann and Vogelsang)

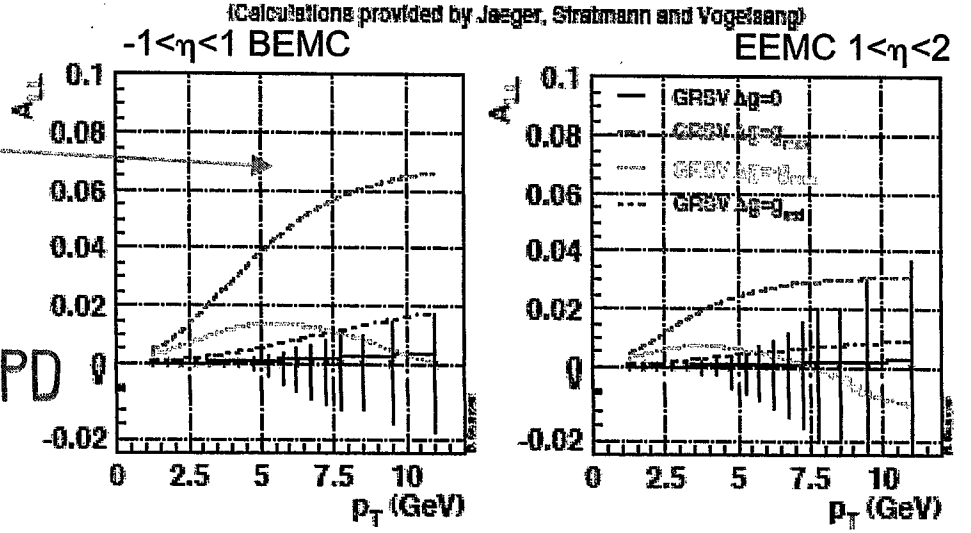

- Only STAR can track vs. η – EMCs+FPD
  - Different partonic contributions
  - Large η→small x

Quark – Gluon Compton Scattering

$\vec{p} + \vec{p} \rightarrow$ Direct γ + Jet

- Compton scattering dominates competing $q\bar{q} \rightarrow g\gamma$ mechanism

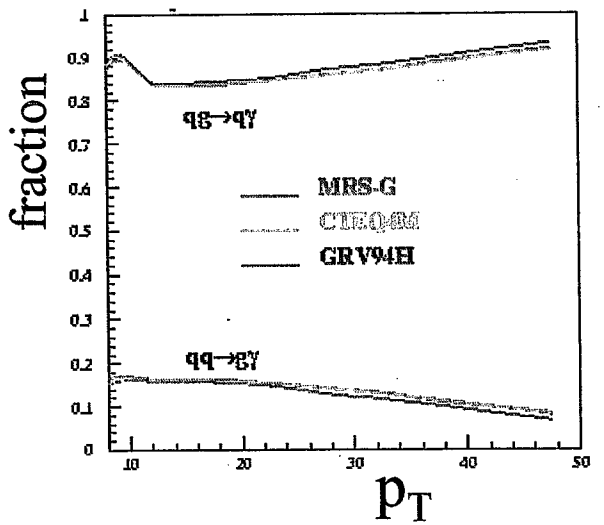

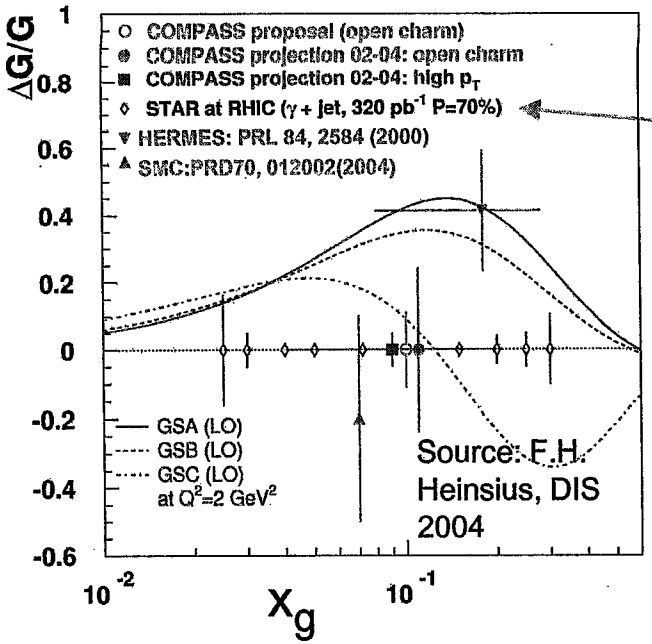

Eventually gives best determ. of $\Delta g(x)$ for existing experiments.

Will get started in 2005 & 2006

- Coinc. γ– jet relatively clean exp. signature
- E_γ, η_γ and η_{jet} determine x_q, x_g, $\hat{\vartheta}$
- Allows extraction of $\Delta g(x)$ →

Simulated full data set $\vec{p}\,\vec{p} \rightarrow \gamma + jet + X$

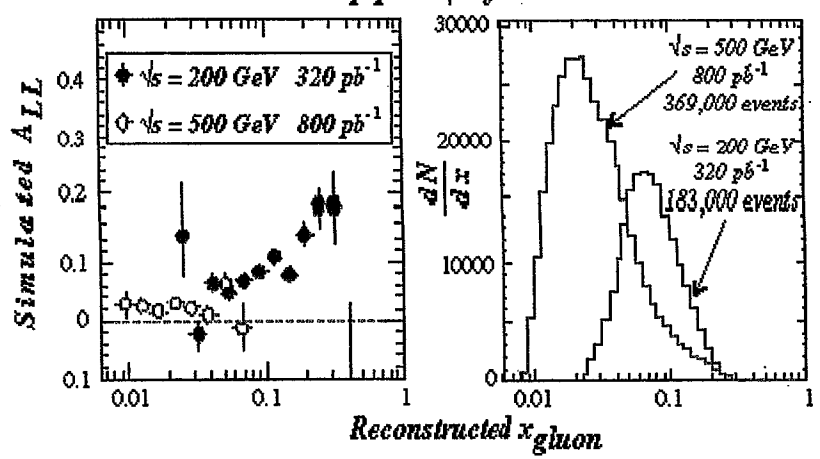

Analyzing Powers at Mid-Rapidity

Do processes invoked in forward scattering show up at large angles?

STAR Collab. Phys. Rev. Lett. **92** (2004) 171801

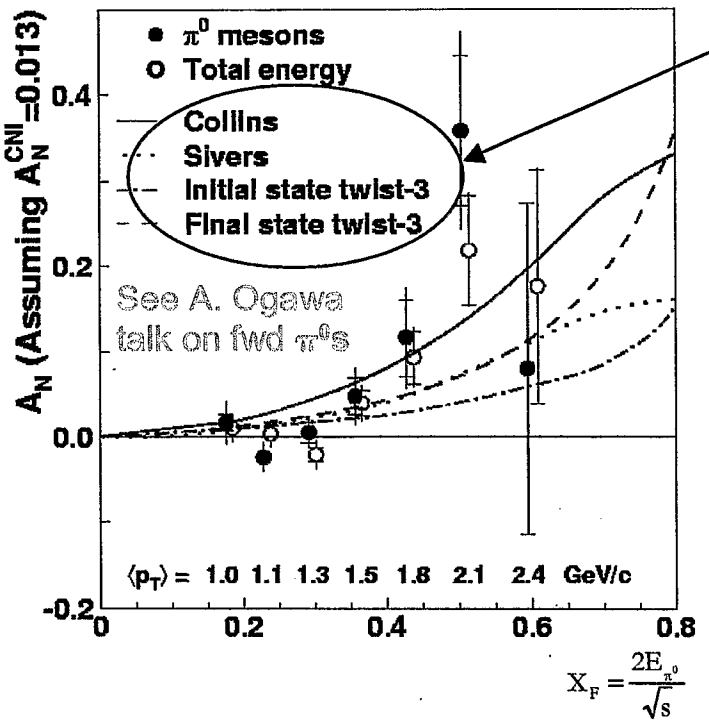

Measure

$$A_N = \frac{1}{Pol}\frac{Y^{\uparrow}_{Dijet} - Y^{\downarrow}_{Dijet}}{Y^{\uparrow}_{Dijet} + Y^{\downarrow}_{Dijet}}$$

Jet

For given parton at some x
$k_T^L \neq k_T^R$

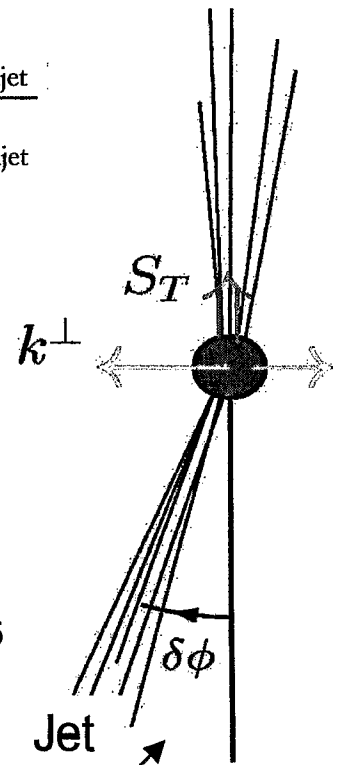

D. Boer and W. Vogelsang, Phys.Rev. D **69** (2004) 094025

Sivers Function – Initial state correlation between k_T and spin

$$f_q(x,k^{\perp},s_P) = f_q(x,k^{\perp}) + \frac{1}{2}\Delta_q^N f_q(x,k^{\perp})\frac{S_P\cdot(P_p\times k^{\perp})}{|S_P||P_P||k^{\perp}|}$$

Partonic k_T from Dijet Analysis

4.1×10^{-4} T. Henry, Quark Matter 2004, J. Phys. G

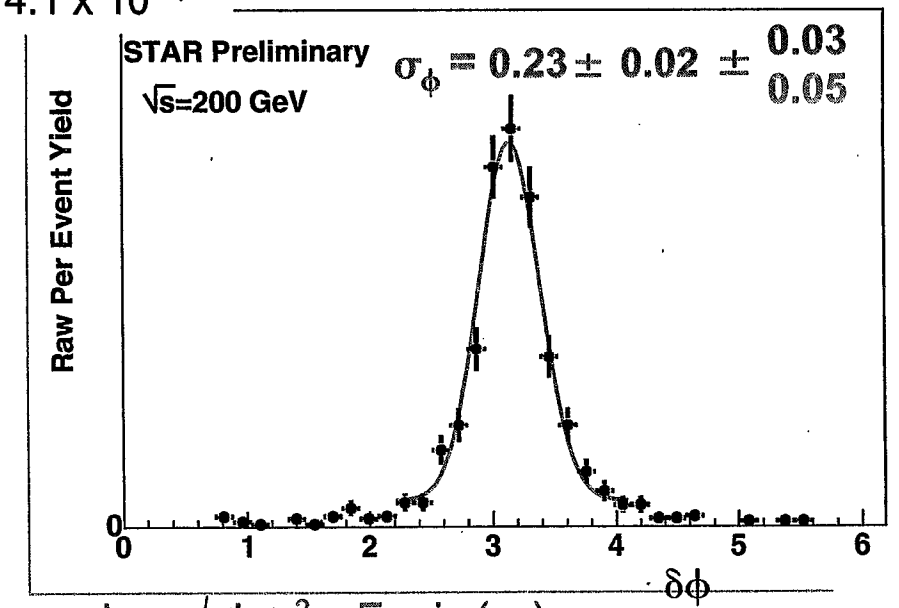

$k_T = \sqrt{\langle k_T \rangle^2} = E_T \sin(\sigma_\phi)$

$E_T = 13.0 \pm 0.7_{sys}$ GeV Trigger Jet

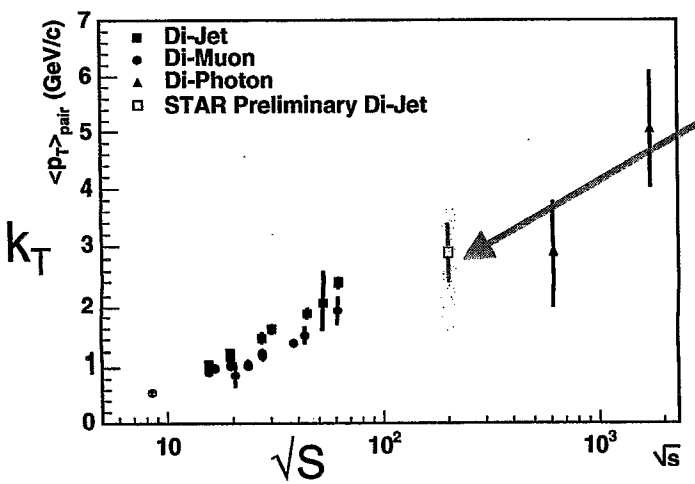

STAR agrees well with World Data on Partonic k_T

Sivers Effect Prediction

D. Boer and W. Vogelsang, Phys.Rev. D **69** (2004) 094025

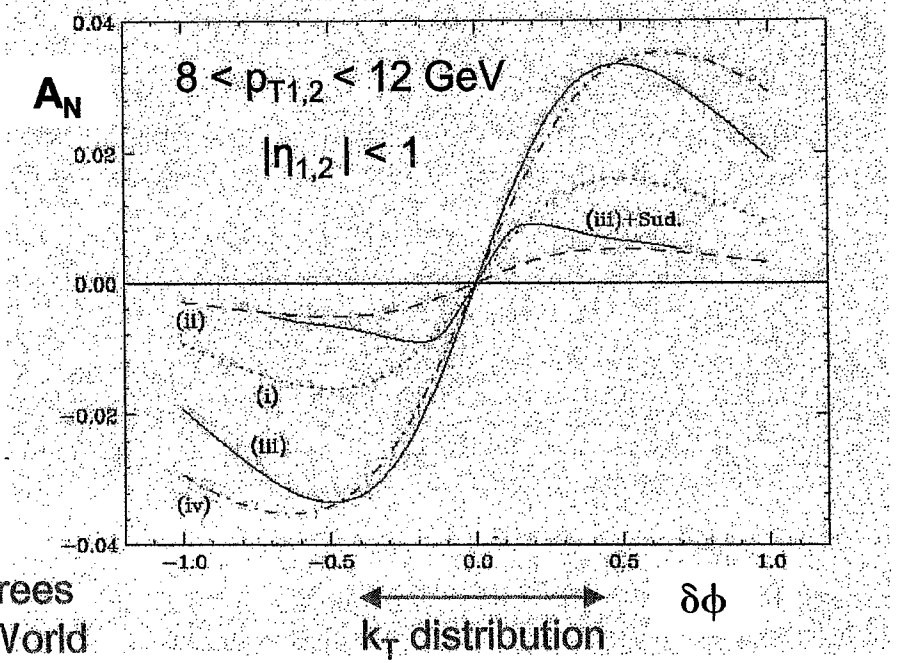

- Curves are for various gluonic Sivers functions
- Connection to partonic orbital angular momentum
- Suppressed by Sudakov effect

STAR

Spin-based physics analyses of 2004 STAR data focused on:

Publishable results and develop techniques for '05 data set

- $A_{LL}(\pi^0)$ in 200 GeV p+p (sensitivity to ΔG in proton) "first look"
- A_{LL}(jets) in 200 GeV p+p (sensitivity to ΔG in proton) "first look"
- Evaluation of efficiency & bias for different jet triggers, + extended coverage for A_{LL}(jets) in 200 GeV p+p
- Search for high-p_T direct photon yield in p+p and Au+Au

π^0 A_{LL} in B & EEMC 1pb^{-1} p=0.4

Jaeger, Stratmann & Vogelsang

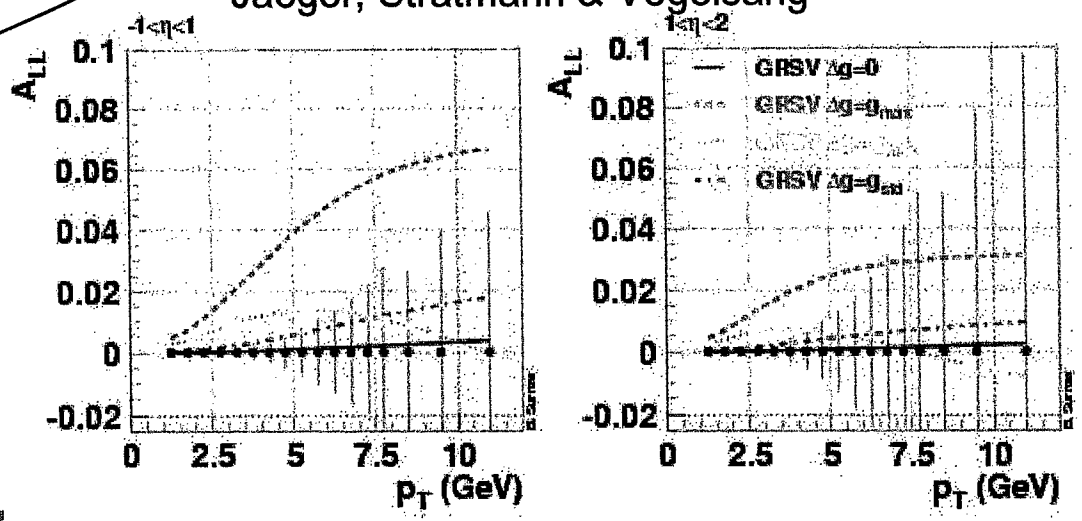

But less than this in '04 & trig & det. ineff. not included

'04 p-p production recently completed, 200 GeV Au-Au ready to go

Conclusions (Beginnings;-)

STAR

- STAR EM calorimeters complete
  - Triggering
  - Large solid angle EM coverage
- 2004 Data
  - provide STAR's "first look" at ΔG
  - Develop techniques for 2005 and beyond
- 2005 Data
  - Important constraints on ΔG expected
    - π^0s
    - Jets
  - Start looking for direct γs
  - Investigations of transverse spin effects

STAR Tracking Upgrades

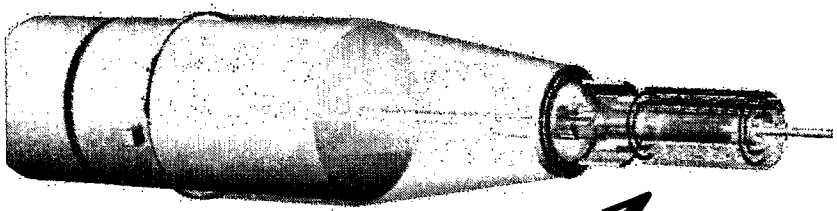

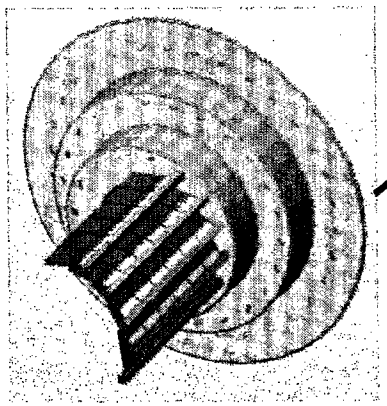

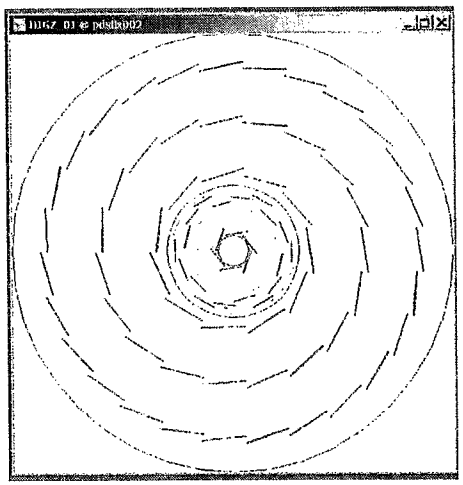

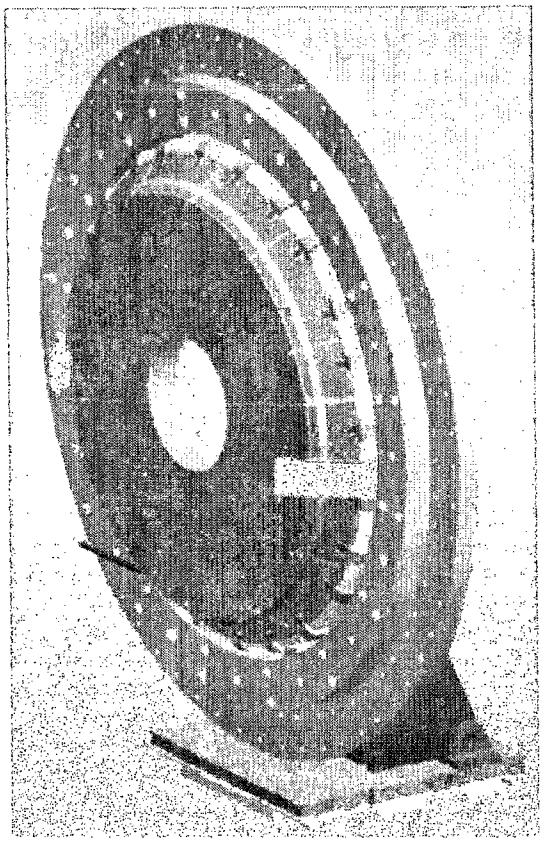

M.L. Miller, MIT
STAR TUP WG

Current STAR Tracking

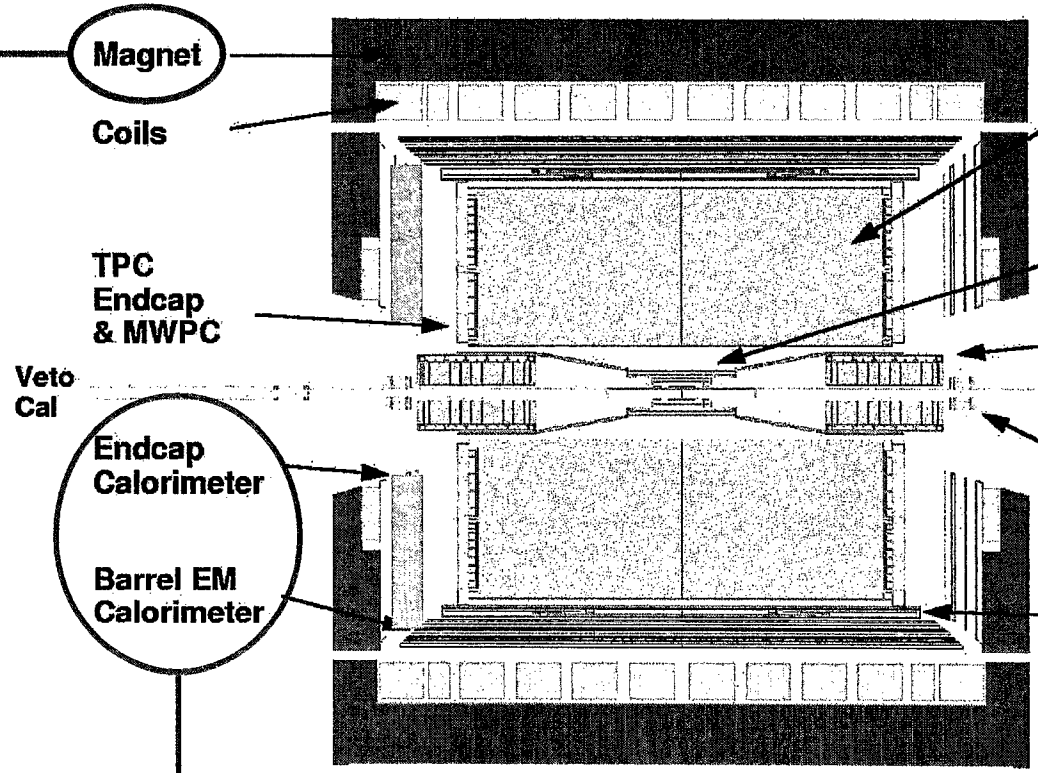

$-1<\eta<2$

These don't match!

3 layer Silicon Drift
+ 1 layer 2-sided Strip
+ 45 Tpc rows
→ $-1<\eta<1$

0.5 T conventional coil

MASSACHUSETTS INSTITUTE OF TECHNOLOGY

Physics Motivation (I): heavy flavor

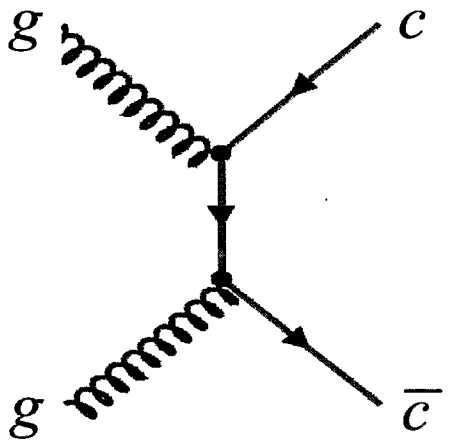

Heavy Ion

- Heavy quark energy loss in medium?
- Charm quark collectivity?
- Does the J/Psi melt?

D^0 $c\tau \approx 124$ mm

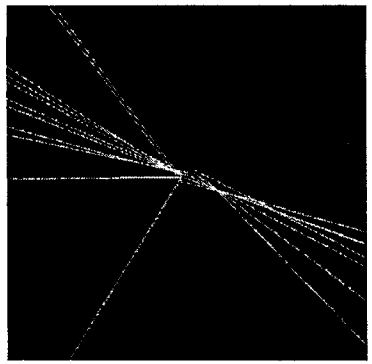

Precision Vertexing

M. Karliner and R.W. Robinett, Phys. Lett. B324 (1994) 209.

STAR Spin

- Unique test of partonic a_{LL} → QCD matrix elements
- Sensitive to gluon helicity
- low background from quark helicities
- NLO formalism available (Bojak and Stratmann)

$$A_{LL} = \frac{(\sigma_{++}+\sigma_{--})-(\sigma_{+-}+\sigma_{-+})}{(\sigma_{++}+\sigma_{--})+(\sigma_{+-}+\sigma_{-+})}$$

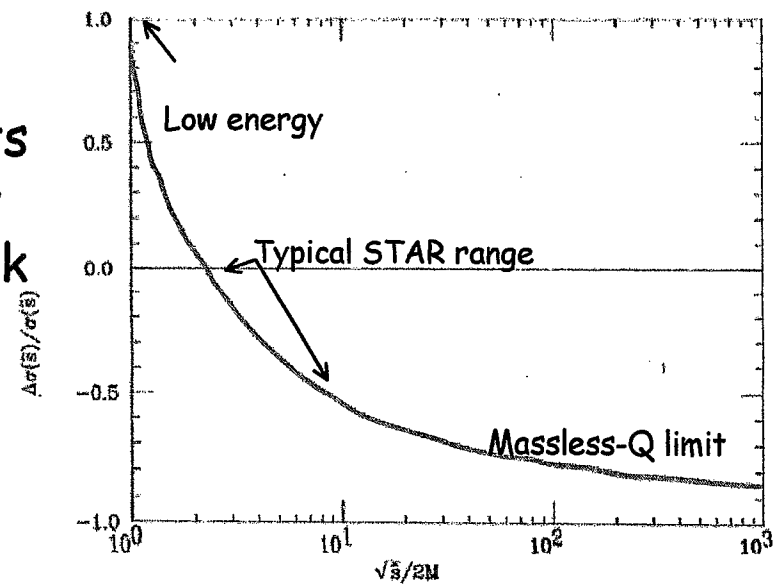

MASSACHUSETTS INSTITUTE OF TECHNOLOGY

Physics Motivation (II): quarks via $W^{\pm}$

- Semi-inclusive DIS - sensitivity reduced by fragmentation functions and e^2_q weighting

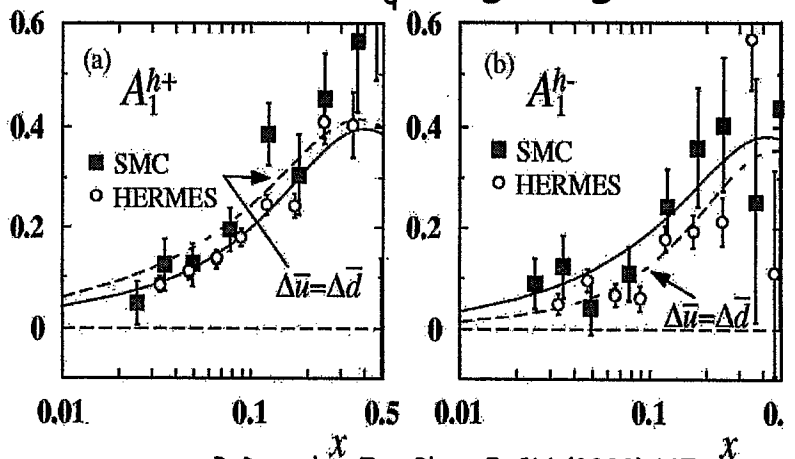

B. Dressler, Eur. Phys. J. C14 (2000) 147.

$$\Delta d + \bar{u} \rightarrow W^- \qquad \Delta\bar{d} + u \rightarrow W^+$$

$$\Delta\bar{u} + d \rightarrow W^- \qquad \Delta u + \bar{d} \rightarrow W^+$$

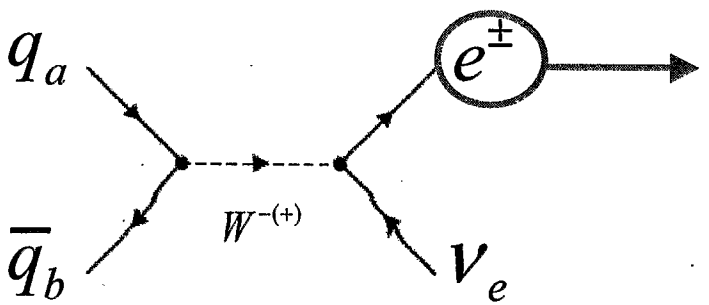

- $p\uparrow p\uparrow \rightarrow W^{\pm}$ - direct measurement

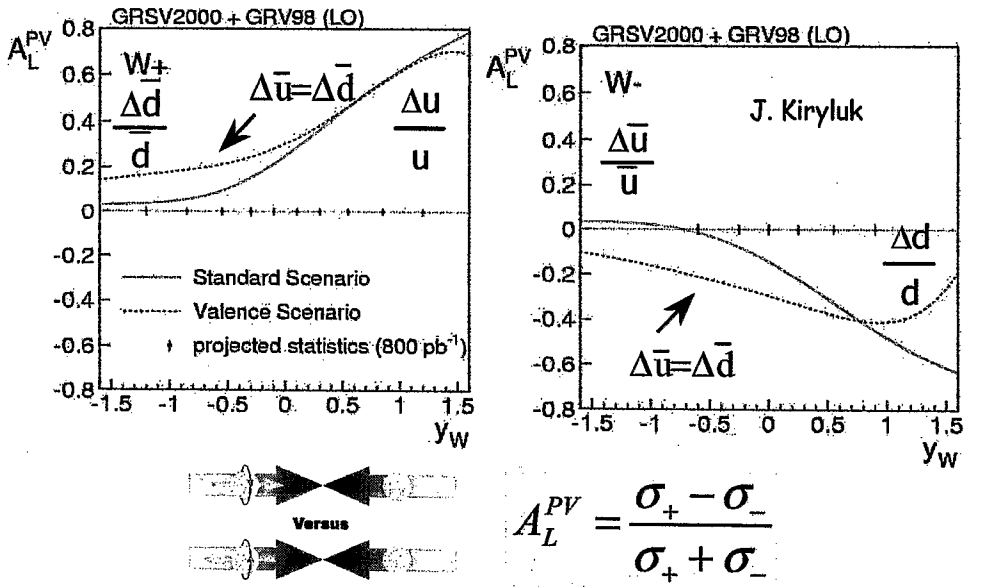

$$A_L^{PV} = \frac{\sigma_+ - \sigma_-}{\sigma_+ + \sigma_-}$$

Barrel EMC or Endcap EMC
Must resolve e^+ from e^-
Endcap: kinematic region of interest
But… poorest tracking in STAR!

Physics Motivation (II): quarks via $W^{\pm}$

$p + p \rightarrow W^{-} + X \quad \sqrt{s} = 500\ \text{GeV (Pythia)}$

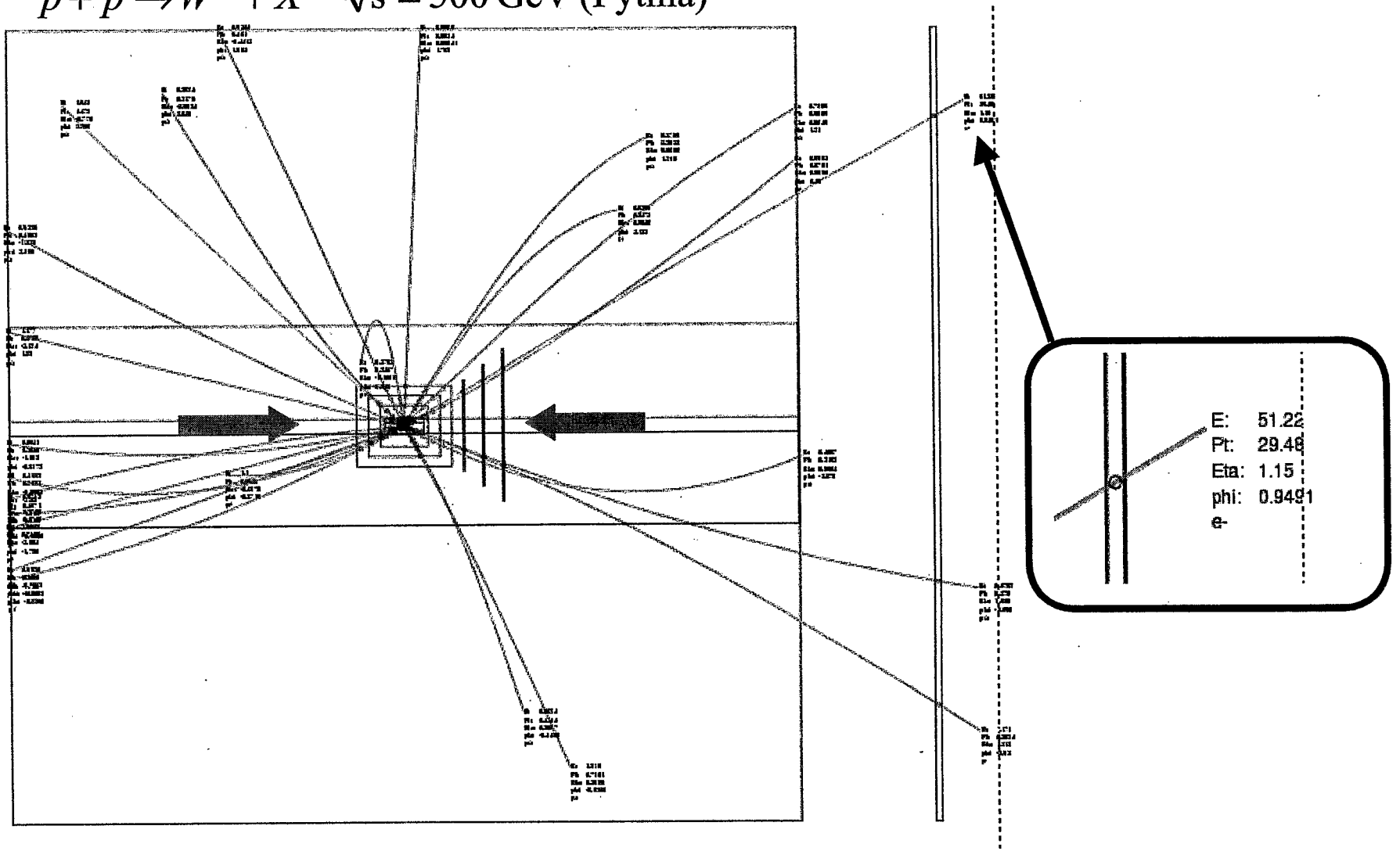

Tracking Requirements

Physics implies new requirements for STAR tracking

→Open charm vertex tagging (*in pileup central Au+Au!*)

→Discriminate 50 GeV/*c* e^+ from e^-

→Provide tracking for photon isolation cut in Endcap EMC

And practical requirements (constrained by TPC and Magnet)

Fast – greater than 100 Hz to deal with design++ luminosity

Efficient – extensive reconstruction studies drive optimal layout → symmetric

Proven Technology – apply standard tech. *or* demonstrate prototype success

~

Layer	σ (μm)	d (cm)	technology
Barrel 1, 2	<10	2, 4	APS Pixel
Barrel 3,4,5	50	7, 12, 17	2xSi Strip
Barrel 6	70	20	SSD (exists)
Forward 1, 2, 3	50	30, 40, 50	Si Strip
Forward 4	50	270	3xGEM

Preliminary Conceptual Layout

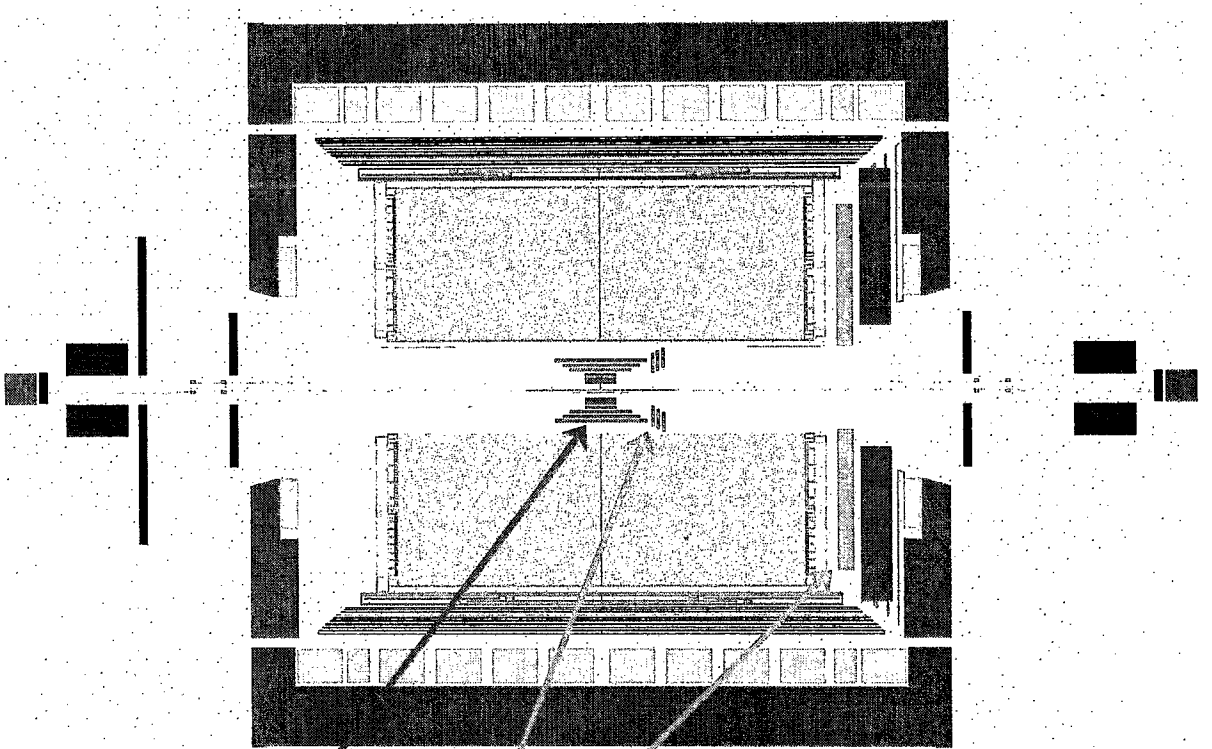

- High Rate - High Quality tracking at $-1<\eta<2$
- 100 Hz+ Inner Si strip barrel tracker
- surrounding a new APS pixel detector
- Add forward Si disk
- Fill small available space with 3xGEM tracker

Stage 1: 3 layers of Si at mid rapidity plus 2 layersAPS pixel detector

Stage 2: Multi-layers of Si and GEM technology at forward rapidity

MASSACHUSETTS INSTITUTE OF TECHNOLOGY

APS Pixel (*Heavy Flavor Tracker*)

Active Pixel Sensor

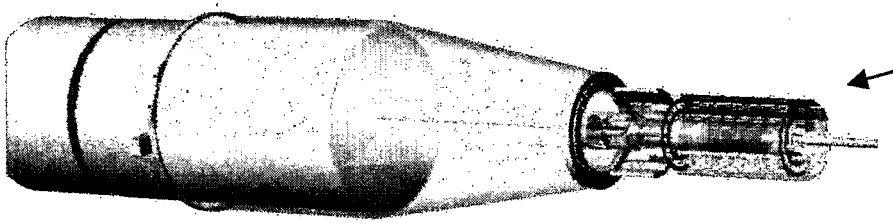

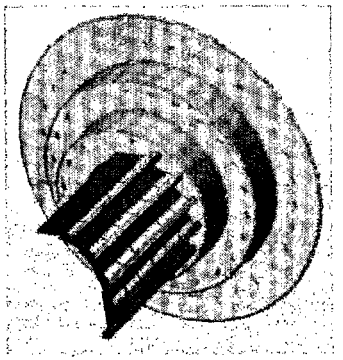

Advanced LBL design:

< 0.2% of rad. length, 30x30 μm^2 pixel size, 5-10 ms readout (but work in progress)

<u>Extensive Tracking Simulation</u>

Central Au+Au events
+ full GEANT + response simulation
+ *current* barrel silicon (will improve)
+ standard STAR ITTF tracking

→ Acceptable efficiency already, new IST barrel + software tune will improve

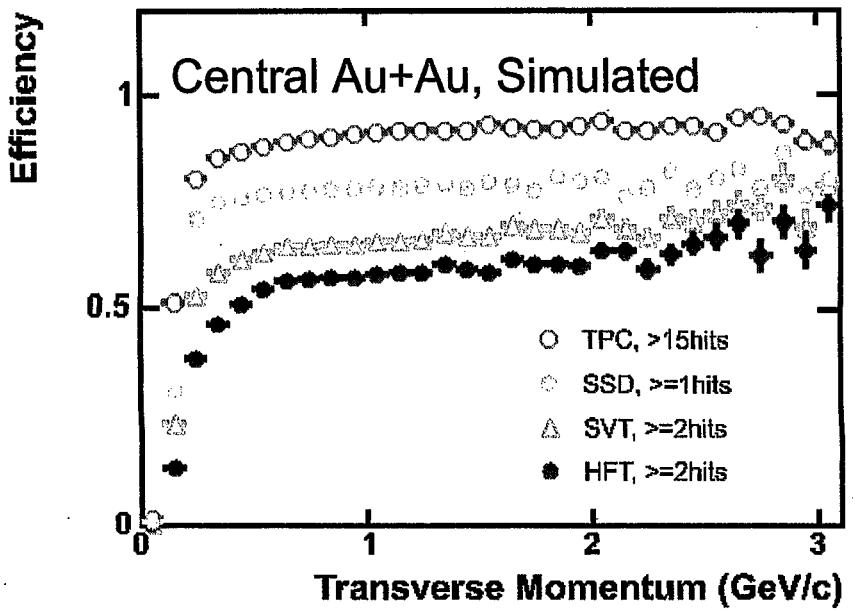

3xGEM Detector

- 50 μm resolution
- Large area (~10 m^2)
- Thin (~4 in)

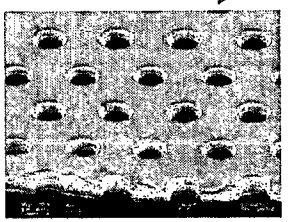

Triple GEM gas detector:
thin gas volume, 3 foils in series
Hole radius: 0.001 in
→ Large gain, excellent resolution

TechEtch Inc.

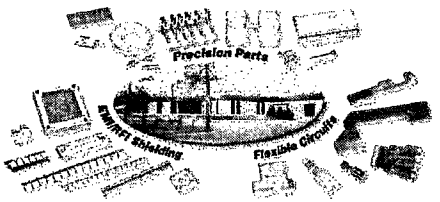

http://www.tech-etch.com

Beam's eye layout

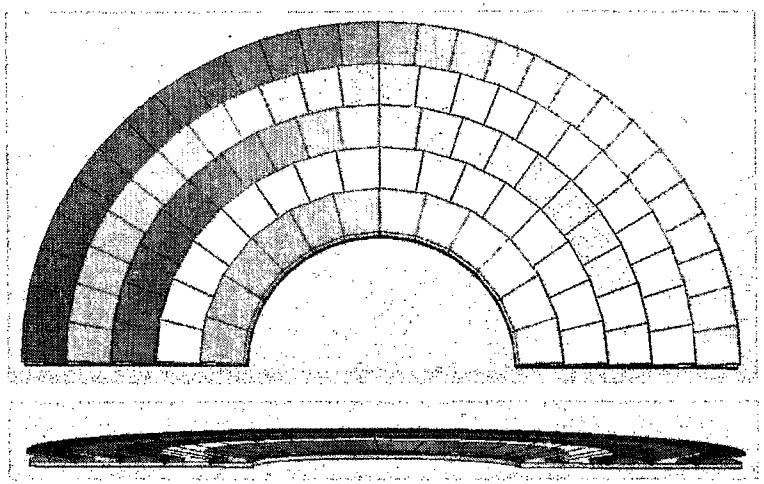

Populate disk with foils of identical dimension

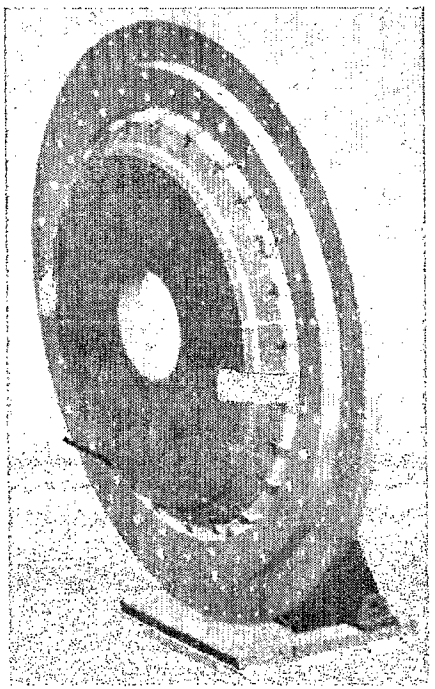

- CERN released tech. to tech-etch (Boston)
- Prototype foils at MIT
- Readout development at MIT-Bates (APV-25)
- R&D funding soon (SBIR)

Silicon Strip Barrel and Disk

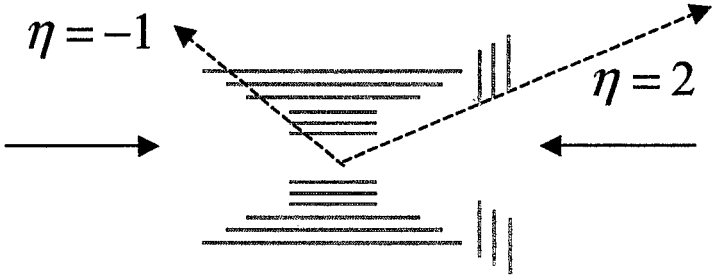

Requirements probably satisfied by standard silicon strip

Either cms-like 2xsingle sided wafers or double sided wafers

Extensive simulation underway

Beam's eye layout

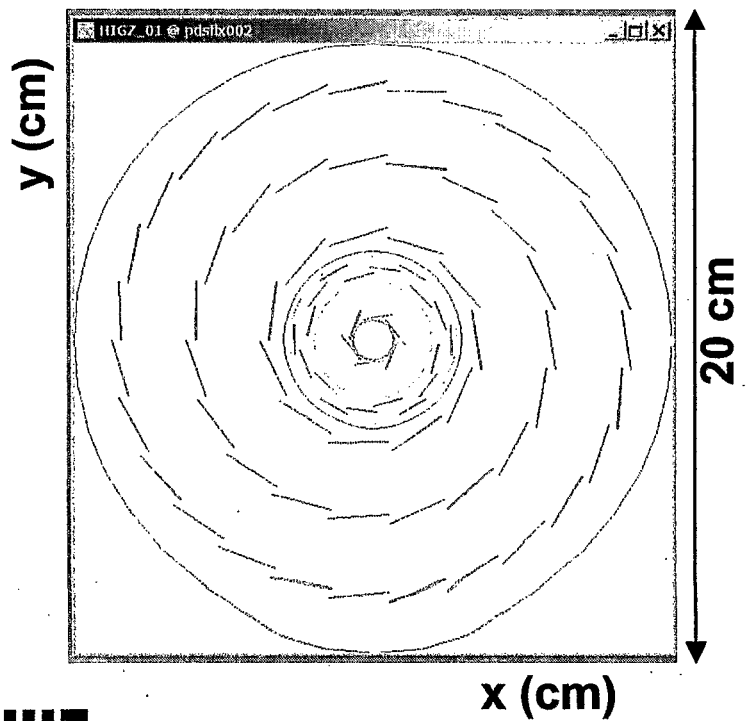

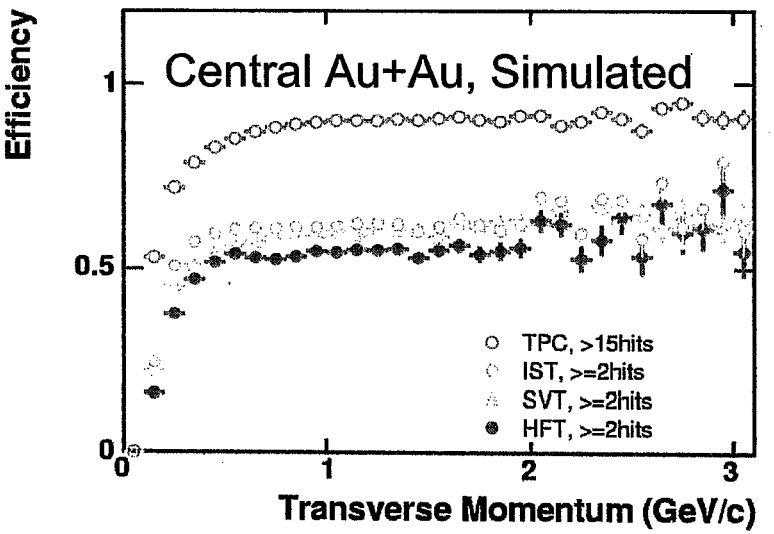

re-use PHOBOS production machinery at MIT

MASSACHUSETTS INSTITUTE OF TECHNOLOGY

Summary

- Physics drives tracking upgrades in STAR
- Barrel heavy flavor
  - standard strip → pointing device for
  - Innovative APS Pixel (or ATLAS pixel)
- Forward $W^{\pm}$ tagging
  - Standard strip → forward disks
  - Innovative 3xGEM tracker

Timeline

- summer 04: conceptual layout
- summer 05: barrel proposal
- summer 06: forward proposal
- summer 08: Pixel + Ist installation
- summer 09: Disk + GEM installation

ARGONNE NATIONAL LABORATORY

INDIANA UNIVERSITY CYCLOTRON FACILITY

BROOKHAVEN NATIONAL LABORATORY

YALE UNIVERSITY

UCLA

WAYNE STATE UNIVERSITY

LNS

USP

MASSACHUSETTS INSTITUTE

APS Pileup Studies

- Heavy flavor studies: Need for fast outer barrel system for pp
- Working numbers:
  - Total cross-section ($\sqrt{s}$=200GeV): 28mb
  - Luminosity: $1 \cdot 10^{32}$ cm^{-2} s^{-1}
    - Integration time: 1ms
- Fast-MC :
  - Two HF layers (30μm pixels, 15 and 40mm radii)
  - One faster detector layer
    - 300μm pxels,
    - 100mm radius,
    - 10-100 faster)
  - Tracking starts from HFT
  - Simple vertexing, +/- 20cm diamond
  - Multiple scattering, digitization
  - No magnetic field included in simulation

2,800 pp interactions within diamond with track density similar to AuAu

Ernst Sichtermann

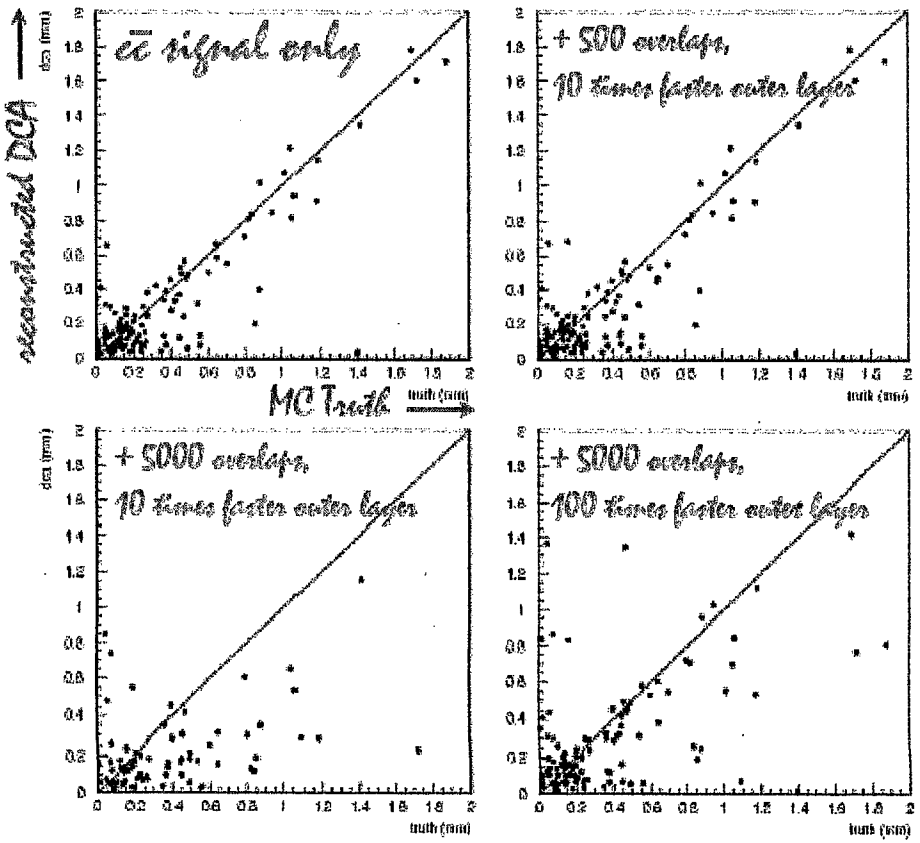

Jet interests at RHIC: $\vec{p} + \vec{p}$

Fragmentation:

$$z \equiv \frac{p_{hadron}}{p_{parton}}$$

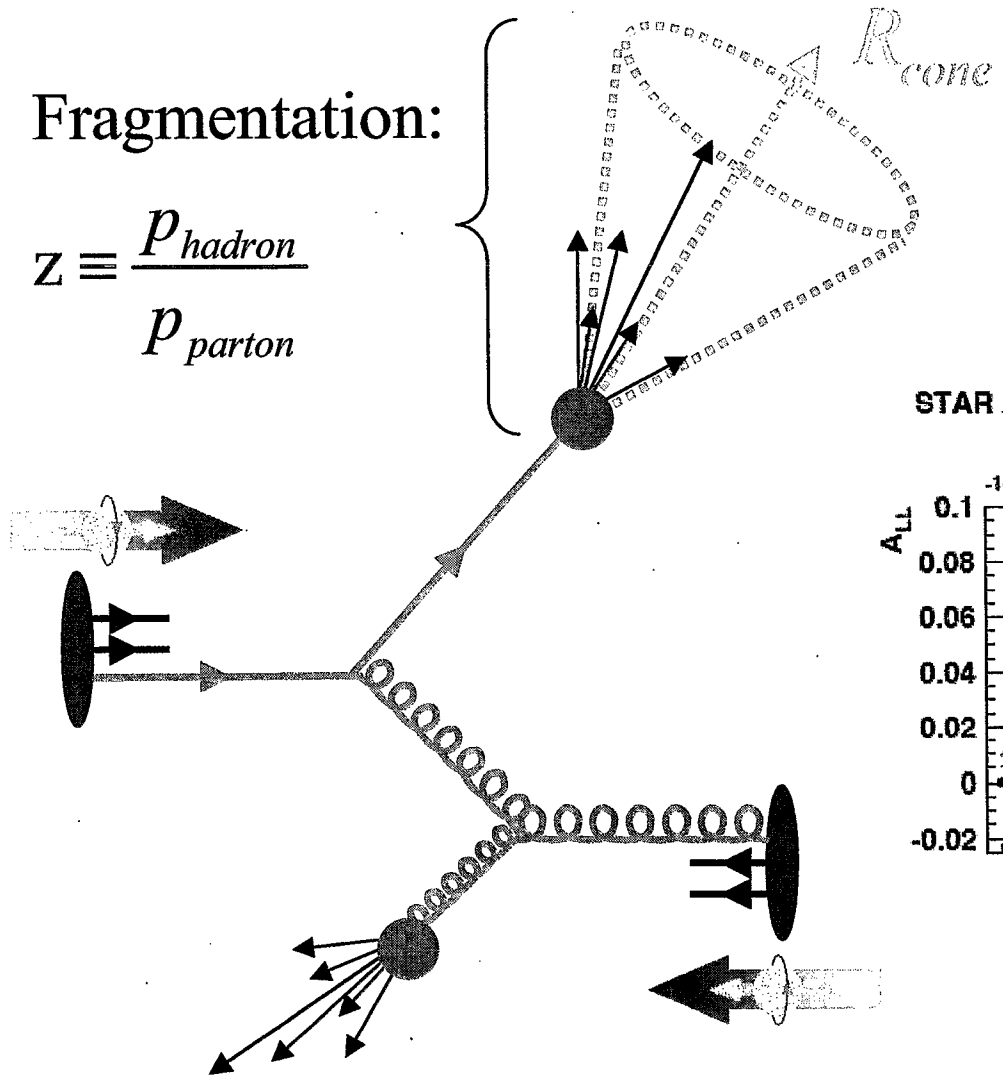

$$\Delta R = \sqrt{\Delta\phi^2 + \Delta\eta^2}$$

A_{LL} :

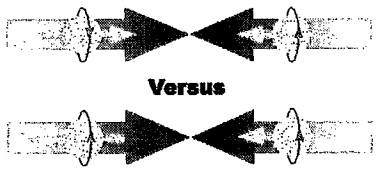

STAR A_{LL} projection (P=0.4 L=7pb^{-1}): Inclusive jet production

(Calculations provided by Jaeger, Stratmann and Vogelsang)

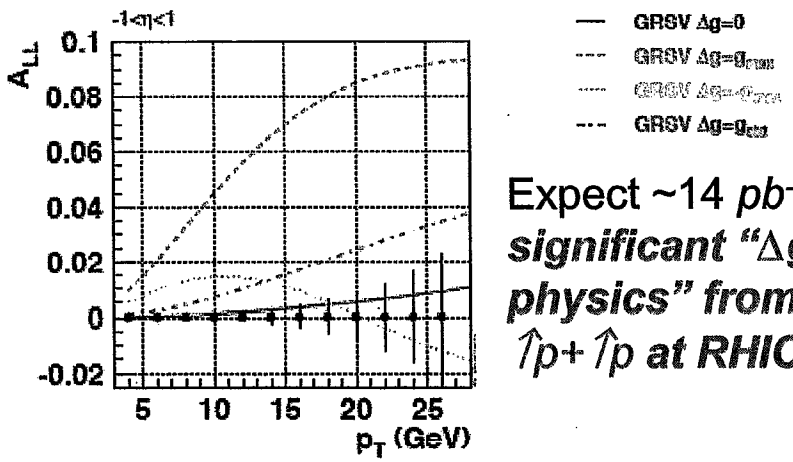

Expect ~14 pb^{-1} → ***significant "Δg physics" from ↑p+↑p at RHIC run5***

But….

Discussion

Physics of Double Spin Asymmetries

Abhay Deshpande & Werner Vogelsang

Possible Points of Discussion:

- Now and next two-three years:
  - A_LL pi0 measurements (Phenix)
  - A_LL direct photon (Phenix)
  - A_LL in Jets by STAR
- Combined analysis of RHIC data to extract fully information on polarized gluon distribution
  - Couple with polarized DIS
- Higher Sqrt(s) running polarized protons:
  - W+/- production
  - Lower x measurements of polarized gluons at high enough pT
- Use of polarized D or He3 for RHIC: polarimetry only? D quark dominance special?
- Theory: issues regarding NLO at fixed-target and colliders, kT

N. Saito

Constraints on $\Delta g/g(x)$

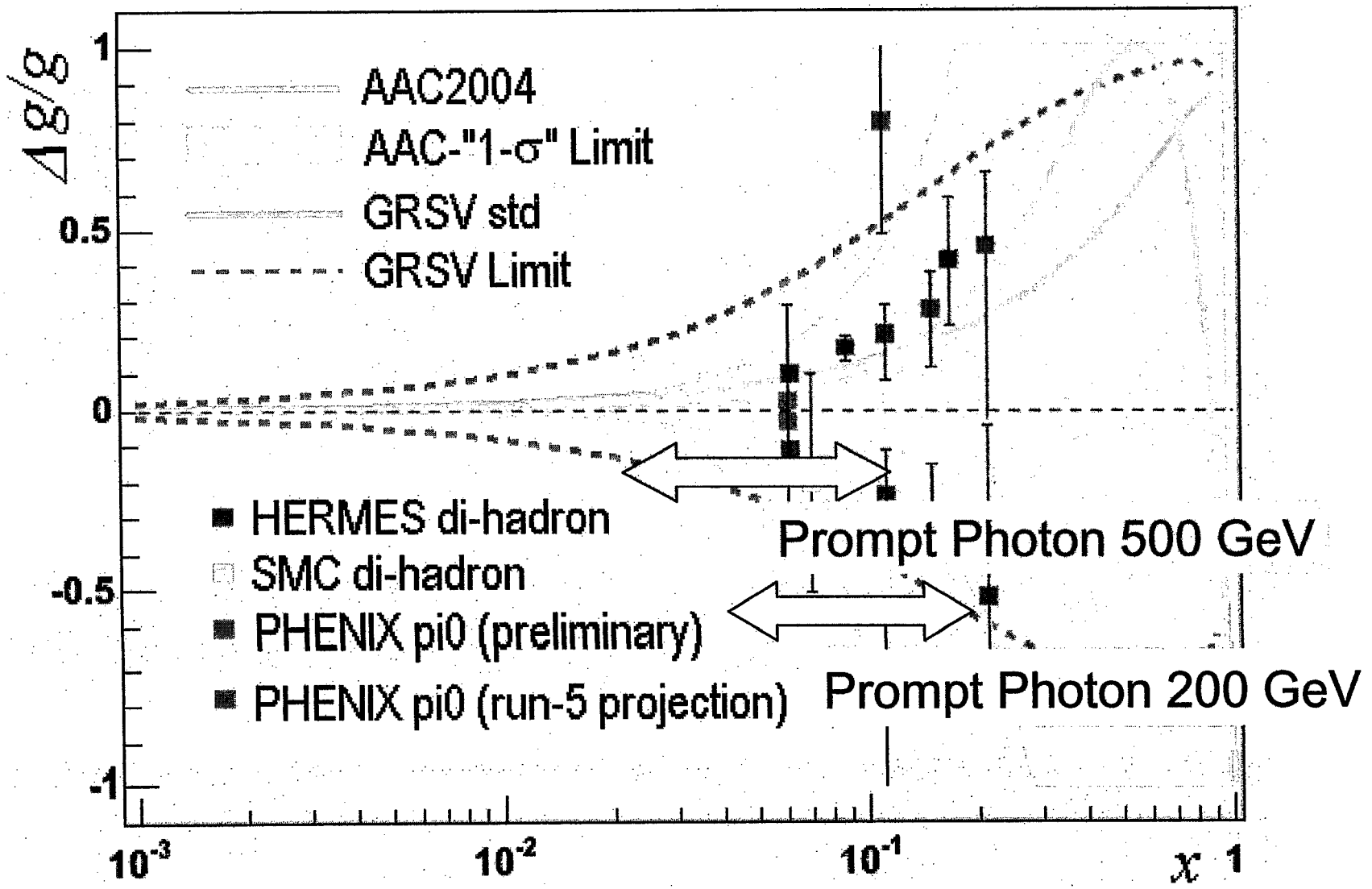

Constraints on $\Delta g/g(x)$

N. Saito

PHENIX – STAR Run-5 (3/pb)

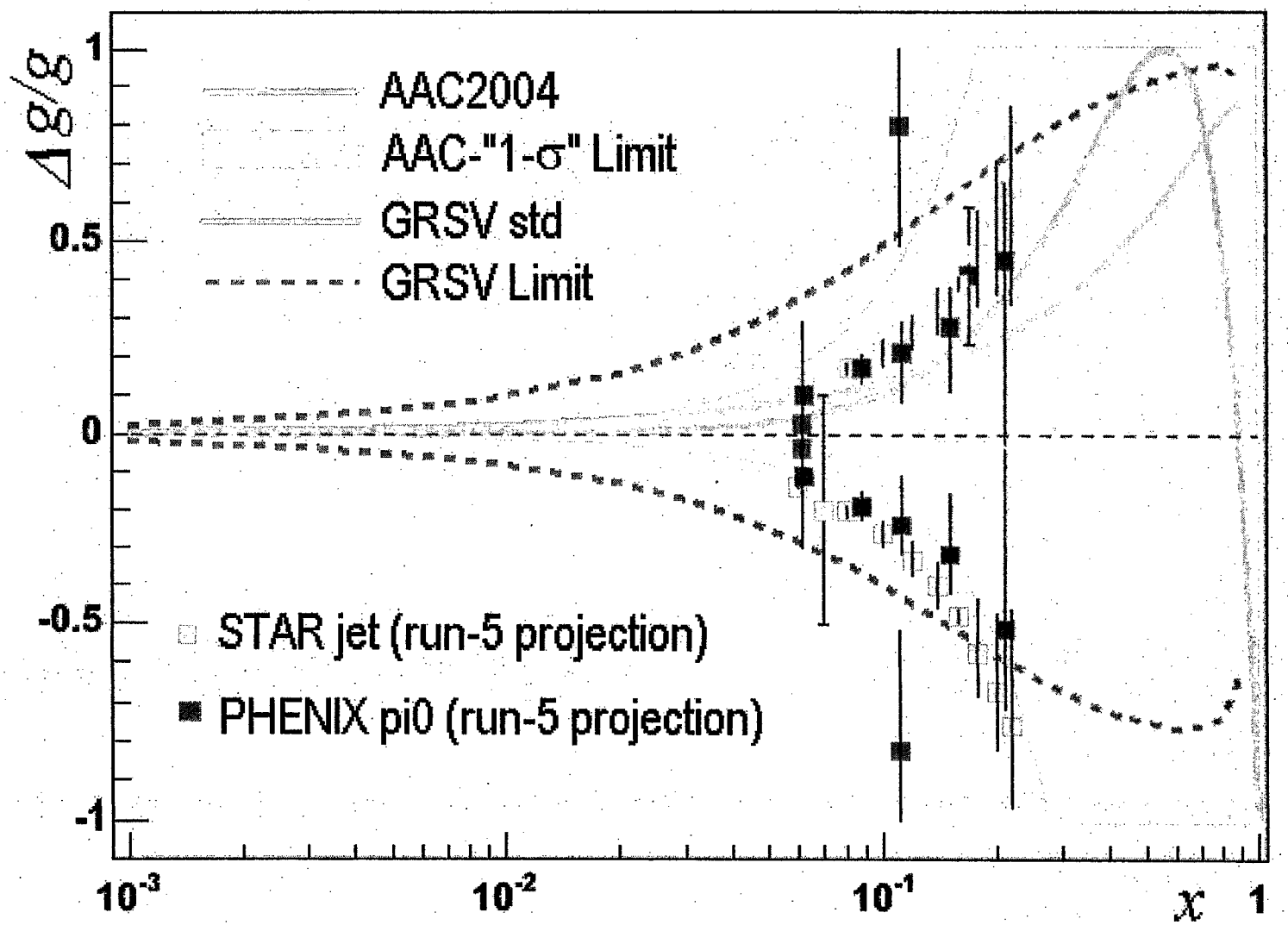

Constraints on $\Delta g/g(x)$

N. Saito

PHENIX Run-6 (100/pb)

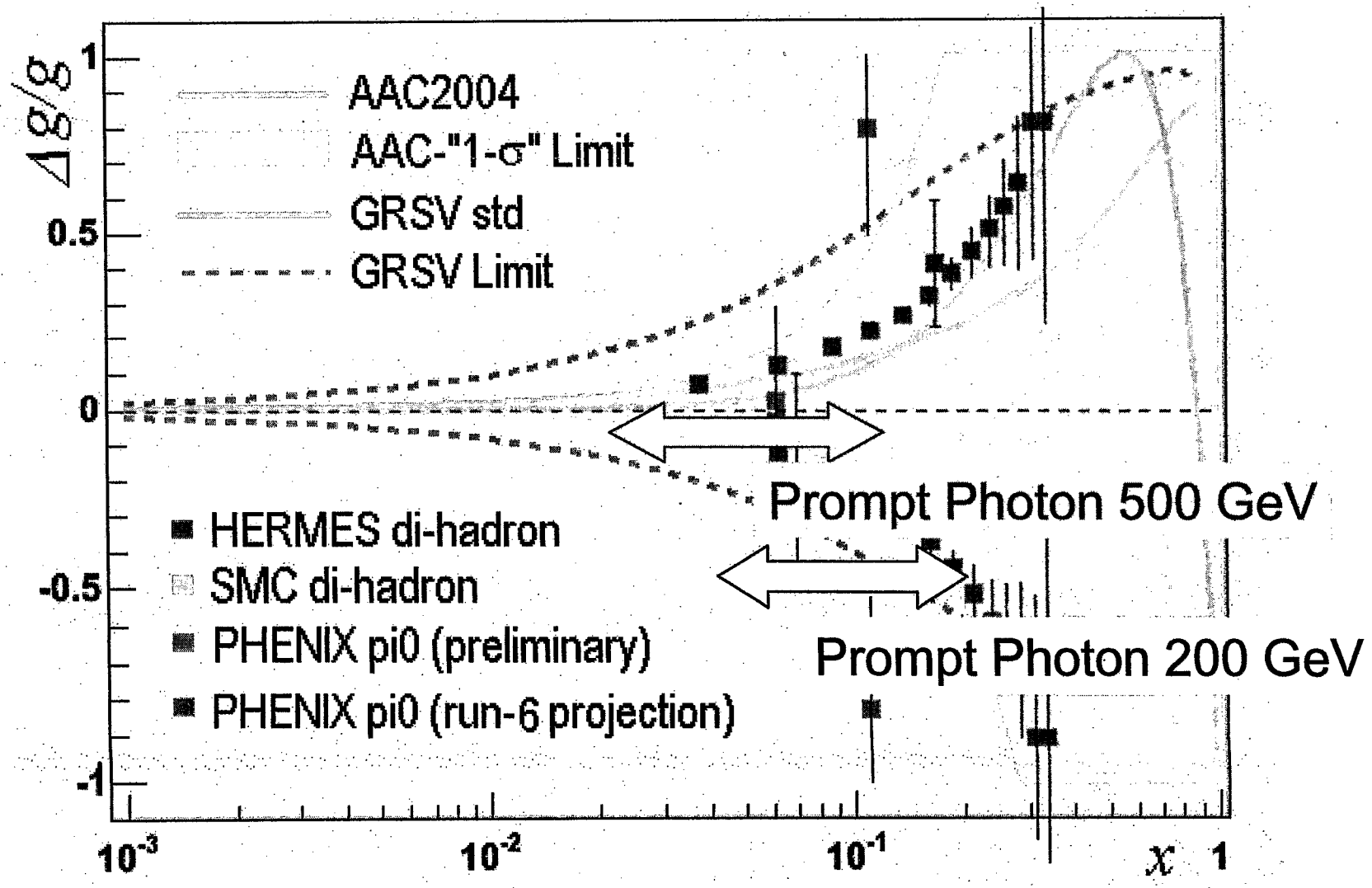

Mike's point: k_T can be measured !

Apanasevich et al.,PRD59, 074007

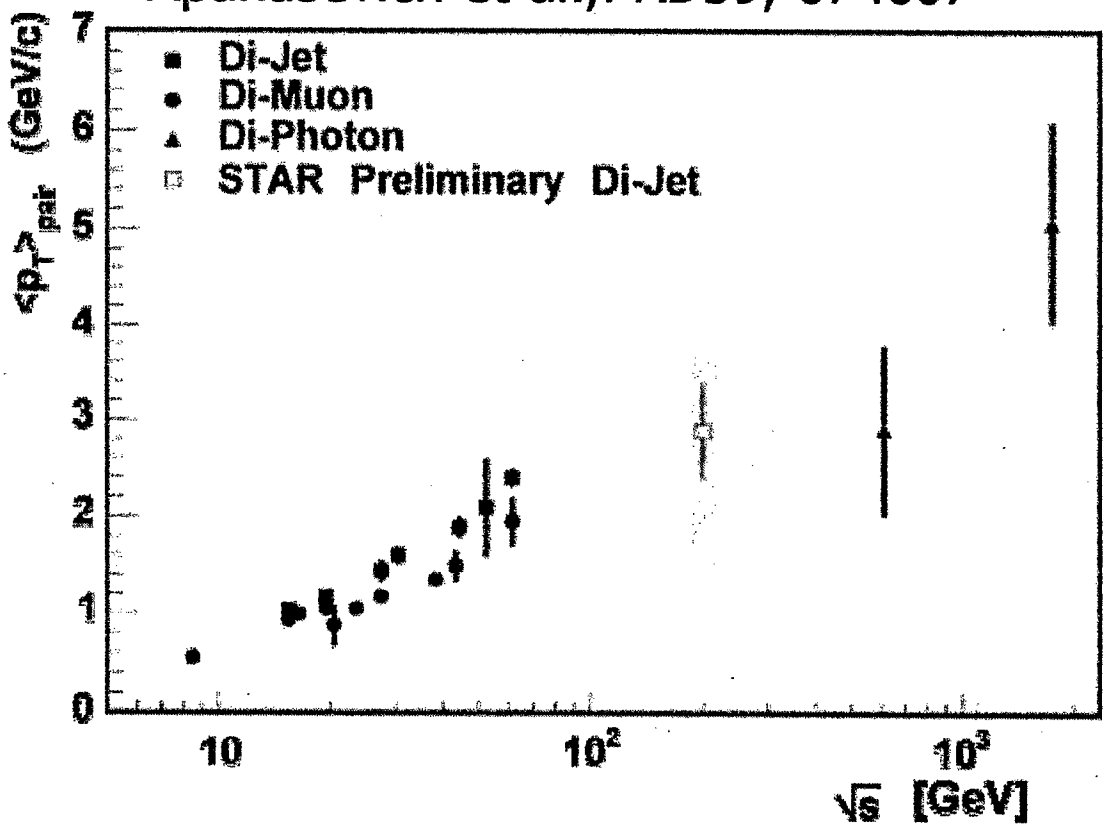

* recent STAR for back-to-back hadrons :

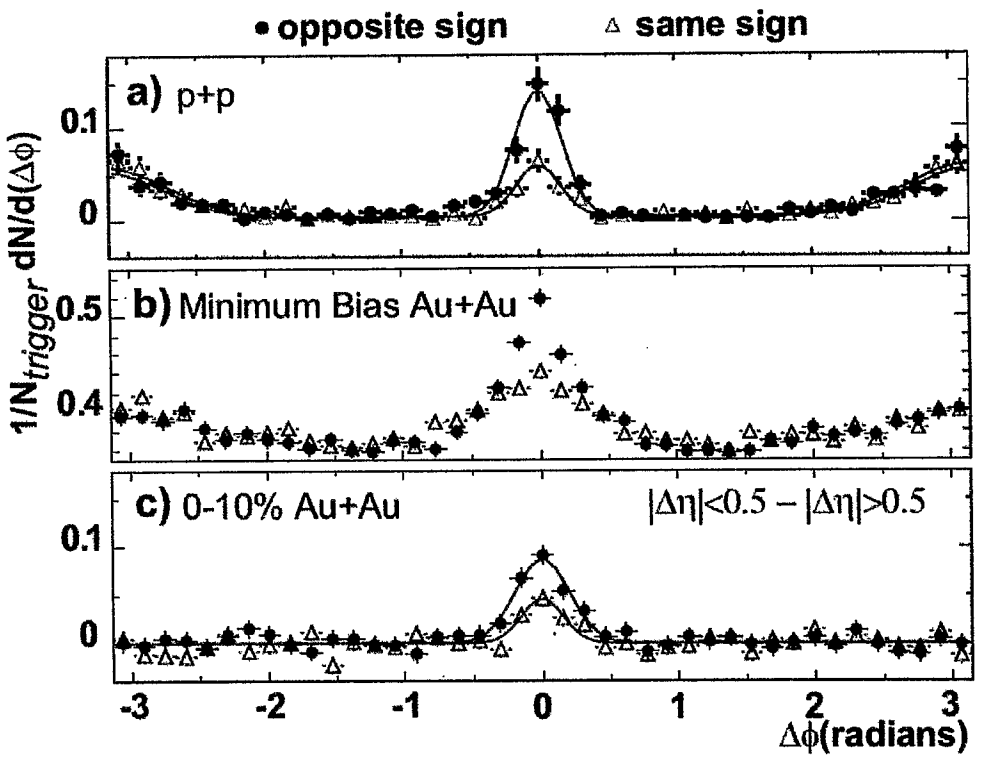

- gluon radiation: Sudakov effects

  in all these observables

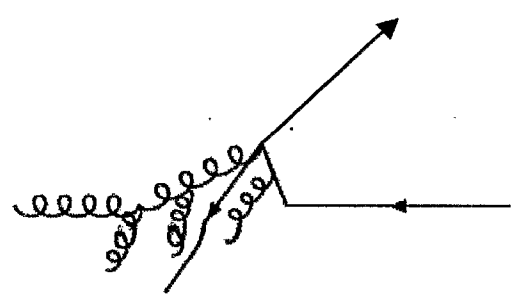

- Gaussian $k_\perp$ distribution for partons yields unpol. correlation :

$$\mathcal{U} \propto e^{a(1+\cos(\delta\phi))}$$

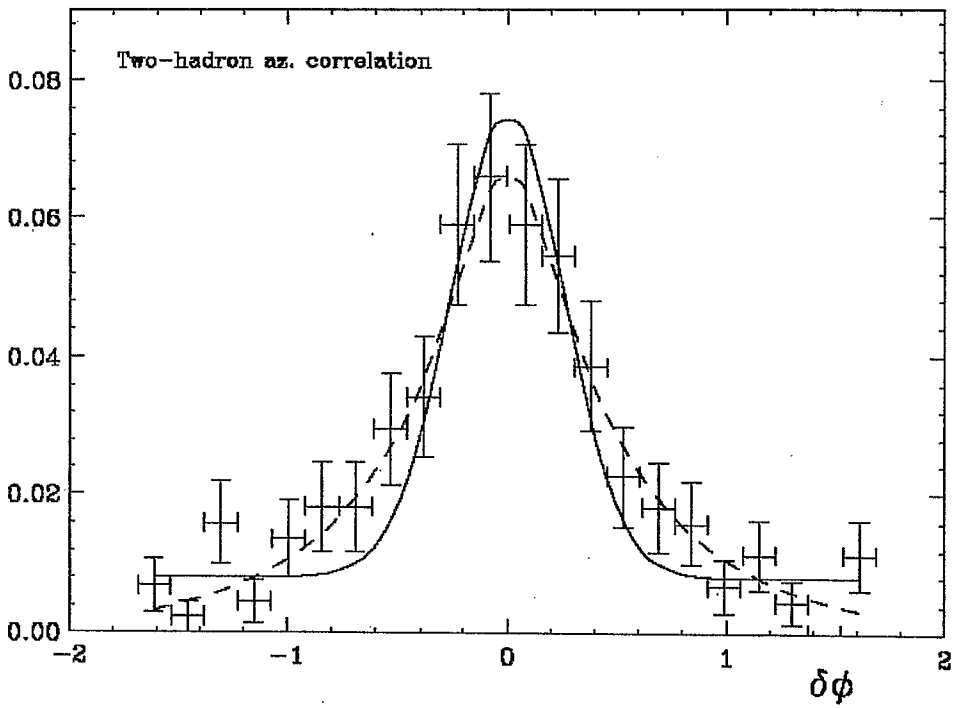

Boer, WV

$\sqrt{\langle k_\perp^2 \rangle} \approx 2$ GeV

STAR

- dashed line: including Sudakov effects
  - markedly better agreement with data; $\sqrt{\langle k_\perp^2 \rangle} \approx 0.9$ GeV

    not Gaussian

→ **how about single-inclusive cross sections ?**

- k_T **effects become "higher-twist"** $\frac{\langle k_T \rangle}{p_T}$

- **often used as model for higher twist AND higher order corrections**

- **no unique way of putting** k_T **into cross sections due to kinematic singularity at** $p_T \sim k_T$

(Contogouris, Gaskell, Papadopoulos; Begel, Huston et al.;
d'Alesion, Murgia; ...
Owens, Fink; Sterman, WV; ...)

$pp \to \pi^0 X$

at lower energies

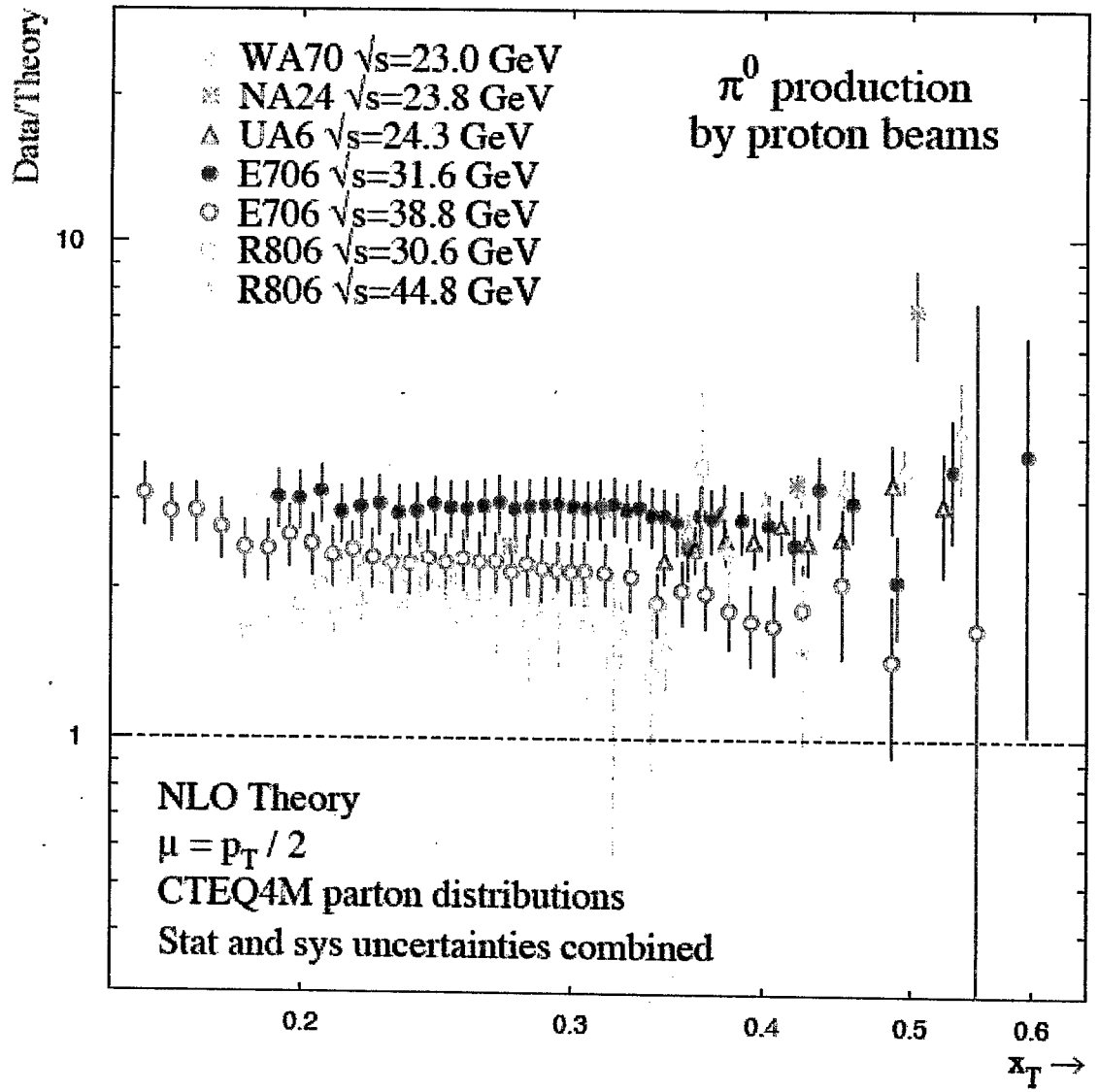

Owens et al.

(see also Aurenche et al.; Bourrely, Soffer)

$pp \rightarrow \pi^0 X$ at RHIC

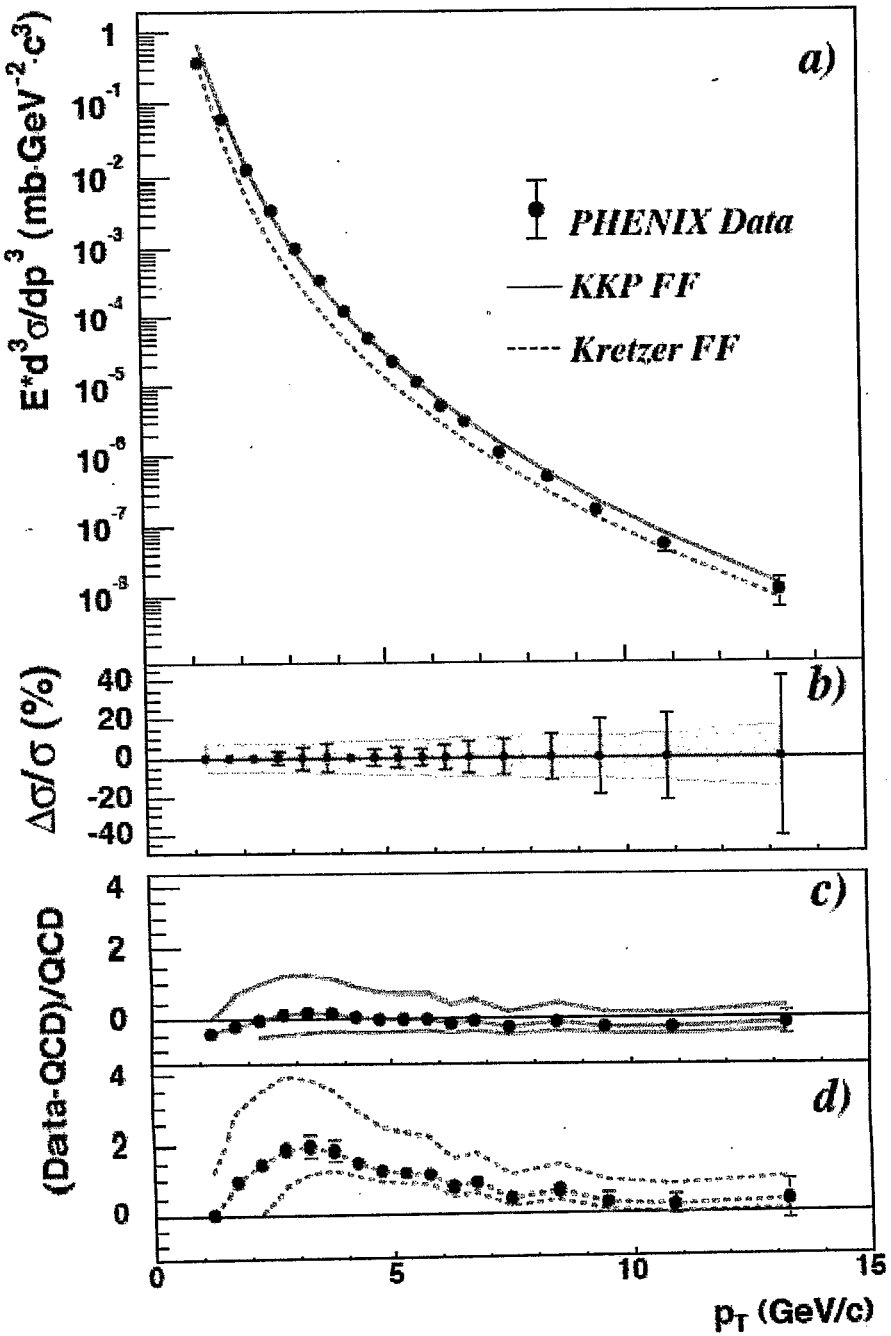

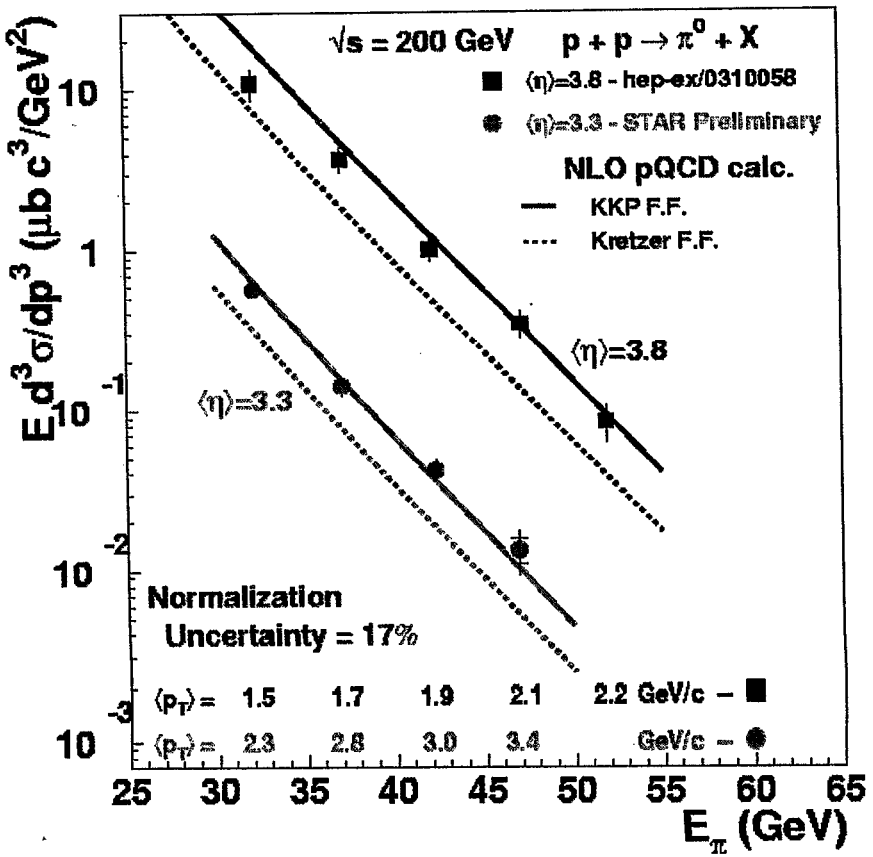

Higher orders are important!

$pp \rightarrow \pi^0 X$

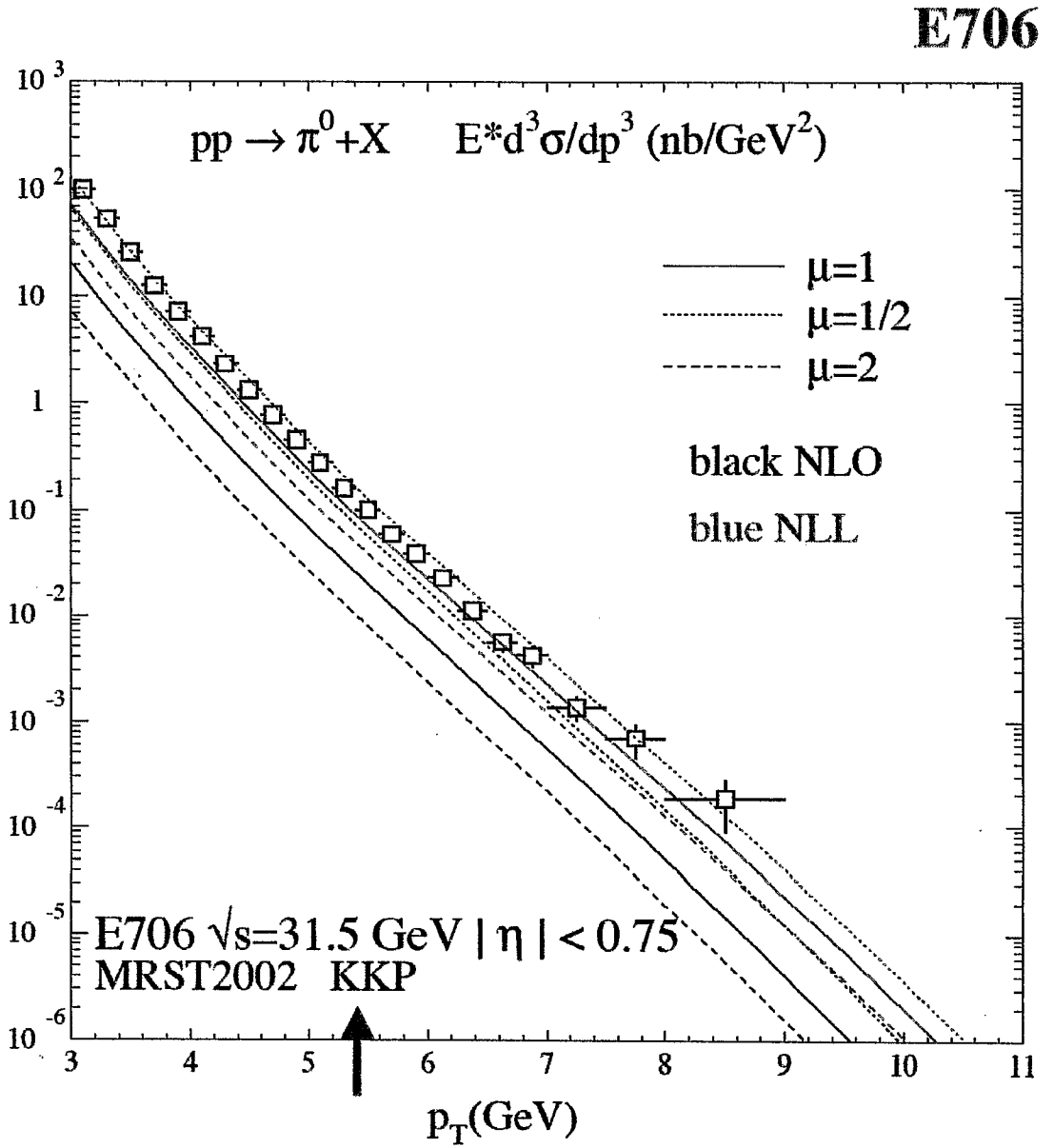

de Florian, WV

WA70

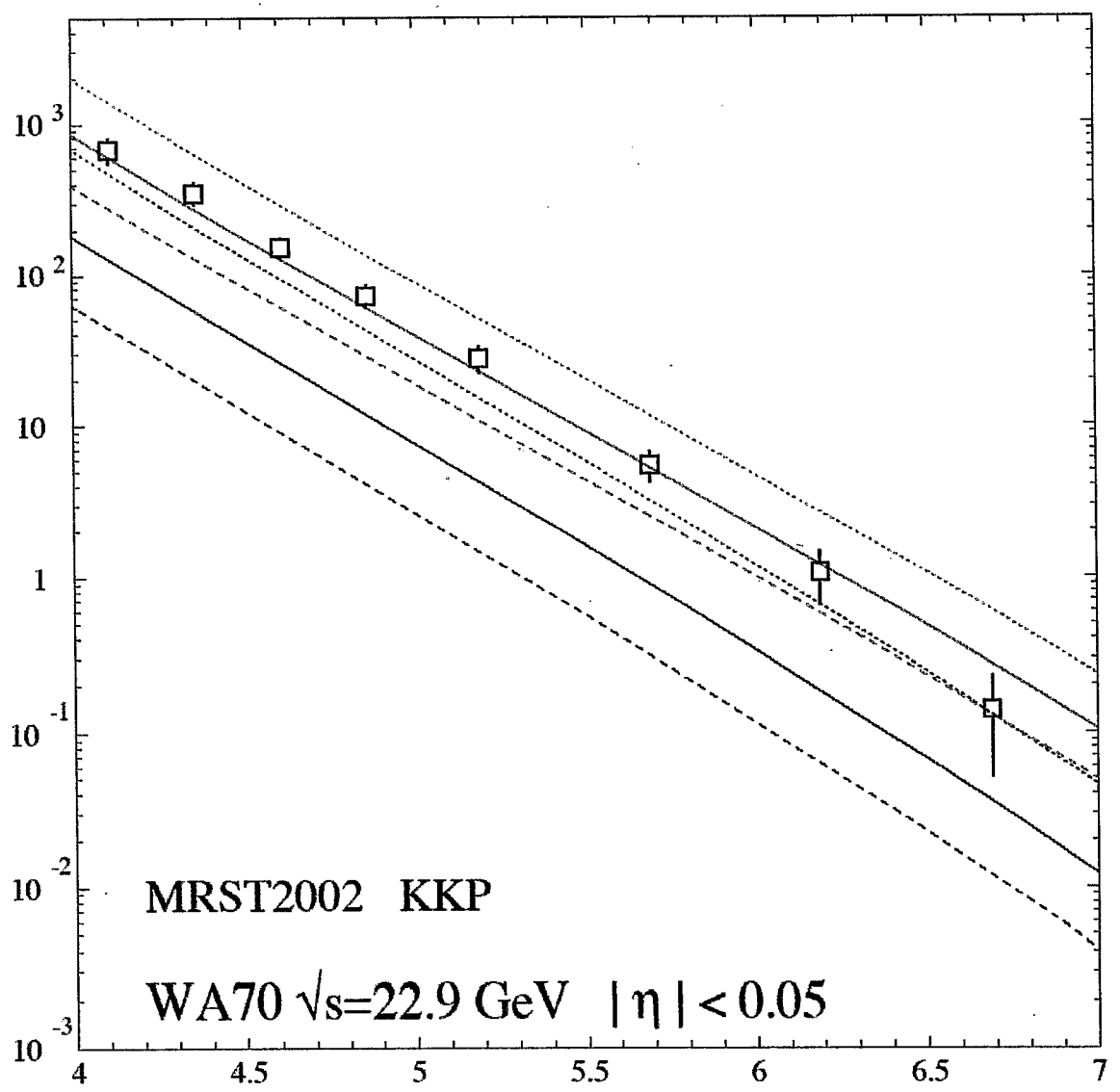
MRST2002 KKP
WA70 √s=22.9 GeV |η| < 0.05
10 3
10 2
10
1
10 -1
10 -2
10 -3
4
4.5
5
5.5
6
6.5
7

How dominant are they ?

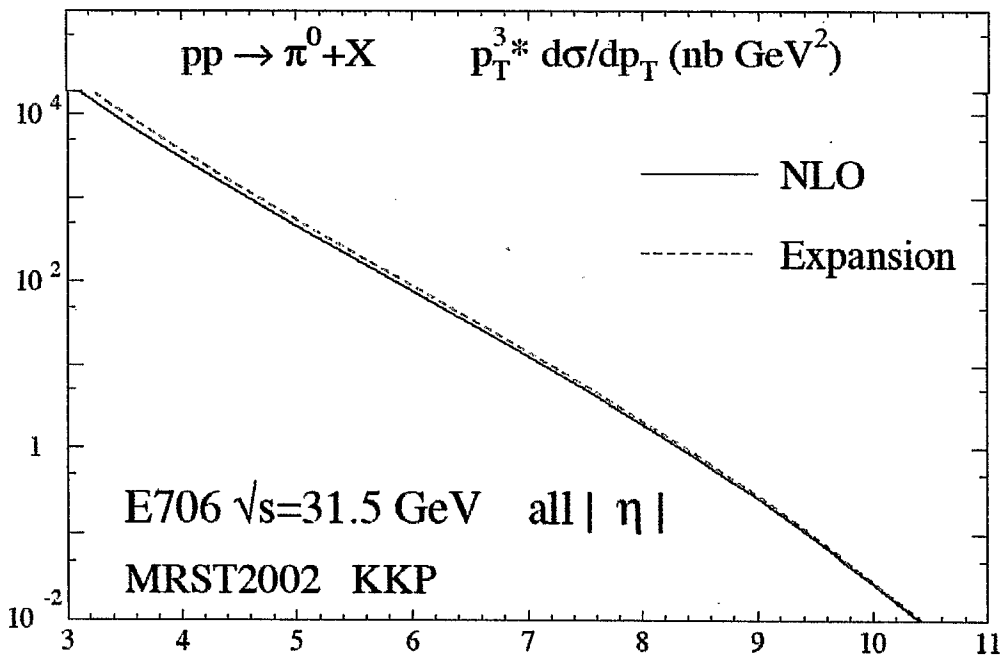

- note, for single-inclusive cross sections $pp \to \gamma X$:

$$Q \leftrightarrow 2p_T$$

$$N \leftrightarrow \frac{1}{\ln x_T^2} \qquad x_T \equiv \frac{2p_T}{\sqrt{s}}$$

- then,

$$\frac{N^2}{Q^2} \sim \frac{1}{p_T^2 \ln^2\left(\frac{4p_T^2}{s}\right)}$$

Sterman,WV

(from Soper's paper)

$$G(\vec{P}_T) = \int d\vec{k}_T \; \rho(\vec{k}_T; P_T) \; G\Big(\vec{P}_T - \frac{1}{2}\vec{k}_T\Big)_{\rm NLO}$$

$$\begin{aligned} G(\vec{P}_T) \;\; \approx \;\; & \int d\vec{k}_T \; \rho(\vec{k}_T; P_T) \; \Big\{ G(\vec{P}_T)_{\rm NLO} \\ & -\frac{1}{2} k_T^i \nabla_i G(\vec{P}_T)_{\rm NLO} + \frac{1}{8} k_T^i k_T^j \nabla_i \nabla_j G(\vec{P}_T)_{\rm NLO} \Big\} \end{aligned}$$

$$\frac{d\sigma}{dE_T} \approx \left(\frac{d\sigma}{dE_T}\right)_{\rm NLO} \left\{ 1 + \frac{(n+1)^2 - n'}{16} \; \frac{\langle k_T^2 \rangle}{E_T^2} \right\}$$

PHENIX: Muon trigger upgrade and Nose Cone Calorimeter

Kenneth N. Barish

RHIC SPIN Meeting - Torino
9 October, 2004

PHENIX

University of California
Riverside

Physics Motivation

Add PHENIX's capabilities at forward rapidity:

- ✓ Probe nucleon structure through W production in polarized p+p
- ✓ Measure ΔG to lower x_G in the prompt-γ channel
- ✓ Study nucleon structure in nuclei at high parton densities in p+A collisions.
- ✓ Significantly extend acceptance for high p_T jet-photon measurements (jet tomography) in A+A.

Upgrade Components

Upgraded muon trigger

- Add momentum information into muon trigger for highest luminosities in p-p, d-A and A-A
- Gives robustness against beam and collision related backgrounds.

Nose cone calorimeter (NCC)

- $0.9 < |\eta| < 3.0$
- Tungsten-Silicon sampling calorimeters
- Electromagnetic and shallow hadronic compartment
- Expands PHENIX's kinematical coverage for jets, inclusive neutral pions, electrons, and photons to forward rapidity
- For p-p, d-A and A-A collisions.

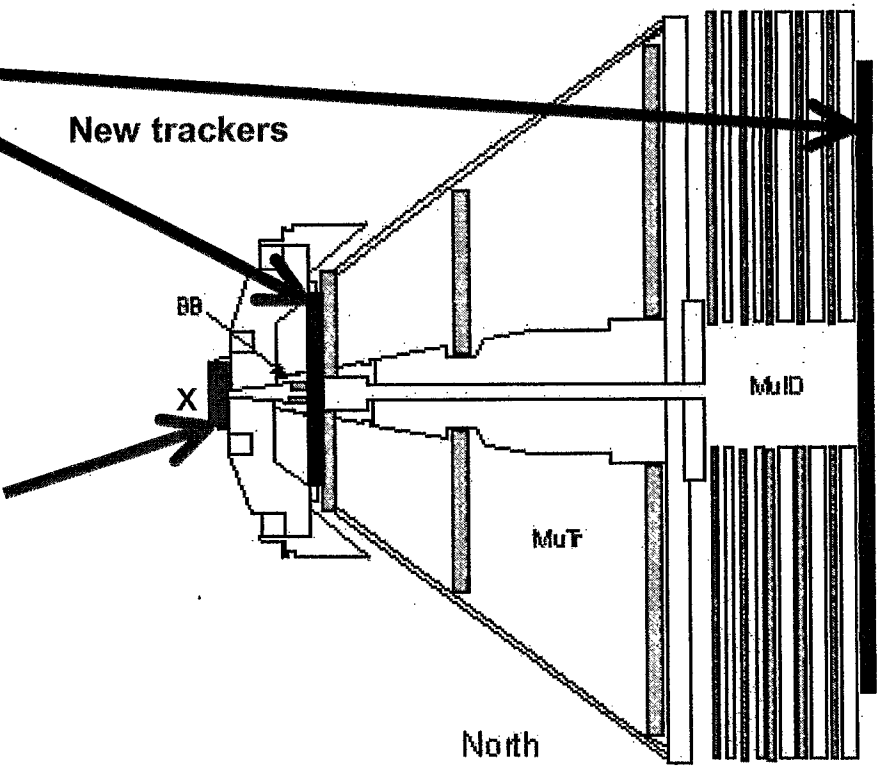

Upgraded muon trigger and NCC also on South side

Understanding proton spin structure

» Pressing issues to understand dynamics of the nucleon spin:

—Contribution of gluons to proton spin - $\Delta G(x)$

—Flavor separation of quark polarization - measure $\Delta\bar{q}(x)/\bar{q}(x)$ and $\Delta q(x)/q(x)$

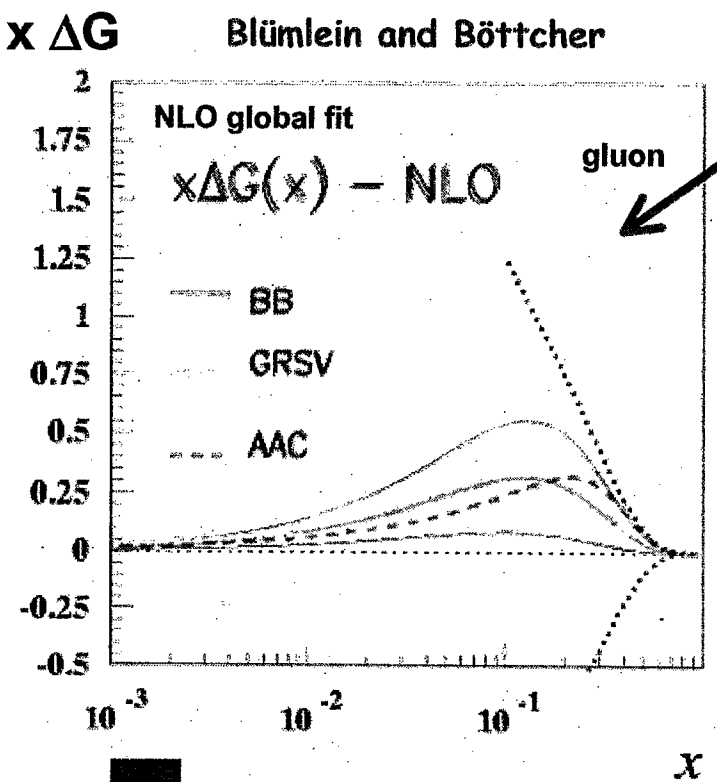

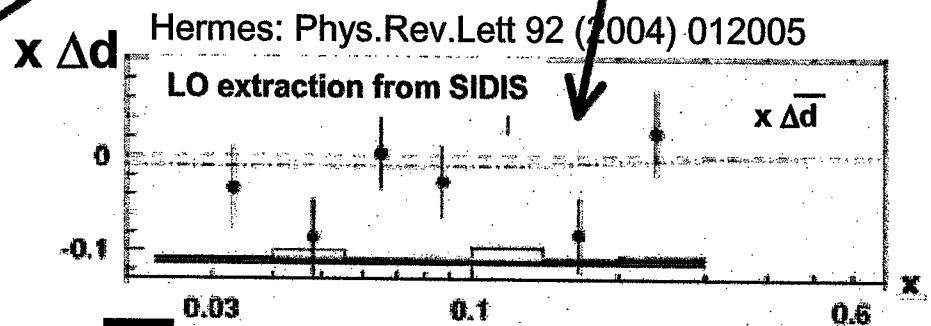

W trigger upgrade!

$\Delta G(x)$ and $\Delta q(x)/q(x)$, $\Delta\bar{q}(x)/\bar{q}(x)$ are currently poorly constrained

Nose Cone Calorimeter!

ΔG using the NCC

- Detection of both hadron jet and final state photon is possible with the NCC and new central arm tracking detectors.
  - Allows the determination of x_G of the gluon on an event-by-event basis (used in conjunction with silicon vertex)

- Significantly extends the range of x_G for the prompt-γ measurement down to ~0.001 at $\sqrt{s}$ =200 GeV
  - Channel with highest analyzing power for gluon polarization in polarized p+p.
  - Sensitivity to shape of polarized gluon distribution over a large x range (important input to extrapolation of ΔG to low x)

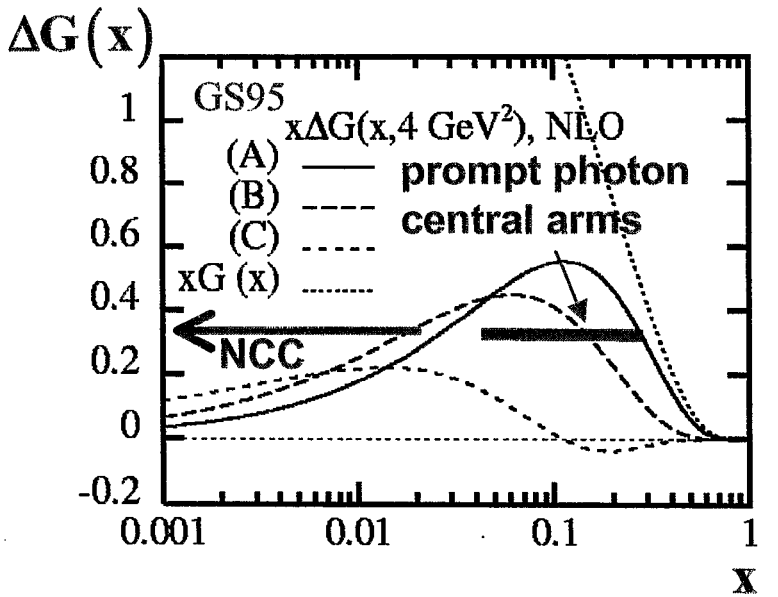

- ΔG with NCC at low-x through jet-γ, π^0, e-μ, open charm.

Flavor decomposition via W's with PHENIX

- The measurement of inclusive single spin muon asymmetries (from W's) is the least biased way to probe $\Delta q/q$, $\Delta \bar{q}/\bar{q}$.
  - Complete theoretical treatment from first principles by Nadolsky and Yuan using re-summation and NLO techniques [NuclPhysB 666(2003) 31].
  - Does not suffer from scale uncertainties

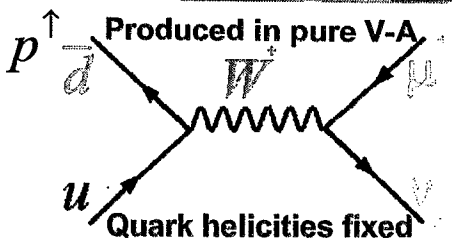

$$A_L = \frac{1}{P}\frac{N^{\uparrow} - N^{\downarrow}}{N^{\uparrow} + N^{\downarrow}}$$

- Experimentally clean measurement .
  - A_L is parity violating → no false physics asymmetries.
  - Does not rely on knowledge of fragmentation functions
- Highest luminosity p+p running at 500GeV required.
  - Prescale factor of 20-50 required without muon trigger upgrade.
  - Significance would go down by prescale factor √

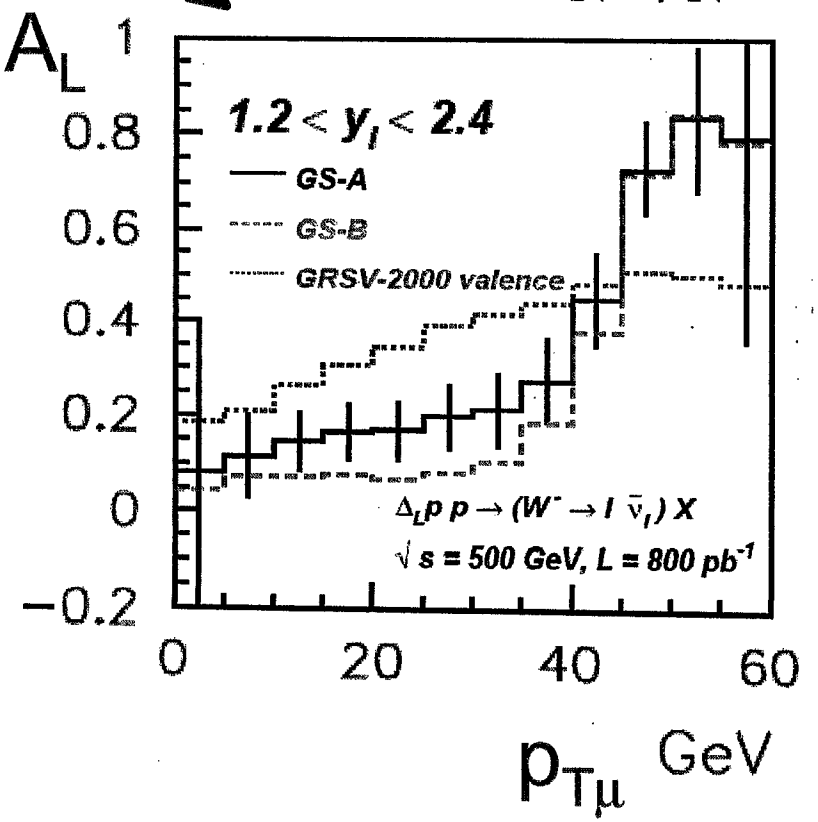

K. Barish

High parton densities in nuclear matter

- ✓ **QCD - High Gluon Densities at low-x**
  - » Onset of gluon saturation?
  - » Initial conditions in Au+Au?
- ✓ **Classical Approx → Color glass condensate**
  - » McLerran, Venugopalan, et al.
  - » Depends on a single scale
    - – $Q_s^2 \propto A^{1/3} \sim (1\text{-}2\ \text{GeV})^2$ at RHIC
  - » Is this the correct theory at RHIC?
  - » Where are the boundaries?

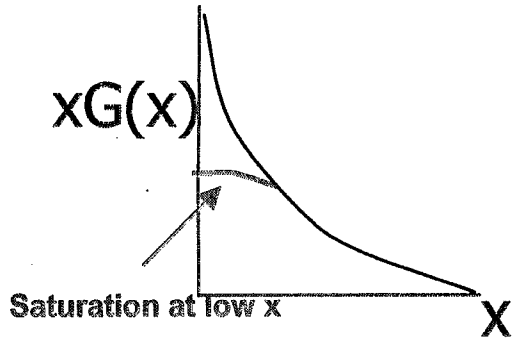

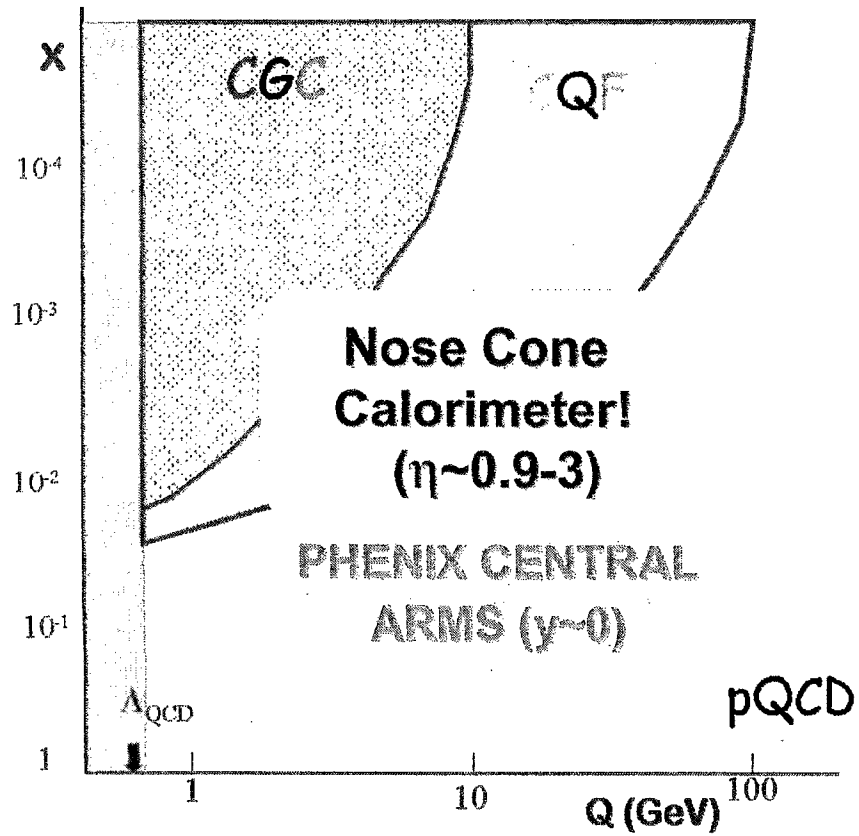

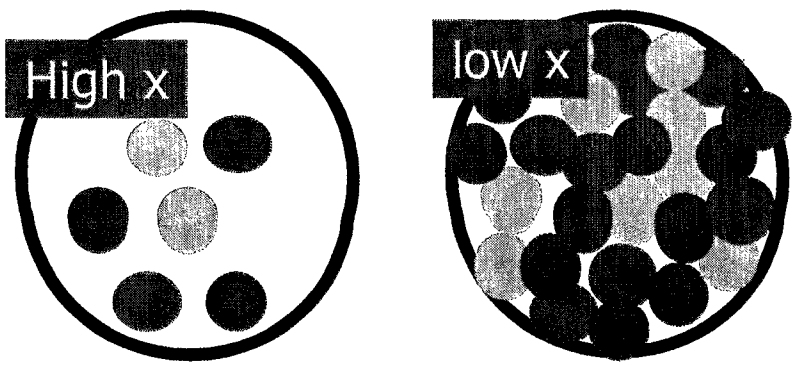

PHENIX

K. Barish

PHENIX Forward Upgrade Components

Nosecone Calorimeter

» Sampling Tungsten-Silicon

» Silicon photon / π^0 identifier layers

Muon trigger

» Upstream tracker (RPC or MuTr)

» Downstream tracker (RPC's)

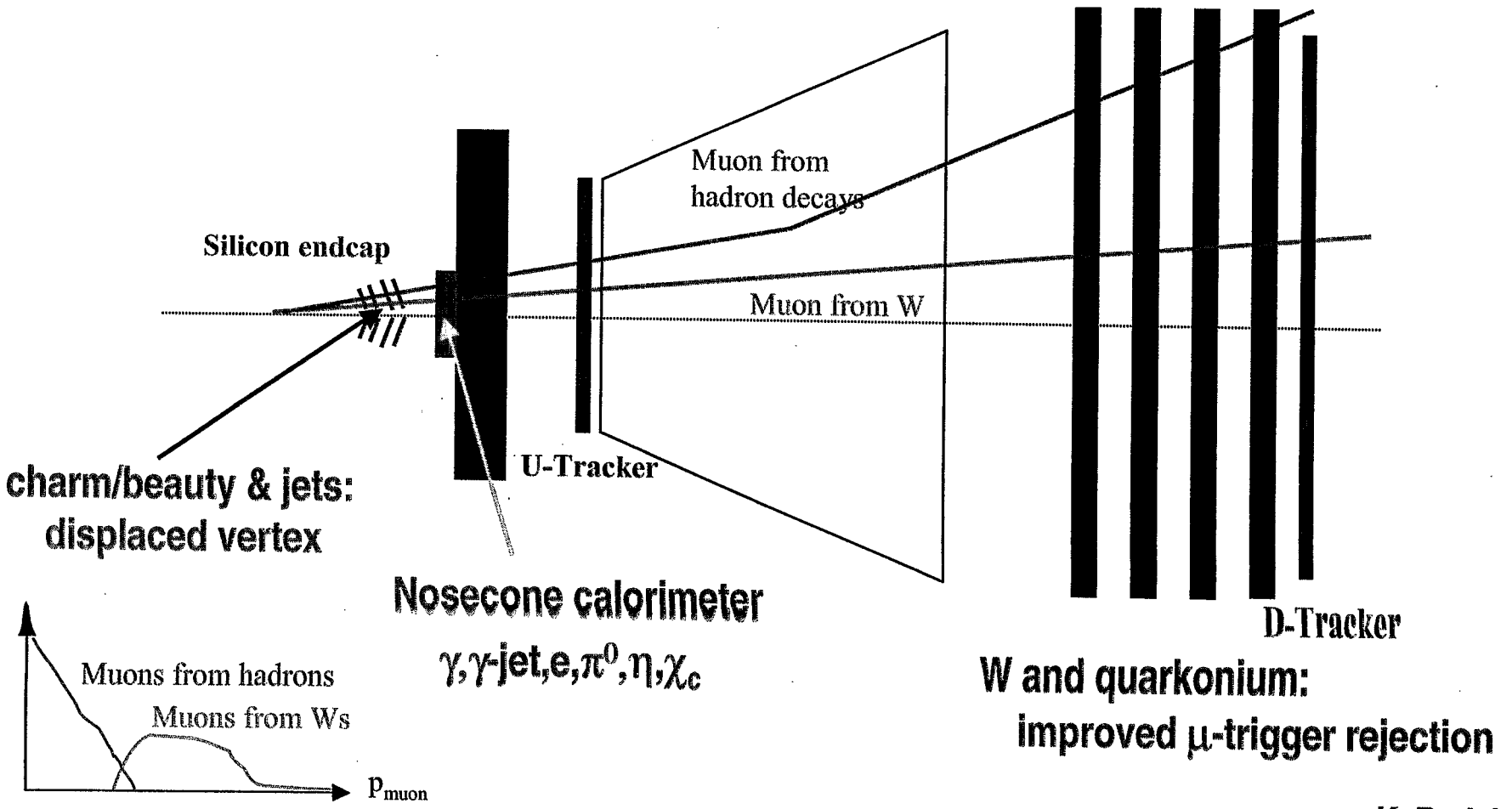

K. Barish

Upgraded muon trigger for W's

» **Current muon trigger:**
- 2.3GeV "deep" muon
- Factor of 20-50 rejection and robustness to background required for p+p at highest luminosities

» **Upgrade needed to add momentum information to trigger:**
- RPC's for new chambers
  - Even modest timing information help remove beam related background.
- Instrument muTR with triggering electronics

» **Detailed simulations with lookup-table algorithms give specifications:**
- Upstream tracker granularity 10x10cm^2 into look-up table
- Downstream tracker granularity 30x30cm^2 into look-up table
- ϕ resolution = 1°

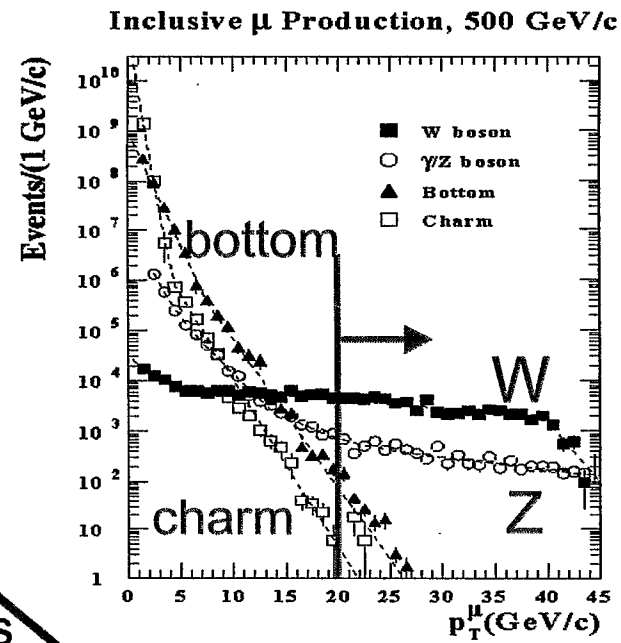

➢ **RPC R&D at UIUC and RBRC prototype for run 5.**

➢ **Tests/studies at Kyoto and UNM to instrument muTR**

Nose Cone Calorimeter

Requirements:

- Good photon measurements
- Reasonable jet measurements
- Triggering capability

Constraints:

» 40 cm from collision point **=> Silicon pixels**

» 20 cm of space is available **=> Tungsten** small Molière R

» Photon / π^0 separation **=> Silicon strip layers**

Challenging technical requirements, but devices with similar specifications have been built for balloon based experiments.

Nose Cone Longitudinal Segmentation

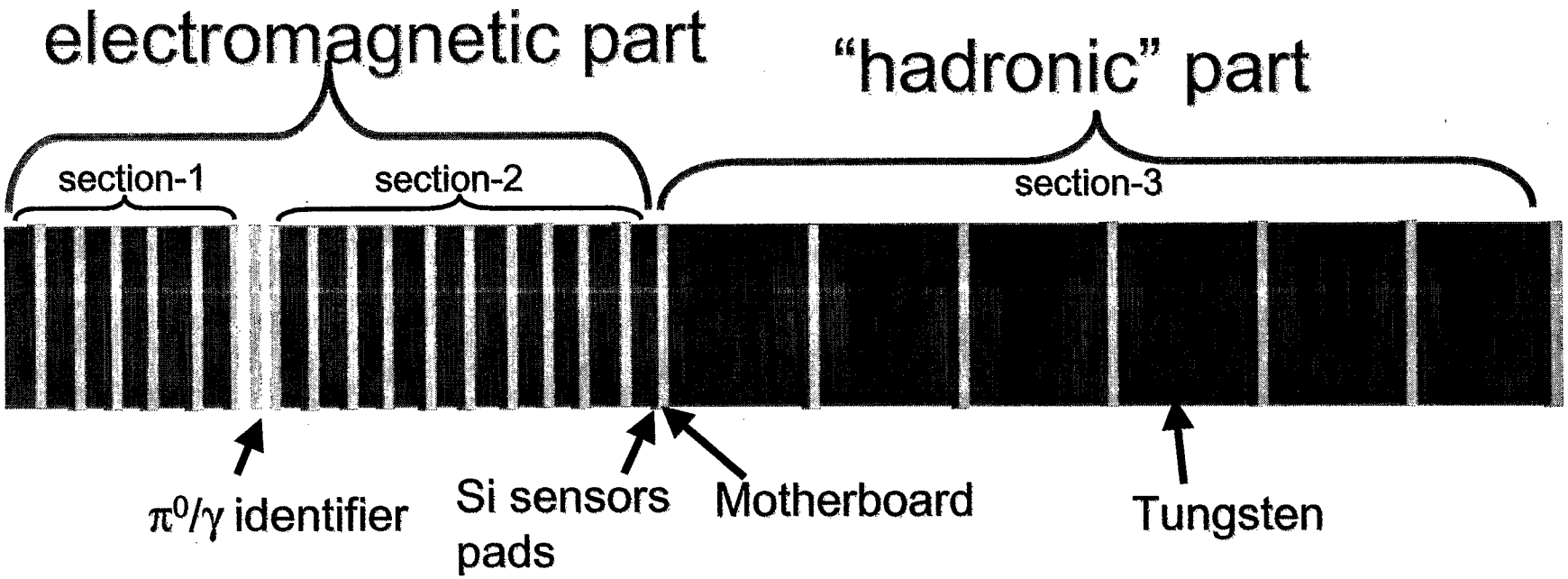

Electromagnetic
- » 16 layers of W 2.5 mm thick ➔ $10X_0$
- » Si 1.5 cm x1.5 cm pads

π^0/γ identifier
- » 2 layers Si , 1.9 mm x 6 cm strips
- » after $4.3X_0$

Hadronic
- » 6 layers W16.6 mm thick
- » Si 1.5 cm x 1.5 cm pads
- » Total (em+had) $40X_0$ $1.5\ \lambda_0$

Readout in 3 longitudinal sections
Molière radius~1.3 cm
EM Energy resolution ~ $20\%/\sqrt{E}$
Hadronic Energy res ~ $100\%/\sqrt{E}$ (?)
2γ "2 track resolution" ~ 4mm (?)

X_0(tungsten)=3.5mm
λ_0=9.5 cm

PHENIX

K. Barish

10 GeV electron in NCC

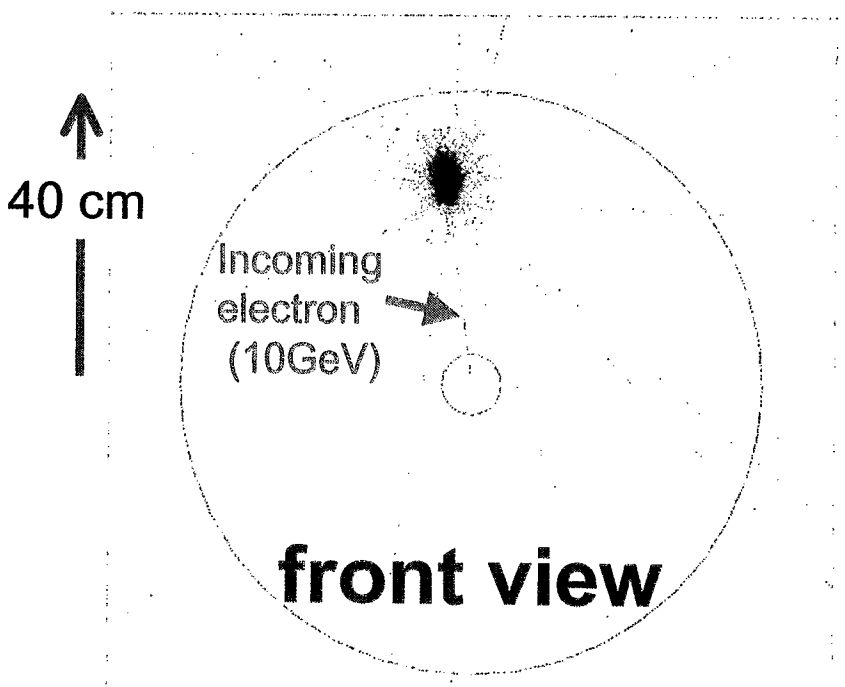

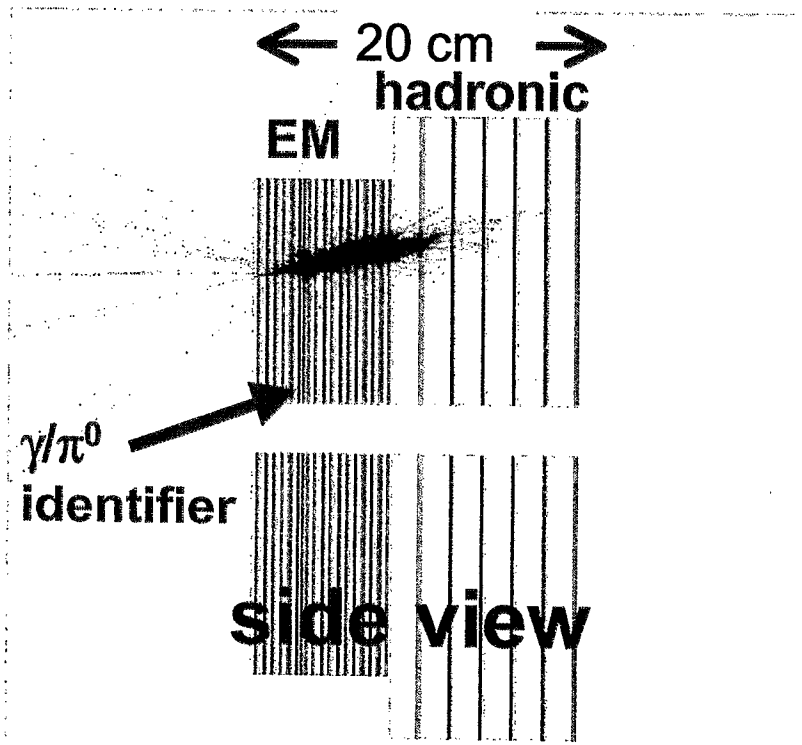

Gluon distribution function

- Pythia input : normal structure function (p+p) and parameterized saturated structure function (p+A) that fit RHIC data.
- Can constrain gluon structure function by making measurements over rapidity and p_t
- Many other observables:
  - E.g. photons jet correlations
    - Constrain kinematics to obtain gluon structure function.
    - Intrinsic k_t.
    - Jet broadening,

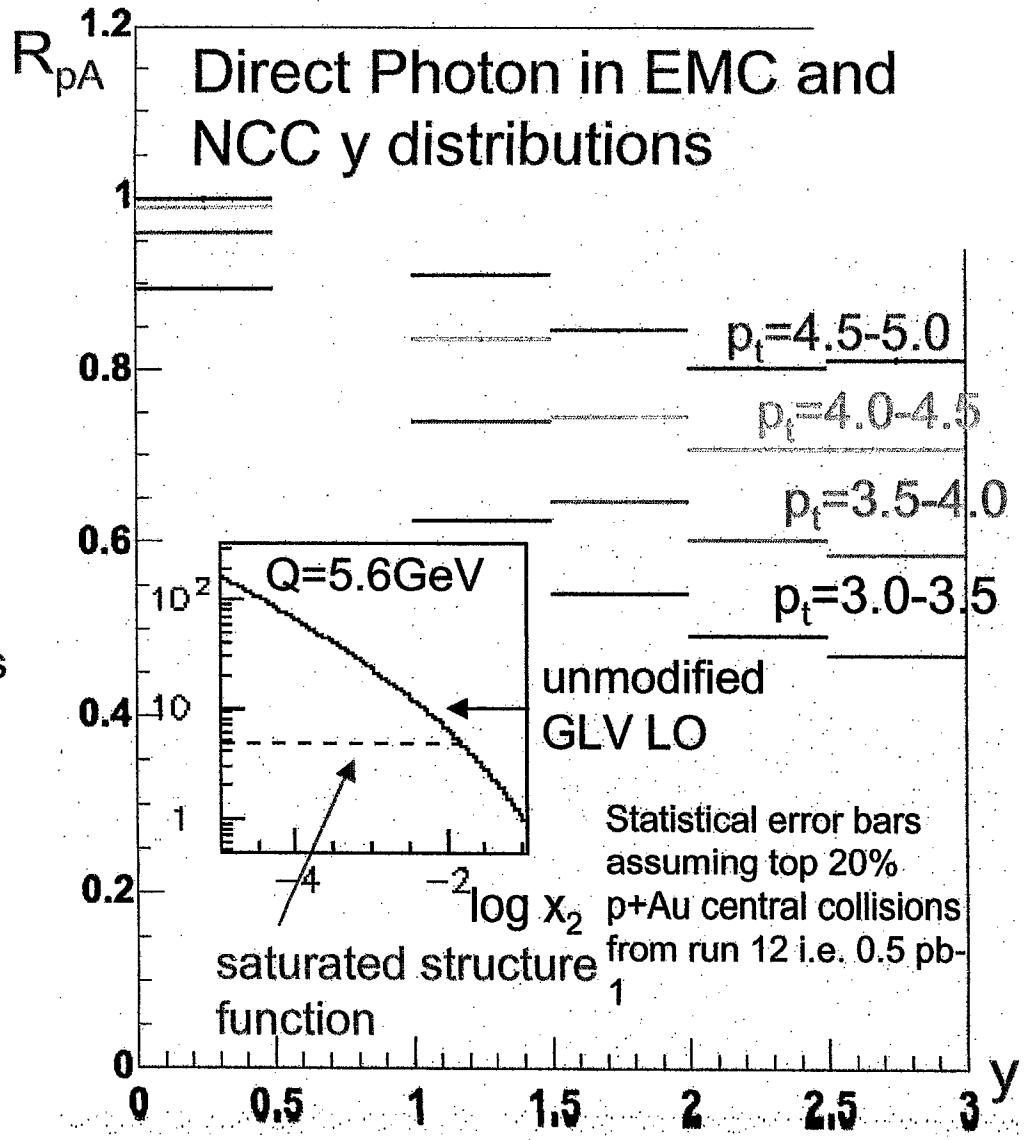

PHENIX

K. Barish

Rough Schedule & Cost

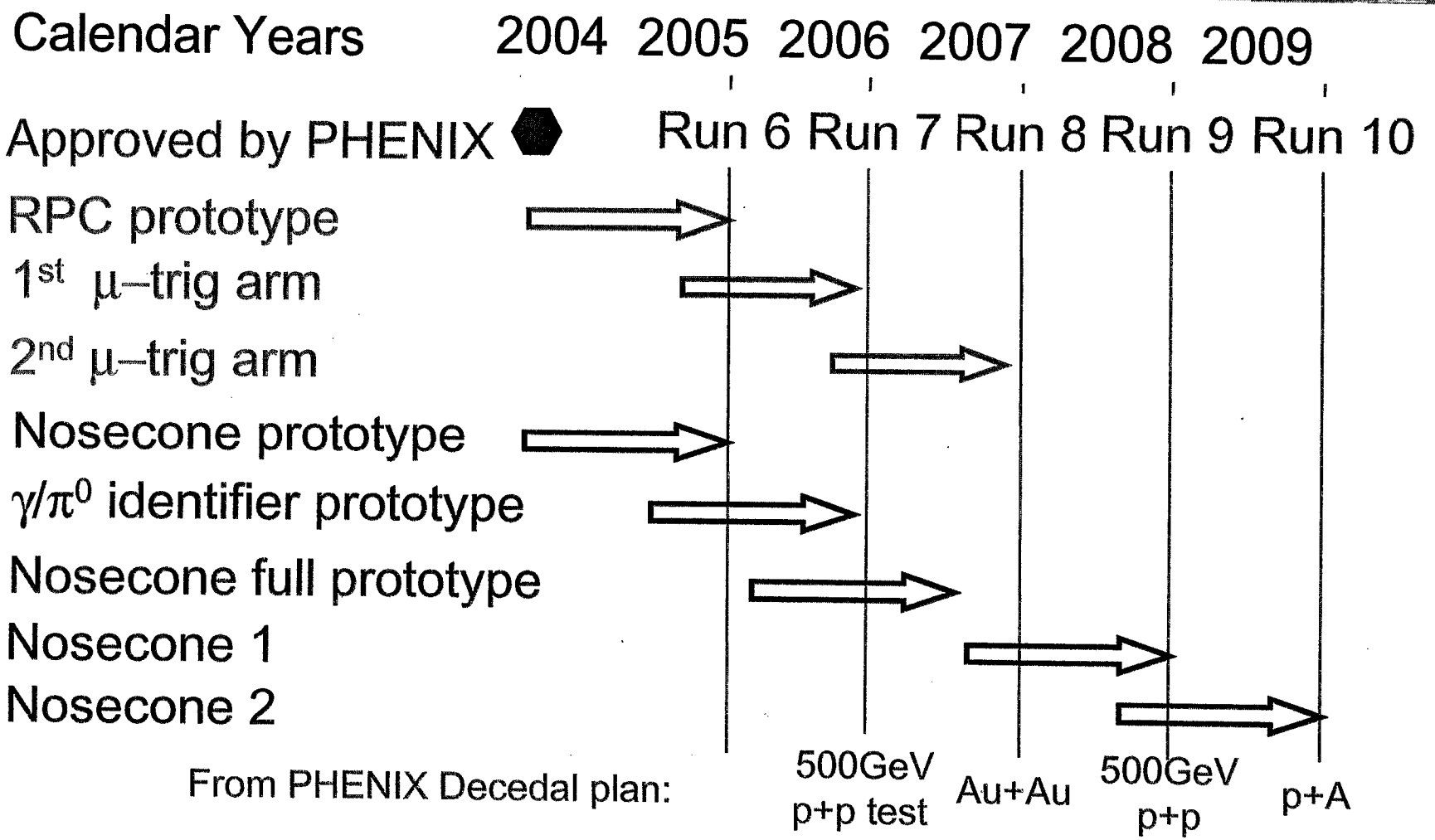

We are now seeking funding & forming an upgrade collaboration.

Initial cost estimates: muon trigger ($2M), NoseCone ($4M/arm)

Summary

- Extend kinematical reach of $\Delta G(x)$ measurements
  - prompt photon down to $x_g \sim 10^{-3} \Rightarrow$ NCC
- Flavor decomposition $\Delta q(\bar{x})/q(\bar{x})$ & $\Delta q(x)/q(x)$.
  - via $W \rightarrow \mu\nu$ theoretically clean measurement
  - Upgraded μ trigger required
- High parton densities in nuclear matter
  - Saturation? CGC?
  - Initial conditions in Au+Au
  - Gluon distribution function forward rapidities $\Rightarrow$ NCC

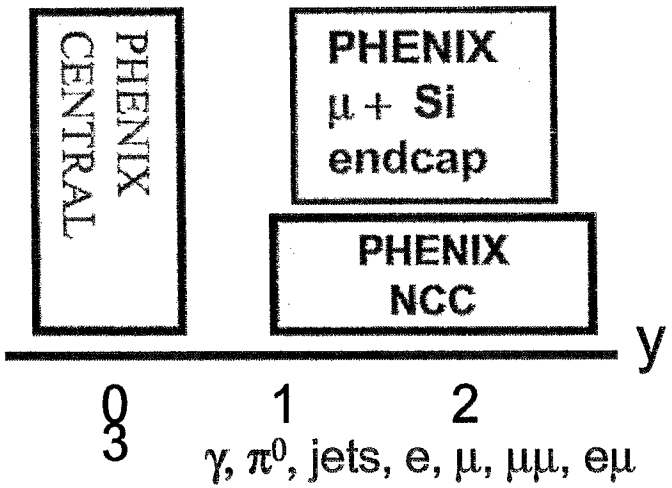

- Extend jet tomography to $\eta \sim 2.5$.
  - photon-jet measurement $\Rightarrow$ NCC (photon or jet in NCC)
- Expand the physics with quarkonia to new states and high luminosity
  - Requires enhanced muon trigger for $\Psi \rightarrow \mu\mu \Rightarrow \mu$ trigger
  - Measurement of $\chi_c \rightarrow J/\psi + \gamma$ may be possible $\Rightarrow$ NCC

Physics takes advantage of highest luminosity p+p, p+A, A+A

Extra slides ...

Expected γ/π^0 separation

Extrapolating PHENIX EMC experience of γ/π^0 separation with central arm EMC to NoseCone EMC:

» PHENIX today has a brute-force pattern recognition that works up to around 15 GeV/c π^0 energy

» NCC is x10 closer to production vertex

1.5 GeV/c

» x10 better lateral granularity and x3 smaller Moliere radius resulting in x 3.5 two photon separation

5 GeV/c

» With 2 mm strips in the silicon layers we can separate two close photons down to ~4 mm compared to ~ 2 cm assumed for NCC itself

~20 GeV/c

Coverage of NCC at 200 GeV

0.5 pb^{-1} pAu (run 12)

$\Delta\log(x_2)\ \Delta Q^2 = 0.1 \times 1\ GeV^2$

Direct photon

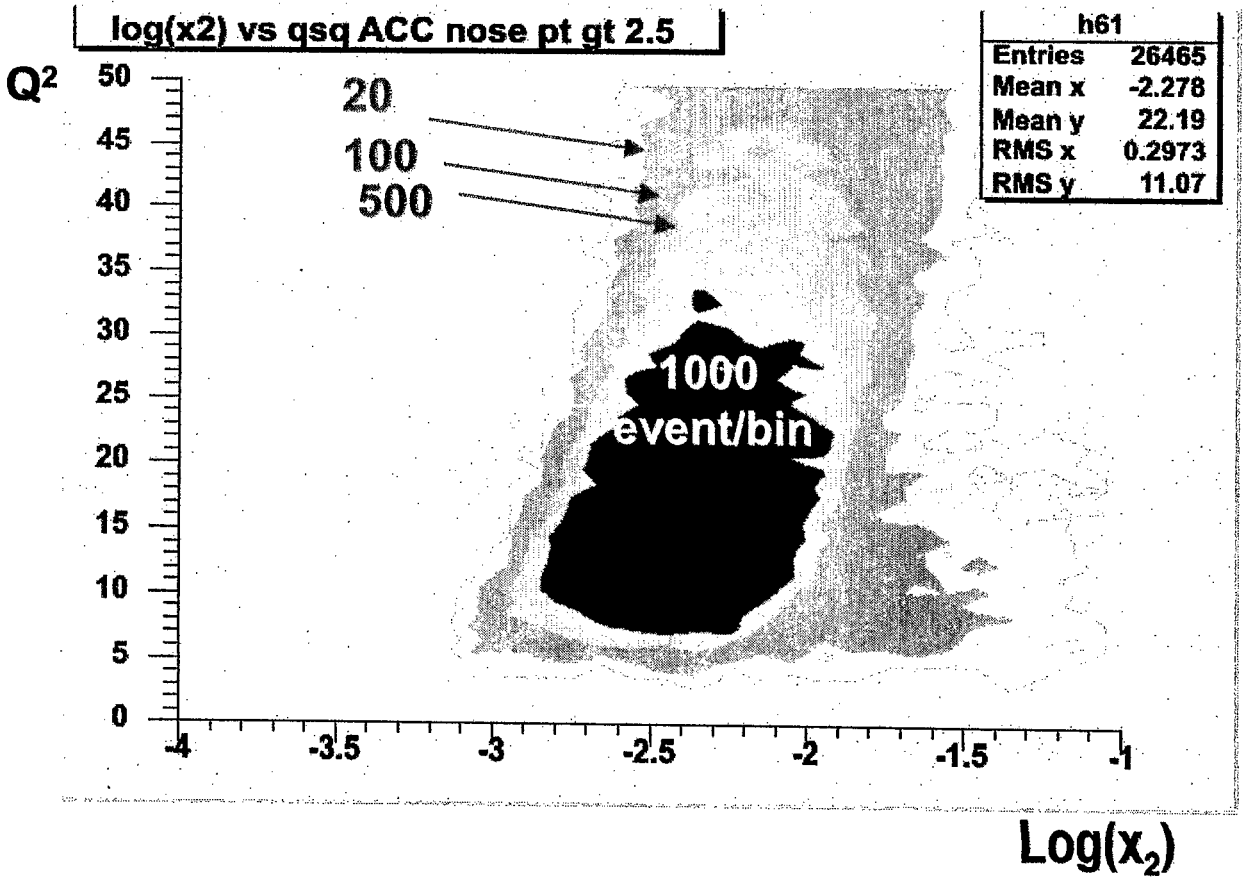

PHENIX

K. Barish

NCC in central Au+Au

- Problem is pile up faking a photon
- Problem worst at high η since the effective segmentation is larger

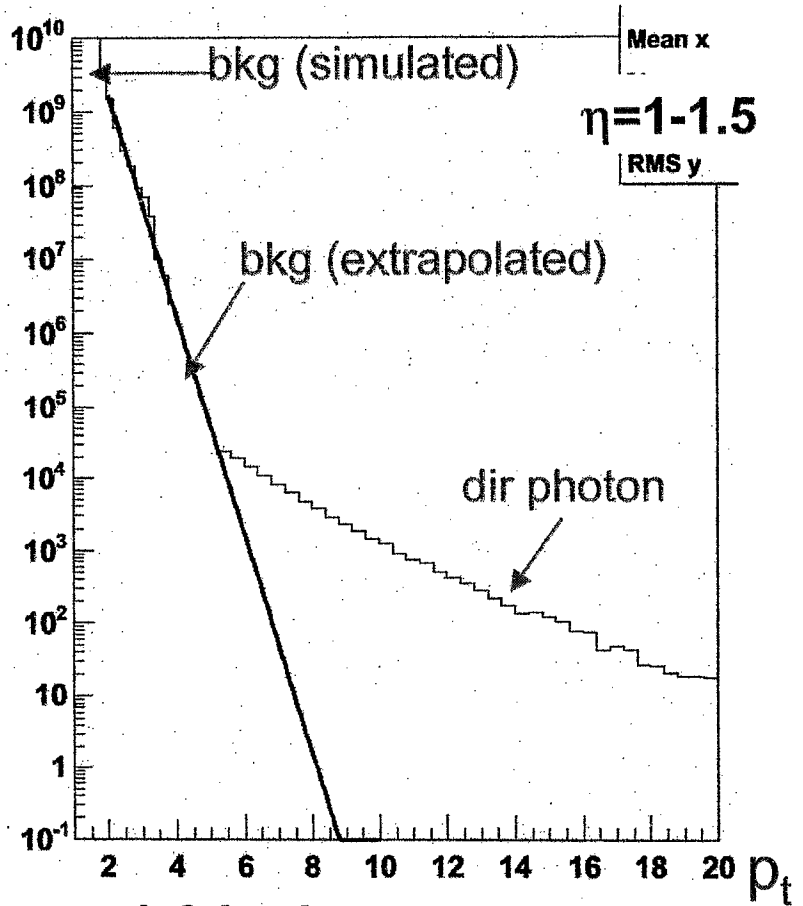

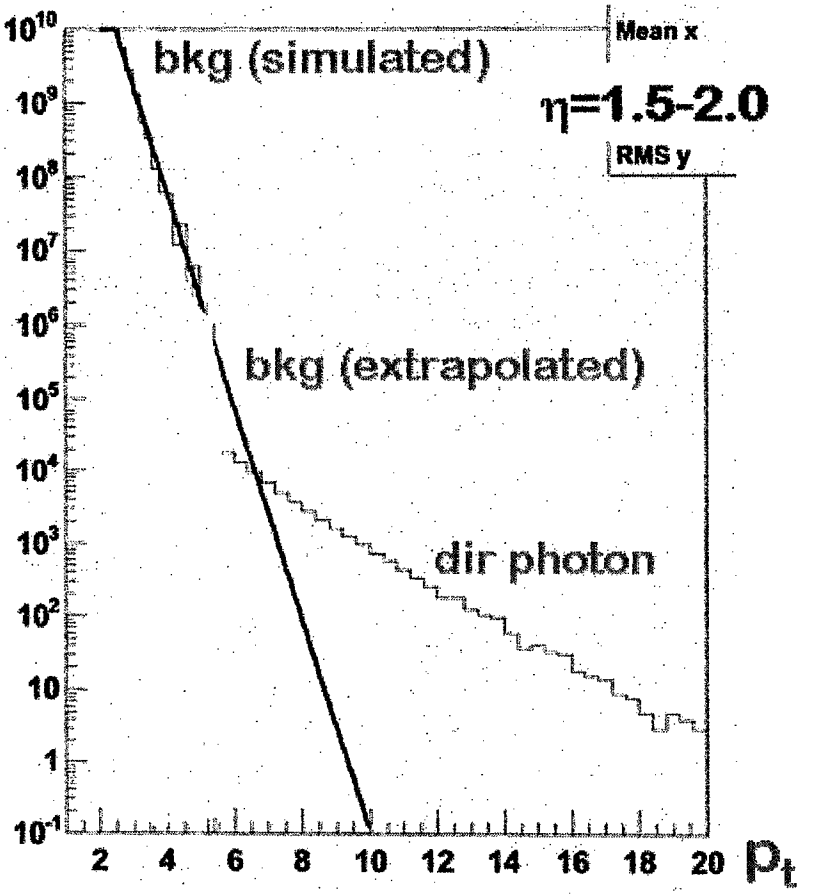

- **y=1-2 looks pretty good, above 2 under study.**

NCC adds kinematic reach for γ-jet measurements

Prompt photons:	central EMCal	$\lvert y\rvert < 0.35$	forward NCC	$0.9 < \lvert\eta\rvert < 3.0$
Jet	central TPC + VTX (charged)	$\lvert\eta\rvert < 1.2$	forward NCC (energy)	$0.9 < \lvert\eta\rvert < 3.0$

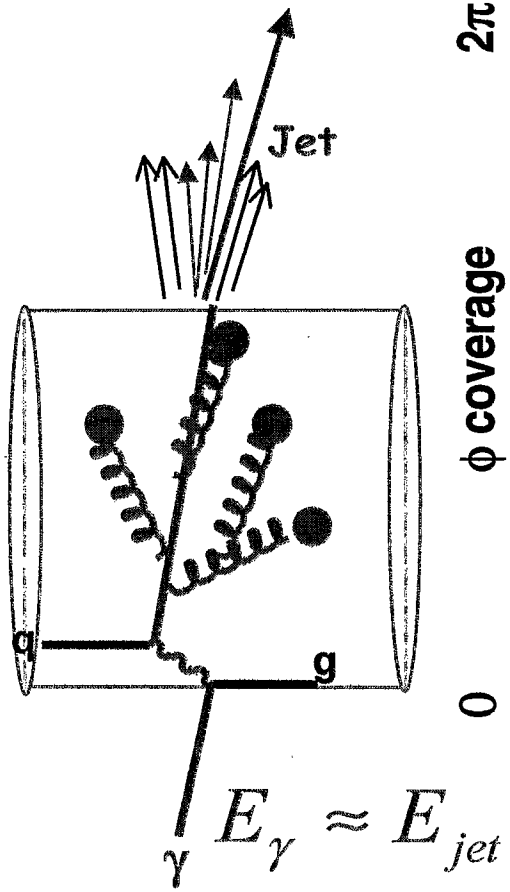

$$E_\gamma \approx E_{jet}$$

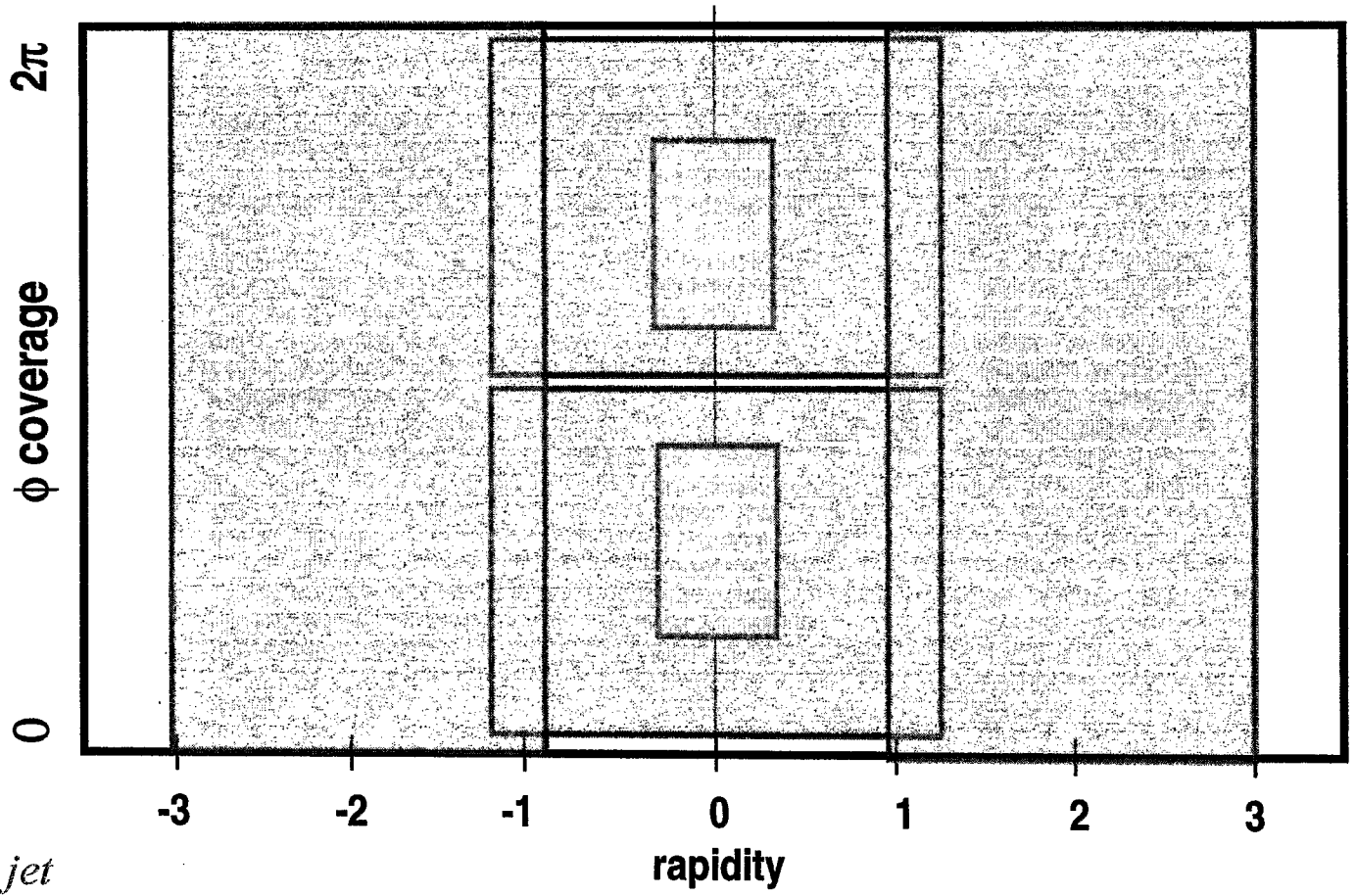

Coverage, presently studying performance

PHENIX

K. Barish

Quarkonium (χ_c & Ψ with NCC & muon trig)

- **Onium system as thermometer**
  - p_T Dependence
  - x_F Dependence
  - Study vs system size and energy

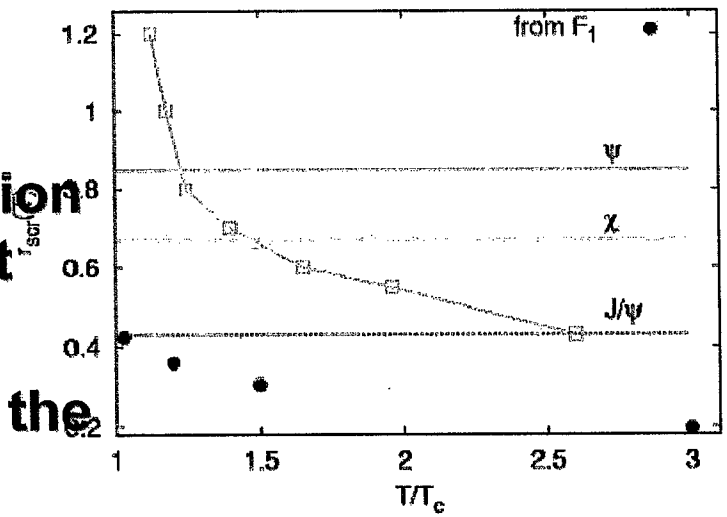

- **Upgraded muon trigger gives rejection needed for $\Psi \rightarrow \mu\mu$ measurements at highest Au+Au luminosities.**
- **Measurement of $\chi_c \rightarrow J/\psi + \gamma$, where the NCC measures γ, is under investigation.**
  - 58% of J/ψ that are accepted in muon arms have photon in NCC.
  - However, the photon is soft, so it will be difficult to measure especially in A+A.

Level-1 triggering scheme

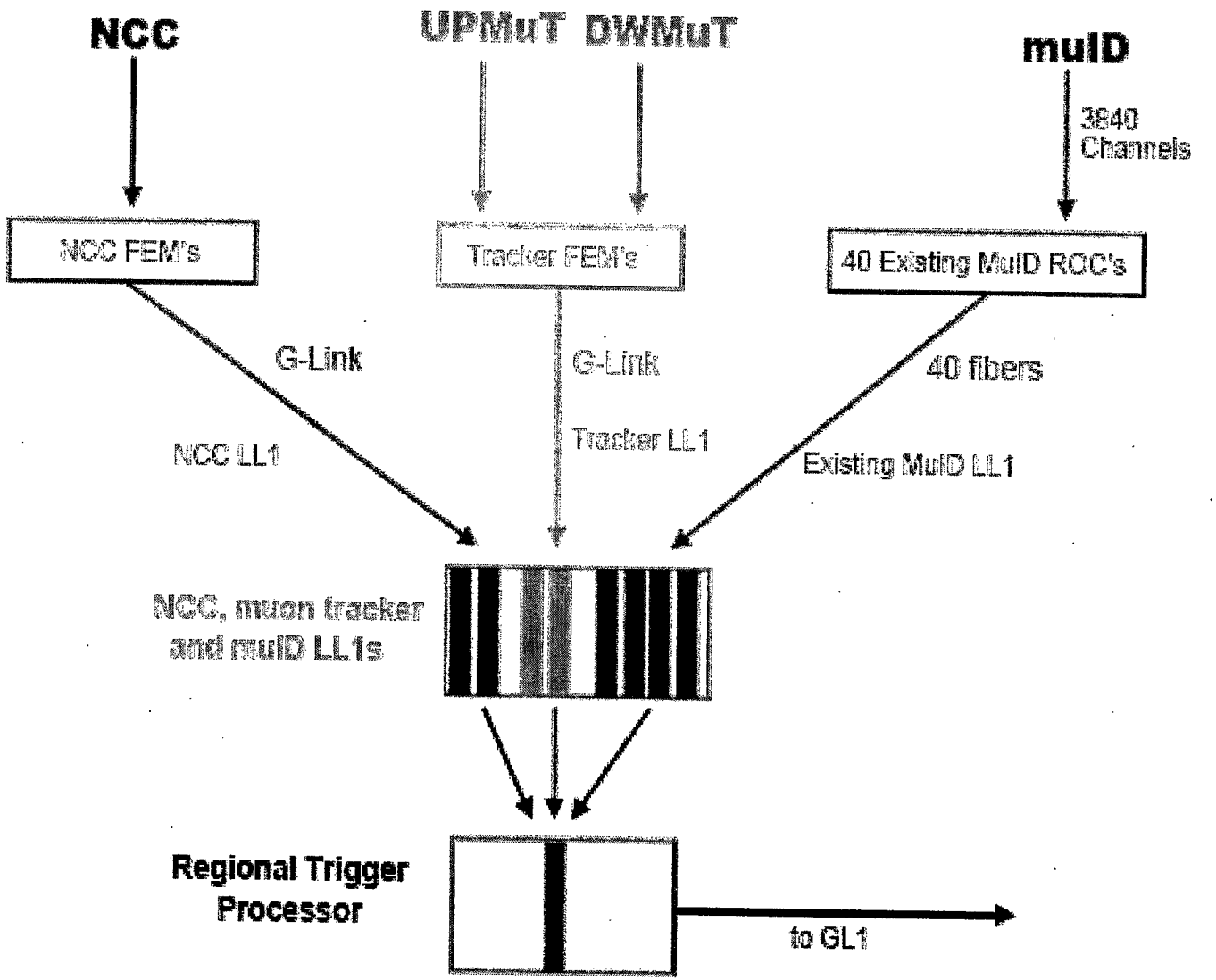

PHENIX

K. Barish

PHENIX VTX Upgade

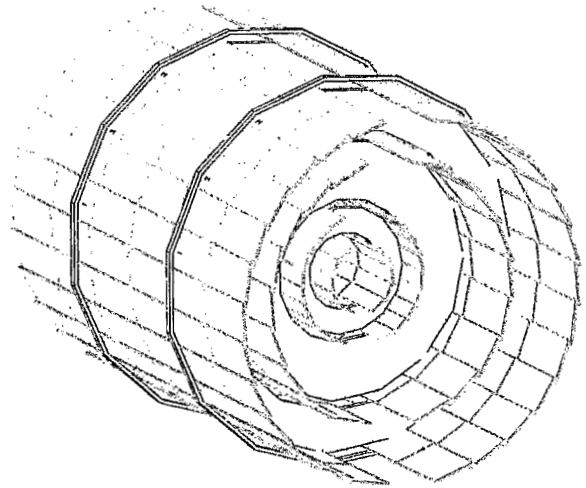

RHIC Spin Collaboration Meeting in Torino

October 9, 2004

Yuji Goto (RIKEN/RBRC)

for the PHENIX Collaboration

Outline

- Review of physics with PHENIX baseline system
  - achieved
  - to be achieved
- Physics with PHENIX VTX upgrade
  - ➔ more in Manabu Togawa's talk in Spin 2004
- status of the VTX development and construction
  - schedule
  - collaboration

Physics with the baseline system

- π^0

Bazilevsky's talk in this meeting and Fukao's talk in Spin2004

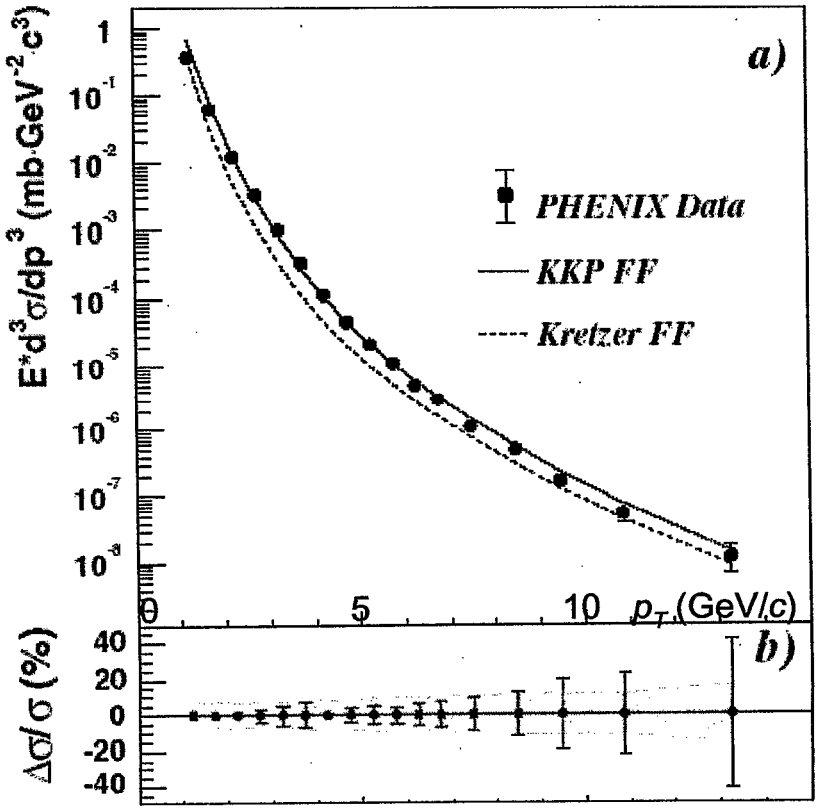

Phys.Rev.Lett. 91 (2003) 241803

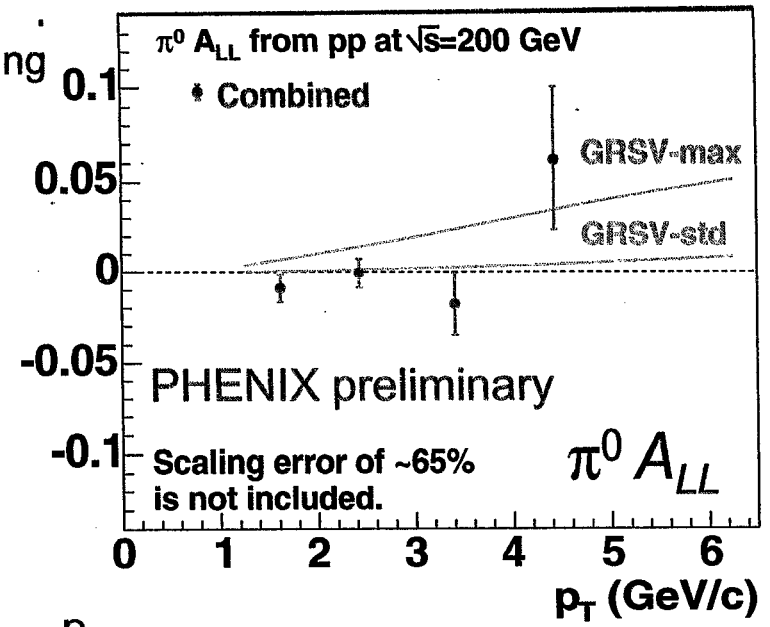

p

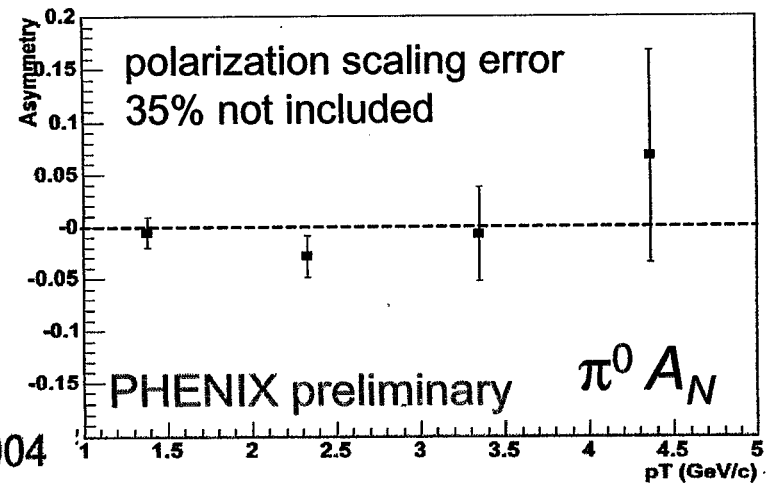

Makdisi's talk in this meeting and Spin2004

Physics with the baseline system

- Charged hadron

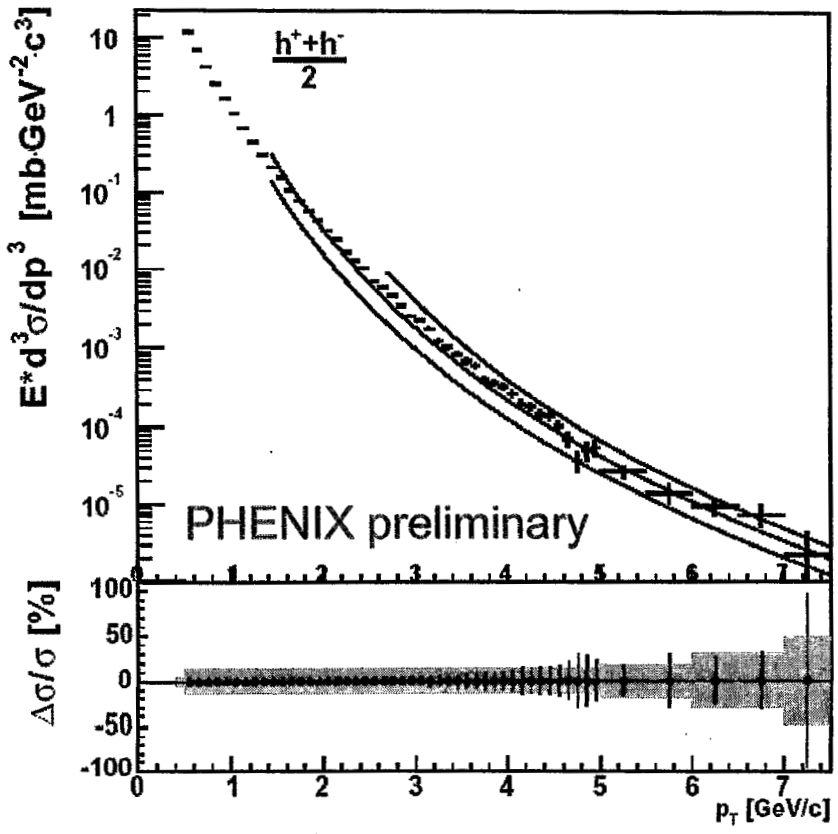

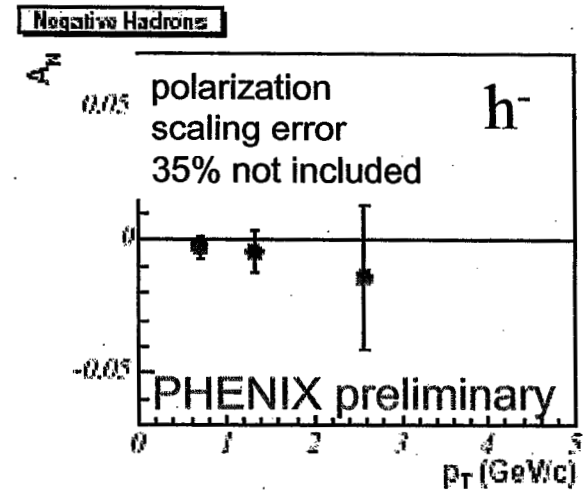

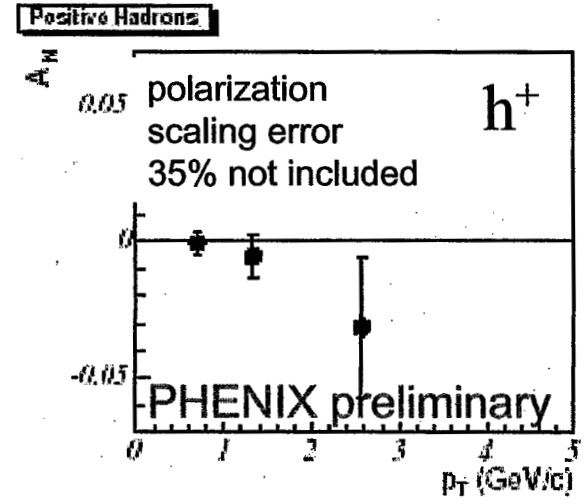

Makdisi's talk in this meeting and Spin2004

566

Physics with the baseline system

- Prompt photon
- Single electron

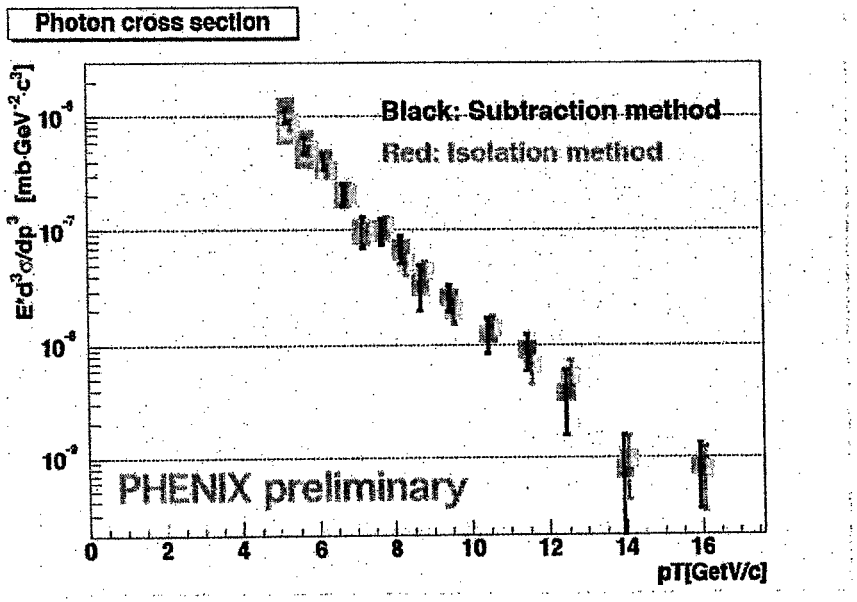

Okada's talk in this meeting and Spin2004

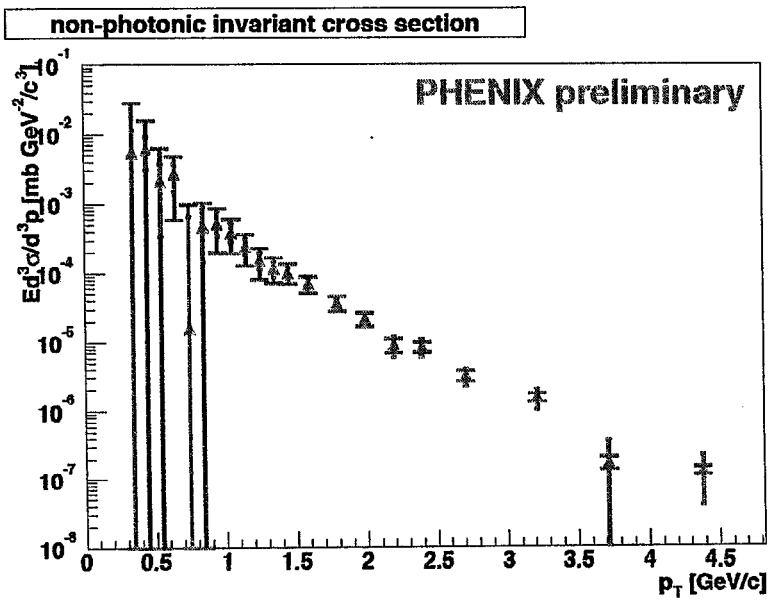

Togawa's talk in Spin2004

Physics with the baseline system

- J/ψ

Phys.Rev.Lett. 92 (2004) 051802

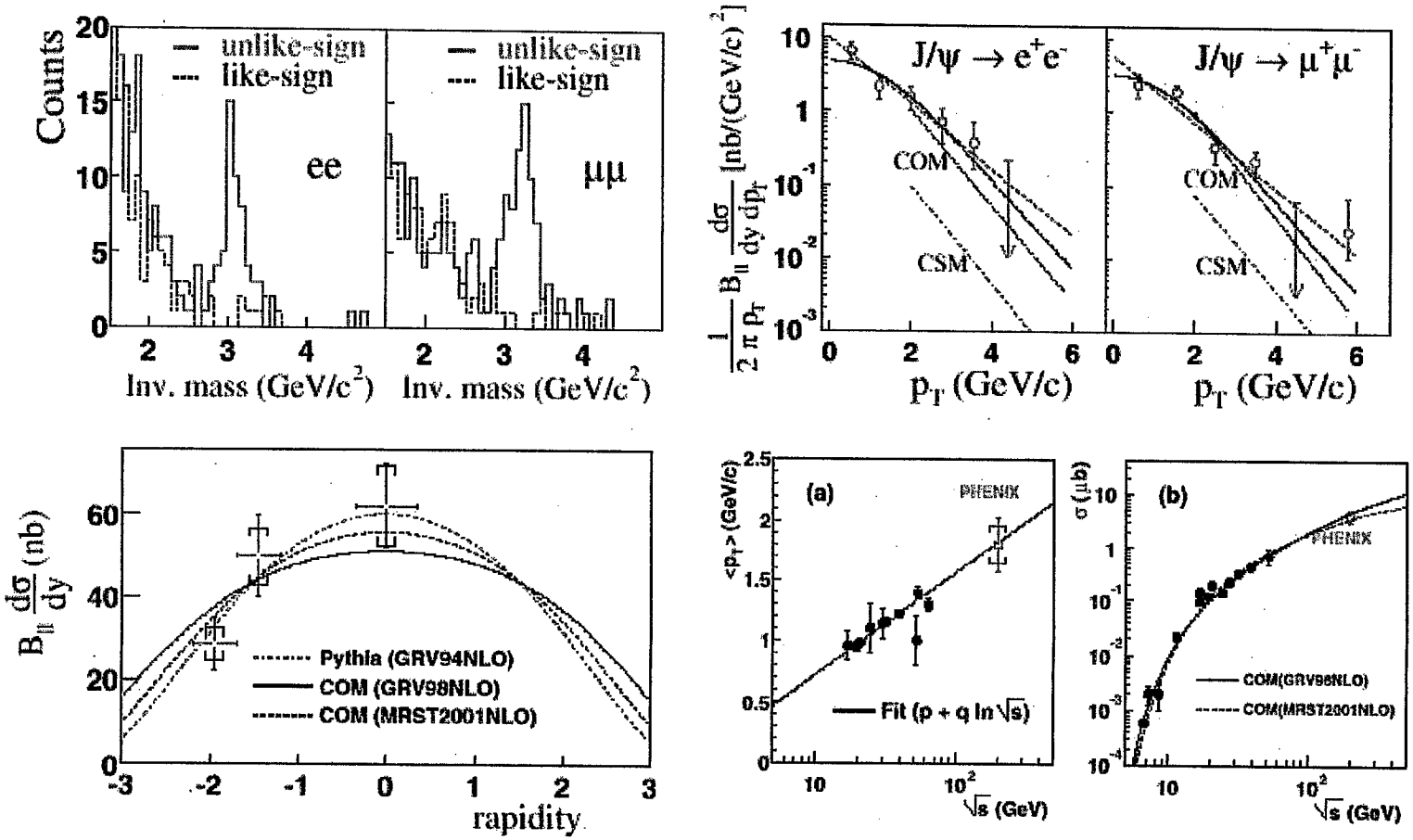

Physics with the baseline system

- Gluon polarization
  - A_{LL} of prompt photon
  - A_{LL} of single electron
- Quark polarization flavor decomposition
  - A_L of weak boson
- Transversity
  - with $\pi^+\pi^-$ interference fragmentation function
  - with Collins effect in jet
- at $\sqrt{s}$ = 200 GeV and 500 GeV

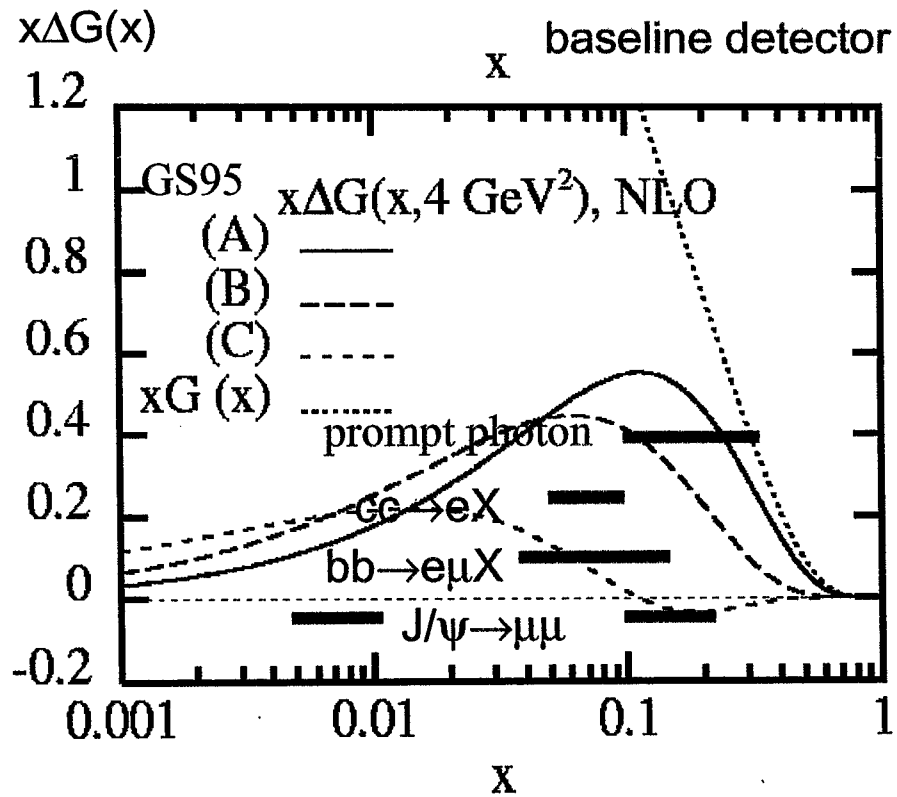

VTX upgrade

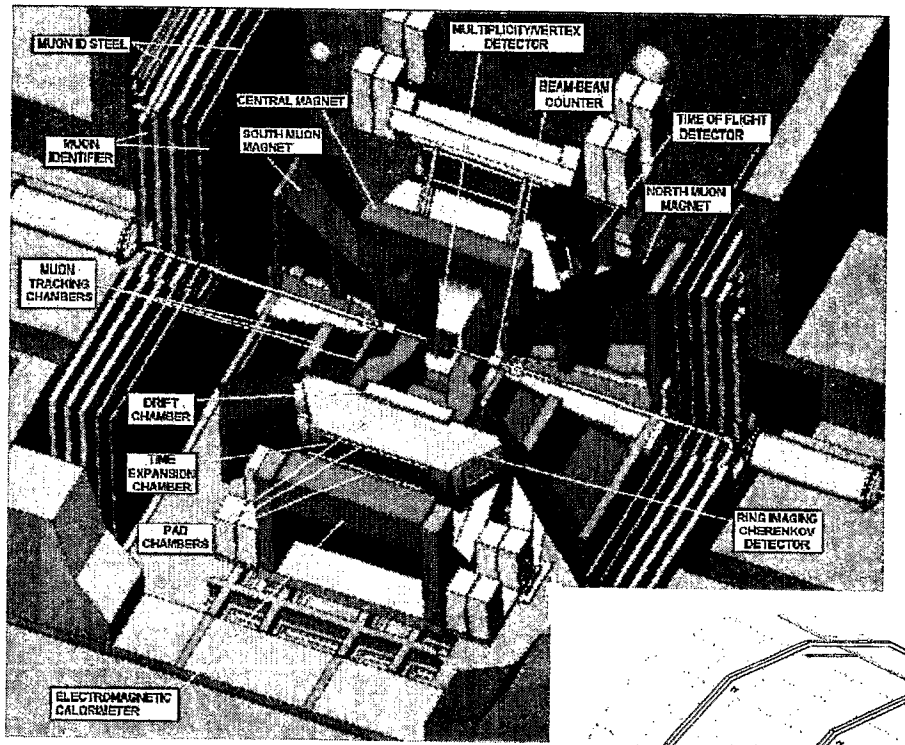
MUON ID STEEL
MULTIPLICITY/VERTEX DETECTOR
CENTRAL MAGNET
BEAM-BEAM COUNTER
TIME OF FLIGHT DETECTOR
MUON IDENTIFIER
SOUTH MUON MAGNET
NORTH MUON MAGNET
MUON TRACKING CHAMBERS
DRIFT CHAMBER
TIME EXPANSION CHAMBER
PAD CHAMBERS
RING IMAGING CHERENKOV DETECTOR
ELECTROMAGNETIC CALORIMETER

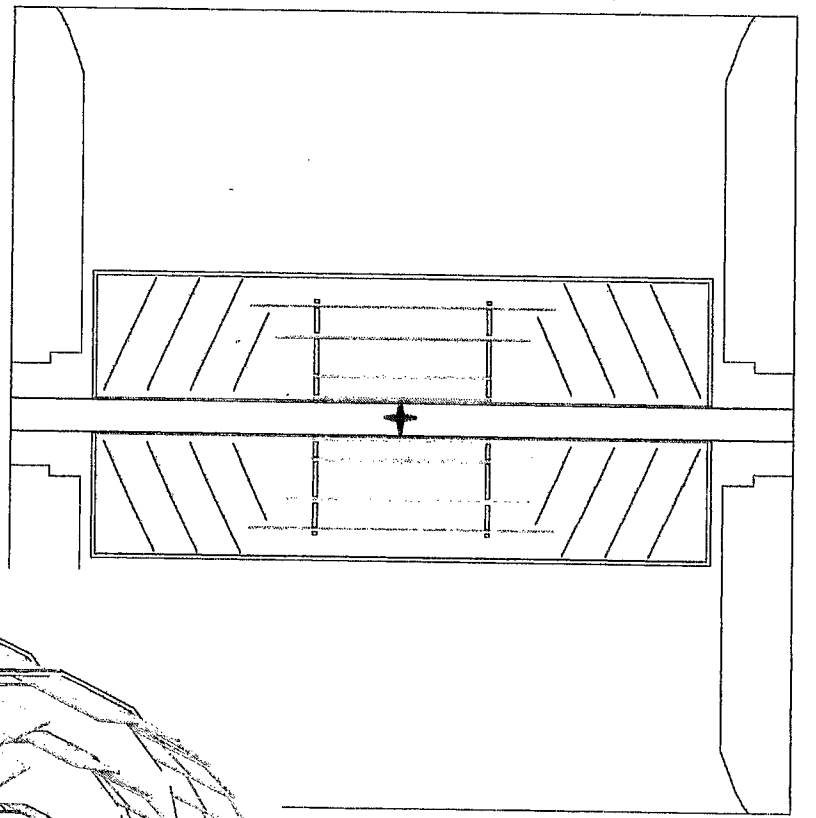

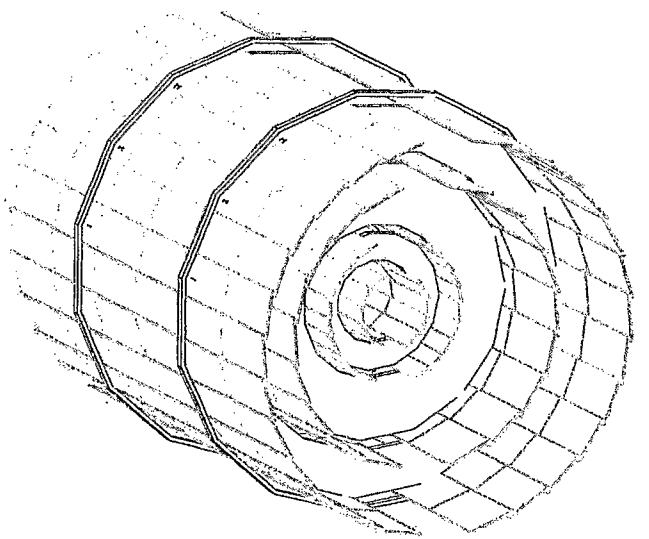

VTX upgrade

- Barrel silicon vertex tracker
  - jet axis measurement and isolation cut by charged particle detection with wider acceptance
  - displaced vertex measurement for heavy flavor tagging

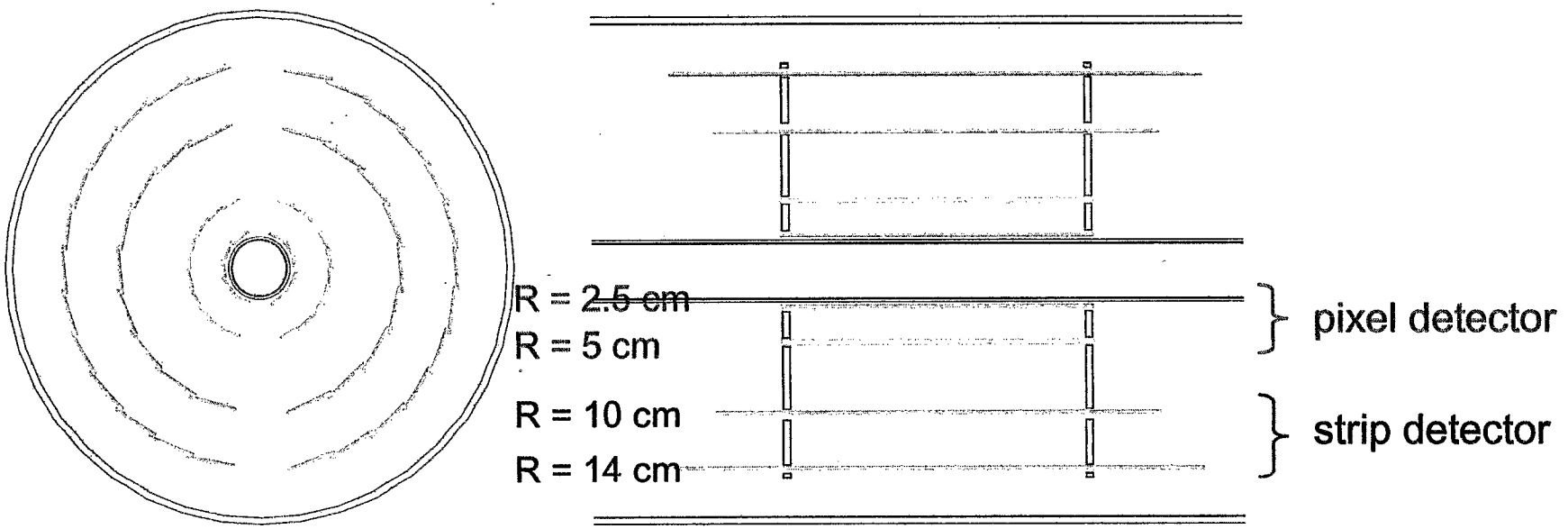

VTX upgrade

VTX	Layer	R1 (pixel)	R2 (pixel)	R3 (strip)	R4 (strip)
Geometrical dimensions	R (cm)	2.5	5	10	14
	Δz (cm)	21.8	21.8	31.8	38.2
	Area (cm^2)	280	560	1240	1600
Channel count	Sensor size R × z (cm^2)	1.28 × 1.36 (256 × 32 pixels)		3.43 × 6.36 (384 × 2 strips)	
	Channel size	50 × 425 μm^2		80 μm × 3 cm (effective 80 × 1000 μm^2)	
	Sensors/ladder	2 × 8		5	6
	Ladders	10	20	18	26
	Sensors	160	320	90	156
	Readout chips	160	320	1080	1872
	Readout channels	1,310,720	2,621,440	138,240	239,616
Radiation length (X/X0)	Sensor	0.2%		0.5 %	
	Readout	0.16%		0.8 %	
	Bus	0.14%			
	Ladder & cooling	0.7%		0.7 %	
	Total	1.2%		2.0 %	

Physics with VTX upgrade

- Gluon polarization
  - photon + jet
  - charm and bottom tagging
- Quark polarization flavor decomposition
  - $W^{\pm}$ with improved isolation cut
- Transversity
  - improved correlation study (near side and far side)
  - with wider acceptance

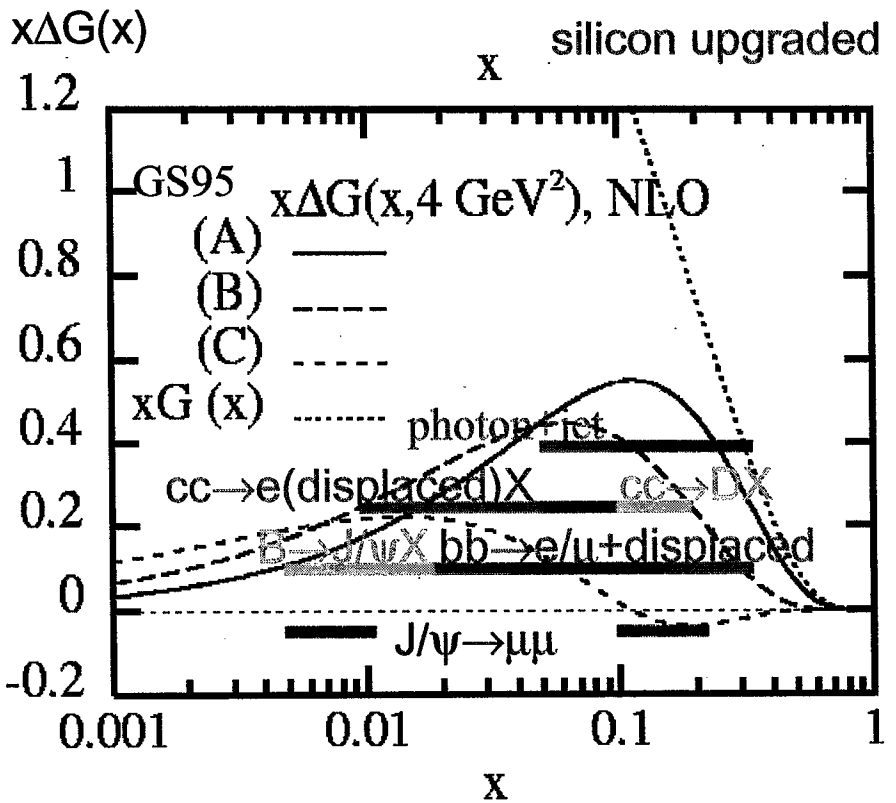

Physics with VTX upgrade

Process	Physics Objectives	Without VTX	With VTX
$c \rightarrow e$	Charm energy loss	$0.5 < p_T < 2.5$ GeV/c	$0.3 < p_T < 6$ GeV/c
$D \rightarrow K\pi$ ($p_T > 2$ GeV/c)	Charm energy loss	No (2σ significance in central Au+Au)	> 7 σ significance in central Au+Au
Total charm yield	Charm production	~ 20 %	~ 10 %
$(c \rightarrow e)/(b \rightarrow e)$ ratio	Search for thermal charm produciton	No	~ 1 %
$b \rightarrow e$	Beauty production Beauty energy loss	$p_T > 3$ GeV/c with model dependence	$1 < p_T < 6$ GeV/c
$B \rightarrow J/\psi$	Beauty production	No	$\Delta\sigma/\sigma \sim$ 10 - 15 %
Total beauty yield	Beauty production	No	~ 10 %
High p_T charged	Light quark energy loss	$p_T \leq 10$ GeV/c	$p_T < 15$ -20 GeV/c
$p+p \rightarrow c \rightarrow e$	$\Delta G(x)$	$0.03 < x < 0.08$	$0.01 < x < 0.15$
$p+p \rightarrow b \rightarrow e$	$\Delta G(x)$	No	$0.02 < x < 0.15$
$p+p \rightarrow \gamma$+jets	$\Delta G(x)$	No	$0.04 < x < 0.3$
$p+A$ $(dA) \rightarrow c/b$	Nuclear shadowing of $G(x)$	$0.03 < x < 0.3$	$0.01 < x < 0.3$

Physics with VTX upgrade

- Gluon polarization
  - photon + jet
    - jet axis measurement
  - charm and bottom tagging
    - with single electron measurement

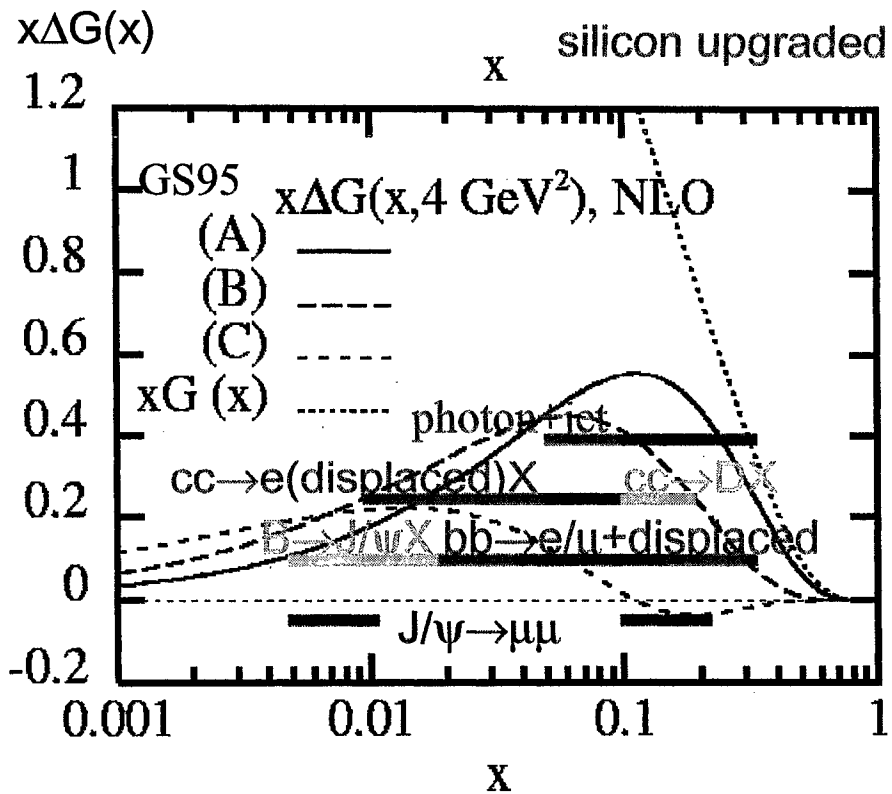

575

Physics with VTX upgrade

- Gluon polarization
  - photon + jet
    - improved gluon's *x* evaluation by kinematic reconstruction with jet axis

$$x_1 = x_2 = x_T = \frac{p_T}{2\sqrt{s}} \qquad x_1 = \frac{p_T}{\sqrt{s}}\left(e^{+\eta_{jet}} + e^{+\eta_\gamma}\right) \; x_2 = \frac{p_T}{\sqrt{s}}\left(e^{-\eta_{jet}} + e^{-\eta_\gamma}\right)$$

Togawa's talk in Spin2004

$\sqrt{s} = 200GeV$

No VTX **With VTX**

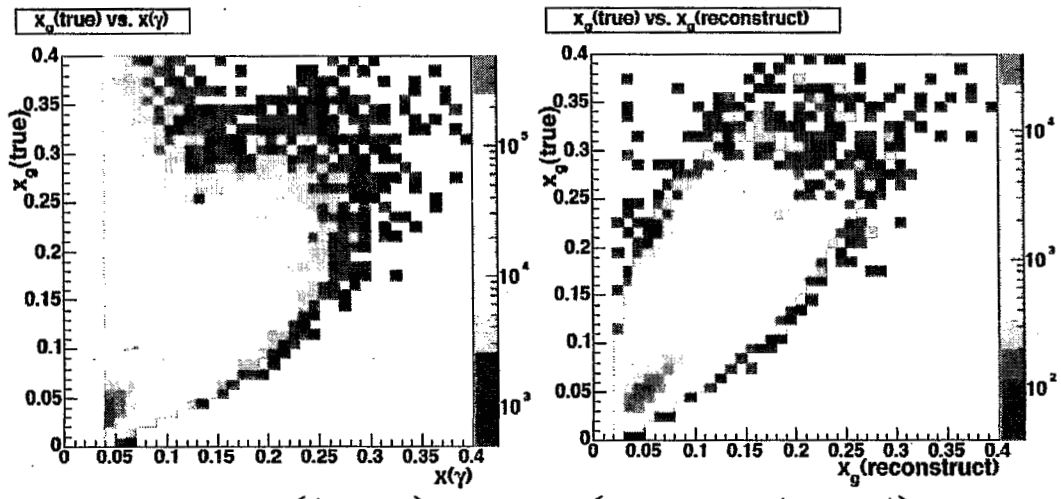

x_g(true) vs. x_g(reconstruct)

- correlation study: "k_T" issue in inclusive photon measurement

576

Physics with VTX upgrade

- Gluon polarization
  - charm and bottom tagging with displaced vertex measurement
  - charm
    - D → single electron
    - D → π K
    - J/ψ → e^+e^-
  - bottom
    - B → single electron
    - B → J/ψ
  - single electron with displaced vertex measurement

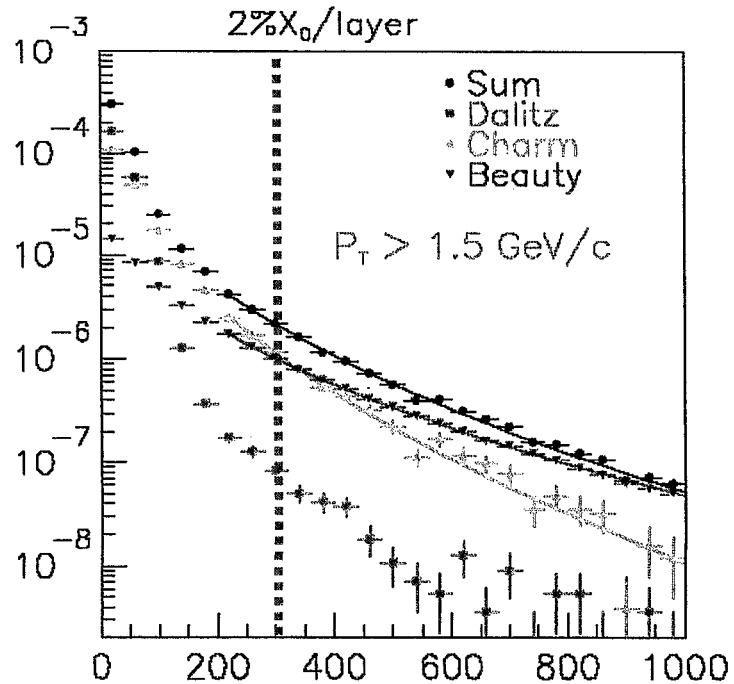

DCA = Distance of Closest Approach (μm)

Physics with VTX upgrade

- Gluon polarization
  - single electron with displaced vertex measurement
    - Dalitz + conversion suppressed
      - $A_{LL}^{\text{Dalitz+Conversion}}$ to be known from $A_{LL}^{\pi 0}$
    - bottom enhanced
      - A_{LL}^{charm} and A_{LL}^{bottom} decomposed

Togawa's talk in Spin2004

no DCA cut

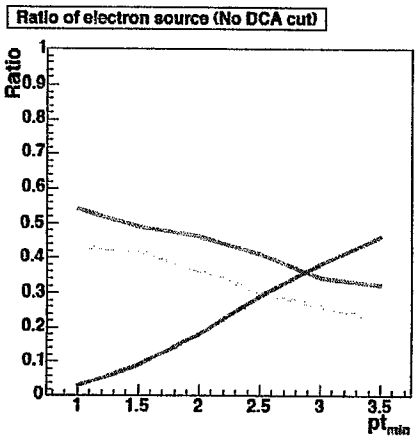

with DCA cut

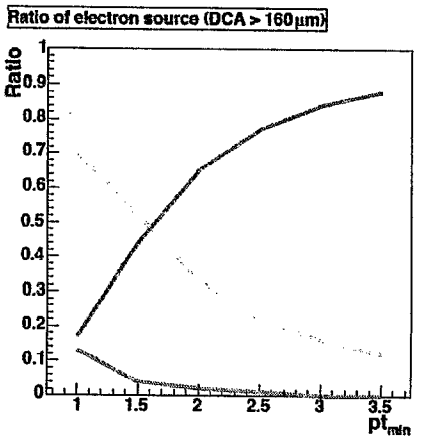

Red : Dalitz+Convesion
Green : Charm
Blue : Beauty

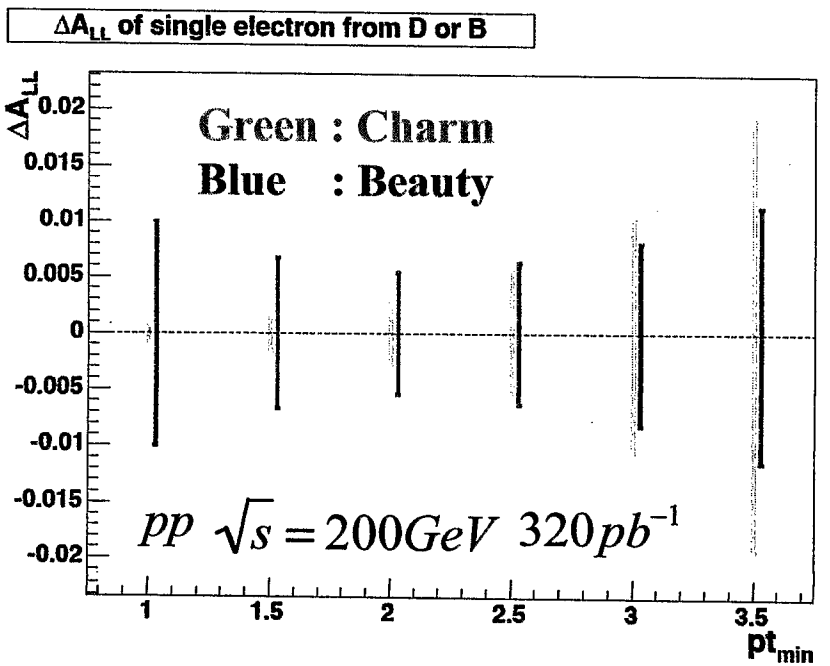

VTX upgrade

- Silicon strip detector
  - final test sensor design (Hamamatsu) + test hybrid module design (ORNL) with SVX4 readout chip (Fermilab)
    - to be built and tested early next year

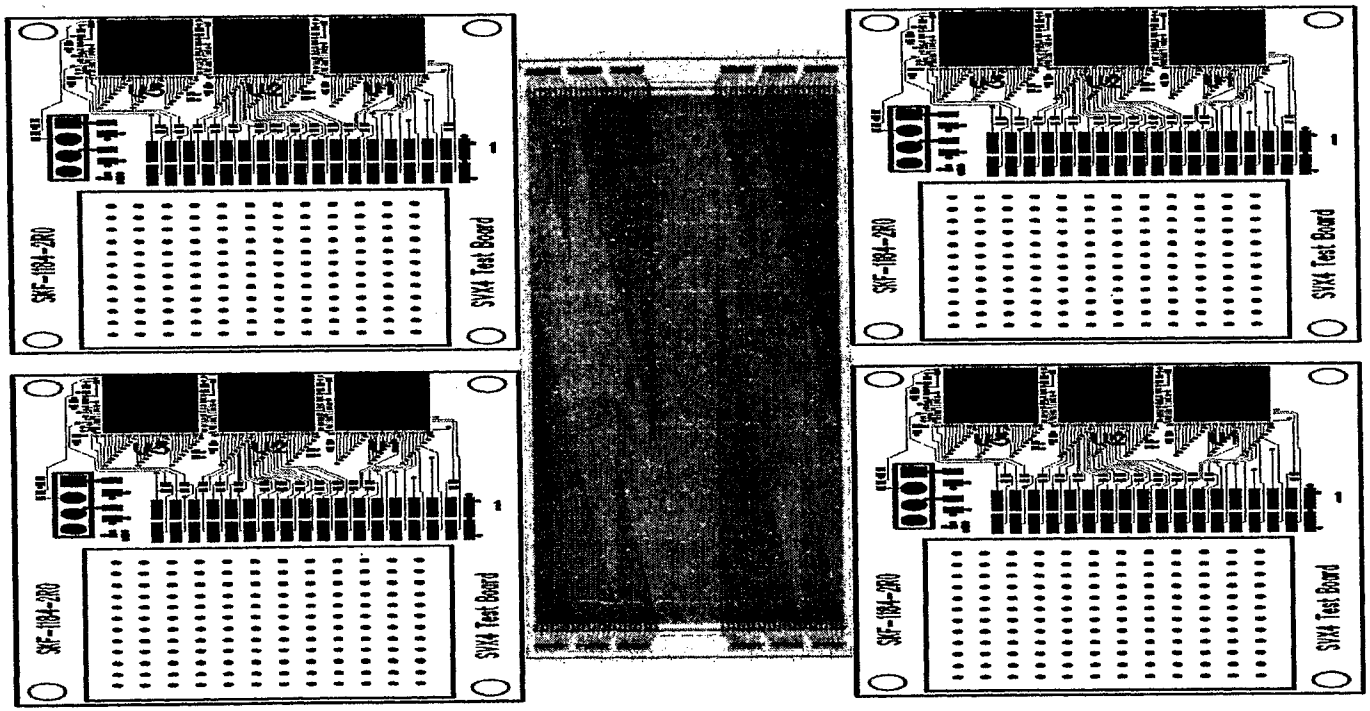

  - final hybrid module will be packaged on the sensor …

VTX upgrade

- Silicon pixel detector
  - ALICE hybrid
    - PHENIX sensor delivered in this month
    - electronics QA done
    - to be bump-bonded in a month or so

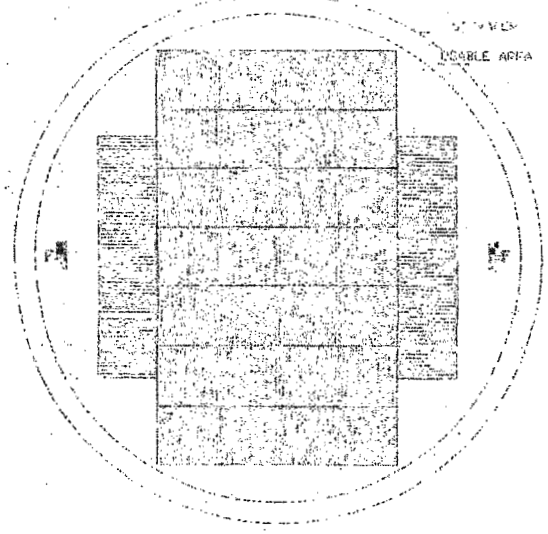

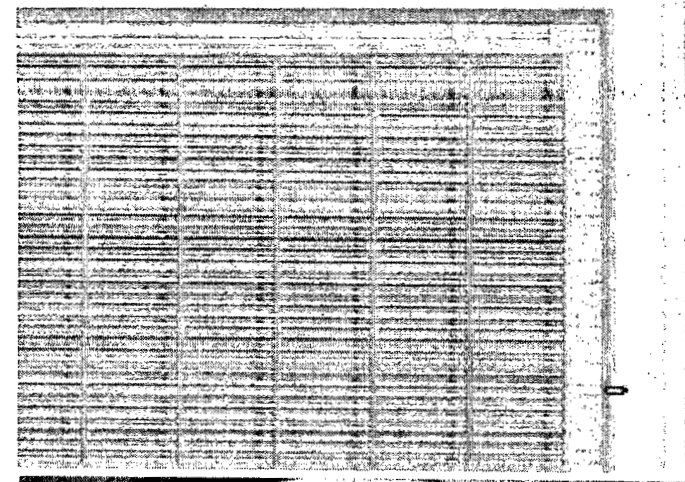

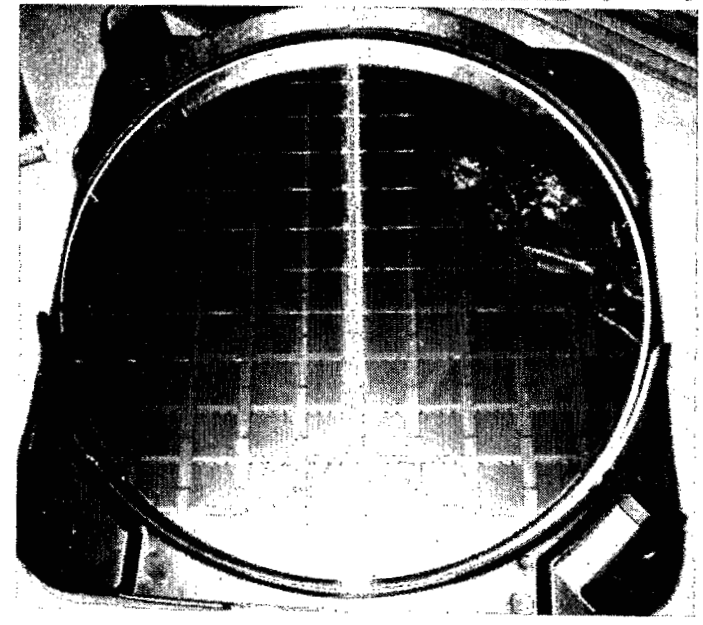

VTX upgrade

– probe station and quality assurance test of pixel readout chips in a clean room laboratory at CERN

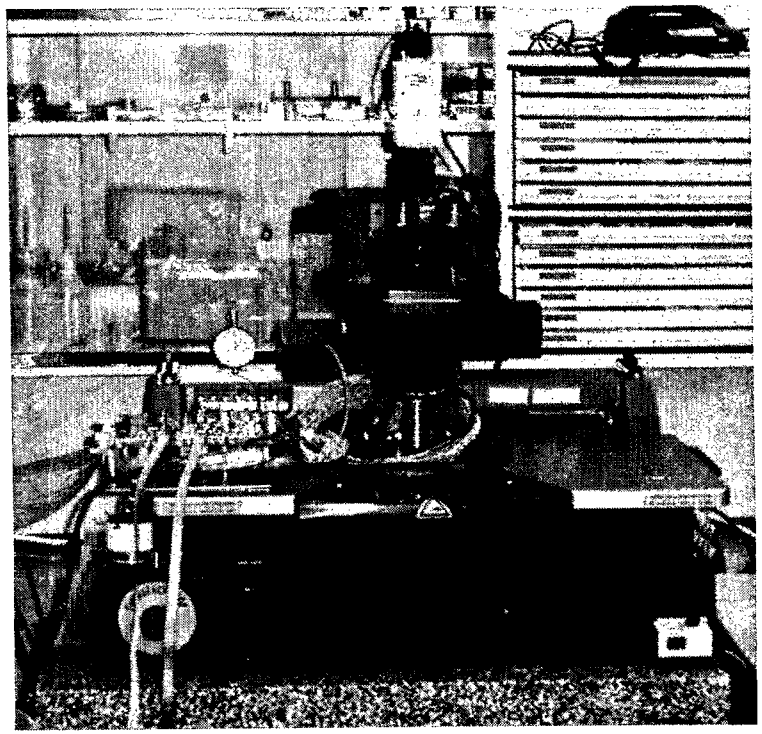

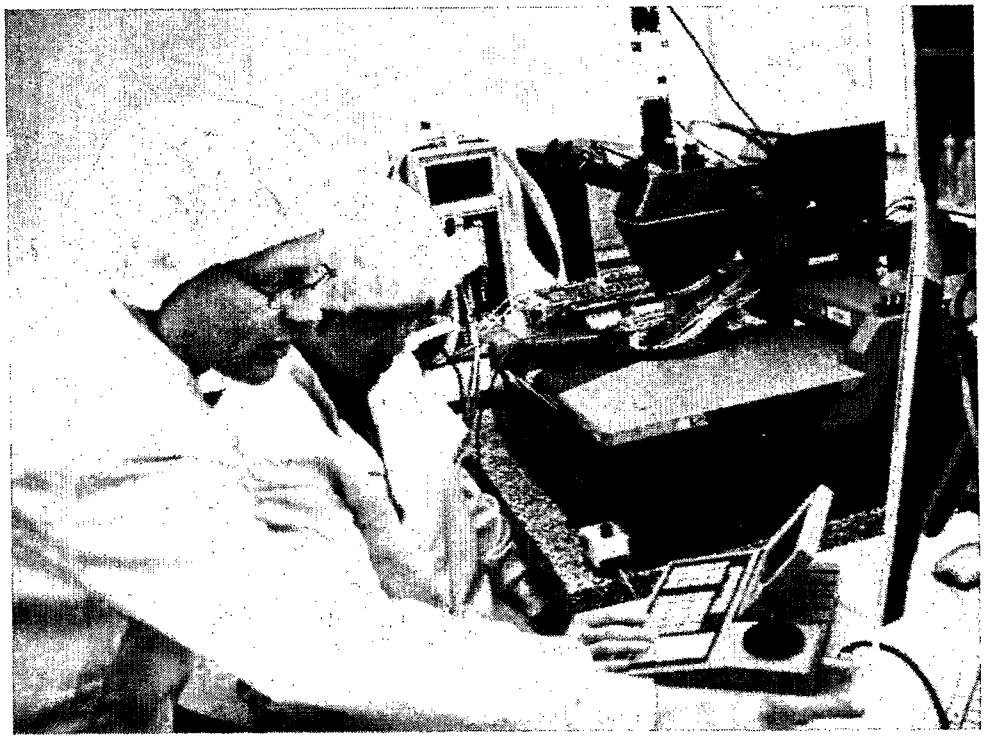

VTX upgrade

– wire bonding facility in a clean room at RIKEN

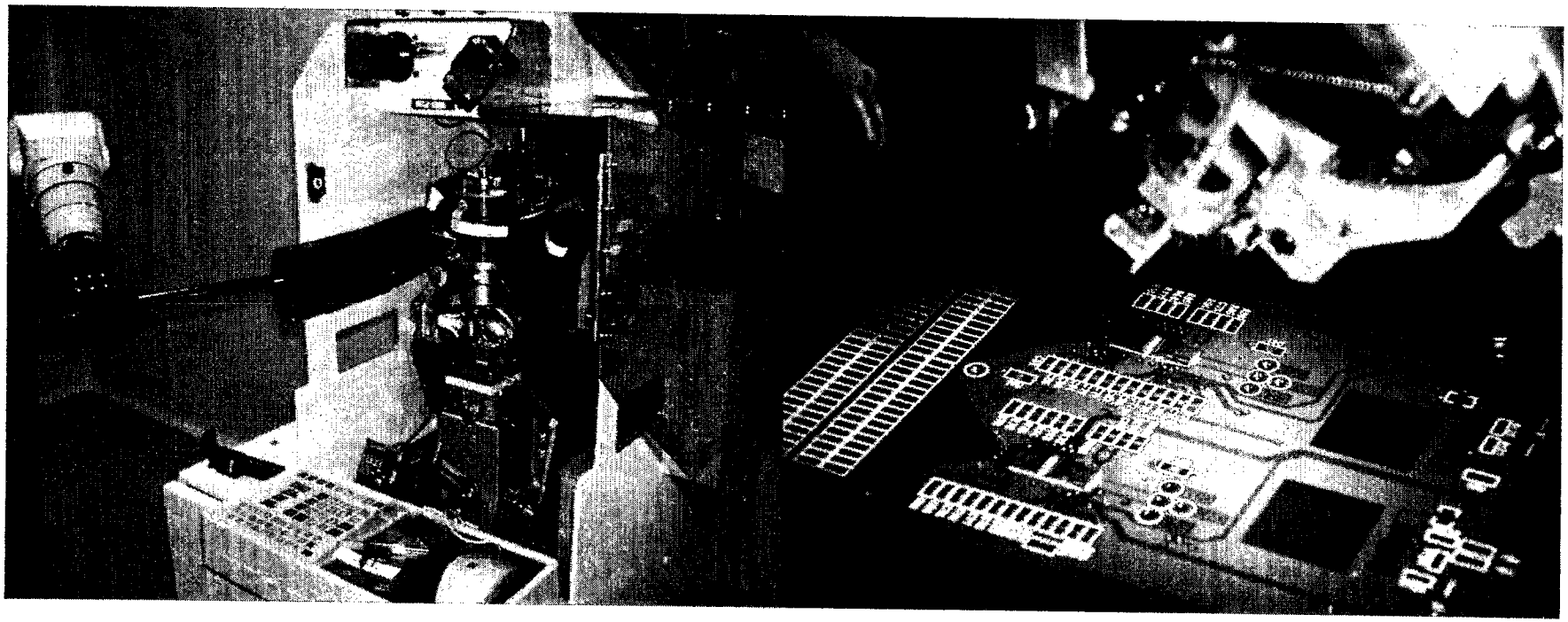

VTX upgrade

- Schedule
  - March 03
    - approved by PHENIX+BNL management
  - endorsed by NSAC sub-committee for RHI
  - September 04
    - proposal submitted to DOE
    - being reviewed …
  - partially funded by RIKEN
    - development and construction underway …
  - summer 06
    - inner pixel layer + part of strip layers installed
  - summer 07
    - full VTX detector completed
    - to be ready for RHIC 2007-2008 run

PHENIX

VTX upgrade

- Collaboration
  - more than 70 people, 14 universities/institutes
    - BNL, Chemistry Department
    - BNL, Instrumentation Division
    - BNL, Physics Division
    - Florida State University
    - Iowa State University
    - KEK
    - Kyoto University
    - LANL
    - Niigata University
    - ORNL
    - RIKEN
    - RIKEN BNL Research Center
    - Stony Brook University
    - University of New Mexico
  - lots of more opportunity for new groups

Summary

- Many measurements have been achieved and will be done with the PHENIX baseline system
  - gluon polarization
  - quark polarization flavor decomposition
  - transversity
- PHENIX VTX will improve those measurements
  - with jet axis measurement: e.g. photon + jet
  - with displaced vertex measurement: e.g. single electron from charm and bottom
- Completion in summer 2007 to be ready for RHIC 2007-2008 run
  - development and construction underway …
  - lots of more opportunity for new groups …

Jet Reconstruction Algorithms for RHIC

M.L. Miller, MIT

"In this, lowest-order approximation, the jets are 'ideal', and consist of a set of exactly parallel-moving hadrons. In realistic cross sections it will be necessary to define what we mean by jets more carefully... It is not, however, completely straightforward to define precisely how many jets are present in a given final state and what their momenta and energies are... Thus a jet cross section is to some extent an artifact... so be it. One must simply give a careful definition how the jet content of the final state is to be measured. Then, one must calculate (perturbatively) the cross section... according to this definition."

-CTEQ Handbook of Perturbative QCD
ala Sterman and Weinberg, 1977-

MASSACHUSETTS INSTITUTE OF TECHNOLOGY

Università degli Studi di Torino

A Brief History…

- Snowmass 1990
  - (Didn't we do this?)
  - Well, not really…
- x-section problems
  - Recombination
  - Missed seeds
  - Collinear "un-safe"
  - Infrared "un-safe"
  - Local minima traps

$$p_\mu^{jet} = \sum p_\mu^{\text{hadron/parton/tower}}$$

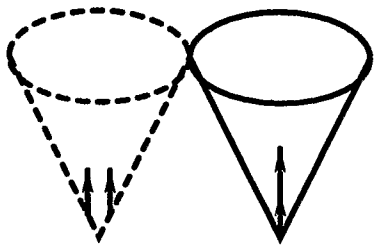

Figures from hep-ex/0005012

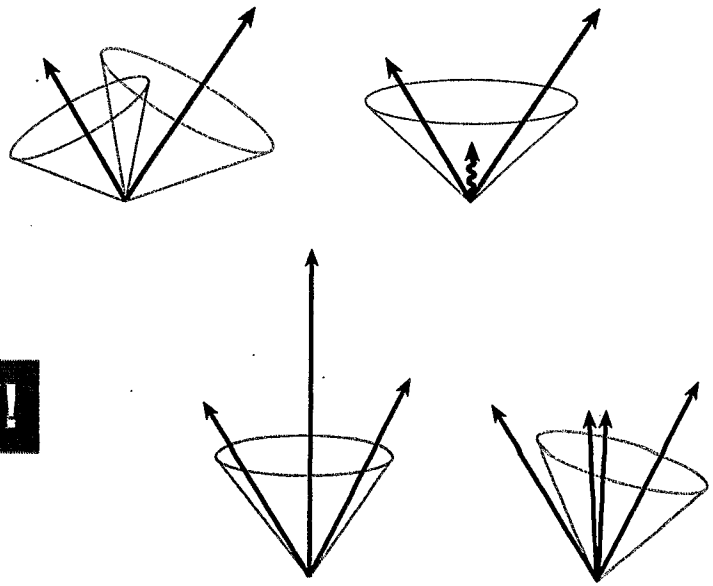

Largest problems for jet p_T<20 GeV!

The Ideal Jet Algorithm for p+p

"Snowmass II" **hep-ex/0005012**

Run II Jet Physics

Gerald C. Blazey[a], Jay R. Dittmann[b], Stephen D. Ellis[c], V. Daniel Elvira[b], K. Frame[d], S. Grinstein[e], Robert Hirosky[f], R. Piegaia[e], H. Schellman[g], R. Snihur[g], V. Sorin[e], Dieter Zeppenfeld[h]

The Ideal Jet Algorithm for p+p

Compare jets at the **parton, hadron** and **detector** level

⇨ **Jet algorithms should ensure**

General

- infrared and collinear safety
- invariance under longitudinal boosts
- fully specified and straightforward to implement
- same algorithm at the parton, hadron and detector level

Theory

- boundary stability (kinematic limit of inclusive jet cross section at $E_T = \sqrt{s}/2$)
- factorization (universal parton densities)

Experiment

- independence of detector detailed geometry and granularity
- minimal sensitivity to non-perturbative processes and pile-up events at high luminosity
- minimization of resolution smearing/angle bias
- reliable calibration
- maximal reconstruction efficiency (find all jets) vs minimal CPU time

(I) k_T Cluster Algorithm (*ala* e^+e^-)

1. p_T ordered list of particles → form the list of $d_i = (p_{Ti})^2$
2. calculate for all pairs of particles, $d_{ij}=\min((p_{Ti})^2,(p_{Tj})^2)\Delta R/d_{cut}$
3. find the minimum of all d_i and d_{ij}
4. if it is a d_i, remove i to jet list
5. if not, combine i and j
6. use combined particle $i+j$ as a new particle in next iteration

- need to reorder list at each iteration → computing time ∝ $O(N^3)$ (N particles)
- proceed until the list of 4-momenta is exhausted
- *Straight forward, formally CIS safe*
- *Only parameter: d_{cut} ~ 1 [radians]*

(II) The Midpoint-Cone Algorithm

$$\Delta R = \sqrt{\Delta\phi^2 + \Delta\eta^2}$$

1. Identify seed
   1. (p_T>0.5 GeV/c)
2. Collect 4-mom in cone
3. Iterate until cone is "stable"
4. Repeat for all seeds
5. Repeat for "midpoints"
6. Disentangle
   1. Split/merge

At fixed order N, 2^N-1 possible locations for stable cones.

Parameters:

1. r_{cone}: ~0.5-1.0 [radians]
2. p_{Tseed}: ~0.5 GeV/c
3. $f_{split/merge}$: 0.5

```
if (E_shared/E_jet<f) →split
else → merge
```

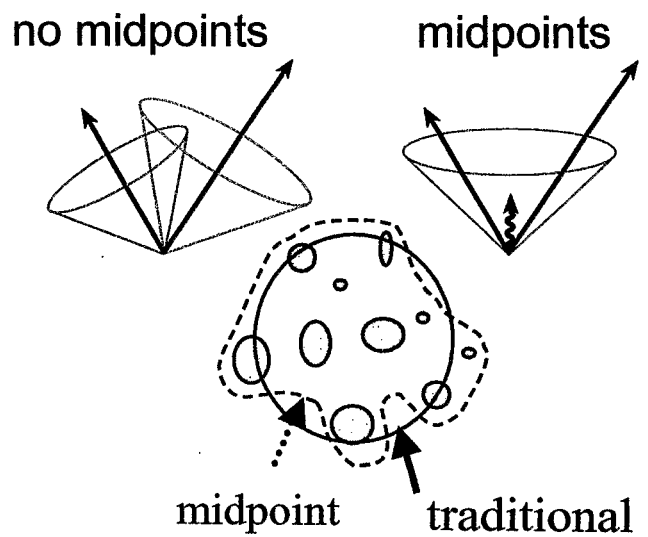

(II) The Midpoint-Cone Algorithm

(or partons or hadrons)

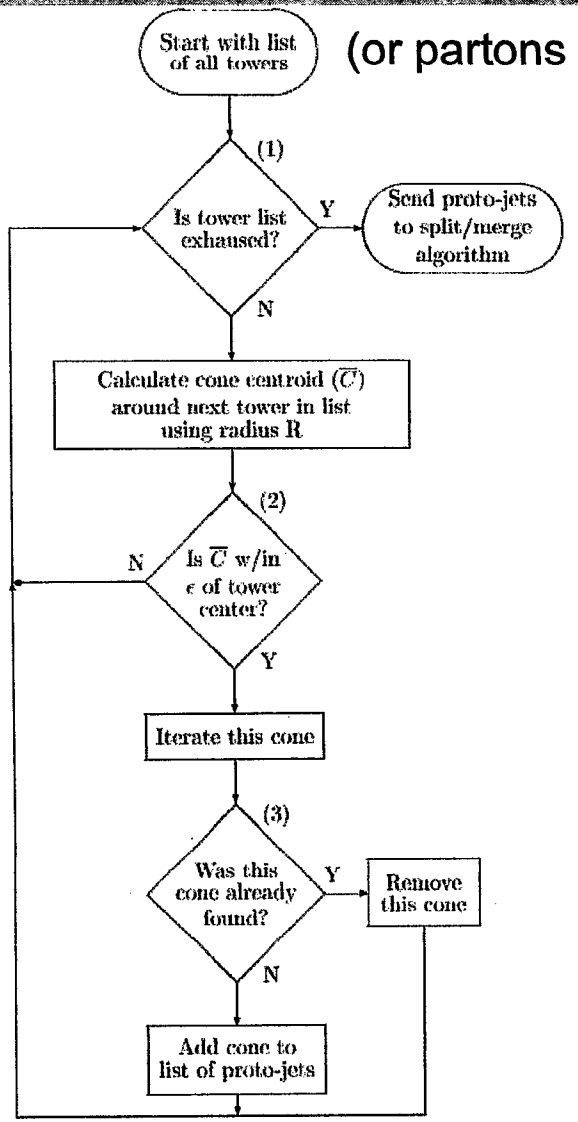

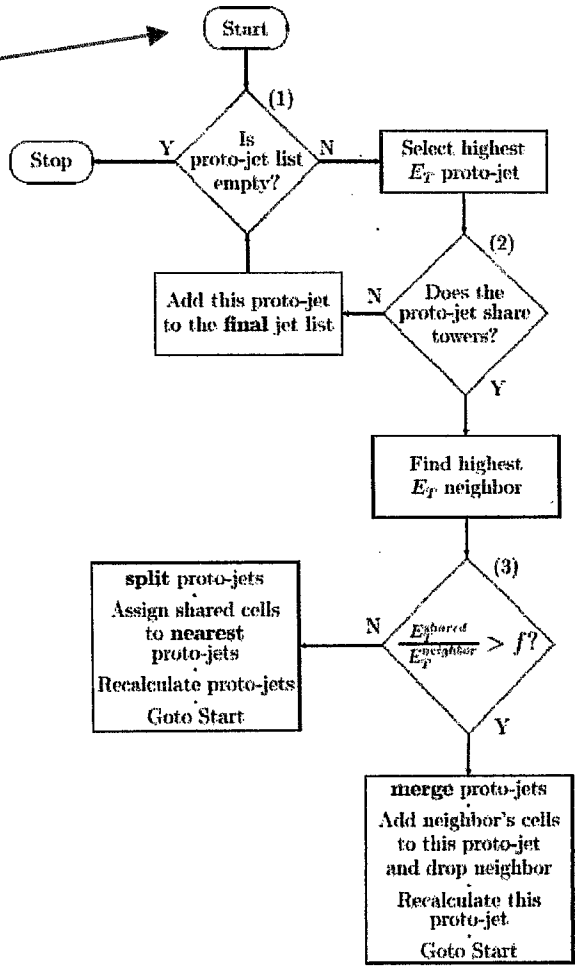

Summary

- Standardized CIS jet algorithms for p+p
  - k_T and midpoint-cone
  - used in Tevatron RunII, LHC
  - Same in theory and experiment, let's do the same
- Both implemented by STAR
  - Stand-alone software
    - standard c++, no ROOT or CLHEP
    - Works for arbitrary list of p^μ
  - open source: www.star.bnl.gov/cgi-bin/cvsweb.cgi/StRoot/StJetFinder/
  - Energy calibration underway in STAR
- Could be easily implemented in PHENIX
  - Of course r_{cone}~.2
- *Test sensitivity of RHIC NLO calculation to jet definition:*
  - Just need a list of partons per event
- and deploy k_T algorithm!

Plans for STAR Forward Calorimetry Upgrade

L.C. Bland
RHIC Spin Collaboration Meeting
Torino, October 2004

STAR Detector

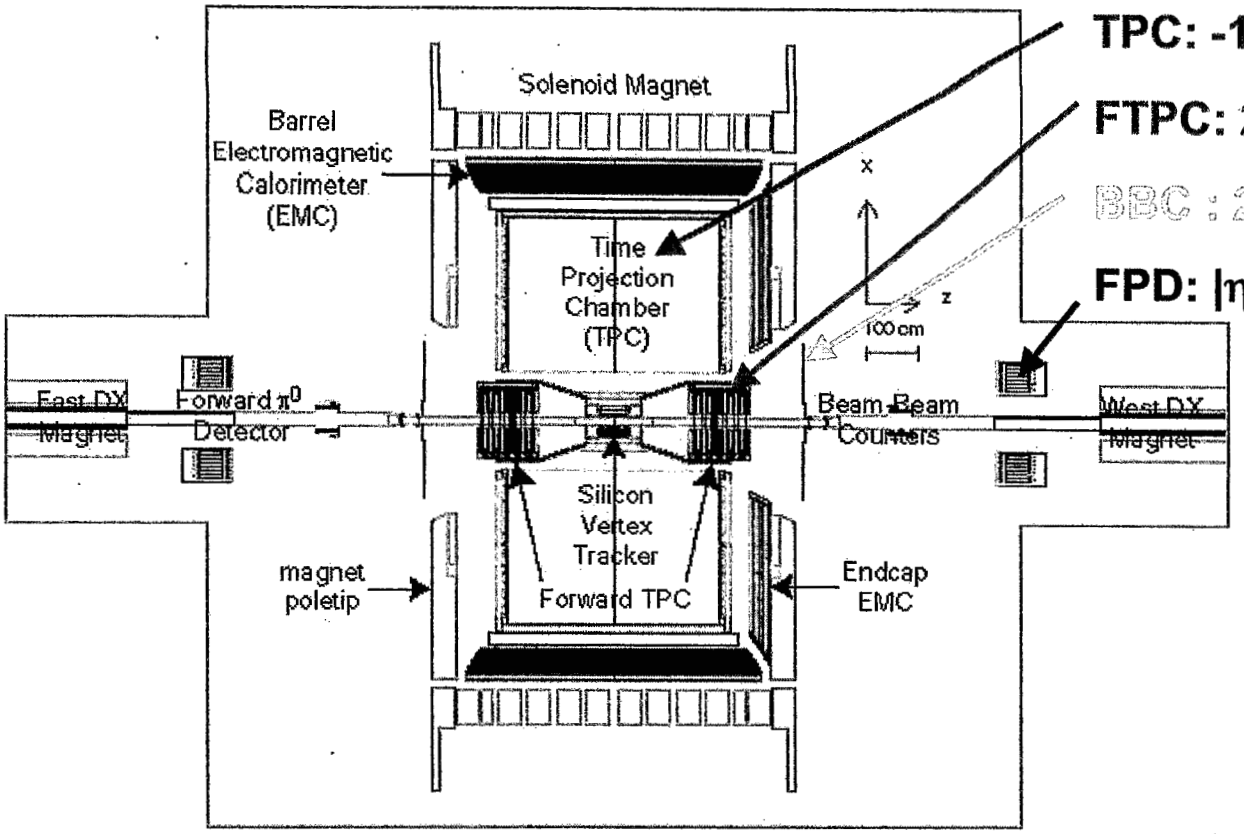

TPC: $-1.0 < \eta < 1.0$

FTPC: $2.8 < |\eta| < 3.8$

BBC : $2.2 < |\eta| < 5.0$

FPD: $|\eta| \sim 4.1$ and ~ 3.6

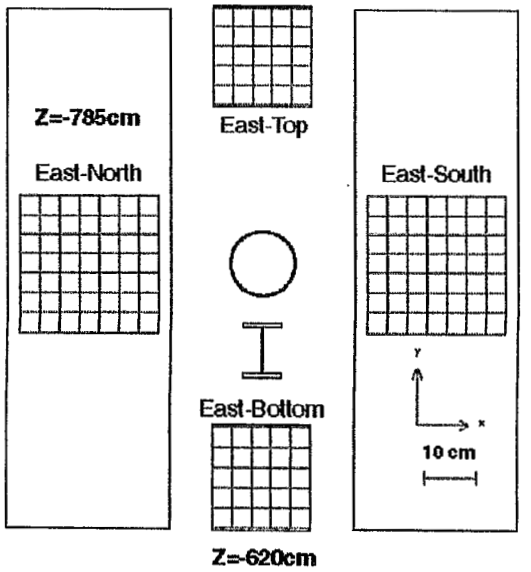

Upgraded Forward π^0 Detector (FPD)

- **Pb-glass EM calorimeter**
- **Shower-Maximum Detector (SMD)**
- **Preshower**

RSC Meeting (Torino)
October, 2004
Akio Ogawa

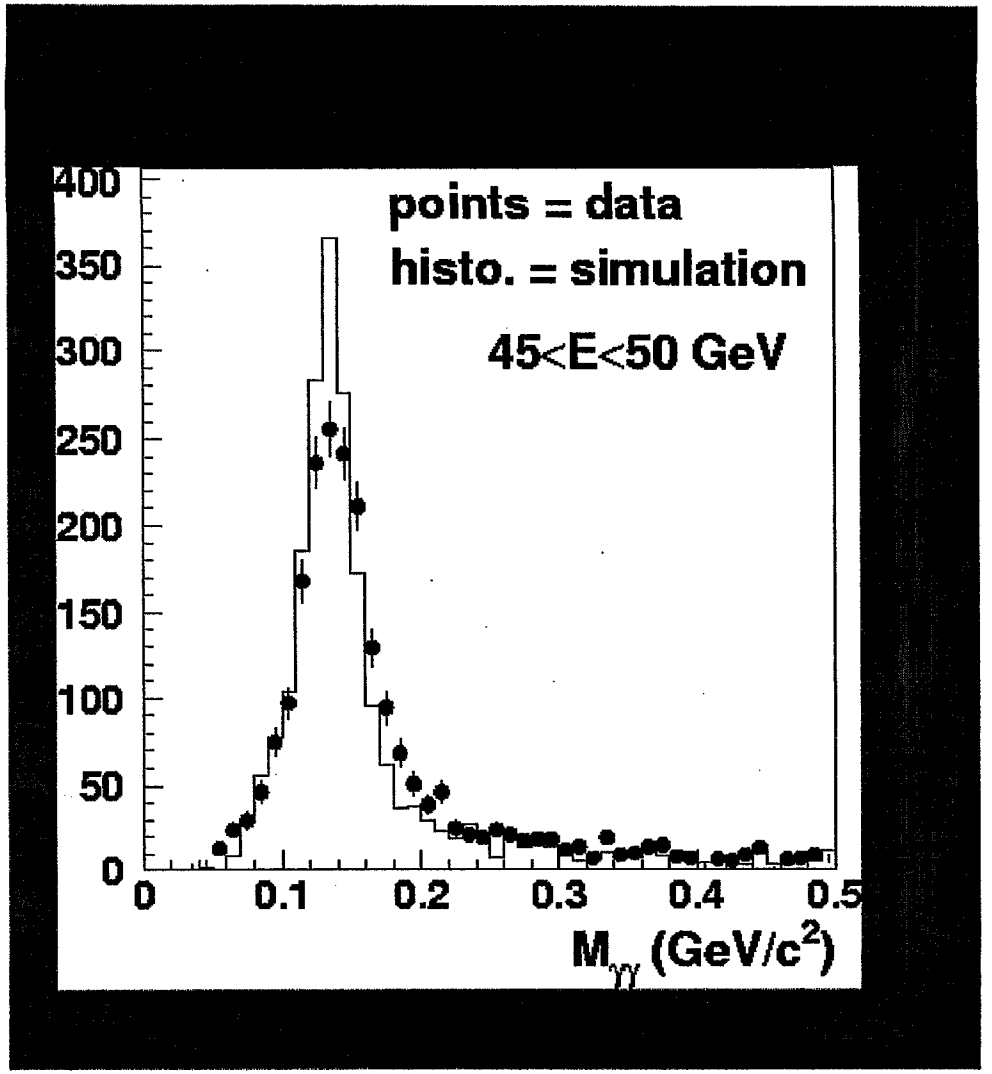

$p+p \rightarrow \pi^0 + X$

$\sqrt{s}=200$ GeV

$\langle\eta\rangle=4.1$

Large Analyzing Powers at RHIC

First measurement of A_N for forward π^0 production at $\sqrt{s}$=200GeV

STAR collaboration, hep-ex/0310058,
Phys. Rev. Lett. **92** (2004) 171801

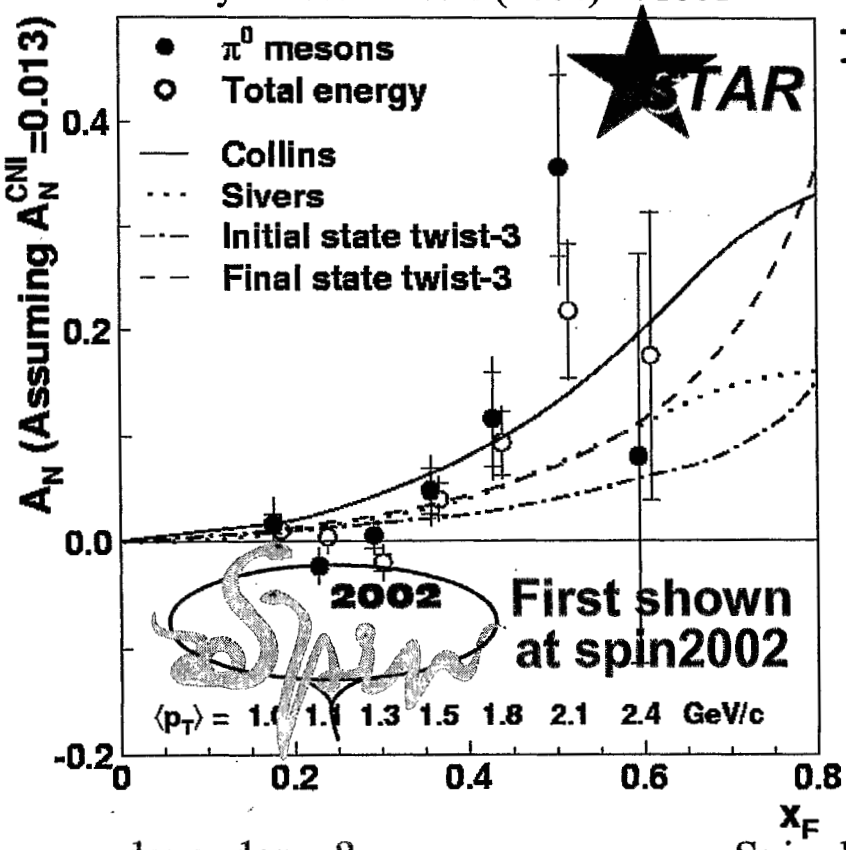

Similar to **FNAL E704** result at $\sqrt{s}$ = 20 GeV

In agreement with several models including different dynamics:

- Sivers: spin and $k_\perp$ correlation in initial state (related to orbital angular momentum?)
- Collins: Transversity distribution function & spin-dependent fragmentation function

  → suppressed? (hep-ph/0408356)
- Qiu and Sterman (initial-state) / Koike (final-state) twist-3 pQCD calculations

- p_T dependence?
- x_F<0?
- A_N with mid-rapidity correlation?
- Spin dependence in jet?
- Heavy flavors??
- Related to "gluon saturation"???

Measurement of A_N

for f 200GeV

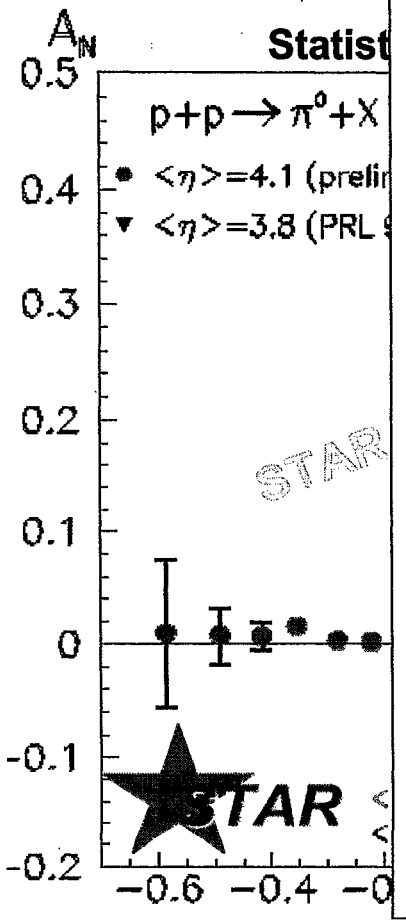

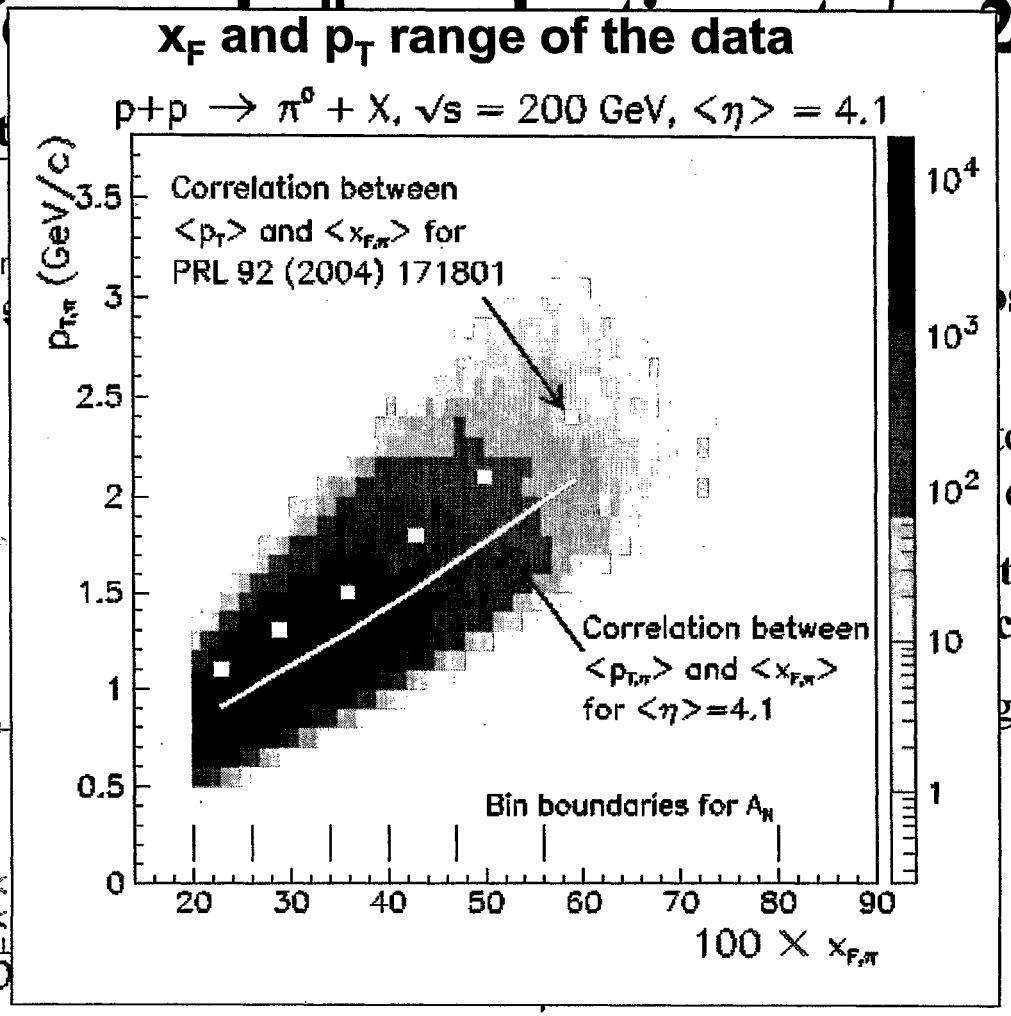

sitive x_F has been

o be non-zero &
data

t of negative x_F A_N
consistent with zero

gluon-gluon

Mapping of A_N in x_F and p_T plane has begun !

d + Au: Possible Color Glass Condensate at RHIC?

$\tau = \ln\left(1/x\right)$ τ related to rapidity of produced hadrons.

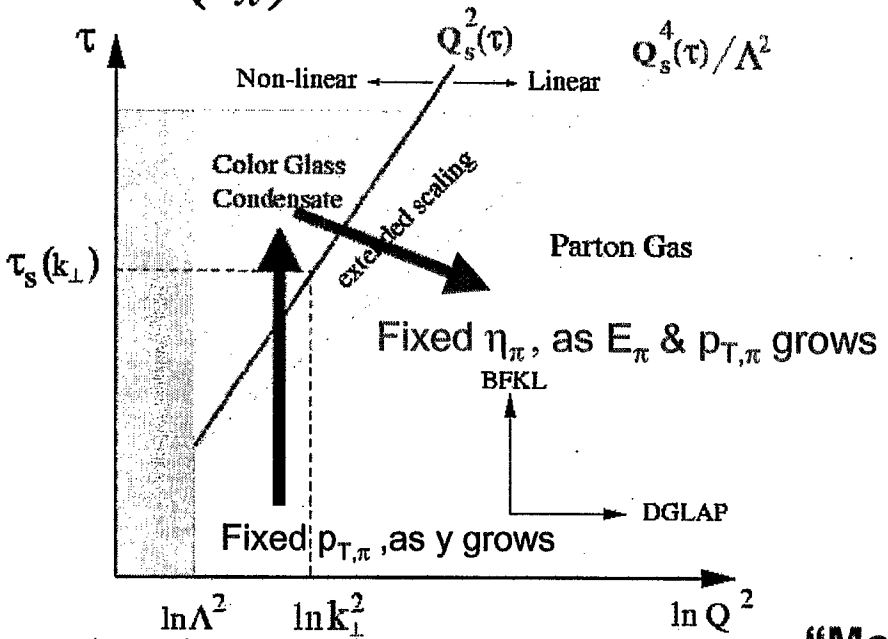

Edmond Iancu and Raju Venugopalan, hep-ph/0303204

General expectations of CGC:

Suppression of forward particle production

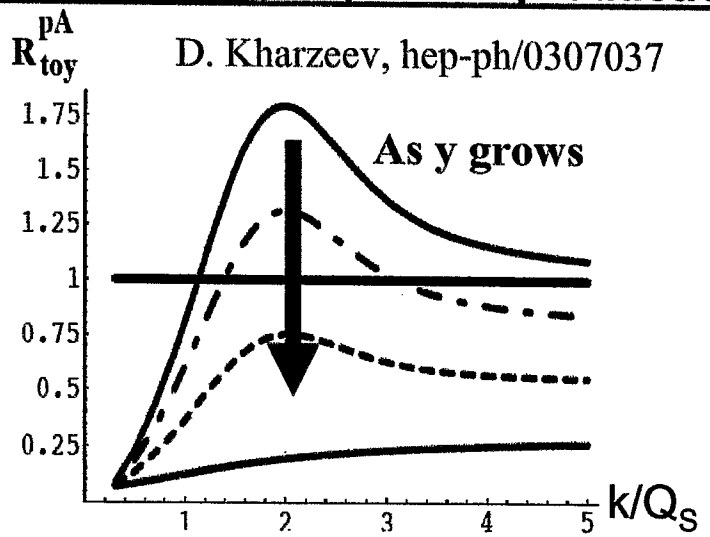

Brahms data shows evidence ?

(nucl-ex/0403005)

"Mono-jet"

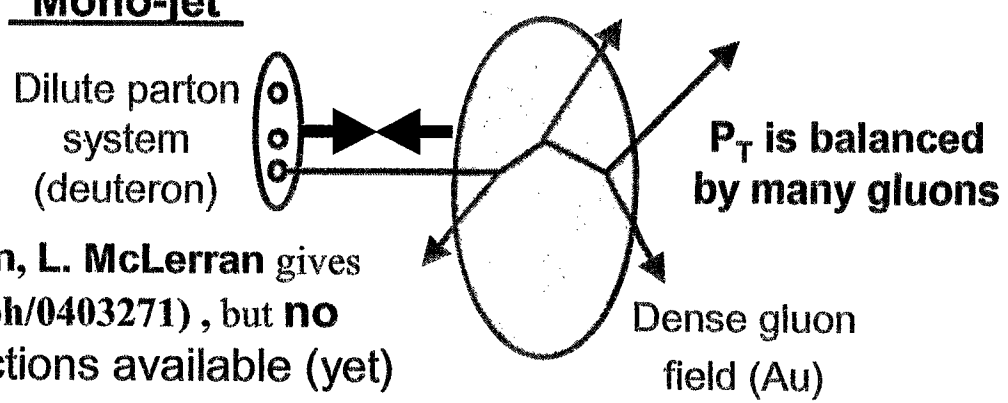

D.Kharzeev, E. Levin, L. McLerran gives physics picture **(hep-ph/0403271)**, but **no** quantitative predictions available (yet)

Results for forward d+Au $h^{\pm}$ production from Brahms

I. Arsene et al. (Brahms Collaboration)

submitted to PRL nucl-ex/0403005

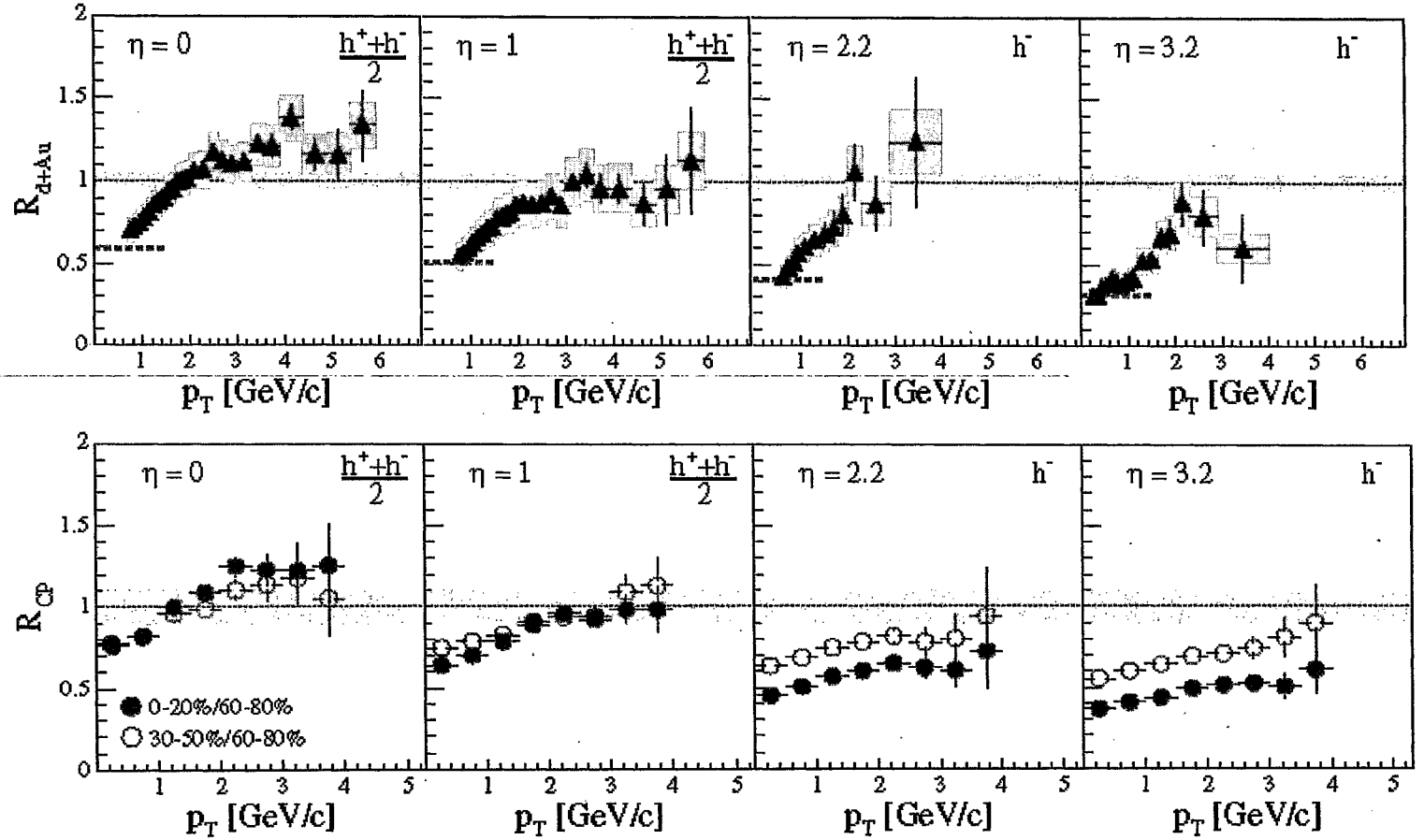

Suppression of inclusive hadron production at forward rapidities of d+Au relative to p+p observed at BRAHMS…

Probing Small-x Gluon Density

- probe the smallest Bjorken-x values by measuring forward di-jets (detected by leading π^0– π^0 pairs) ⇒ probe $x_{gluon} \leq 0.004$
- measure rapidity (η_2) distribution of π^0 in STAR barrel/endcap EMC, for events tagged with forward π^0 ($2.5<\eta_1<3.5$) ⇒ probe *monojet hypothesis* of the Color Glass Condensate
- increased acceptance of large-rapidity calorimetry ⇒ allow measurements of direct γ and heavier mesons ($\eta, K_S, \omega, \eta', D^0$) decaying to all γ final states.

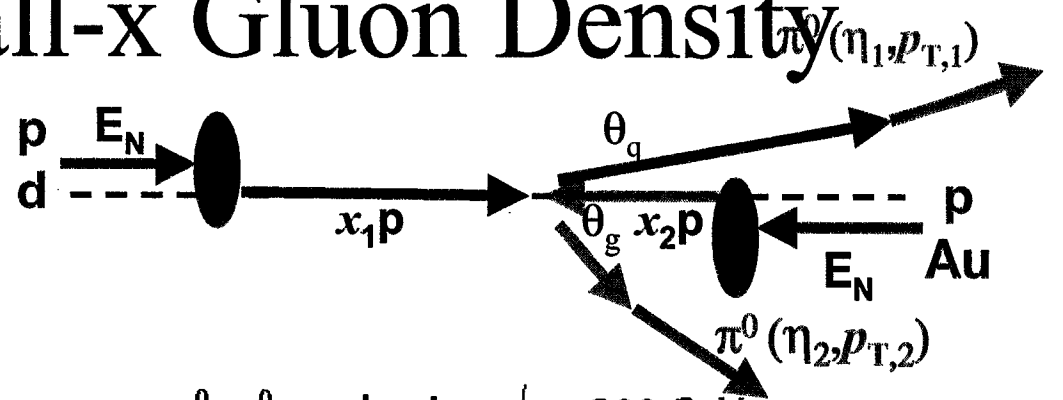

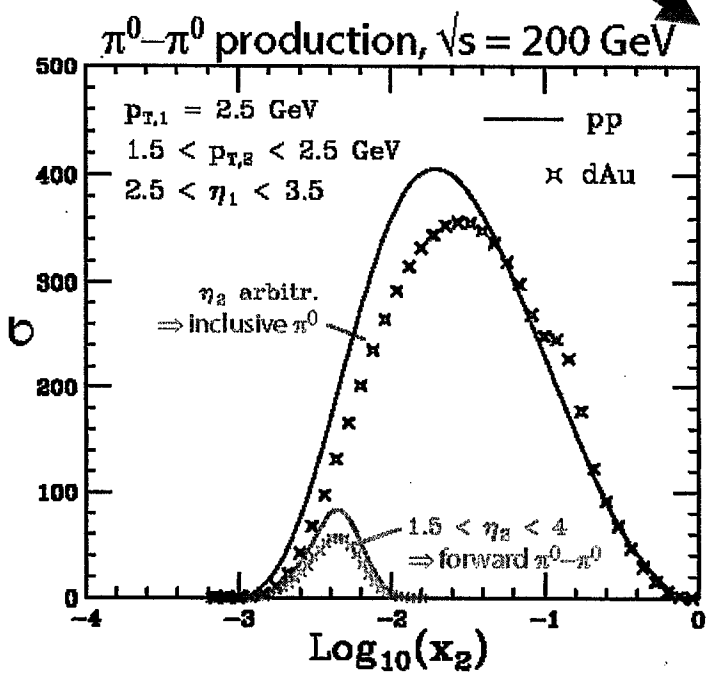

V. Guzey, M. Strikman and W. Vogelsang (hep-ph/0407201)

Forward Physics at STAR

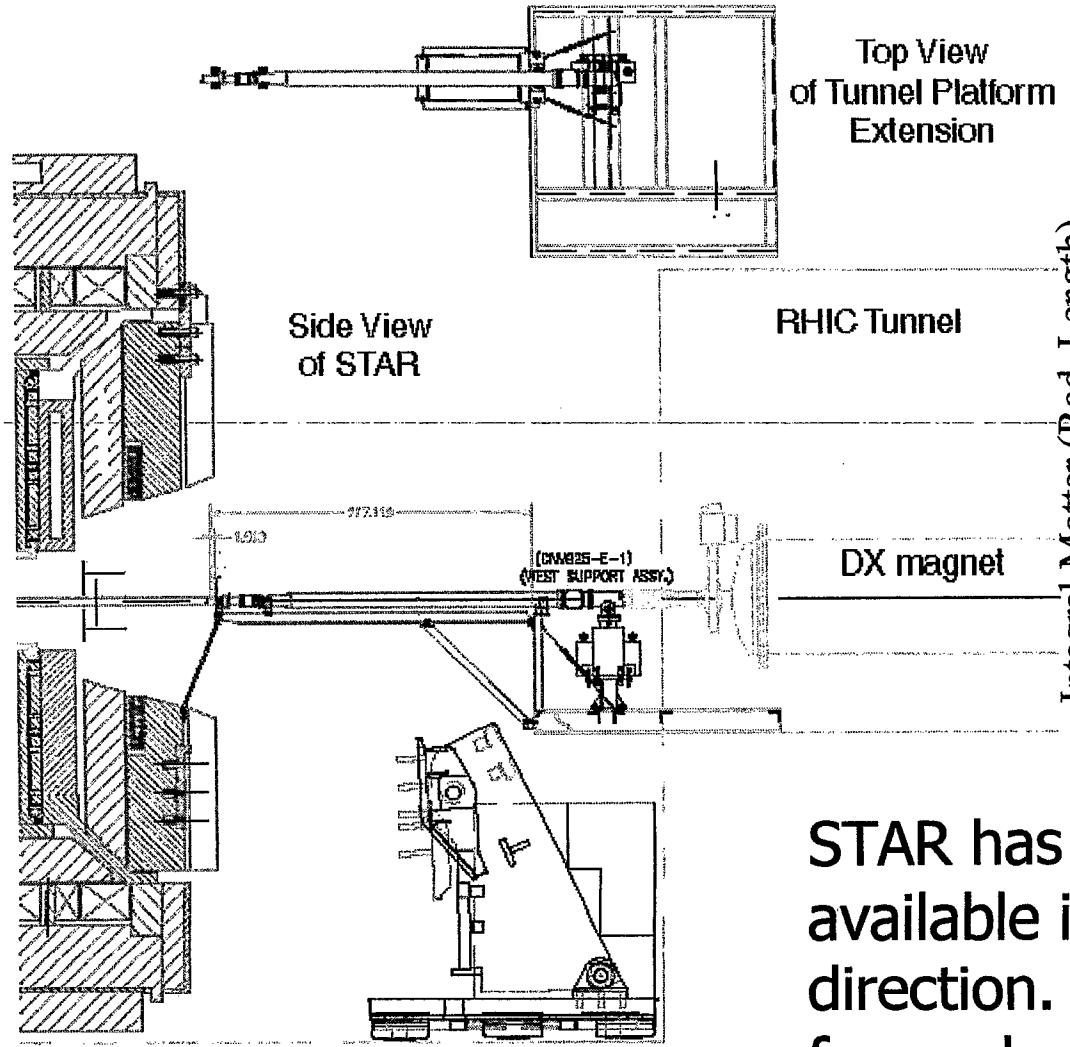

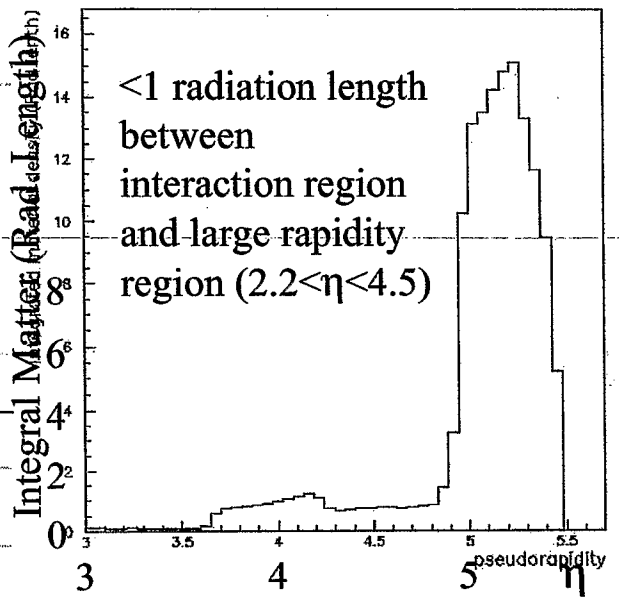

STAR has significant space available in the forward direction. ⇒ well suited to forward particle detection.

Forward Meson Spectrometer

Conceptual Design

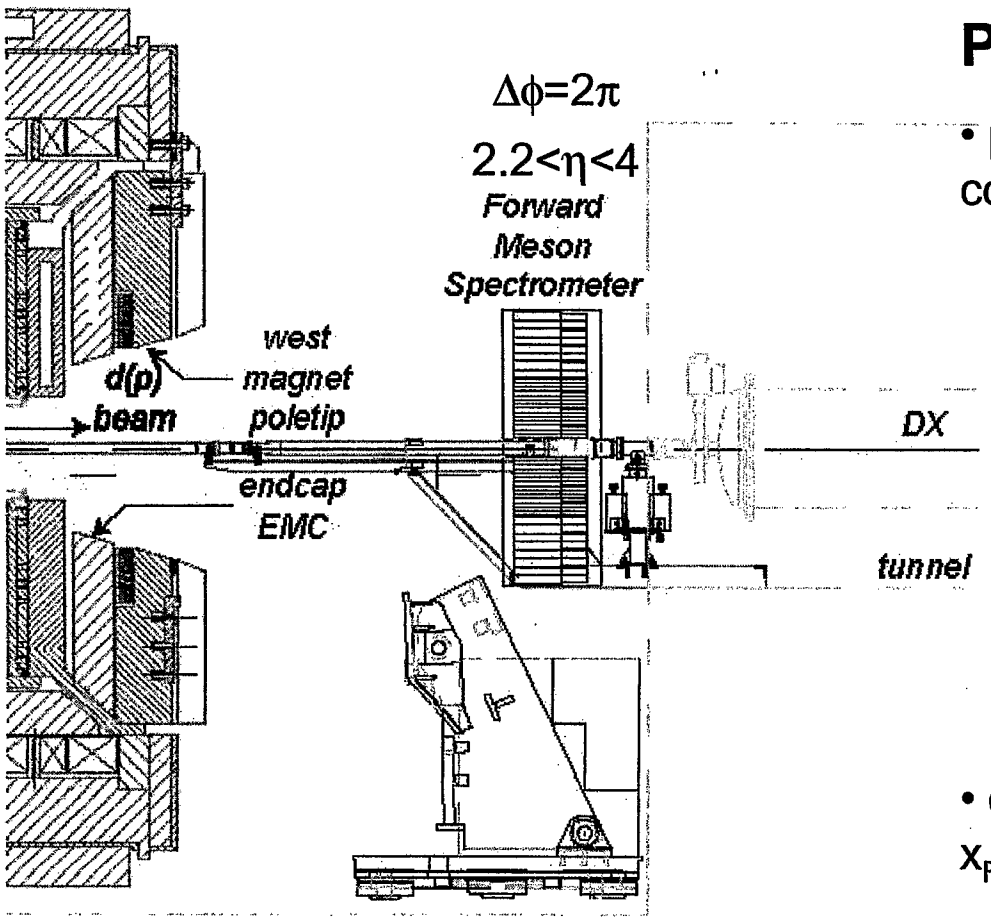

Physics Motivation:

- probing gluon saturation in p(d)+A collisions via…
  - large rapidity particle production ($\pi^0,\eta,\omega,\eta',\gamma,K^0,D^0$) detected through all γ decays.
  - forward di-jet surrogates (π^0–π^0) probe gluons with smallest Bjorken-x in Au nucleus
  - di-jets with large rapidity interval (Mueller-Navelet jets)
- disentangling dynamical origins of large x_F analyzing power in $p_\uparrow$+p collisions.

Forward Meson Spectrometer

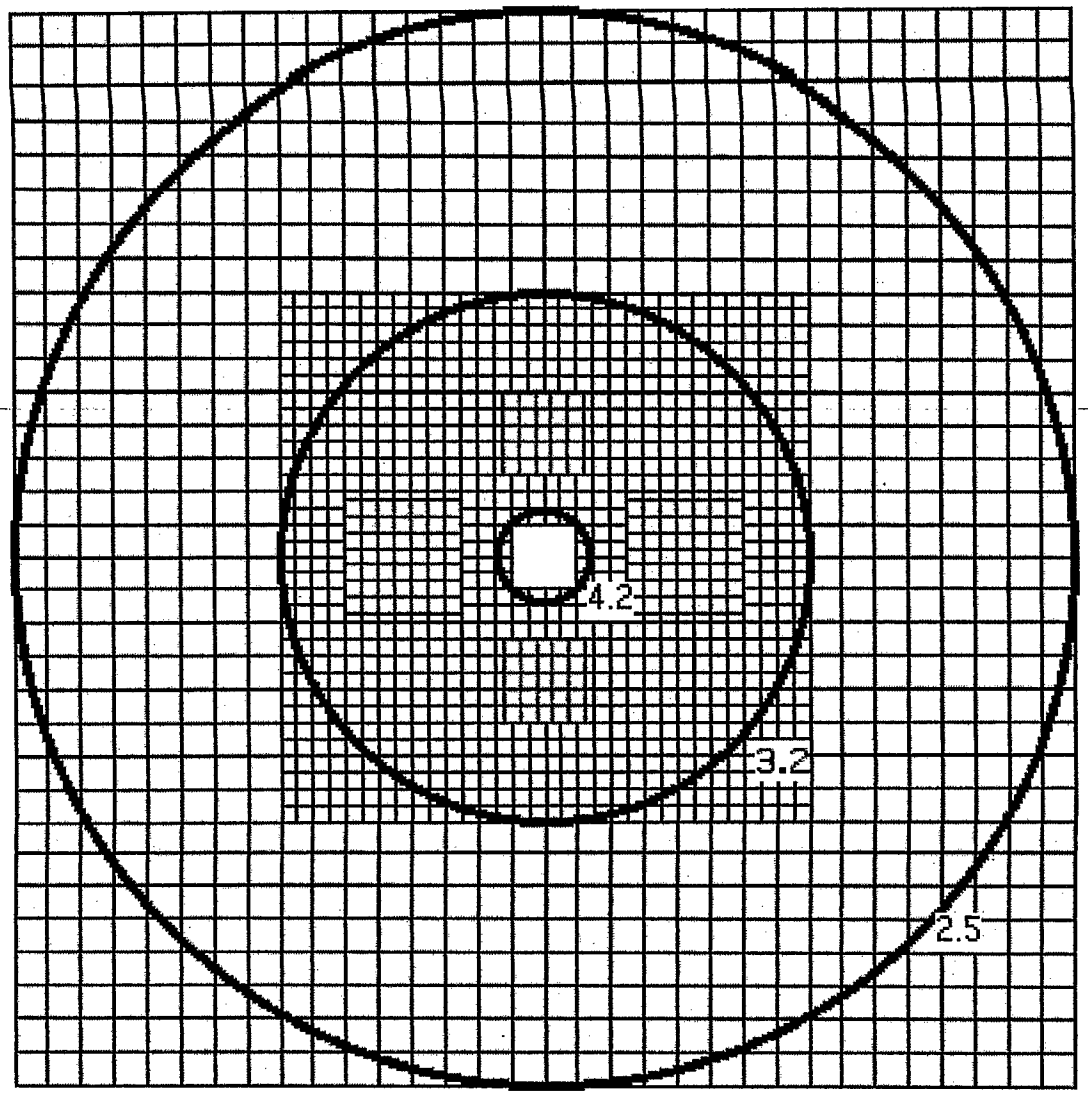

~2.4m square

~1500 PMTs

3.8 cm inner
7.6 cm outer

Forward Meson Spectrometer

Status

- **Timing**
  - STAR Forward Workshop (6/9/04) to establish scope
  - STAR Upgrades Workshop (6/15-17/04) for development of overall upgrades plan
  - Completion of Proposal (Fall, 2004)
  - Commissioning (Fall, 2006)
- **Cost**
  - Depends critically on availability of existing calorimetry (Pb glass).
  - If existing calorimetry can be employed, costs are dominantly readout/triggering electronics, high-voltage distribution, and mechanical design.
    Rough estimate ~ $0.8M

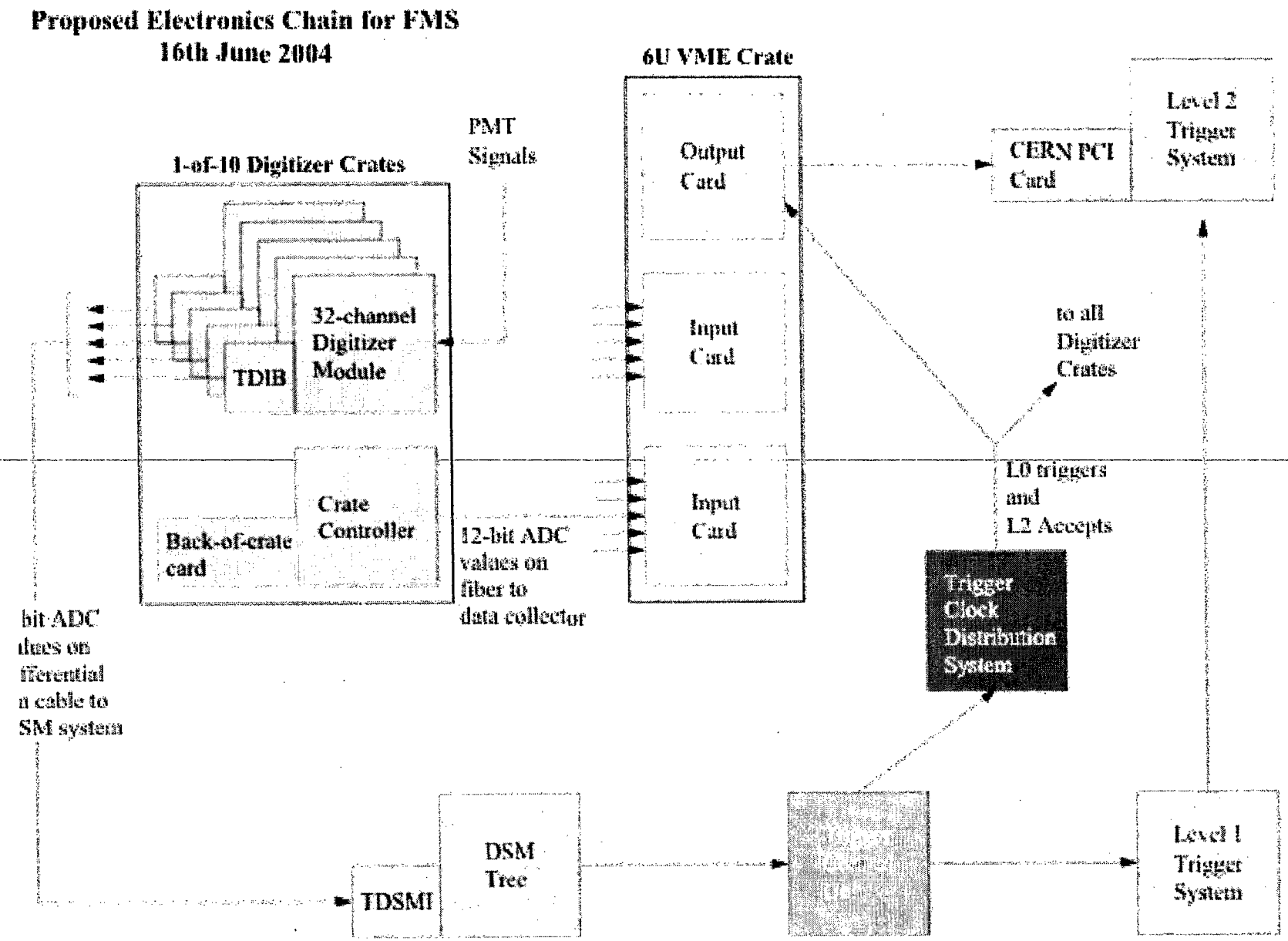

Use existing FPD L0 electronics - trigger on geometrical E

RHIC Spin Collaboration Meeting XXIX
Torino, Italy
October 8-9, 2004

LIST OF PARTICIPANTS

NAME	Affiliation	e-mail
I. Alekseev	ITEP	alekseev@vitep5.itep.ru
M. Anselmino	INFN	mauro.anselmino@to.infn.it
M. Bai	BNL	mbai@bnl.gov
K. Barish	UCR	barish@phyun0.ucr.edu
A. Bazilevsky	BNL	shura@bnl.gov
L. Bland	BNL	bland@iucf.indiana.edu
M. Boglione	INFN	elena.boglione@to.infn.it
G. Bunce	BNL	bunce@bnl.gov
N. Buttimore	Dublin	nigel.buttimore@tcd.ie
U. D'Alesio	INFN Cagliari	umberto.dalesio@ca.infn.it
A. Deshpande	Stony Brook	abhay@bnl.gov
A. Efremov	JINR	efremov@thsun1.jinr.ru
H. En'yo	RIKEN	enyo@riken.go.jp
D. Fields	New Mexico	fields@unm.edu
Y. Fukao	Kyoto/RIKEN	fukao@bnl.gov
L. Gamberg	Penn State Berks	lpg10@psu.edu
Y. Goto	RIKEN	goto@bnl.gov
W. Guryn	BNL	guryn@bnl.gov
D. Hasch	Frascati	hasch@mail.desy.de
R. Hobbs	New Mexico	rhobbs@unm.edu
H. Huang	BNL	huanghai@bnl.gov
K. Imai	Kyoto	imai@nh.scphys.kyoto-u.ac.jp
O. Jinnouchi	RBRC	josamu@bnl.gov
D. Kawall	RBRC / BNL	dave.kawall@bnl.gov
A. Kotzinia	Torino Univ.	aram.kotzinian@cern.ch
E. Leader	Imperial C.	e.leader@imperial.ac.uk
A. Lehrach	Julich	a.lehrach@fz_juelich.de
Y. Makdisi	BNL	makdisi@bnl.gov

RHIC Spin Collaboration Meeting XXIX
Torino, Italy
October 8-9, 2004

LIST OF PARTICIPANTS

M. Miller	MIT	mlmiller@mit.edu
A. Ogawa	BNL	akio@bnl.gov
H. Okada	Kyoto	okadah@bnl.gov
K. Okada	RBRC	okada@bnl.gov
A. Prokudin	INFN	prokudin@to.infn.it
V. Ptitsyn	BNL	vadimp@bnl.gov
P. Ratcliffe	dell'Insubria	philip.ratcliffe@uninsubria.it
V. Rykov	RIKEN	rykov@riken.go.jp
N. Saito	Kyoto	saito@spin.riken.bnl.gov
R. Seidl	UIUC	rseidl@uiuc.edu
J. Sowinski	IUCF	sowinski@iucf.indiana.edu
M. Stratmann	Regensburg	marco.stratmann@physik.uni-regensburg.de
D. Svirida	ITEP	svirida@vitep5.itep.ru
M. Tannenbaum	BNL	mjt@bnl.gov
O. Teryaev	JINR	teryaev@thsun1.jinr.ru
M. Togawa	Kyoto	togawa@nh.scphys.kyoto-u.ac.jp
L. Trueman	BNL	trueman@quark.phy.bnl.gov
D. Underwood	ANL	dgu@gate.hep.anl.gov
W. Vogelsang	BNL	wvogelsang@bnl.gov
M. Wagner	Kyoto/RIKEN	mwagner@rcf.rhic.bnl.gov
A. Zelenski	BNL	zelenski@bnl.gov

RHIC Spin Collaboration Meeting XXIX
October 8 & 9, 2004 ~ Torino, Italy

AGENDA

Most talks are 20min + 10min (discussions) unless specified otherwise.
There are 3 discussion sessions, each ~30mins and led by 2 "discussion leaders".

October 8 (Friday)

***Opening Session (chair A. Ogawa)

09:00-09:10 Welcome, M. Anselmino
09:10-09:50 RHIC Status & Plan (30+10min), M. Bai
09:50-10:20 Gas-jet Target Polarimeter, A. Zelinski
10:20-10:50 Polarized Beam at COSY and HESR, A. Lehrach

coffee break

*** 11:00 Elastic Scattering (chair Y. Makdisi)

11:00-11:30 pp Polarimeter (backup), H. Okada
11:30-12:00 pp2pp, I. Alekseev
12:00-12:30 pC Polarimeter, O. Jinnouchi

lunch

13:30-14:00 Theory, L. Trueman
14:00-14:30 Spin Dynamics for High Energy Protons, N. Buttimore
14:30-15:00 Discussions led by E. Leader & Y. Makdisi

coffee break

***Transverse Spin (chair M. Anselmino)

15:15-15:45 HERMES, R. Seidl
15:45-16:00 Short Comment on the HERMES Transversal Spin Asymmetries (15 mins), A. Efremov
16:00-16:15 Disentangling of the Sources of Transverse Spin Asymmetries (15 mins), O. Teryaev
16:15-16:45 Suppression of Collins Mechanism for SSA in $p^¥uparrow p ¥to ¥pi X$, U. D'Alesio
16:45-17:15 PHENIX A_N, Y. Makdisi
17:15-17:45 STAR A_N from Forward pi0, A. Ogawa

20:00 Meeting Dinner at "Trattoria del Cardo Gobbo" (Piemontese Cuisine)

RHIC Spin Collaboration Meeting XXIX
October 8 & 9, 2004 ~ Torino, Italy

AGENDA

October 9 (Saturday)

***Transverse Spin (continuned) (chair M. Anselmino)

09:00-09:30 Transversity Properties of Quarks and Hadrons in SIDIS and Drell Yan, L. Gamberg
09:30-09:45 A_N in D Production and Sivers Gluon pdf at RHIC (15 mins), M. Boglione
09:45-10:00 A Critique of the Angular Momentum Sum Rules and a New Angular Momentum Sum Rule (15 mins), E. Leader
10:00-10:30 Discussions led by M. Anselmino & L. Bland

coffee break

***Longitudinal Spin (chair A. Deshpande)

10:50-11:20 HERMES, D. Hasch
11:20-11:40 LEPTO and Polarized SIDIS (15+5mins), A. Kotzinian
11:40-12:10 Spin Asymmetries for high-pt Pions and Jets, M. Stratmann

lunch

13:15-13:45 PHENIX pi0 A_LL, A. Bazilevsky
13:45-14:05 PHENIX direct photon xsection (15+5min), K. Okada
14:05-14:35 Longitudinal Progress at STAR, J. Sowinski
14:35-14:55 STAR jet algorithms (15+5min), M. Miller
14:55-15:25 Discussions led by A. Deshpande & W. Vogelsang (additional slides)

coffee break

***Upgrades (chair K. Imai) (all talks in this session are 15+5mins)

15:40-16:00 PHENIX forward upgrade, K. Barish
16:00-16:20 PHENIX tracking upgrade, Y. Goto
16:20-16:40 STAR forward tracking upgrade, M. Miller
16:40-17:00 STAR foward calorimetry upgrade, L. Bland

Meeting adjourns

Additional RIKEN BNL Research Center Proceedings:

Volume 66 – RHIC Spin Collaboration Meeting XXIX, October 8-9, 2004, Torino Italy – BNL-

Volume 65 – RHIC Spin Collaboration Meetings XXVII (July 22, 2004), XXVIII (September 2, 2004), XXX (December 6, 2004) - BNL-

Volume 64 – Theory Summer Program on RHIC Physics – BNL-73263-2004

Volume 63 – RHIC Spin Collaboration Meetings XXIV (May 21, 2004), XXV (May 27, 2004), XXVI (June 1, 2004) – BNL-72397-2004

Volume 62 – New Discoveries at RHIC, May 14-15, 2004 – BNL- 72391-2004

Volume 61 – RIKEN-TODAI Mini Workshop on "Topics in Hadron Physics at RHIC", March 23-24, 2004 – BNL-72336-2004

Volume 60 – Lattice QCD at Finite Temperature and Density – BNL–72083-2004

Volume 59 – RHIC Spin Collaboration Meeting XXI (January 22, 2004), XXII (February 27, 2004), XXIII (March 19, 2004)– BNL-72382-2004

Volume 58 – RHIC Spin Collaboration Meeting XX – BNL-71900-2004

Volume 57 – High pt Physics at RHIC, December 2-6, 2003 – BNL-72069-2004

Volume 56 – RBRC Scientific Review Committee Meeting – BNL-71899-2003

Volume 55 – Collective Flow and QGP Properties – BNL-71898-2003

Volume 54 – RHIC Spin Collaboration Meetings XVII, XVIII, XIX – BNL-71751-2003

Volume 53 – Theory Studies for Polarized *pp* Scattering – BNL-71747-2003

Volume 52 – RIKEN School on QCD "Topics on the Proton" – BNL-71694-2003

Volume 51 – RHIC Spin Collaboration Meetings XV, XVI – BNL-71539-2003

Volume 50 – High Performance Computing with QCDOC and BlueGene – BNL-71147-2003

Volume 49 – RBRC Scientific Review Committee Meeting – BNL-52679

Volume 48 – RHIC Spin Collaboration Meeting XIV – BNL-71300-2003

Volume 47 – RHIC Spin Collaboration Meetings XII, XIII – BNL-71118-2003

Volume 46 – Large-Scale Computations in Nuclear Physics using the QCDOC – BNL-52678

Volume 45 – Summer Program: Current and Future Directions at RHIC – BNL-71035

Volume 44 – RHIC Spin Collaboration Meetings VIII, IX, X, XI – BNL-71117-2003

Volume 43 – RIKEN Winter School – Quark-Gluon Structure of the Nucleon and QCD – BNL-52672

Volume 42 – Baryon Dynamics at RHIC – BNL-52669

Volume 41 – Hadron Structure from Lattice QCD – BNL-52674

Volume 40 – Theory Studies for RHIC-Spin – BNL-52662

Volume 39 – RHIC Spin Collaboration Meeting VII – BNL-52659

Volume 38 – RBRC Scientific Review Committee Meeting – BNL-52649

Volume 37 – RHIC Spin Collaboration Meeting VI (Part 2) – BNL-52660

Volume 36 – RHIC Spin Collaboration Meeting VI – BNL-52642

Volume 35 – RIKEN Winter School – Quarks, Hadrons and Nuclei – QCD Hard Processes and the Nucleon Spin – BNL-52643

Volume 34 – High Energy QCD: Beyond the Pomeron – BNL-52641

Volume 33 – Spin Physics at RHIC in Year-1 and Beyond – BNL-52635

Additional RIKEN BNL Research Center Proceedings:

Volume 32 – RHIC Spin Physics V – BNL-52628
Volume 31 – RHIC Spin Physics III & IV Polarized Partons at High Q^2 Region – BNL-52617
Volume 30 – RBRC Scientific Review Committee Meeting – BNL-52603
Volume 29 – Future Transversity Measurements – BNL-52612
Volume 28 – Equilibrium & Non-Equilibrium Aspects of Hot, Dense QCD – BNL-52613
Volume 27 – Predictions and Uncertainties for RHIC Spin Physics & Event Generator for RHIC Spin Physics III – Towards Precision Spin Physics at RHIC – BNL-52596
Volume 26 – Circum-Pan-Pacific RIKEN Symposium on High Energy Spin Physics – BNL-52588
Volume 25 – RHIC Spin – BNL-52581
Volume 24 – Physics Society of Japan Biannual Meeting Symposium on QCD Physics at RIKEN BNL Research Center – BNL-52578
Volume 23 – Coulomb and Pion-Asymmetry Polarimetry and Hadronic Spin Dependence at RHIC Energies – BNL-52589
Volume 22 – OSCAR II: Predictions for RHIC – BNL-52591
Volume 21 – RBRC Scientific Review Committee Meeting – BNL-52568
Volume 20 – Gauge-Invariant Variables in Gauge Theories – BNL-52590
Volume 19 – Numerical Algorithms at Non-Zero Chemical Potential – BNL-52573
Volume 18 – Event Generator for RHIC Spin Physics – BNL-52571
Volume 17 – Hard Parton Physics in High-Energy Nuclear Collisions – BNL-52574
Volume 16 – RIKEN Winter School - Structure of Hadrons - Introduction to QCD Hard Processes – BNL-52569
Volume 15 – QCD Phase Transitions – BNL-52561
Volume 14 – Quantum Fields In and Out of Equilibrium – BNL-52560
Volume 13 – Physics of the 1 Teraflop RIKEN-BNL-Columbia QCD Project First Anniversary Celebration – BNL-66299
Volume 12 – Quarkonium Production in Relativistic Nuclear Collisions – BNL-52559
Volume 11 – Event Generator for RHIC Spin Physics – BNL-66116
Volume 10 – Physics of Polarimetry at RHIC – BNL-65926
Volume 9 – High Density Matter in AGS, SPS and RHIC Collisions – BNL-65762
Volume 8 – Fermion Frontiers in Vector Lattice Gauge Theories – BNL-65634
Volume 7 – RHIC Spin Physics – BNL-65615
Volume 6 – Quarks and Gluons in the Nucleon – BNL-65234
Volume 5 – Color Superconductivity, Instantons and Parity (Non?)-Conservation at High Baryon Density – BNL-65105
Volume 4 – Inauguration Ceremony, September 22 and Non -Equilibrium Many Body Dynamics –BNL-64912
Volume 3 – Hadron Spin-Flip at RHIC Energies – BNL-64724
Volume 2 – Perturbative QCD as a Probe of Hadron Structure – BNL-64723
Volume 1 – Open Standards for Cascade Models for RHIC – BNL-64722

For information please contact:

Ms. Pamela Esposito
RIKEN BNL Research Center
Building 510A
Brookhaven National Laboratory
Upton, NY 11973-5000 USA

Phone: (631) 344-3097
Fax: (631) 344-4067
E-Mail: pesposit@bnl.gov

Mrs. Tammy Stein
RIKEN BNL Research Center
Building 510A
Brookhaven National Laboratory
Upton, NY 11973-5000 USA

(631) 344-5864
(631) 344-2562
tstein@bnl.gov

Homepage: http://www.bnl.gov/riken

RIKEN BNL RESEARCH CENTER

RHIC Spin Collaboration Meeting XXIX

October 8-9, 2004 ~ Torino, Italy

Li Keran

Nuclei as heavy as bulls
Through collision
Generate new states of matter.
T.D. Lee

Copyright©CCASTA

Speakers:

I. Alekseev	M. Anselmino	M. Bai	K. Barish
A. Bazilevsky	L. Bland	M. Boglione	N. Buttimore
U. D'Alesio	A. Deshpande	A. Efremov	L. Gamberg
Y. Goto	D. Hasch	O. Jinnouchi	A. Kotzinian
E. Leader	A. Lehrach	Y. Makdisi	M. Miller
A. Ogawa	H. Okada	K. Okada	R. Seidl
J. Sowinski	M. Stratmann	O. Teryaev	L. Trueman
W. Vogelsang	A. Zelinsky		

Organizer: A. Ogawa